UNIVERSITY OF LONDON THESIS

Degree PhD Year 2007 Name of Author SPASIS, George

Heating, Ventilation and Air Conditioning System Optimization:

A study of the effect of climate, building design, system selection and control strategy on the energy consumption of a typical office building in London and Athens

Georgios Spasis

The Bartlett School of Graduate Studies

University College London

A thesis submitted for the

degree of Doctor of Philosophy

University of London

2007

ProQuest LLC
789 East Eisenhower Parkway
P.O. Box 1346
Ann Arbor, MI 48106-1346

Declaration that the work presented in the thesis is the candidate's own

I, Georgios Spasis, confirm that the work presented in this thesis is my own. Where information has been derived from other sources, I confirm that this has been indicated in the thesis.

Signature

Abstract

The increasing demand for air conditioning in commercial buildings imposes a serious threat to Europe's CO_2 reduction targets. Architects and engineers are therefore in a key position to help reduce the impact of buildings on the environment by taking appropriate decisions concerning the design of the building and the associated heating, ventilation and air conditioning (HVAC) system.

The thesis studies the effect of a number of building and HVAC system related design factors on the energy performance of a notional air-conditioned office building employing either a variable air volume (VAV) system with terminal re-heaters, or a four-pipe fan coil unit (FCU) system with fresh air supply from a central plant, using mainly a dynamic simulation tool and the response surface methodology. The evaluation of the energy performance of the HVAC systems is for two types of climate, using typical weather data for London (UK) and Athens (Greece).

It has been found that the design variables associated with the solar radiation through the transparent building elements and the internal heat gains should be the main concern of the building designer. On the other hand, the HVAC system engineer should give emphasis to the parameters associated with the plant performance and operation, as well as the temperature control set-points. It has been shown that it is possible to reduce the carbon emissions of the base case scenario by up to 88% depending on the HVAC system and the climate for which it is simulated. The carbon savings, however, are reduced by up to 22% where humidification is provided. This reduction differs depending on the HVAC system and the climatic conditions.

The VAV system is more energy efficient than the FCU system, mainly due to the exploitation of the free cooling capacity of the outdoor air. The difference in carbon emissions between the two systems drops when both of them are simulated for the Athens as opposed to the London typical weather conditions. It has been found that it is possible to turn the carbon scales in favour of the FCU system when humidification to a high RH set-point is provided throughout the year, since the adjustment of the RH of the air is particularly energy wasteful for the VAV system.

Acknowledgements

The first words of this text should be words of gratitude to all those who helped to make this thesis possible. Above all, I would like to thank my supervisor Dr. Alan Young for encouraging me to do a PhD. I feel deeply grateful for his advice and guidance throughout the period of this study. I could not have imagined having a better mentor for my PhD, and without his knowledge, perceptiveness and invaluable suggestions working on this project would have been much more difficult. My gratitude also goes to Dr. Ben Croxford for his useful comments on this work. I am most indebted to Prof. Georgios Skarakis and Xaralambos Kotzamanidis for introducing me to the field of statistics. I sincerely thank Alexandros Vakalopoulos for his advice on the duct sizing calculations and the HVAC system design. Finally, I warmly thank my family for their understanding, endless patience and continuous support during all these years.

Table of Contents

List of Figures

List of Tables

Chapter 1: Introduction

1.1 The use of air conditioning in the commercial building sector

Air-conditioning can be defined as the provision and maintenance of a desirable internal environment irrespective of the external conditions or casual internal gains [1]. Traditionally, the term 'air-conditioning' is associated with the provision of cooling during the warm periods of the year [2]. However, due to modern building forms and the high standards of living and working conditions expected, a number of advanced HVAC systems have been produced, which can provide close control of temperature, humidity and air quality to guarantee a satisfactory internal environment all year round [1], [2].

The use of air-conditioning in the United Kingdom has shown an accelerating growth during the last 20 years, with the commercial sector being the leader in terms of cooled floor space [3]. The average market growth in the 1970s and early 1980s was only around 100-150 MW of installed cooling power per year. Within ten years, during the early 1990s, the installed cooling power accelerated to approximately 1000 MW per year. The belief of developers and owners that air-conditioned spaces can guarantee more satisfied and productive employees as well as higher rental values was the main market driver behind this growth in air-conditioning use. However, this huge demand for air-conditioning was certainly not completely unjustified. The implementation of fully glazed facades, the use of lighting and personal computers in combination with the outdoor air pollution and traffic noise contributed to an increasing likelihood of overheating at least for a part of the year.

Over the last decade, the use of air conditioning has followed a similar pattern. Thus, UK sales (by volume) for A/C chiller-units have more than tripled between 1988 and 2001. Almost all of these units were sold to the commercial sector, with around 45% installed in commercial offices [25].

At present, buildings contribute 46% of UK carbon emissions with 19% originating from non-domestic buildings [15]. A BRE paper [3] on projections for future use of air conditioning in buildings predicted that by 2020 about 40% of commercial floor space will be air-conditioned, as opposed to 10% in 1994 [6]. This prediction was based on the assumption that the market drivers stay the same, the technology used does not alter significantly, and the area of cooled space develops along a classic S-curve, with first time sales declining when a level of market saturation is reached [3]. The projected trend in air-conditioning energy consumption and the associated carbon emissions until 2020 can be seen figures 1-1 and 1-2, respectively:

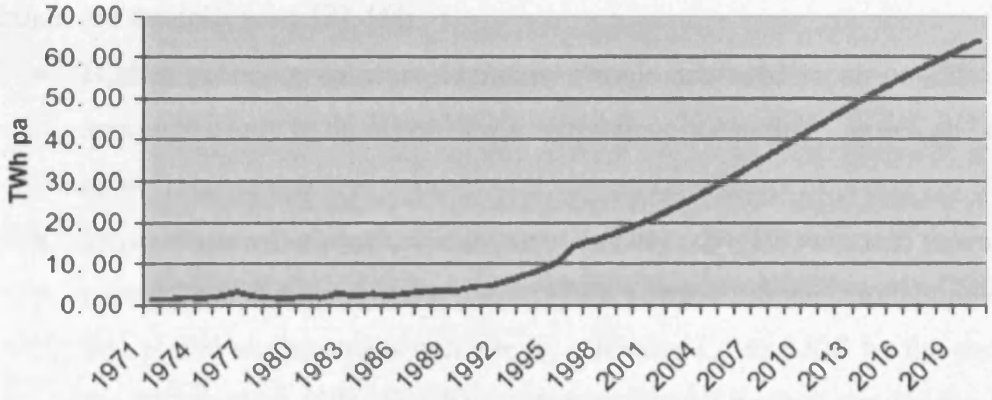

Figure 1-1: Projected trend in cooling electricity use [3]

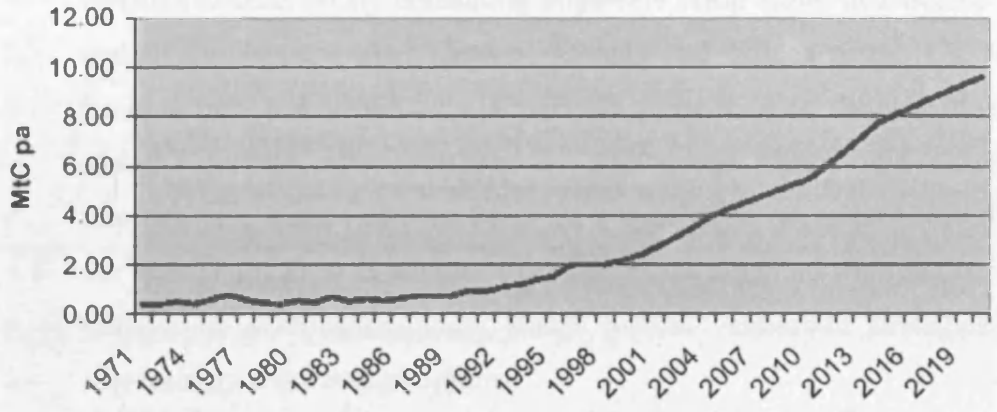

Figure 1-2: Projected trend in carbon emissions from air-conditioning [3]

It is clear that the predicted increase in electricity use (by 2020) and the consequent carbon emissions associated with air conditioning conflicts with both the UK's commitment to reduce greenhouse gas emissions by 12.5% below 1990 levels over the period 2008 – 2012 under the Kyoto Protocol [10] and the UK government's additional goal to reduce carbon dioxide emissions by 60% before 2050, as stated in the Energy White Paper [11], [12], published in February 2003, which acknowledges that climate change is real and that action is needed to mitigate the impact.

The reasons, which have induced this rapid demand for air-conditioning during the last 20 years, and which are likely to maintain this trend until 2020 or even further, are the following [3], [6]:

- Higher occupant comfort demands. People are used to air-conditioned spaces not only in their working environment but in their houses and cars as well, becoming less tolerant to relatively high temperatures.
- Expectation of a warmer climate. Globally, the 10 warmest years on record have occurred since 1990, while current climate models predict that global temperatures will rise by a further 1.4 to 5.8°C by the end of the 21st century [20]. The latest climate change projections for the UK indicate that peak summer temperatures could be up to 7°C warmer than today by the later decades of this century [21]. Also, the results of research conducted by consulting engineers Arup show that before the end of the century many homes, schools and offices in the UK will become unbearably hot for a significant proportion of the year due to global warming. For example, by 2080 some offices will have an internal temperature of over 28°C for a quarter of occupied hours over the year [7], [22]. It is obvious that the impact of global warming on the number of overheating hours makes natural ventilation strategies an increasingly risky design option.
- Higher standards of air tightness and thermal insulation currently implemented in buildings, in combination with the increasing use of office equipment and computer-intensive operations with a lot of internal

heat generation, which results in most buildings being in cooling mode for most of the year.

- Effect of air-conditioning on the rental value of floor space. For example, in U.S. offices, once 20% of the office space in a city is air-conditioned, it sets the rental value, and the uncooled space can only be let at a discount. It is, therefore, obvious why both the HVAC industry and market are increasing the pressure towards air-conditioning.

The energy use in the building sector in other countries is following a similar pattern. The 160 million buildings in the European Union use more than 40% of Europe's energy and create more than 40% of its CO_2 emissions [16]. A recent report which attempted to quantify the energy use in 13 industrialized countries, including Germany, France, Canada and U.S.A., illustrated that 39% of the annual primary energy consumption of the 13 nations is used in residential and commercial buildings, while 68% of the energy delivered to these types of buildings is attributed to space conditioning energy [5]. Similarly, the final energy demand in Greece in 2000 totaled 18.9 Mtoe of which 37% was used by the residential and tertiary sector. It should be stressed that the amount of energy used by this sector increased by 44% over the time period 1990 - 2000. This energy was primarily used for space heating and cooling, and domestic hot water production in residential, public and commercial premises [8].

It is obvious that buildings have a substantial share of the energy consumption all over the world. Scientific opinion that the burning of fossil fuels is responsible for global warming is now almost unanimous [18]. Given the predicted impact of global warming on the weather systems and ecology, a number of legislative instruments have been introduced to reinforce the need to reduce greenhouse gas emissions like the Kyoto Protocol and the Energy White Paper (in UK), mentioned earlier [18]. The EU is also making a determined effort to reduce the amount of energy used in buildings through the introduction of the Energy Performance of Buildings Directive (EPBD). The EPBD, which must be transposed into law in each member state with effect from January 2006, imposes on member states an obligation to establish a methodology for calculating the energy performance of buildings and in setting energy

performance standards for both new and existing buildings [17]. The major responsibility for practical measures to meet the requirements of the European Directive will obviously fall on architects and engineers [16].

The choice and design of HVAC systems is an aspect of the whole building design, which has a major impact on the environmental performance of the final project. On the other hand, the energy requirements of the chosen HVAC system also depend on the control strategy and the operation schedule as well as the climate that influences the thermal performance of the building and its design. It is, therefore, clear that architects / engineers are in a key position to help reduce the carbon emissions and the corresponding impact of buildings on global warming by taking thorough long-term decisions concerning the design of the building and the associated HVAC system. It should be stressed, however, that the impact of such decisions on the thermal performance of a building diminishes along the different stages over its life (i.e. sketch phase, architectural design, engineering design, construction, operation & maintenance) [9]. In other words, the design decisions made during the early stages of the design process usually carry the most effect. Therefore, the designer needs to consider a large number of alternative design options at the outset of the design process in order to identify the solution that best meets the objectives of the design project.

Information on the relationship between the design factors and the objectives of the design project is clearly required in order to make the best design decision. Building designers have traditionally reached such decisions based mainly on past experience [13]. However, total reliance upon an individual's experience may lead to unsatisfactory results [13]. The implementation of statistical and optimization techniques in building design can be particularly useful since they allow for systematic analysis of the decision-making problems faced by designers at the early stages of the design process. The complexity of the building systems and their ill-defined nature as well as their dynamic thermal behavior, were some of the factors responsible for the limited use of the aforementioned techniques in the analysis of the thermal performance of buildings [9]. However, the developments in computer technology and the availability of suitable energy simulation programs have allowed the integration

of simulation models and optimization techniques within the thermal design of buildings for decision-making purposes [9]. The most common approach involves the use of statistical techniques to build approximations of the detailed computer analysis codes, called 'metamodels' (e.g. low order polynomials), which are more efficient to run and help to uncover the functional relationship between the design factors and the performance indicator of interest, (e.g. the annual building energy consumption, the peak design loads, etc), while they also provide fast analysis tools for numerical optimization [4]. As a result, the designer is able to analyze the interaction between different design variables and choose the likely best combination, which will lead to the optimum energy use for different building or HVAC system types in different climates [9].

1.2 Aims of the study

The main aim of this theoretical study is to assess, through computer simulation, the effect of a number of design factors on the energy performance of a notional air-conditioned office building employing either a VAV system with terminal re-heaters or a four-pipe fan coil system with fresh air supply from a central plant, which are two of the most popular HVAC systems in the UK. The evaluation of the energy performance of the chosen systems is for two types of climate, using typical weather data for London (UK) and Athens (Greece). The chosen design variables are categorized into a number of groups associated with the design & operation of (a) the building and (b) the HVAC systems. The relationship between each of the chosen groups of factors and the energy performance of the HVAC systems is analysed using regression modeling techniques, while the design options minimizing the impact of the systems on the environment are identified using numerical optimization. Each group of parameters is first treated separately in order to understand how the factors under consideration affect the annual heating and cooling energy use, depending on the chosen HVAC system and the climate for which it is simulated, and to identify the parameters that should be the main concern of architects / engineers. The combination of factor levels of each group minimizing the total carbon emissions is identified, while the alternative design options or control strategies that can be

used to improve the carbon performance of the base case scenario (BCS) are displayed graphically. The findings obtained from each group of factors are finally combined in order to reach the overall optimum design solution for both HVAC systems, evaluated for the climates mentioned above. Based on the results, the appropriate designs and strategies are proposed in order to optimize the environmental performance of air-conditioned office buildings without compromising the thermal comfort of the occupants.

A secondary objective of this study is the comparison of the HVAC systems in question in order to determine which proves to be the most efficient both in terms of energy use and carbon emissions in each type of climate.

1.3 Outline of the methodology

The main concept behind this study is the consideration of a notional air conditioned office building which is simulated for two types of climate, using a sophisticated thermal analysis software tool. Two notional air conditioning systems are installed in the case study building model to assess their performance using an advanced HVAC system analysis tool. The effect of a number of design factors on the annual energy use and carbon emissions depending on the HVAC system and the climate for which it is simulated is analysed in detail, while the combinations of factor levels minimizing the impact of the HVAC systems on the environment are identified using a powerful statistical software package.

The procedure followed throughout this study can be summarized in the following:

- Three of the most popular building energy simulation programs (including TAS, APACHE and EnergyPlus) are considered in order to decide which is the most suitable for this study[1].
- The case study is a 6-floor notional deep-plan air-conditioned office building. The thermal performance of this building is evaluated in A-TAS, a dynamic thermal simulation software tool, using good practice

[1] **Note:** The study on the comparison of the three simulation tools can be found in appendix M.

values for the fabric construction, glazing ratio and internal conditions in order to reach a performance as similar as possible to a contemporary office building complying with the Building Regulations Part L (2002).

- The case study building employs either a VAV system with terminal re-heaters or a four-pipe fan coil system with fresh air supply from a central plant. B-TAS, a component-based simulation tool, is used for the assessment of both systems.
- Duct sizing calculations are carried out using mainly an Excel spreadsheet based on the equation of Colebrook-White [23] and the pressure loss factors supplied by CIBSE Guide C: Reference Data (2002) [24] in order to estimate the sizes of the fans for the chosen HVAC systems. The fan total pressure of the supply and return fans along with the simulation output file from A-TAS are then input into B-TAS to assess the energy performance of the HVAC systems, as mentioned above.
- The simulation of the systems in question is carried out using the latest Test Reference Years for London (UK) and Athens (Greece).
- The chosen design factors are categorized into eight groups related to the design and operation of the building and the associated HVAC systems.
- The Response Surface Methodology is used to model the relationship between each group of design factors and the annual energy use, as well as to identify the design options that minimize the impact of each HVAC system on the environment. Design-Expert is a statistical software package for specialized use in the design of experiments involving a set of predictor variables and one or more response functions. In general, the procedure that is followed can be described in the following two steps:

  1. The specification of the experimental design strategy, by which purposeful changes are made to the design factors in order to observe the effects on the TAS simulation output of interest [14], takes place in Design-Expert.

  2. The required simulations are carried out in A and B-TAS, as described above, and the predicted energy consumption data are input into Design-Expert which carries out step-by-step statistical analysis

providing the regression model that best fits the data, as well as, a variety of 2D or 3D plots (i.e. graphical representations of the response function) that aid the analysis of the results. The combinations of factor levels optimizing the performance of both systems in each of the chosen climates are also provided by Design-Expert, which makes use of the optimization technique developed by Derringer and Suich [19].

- The findings obtained from each group of parameters are finally combined through a number of scenarios simulated in TAS, in order to reach gradually the overall optimum design solution which maximises the total carbon savings over the BCS, depending on the HVAC system and the climate for which it is simulated.

Further details of the methodology described above are given in chapter 3.

1.4 Structure of the thesis

The thesis is structured as follows:

- A critical review of a number of past studies on the assessment of the design factors that affect the energy performance of air-conditioned buildings using mainly a computer simulation tool, is provided in chapter 2. This chapter also identifies the main points that a new study on this subject should consider.
- The methodology used to study the relationship between the design factors contained in each of the eight chosen groups and the energy consumption of the HVAC systems depending on the climate for which they are simulated as well as to identify the optimum factor settings is described in detail in chapter 3.
- The assessment of the effect of each group of factors on the energy performance of the FCU system and the VAV system, when they are simulated for the London and the Athens climate respectively, takes place in chapter 4. The combinations of factor levels minimizing the heating &

cooling energy consumption of each system depending on the climate for which the simulations are carried out, are also provided in this chapter.

- The factor settings of each group minimizing the overall carbon emissions of the HVAC systems in each climate and the associated reduction over the carbon performance of the BCS, are presented in chapter 5. Recommendations concerning the alternative combinations of factor levels resulting in near-optimum carbon performance are also given in this chapter.
- The findings derived from the study of each group of parameters are combined in chapter 6 through eight scenarios simulated in TAS, in order to reach gradually the overall optimum design solution. The simulation results of these scenarios are discussed, while the maximum total carbon savings over the BCS, depending on the type of HVAC system and the climate under consideration, are also provided in this chapter.
- The conclusions of the thesis along with a few recommendations concerning future research on the design of low-energy buildings through computer simulation are finally presented in chapter 7.

References

[1] Martin P L and Oughton D R, editors, *Faber and Kell's Heating and Air-Conditioning of Buildings*, Butterworths, London, 8th edition, 1995.

[2] McQuiston F C, Parker J D, Spitler J D, *Heating, Ventilating and Air-Conditioning: Analysis and Design*, 4th edition, 2000

[3] E.R. Hitchin, C.H. Pout, *Local Cooling: Global Warming? – UK Carbon Emissions form Air-Conditioning in the Next Two Decades*, BRE Client Report, June 2001

[4] T. W. Simpson, J. D. Peplinski, P. N. Koch, J. K. Allen, Metamodels for Computer-base Engineering Design: Survey and Recommendations, Engineering with Computers 17: 129 – 150, 2001

[5] M. Orme, *Estimates of the energy impact of ventilation and associated financial expenditures*, Energy and buildings 33, 2001, 199-205

[6] David Butler, *Trends in air conditioning*, Building Services Journal, June 2001, pg. 43-47

[7] UK will be too hot for comfort, Building Services Journal, September 2004, pg. 6

[8] Third National Communication to the UNFCCC (United Nations Framework Convention on Climate Change), February 2003, Climate Change – Official reports, National Observatory of Athens: http://www.climate.noa.gr/Reports/CC_reports.htm

[9] Mohammad Saad Al-Homoud, *Computer-aided building energy analysis techniques*, Building and Environment 36, (2001), 421-433

[10] Climate change – Action to tackle global warming: www.defra.gov.uk/environment/climatechange/02.htm#energywp

[11] Energy White Paper: Our energy future – creating a low carbon economy: www.dti.gov.uk/energy/index.htm.

[12] G. N. Dunn, I. P. Knight, E.R. Hitchin, *Measured Chiller Efficiency In-Use: Liquid Chillers & Direct Expansion Systems within UK Offices*, International Conference on Electricity Efficiency in Commercial Buildings, Frankfurt, Germany, 21-22 April 2004

[13] Mohammad S. Al-Homoud, Optimum Thermal Design of Air-Conditioned Residential Buildings, *Building and Environment*, Vol. 32, No. 3, 203-210, 1997

[14] Shari L. Kraber, Patrick J. Whitcomb, Mark J. Anderson, Handbook for Experimenters, Stat-Ease, Inc., www.statease.com, 2002

[15] Mott Green & Wall, Energy Efficient Ventilation Systems, Building Services Journal, January 2003, pg. 18-20

[16] Terry Welch, Energy Labelling of Buildings, Building Services Journal, October 2004, pg. 79-81

[17] Alan Fieldsend, Legislation for sustainability, Building Services Journal, September 2004, pg. 21

[18] Terry Dix, Time to Deliver, Building Services Journal, November 2003, pg. 37-38

[19] R.H. Myers, D.C. Montgomery, Response Surface Methodology: Process and Product Optimization Using Designed Experiments, Second Edition, 2002

[20] Jacqui Harman, The impact of climate change on modern building services, Modern Building Services, September 2004, (available from: http:// www.modbs.co.uk/news/fullstory.php/aid/370/The_impact_of_climate_change_ on_modern_building_services.html)

[21] Hacker J.N., Belcher S.E. and Connell R.K., Beating the Heat: Keeping UK Buildings Cool in a Warming Climate, UKCIP Briefing Report, UK Climate Impacts Programme and Arup, Oxford, September 2005, (available from: http://www.ukcip.org.uk /resources/publications/pub_dets.asp?ID=69)

[22] Hacker J.N., Holmes M.J., Belcher S.E. and Davies G, Climate Change and the Indoor Environment: Impacts and Adaptation, CIBSE TM36, Chartered Institution of Building Services Engineers, London, February 2005

[23] Jones W P, Air Conditioning Applications and Design, Arnold, London, 2nd edition, 1997

[24] CIBSE Guide C: Reference Data, The Chartered Institution of Building Services Engineers, London, 2001, Section 4.10: Pressure loss factors for ductwork, pages 96 -117.

[25] Joanne Wade, Jacky Pett, Lotter Ramsay, Energy Efficiency in Offices: Assessing the Situation, A scoping paper commissioned by the Carbon Trust and published by the Association for the Conservation of Energy, 2003.

Chapter 2: Approaches to the assessment of factors affecting the energy performance of buildings

2.0 Aims of the chapter

Building design is a process that should be considered as a whole, with an implementation of parts acting together to determine the performance of the building [1]. It is obvious that all the design parameters do not have the same effect on the building energy performance. However, it is important for the building designer to understand the relevant importance of these parameters. For example, it is essential to know to what extent the annual energy use is responsive to a change in the window surface area or the choice of HVAC system, in order to produce a more energy efficient building [2].

This chapter provides a critical review of past studies on the assessment of a number of design factors associated mainly with the design of the building envelope, the choice of the HVAC system and the characteristics of the climate on the energy performance of air-conditioned buildings through computer simulation, and identifies the main points that a new study on this subject should consider.

2.1 Structure of the chapter

An early pilot study on the effect of several design parameters on the energy consumption of an air-conditioned commercial building employing a computer simulation tool was carried out in 1980 and is presented in section 2.2. Another, more recent study that attempted to assess the effect of a number of design factors on the energy performance of two office buildings through computer simulation is presented in section 2.3. The principles of sensitivity analysis are briefly described in section 2.4, where important design parameters are identified and analyzed from the point of view of annual energy consumption and peak

design loads of a generic air-conditioned office building in Hong Kong. Section 2.5 illustrates the use of regression analysis techniques to correlate various design parameters with the energy consumption of an office building again in Hong Kong. Section 2.6 involves a study of the performance of several HVAC systems commonly incorporated in high-rise office buildings, to help the designer choose the system which can achieve low energy consumption combined with satisfactory thermal comfort conditions, while the studies presented in section 2.7, deal with the effect of different types of climate on the energy performance of air-conditioned residential and office buildings. Section 2.8 briefly discusses a number of studies that focus on the combination of optimization techniques and building simulation programs for the design of low-energy buildings. Finally, in section 2.9, a summary of the weaknesses of all these studies takes place, indicating the areas of this topic that require further investigation.

2.2 The application of a parametric analysis to the evaluation of the energy performance of a commercial air-conditioned building [11]

This study by Oughton (1980) [11] adopted a modular approach to estimate the energy consumption of a notional commercial air-conditioned building, based on computer simulation techniques, which allowed the effects of several factors of both architectural and engineering nature to be assessed. ENPRO, a computer program marketed by Faber Computer Operations was employed in the study. The architectural aspects of the design that were examined included the building orientation, the window-to-wall area, the glazing properties and the thermal properties of the opaque structure. Concerning the building services, a comparison was made between the energy consumption of a variable air volume (VAV) system and an induction unit system.

The case study was a typical air-conditioned building, with three alternative envelopes, two of them complying with the regulations of part FF (1978) and one based on the CIBS Energy Code Part 1 (1977). The floor plan of this building was divided into eight perimeter zones and one core zone module. The

meteorological data used for the simulations contained average hourly conditions of dry-bulb temperature, wet-bulb temperature and solar irradiation for Wethersfield, Essex.

The simulation results included the energy consumed by boilers and auxiliaries, chillers and cooling towers, fans and pumps. The energy used by lighting and small power was excluded, but the indirect effect of these as heat gains to the space was included. Some of the findings derived from the study of the effect of the design variables under consideration on the building energy performance are described in the following paragraphs.

Concerning the effect of the different envelopes it was found that if the effectiveness of window blinds was kept constant, an increase in window area would cause an increase in the total energy consumption. In the same sense, a reduction in the effectiveness of window blinds would increase again the building energy use.

It was found that over-insulation of the fabric of the air conditioned case study building did not produce a significant increase of the cooling energy, for normal levels of internal gains. However, a rise of the level of internal gains incurred a much greater increase of the building energy consumption.

Studying the energy requirements of the differently orientated zones of the building, it was found that the north facing modules had rather low energy consumption notwithstanding the higher heating load during the winter period, arising from the limited solar gains. The reason for this was that the energy consumption of an air-conditioned building complying with the building regulations part FF, (valid for 1980 when the study took place), was dominated by the cooling function. Thus, the total energy consumption of the case study building had lower values for the north facing zones and was greater for perimeter zones facing towards directions in the south to west quadrant, due to increased solar effects.

A limited study was also conducted to compare the energy consumed by a VAV system and an Induction Unit system. The primary energy consumption of the two systems is shown in figure 2-1, which illustrates that the Induction Unit system consumed more energy than the VAV system. This excess varied with the level of internal gains and the type of envelope. In general, as the internal gains increased so did the total energy consumption for both systems.

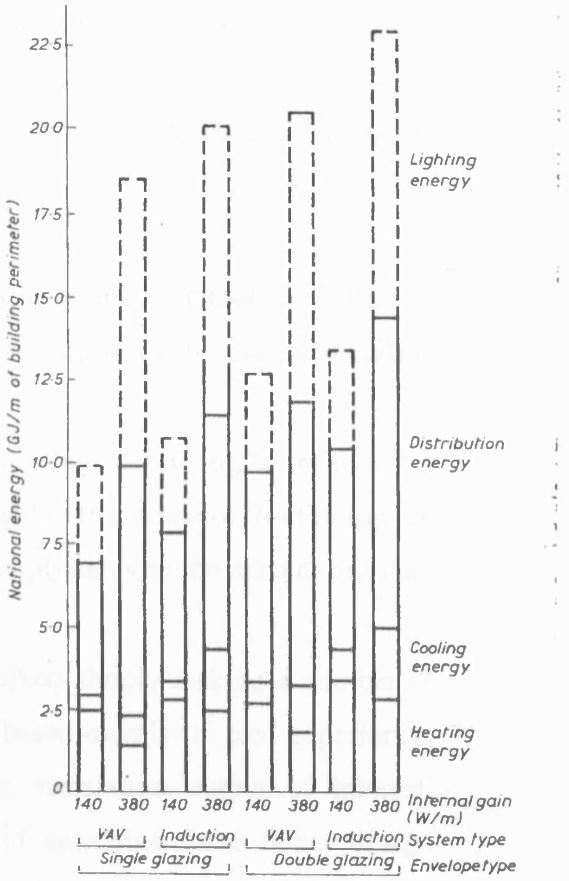

Figure 2-1: Components of average energy use in air conditioning systems – based on national energy [11]

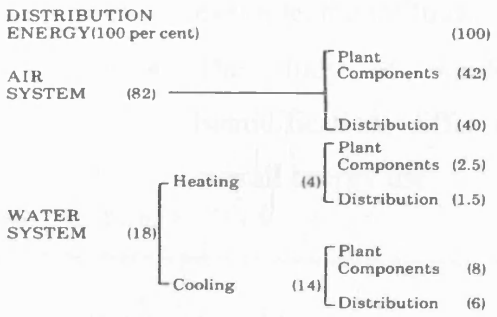

Figure 2-2: Components of the distribution energy in a typical variable air volume system [11]

Also considered was the distribution energy, which forms a significant part of the total energy consumption, as illustrated in figure 2.2 for a typical VAV system, related to the pressure drop across plant items, and through the ductwork and pipework circuits. This indicated the parts of an HVAC system that should receive critical examination during the design process.

To conclude, this study illustrated that there are certain factors associated mainly with the building envelope, as well as the design of the HVAC systems that should be given critical attention at the early steps of the design process, to achieve an energy efficient building. Nevertheless, there are many parts of the study that could now be criticized, such as, for example:

- The fact that it is based on a quite old simulation tool with limited capabilities, particularly given the sophistication of the current building simulation programs.
- The implementation of a case study building complying with an older version of the regulations. It is quite possible that some of the findings of this study are not valid for a building complying with the current building regulations.
- The approach adopted in this study involved simply making a number of changes to one or more design factors, based mainly on past experience, in order to observe the effect on the simulation output of interest. However, this trial and error process of searching for a better design solution is time-consuming and ineffective since the functional relationship between the design factors and the response variable is not uncovered, while the designer has to base his design decisions on a few trials leaving many promising solutions unexplored.
- There are several building related factors that were not examined, for example, the infiltration rate, the design of shading devices, etc.
- The study of building services systems ignored the effect of humidification, different set-points and other control strategies on the overall energy use.

2.3 Design of low energy buildings through computer simulation [30]

A recent study by Gratia, et al. (2003) [30] attempted to assess the effect of a number of design factors, such as the internal heat gains, the thermal characteristics of the walls and windows, the orientation and the area of windows, the building form, the external shading, the thermal mass of the building structure and the provision of natural ventilation on the thermal

performance of two air-conditioned[1] office buildings through computer simulation. Two simulation programs were used to this end. The first was OPTI a fast analysis tool, requiring a small number of input data to evaluate the impact of certain design choices on the energy use of a building, while the second was TAS, a dynamic simulation tool for the thermal analysis of buildings. The simulations were carried out for 12 actual months representative of the average climatic conditions in Uccle (Belgium).

The methodology used to carry out the above investigation, however, was particularly complicated, while the analysis of the simulation results was in most cases incomplete and confusing. For example, two office buildings were considered, while two simulation programs were used for no apparent reason. The basis of the selection of the design factors to be studied in each case was not given. Although each section of the paper under consideration was supposed to be dealing with one or two design factors, the associated simulation scenarios involved random changes in a large number of parameters[2], while the response variable was not always the same (e.g. the response variable could be the heating or cooling load of the buildings, the resultant or the air temperature of a chosen zone, the primary energy consumption, or the energy cost). It was therefore extremely difficult to analyze the results, which were usually presented through a number of rather unclear graphs, none of which was actually explained. Only some of the results were discussed, but the analysis was in most cases confusing, giving the impression that some of the final conclusions were not actually derived from the parts of the study presented in paper [30]. It is therefore clear that this is a rather poor study on the assessment of the design factors that make buildings energy efficient, which illustrates that the utilization of a sound

[1] **Note:** The temperature set-points and the operation schedule of the HVAC system were different in each building. Details concerning the type of HVAC system installed in each building were not given.

[2] **Note:** For example, the effect of the insulation level of the external building envelope on the heating & cooling load, the primary energy use as well as the energy cost of the first case study building was studied through 10 scenarios simulated in OPTI. However, these scenarios were changing at the same time the insulation thickness of the walls, floor and roof, the infiltration rate, the type of glazing and the thermal mass of the building structure, while the last six scenarios also considered the provision of ventilation and the addition of external blinds to the windows. On top of this, the effect of all these scenarios on the response variables under consideration was given for different levels of internal heat gains. The findings of this investigation were not discussed in detail. (In fact, the simulation results of most of these scenarios were not discussed at all). It was simply stated that insulation is beneficial in winter, but it can create overheating problems in summer.

methodology and the coherent analysis of the simulation results are essential aspects of a good investigation that will lead to clear and understandable conclusions.

2.4 Sensitivity analysis of the energy performance of office buildings [3]

This paper by Lam, et al. (1996) [3] involved a study of the factors that affect the energy consumption of a typical air conditioned office building in Hong Kong, using DOE-2, a building simulation program developed by Lawrence Berkeley National Laboratory (USA). Sensitivity analysis techniques were employed to aid the identification of the design elements that should receive major attention during modeling.

The general aim of sensitivity analysis is to observe the system response following a modification in a given design parameter. A measure of the sensitivity of each parameter is the influence coefficient (IC), which is derived as the partial derivative of one variable with respect to another variable in a system [4]. In building energy simulation, the IC quantifies the influence of an input parameter on a simulation result as follows:

$$IC = \frac{\partial OP}{\partial IP} \approx \frac{\Delta \mathrm{OP}}{\Delta IP}$$

where OP is the output and IP is the input.

The sensitivity coefficients appear in five forms, which can either have dimensions or not, as can be seen in table 2-1:

Form	Formulae	Dimensions	Common name(s)
1	$\frac{\Delta OP}{\Delta IP}$	with dimension	Sensitivity coefficient, influence coefficient
2a	$\frac{\Delta OP \div OP_{BC}}{\Delta IP \div IP_{BC}}$	$\frac{\%\ OP \text{ change}}{\%\ IP \text{ change}}$	Influence coefficient, point elasticity
2b	$\frac{\Delta OP \div OP_{BC}}{\Delta IP}$	with dimension	Influence coefficient
3a	$\frac{\Delta OP \div \left(\frac{OP_1 + OP_2}{2}\right)}{\Delta IP \div \left(\frac{IP_1 + IP_2}{2}\right)}$	$\frac{\%\ OP \text{ change}}{\%\ IP \text{ change}}$	Arc mid-point elasticity
3b	$\left(\frac{\Delta OP}{\Delta IP}\right) \div \left(\frac{\overline{OP}}{\overline{IP}}\right)$	$\frac{\%\ OP \text{ change}}{\%\ IP \text{ change}}$	(see note 2)

1. ΔOP, ΔIP = changes in output and input respectively.
OP_{BC}, IP_{BC} = base case values of output and input respectively.
IP_1, IP_2 = two values of input.
OP_1, OP_2 = two values of the corresponding output.
$\overline{OP}$, $\overline{IP}$ = mean values of output and input respectively.
2. For the form (3b), the slope of the linear regression line divided by the ratio of the mean output and mean input values will be taken for determining the sensitivity coefficient.

Table 2-1: Different forms of sensitivity coefficients [3]

Although all five forms of the sensitivity coefficients displayed in table 2-1 can be used in computer simulation, forms (1), (2a) and (3b) are more useful for the assessment of sensitivity using building energy simulation methods [3].

The procedure followed in this paper to study the energy characteristics of an air-conditioned office building in Hong Kong, was based on the sensitivity theory briefly described above.

The base case building, which forms an important aspect of the study, since all subsequent calculations and analyses are based on the comparison with it, was established from a survey of local construction and engineering practices in Hong Kong. It was a 40-storey square office building (35 x 35 m) with a curtain wall construction, served by a terminal reheat VAV system. A plan and section through a typical floor can be seen in figure 2-3.

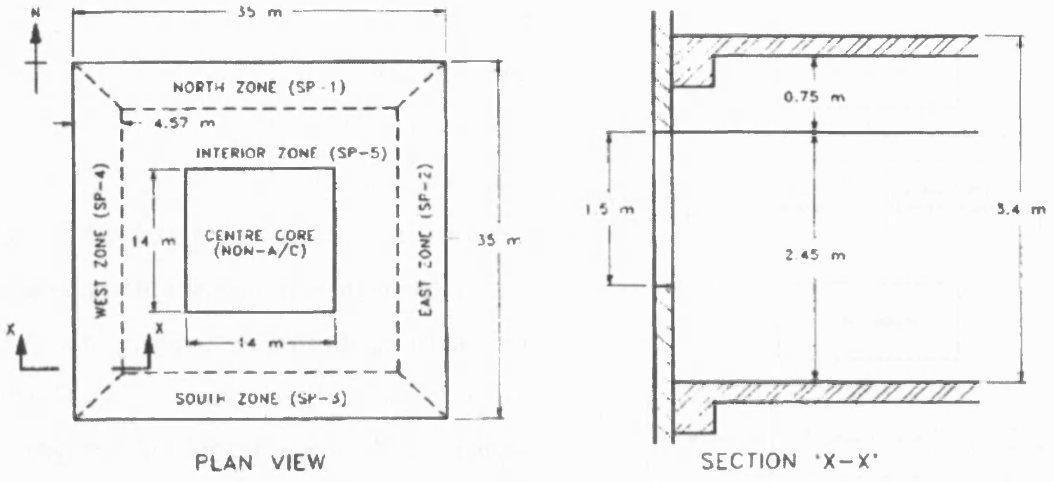

Figure 2-3: Plan and section of a typical floor of the base case building [3]

The simulations were carried out using hourly weather data for the year 1989, which was considered to be representative of the prevailing local climatic conditions [6], [7].

It is worth mentioning that the analysis of the base case building energy performance indicated that the annual energy consumption was dominated by the cooling energy use (52%). The heating energy consumption, on the other hand, was considered insignificant, accounting for only 0.3%

The next step involved the breakdown of the factors, which were essential to the design of office buildings in Hong Kong, into basic parameters. A list of 62 design parameters was formed. These parameters were categorized into 3 main groups: 1) Building Load, 2) HVAC systems and 3) HVAC refrigeration plant. Each of these groups was also sub-divided into different sub-groups as can be seen in figure 2-4. By categorizing the input design parameters a clear picture of the energy related factors can be established.

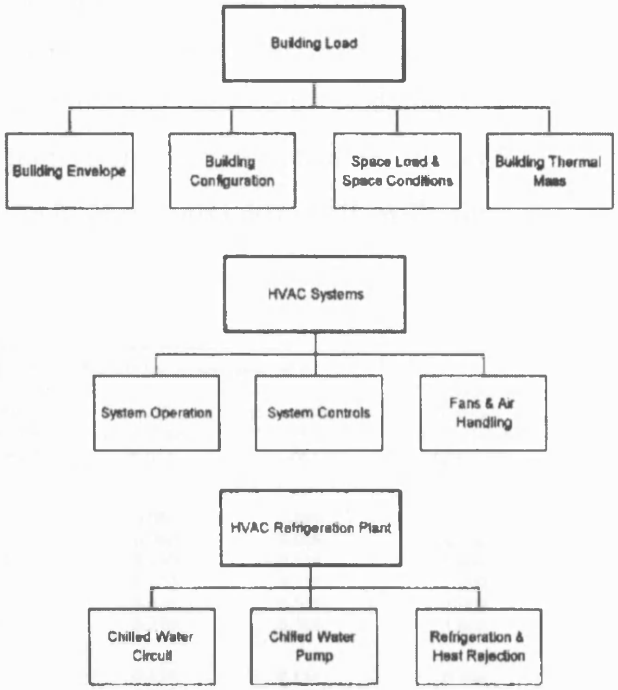

Figure 2-4: Parameterisation of input parameters [3]

The breakdown of the factors was based on the input building description language of DOE-2, to ensure maximum effectiveness and compatibility. However, a close look at each of the 62 chosen parameters gives the impression that some of them were chosen just because they were part of the input parameters of DOE-2, and not because they actually represented factors that could possibly be considered critical for the design process.

The third step involved the choice of the objective function. In this study, the simulation outputs chosen for the sensitivity analysis included the annual energy consumption and the peak design loads.

Having determined input and output parameters, a large number of simulations, (approximately 400), was performed in order to assess the effect of each of the 62 input parameters on the simulation outputs. In each simulation, all the input data were kept the same except from the parameter under consideration, which was assigned a range of different values, one at a time. The analysis of the results was focused on the most significant parameters, which were identified calculating the sensitivity coefficients, as mentioned earlier.

The sensitivity of the total energy consumption to the design variables was assessed via the single parametric analysis described above. The effect of each input parameter on the annual energy consumption was realized by studying the sensitivity coefficients and the results of regression analysis. In table 2-2 are presented the most significant factors, which also correlated well with the building energy consumption.

Abbreviation	Input parameter	Sensitivity coefficients for annual elec. MWh*			Coefficient of determ. R^2 for linear regression
		Form (1) (MWh per input unit)	Form (2a) (% *OP* per % *IP*)	Form (3b) (% *OP* per % *IP*)	
1. *Building load*					
SC	shading coefficient of windows	1670	0.083	0.099	0.997
WR	window-to-wall ratio	1101	0.060	0.069	0.996
AT	space air temperature (°C)	−44.2	−0.140	−0.138	0.996
EQ	equipment load (W/m²)	135	0.252	0.251	1.000
LL	lighting load (W/m²)	168	0.418	0.349	1.000
OC	occupancy density (psn/m²)	8453	0.210	0.308	1.000
2. *HVAC system*					
OA	outdoor air flow rate (l/s per psn)	131	0.114	0.151	0.996
TS	summer therm. setpoint (°C)	−283	−0.900	−0.851	0.981
FE	fan efficiency†	640	0.145	0.234	1.000
FS	fan static pressure (Pa)	0.869	0.148	0.177	1.000
3. *HVAC refrig. plant*					
CH	chw. supply temperature (°C)	−164	−0.136	−0.131	0.931
CP	chiller coeff. of performance (kWr output/kWe input)†	8560	0.363	0.350	1.000

Table 2-2: Sensitivity coefficients[3] for annual electricity (MWh) for the most important parameters [3]

Studying the effect of some of the factors under consideration on the building energy consumption it was concluded that:

- The annual energy consumption decreases exponentially with the increase in the projection ratio of the external shading devices, indicating that external shading up to a projection ratio of about 1.5 can be an effective measure for energy-conserving design.
- The characteristics of window design such as the shading coefficient of the glazing or the window-to-wall ratio have a significant impact on the building energy consumption.
- The building energy consumption decreases with an increase in the U-value of windows. It seems that windows help lose some of the heat

[3] **Note:** It should be stressed that direct comparison of the sensitivity coefficients is not always feasible because the parameters may have different dimensions, units of change and base case values. The coefficients are directly comparable only in the case that the input parameters are measured in the same units and are of the same nature [3].

particularly during the night when the outdoor temperature is lower than the indoor design temperature [6] resulting in lower cooling energy consumption.

A single parameter analysis was performed again to assess the effect of the design parameters on the peak design loads of the building, which determine the equipment sizes and plant capacities[4]. A few interesting conclusions derived from this study were the following:

- The peak loads of the building decrease with an increase in the weight of the floor slab due to the effect of the thermal mass of the building structure.
- The peak design loads are affected by the coincidence of block loads (i.e. the individual load components such as the internal gains from people, equipment and lights, the solar gains, etc), most of which tend to peak in the summer months, (when the internal loads coincide with peak solar gains, external temperatures higher than 25°C and mean relative humidity higher than 70% [7]), and the peak time of the building is dictated by the external weather conditions.

To sum up, this report attempted to study the thermal response of a typical office building in Hong Kong to a large number of design variables, employing sensitivity methods and regression analysis techniques. The procedure that was followed involved a large number of simulations, where each input parameter was assigned a range of values based on design practice.

However, the decision to study the effect of changes in one input parameter at a time on the output can be criticized, since the interactions between design factors were ignored. In general, the one-factor-at-a-time approach provides an estimate of the effect of a single variable at selected fixed conditions of the other parameters under consideration. However this estimate has general relevance only if it is assumed that the effect will be the same at other settings of the rest of

[4] **Note:** The maximum demands are not, however, the only factors determining the equipment and plant sizes. Other factors, like standby capacities, safety margins, etc, should also be considered [3].

the parameters [14]. As a result, this method has been replaced by factorial studies[5], which have, in comparison with the one-factor-at-a-time method, the following advantages [13]:

- They provide greater precision for estimating overall factor effects.
- They enable the interactions between different factors, which allow for the identification of near-optimum combinations of factor levels, to be explored.
- They allow the range of validity of the conclusions to be extended by the insertion of additional factors.

Another point that should be stressed is that the study was limited to only one HVAC system, ignoring the effect of different systems on the building energy performance, which might have been significant, considering that the cooling requirement dominated the energy consumption of the case study building. Also, recommendations concerning the values that the critical design parameters should take in order to reduce the annual energy consumption or the peak design loads were not given.

Despite its limitations, this project helped to identify the factors that should receive critical examination in the design of office buildings in Hong Kong. It was found that the annual energy consumption and the peak design loads are sensitive mainly to measures affecting the internal loads, the window-to-wall area, the shading coefficient of the windows, the temperature set-points and the plant efficiencies.

[5] **Note:** More details regarding the factorial designs can be found in chapter 3, section 3.2.1.

2.5 The development of energy prediction equations for air-conditioned office buildings in Hong Kong [8]

The aim of this study by Lam, et al. (1997) [8] was to develop energy prediction equations for a typical air-conditioned office building, employing multiple regression analysis techniques.

Being conducted by the same authors as the previous study, this work was based on part of the data used in that study. Thus, the case study building, the computer simulation tool and the chosen weather data were the same in both studies. Similarly, it was decided to study the effect of 62 design parameters, which were categorized into three main groups, (Building load, HVAC system and HVAC plant, as in the previous study), on the total energy consumption of the case study building. However, a different procedure was followed this time, to develop the energy prediction equations.

First of all, a single-parameter study was conducted to identify the principal forms of relationship between each of the 62 input parameters and the building energy use. Regression analysis was used to this end. Twenty-eight parameters were found to correlate well with the annual energy consumption. First-order regression models provided good fit between many of the building load parameters and the annual energy consumption, whereas quadratic equations were applied to many HVAC system and plant variables. It should be noted that the coefficient of determination[6] R^2, which is a measure of 'goodness of fit', was higher than 0.9 for all 28 parameters.

The second step involved a sensitivity analysis on the 28 parameters to identify the ones that should be given primary attention in the design process. The sensitivity coefficients indicated that the annual energy consumption was most sensitive to 12 parameters (6 from the building load, 4 from the HVAC system and 2 from the HVAC refrigeration plant). These 12 parameters were considered in the detailed analysis using multiple regression techniques.

[6] **Note:** The R^2 factor estimates the fraction (a number between zero and one) of the overall variation in the data accounted for by the model [15].

The third step involved the development of simple energy prediction equations for each of the three main groups, using their respective parameters. The range of values assigned for these factors[7] and the total number of simulations performed are given in table 2-3.

Building load	SC	WR	AT (°C)	EQ (W/m^2)	LL (W/m^2)	OC (psn/m^2)
($3^6 = 729$ runs)	0.1	0.1	21	0	0	1
	0.55	0.5	25.5	15	15	5.5
	1.0	0.9	30	30	30	10
HVAC system	OA (l/s/psn)	TS (°C)	FE	FS (Pa)		
($4^4 = 256$ runs)	2	21	0.1	0		
	8	24	0.4	1000		
	14	27	0.7	2000		
	20	30	1.0	3000		
HVAC refrig.plant:	CH (°C)	CP				
($4^2 = 16$ runs)	4	0.142				
	6	0.284				
	8	0.427				
	10	0.568				

Table 2-3: Factor levels and number of simulation runs for multiple regression analysis [8].

The energy consumption data predicted by DOE-2.1E in each simulation run were submitted to the SPSS statistical package to conduct the multiple regression analysis. The R^2 for the 3 derived equations, were all higher than 0.96, indicating that at least 96% of the variation in the annual electricity expenditure due to changes in the 12 selected parameters can be explained using the 3 regression models.

The predictive power of the equations was tested using a database containing randomized input values for the parameters. The comparison of the DOE simulation output with the predictions of the 3 equations for this database showed that the regression models are quite good in estimating the annual electricity expenditure for the randomized input data.

[7] **Note:** *SC* = Shading Coefficient, *WR* = Window-to-Wall ratio, *AT* = Space air temperature, *EQ* = Equipment load, *LL* = Lighting load, *OC* = Occupant density, *OA* = Outdoor air flow rate, *TS* = Thermostat set-point (summer), *FE* = Fan efficiency, *FS* = Fan static pressure, *CH* = Chilled water supply temperature, *CP* = Chiller COP.

The final step involved the development of a single equation for the prediction of the annual electricity consumption of the case study building, using all 12 parameters of the three groups.

A problem that usually occurs when the number of parameters is too large is the number of simulations required to generate the data for the regression analysis. (For example, if each of the 12 parameters has 3 levels, the number of required simulations is 3^{12} = 531,441). On the other hand, as the number of simulations increases, (to generate more data points), the more representative the regression model is going to be. In the present study, it was decided to use randomized simulation inputs for the parameters so that a manageable number of simulations, (100 in this case), could be run to generate the data required for the regression analysis. However, an actual criterion to determine the minimum number of simulations required to obtain a good regression model was not really considered.

The final energy prediction equation (involving an R^2 value of 0.988) was the following [8]:

(Annual Energy Consumption) =

$$(-1.38 - 7.3 \times SC \times WR - 0.0151 \times AT - 0.167 \times EQ - 0.206 \times LL - 9.60 \times C) \times$$
$$(-340 - 73.7 \times OA - 412 \times FE - 0.406 \times FS - 0.0000384 \times FS \times FS$$
$$- 0.644 \times TS \times TS + 2.49 \times OA \times TS + 16.7 \times TS \times FE + 0.0215 \times TS \times FS - 0.0872 \times FS \times FE)$$
$$\times (0.508 - 0.0109 \times CH + 1.093 \times CP)$$

The predictive power of this equation was tested using again a randomized input database. The comparison between the simulation results and the model predictions for the aforementioned database indicated that the final regression model could predict the annual energy consumption quite well.

In general, this study demonstrated the potential of expressing the building energy performance in terms of a number of design variables, which are considered critical during the design process, using multiple regression techniques. It was stressed that the role of such prediction models is to offer a simplified design tool for the comparison of the energy performance of different

design schemes during the early design stages. It should be mentioned, however, that the equations established in this paper are valid only for office buildings of similar characteristics with the case study building situated in Hong Kong.

Some parts of this study that could be criticized are the following:

- The number of simulations that was carried out to correlate the most significant parameters from each of the three main groups (i.e. the Building load, the HVAC system and the HVAC plant group) with the energy consumption was particularly large, as can be seen from table 2-3. This number would have been significantly smaller had a 2-level factorial design or a central composite design been used[8]. For example, to correlate the 4 parameters derived from the HVAC system category with the annual energy consumption using a central composite design[9], the total number of simulation runs would have been $2^4 + 2\times4 + 6 = 30$, which is considerably smaller than the $4^4 = 256$ runs used in this study. Also, some form of planned experimentation should have been used to develop the final prediction equation instead of arbitrarily selecting 100 simulation runs.
- In order to get a better regression fit, several different forms of models were tested by adding new terms (e.g. single variables or interaction terms) one by one. The final models correlating the most significant parameters from each of the three main categories or all 12 parameters with the annual energy use were chosen based on a balance between accuracy (in terms of the coefficient of determination R^2) and ease of use (in terms of simplicity). However, it should be stressed that a high value for R^2 can often be misleading. Adding a new variable to the model will never make R^2 worse, only the same or larger, regardless of whether this variable is statistically significant or not. This could result in a model having a high value for R^2 but yields poor predictions of new observations or estimates of the mean response [12]. When comparing

[8] **Note:** The former type of experimental design could have been useful, for example, for the HVAC refrigeration plant category where a first order model was fitted, while the latter could have been applied to the HVAC system group of factors where a second-order model was developed.

[9] **Note:** Details regarding the response surface methodology and the central composite designs can be found in chapter 3, section 3.2.1.

models with different number of predictors, it is recommended to take into consideration the adjusted–R^2 statistic, which is a modified R^2 that has been adjusted for the number of terms in the model. It is $(adjusted - R^2) = 1 - \frac{n-1}{n-p} \times (1 - R^2)$, where n is the number of observations on the response variable y and p is the number of model parameters [12]. This statistic does not always increase as new terms are added to the model. In fact it will often decrease, if unnecessary terms are added. As a result, when the R^2 and the adjusted-R^2 differ dramatically there is a good chance that non-significant terms have been included in the regression model [12]. Another statistic that should also be considered is the Predicted-R^2, which is a measure of the amount of variation in new data explained by the model[10] [12].

- The final stages of the study focused on the development of energy prediction equations that could possibly be useful for the designer at the early stages of the design process when a large number of alternative design options is usually considered. However, there was no attempt to analyze the derived regression models and provide the designer with practical advice regarding the relative importance of the design variables and the way that they affect the annual energy use. Of course, the analysis of the final energy prediction equation would have been particularly difficult due to the large number of factors (i.e. 12) involved. Moreover, the use of optimization techniques to obtain the combinations of factor levels minimizing the annual electricity consumption was not considered.

[10] **Note:** More details about this statistic can be found in appendix H.3.

2.6 Evaluation of different types of HVAC systems using computer simulation techniques [9]

This study by Sekhar, et al. (1998) [9] adopted the energy simulation approach to evaluate the performance of five commonly employed air-conditioning systems for high-rise office buildings. The simulation tool used was DOE-2.1E, while the five HVAC systems were the following:

- a Variable Air Volume System (VAVS)
- a Constant Air Volume System (CAVS) without reheat
- a Two Pipe Fan Coil System (TPFCS)
- a Two Pipe Induction Unit System (TPIUS)
- and a Packaged Variable Air Volume System (PVAVS)

The main difference of this study, with the previous two, was that the building modeled had a fixed set of characteristics such as dimensions, orientation, materials, internal gains, etc, representing a generic (but typical) high-rise office building. Thus, the results were representative of the effect of each of the selected HVAC systems on a generic office building, providing the designer with useful information regarding the thermal and energy performance of some widely adopted HVAC systems, without taking into consideration the effect of the architectural or operational characteristics of the building on the HVAC system performance.

The case study was a 20-storey office building with an aspect ratio of 1:1.5. A typical floor plan is presented in figure 2-5:

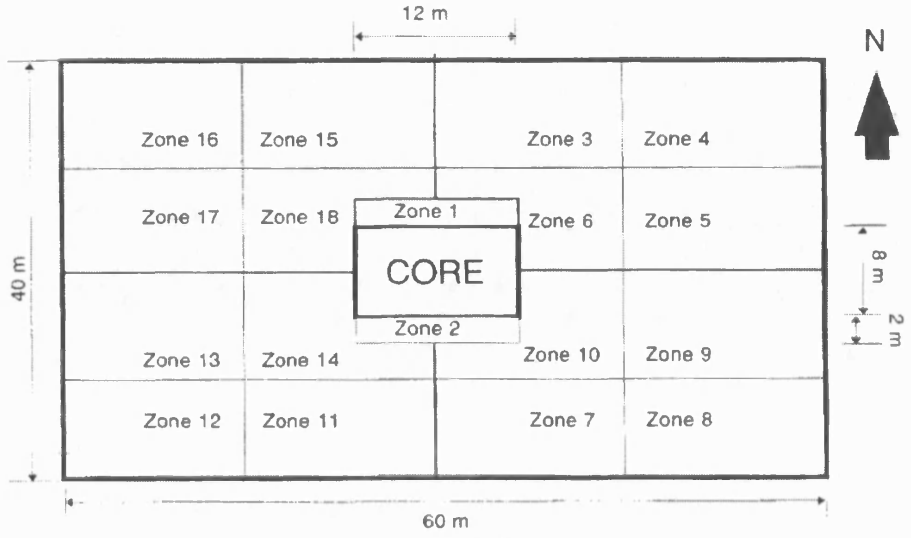

Figure 2-5: Typical floor plan of the base case building [9]

As can be seen from figure 2-5, each floor was divided into 18 zones, considering that a floor space of 150 m^2 per zone would be required for a detailed analysis of the building performance. The core zone, unlike the rest of the zones, was not air-conditioned, representing the total unconditioned space of the building. The rest of the building characteristics can be considered typical of a high-rise office building.

Regarding the five HVAC systems, it is worth mentioning that the design temperature set-point was set to 23.9°C throughout the whole year, while no separate humidity control was employed in any of them. The relative performance of the systems was compared in terms of thermal comfort conditions and energy consumption.

The maximum and minimum space temperatures in each zone indicated that the PVAVS and the CAVS had the highest temperature variation within a zone, (see figure 2-6), which means that they either could not cope with the maximum cooling requirements or they were not responsive to load variations. In general, high fluctuations in temperature are undesirable since they can create thermal discomfort, especially when they happen in a short period of time. The other three systems were able to respond to the load variation and provide stable conditions, with the TPFCS illustrating the best performance.

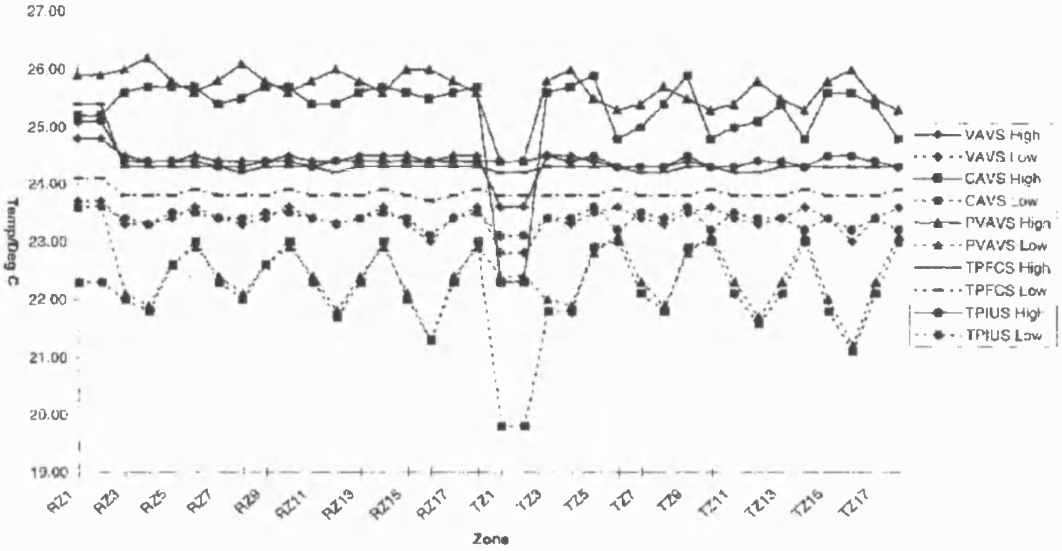

Figure 2-6: Maximum and minimum temperatures within zones [9]

Considering the difference between the zone with the maximum annual average temperature (AAT) and the zone with the minimum AAT, it was shown that all the systems apart from the CAVS were able to keep the temperature fairly stable and close to the desired set-point for all the zones throughout the year. The CAVS showed the worst performance, since it was not capable of keeping the temperature difference between the zones to low levels when the cooling requirements were not the same. The main reason for this was that the volume of the supply air was kept constant and passed through the same coil, which cooled the air down in order to satisfy the zone with the highest demand, overcooling the rest of the zones[11].

The TPFCS and TPIUS on the other hand, performed well in terms of minimizing both the fluctuation of temperature within a particular zone and the temperature difference across different zones, since they are terminal systems, which means that they are capable of responding to varying requirements of different zones or to changes in load of the same zone.

The only central system that showed a similar performance to the two terminal systems was the VAVS, which employed VAV boxes and variable-speed supply

[11] **Note:** Obviously, if only low demands were met, the higher demands would not have been satisfied.

fans. This system was, therefore, capable of responding to the varying zone cooling requirements by adjusting the volume of the supply air.

As mentioned earlier, the performance of the five HVAC systems was also evaluated in terms of annual energy consumption, which was broken down into the electricity consumed by the chiller, the cooling tower, the pumps, and the central or terminal fans. The energy consumption for each of the 5 HVAC systems can be seen in table 2-4:

	Annual Energy Used MWH				
Category	VAVS	CAVS	PVAVS	TPFCS	TPIUS
Area Lights	2837	2837	2837	2837	2837
Space Cool	2103	2293	3287	2099	2106
Heat Reject	427	406		354	350
Pumps and Misc	180	168		147	144
Vent Fans	339	460	314	715	309
Total	5886	6163	6437	6152	5746
Total less *Lights*	3049	3326	3600	3315	2909
Index (VAVS as base)	100.0	109.1	118.1	108.7	95.4

Table 2-4: Building energy performance summary [9]

It was found that the CAVS consumed about 10% more cooling energy than the VAVS, TPFCS and TPIUS. The high energy consumption for the CAVS was attributed to the uneconomical constant delivery of air volume, which also resulted in over-cooling, as mentioned earlier.

Concerning the fan energy use, the simulation results indicated that the supply fan of the CAVS consumed 35% more electricity than the variable speed fan of the VAVS, due to the constant airflow supplied, regardless of the actual zone requirements.

Also, the amount of electricity used for all the supply fans of the TPFCS was almost double that of any other system, suggesting that the sum of the energy requirements of all the terminal units exceeded the energy requirement of the supply fan in other systems.

Summarizing the findings of this study it can be concluded that the VAVS and the TPIUS had the best overall performance, demonstrating low annual energy use and maintaining a small fluctuation of temperature throughout the year, as well as, fairly stable temperature across the building.

The TPFCS, which is a terminal unit system, had about 10% higher energy consumption than the VAVS. In terms of thermal comfort, the system performed better than the central air systems.

The CAVS, finally, not only consumed 10% more energy than the VAVS, but it also failed to keep the temperature stable throughout the year, or across the building, tending to over-cool a number of zones in an attempt to meet the higher cooling requirement of others.

It is clear that parts of this study could be criticized and other parts require further research, for example:

- The thermostat set-point was kept constant throughout the year for all the systems, whereas in real life set-points are adjusted to achieve the desired condition in each season [9].
- The temperature results were generated on a monthly basis. It is, therefore, possible that the occupants would not actually experience rapid temperature fluctuations, since they could be a result of oscillating temperatures before meeting the heat balance [9]. In any case, though, wide fluctuation in the temperature of a zone can be considered as an indication for a poor performing system.
- The architectural and operational characteristics of the case study building were kept the same, ignoring their effect on the energy performance of the air-conditioned building.
- Similarly the characteristics of the HVAC systems were kept the same, ignoring the effect of different control strategies or variations of the systems studied, (e.g. a four-pipe fan coil system with central air supply), on the building energy consumption.

- The effect of humidification on the energy consumption or thermal comfort sensation was not taken into consideration.

Nevertheless, the study gave a quite detailed picture of the energy characteristics of five commonly used HVAC systems, providing also some useful guidelines regarding the choice of the HVAC system for a high-rise commercial building in South-East Asia.

2.7 The effect of climate on the thermal design of air-conditioned residential and office buildings [10], [17]

The first study by Al-Homoud (1997) [10] considered in this section, dealt with the application of an optimization technique to the thermal analysis of a typical air-conditioned residential building, in order not only to minimize its energy consumption but also to provide the designer with valuable information regarding the likely best combination of building envelope related design variables for four types of climate.

The optimization tool used in the study was ENEROPT, which utilizes a direct search optimization technique coupled with a building energy simulation model, called ENERCALC, to optimize 14, mainly building envelope related design parameters, subject to upper and lower constraints imposed by the designer. The objective of the optimization was to minimize the energy consumption of a typical 223 m^2 residence in the USA and Saudi Arabia. The base case values and the upper and lower limits of the 14 design parameters are given in table 2-5.

Variable	Initial value	Lower bound	Upper bound
Wall U-value (BTU h $^{-1}$ F $^{-1}$ ft $^{-2}$)	0.33	0.06	1.10
Absorptance	0.26	0.10	0.98
Time lag (h)	5.00	1.00	10.00
Roof U-value (BTU h^{-1} F^{-1} ft^{-2})	0.34	0.04	1.10
Glass U-value (BTU h^{-1} F^{-1} ft^{-2})	0.33	0.25	1.10
Shading coefficient	0.35	0.20	1.00
Emittance	0.36	0.20	0.98
% glass area N	20.00	15.00	99.00
E	20.00	15.00	99.00
S	20.00	15.00	99.00
W	20.00	15.00	99.00
Infiltration rate (ach h $^{-1}$)	0.70	0.50	3.00
Internal mass (lb ft^{-2})	75.00	50.00	150.00
Orientation (from south)	0	0	360

1 BTU h $^{-1}$ F^{-1} ft^{-2} = 5.679 W m^{-2} C $^{-1}$; 1 lb ft^{-2} = 4.883 kg m $^{-2}$.

Table 2-5: Optimisation variables' initial (i.e. base case) values and limiting constraints [10]

Regarding the selection of weather data, it was decided to adopt Olgyay's categorization of climate types into four climatic regions, which are the following:

- Cool climate, (represented by Madison, Wisconsin), which is characterized by severe cold temperatures with short hot summers.
- Temperate climate, (represented by Medford, Oregon), which is characterized by a very mild climate with cool winter temperatures and frequent rain with overcast skies.
- Hot-arid climate, (represented by Phoenix, Arizona and Riyadh, Saudi Arabia), which is dominated by extremely hot and dry summers with very large diurnal temperature ranges and moderately cold winters.
- Hot-humid climate, (represented by Houston, Texas and Jeddah, Saudi Arabia), which is characterized by long, hot and humid summers with very small diurnal temperature ranges and short, mild winters.

It is worth mentioning that the average computer optimization run took 300 stages with approximately 700 hourly simulation runs to reach the optimum solution. The building energy simulation program was run in an abbreviated

mode that permits the simulation of less than full months (i.e. only a certain number of days per month was considered by the program) and still maintains its statistical integrity for energy calculations [1]. This feature of ENERCALC makes it more efficient in optimization where hundreds of simulations need to be carried out to reach the optimum solution, as shown above [1].

The energy consumption and the peak loads for a typical two-storey residence and the optimized solution are presented in figures 2-7 and 2-8.

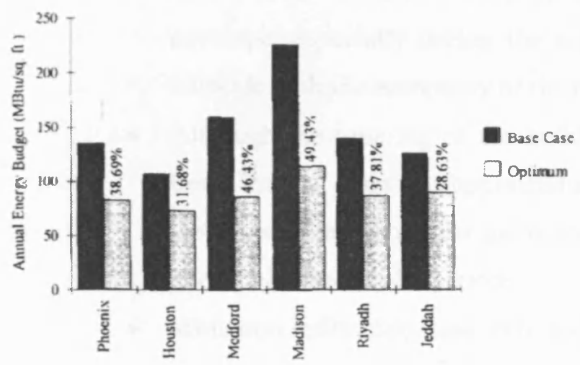

Figure 2-7: Optimum and base case annual energy consumption in different climates for a typical two-storey residence [10] (1 BTU ft^{-2} = 11.356 kJ/m^2)

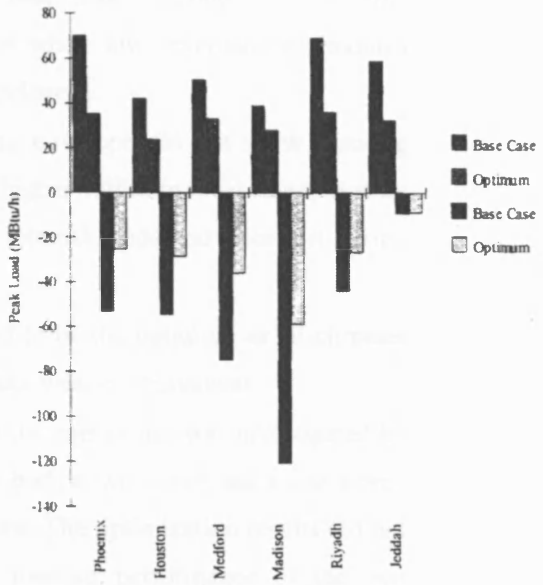

Figure 2-8: Optimum and base case heating and cooling peak loads in different climates for a typical two-storey residence [10] (1 BTU ft^{-2} = 11.356 kJ/m^2)

As can be seen from figures 2-7 and 2-8, the optimization technique employed in the thermal design of this building allowed for significant energy savings, and lower peak heating and cooling loads.

Some interesting observations derived from the optimization results, which can be used as recommendations for the thermal design of residential buildings in different climates, are summarized in the following:

- Building orientation with the long exposure facing south was the optimum for all climates. There was, however, a tendency towards an optimum southwestly orientation for cold and temperate climates.

- The most desirable glass exposure for all climates was found to be the south exposure, to benefit from winter sun and minimize summer overheating. There was a general trend, on the other hand, to minimize east, west and north glass areas.
- Minimum shading coefficients were needed, especially in hot climates, to deal with solar gains. Low glass U-values were also the trend of optimization for all climates.
- High wall and roof insulation levels were recommended for buildings in all climates to reduce conduction heat losses through the building envelope, especially during the night when low external temperatures coincide with the occupancy of the residences.
- Although the time lag of the building envelope did not show a strong trend, internal mass was optimized at higher values in most cases, to store the excess heat from solar gains and internal loads and release it during unoccupied and cooler periods.
- Minimum infiltration rates were found to be the optimum in all climates and careful treatment of cracks and leaks was recommended.
- The effect of building form on the annual energy use was investigated by repeating the optimization process for both a two-storey and a one-storey residence with the same gross floor area. The optimization results did not show significant differences in the thermal performance of the two houses.

Another important observation obtained from the integration of optimization in building thermal design was that the optimum solution for each type of climate is not unique. Several combinations of the building elements and their arrangements were identified resulting in near-optimum thermal performance. This was attributed to the interactions between the design variables which could not be studied using a variable by variable investigation of alternatives. It was concluded that the application of optimization in building design is worthwhile for exploring new design possibilities, instead of relying on trial and error investigation of alternative design options.

In general, this study demonstrated that the climate influences significantly the energy consumption of residential air-conditioned buildings, requiring, in certain cases, different design approaches for different types of climate, to achieve energy efficiency. The optimization results were quite impressive, allowing for energy savings up to 49% and 56% for the two-storey and the one-storey residence, respectively. However, it should be borne in mind that residential buildings are mainly 'skin-load' dominated, while internal loads are relatively insignificant, compared to commercial buildings. As a result, their thermal performance is more significantly influenced by the climatic conditions, while architectural decisions based on the optimization of the building envelope are guaranteed to have a considerable impact on the energy consumption.

In another study by Al-Homoud (1997) [17], the same method was used to optimize the design of the building envelope of three office buildings. The case study buildings were considered to be representative of a typical small (465 m^2, 2 floors), medium (4,710 m^2, 6 floors) and large (13,000 m^2, 7 floors) office building respectively. The optimization tool, the building energy simulation program and the weather files used for the simulations were the same in both studies discussed in this section. The fourteen design variables displayed in table 2-5 were optimized for each office building with the objective of minimizing the annual energy consumption.

The optimum combinations of factor levels resulted in up to 22%, 26% and 50% energy savings for the large, the medium and the small office building respectively. On the other hand, the cold climate resulted in the maximum building energy savings, followed by the temperate climate, the hot-arid climate and finally the hot-humid climate.

The recommendations concerning the optimum values of the 14 envelope related design variables were approximately the same for both the typical residences and the typical office buildings involved in the first [10] and the second [17] study considered in this section respectively. In addition, the maximum energy savings were close to 50% for both the two-storey residence and the small office building considered in studies [10] and [17] respectively. It

seems that the energy requirements of both the small office building and the two-storey residence were more climate-dependent as a result of having less internal heat generation and a greater surface-to-volume ratio than the medium and large office buildings considered in study [17]. The maximum energy savings were relatively lower for both the medium and the large office building, on the other hand, due to the dominating effect of the internal heat gains on the overall building thermal performance. Despite this fact, however, the potential improvement in energy use that can be achieved through proper control of artificial lighting or through the installation of energy efficient lights and office equipment was not considered in study [17]. Also, the effect of the parameters associated with the glazing system (i.e. the glazing percentage and the total shading coefficient) on the daylight levels inside the perimeter zones of the office buildings was not investigated. The utilisation of daylight to reduce the amount of electricity consumed by lights was not considered as well, since this is what usually happens in most actual office buildings, as stated in study [17].

It should also be stressed that it is quite strange that the same base case, lower and upper values were adopted for all the 14 design parameters displayed in table 2-5, in both studies. It is considered unlikely that a typical residence and a typical office building will have exactly the same base case values for all the parameters associated with the design of their envelope, while the minimum or maximum level for some of these design factors may not be appropriate for both types of building. For example, a fully glazed (i.e. the maximum value of the glass area for all building facades, as shown in table 2-5) office building is quite common, but a fully glazed residence is rather unlikely. In addition, the base case value assumed for this parameter (i.e. 20%) seems to be small for both a typical office building and a typical residence.

Also, there are other parameters, which affect the performance of an air-conditioned residential and/or office building that were not taken into consideration in the present studies, like the provision of night ventilation, the utilization of shading devices and the type and pattern of use of the HVAC system.

Nevertheless, both studies still succeeded in providing the designers with valuable information regarding the design of the components of the building envelope during the initial stages of the building design, when the decisions of the architect or the engineer have a significant impact on the building energy performance.

2.8 The combination of optimization techniques (genetic algorithms) and simulation programs for the design of low-energy buildings

Building simulation programs are valuable tools in the process of low energy design, allowing designers to assess building performance in terms of energy use, thermal comfort, lighting, acoustics, etc. However, since no optimization routine is contained in current building simulation programs, the user must explore the design space manually to identify one or more design options satisfying the requirements of the design project [24]. This section presents a number of studies that dealt with the coupling of an optimization algorithm with a building simulation program to automatically search for the optimal or near-optimal solutions in the design space.

There are several applications of optimization techniques to different building design problems. Such applications range from spatial allocation problems to the design of structural and mechanical systems in buildings with different degrees of success [17]. Some of the optimization techniques that have been applied to building thermal design include the method of Hooke and Jeeves [25], the lattice method for global optimization [26] and the optimization search technique of Nelder & Mead and Himmilblau [1] that was used in both studies discussed in the previous section. However, one of the most popular optimization algorithms that is capable of handling non-linear, ill-defined problems of many dimensions in search spaces with many local minima is the genetic algorithm (GA) [19]. GA is a population-based stochastic global search technique inspired from the biological principles of natural selection and genetic recombination [23]. In GA, a variable value is usually coded into a string of fixed length of bits consisting of '1' and '0'. The binary codes of all variable values are concatenated to form a

binary string (i.e. a chromosome), representing a potential solution to the optimization problem [24]. GA maintains and operates on a set of chromosomes, called a population of individuals. Typical population sizes range from 30 to 200, while they can reach 2000 individuals (i.e. potential solutions to the problem) [18], [19]. The first generation of the population is usually randomly generated while the remaining generations are produced through three genetic operations: selection, crossover, and mutation. Selection favors those robust individuals by giving them higher opportunity to reproduce. Crossover and mutation operations are applied on the selected individuals to form a new generation of population. The above genetic operations are applied on the new population and repeated until reaching a predefined stopping criterion such as the maximum number of generations or the maximum number of consecutive generations for which the optimal solutions remain unchanged [24].

There are many variations of GAs, which are suitable for different types of problems, while it should be stressed that the performance of the optimization algorithm under consideration depends on the chosen values of the algorithm parameters [27]. A few typical characteristics of an optimization problem for which GAs are suitable are the following [23]:

- The problem is multi-objective with conflicting criteria.
- The problem includes a large number of both continuous and discrete variables.
- Variables are at different hierarchical levels. For example, wall type and wall layers are variables at different hierarchical levels. The wall type determines the sequence and the material types of all contained layers. If there are several alternative wall types, only the layers belonging to the active wall type should be used.

An optimization algorithm (called micro-GA) was coupled with DOE2.1E, an hourly thermal simulation program, in the study by Galdas, et al. (2002) [18] to identify the window dimensions that lead to the minimum total energy consumption of an office building. The hypothetical office building module considered in this study consisted of a square core zone, surrounded by four

identical perimeter zones. DOE 2.1E was used to carry out daylighting calculations and estimate the annual energy consumption of the building for all the potential design solutions generated by the GA. It is worth mentioning that the artificial lighting system was set to provide just enough light to make up for the difference between available daylighting and required light levels. The optimization variables included the window dimensions for each of the four cardinal orientations. Both the width and the height of each window were allowed to range from 0.3 to 2.4 m at discrete steps of 0.3 m, resulting in a solution space of 8^8 design points. The window size was optimized for both a cooling-dominated climate (Phoenix, Arizona) and a heating-dominated climate (Chicago, Illinois). The optimization process was carried out 5 times to compare the results from different trials. A maximum number of 100 generations and a population size of 5 (which is very small) were specified for each experiment (or, in other words, the maximum number of simulations for each optimization experiment was 500).

Five somewhat different design solutions (one for each optimization experiment) with similar energy performance were obtained for each climate. The results were considered satisfactory in most cases. For example, a large north window (2.1 x 2.1 m) was chosen in the cooling-dominated climate of Phoenix to take advantage of daylight without creating overheating problems due to high solar heat gains in the summer. The chosen window dimensions were rather unusual in a few cases, however, like the west window in the heating-dominated climate, which was reduced to a horizontal strip (i.e. 2.4 x 0.3 m) to allow for some daylighting while preventing excessive heat losses. In addition, all the design solutions were clearly dependent on the characteristics of the chosen window construction, (i.e. the U-value, the shading coefficient, etc), which were held constant during the optimization to keep this study as simple as possible.

The study by Coley, et al. (2002) [19] coupled a population-based optimization algorithm to a dynamic thermal model (EXCALIBUR) with the idea of identifying a large number of low-energy designs with architectural appeal for a community hall. The optimization variables included the shape of the perimeter

and the pitch of the roof, as well as the constructional details of the external walls, floor, roof & windows, the location of windows and shading, and the orientation of the building. The only pre-defined constraints regarding the geometry of the building included the floor area, which was set to 200 m^2 and that the design should be a single-storied one. A single zone of the building was simulated in EXCALIBUR, while the only performance measure was the annual (heating & cooling) energy consumption. It was stressed that the advantage of using a simplified dynamic thermal model is that a whole year simulation can be run fairly quickly, allowing a large number of potential designs to be processed [19].

As mentioned above, the aim of this study was not just to minimize the annual energy use, but to maximize the architectural appeal of the design project as well. However, no attempt was made to include the architectural appeal in the optimization algorithm, since it is a non-numerical measure of the design performance. It was, therefore, decided to obtain an extensive range of low-energy designs instead of being limited to a small number of designs leading to optimum or near-optimum energy use, allowing the designer to make the final choice on the basis of other important non-optimized criteria (such as the architectural appeal). In short, the procedure that was used in this study involved the filtering of the set of all designs generated by the GA to remove the ones leading to energy use more than v% (typically v = 5 – 10%) higher than the minimum energy consumption. The chosen designs were then presented in the form of a visual summary (a stacked histogram was used) for further judgment by the design team as to potential use. However, the final stacked histogram (a fragment of which was only presented, involving 100 design solutions) was particularly complicated, making the evaluation of the chosen designs a difficult task. Thus, the authors very briefly discussed a sketch of only two of the 100 designs, which illustrated that it is possible to achieve similar environmental performance using very different design options.

The study by Wright, et al. (2002) [20] investigated the application of a multi-objective genetic algorithm (MOGA) search method in the identification of the optimum pay-off characteristic (i.e. the trade-off relationship) between the

operating energy cost of a single-zone "all outside air" HVAC system and the occupant thermal discomfort. The system consisted of a regenerative heat exchanger, a cooling coil, a heating coil, and a supply fan. The performance of each candidate design solution generated by the optimization algorithm was evaluated through a thermal performance simulation of the building and the associated HVAC system. The case study was only a south facing mid-level zone (with one window on the south façade) of a multi-storey building. A single zone lumped capacitance model was used to represent the thermal response of this zone. The simulations were carried out for three design days of operation (a winter design day, a summer design day and a day in the intermediate season). UK climate data were used for the simulations, without giving any details regarding the exact location and the characteristics of the chosen weather file.

The problem variables were formed from the control set-points and the size of the HVAC system components (e.g. width, height, number of rows of each coil, etc). Separate variables were specified for the supply air temperature and flow rate set-points in each hour of the day. As a result, the total number of design variables for all three design days was equal to 200. The total energy consumption (and, hence, the operating energy cost) of the HVAC system for the three design days was estimated through a thermal simulation of the case study building, as described above. The second objective function was the zone thermal discomfort (during the occupancy period), which was represented by the maximum "predicted percentage of dissatisfied" (PPD) for each design day. The hourly values of the zone air temperature and the mean radiant temperature were only used for the calculation of the PPD (%), while all the other thermal comfort parameters, (metabolic rate, air velocity, and zone relative humidity), were assigned constant values. It seems that the thermal simulation model employed in this study could not estimate the relative humidity in the building zone. The final optimization criterion was an aggregated value of all the design constraints (i.e. restrictions on the design of the coils, the performance envelop of the supply fan, etc), which was used as a means of finding and maintaining feasible solutions.

In order to determine the trade-off relationship between the energy cost and zone thermal discomfort, the multi-criterion genetic algorithm was run with a

population of 200 sample solutions, and was allowed to run for a 1000 generations. In other words, the maximum number of simulations was 200,000.

The analysis of the results focused on the HVAC system control strategy and the thermal comfort conditions over the summer design day. It was concluded that the lowest energy cost (and the highest thermal discomfort) solution, which resulted from a set-point schedule that demanded no mechanical cooling and flow rates set to the minimum allowable value is the best choice, considering that the corresponding maximum thermal discomfort was only 15.0% PPD.

Some variations of the study discussed above were also carried out by the same authors [21], [22]. In one of these studies by Wright, et al. (2001) [21], the building construction (i.e. light-weight, medium-weight or heavy-weight) was assumed to be a problem variable. In addition, each building construction could have one of two possible glazing types (i.e. clear glass or low emissivity glass), while three possible areas of glazing were specified for the south facade (i.e. 10%, 20% or 30%). This resulted in 3 additional optimization variables (building construction / weight, glazing type, glazed area), and a total of 203 problem variables. The aim of this study was to minimise only the energy cost of the HVAC system, (single-criterion optimization), with the maximum thermal discomfort of 10% PPD set as a constraint on the optimization.

The GA correctly identified the construction with the minimum energy cost (heavy-weight, low emissivity glass, 10% glazing percentage). The analysis of the optimum control strategy for the design summer day illustrated that during most of the morning the temperature set-points matched the ambient temperature so that the system could operate in a free cooling mode, while mechanical cooling was required in the late afternoon in order to maintain thermal comfort. The corresponding thermal discomfort profile showed that the chosen control strategy managed to satisfy the thermal comfort requirements of the occupants, with the peak PPD of 10% occurring in the late afternoon, when the thermal heat gains were the highest.

The final two studies by Wang, et al. (2005) [23], [24] considered in this section, employed a multi-objective genetic algorithm to optimize the life-cycle cost (LCC) and the life-cycle environmental impact[12] (LCEI) of a single-storey office building located in Montreal, Canada. A simulation program based on the ASHRAE toolkit for building load calculations was used to estimate the operating energy consumption. This was then used to calculate the environmental impacts due to the operation phase of the life-cycle of the building, and the operating energy cost. The environmental impacts due to the pre-operation phase, (including natural resource acquisition, material manufacturing, on-site construction, and the transportation associated with the above processes), and the initial construction cost were derived directly from the building description, construction cost and embodied impact data of building materials/products[13].

The optimization variables in both studies were associated mainly with the design of the building envelope, including the aspect ratio of the building plan, the building orientation, the wall construction, the roof construction, and the glazing percentage of each building façade. Some additional variables considered in the second study by Wang, et al [24] included the shape of the building plan, the overhang depth and the type of window for each façade of the building. Most of the above design factors were specified as discrete and hierarchical[14] variables.

The simulation program was coupled with and called by the optimization algorithm. Due to the inherent randomness of GA, the optimization process was

[12] **Note:** Exergy is a concept from thermodynamics that represents the maximum theoretical work that can be done by a system with respect to the reference environment, which was employed in both studies under consideration to evaluate the life-cycle environmental impacts with expanded cumulative exergy consumption as the indicator. This indicator consists of two items: cumulative exergy consumption and abatement exergy consumption. The first item expresses the sum of exergy of all natural sources consumed by a building throughout its whole life-cycle covering resource extraction, material manufacturing, on-site construction, operation, and transportation between the previous phases. The second item is the exergy required by necessary operations if the wastes produced in the life-cycle phases of a building are removed or recovered to avoid their release to the environment [24].

[13] **Note:** Maintenance and demolition were two building life-cycle phases that were not considered, because the corresponding environmental impact data could not be found for many building materials or assemblies [23].

[14] **Note:** For example, there were two possible wall types in study [24]: a concrete block wall and a steel-stud wall. Each of these wall types had different compositions in terms of material types and sequence of layers. Only the layers of cladding and insulation were part of the optimisation variables. Thus, if a concrete wall was considered, the insulation layer could be 102 mm expanded polystyrene, 127 mm extruded polystyrene, etc, while if a steel-stud wall was chosen the insulation layer could be 102 mm fibreglass, 102 mm rockwool, etc [24].

run three times. The population size was 40, while the maximum number of generations was equal to 200 in the first study [23] and 300 in the second [24].

The optimization procedure identified 29 near-optimum solutions in study [23] and 15 near-optimum solutions in study [24] allowing some trade-off between the two objective functions. In short, in both studies it was shown that the building should be elongated on the east-west axis, while the aspect ratio was allowed to take a wide range of values. A square shape was favourable for cost reduction since it has the minimum exterior envelope surface, while a rectangular shape with the long side towards the south was better in terms of energy use. The glazing percentage was set to the minimum specified value on all facades of the building in study [23], while in study [24] it was allowed to take higher values only on the south façade of the building to take advantage of the solar gains during the winter period. An overhang was specified for the south facing window[15], while the addition of side-fins to the east and west orientated windows was not investigated. Finally, the optimum choice of wall or roof construction was discussed depending on the trade-off between the operating energy use, the environmental impacts due to material production & construction and the initial cost[16].

The studies discussed in the previous paragraphs demonstrated that the combination of an optimization algorithm with a building simulation program allows for the exploration of a large design space to locate the optimal or near optimal solutions. The problems associated with the utilisation of such a method in the design of a building along with some criticisms that can be applied to most of the studies under consideration are summarised in the following:

- The integration of an optimization technique into the thermal design of buildings requires good knowledge of optimization theory. The appropriate optimization algorithm should be selected carefully based on the characteristics of the problem under consideration. In addition,

[15] **Note:** It is worth mentioning that the optimum value of the overhang depth increased as the glazing percentage specified for the south façade of the building was getting higher [24].
[16] **Note:** For example, in study [23], it was shown that a steel-frame wall is more favourable for economical performance, while a heavy masonry cavity wall is better in terms of environmental performance.

several trial runs may be required for the selection of the values of the various parameters of the chosen optimization algorithm [24].

- Optimization and building simulation programs need to share the values of variables and functions (usually through files). The optimizer transfers the variable values (that represent a design option) to the simulation program, which uses these values to calculate the objective functions[17] or functional constraints and returns the results to the optimizer. The above procedure is iterated until a predefined criterion is satisfied [24]. The user should therefore have some computer programming related knowledge to ensure proper communication between all the programs under consideration so that the entire optimization process can be carried out automatically.
- A large number of simulations is usually required to solve an optimization problem and substantial computation time can be consumed to obtain the simulation results. For example, each optimization run carried out in the study by Wang, et al. [24] took approximately 70 hrs on a fairly powerful computer with Windows XP (3.06 GHz Pentium-IV processor, 512 MB RAM).
- The computation time required to obtain the optimum solution(s) depends not only on the chosen optimization algorithm[18], or the number & type of the design variables considered, but on the simulation program and the complexity of the building model as well. The studies discussed in this section employed a simplified simulation program and/or a simple building model (e.g. a single-zone or just one floor of the case study building), while in some cases full year simulations were avoided to

[17] **Note:** More complicated situations may arise in low-energy building design optimization, in case the values of objective functions or functional constraints cannot be directly obtained from the available simulation program. The simulation results must then be post-processed in order to obtain the required function values. For example, to minimize the greenhouse gas emissions due to the operation of a building, the annual energy consumption estimated by a building energy simulation program must be processed further to consider the primary energy sources and their emission factors to derive the greenhouse gas emissions. This calculation must be carried out through a user-developed program which should communicate with the main simulation program and the optimizer in order to carry out the optimization process as described above [24].

[18] **Note:** A comparison of the performance of a number of optimization algorithms in solving the same optimization problem that was carried out by Wetter, et al, (2004) [27], illustrated that the total number of simulations ranged from 195 to 2330 depending on the algorithm used.

speed-up the optimization process. The downside of the above simplifications is the impact on the accuracy of the simulation results.

- Most of the studies presented earlier involved a large number of design factors. However, in some cases the specification of the design variables made the optimization process unnecessarily complicated since no practical benefit was obtained from the optimization results. For example, the consideration of separate HVAC system control variables for each hour of the day in the three studies by Wright, et al. [20], [21], [22] resulted in a huge design space. As a result, it was practically impossible to carry out the optimization process for a complete (simulation) year, (8760 independent variables would have been required for each HVAC system control set-point in such a case), while the conclusions derived from the three-day simulations were of limited use to the designer. Also, the specification of different types of window depending on the façade of the case study building in the study by Wang, et al. [24] is not really necessary since it is uncommon to install different window constructions on each façade of an actual building.
- As mentioned in both studies by Wang, et al. [23], [24], the use of optimization is particularly useful at the conceptual stage of the design process when a large number of design options needs to be considered. However, the detailed description of a limited number of different wall constructions and materials or window types in both these studies seems to be in contrast with the above notion, since not only does it increase the complexity of the optimization problem, (due to the use of hierarchical variables), but it clearly limits the choices of the designer. In addition, changing, for example, the type of window construction affects a large number of parameters associated with the thermal performance of the glazed building elements, like the U-value and the total shading coefficient, preventing the designer from gaining a clear understanding of the design factors that make buildings energy efficient.
- Some of the studies considered in this section (such as [19], [20], [21] and [22]) obtained a large number of design options attempting to study the trade-off relationship between the objective functions, while the rest

concentrated on a small number of near-optimum design solutions. In both cases, however, the discussion of the results was rather poor, since it proved difficult to analyze the optimization results in depth and provide designers with some practical guidelines. The reason is that even though the direct coupling of an optimization technique with a building energy simulation program takes into account the interactions between the design variables providing a number of near-optimum design solutions, the functional relationship between the design factors and the objective function(s) cannot be uncovered. For example, it is not clear which design factor has the highest effect on the objective function(s), while it is not possible to quantify the impact that changing one or more design variables has on the response variable under consideration.

Although the direct coupling of an optimization algorithm with a building simulation tool to achieve low energy buildings looks promising, there are several problems, as discussed in the above bullet points, questioning whether it would be practical to apply such complicated and time consuming techniques to an actual design project. However, most of the above issues can be resolved through the use of metamodeling techniques (such as the response surface methodology), which allow for the development of approximations of the detailed computer codes, called 'metamodels' [28]. These approximations are then used in place of the computer program to help designers to understand the functional relationship between the design variables and the simulation output of interest, while they also provide fast analysis tools for optimization and design space exploration [29]. It is therefore possible to reduce the number of simulations and the required computation time for the identification of the optimum solution(s) allowing the designer to carry out full year simulations using a sophisticated simulation program along with a detailed model of the building and the associated HVAC system. More details on the metamodeling techniques and the response surface methodology can be found in chapter 3.

2.9 Summary and Conclusions

All the reports presented in sections 2.2 to 2.8 are based on the concept that buildings are major energy consumers mainly due to the increasing use of air-conditioning. As a result, they all study the effect of a number of design variables on the annual energy consumption using mainly a computer simulation tool, in an attempt to understand the factors that make buildings energy efficient. However, the methodology used to reach the solution of the problem is different for each study.

The report presented in section 2.2, is really a pilot study, which adopted a trial and error approach to study the effect of a number of parameters of both an architectural and an engineering nature on the energy performance of a commercial air-conditioned building without employing any form of planned experimentation, statistical procedures or optimization techniques for the analysis of the results.

Section 2.3 presented a poor attempt on the assessment of the effect of a number of design factors on the energy performance of two office buildings through computer simulation, illustrating that the employment of a sound methodology and the systematic analysis of the simulation results are essential aspects of a good research that will lead to clear and understandable conclusions.

The authors of the papers presented in sections 2.4 and 2.5 studied a large number of design variables, making use of sensitivity and regression analysis techniques, to identify the most significant parameters and their correlation to building energy consumption, as well as to develop some energy prediction equations. However, there are some parts of the methodology used in these studies that could be criticized, such as, for example, the use of an unnecessarily large number of simulations to correlate a relatively small number of parameters with the response under consideration, as shown in section 2.5, or the adoption of the one-factor-at-a-time approach, as explained in section 2.4. Moreover, the authors claim that the aim of the final energy prediction equations is to aid the design process during the early stages, when several alternative design schemes

and concepts need to be evaluated, while the use of detailed simulation tools is often considered time consuming. However, both reports fail to provide architects or engineers with any practical design guidelines. In addition, it should be borne in mind that the energy equations developed in section 2.5 are appropriate only if considered with the assumptions made in this study, regarding mainly the characteristics of the base case building and the associated HVAC system, as well as the selected climatic conditions. Finally, while both studies realize that the use of mechanical cooling dominates the total energy consumed in commercial buildings in Hong Kong, they ignore the effect of different HVAC systems on the annual energy consumption.

The studies presented in sections 2.6 and 2.7 concentrate on the effect of different types of HVAC systems and climates respectively, on the energy consumption of buildings. Although both studies ignore a large number of parameters that could possibly affect the building energy consumption (e.g. the effect of shading devices, the effect of different control strategies of HVAC systems, etc), they indicate that the choice of the HVAC system (section 2.6) and the type of climate (section 2.7) have a significant impact on the building thermal performance.

Finally, the studies included in section 2.8 indicate that it is possible to couple an optimization algorithm with a simulation program in order to automatically search for the optimal or near-optimal solutions in the design space. However, there are several issues, (e.g. the huge number of simulations, the substantial computation time, the use of several simplifications in the simulation of the building and the associated HVAC system to make the optimization process feasible, the difficulties in the analysis of the relationship between the design factors and the response variables, etc), most of which can be resolved using a metamodeling technique, as explained in section 2.8.

Although all the previous studies have reached some interesting conclusions, regarding the reduction of the energy consumed in air-conditioned buildings, none of them can be considered complete, since in each there are topics that require further research. New research work on this subject should be aware of

both the weaknesses and failures of the previous studies, to avoid repeating the same mistakes, and be able to offer a more comprehensive and practical solution to this problem. As a result, any new study, which aims to minimize the energy consumption in buildings should:

- take into consideration the most important design factors of both an architectural and an engineering nature that affect the building thermal performance. However, any new study can certainly benefit from the findings of previous studies, since most of them agree on certain design variables which are likely to have a significant impact on the building energy consumption (e.g. the window-to-wall ratio, or the shading coefficient of the window). Therefore, in a new study it is not necessary to consider all the input parameters of the selected simulation tool, (some of which may not represent actual design factors), thereby avoiding the waste of both effort and time, as well as the increase of the possibility of input errors.
- study the effect of different HVAC systems on the annual energy consumption of the case study building, while bearing in mind that the cooling requirement of commercial buildings dominates the total energy use.
- examine in detail factors that affect the energy performance of the HVAC systems, such as different temperature set-points and schedules, the provision of humidification, the provision of night ventilation, etc.
- study the effect of different types of climate on the building energy consumption. Moreover, concentration should not only be on the design of the building envelope to reduce the sensitivity of the building thermal performance to the weather conditions, but also to the selection of the system that would be more suitable for each type of climate.
- use a sophisticated dynamic simulation tool which can assess the energy performance of a multi-zone building model and the associated HVAC system in detail throughout a complete simulation year.
- provide both engineers and architects with some practical guidelines to aid the design process and produce more energy efficient buildings.

Finally, it should be stressed that a new study that attempts to understand the functional relationship between the chosen design factors and the energy used in buildings should make use of the Response Surface Methodology which combines (a) the experimental strategy to explore systematically the space of the design variables under consideration, (b) the statistical techniques required to correlate the chosen design factors with the dependent variable(s) of interest (e.g. the annual heating or cooling energy consumption) and (c) the optimization methods for the identification of the factor settings that optimize the dependent variable(s) [12], instead of testing only a limited number of alternative designs, based mainly on past experience, since that can prove time-consuming and cumbersome, while there is always the possibility of leaving out a potential solution to the problem. Also, detailed analysis of the interactions between the design factors should be carried out to explore new design possibilities and identify potential alternative combinations of factor levels resulting in near-optimum energy performance.

The methodology used for the assessment of the effect of the chosen design parameters on the HVAC system energy consumption in this research work is described in detail in chapter 3.

References

[1] Mohammad Saad Al-Homoud, Computer-aided building energy analysis techniques, Building and Environment, Vol. 36, 421-433, 2001

[2] G. Gammarata, A. Fichera, L. Marletta, Sensitivity Analysis for Room Thermal Response, International Journal of Energy Research, Vol. 17, 709-718, 1993

[3] Joseph C. Lam, Sam C. M. Hui, Sensitivity Analysis of Energy Performance of Office Buildings, Building and Environment, Vol. 31, No. 1, 27-39, 1996

[4] Jeffrey D. Splitler, Daniel E. Fisher, David C. Zietlow, A Primer on the Use of Influence Coefficients in Building Simulation, Proceedings of Building Simulation '89 Conference, pp. 299-304, Vancouver, 23-24 June 1989, The International Building Performance Association, Belgium (1989)

[5] S. K. Chou, W. L. Chang, Y. W. Wong, Effects of Multi-Parameter Changes on Energy Use of Large Buildings, Int. J. Energy Res., 17 (1993) 885

[6] Joseph C. Lam, Sam C. M. Hui, Computer Simulation of Energy Performance of Commercial Buildings in Hong Kong, Proc. IBPSA Building Simulation '93 Conference, Adelaide, Australia, 1993, pp.129-143

[7] Joseph C. Lam, Climatic Influences on the Energy Performance of Air-Conditioned Buildings, Energy Conversion & Management, Vol. 40, 39-49, 1999

[8] Joseph C. Lam, Sam C. M. Hui, Apple L. S. Chan, Regression Analysis of High-Rise Fully Air-Conditioned Office Buildings, Energy and Buildings, Vol. 26, (1997), 189-197

[9] Sekhar S C., Chung J Y., Energy Simulation Approach to Air-Conditioning System Evaluation, Building and Environment, Vol. 33, No. 6, 397-408, 1998

[10] Mohammad S. Al-Homoud, Optimum Thermal Design of Air-Conditioned Residential Buildings, Building and Environment, Vol. 32, No. 3, 203-210, 1997

[11] D.R.Oughton, Predicted energy consumption for air conditioning systems related to the building envelope and form, **B**uilding Services Engineering, Research & Technology (BSERT), Vol 1, No 4, pp 189-198, 1980

[12] R.H. Myers, D.C. Montgomery, Response Surface Methodology: Process and Product Optimization Using Designed Experiments, Second Edition, 2002

[13] D.R.Cox, Planning of Experiments, Wiley Classics Library Edition, 1992

[14] G.E.P. Box, W.G. Hunter, J.S. Hunter, Statistics for Experimenters: An Introduction to Design, Data Analysis and Model Building, 1978

[15] R Mark J. Anderson & Patrick J. Whitcomb, RSM Simplified: Optimizing Processes Using Response Surface Methods for Design of Experiments, Productivity Press, 2005

[16] Hui, S. C. M., A randomised approach to multiple regression analysis of building energy simulation, In Proc. of the IBPSA Building Simulation '97 Conference, 8-10 September, 1997, Prague, Czech Republic, Volume II, pp. 133-140

[17] Mohammad S. Al-Homoud, Optimum Thermal Design of Office Buildings, International Journal of Energy Research, Vol. 21, 941-957, 1997

[18] Galdas L.G., Norford L.K., A design optimization tool based on a genetic algorithm, Automation in Construction, Vol. 2, No.11, 173-184, 2002

[19] Coley D.A., Schukat S., Low-energy design: combining computer based optimization and human judgement. Building and Environment, Vol. 12, No. 37, 1241–7, 2002

[20] Wright J.A., Loosemore H.A., Farmani R., Optimization of building thermal design and control by multi-criterion genetic algorithm. Energy and Buildings, Vol. 9, No. 34, 959–72, 2002

[21] Wright J., Farmani R., The simultaneous optimisation of building fabric construction, HVAC system size and the plant control strategy, Proceedings of Building Simulation, 7th International IBPSA Conference, Rio de Janeiro, August, 2001

[22] Wright J., Loosemore H., The multi-criterion optimisation of building thermal design and control. Proceedings of Building Simulation, 7th International IBPSA Conference, Rio de Janeiro, August, 2001

[23] Wang W., Zmeureanu R., Rivard. H., Applying multi-objective genetic algorithms in green building design optimization, Building and Environment, Vol. 40, 1512-1525, 2005

[24] Wang W., Rivard. H., Zmeureanu R., An object-orientated framework for simulation-based green building design optimization with genetic algorithms, Advanced Engineering Informatics, Vol. 19, No.1, 5-23, 2005

[25] Peippo K., Lund P.D., Vartiainen E., Multivariate optimization of design trade-offs for solar low energy buildings. Energy and Buildings, Vol. 2, No.29, 189–205, 1999

[26] Saporito A., Day A.R., Karayiannis T.G., Parand F., Multi-parameter building thermal analysis using the lattice method for global optimization, Energy and Buildings,Vol. 33, No. 3, 267-274, 2001

[27] Wetter M., Wright J., A comparison of deterministic and probabilistic optimization algorithms for nonsmooth simulation-based optimization, Building and Environment, Vol. 39, No. 8, 989-999, 2004

[28] T. W. Simpson, J. D. Peplinski, P. N. Koch, J. K. Allen, Metamodels for Computer-base Engineering Design: Survey and Recommendations, Engineering with Computers 17: 129 – 150, 2001

[29] Timothy W. Simpson, John J. Korte, Timothy M. Mauery, Farrokh Mistree, Comparison of Response Surface and Kriging Models for Multidisciplinary Design Optimization, (AIAA-98-4755), 7th Symposium on Multidisciplinary Analysis and Optimization, St. Louis, MI, September 2-4, 1998

[30] Elisabeth Gratia, Andre De Herte, Design of low energy buildings, Energy and Buildings, Vol.35, pg. 473-491, 2003

Chapter 3: Methodology used for the assessment of the effect of the chosen design factors on the HVAC system energy consumption

3.0 Aims of the chapter

The aim of this research work is to study the effect of 25 design factors on the annual energy consumption of a notional air-conditioned office building employing either a VAV system with terminal re-heaters or a four-pipe FCU system with fresh air supply from a central plant, through computer simulation. The evaluation of the energy performance of the chosen systems is for two types of climate. The design factors are categorized into 8 groups related to the design & operation of the building and the associated HVAC system. The Response Surface Methodology (RSM) is used to model the relationship between the parameters of each group and the annual energy use, as well as to identify the combinations of factor levels that optimize the energy performance of both systems depending on the climate for which they are simulated. This chapter describes the procedure required to perform all these tasks.

3.1 Structure of the chapter

A short description of the RSM is given in section 3.2 of this chapter. The experimental designs, which provide an efficient procedure for planning experiments so that the data obtained can be analyzed to yield valid and objective conclusions [50], are presented in section 3.2.1. A short description of Design-Expert, the statistical software package used in this study, is also provided in this section. The various techniques which can be used in order to optimise one or more response variables are described in section 3.2.2. The application of the RSM to experiments carried out using computer models is discussed in section 3.2.3.

The factors studied in the thesis and their range of values are presented in section 3.3. Section 3.3.1 contains all the building related groups of parameters, while section 3.3.2 includes the HVAC system associated groups of factors.

A short description of A-TAS and the characteristics of the case study building as introduced into the thermal simulation program are provided in sections 3.4.1 and 3.4.2, respectively. The simulation concept behind B-TAS is discussed in section 3.5.1, while the main components of both the VAV system and the FCU system as designed in B-TAS are described in sections 3.5.2 and 3.5.3, respectively. The main features of the duct sizing methodology used to estimate the total pressure of the central fans of the HVAC systems are presented in section 3.6.

Sections 3.7.1 and 3.7.2 contain a short description of the Test Reference Years for London and Athens respectively, which are used for the simulation of the chosen HVAC systems. Finally, section 3.8 analyses the overall carbon performance of the case study office building in the base case scenario.

3.2 Response Surface Methodology

3.2.1 Response Surface Designs: Central Composite and Face Centered Designs

A common problem faced by scientists in many technical fields is the mathematical representation and study of the relationship between a set of predictor (or independent) variables x_1, x_2, ..., x_k subject to the control of the experimenter, and a response (or dependent) variable of interest y. In most cases the nature of this relationship is not known in advance. Thus, the experimenter must approximate the unknown correlation between y and the x's with an appropriate empirical model of the form $y = f(x_1, x_2, \ldots, x_{k)} + \varepsilon$, where ε is the "error" in the system [1]. This empirical model is called a response surface model, and it can be used for the development of graphical representations of the relationship between the response variable y and the independent variables x_1, x_2, ..., $x_{k,}$, and the identification of the factor levels that optimize the response function.

The response surface methodology (RSM) is a collection of statistical and mathematical techniques which can be used to perform all the tasks mentioned above. Thus, the field of RSM comprises of (a) the experimental strategy to explore the space of the independent variables, (b) the statistical techniques required to develop an appropriate approximating relationship between the response y and the independent variables x_1, x_2, ..., x_k, and (c) the optimization methods for the identification of the factor levels that produce desirable values of the response variable y (e.g. the combinations of factor levels that minimize or maximize y) [1].

As mentioned above, the form of the response function f is not known in advance, so it is usually approximated by a first-order or a second-order model. The first-order model is likely to be appropriate when the true response surface is approximated over a small region of the independent variables space, in a location where there is little curvature in f [1]. The simplest form of the first-

order regression model is $Y = \beta_0 + \sum_{i=1}^{\kappa} \beta_i x_i + \varepsilon$, which includes only the main effects of the independent variables x_1, x_2, …, x_k. However, if there is an interaction between the independent variables the model takes the form: $Y = \beta_0 + \sum_{i=1}^{\kappa} \beta_i x_i + \sum_{i<j=2}^{k} \sum \beta_{ij} x_i x_j + \varepsilon$, where $\beta_1, ..., \beta_\kappa$ are the linear main effect coefficients and $\beta_{12}, \beta_{13}, ..., \beta_{\kappa-1,\kappa}$, are the interaction effects coefficients.

Factorial designs[1] can be used in order to estimate all the terms of the first-order model (i.e. both linear and interaction terms). To perform a general factorial design the experimenter must choose a fixed number of levels for each independent variable and then study all the possible combinations. For example, if there are l_1 levels for the independent variable x_1, l_2 for the variable x_2 and l_k for the x_k variable, the total number of combinations (and, consequently, the total number of experimental runs) will be $l_1 \times l_2 \times ... \times l_k$ [2].

A very important class of factorial designs is that where each independent variable has two levels. Assuming that the total number of factors is k, the number of experimental runs will be 2^k. The 2^k factorial designs are of great importance for a number of reasons, some of which are the following [1], [2]:

- They require a relatively small number of runs.
- They can be augmented with a suitable number of design points to form central composite designs which can be used to fit second-order response surface models.
- The interpretation of the observations produced by these designs can proceed mainly by using common sense and basic arithmetic.

It is also worth mentioning that the factorial designs have practically replaced the "one-factor-at-a-time" method, another more traditional form of planned experimentation, which was formerly used in most research projects. The "one-

[1] **Note:** To estimate the coefficients β, data must be collected on the system or process being studied. Experimental designs are used to this end. An experimental design represents a sequence of experiments to be carried out, expressed in terms of factors set at specified levels [44]. The layout of a design consists of an array of values presented in rows and columns. The columns usually represent design factors, while the values in the rows represent settings for each factor in the individual runs of the design [43], [48].

factor-at-a-time" method provides an estimate of the effect of a single independent variable on the response variable y, at chosen fixed levels of the rest of the independent variables. However, this estimate is correct only when it is assumed that the effect is the same at other settings of the rest of the independent variables, which means that over the ranges of interest, the variables act on the response additively. However, when the variables do not act additively, the factorial designs, unlike the "one-factor-at-a-time" method, can detect and estimate interactions that measure non-additivity. Moreover, even when the independent variables do act additively, the factorial designs can perform the same task with more precision [2].

The interaction terms in the full first-order model presented earlier introduce curvature into the response function. However, in many cases the curvature in the true response surface is so strong that the first-order model (including the interaction terms) is not adequate [1]. In such a case a second-order model might be required. The second-order model has the form: $Y = \beta_0 + \sum_{i=1}^{\kappa} \beta_i x_i + \sum_{i=1}^{\kappa} \beta_{ii} x_{ii}^2 + \sum_{i<j=2} \sum^{\kappa} \beta_{ij} x_i x_j + \varepsilon$, where $\beta_{11},...,\beta_{\kappa\kappa}$, are the quadratic effect coefficients.

The second order model is widely used in RSM for the following reasons [1]:

- It can take on a great variety of functional forms, so in most cases it will provide a very good approximation of the true response surface.
- The coefficients β in the second order model can be easily estimated[2] using linear regression analysis.
- There is substantial practical evidence indicating that second-order models work well in solving real response surface problems.

[2] **Note:** The least squares method is typically used to estimate the regression coefficients in a multiple linear regression model. This method chooses the best-fitting model to be that model which minimizes the sum of squares of the distances between the observed responses and those predicted by the fitted model. In general, the better the fit the smaller will be the deviations of observed from predicted values [40].

The minimum requirements to fit a second-order response surface model are the following [1], [2]:

- Each design variable must have at least three levels.
- The number of distinct design points must be equal to $1+2k+k\times(k-1)$ at least.

There is a variety of response surface designs not only meeting the two minimum requirements but also displaying a number of additional properties which serve different purposes (e.g. there are experimental designs that aim for cost effectiveness, good distribution of the prediction variance, etc) [1]. However, the most popular class of second-order designs is by far the Central Composite Design (CCD), which was introduced by Box and Wilson (1951) [1]. A CCD is basically a two-level (full or fractional) factorial design which has been augmented with a small number of carefully chosen design points (i.e. axial and centre points), to allow the estimation of the second-order response surface model [5], as can be seen in figure 3-1[3]:

[3] **Note:** It should be stressed that the natural independent variables are transformed in coded variables X_1, X_2, X_3,...,X_k which are usually defined to be dimensionless with mean zero and the same spread or standard deviation [1]. The levels of each factor X_j are typically coded as follows [3]:

$$X_j = \frac{Actual - \frac{High + Low}{2}}{\frac{High - Low}{2}}$$

This coding scheme results in coded values of:

- −1 for the low level of each factor X_j
- 0 for the mid-level of each factor X_j
- +1 for the high level of each factor X_j

The coding scheme helps to eliminate any spurious statistical results due to the different measuring scales for the various factors. Since coding the factors removes their units of measure, the model coefficients, in coded format, can be directly compared as a measure of their relative impact. Also, using uncoded factors sometimes leads to colinearity among the terms of the model. This inflates the variability in the coefficient estimates and makes them difficult to interpret. It is, therefore, recommended to use coded variables since it helps to get rid of such problems [3].

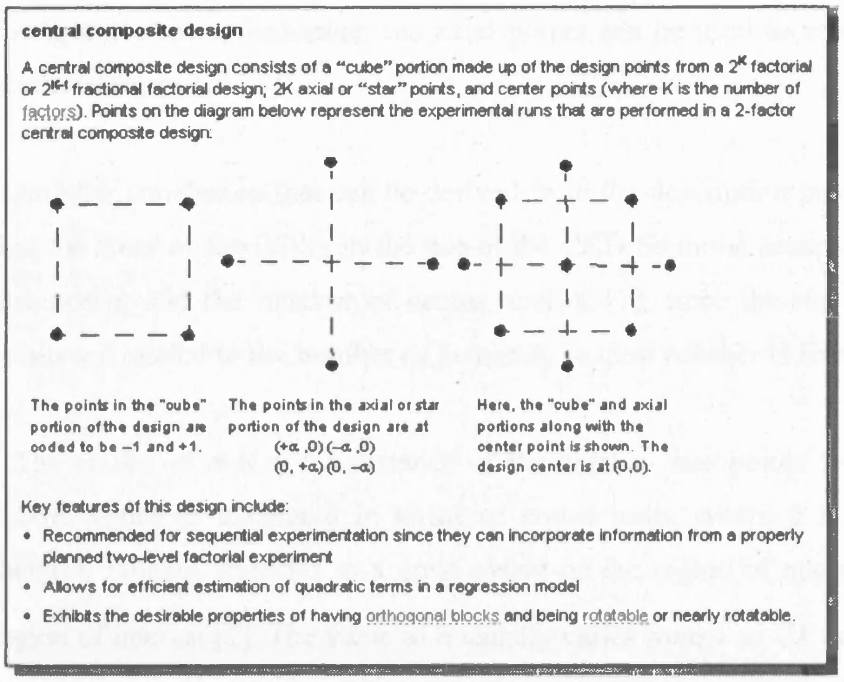

Figure 3-1: The design points constituting a CCD involving two factors [3].

The CCD consists of three components (i.e. groups of design points), which play important and somewhat different roles [1]:

- 2^k factorial points, (where k is the number of parameters), which are used to estimate both the linear terms and the two factor interactions[4].
- 2k axial or star points, which contribute in a large way to the estimation of quadratic terms[5]. The term "axial" stems from the fact that each of these points lies either on the x_1 or the x_2 axis, at a distance α from the design centre, as illustrated in figure 3-1.
- n_c centre points, which provide an internal estimate of error (pure error) and contribute towards the estimation of the quadratic terms.

The sequential nature of the CCD becomes clear from the description of the various design points provided above. Thus, the factorial points allow for the estimation of the first-order plus two-factor interaction model, while the centre runs provide information about the existence of strong curvature in the system. If

[4] **Note:** It should be stressed that the factorial points are the only design points contributing to the estimation of the interaction terms.

[5] **Note:** Without the axial points, only the sum of the quadratic terms, $\sum_{i=1}^{k} \beta_{ii}$ can be estimated.

strong curvature is indicated, the axial points can be used to estimate the pure quadratic terms [1].

Another conclusion that can be derived from the description provided above is that the areas of flexibility in the use of the CCD lie in the selection of the axial distance α, and the number of centre runs n_c [1], since the rest of the design points are related to the number of factors k, so their number is fixed[6].

The choice of α (i.e. the distance of the axial or star points from the design centre, which is measured in terms of coded units, where ± 1 represents the factorial ranges), depends to a great extent on the region of operability and the region of interest [1]. The value of α usually varies from 1 to $\sqrt{k}$ or $\sqrt[4]{2^k}$.

When $\alpha = \sqrt{k}$, the axial points are placed on a common sphere, surrounding the cuboidal proportion of the design consisting of the factorial and centre points, as can be seen in figure 3-2:

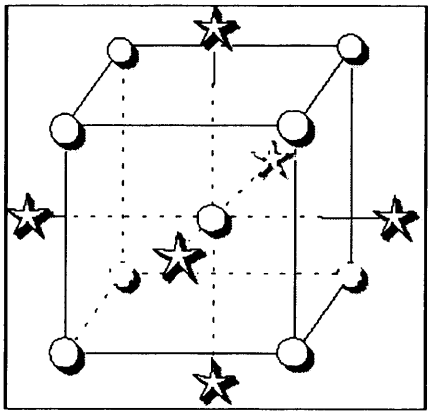

Figure 3-2: Central composite design for k=3 factors, where the axial distance is $\alpha = \sqrt{k}$ [4]

When $\alpha = \sqrt[4]{2^k}$, (where 2^k is the number of the factorial points), the property of rotability is ensured. In general, a rotatable design is one for which the prediction variance has the same value at any two locations that are at the same distance from the design centre. In other words, the prediction variance is constant on spheres [1]. It should be stressed, however, that a rotatable design does not imply stability throughout the design region. To achieve stability throughout the design region it is necessary to use a certain number of centre points n_c [1]. Five centre points or more are necessary to achieve relatively uniform precision inside the factorial ranges [43].

[6] **Note:** For example, a CCD involving k=3 factors will contain $2^3 = 8$ factorial points, and $2 \times 3 = 6$ axial points.

As mentioned earlier, the region of operability, and the region of interest play also a very important role on the choice of α. In many cases the region of interest is smaller than the region of operability, which is the area where it is theoretically possible to carry out the experiment and observe response values. However, there are some situations where the ranges of the design variables specified by the scientist or the engineer are strict [1]. In such a case, the axial distance α cannot be extended beyond the experimental region defined by the upper and lower limits of each factor (i.e. $\alpha \leq 1.0$) [5]. As a result, the region of interest and the region of operability are practically the same, which means that the obvious region for such a design is a cube (and not a sphere) [1].

In the case of a cuboidal design region[7], the axial points are placed at the centre of the faces of the cube (in other words α = 1.0), as illustrated in figure 3-3. Designs of this type are called Face Centered Designs (FCD), and are very effective second-order designs [1].

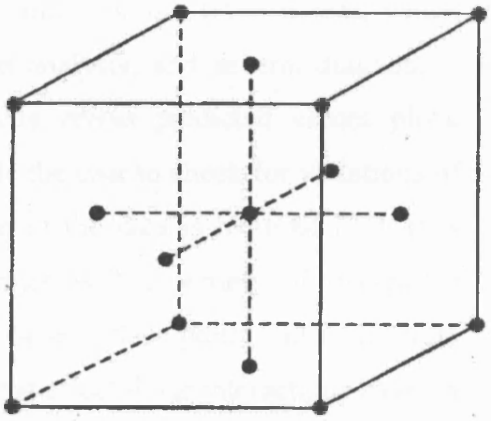

Figure 3-3: Face centered central composite design for k=3 factors, where the axial points are placed at the centre of the faces of the cube (i.e. α = 1) [43]

[7] **Note:** It should be stressed that when the design region is cuboidal, it is important to push the design points to the extreme of the experimental region (i.e. the axial distance α should be equal to 1.0). This results in the most attractive distribution of the prediction variance, since the design region is covered in a symmetrical fashion [1]. The FCD described above accomplishes this, but it is still not a rotatable design. However, the property of rotability is not an important priority when the region of interest is clearly cuboidal [1].

The design and statistical analysis of the experiments carried out in this study is performed using Design Expert[8] (version 6.0.10), a statistical software package specializing in the design of experiments involving a number of independent variables (categorical or numerical) and one or more dependent variables. This program provides a variety of experimental designs including standard two-level full or fractional factorial designs, general multilevel factorial designs, Response Surface Method designs, etc [4].

Having identified the design that best suites the objectives of the user, Design-Expert performs step-by-step statistical analysis of the experimental data, suggesting which type of regression model provides best fit for the data, producing ANOVA (Analysis of Variance) tables for the fitted model, which summarize the results of multiple regression analysis, and several diagnostics plots (e.g. normal probability plots, residuals versus predicted values plots, outlier plots, Box-Cox plots, etc) which enable the user to check for violations of statistical assumptions, or if a transformation of the data is required [23]. It is also possible to visualize the response surface with a variety of two-factor interaction plots, 2D contour plots or 3D response surface plots, which illustrate how the independent variables interact and what effect those interactions have on the response[9] [24]. Finally, Design Expert provides both graphical and numerical functions for the optimization of a single or a number of dependent variables. The optimization technique used by the program is described in the following section.

[8] **Note:** Two other statistical software tools were considered, including SPSS (version 11.0.1) and MINITAB (version 13), but Design Expert proved to be the most suitable program for the objectives of this study, as well as the most user-friendly.

[9] **Note:** This is the procedure used to correlate the building & HVAC system related design factors contained in each of the 8 chosen groups with the energy performance of the HVAC systems and analyse their effect on the annual heating and cooling energy use. All the response surface models developed in this study can be found in appendix H, while an example of the procedure required to fit each of these models is given in section H1.1.

3.2.2 Various techniques for the optimization of the response

The general form of a second-order response surface model, as also explained in section 3.2.1, is the following:

$$Y = \beta_0 + \sum_{i=1}^{K} \beta_i x_i + \sum_{i=1}^{K} \beta_{ii} x_{ii}^2 + \sum_{i<j=2} \sum^{K} \beta_{ij} x_i x_j + \varepsilon$$

The nature of the response surface, (e.g. minimum or maximum point), depends on the signs and magnitudes of the coefficients in the model displayed above. In particular, the interaction and pure quadratic terms play a vital role [1].

There are some occasions, especially when the number of factors is small ($k \leq 2$), that a contour plot[10] can clearly show if there is a maximum or minimum point close to the centre of the design region. However, in most cases a more formal analytical approach must be adopted to identify the nature of the response surface system and the location of the minimum or maximum point. Moreover, it might be necessary to use constrained optimisation to arrive at potential operating conditions when the goal of the analysis is to determine the nature of the system inside or on the perimeter of the design region, or when several response variables must be considered [1].

The simultaneous consideration of multiple responses involves first fitting an appropriate response surface model for each response and then trying to identify a set of operating conditions that in some sense optimizes all the responses or at least keeps them within desired ranges [1]. The most popular approach to multiple response optimization is to formulate and solve the problem as a constrained optimization problem. One of the numerical techniques, (sometimes referred to as nonlinear programming methods), that can be used to solve this problem is the simultaneous optimization technique developed by Derringer and Suich [1], [4]. This technique is utilized by the Design Expert statistical software.

[10] **Note:** The contour plot is a two-dimensional graphical representation of the response surface, where the points that have the same response are connected to produce contours lines of constant responses [3].

The optimization method developed by Derringer and Suich, is based on the desirability functions d_i. Each response y_i is first converted into an individual desirability function that varies over the range $0 \leq d_i \leq 1$. In general, if an individual response y_i is at its target, the desirability is d_i = 1.0, while if the response is outside an acceptable region the desirability d_i = 0.0. The simultaneous objective function is a geometric (i.e. multiplicative) mean of all the transformed responses: $D = (d_1 \times d_2 \times ... \times d_n)^{1/n}$, where n is the number of the responses being optimised, and it also has a range of 0 to 1. In other words, the overall desirability D is a measure of how well the combined goals for all the responses have been satisfied. Averaging multiplicatively, instead of additively, causes an outcome of zero (i.e. D = 0), in case that any of the individual responses falls outside its desirability range [43]. It is obvious that the optimum solution involves the factor levels that maximize the overall desirability (i.e. bring D as close to 1.0 as possible) [1], [4].

The same numerical method can also be used to optimize a single response or a single response subject to upper and/or lower constraints on other responses. The goal for the optimization of the response variable [11] can be "maximum", "minimum", "target" (i.e. when the response must be equal to a certain value), or "in range" (i.e. when the response must fall within a specific range of values) [4]. Moreover, for simultaneous optimization each response must have a low and high value assigned to each goal. These values establish the points at which the desirability index becomes 0 or 1 [48]. For example, when the objective is to maximize the response y_i, the desirability is defined by the following formulas [4]:

$$d_i = \begin{cases} 0 & y_i \leq Low_i \\ \left(\dfrac{y_i - Low_i}{High_i - Low_i}\right)^{wt_i} & Low_i < y_i < High_i \\ 1 & y_i \geq High_i \end{cases}$$

[11] **Note:** It is also possible to set goals for the factors. Factors are normally constrained within the ranges experimented upon [43]. In such a case the goal is "in range" and the factors are left free to vary within their experimental region. However, it may be necessary, for example, that one or more factors are held close to their minimum or maximum level during the optimisation of the response variable(s).

The desirability curves, when the objective is to maximize the response are illustrated in figure 3-4:

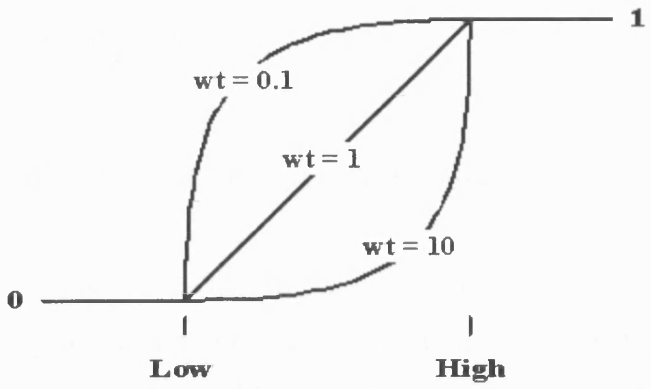

Figure 3-4: Desirability curves when the goal is to maximise the response function [4]

As can be seen from figure 3-4 the shape of the desirability function depends on the weight (*wt*). For the default value of $wt = 1.0$, the desirability function is linear. However, choosing $wt > 1.0$ places more emphasis on the target value, while choosing $0 < wt < 1.0$ places less emphasis on the goal [4].

It is also possible to change the importance[12] (r_i) of one goal in relation to the other goals. In the overall desirability function (D), each response is assigned an importance (r_i), relative to the other responses, which varies from the value of 1 (least important) to the value of 5 (most important). The default is for all goals to be equally important at a setting of $r_i = 3$. However, varying degrees of importance can be assigned to the different responses (e.g. if one goal is more important than the rest, a level of importance equal to 5 can be assigned to it). In such a case the overall desirability function will be: $D = (d_1^{r_1} \times d_2^{r_2} \times ... \times d_n^{r_n})^{1/\sum r_i}$ [4].

One of the objectives of this study is to determine the values that the design variables contained in each group should take in order to minimize either or both the heating and the cooling energy use (or, in other words, the total carbon emissions) over the simulation period, depending on the HVAC system and the

[12] **Note:** The importance (r_i) is a relative scale for weighting each of the resulting d_i in the overall desirability product [4].

climate for which it is simulated. The optimization technique developed by Derringer and Suich is, therefore, used to identify the combination(s) of factor levels within the design region that minimize the impact of the HVAC systems on the environment.

3.2.3 The application of RSM to deterministic computer experiments

Statistical techniques are widely used in engineering design to construct approximations of detailed computer analysis codes, called 'metamodels' [44]. These approximations are then used in place of the actual computer simulation codes to yield insight into the functional relationship between the input design parameters x and the output response variables of interest y, while they also provide fast analysis tools for optimization and design space exploration [47]. The metamodels are particularly useful at the early stages of the design, when it is necessary to evaluate several potential conceptual configurations in order to obtain the ones that best meet the design objectives.

In general, metamodeling involves (a) choosing an experimental design, which represents a sequence of experiments (or, in other words, computer simulations) to be performed to collect data from the simulation model in an organized way (sample points), (b) choosing a model to represent these data and (c) fitting the model to the observed data [44]. The four, most prevalent in the literature, metamodeling techniques are the following [44]:

- Response Surface Methodology, which is a collection of mathematical and statistical techniques for empirical model building and exploration of a region of design variables in order to identify the optimum factor settings, as explained in detail in sections 3.2.1 and 3.2.2.
- Neural Networks which are composed of neurons, or in other words, multiple linear regression models with a nonlinear (typically sigmoidal) transformation of y. Typical applications of neural networks are speech recognition and handwritten character recognition where the data is complex and of high dimensionality. Networks with tens of thousands of parameters have been used but the necessary gathering of training data

and evaluation of model parameters can be extremely computationally expensive.

- Inductive Learning, which is a modeling technique most appropriate when both input and output factors are primarily discrete-valued. The prediction model comes in the form of condition - action rules or a decision tree, which means that it may lack the mathematical insight, required for engineering design applications.
- Kriging, which is an interpolation method capable of handling deterministic data. This method is very flexible due to the wide range of correlation functions that may be chosen, but it has found limited use in engineering applications due to the complexity of fitting a kriging model or the additional effort required to use such a model, in combination with the lack of readily available software to construct kriging models.

The RSM is the most well established metamodeling technique [44]. Most metamodeling applications involve the development of a low order polynomial using CCDs and least squares regression. Some of the reasons for the increased popularity of this approach include the maturity of RSM, its simplicity and the availability of accessible software tools [44]. However, this method should not be applied blindly to computer experiments. This is due to the fact that, in most cases, there is no measurement error or no variability in the computer analysis outputs given a specific set of input variables [46]. In other words, the output of experiments carried out using computer models is deterministic. As a result, the classical notions of experimental blocking, replication and randomization are not applicable to computer experiments. In addition, statistical testing of model and parameter significance, based on F-values or P-values[13], is not appropriate for computer experiments which lack random error [44]. Nevertheless, much of the standard statistical analyses remain relevant, including measures of model fit such as $R^2_{adjusted}$ which takes into account the number of parameters in the model, $R^2_{predicted}$ which measures the amount of variation in new data explained by the

[13] **Note:** The F-distribution is a probability distribution used to compare variances by examining their ratio. If they are equal, the F-value is 1. The F-value in the ANOVA table is the ratio of the model mean square to the appropriate error mean square. The larger their ratio, the larger the F-value and the more likely that the variance contributed by the model is significantly larger than random error. The probability value or P-value relates to the risk of falsely rejecting a given hypothesis. Generally, a probability<0.05 is considered significant [43].

model and PRESS which is a measure of how well the model fits each point in the design [43], [44]. Residual plots may also be helpful for verifying model adequacy, identifying trends in data, examining outliers, etc [44]. Finally, model validation using a separate (different to the original) set of data points is recommended [44]. The average absolute error, the maximum absolute error and the root mean square error[14] can be estimated for the validation data points in order to assess the model accuracy.

There are several applications of RSM in computer experiments, most of which come from aerospace and mechanical engineering. For example, aerospace engineers wanted to understand how wing weight varies with changes in wing geometry of a lightweight fighter jet [45]. The relationship between the wing weight and the three design variables associated with the wing geometry was approximated by a second order model. The coefficients of this model were estimated using least squares regression of computer simulated data, which was provided in an organized manner through a face centered design. The validation test, which involved a maximum absolute error just under 7%, indicated that the response surface equation is a good predictor of the exact relationship between wing weight and wing geometry. A recent review of several engineering applications of response surface models can be found in reference [44].

Also, the use of second order response surface models has been compared with the utilization of kriging models for approximating deterministic computer analyses [47]. It was found that the RS and kriging models yield comparable results with minimal difference in predictive capability. Another study that compared the performance of experimental design methods for approximation model building for deterministic computer models, in terms of (a) the quality of fit and (b) the number of design points required, found that CCDs work well for problems with five or less design parameters [46].

As mentioned in the previous sections, this study uses the RSM to approximate the relationship between a number of building & HVAC system related design

[14] **Note:** The definition of these three model validity measures, along with a detailed description of PRESS and $R^2_{predicted}$ mentioned earlier, can be found in appendix H.3.

factors, classified into eight groups of 3 or 4 parameters, and the energy performance of two types of HVAC systems, which is predicted by TAS, a dynamic thermal simulation software (i.e. a deterministic computer model). The 54 polynomial approximations or 'metamodels' developed throughout the thesis can be found in appendix H. A number of summary statistics (including $R^2_{predicted}$ and PRESS) along with the model accuracy measures computed for a separate validity data set, as described earlier, are presented in table H-3 of this appendix. The validation results, involving a maximum absolute error lower than 5% for most of the fitted polynomials, suggest that the response surface models predict the TAS simulation output of interest with reasonable accuracy within the design region studied. In other words, the response surface equations are good predictors of the true relationship between the building & HVAC system related design factors and the energy performance of the HVAC systems under consideration.

3.3 Factors to be studied and their range of values

The main objective of the thesis is to study the effect of 25 factors of both an architectural and engineering nature on the energy performance of two HVAC systems. The basis of selection of these parameters is that they should represent actual design factors which are considered critical by both engineers and architects in the design process. It should also be stressed that past parametric studies have been taken into consideration in this work, since most of them agree on certain design variables, which are likely to have a significant impact on the annual energy use (e.g. the glazing percentage or the shading coefficient of the window). Therefore, it is not necessary to consider all the input parameters of TAS, thereby avoiding the waste of both effort and time, as well as the increase of the possibility of input errors, as also explained in section 2.9 (chapter 2).

However, the simultaneous consideration of all the chosen factors would still lead to a huge number of simulations, (e.g. assuming that each HVAC system related factor has three levels, the total number of simulations in order to assess all the combinations of the 15 chosen factors would be 3^{15} = 14,348,907), and a complicated regression model[15] which would be extremely difficult to interpret. To overcome these two problems, the parameters have been categorized into eight small groups, (using some subject related knowledge so that each group is of particular interest to architects and/or engineers), keeping the simulations to a manageable number and leading to models which are easier to visualize and interpret. As a result, building designers gain a better understanding of the effect of the parameters associated with, say, the solar gains through the windows or the thermal resistance and the air tightness of the building envelope on the annual (heating or cooling) energy consumption of the HVAC systems, and are able to achieve energy efficiency via the proper choice of design variables.

[15] **Note:** In other words, the result would be an energy prediction equation such as the one developed in the paper reviewed in section 2.5 (chapter 2). However, the aim of this research work is not to develop a complicated equation that could be used in place of a building simulation program in order to predict the annual energy use, but to provide designers with some practical guidelines towards energy efficient buildings.

The 25 design factors studied in the thesis and their range of values are presented in sections 3.3.1 and 3.3.2, respectively. Moreover, a short discussion regarding the basis of selection of the minimum, maximum and standard values for each factor, (as well as their sources, when this is necessary), is provided.

In general, the 'standard' value mentioned above indicates the value of each parameter in the base case scenario (i.e. the simulation of the case study building and the associated HVAC system in TAS). This value usually corresponds to the requirements of the Part L Building Regulations (2002) or to standard design practices for air conditioned office buildings. An attempt has also been made so that both the minimum and the maximum values of each parameter respond to real design practices (even if in some cases these values are not considered to be very common).

3.3.1 Building load parameters

In general, the total cooling load of the building consists of two main components, namely the internal cooling load and the building envelope cooling load [39]. The internal cooling load is affected by the heat gains from occupants, equipment and lighting. The building envelope cooling load is affected by factors associated with the solar heat gains through the windows (e.g. the total shading coefficient or the glazing ratio), and also, by factors associated with air infiltration and the heat conduction through the building envelope (e.g. the wall U-value). Keeping this in mind, the parameters classified in this category were divided into the following 3 groups:

Group A: Window design and shading devices

This group contains four parameters associated with the solar gains through the transparent building elements:

Factors	Values		
	Standard	Minimum	Maximum
Factor A: Glazing percentage (%)	40%	25%	95%
Factor B: Total shading coefficient (TSC)	0.74	0.16	0.88
Factor C: Overhang depth (m)	-	0.0	2.0
Factor D: Side-fin depth (m)	-	0.0	2.0

Table 3-1: The range of values of the factors associated with the solar gains through the windows

Glazing percentage: The standard value of this factor corresponds to the requirement of the Part L document [12], which specifies a maximum allowable glazing area equal to 40% for office buildings, following the Elemental method. The maximum value of this parameter refers to fully glazed office buildings, while a minimum value lower than 25% is considered unusual.

Total Shading Coefficient (TSC): The TSC expresses the fraction of solar radiation at normal incidence that is transferred through the window construction by all means [11]. A TSC of 0.74 is considered to be the most common value, while the minimum and maximum values correspond to high performance glazing and single glazed windows, respectively [11].

Overhang & Side-fin depth: The base case building model does not incorporate any external shading devices. The minimum value of these parameters is also set to zero. On the other hand, an overhang or side-fin depth (i.e. the distance between the wall and the outer edge of the overhang or the side-fin) greater than 2.0 m is considered unlikely due to the inevitable reduction of daylight levels as well as the negative impact on the appearance of the building. It should also be stressed that overhangs are placed only on the south façade of the building, while side-fins are placed on the east and west facades.

Group B: Thermal resistance and air tightness of the building envelope

This group contains three design variables associated with the air tightness and the U-value of the building envelope:

Factors	Values		
	Standard	Minimum	Maximum
Factor A: Wall U-value (W/m^2K)	0.35	0.18	0.70
Factor B: Infiltration rate (ach)	0.50	0.25	2.00
Factor C: Window U-value (W/m^2K)	2.10	1.20	5.80

Table 3-2: The range of values of the factors related to the air tightness and the U-value of the building envelope

Wall[16] *U-value:* To comply with the Building Regulations Part L (2002) [12], following the Elemental method, the wall insulation should be no worse than 0.35 W/m^2K. The U-value of 0.18 W/m^2K, which characterizes a highly insulated external wall, corresponds to the minimum requirements of the more stringent Swedish building regulations [7]. The chosen maximum value[17] refers to a poorly insulated wall.

Infiltration: The standard, minimum and maximum infiltration levels shown in the table above correspond to a typical, airtight and leaky office building, respectively.

Window U-value: The Part L document [12] (following the Elemental method) specifies a window U-value of 2.0/2.2 W/m^2K if wood or metal frames are used, respectively. The minimum value of 1.2 W/m^2K corresponds to high performance windows. Moreover, U-values of this order correspond to the

[16] **Note:** Different insulation levels for the floor or the roof of the building are not investigated since their contribution to the annual heating or cooling energy consumption is not expected to be significant. This is due to the fact that the area of the roof or the ground floor is a small percentage of the total area of the external envelope of the six-floor case study building. Past parametric studies have also reached similar conclusions [39].

[17] **Note:** It is worth mentioning that the Elemental method [12], allows parts of an exposed wall or floor to have a U-value of 0.70 W/m^2K provided that other compensating measures are taken.

minimum requirements of other European countries [6]. The maximum value refers to single glazed windows [11].

Group C: Internal heat gains

This group contains three parameters associated with the internal heat gains of the building:

Factors	Values		
	Standard	Minimum	Maximum
Factor A: Equipment gains (W/m^2)	15.0	10.0	25.0
Factor B: Lighting gains (W/m^2)	12.0	6.5	20.0
Factor C: Occupancy density (m^2 per person)	10	5	20

Table 3-3: The range of values of the factors related to the internal heat gains of the building

Equipment heat gains: The BCO Guide 2000 [25], which provides concise guidance for the specification of offices, states that when diversified over 1000 m^2 or more, the power consumption for office equipment rarely exceeds 15 W/m^2, but points out that offices should have the ability to upgrade to 25 W/m^2. The good practice recommendation of ECON 19 [8] for the equipment gains of an air-conditioned office building also equals 15 W/m^2. Moreover, the office equipment heat gains were calculated [18] for the BCS, using the worksheet provided in appendix 1 of the Good Practice Guide 276 [5]. It was found that the equipment gains are equal to 20 W/m^2, when energy saving features are not enabled, while they can be reduced to 13 W/m^2, when all the energy saving features are enabled. As a result, the equipment heat gains in a typical office building usually range between 13 - 20 W/m^2. The standard value for the office equipment gains was, therefore, set to 15 W/m^2, while the maximum value was set to 25 W/m^2. Finally, the minimum value shown in table 3-3, is the best practice value adopted in TM29 [3], which corresponds to contemporary low energy IT office equipment.

[18] **Note:** Details concerning this calculation can be found in Appendix E.

Lighting gains: The standard and maximum values of this parameter correspond to the good practice[19] and typical indices of ECON 19 [8], respectively, for an air conditioned office building. The minimum value corresponds to the recommendations of TM 29 [6], where air handling luminaires are considered, which allow a proportion[20] of the heat gains to be transferred through the ceiling void to be handled at the central plant. (This means only 6.5 W/m^2 is considered as space heat gain).

Occupancy density: It should be stressed that the occupant density (in m^2 per person) is not part of the TAS input parameters. However both the occupant sensible gains (in W/m^2) and the occupant latent gains (in W/m^2) must be specified in *A-TAS: Internal Conditions*. Keeping in mind that a sedentary person emits 100 W sensible and 40 W latent heat [14], the occupant sensible & latent gains for each of the chosen values of the occupant density, (i.e. the minimum, maximum and standard value), are presented in table 3-4:

Factors	Values		
	Standard	Minimum	Maximum
Occupancy density (m^2 per person)	10	5	20
Occupant sensible gains (W/m^2)	10	20	5
Occupant latent gains (W/m^2) = 0.4 x Occupant sensible gains	4	8	2

Table 3-4: Occupant sensible and latent gains for each of the chosen values of the occupant density

The minimum and maximum values for the occupancy density are based on the Energy Consumption Guide 35 [9], where a survey was carried out to understand how energy is used in offices. Among the findings of this study was that the occupation densities varied from 5 m^2 to 30 m^2 per person, while the majority was between 8 and 16 m^2 per person. However, it is considered that a value of 30 m^2 per person is unlikely nowadays in an air-conditioned office building. (The

[19] **Note:** The good practice index of 12 W/m^2 is based on a level of 350-400 lux, which is a good compromise between screen and paper-based tasks [8]

[20] **Note:** The part of the lighting load that is extracted from the space via air handling luminaires, (the total lighting load is 10 W/m^2 but 35% or 3.5 W/m^2 is removed via air handling luminaires [6]), when the lighting gains are set to their minimum level has been ignored, (assuming that no air from the ceiling plenum is re-circulated back to the room), in order to study the impact of the reduced lighting heat gains (i.e. the minimum value, which is 6.5 W/m^2) on the energy performance of the HVAC systems.

survey was conducted in 1992 [9]). It was, therefore, decided to keep the minimum value at 5 m^2 per person and set the maximum value to 20 m^2 per person. The standard value of 10 m^2 per person is a typical value taken for most office buildings.

3.3.2 HVAC system parameters

This category includes the parameters associated with the design and operation of the chosen HVAC systems. The 5 groups of design variables presented in this section are common for both the VAV and the FCU system. However, in a few cases there are differences in the range of values for one or more parameters. In such a case the range of values for these parameters is specified separately for each system.

Group D: Temperature control set-points for the supply air quantity and the zone air

This group involves three parameters associated with the control of the internal air temperature. The range of values of these parameters for the VAV system is shown in table 3-5:

HVAC system	Factors	Values		
		Standard	Minimum	Maximum
VAV system	Factor A: Heating zone air temperature (°C)	20	18	22
	Factor B: Cooling zone air temperature (°C)	24	22	26
	Factor C: Temperature difference (ΔT) between the supply and the zone air (°C)	8	6	10

Table 3-5: The range of values for the factors related to the VAV system temperature control set-points

Heating & Cooling zone temperature set-point: The heating zone temperature set-point (factor A), which is the limit below which heating is provided, ranges from 18°C to 22°C, while the cooling zone air temperature (factor B), or, in other words, the temperature threshold above which cooling becomes available, ranges from 22°C to 26°C. Both the minimum and the maximum values of these

parameters have been chosen so that the thermal comfort of the occupants is not compromised.

Temperature difference (ΔT) between the supply and zone air: The ΔT between the supply and zone air ranges between 6°C and 10°C. Setting this temperature difference higher than 10°C would create cold draughts. The standard value of this parameter corresponds to the most common control strategy adopted for a typical VAV system.

The range of values of the parameters under consideration for the FCU system is presented in table 3-6:

HVAC system	Factors	Values		
		Standard	Minimum	Maximum
FCU system	Factor A: Heating zone air temperature (°C)	20	18	22
	Factor B: Cooling zone air temperature (°C)	24	22	26
	Factor C: Temperature difference (ΔT) between the supply and the zone air (°C)	8	0	8

Table 3-6: The range of values for the parameters associated with the temperature control settings of the FCU system

Heating & Cooling zone temperature set-points: The range of values for these parameters is the same for both HVAC systems.

Temperature difference (ΔT) between the supply and zone air: The ΔT between the supply fresh air quantity and the zone air ranges from 0°C to 8°C for the FCU system. Supplying the fresh air at the zone air temperature is a common control strategy for this HVAC system, while setting the ΔT between the supply and zone air to 8°C allows for the 'free' cooling capacity of the fresh air to be utilized. The standard value of this parameter is also set to 8°C [19].

Group E: Night ventilation

This group contains two parameters associated with the night ventilation strategy implemented over the summer period (i.e. June, July and August):

Factors	Values		
	Standard	Minimum	Maximum
Factor A: Ventilation rate (ach)	-	5.0	10.0
Factor B: Duration of ventilation (hours)	-	4	10

Table 3-7: The range of values of the parameters related to the night ventilation strategy

Ventilation rate: The fresh air ventilation rate ranges from 5.0 to 10.0 ach, as illustrated in table 3-7. The control over the ventilation rate of the incoming fresh air was achieved by changing the infiltration rate of the building in A-TAS. It is assumed that the fresh air is introduced to the perimeter zones of the building through a number of apertures located around the perimeter of the building, while the core zones are served using the central fans of the HVAC systems[21]. The impact of the chosen night ventilation strategy on the energy performance of the HVAC systems is assessed in section 4.2.2, (chapter 4), while appendix D contains a short investigation on the effect of a number of night ventilation strategies, (based on automatic or manual control of the windows), simulated in TAS, on the internal temperature and energy use. It should be stressed that night ventilation is not provided in the BCS.

Duration of ventilation: It should be remembered that the HVAC system operates between 7:00 – 17:00. As a result, when night ventilation is provided for 10 hours, (i.e. the maximum value) it means that fresh air enters the building between 21:00 – 7:00. Similarly, when the duration of night ventilation equals 4 or 7 hours, (i.e. the minimum and mid-value of this parameter), the fresh air is supplied between 3:00 – 7:00 and 0:00 – 7:00, respectively.

[21] **Note:** Keeping in mind that the case study is a deep plan office building, it is realised that it would be difficult to treat the core zones using a natural ventilation strategy. The amount of energy consumed by the central fans of the HVAC systems serving the core zones of the building over the night is estimated in section 4.2.2-1 (chapter 4).

Group F: Plant operation schedule and performance

This group involves three parameters associated with the efficiency and the operation schedule of the plant:

Factors	Values		
	Standard	Minimum	Maximum
Factor A: Boiler efficiency (%)	85%	75%	95%
Factor B: Chiller COP	2.5	1.9	5.2
Factor C: HVAC system operation schedule (hours)	10	9	17

Table 3-8: The range of values of the design variables related to the plant performance and operation

Boiler efficiency: This is the full load fractional efficiency of the boiler, i.e. the output power divided by the input power at full load [13]. In BSRIA Technical Note 8/86 [26], it is stated that the full-load efficiency of commercial conventional boilers ranges between 75% and 85%, while the full-load efficiency of a condensing boiler is usually between 85% and 95%. Moreover in "Rules of Thumb, 3rd edition" [27] it is stated that the typical seasonal efficiency of condensing boilers varies between 85% - 90%, while the seasonal efficiency of non-condensing boilers can go up to 80% - 82% for modern high efficiency boilers. The upper limit for the boiler efficiency is, therefore, set to 95% (condensing boiler), while the lower limit is set to 75% (conventional boiler). The boiler efficiency for the BCS is taken equal to 85%, corresponding to either a condensing boiler or a high performance conventional boiler.

Chiller COP: This is the Coefficient of Performance of the chiller, i.e. the output power divided by the input power when it is working at full load [13]. In GPG 291 [28], it is stated that the large central plant chillers may be either water or air cooled. Typical figures for the COP of air and water cooled machines are as follows [28]:

- Air cooled chillers: Seasonal COP: 2.5 – 2.7
- Water cooled chillers: Seasonal COP: 4.0 – 5.2

Moreover, in the paper "Guidance for the use of the Carbon Emissions Calculation method" [35], it is stated that the elemental Carbon Performance Rating [12] is based on the performance at the midpoint of the ECON 19 distribution, which is illustrated in figure 3-5:

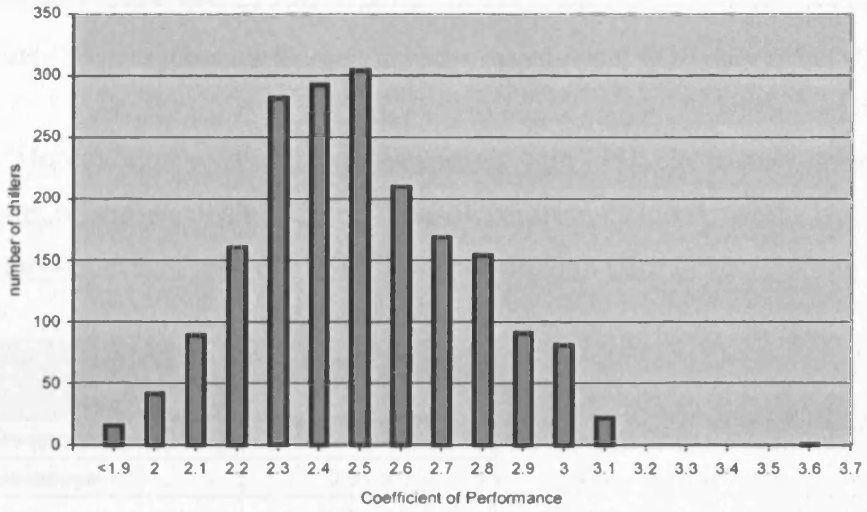

Figure 3-5: Frequency distribution of the Coefficient of Performance for a number of HVAC systems [35]

As can be seen from figure 3-5 (ECON 19), the COP for air cooled chillers ranges from 1.9 to 3.6, with most having a COP of 2.5, which is also the mid-point of the range from <1.9 to 3.1.

Regarding the COP of water cooled chillers, the figures provided by GPG 291 seem to be rather high. However, in the web-site of the Edison Electric Institute[22] [37], it is stated that electric water-cooled chillers have made impressive efficiency gains over the last 25 years, despite the phase out of CFC refrigerants, which took place a few years ago. The chiller efficiency at peak loading conditions since 1976 is shown in the following table derived from the ASHRAE Journal (September 1997):

[22] **Note:** EEI or Edison Electric Institute is the association of United States shareholder-owned electric companies, international affiliates and industry associates worldwide, which provides authoritative analysis and critical industry data to its members, and investigates strategies to advance the industry and ensure a competitive position in the market place [37].

Year	Average Peak Load COP	"Best" Peak Load COP
1976	3.9	4.4
1980	4.7	5.0
1990	5.0	5.4
1993	5.6	6.4
1996	5.9	>7.0
1998 (estimated)	6.0	>7.2
2001 Standard	6.1	>7.3

Table 3-9: The dramatic increase in water-cooled chiller COP since 1976 [37]

Moreover, at www.siliconvalleypower.com [38], electrically driven chillers are categorized according to the type of compressor used, while typical efficiency ranges for each type of chiller[23] are provided in table 3-10.

Compressor type	Typical COP range
Air-Cooled	
Reciprocating	2.7 - 3.5
Centrifugal	3.9 - 5.0
Screw	2.9 - 5.0
Scroll	up to 2.9
Water-Cooled	
Reciprocating	3.9 - 4.4
Centrifugal	4.4 - 7.0
Screw	5.0 - 5.9

Table 3-10: Typical COPs according to the type of compressor [38]

Also, it is mentioned that water chillers (where a separate water loop is utilized at the condenser to remove heat from the refrigerant) have in general higher efficiencies than air cooled units (where an air-to-refrigerant heat exchanger is utilized), due to the more efficient heat transfer and consequently the lower condensing temperatures [38].

It is clear that the COP can take a wide range of values depending on the characteristics of the chiller (mainly the characteristics of the compressor). In particular, the water cooled chillers can reach COPs as high as 7.0 for certain entering condensing temperatures & leaving chilled water temperatures and chiller model characteristics.

[23] **Note:** It must be stressed that when comparing chillers for energy efficiency, auxiliary energy requirements such as chilled water pumps, cooling tower fans, as well as the cost of water treatment are not taken into consideration [38].

Therefore, the standard value for the chiller COP is set to 2.5, while the minimum value is taken equal to 1.9, according to the ECON 19 distribution of COP values for air-cooled chillers, illustrated in figure 3-5. Finally, the maximum value is set to 5.2 representing a water cooled chiller, in accordance with the typical values provided by GPG 291 [28].

HVAC system operation schedule: The HVAC system operates for 10 hours (per day) in the BCS, (i.e. 7:00 – 17:00, or, in other words, it starts two hours in advance of the occupancy period). The minimum value for the plant operation schedule is set to 9 hours (i.e. 8:00 – 17:00), while, the maximum value for this parameter is set to 17 hours, (i.e. the plant starts at midnight and stops at 17:00). A recent study that monitored the energy consumption in over 30 air conditioning systems in real office buildings, over a three year period, illustrated that the run-hours of many of the systems bore no relation to the times they were actually needed [49]. It was found that on average most systems ran twice as long as the most conservative estimate of the occupancies served [49]. The large value chosen for the maximum level of the HVAC system operation schedule (i.e. 17 hours) will show the impact of such a poor control strategy on the energy use of each HVAC system.

Group G: Fan characteristics (size and efficiency)

This group includes four design variables associated with the size and efficiency of the fans used to move the air throughout the case study building. The range of values of these parameters for the VAV system, is presented in table 3-11:

HVAC system	Factors	Values		
		Standard	Minimum	Maximum
VAV system	Factor A: Fan Efficiency (%)	78%	45%	90%
	Factor B: Motor Efficiency (%)	90%	75%	95%
	Factor C: Fan Total Pressure (FTP) - Supply Fan (Pa)	677	500	1500
	Factor D: Fan Total Pressure (FTP) - Extract Fan (Pa)	162	120	360

Table 3-11: The range of values for the parameters related to the characteristics of the VAV system central fans

There are fifteen different fan types stored in the B-TAS database, including variable speed – eddy current coupling, variable speed – variable frequency, variable speed – variable voltage, centrifugal – damper control, etc, which are suitable for VAV systems. It should be stressed that the parameters stored in the TAS database for a particular fan type are not parameters of the fan alone, but of the fan taken together with the system it is installed in, including all the mechanisms used to control air flow [13].

In the BRE report "Supply fan energy savings in VAV air-conditioned buildings" [29], it is stated that in modern VAV systems the most energy efficient way of varying the capacity of the fans is to control their speed directly. This is usually achieved by employing a mains frequency inverter in the drive motor mains supply.

In the BSJ article "Variable Speed Drives" [30], it is also noted that the use of variable speed drives for fans in HVAC systems is becoming more widespread, while in the Danfoss website [33] it is explained that the use of an adjustable frequency drive can reduce complexity, improve system control, and save fan energy. Finally, in "VAV air conditioning systems" by Keith Sepherd [31] it is

also stated that the combination of a centrifugal fan equipped with an AC inverter variable-speed drive is increasingly becoming the first choice for VAV systems. Regarding the extract fans, modern design practice dictates the use of either a centrifugal fan with AC inverter variable-speed drive or a variable pitch blade axial fan [31].

It was, therefore, decided to employ a centrifugal fan with an adjustable frequency variable speed drive for both the supply and extract fans of the VAV system installed in the case study building. The characteristics of the central fans of this HVAC system are described in the following:

Fan efficiency (%): This is the efficiency of the fan in transferring mechanical power from the fan shaft to the air stream, when running at the design flow rate. Typical efficiencies of centrifugal fans are 45% - 70% for forward curved fans, 65% - 85% for backward curved fans and 80% - 90% for the aerofoil type [32]. The minimum value for the fan efficiency is, therefore, set to 45%, and the maximum is set to 90%. The standard value equals 78% (i.e. the default value in the TAS database), corresponding to a backward curved centrifugal fan.

Motor efficiency (%): This is the efficiency of the fan motor in converting electrical power into mechanical power. In "Air handling efficiency and design practices" by Lars J. Nilsson [16], it is stated that typical efficiencies for small size motors are 75% - 85%, while for large size motors are 90% - 95%. Therefore, the minimum value for the motor efficiency is set to 75%, while the maximum value is taken equal to 95%. The standard value equals 90%, and is the default value for the fans contained in the TAS database.

Fan Total Pressure (supply and extract fan): This is the total pressure that must be developed by the fan to overcome friction losses in straight ducts, plant components including terminal units and duct fittings, through which the air is transported [15]. The standard values for the FTP of the supply and return fans of the VAV system were estimated via duct sizing calculations (section 3.6). It is worth mentioning that the values displayed in table 3-11 refer to the fans located in the first AHU serving the ground and first floors of the case study building.

The sizes of the fans installed in the remaining two AHUs serving the rest of building are slightly lower than the fans presented in table 3-11. Details regarding the specification of the AHUs are provided in appendix A.1.1, while the duct sizing results for the VAV system are presented in appendix A.4.1[24].

In "Air handling efficiency and design practices" by Lars J. Nilsson [16], it is stated that the total pressure across individual fans in Switzerland typically ranges from 300 Pa to 1500 Pa, depending of course on the application, while in Swedish practices the fan total pressure ranges from 500 Pa to 1300 Pa. Assuming that the range of fan sizes will be similar in the UK, since the duct sizing methods and rules of thumb (e.g. maximum pressure drop or velocity limits) used in most countries are more or less the same [16], the minimum value for the supply FTP is taken equal to 500 Pa, while the maximum value is set to 1500 Pa[25]. By changing the size of the central fans it is possible to assess the effect of energy efficient or bad ductwork design on the energy performance of the HVAC systems. In other words, the increase or reduction in the FTP is due to the use of, say, plant and system components incurring higher or lower pressure losses to the ductwork system respectively, while the flow rate remains unchanged, as does the ability of the system to meet the cooling/heating demands.

Moreover, the FTP of the return fans was found to be approximately 24% of the size of the supply fans, in the duct sizing calculations carried out for the BCS, as can be seen from table 3-11. Thus, it was decided to maintain the same ratio of return FTP / supply FTP for both minimum and maximum levels selected for the return fans in this investigation (e.g. for the minimum level of the return fans: 120 Pa = 0.24 x 500 Pa).

[24] **Note:**The standard values for the FTP of the central fans of the VAV system displayed in table 3-11 refer to the simulations carried out for the CIBSE TRY. The size of the fans in the BCS was re-calculated for the NOA TRY. The duct sizing results for both climates can be found in appendix A4.1. The range of values for all the parameters of this group, however, was kept the same for both the CIBSE TRY and the NOA TRY to make the comparison between the two climates easier.

[25] **Note:** The minimum and maximum values for both the supply and return fans shown in table 3-11 are common for all the fans serving the case study office building.

The range of values of the parameters of group G for the FCU system is illustrated in table 3-12:

HVAC system	Factors	Values		
		Standard	Minimum	Maximum
FCU system	Factor A: Fan Efficiency (%)	78%	45%	90%
	Factor B: Motor Efficiency (%)	90%	75%	95%
	Factor C: Fan Total Pressure (FTP) - Supply Fan (Pa)	421	300	900
	Factor D: Fan Total Pressure (FTP) - Extract Fan (Pa)	197	140	420

Table 3-12: The range of values of the parameters related to the central[26] FCU system fans

Fan and Motor efficiency: The range of values for these parameters is the same for both HVAC systems.

Fan Total Pressure (supply and extract): The standard values for the FTP of the central fans of the FCU system were also estimated via duct sizing calculations[27]. It is obvious that both the range of values and the standard level for the FTP of the fans moving the air throughout the case study building are different depending on the HVAC system that is installed. This is due to the fact that the central AHU[28] supplies only the minimum fresh air quantity around the building when the FCU system is installed, while the VAV system varies the supply air quantity depending on the requirements of the building zones. Therefore, the minimum and maximum values for the central supply fan of the FCU system were taken equal to 60% of the respective minimum and maximum values displayed in table 3-11, since the ratio of the FTP of the supply fans serving the case study building when the FCU system and the VAV system is considered respectively, is also approximately 60%[29] (i.e. FCU supply FTP / VAV supply FTP = 421 / 677 ≈ 60%). Moreover, the FTP of the extract fan was found to be approximately 47% of the supply fan, in the duct sizing calculations carried out

[26] **Note:** The characteristics of the small fans located in the fan coil units are fairly standard, (e.g. the FTP of these fans usually ranges from 50 Pa to 70 Pa, as explained in appendix A.4.2) so it would not really make sense to study their effect on the FCU system energy performance.

[27] **Note:** The standard values for the FTP of the central fans of the FCU system shown in table 3-12, refer to the simulations carried out for the CIBSE TRY. The size of these fans in the BCS was also estimated for the NOA TRY. The duct sizing results for both climates are presented in appendix A4.2.

[28] **Note:** The case study office building is served by one AHU when the FCU system is studied, since only the minimum fresh air quantity, for ventilation purposes, is supplied throughout the various building zones as also explained in appendix A.1.2.

[29] **Note:** This way it is ensured that the range of values for the FTP of the supply fans of the FCU system is lower than the range of values for the FTP of the VAV fans.

for the FCU system, as illustrated in table 3-12 (standard values). As a result, it was decided to maintain the same ratio of return FTP / supply FTP for both the minimum and the maximum levels of the extract fan of the FCU system (e.g. minimum level of the extract FTP = 0.47 x 300 ≈ 140 Pa).

Group H: Humidification of the supply air

This group contains three parameters associated with the control of the relative humidity (RH) of the supply air:

Factors	Values		
	Standard	Minimum	Maximum
Factor A: Humidification set-point (%)	-	40%	50%
Factor B: Proportional band (%)	-	5%	10%
Factor C: Period of humidification	-	Heating season	All year

Table 3-13: The range of values of the factors associated with the humidification of the supply air

Humidification set-point & Proportional band: The RH control set-points investigated range from 40% to 50%. These set-points are also modified using a proportional band that ranges from 5% (± 2.5%) to 10% (or ± 5%).

Period of humidification: The steam humidifier is set to operate either for the heating period (i.e. for 6 months including October, November, December, January, February and March), or throughout year (i.e. for 12 months). The supply air quantity is not humidified in the BCS, since humidity control is not usually necessary within the base office scheme, unless a particularly high rate of fresh air per occupant must be supplied [25].

3.4 Simulation of the case study building in A-TAS

3.4.1 A short description of the thermal simulation program

A-TAS is a thermal simulation program, which is used for the assessment of the thermal behavior and energy performance of naturally ventilated or air-conditioned buildings. It provides a detailed picture of the performance of the building model using a simulation technique, which is based on the tracing of the thermal state of the building through hourly snapshots [11]. This procedure allows the influences of all the thermal processes that occur in the building to be properly assessed on an hourly basis for the simulation period, which ranges from a single day to a whole year [11]. At the end of the simulation process the program can produce a variety of output reports including air or surface temperatures, room loads, etc. Detailed description of the features of A-TAS can be found in appendix M, section M.4.1.

3.4.2 Characteristics of the case study building

The case study building model is designed in 3D-TAS, while the details concerning the thermal properties of the building envelope, the internal loads, the occupancy pattern, etc are specified in A-TAS. In detail, the simulation of the base case scenario is based on the following:

Building geometry: The case study is a six floor deep-plan air conditioned office building with a total floor area of 12,000 m^2. The area of each of the 6 floors equals 2,000 m^2, while the plan shape ratio is 2:1 (i.e. the floor plate is approximately 63 × 32 m). The long axis of the building is orientated in an east-west direction (figure 3-6). The finished floor to floor height is taken equal to 3.5 m, while the finished floor to ceiling height is approximately 2.8 m.

It is worth mentioning that analyses of the "Valuation Support Application" database, which was compiled by the Valuation Office to aid the revaluation of non-domestic premises in England and Wales during 1995, illustrated that there

is a marked relationship between the incidence of air conditioning and the size and age of UK office buildings [51]. The incidence of air conditioning increases steadily as the premises get larger, while newer buildings are more likely to be air conditioned. As a result, approximately 90% of UK office buildings in the post 1990 age band and over 10,000 m^2 are fully air conditioned [51]. Also, analyses of the database developed by the Non-Domestic Building Stock project, which has provided detailed information on the entire non-domestic building stock of England and Wales, indicated that offices are mainly found in sidelit and deep-plan buildings [52]. It is therefore clear that the case study building has similar characteristics with a typical air conditioned office building in the UK.

Thermal zoning: Each floor is similarly divided into 9 zones, resulting in a total of 54 zones for the whole building. There are 8 perimeter zones with a standard depth of 6 m, (representing all possible orientations), and a single core zone, as can be seen in figure 3-6, which illustrates the zones of a typical floor of the case study building:

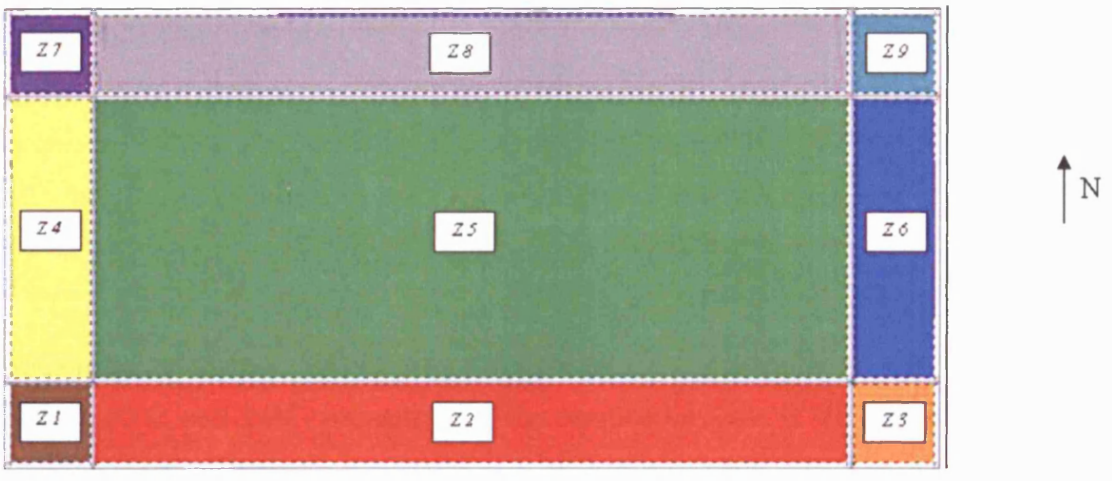

Figure 3-6: The 9 zones[30] of a typical floor of the case study building.

[30] **Note:** The zone numbers specified in this figure refer to the ground floor of the building.

Thermal resistance and airtightness of the building envelope: The fabric design U-values of the individual building elements are illustrated in table 3-14:

Building Element	U-value (W/m^2 K)	Building Regulations Part L 2002 Edition (W/m^2K)
Ground Floor	0.25	0.25
Flat Roof	0.25	0.25
External Wall	0.35	0.35
Window	2.10	2.0/2.2

Table 3-14: U-values of the building elements, which are in line with the Building Regulations Part L [12] requirements

The infiltration rate is defined in A-TAS as the fresh air leakage into a zone in air changes per hour [11]. It is taken equal to 0.5 ach for the perimeter zones and 0.0 ach for the core zones.

Internal loads: The base case values of the internal heat gains from occupants, lighting and equipment have been presented in tables 3-3 and 3-4.

Occupancy period: The building is occupied between 9:00 – 17:00 (8 hours), while the HVAC system operates between 7:00 – 17:00 (10 hours) for 5 days a week and 52 weeks a year, as also mentioned in section 3.3.2.

Zone design conditions: The heating and cooling zone temperature set-points are equal to 20°C and 24°C respectively. The simulation year is divided into the following three periods:

- Heating period: January, February, March, October, November and December. Both heating and cooling are available for the heating period.
- Cooling period: June, July and August. Only cooling is available for this period.
- Intermediate period: April, May and September. Both heating and cooling are available for this period. However, heating will only be required for a few hours, mainly during the beginning of the

occupancy period, so the heating energy consumption is expected to be low for these months.

The simulation year was divided into these periods using the 'calendar' function of A-TAS, while the thermal performance of the case study building was assessed to ensure that the internal temperature is maintained between 20°C and 24°C throughout the year, providing satisfactory internal conditions for the occupants. Details concerning the specification of the heating, cooling and intermediate period can be found in appendix C.

3.5 Simulation of the HVAC systems in B-TAS

3.5.1 A short description of the detailed air-conditioning analysis software

B-TAS is a component based system simulation tool used for the detailed analysis of various HVAC systems. The program allows the performance of the system to be assessed in relation to the dynamic simulation of the building, using a loads file generated by A-TAS, (BSO file), which contains sensible loads, internal gain schedules and other building-related information. It then traces the thermal state of both the system and the building in which it is installed through hourly snapshots, providing a detailed picture of the system performance and the internal zone conditions over the simulation period [12]. A detailed description of the features of B-TAS can be found in appendix M, section M.4.2.

3.5.2 VAV system with terminal re-heaters

The VAV system schematic as designed in B-TAS is presented in figure 3-7:

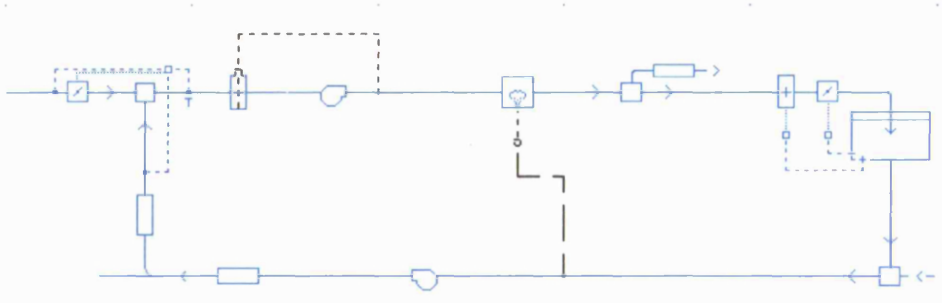

Figure 3-7: An example of the VAV system with terminal re-heaters as designed in B-TAS

The main components of the system are the following[31]:

[31] **Note:** It should be remembered that all the temperature set-points mentioned both in this section and section 3.5.3 refer to the base case scenario.

- Temperature optimiser: The temperature optimiser is basically a mixing box which has been supplemented with a temperature controller. Thus, the two entering air streams (fresh and re-circulated air) are mixed in variable proportions, (the damper regulates the air quantities), with the aim of achieving a temperature as close as possible to the target temperature set as the parameter of the sensor [13]. The target temperature is set to 14°C with a proportional band of 4°C (or ± 2 °C). As a result, the temperature of the mixed air varies between 12°C and 16°C which is the desired supply air temperature when heating and cooling is provided[32] respectively. It should also be stressed that the optimisation process is subject to a minimum flow through the intake duct, which is set as the minimum fresh air requirement of the zones for ventilation purposes (i.e. 8 l/s per person). The benefit of the temperature optimiser is quite obvious, since, depending on the external conditions, it can make use of the free cooling potential of the fresh air and reduce both the cooling and the heating loads of the system.

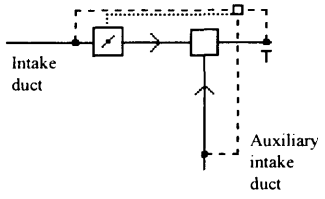

- Cooling coil: The cooling coil extracts a certain amount of heat from the supply air stream in order to achieve a target temperature set as the parameter of the sensor to which it is connected [13]. The target temperature that the cooling coil aims for is set to 16°C, which is 8°C lower than the cooling zone temperature set-point. The capacity of the coil is calculated by the program. Although mechanical cooling is available throughout the year (to avoid potential overheating problems), most of the total cooling energy is consumed mainly during the summer months, when free cooling is not available (i.e. during the summer period the temperature of the supply mixed air quantity is usually higher than 16°C. As a result, the cooling coil is required to condition the supply air quantity).

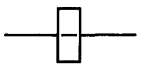

[32] **Note:** B-TAS does not allow the user to specify different set-points for the temperature controller depending on the period of the year (or the part of the day) that heating or cooling is available, so the proportional band is used to ensure that the supply air temperature varies between 12°C and 16°C throughout the year.

- Steam humidifier: 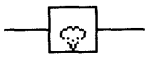 This injects an amount of steam to the supply airstream to ensure that the RH in the zones will not fall below a certain limit. To achieve this the humidifier is connected to a RH sensor that measures the average RH of all the zones in the common return air duct and controls the supply air's RH with respect to that. As mentioned in section 3.3.2, the air is not humidified in the BCS.
- Fans: There is a supply and a return fan in each of the three AHUs serving the case study building. The fan total pressure of these fans is calculated using an Excel spreadsheet based on the equation of Colebrook-White, as explained in section 3.6. The estimated FTP for these fans can be found in appendix A - section A.4.1.

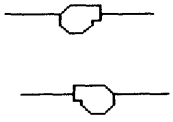

- Zone parameters: The zone[33] contains two inbuilt proportional controllers that sense the zone temperature and generate control signals in accordance with the parameters set for them [13].

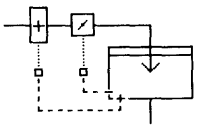

These controllers are fed into other system components by attaching temperature sensors to them: the heating controller is connected to a heating coil, which is contained in each terminal unit (re-heater), and the cooling controller is connected to a damper. The air supply rate is determined by the damper in the supply duct in order to meet the cooling requirements of each zone. The cooling control set-point is set to 24°C. Similarly, the heating coil generates an amount of heat with respect to the heating control set-point, which is 20°C. As explained in section 3.4.2, heating is available during the heating and intermediate period, while cooling is available throughout the year. According to the results of the various simulations for the VAV system, the heating coil operates mostly for the first morning hours of the working day, while for the rest of the time there is a net cooling demand for all the zones.

[33] **Note:** It should be stressed that the zone icon shown in figure 3-7 represents only one of the 54 zones of the case study building. In general, B-TAS allows the use of a single graphic icon for the representation of a number of repeating system components. This way it is possible to simulate HVAC systems serving multi-zone buildings with a large number of floors, avoiding complicated HVAC system schematics. A detailed description of the features of B-TAS can be found in appendix M, section M.4.2, as also mentioned earlier.

3.5.3 Four-pipe fan coil system with fresh air supply from a central plant

The fan coil system schematic as designed in B-Tas is shown in figure 3-8:

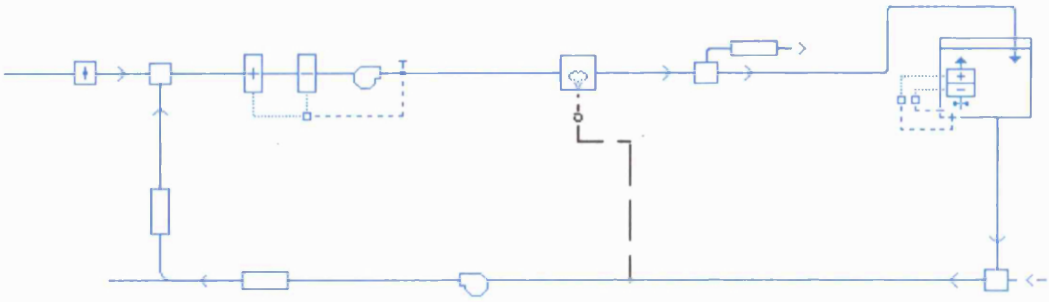

Figure 3-8: An example of the fan coil system as designed in B-TAS

The main components of the system as would be employed in the base case scenario are the following:

- Mixing box: Normally it is used to mix the two entering air streams (i.e. the fresh air and the re-circulated air), either in fixed proportions or in variable proportions in order to achieve a target temperature, RH or enthalpy. However, in the fan coil system that is studied here, the AHU supplies only the minimum fresh air quantity for ventilation purposes[34], while the four-pipe fan coil units installed throughout the building re-circulate the room air providing heating or cooling depending on the requirements of each zone. Therefore, in this case, the two airstreams are not mixed.

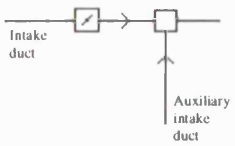

- Heating coil: This delivers a certain amount of heat to the supply air stream to achieve a target temperature set as a parameter for the sensor to which it is connected. The capacity of the coil is calculated by the

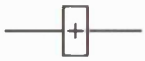

[34] **Note:** It should be remembered that the minimum fresh air quantity drawn through the intake duct is calculated assuming a minimum fresh air requirement of 8 l /s per person as well as an occupant density of 1 person per 10 m^2.

program, while the set-point of the temperature sensor is taken as 12°C, i.e. 8°C lower than the respective heating zone temperature set-point[35]. The central heating coil operates during the heating and intermediate periods.

- Cooling coil: A description of this AHU component has been provided in section 3.5.2. It should be stressed that the cooling coil aims for a target temperature of 16°C, i.e. 8°C lower than the respective cooling zone temperature setpoint[34]. The central cooling coil operates throughout the year.

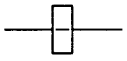

- Fans: There is a supply and a return fan in the main circuit, as well as a small fan located in each fan coil unit. The FTP of the central fans is estimated via duct sizing calculations. The results are presented in appendix A – section A.4.2. The FTP of the fan located in each fan coil unit is taken as 60 Pa, which is considered to be a typical value for fan coil units. Details concerning the selection of this value as well as the number of fan coil units per zone are provided in appendix A.4.2.

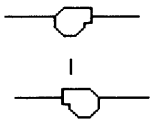

- Steam humidifier: As short description of the humidifier has been provided in section 3.5.2.

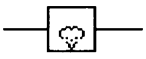

- Zone parameters: The minimum fresh air quantity is delivered to each zone via the supply duct, where it is mixed with the room air, which is re-circulated by the fan coil units that heat or cool the room air to the temperature settings specified in the controller parameters. The heating and cooling zone temperature set-points equal 20°C and 24°C

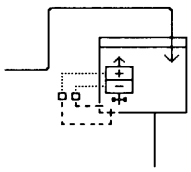

[35] **Note:** It is worth mentioning that the set-points of the central coils were specified through an investigation of different temperature control strategies for the FCU system that was carried out in reference [19]. The B-TAS simulations carried out in reference [19] established a net cooling demand for most of the year (apart from the first morning hours mainly during the heating period). It was shown that keeping the temperature of the fresh air 8°C lower than the zone design condition to take advantage of the 'free' cooling capacity of the fresh air quantity, reduces the annual energy use of this system [19].

respectively. The fan coil units provide heating for both the heating and the intermediate period, and cooling throughout the year.

A detailed description of the main characteristics of both the VAV and the FCU system can be found in appendix L, sections L.2 and L.3, respectively.

3.6 Duct sizing methodology – Calculation of the Fan Total Pressure

The fan total pressure of both the supply and the extract fans is estimated using mainly an Excel spreadsheet [19]. It is then introduced into B-TAS to perform the simulation of the HVAC systems, as described in sections 3.5.2 and 3.5.3.

In general, the concept of duct sizing is based on the equation $Q = A \times V$, where [15]:

- Q is the volumetric flow rate in m^3/s
- A is the duct area in m^2
- V is the air velocity in m/s

The CIBSE also publishes a chart used in duct sizing calculations which is based on the equation of Colebrook – White [15]:

$$Q = -2.0279 \cdot \Delta P \cdot d^{2.5} \times \log_{10}\left(\frac{4.0541 \times 10^{-5}}{d} + \frac{2.9164 \times 10^{-5}}{\sqrt{\Delta P} \cdot d^{1.5}}\right)$$, where:

- ΔP is the rate of pressure drop in Pa/m
- d is the internal diameter of the duct in m

The volumetric flow rate Q is in most cases the only quantity known in advance (e.g. it could be the minimum fresh air quantity for ventilation purposes or the quantity of air required to offset a specific sensible load), so the problem is reduced to the choice of a suitable velocity or pressure drop rate.

There are three basic methods for duct sizing [15], [16]:

- The constant velocity method, where a suitable mean velocity is chosen for a section of the system, (usually the main duct after the fan discharge), which is considered to be critical in terms of noise, and the rest of the ductwork system is sized according to this velocity limit.
- The equal pressure drop or equal friction method, where the ducts are designed so that the pressure drop per unit length of duct remains constant.
- The static regain method, where the ducts are designed so that the static pressure regain at each branch is equal to the pressure drop in the downstream ducting section.

It is also very common to use both velocity and pressure drop limits (i.e. a combination of the constant velocity and the equal friction methods) to size a ductwork system. Moreover, when the minimisation of the life-cycle cost of the ductwork system is also required, more recent duct sizing techniques like the T-method [17] or the Dynamic Programming Method (DPM) [18], which make use of cost optimisation theory, should be used.

The main parts of the duct sizing procedure followed in this study are the following [19]:

- A single line layout is drawn for both the supply and the extract ductwork system on the building plans for each HVAC system. The design concept is based on the assumption that each supply-air diffuser can serve a 36 m^2 area, which means that the maximum throw[36] for each of the four main directions is taken as 3.0 m. The duct layouts for both HVAC systems are presented in appendix A - sections A.1.1 and A.1.2.
- The supply and extract ductwork systems for each HVAC system are sized using both velocity and pressure drop limits, as mentioned earlier. The velocity and pressure drop rate limits used to size the FCU system and VAV system, respectively, are presented in table 3-15:

[36] **Note:** The term 'throw' stands for the distance from the terminal to the point where the velocity has decayed to 0.5 m/s [14]

HVAC System	System type		Duct shape	Velocity (m/s)	Pressure drop rate (Pa/m)
FCU system	Supply:	Low velocity	Rectangular	5.0	1.0
	Extract:	Low velocity	Rectangular	5.0	1.0
VAV system	Supply:	High velocity	Circular	15.0 (vertical ducts)	2.0
				10.0 (main ducts)	2.0
				6.0 (duct branches)	2.0
	Extract:	Low velocity	Rectangular	5.0	1.0

Table 3-15: Duct sizing limits for both the FCU and the VAV system

The calculation is carried out using an Excel spreadsheet based on the equation of Colebrook-White, which can be solved using a trial and error method. The calculation methodology is explained in appendix A.3.

- The pressure losses arising from the presence of duct fittings are expressed as a fraction of the velocity pressure at the point of the system where they occur, using the appropriate pressure loss factors for each fitting [14]. The pressure loss factors used to perform the duct sizing calculations are derived from the CIBSE Guide C: Reference Data (2001) [41], in which an extensive review of pressure loss factors from various sources has been undertaken, in order to present the data considered to be the most reliable. A thorough investigation has also been carried out on the variations in FTP depending on the choice of duct fittings (including duct fittings derived from both the old and the new version of CIBSE Guide C) and the associated energy implications. Details regarding this study can be found in appendix B.
- The pressure losses due to the presence of various plant or system components are usually quoted in Pa by the manufacturers [14]. A list of the figures for equipment losses used in this study is provided in appendix A.2.

3.7 Weather data used for the simulation of the case study building

TAS uses hourly weather datasets (usually for a period of one year) to perform a dynamic simulation of the building model and the associated HVAC system. The program comes with a climate database, which contains several weather files covering many different regions of the world. The choice of weather data for a specific location depends mainly on the objective of the study. Thus, extreme weather years are more suitable when peak load sizing is involved, while typical weather years, such as Test Reference Years (TRYs), are used for analysing and comparing the energy use and overall environmental performance of different design options, since any non-typical weather conditions can favour one type of plant, building or energy supply [22]. For example, a fully-glazed building will be more susceptible to solar radiation than one with moderate levels of glazing. As a result, the selection of a weather file containing untypically low hours of sunshine can affect the comparison of the energy performance of the two design options, leading to wrong results [35].

The TRYs provide hourly data for several weather variables (including air temperature, solar radiation, wind speed, etc), for a period of one year, representing climatic conditions considered to be typical for a location over a long-time period [21], and are suitable for the assessment of the energy performance and indoor climate conditions of a building using dynamic thermal simulation programs [11]. Various methods have been developed for the generation of TRYs for several locations around the world. Most of these methods involve complex statistical analysis and selection of weather variables from a long period of measured weather data, to compose a weather file which covers all seasons of the year as a form of overall average, but retaining, at the same time, realistic short term patterns and variations, as well as true correlation between the different weather elements [20], [34].

It is clear that the use of typical weather data suits best the objectives of this study. A short description of the characteristics of the chosen TRYs for London (UK) and Athens (Greece) is provided in sections 3.7.1 and 3.7.2, respectively.

3.7.1 CIBSE Test Reference Year (TRY) for London

The development of several methodologies for the generation of typical weather data resulted in a large number of typical weather years for various UK locations obtainable from different sources and under different conditions (e.g. European TRYs for four UK sites, CIBSE Example Weather Years (EWYs) for 15 UK sites, PCL TRY for Kew, etc) [20]. As a result CIBSE, recognising the need for a single representative weather year as a basis for predicting and comparing the energy use at the design stage, decided to develop a TRY for three UK locations (i.e. London, Manchester and Edinburgh), based on high quality, recent, measured weather data, using a new more sensitive method of selection in which chosen daily source weather data from the parent weather dataset are analysed for conformity with the long-term mean and variance [20].

The new CIBSE TRY is a composite year, i.e. a sequence of the most typical months from a 20-year period, with some smoothing in the hours either side of the month-to-month boundaries (i.e. to smooth the transition between the different chosen months) [20]. The parent weather dataset is the 20-year period 1976 – 1995. It would be possible to use a larger period of recorded data, but taking into consideration the significant changes in the character of UK weather in different decades (either due to natural variability or due to climate change), it was decided to use a short, recent period rather than a longer period in which contrary trends in earlier years could have negated important characteristics of later years [20]. A detailed description of the methodology used to select the individual months from the 20-year parent weather dataset can be found in reference [20].

It is worth mentioning that the impact of the new CIBSE TRY on the design of low energy buildings was investigated in a recent paper, which compared the effect of this weather file (for Manchester and London), and the older CIBSE EWY[37] on the internal comfort conditions of a typical naturally ventilated office

[37] **Note:** The EWY is an actual year (1984-85 for the north region and 1979-80 for the south region of the UK), considered to be representative of the average weather conditions of a large weather period of measured data. It has been widely used for building thermal simulation and energy assessment in the UK, for a long time [36].

building, using dynamic thermal modeling [36]. The effect of the external weather conditions on the cooling energy consumption of the same building, when mechanical cooling was required to meet the internal thermal comfort criteria (mixed mode strategy), was also considered.

It was found that the use of the new CIBSE TRY in place of the EWY would result in a reduction in both heating plant capacity and heating energy consumption. The percentage reduction in total heating demand was higher than the percentage reduction in peak heating load, so the annual heating energy use was reduced to a greater extent than the heating plant capacity. On the other hand, the cooling demand was increased when the new weather data were applied, since there are more hours of higher dry bulb temperature in the CIBSE TRY than in the EWY. It was concluded that designers should be aware of the fact that the use of the new CIBSE weather data can have a significant impact on the internal thermal comfort conditions or the energy performance[38] of the design project. Of course, the magnitude of this impact depends on a number of factors, like the fabric or the usage of the building. Thus, it was stated that a design project based on natural ventilation that performs well when the EWY is used, may not meet the internal thermal comfort criteria when it is evaluated using the new CIBSE TRY. In such a case mixed mode strategies may be required to ensure satisfactory internal conditions [36].

The CIBSE TRY is the chosen weather file for this study. It is representative of typical climatic conditions in London and is used to perform the simulations of the case study building and the chosen HVAC systems in A-TAS and B-TAS, respectively.

---

[38] **Note:** In general, the use of the CIBSE TRY for energy simulation in comparison with the use of the EWY, is expected to predict lower heating energy use and higher energy consumption for the cooling plant [36].

3.7.2 NOA Test Reference Year (TRY) for Athens

The first TRY for Athens was developed by Pissimanis in 1988, using a database containing weather data from 1966 to 1982 (i.e. 17 years in total). The final selection criterion for this TRY was based on the comparison of global solar radiation values. However, typical meteorological years are also used for the prediction of the thermal performance of various sophisticated solar and building energy systems [21]. It is clear that the thermal performance of such applications does not depend only on global radiation or air temperature, but also on other meteorological parameters including diffuse solar radiation, relative humidity and wind velocity [21]. Therefore, more comprehensive TRYs, where the selection criteria are based on a variety of weather variables, are required.

As a result, another TRY for Athens was developed in 1998, applying all the major methodologies for the generation of TRYs reported in the literature to a 20-year weather database covering the period 1977 – 1996, which was provided by the National Observatory of Athens (NOA) [21]. This resulted in 17 TRYs in total. The selection of the final TRY was based on comparisons of the results obtained from detailed simulations of the annual performance of typical energy systems, including a solar water heating system, a building, a photovoltaic system and a large scale solar heating system with interseasonal storage [21]. The best performing TRY was considered to be the one providing the closest performance to the average performance of the chosen energy systems as predicted using the 20-year measured weather data. A detailed description of methodology used to develop the TRY for Athens, is provided in reference [21].

The NOA TRY, which is representative of the typical weather conditions in Athens (Greece), is the second weather file used in this study to carry out the simulations of the case study building and the associated HVAC systems.

3.8 Contribution of the various energy uses to the overall carbon emissions of the case study office building in the base case scenario

The breakdown of the overall carbon emissions of the case study building in the BCS into five components, given that lights, office equipment, fans and cooling run on electricity (i.e. a value of 0.127 kg C/ kWh of delivered energy is assumed [8]), while heating operates on gas (i.e. a value of 0.052 kg C/ kWh of delivered energy is assumed [8]) is presented in figures 3-9 to 3-12, depending on the HVAC system and the climate under consideration:

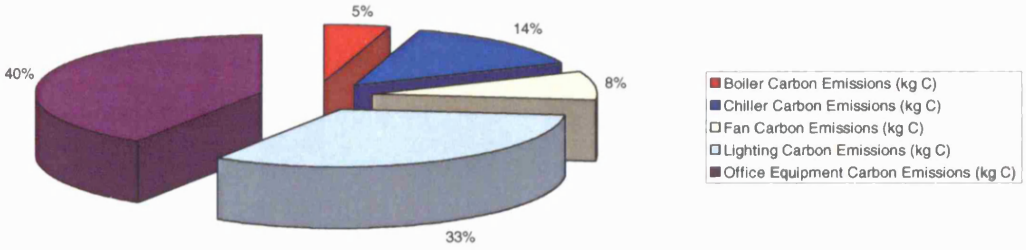

Figure 3-9: Analysis of the overall carbon emissions of the BCS when the VAV system is simulated for the CIBSE TRY

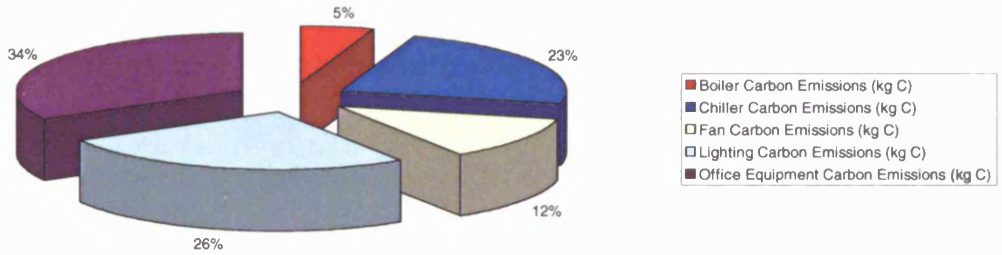

Figure 3-10: Analysis of the overall carbon emissions of the BCS when the FCU system is simulated for the CIBSE TRY

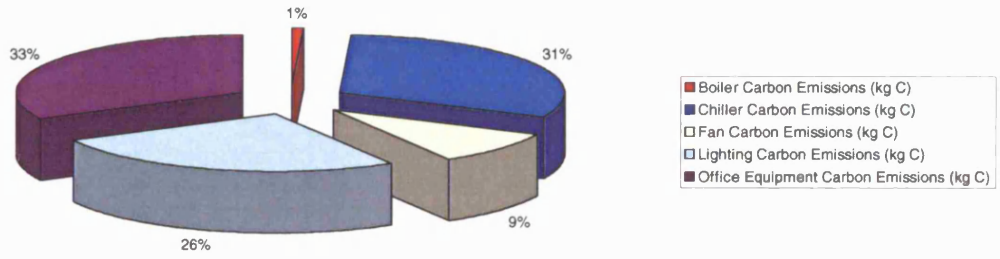

Figure 3-11: Analysis of the overall carbon emissions of the BCS when the VAV system is simulated for the NOA TRY

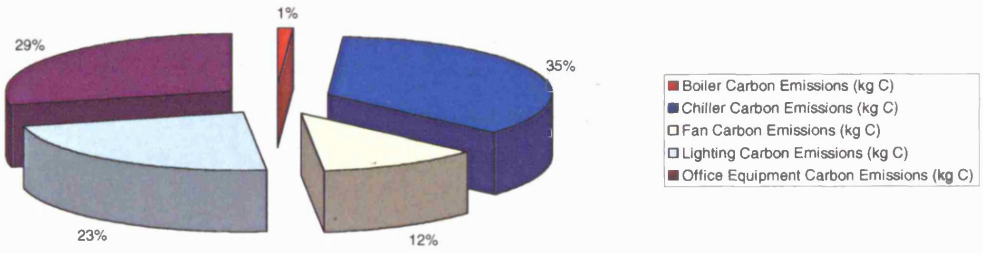

Figure 3-12: Analysis of the overall carbon emissions of the BCS when the FCU system is simulated for the NOA TRY

As can be seen from the above figures, the carbon emissions associated with the use of office equipment & lights have the highest environmental impact. It should be stressed, however, that the energy used by lighting and office equipment is roughly estimated in this theoretical study, by simply multiplying the good practice recommendations of ECON 19, (i.e. lighting heat gains of 12 W/m^2 and office equipment heat gains of 15 W/m^2), by the total run hours, assuming that both lights & office equipment are constantly on during the occupation period, without taking into consideration factors such as occupancy and daylight sensors or varying patterns of use for the equipment. Thus, the lighting and office equipment energy consumption data should be taken mainly as an indication that the installation of energy efficient lights & office equipment and good management of their operation are very important since they can reduce the amount of electricity consumed by them. Furthermore, the effect of the lighting and equipment heat gains on the energy / carbon performance of the HVAC system installed is investigated in detail in chapters 4 and 5.

Excluding the above two energy uses, it becomes clear that use of mechanical cooling should receive critical attention in the design process, particularly when the simulations are carried out for the Athens climate[39], followed by the fan and heating energy consumption. Keeping in mind that TAS is capable of estimating the amount of energy consumed by boilers, chillers and fans, throughout the year, in detail, chapter 4 studies the effect of each of the 8 chosen groups of design factors on the energy performance of the FCU system and the VAV system in both climates for which they are simulated.

[39] **Note:** In fact the use of mechanical cooling dominates the total carbon emissions of the BCS when the FCU system is simulated for the NOA TRY, even when the lighting and equipment energy uses are taken into account, as shown in figure 3-12.

References

[1] R.H. Myers, D.C. Montgomery, Response Surface Methodology: Process and Product Optimization Using Designed Experiments, Second Edition, 2002

[2] G.E.P. Box, W.G. Hunter, J.S. Hunter, Statistics for Experimenters: An Introduction to Design, Data Analysis and Model Building, 1978

[3] MINTAB 13 User's Manual, 2000

[4] Design-Expert version 6 User's Guide, Stat-Ease (2000)

[5] Neter J., Kutner M.H., Nactsheim, C.J. & Wasseman, W., Applied Linear Statistical Models, pp. 1280-1310, Chicago: The McGraw-Hill Companies, Inc. ISBN 0256117365.

[6] CIBSE TM29: HVAC strategies for well-insulated buildings, CIBSE, 2001

[7] Helena Bulow-Hube, The effect of glazing type and size on annual heating and cooling demand for Swedish offices, Lund University, Institute of Technology, Dept. of Building Science

[8] Energy Consumption Guide 19: Energy use in offices, Best Practice Programme

[9] Energy Consumption Guide 35: Energy Efficiency in Offices-Small Power Loads, Best Practice Programme.

[10] Good Practice Guide 276: Managing for a better environment, Best Practice Programme

[11] A-Tas Reference Manual, EDSL Documentation

[12] The Building Regulations Approved Document L2: Conservation of fuel and power in buildings other than dwellings, 2002 Edition.

[13] B-Tas Reference Manual, EDSL Documentation

[14] Martin P L and Oughton D R, editors, Faber and Kell's Heating and Air-Conditioning of Buildings, Butterworths, London, 8th edition, 1995

[15] Jones W P, Air Conditioning Applications and Design, Arnold, London, 2nd edition, 1997

[16] L.J.Nilsson, Air-handling energy efficiency and design practices, Energy and Buildings 22 (1995) 1-13

[17] E.H. Mathews, D.T. Claassen, A new duct design software tool, Building and Environment 38 (2003) 521-531

[18] Huan-Ruei Shiu, Feng-Chu Ou, Sih-Li Chen, Optimization design of exhaust duct system in semiconductor factory using dynamic programming method, Building and Environment 38 (2003) 533-542

[19] Spasis George, Building Services Strategies and Energy Consumption in Offices, A dissertation submitted in part fulfilment of the degree of Master of Science Built Environment: Environmental Design and Engineering, Bartlett School of Graduate Studies, University College London, 2001

[20] CIBSE Guide J: Weather, Solar and Illuminance data, CIBSE 2002

[21] A. Argiriou, S. Lykoudis, S. Kontoyiannidis, C.A. Balaras, D. Asimakopoulos, M. Petrakis, P. Kassomenos, Comparison of methodologies for TMY generation using 20 years data for Athens, Greece, Solar Energy Vol. 66, No 1, pp. 33-45, 1999

[22] Holmes M J and Hitchen E R, An example weather year for the calculation of energy demand in buildings, Building Services Engineer 45, 186-189, (1978)

[23] A. Dentener, Design-Expert DOEs it better, Food Technology in New Zealand, Vol 37 (9): 12-14, September 2002

[24] E. Claekson, Understanding you process, Desktop Engineering, June 1998

[25] BCO Guide 2000 – Best Practice in the specification for offices, British Council for Offices, 2000

[26]: BSRIA Technical Note 8/86: Condensing Boilers

[27]: BSRIA Technical Note 15/200, Rules of Thumb: Guidelines for assessing building services, UK 3rd edition

[28]: Good Practice Guide 291: A designer's guide to the options for ventilation and cooling, Best Practice Programme

[29] BRE Report Technical File, Supply fan energy savings in VAV air-conditioned buildings, Building Services Journal, May 1998

[30] Tim Dwyer, The cpd collection, Variable Speed Drives, Building Services Journal, February 2003, pg. 68-69

[31] Keith Sepherd, VAV Air Conditioning Systems, Blackwell Science, 1999

[32] Mott Green & Wall, Energy Efficient Ventilation Systems, Building Services Journal, January 2003, pg. 18-20

[33] Danfoss website: http://www.danfoss.com/drives

[34] Ernst Muller, Development of a Test Reference Year on a Limited Database for Simulations on Passive Heating and Cooling in Chile, Seventh IBPSA Conference, Rio de Janeiro, Brazil, August 13-15, 2001

[35] CIBSE TM32, Guidance for the use of the Carbon Emissions Calculation Method, 2003

[36] M. J. Ren, G. Levermore, N. Doylend, The impact of the new CIBSE weather data on natural ventilation design, Building Serv. Eng. Res. Technol. 24, 2 (2003), pp. 83-91

[37] Edison Electric Institute, www.eei.org

[38] Silicon Valley Power: www.siliconvalleypower.com

[39] Danny H.W. Li, S.L. Wong, Joseph C. Lam, Climatic effects on cooling load determination in subtropical regions, Energy Conversion and Management 44 (2003) 1831 – 1843.

[40] David G. Kleinbaum, Laurence L. Kupper, Applied Regression Analysis and Other Multivariate Methods, The University of North Carolina at Chapel Hill, Duxbury Press, North Scituate, Massachusetts, 1978.

[41] CIBSE Guide C: Reference Data, The Chartered Institution of Building Services Engineers, London, 2001, Section 4.10: Pressure loss factors for ductwork, pages 96 -117.

[42] TRNSYS: http://www.trnsys.com/

[43] R Mark J. Anderson & Patrick J. Whitcomb, RSM Simplified: Optimizing Processes Using Response Surface Methods for Design of Experiments, Productivity Press, 2005

[44] T. W. Simpson, J. D. Peplinski, P. N. Koch, J. K. Allen, Metamodels for Computer-base Engineering Design: Survey and Recommendations, Engineering with Computers 17: 129 – 150, 2001

[45] Scott P. Zink, Dimitri N. Mavris, Peter M. Flick, Michael H. Love, Impact of Active Aeroelastic Wing Technology on Wing Geometry Using Response Surface Methodology, Presented at CEAS/ AIAA/ ICASE/ NASA Langley International Forum on Aeroelasticity and Structural Dynamics, Williamsburg, VA, June 22-25, 1999

[46] Resit Unal, Roger A. Lepsch, Mark L. McMillin, Response Surface Building and Multidisciplinary Optimization Using D-Optimal Designs, (AIAA-98-4759), Collection of Technical Papers for 7th Annual AIAA/NASA/ISSMO Symposium on Multidisciplinary Analysis and Optimization, pp. 405-411, September 1998.

[47] Timothy W. Simpson, John J. Korte, Timothy M. Mauery, Farrokh Mistree, Comparison of Response Surface and Kriging Models for Multidisciplinary Design Optimization, (AIAA-98-4755), 7th Symposium on Multidisciplinary Analysis and Optimization, St. Louis, MI, September 2-4, 1998.

[48] Shari L. Kraber, Patrick J. Whitcomb, Mark J. Anderson, Handbook for Experimenters, Stat-Ease, Inc., www.statease.com, 2002

[49] Ian Knight, Gavin Dunn, Size does matter, Building Services Journal, August 2004, pg. 34-36

[50] Engineering Statistics Handbook:
http://www.itl.nist.gov/div898/handbook/pri/section1/pri11.htm

[51] Peter Rickaby, Harry Bruhns, Nigel Mortimer, Emma Clark and Philip Steadman, Mechanical Ventilation and Air Conditioning Systems in UK Buildings, Volume 2: Investigations, analyses and surveys, Department of the Environment Research Project 12B, Scooping Study for HVAC systems, Centre for Configurational Studies, The Open University Resources Research Unit, Sheffield Hallam University, Rickaby Thompson Associates Architects and Energy Consultants, Keith Gordon Services, November 1995

[52] Harry Bruhns, Philip Steadman, Horace Herring, A database for modeling energy use in the non-domestic building stock of England, Applied Energy 66, pp. 277 - 297, 2000

Chapter 4: The effect of each of the eight chosen groups of design factors on the energy performance of the HVAC systems

4.0 Aims of the chapter

This chapter discusses the effect of each of the eight chosen groups of design variables on the energy performance of the FCU system and the VAV system, when they are simulated for the CIBSE TRY and the NOA TRY respectively. A short description of the statistical analysis of the results is provided mainly through a number of plots and tables illustrating the way the factors under consideration affect the annual heating & cooling energy use of the HVAC systems in each climate. The combinations of factor levels minimizing the heating & cooling energy consumption and the associated reduction over the energy performance of the base case scenario (BCS), depending on the type of HVAC system and the climate for which it is simulated, are also provided.

Sections 4.1.1 to 4.1.3 discuss the effect of each of the groups of factors associated with the building load (i.e. groups A, B and C) on the energy performance of the HVAC systems when the simulations are carried out for the CIBSE TRY and the NOA TRY respectively. Sections 4.2.1 to 4.2.5 analyze the effect of each of the groups of parameters related to the design & operation of the HVAC systems (i.e. groups D, E, F, G and H) on the energy consumption of the FCU system & the VAV system, when they are studied for the London and the Athens typical weather data respectively. Finally, section 4.3 briefly summarizes the findings derived from the study of each group of factors.

4.1 Building load related parameters

4.1.1 The effect of the design variables related to the solar gains through the transparent building elements (group A) on the energy performance of the HVAC systems

The aim of this study is to yield insight into the functional relationship between the parameters associated with the solar gains through the transparent building elements and the energy performance of the FCU system and the VAV system, when the simulations are carried out for the CIBSE TRY (London) and the NOA TRY (Athens), respectively. Secondary aims include the identification of factor levels that minimize the annual heating and cooling energy consumption of each system in both climates.

The parameters of this group and their range of values are presented in table 4.1.1-1:

Factors	Values		
	Standard	Minimum	Maximum
Factor A: Glazing percentage (%)	40%	25%	95%
Factor B: Total shading coefficient (TSC)	0.74	0.16	0.88
Factor C: Overhang depth (m)	-	0.0	2.0
Factor D: Side-fin depth (m)	-	0.0	2.0

Table 4.1.1-1: The range of values of the four parameters of group A

The chosen response variables include the annual heating and cooling energy consumption of the HVAC systems. Using a Face Centered design two different response surface models are developed approximating the relationship between the four factors shown in table 4.1.1-1 and each of the response variables under consideration. This procedure is repeated for both HVAC systems simulated for each of the climates mentioned above, so eight regression models are developed in total. It should be remembered that the description of the Response Surface Methodology used in this study can be found in chapter 3. The fitted regression

models and the procedure required for their development are presented in appendix H, section H.1.1.

Sections 4.1.1-1 and 4.1.1-2 analyse the effect of the design factors related to the solar gains through the transparent building elements on the annual heating and cooling energy use of the HVAC systems respectively, in both climates for which they are simulated. The findings of this study are summarized in section 4.1.1-3.

4.1.1-1 The effect of the parameters of group A on the heating energy consumption of the HVAC systems when they are simulated for the CIBSE TRY and the NOA TRY respectively

The effect of all the parameters associated with the solar gains through the transparent building elements (group A) on the heating energy consumption of the FCU system for the CIBSE TRY is illustrated in figure 4.1.1-1, which indicates how the response changes as each factor moves from a reference point, (which in this case is the standard value of each parameter or, in other words, the value of each parameter in the BCS), with all the other factors held constant at this reference value.

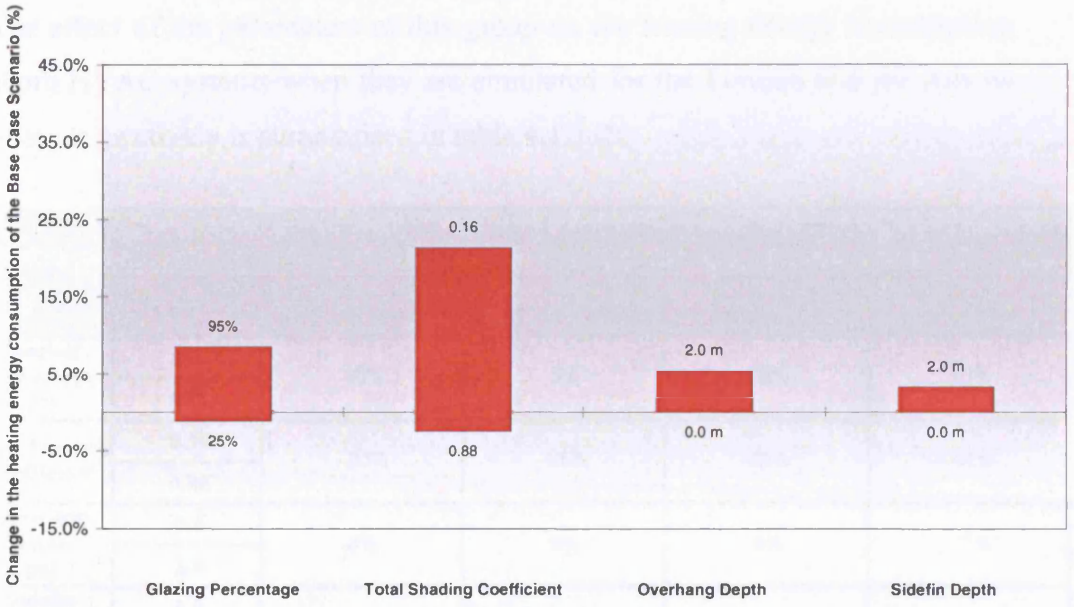

Figure 4.1.1-1: The effect of all the parameters of group A on the annual heating energy consumption of the BCS, when the FCU system is simulated for the CIBSE TRY

Figure 4.1.1-1 shows that the TSC (factor B) and the glazing percentage (factor A) have a relatively higher impact on the annual heating energy consumption than the overhang and the side-fin depth (i.e. factors C and D).

The decrease in heating energy use reaches 20% as the TSC of the windows rises from 0.16 to 0.88. It is obvious that high values of this factor allow most of the incident solar radiation to pass through the window constructions reducing

the heating requirement during the winter period. On the other hand, increasing the glazing percentage of the building leads mainly to higher heat losses to the external environment that overcome the desirable solar gains during the winter months. As a result, the heating energy use rises by 10% when the glazing percentage is set to 95% as opposed to 25%. As also shown in figure 4.1.1-1, the addition of 2.0 metre overhangs to the south windows leads to 4.0% higher heating energy use, while the addition of 2.0 metre side-fins to the east & west windows results in 2.0% higher heating energy consumption respectively. It seems that the utilisation of external shading devices of such a depth, blocks a small part of the incoming solar radiation resulting in slightly higher heating energy use.

The effect of the parameters of this group on the heating energy consumption of both HVAC systems when they are simulated for the London and the Athens climate respectively is summarised in table 4.1.1-2:

Factor	Min and Max Level	Impact on heating energy use (%)			
		FCU system		VAV system	
		CIBSE TRY	NOA TRY	CIBSE TRY	NOA TRY
Glazing Percentage (%)	25%	10%	5%	28%	15%
	95%				
Total Shading Coefficient	0.16	-20%	-35%	-32%	-51%
	0.88				
Overhang Depth (m)	0.0	4%	9%	6%	17%
	2.0				
Sidefin Depth (m)	0.0	2%	4%	5%	6%
	2.0				

Table 4.1.1-2: Change in the heating energy consumption, depending on the HVAC system and the climate for which the simulations are carried out, when each factor of group A rises from its minimum to its maximum level, while the remaining parameters are set to their respective standard level.

As can be seen from table 4.1.1-2, the heating energy consumption of both systems is more sensitive to factors B, C and D and less sensitive to factor A when the simulations are carried out for the NOA TRY in place of the CIBSE TRY. This is due to the fact that the former involves higher levels of solar

radiation and external temperatures than the latter of the two climates. Thus, for example, the increase in heating energy use as the glazing percentage rises from 25% to 95%, drops when either the FCU system or the VAV system is simulated for the NOA TRY as opposed to the CIBSE TRY, due to the combination of higher solar gains and reduced heat losses to the external environment.

In addition, the heating energy consumption of the VAV system is more sensitive to the design factors of this group than the heating energy use of the FCU system, in both climates, as shown in table 4.1.1-2. The main reason is that a significant part of the total heating load is handled by the central heating coil in the FCU system. Therefore, potential changes related to, say, the area of glazing or the TSC of the window construction affect mainly the part of the total heating energy consumed by the fan coil units located around the zones of the building, while the amount of heating energy consumed by the central AHU, supplying the minimum fresh air quantity throughout the building, remains approximately the same. On the other hand, the VAV system handles the heating requirement of the building via terminal re-heaters located in the perimeter zones. As a result, the total heating energy use of this system is affected by the parameters of this group.

4.1.1-1.1 The factor settings of group A minimising the heating energy consumption depending on the HVAC system and the climate for which it is simulated

The design option resulting in the minimum heating energy consumption[1] and the associated energy savings over the BCS, depending on the HVAC system and the climate under consideration are shown in table 4.1.1-3:

HVAC system	Climate	Scenario	Factor Levels				Reduction in heating energy over the BCS (%)
			Glazing Ratio (0 -1)	Total Shading Coefficient	Overhang Depth (m)	Sidefin Depth (m)	
FCU system	CIBSE TRY	Base case scenario	0.40	0.74	0.00	0.00	-
		Minimum heating energy consumption	0.25	0.88	0.00	0.00	-4%
	NOA TRY	Base case scenario	0.40	0.74	0.00	0.00	-
		Minimum heating energy consumption	0.25	0.88	0.00	0.00	-4%
VAV system	CIBSE TRY	Base case scenario	0.40	0.74	0.00	0.00	-
		Minimum heating energy consumption	0.25	0.88	0.00	0.00	-10%
	NOA TRY	Base case scenario	0.40	0.74	0.00	0.00	-
		Minimum heating energy consumption	0.25	0.88	0.00	0.00	-8%

Table 4.1.1-3: The combination of factor levels minimising the requirement for space heating and the associated reduction over the heating energy consumption of the BCS, depending on the HVAC system and the climate for which the simulations are carried out

As can be seen from this table, the minimum heating energy consumption occurs when the TSC of the windows is maximised, while the building model does not incorporate any external shading devices. It is obvious that in such a case the maximum amount of solar radiation passes through the transparent building elements into the occupied space reducing the demand for space heating mainly during the winter months. On the other hand, the glazing percentage of the building is set to 25%, since larger window areas would result in high heat losses to the external environment, especially during the night, increasing the heating energy use for the first hours of the next morning before casual gains kick in.

[1] **Note:** The optimization technique developed by Derringer and Suich is utilised by Design-Expert to obtain the combinations of factor levels minimising the response variable under consideration, as explained in section 3.2.2, chapter 3.

4.1.1-2 The effect of the parameters of group A on the cooling energy consumption of the HVAC systems when they are simulated for the CIBSE TRY and the NOA TRY respectively

The effect of all the parameters of this group on the cooling energy consumption of the FCU system for the CIBSE TRY is shown in figure 4.1.1-2:

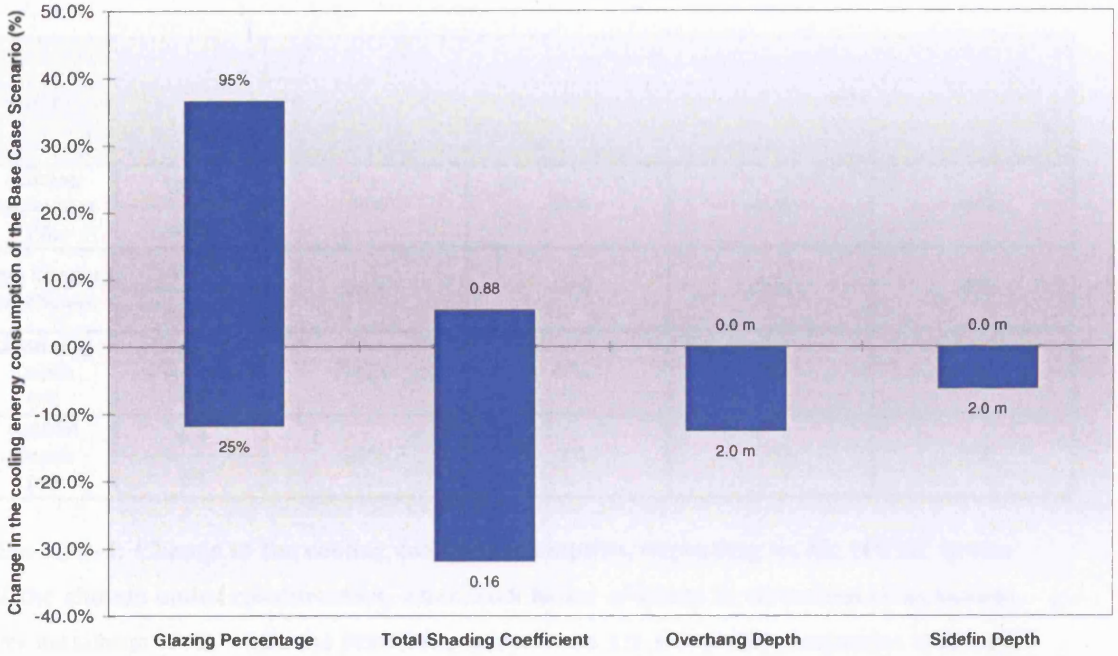

Figure 4.1.1-2: The effect of all the parameters of group A on the cooling energy consumption of the BCS, when the FCU system is simulated for the CIBSE TRY

The cooling energy use of the FCU system increases by 55% as the TSC of the windows rises from 0.16 to 0.88, as can be seen from figure 4.1.1-2. It is obvious that the increase of the TSC of the window construction limits the control over the incoming solar radiation, leading to overheating problems mainly during the summer period. Similarly, the increase of the glazing percentage of the building results in high solar gains that overcome the heat losses to the external environment, (which are certainly smaller during the summer than the winter period), generating an excessive demand for mechanical cooling. As a result, the cooling energy consumption increases by approximately 55% when the glazing percentage rises from 25% to 95%. On the other hand, the external shading devices block part of the incoming solar radiation, reducing the cooling energy

use by 10% when 2.0 metre overhangs are utilised and 3% when 2.0 metre side-fins are used respectively, as can be seen from this figure.

The effect of the design factors associated with the solar gains through the transparent building elements on the cooling energy consumption of both HVAC systems when they are simulated for the CIBSE TRY and the NOA TRY respectively is summarised in table 4.1.1-4:

Factor	Min and Max Level	Impact on cooling energy use (%)			
		FCU system		VAV system	
		CIBSE TRY	NOA TRY	CIBSE TRY	NOA TRY
Glazing Percentage (%)	25%	55%	51%	50%	45%
	95%				
Total Shading Coefficient	0.16	55%	44%	51%	39%
	0.88				
Overhang Depth (m)	0.0	-10%	-9%	-8%	-8%
	2.0				
Sidefin Depth (m)	0.0	-3%	-3%	-3%	-2%
	2.0				

Table 4.1.1-4: Change in the cooling energy consumption, depending on the HVAC system and the climate under consideration, when each factor of group A rises from its minimum to its maximum level, while the remaining parameters are set to their respective standard level.

Each of the response surface models approximating the relationship between the parameters of this group and the cooling energy consumption of the FCU system or the VAV system for the CIBSE TRY and the NOA TRY respectively, (presented in appendix H), contains a number of two-factor interaction terms. The effect of each of these terms on the cooling energy use can be illustrated using interaction plots, which show the impact that changing the settings of one factor has on the other factor. The effect of the 'strongest' interaction term (i.e. the interaction term with the highest model coefficient) involving the glazing percentage (factor A) and the TSC (factor B) on the cooling energy use of the FCU system for the CIBSE TRY is presented in figure 4.1.1-3:

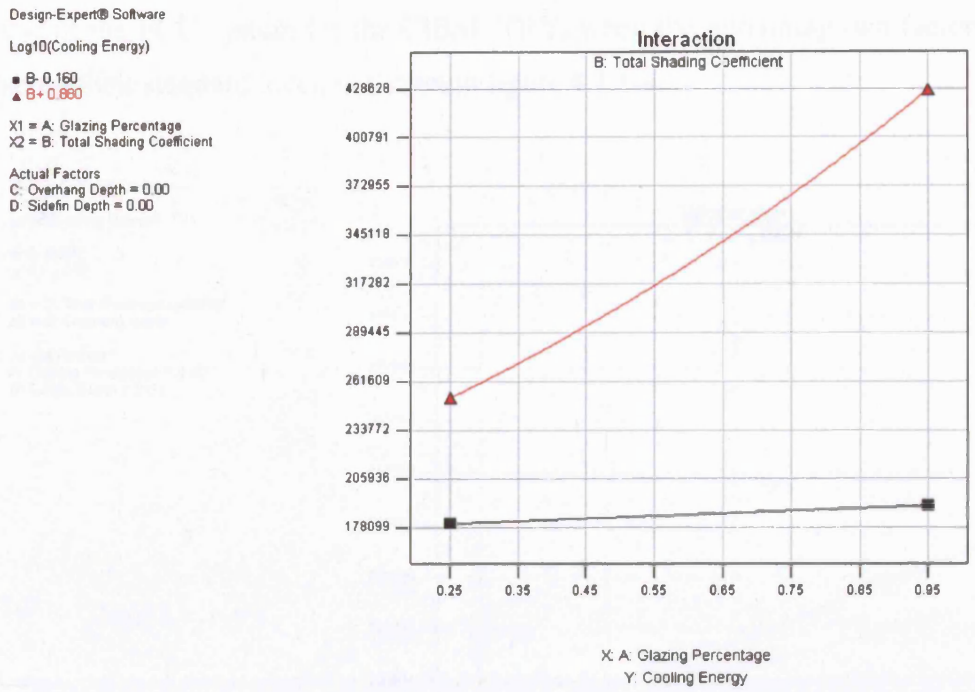

Figure 4.1.1-3: The effect of the TSC (factor B) and the glazing percentage (factor A) on the cooling energy consumption of the FCU system for the CIBSE TRY, when both the overhang (factor C) and the side-fin (factor D) depth are held constant at 0.0 m

Figure 4.1.1-3 shows the effect of the glazing percentage on the cooling energy use for two values of the TSC (i.e. the chosen minimum and maximum values), assuming that the case study building does not incorporate any external shading devices. The glazing percentage has a considerably higher impact on the cooling energy use when the TSC of the windows equals 0.88 as opposed to 0.16, as suggested by the steeper slope of the red line in comparison with the black line shown in this figure. Obviously, opting for windows with a high TSC and a fully glazed building maximises the solar gains through the transparent building elements, resulting in excessive use of mechanical cooling (red line). On the other hand, the installation of window constructions with a low TSC provides very effective control of the incoming solar radiation and, thus, helps to maintain the cooling energy consumption at approximately the same level, regardless of the glazing percentage (black line).

Moreover, both the overhang depth (factor C) and the side-fin depth (factor D) interact with the TSC (factor B) of the windows in their effect on the cooling

energy consumption. The effect of the interaction term BC on the cooling energy use of the FCU system for the CIBSE TRY, when the remaining two factors are set to their standard level, is shown in figure 4.1.1-4:

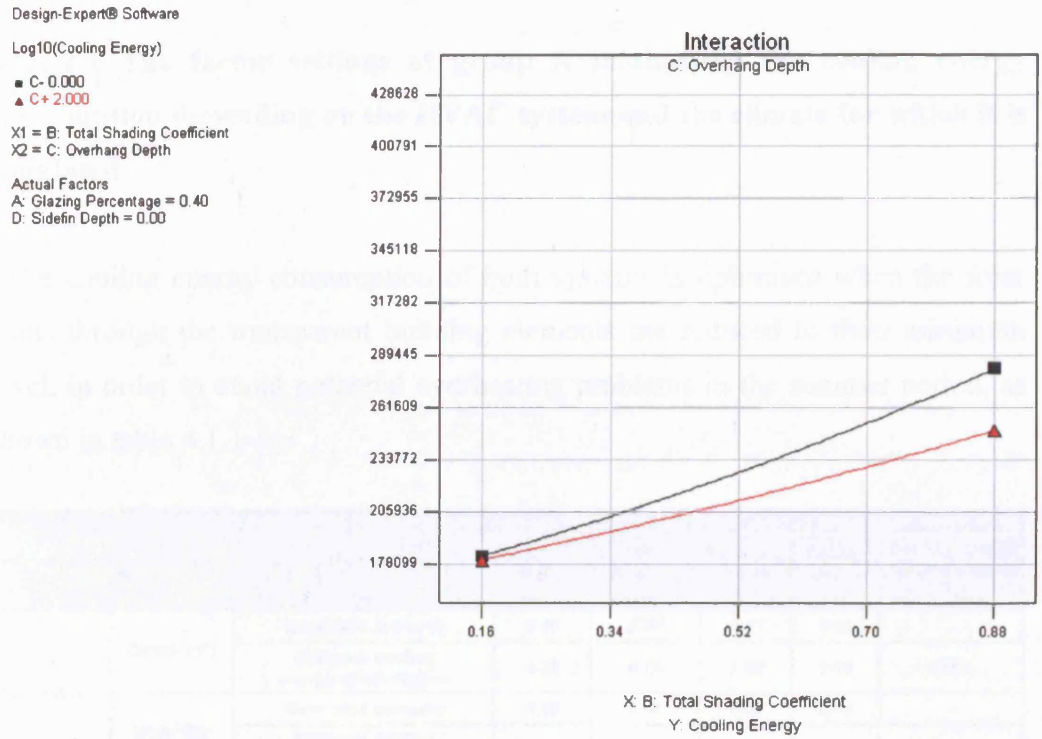

Figure 4.1.1-4: The effect of the TSC (factor B) and the overhang depth (factor C) on the cooling energy consumption of the FCU system for the CIBSE TRY, provided that the glazing percentage (factor A) equals 40% and the side-fin depth (factor D) is 0.0 m

As can be seen from figure 4.1.1-4, the cooling energy savings due to the addition of overhangs gradually increase as the TSC of the windows rises from 0.16 to 0.88. It is obvious that the maximum benefit from the addition of an external shading device is realised when the TSC is 0.88. In such a case, the addition of 2.0 metre overhangs to the south orientated windows of the building reduces the cooling energy use by approximately 33,000 kWh. Alternatively, the cooling energy consumption is not really affected by the presence of overhangs when the TSC of the window construction is reduced to 0.16[2], as illustrated in this two-factor interaction plot.

[2] **Note:** The cooling energy use drops by only 2,200 kWh when 2.0 metre overhangs are constructed for the south windows and the TSC equals 0.16.

The interaction term BD, involving the TSC of the windows and the side-fin depth, affects the cooling energy consumption of the FCU system in a similar way.

4.1.1-2.1 The factor settings of group A minimising the cooling energy consumption depending on the HVAC system and the climate for which it is simulated

The cooling energy consumption of both systems is optimised when the solar gains through the transparent building elements are reduced to their minimum level, in order to avoid potential overheating problems in the summer period, as shown in table 4.1.1-5:

HVAC system	Climate	Scenario	Factor Levels				Reduction in cooling energy over the BCS (%)
			Glazing Ratio (0 -1)	Total Shading Coefficient	Overhang Depth (m)	Sidefin Depth (m)	
FCU system	CIBSE TRY	Base case scenario	0.40	0.74	0.00	0.00	-
		Minimum cooling energy consumption	0.25	0.16	2.00	2.00	-33%
	NOA TRY	Base case scenario	0.40	0.74	0.00	0.00	-
		Minimum cooling energy consumption	0.25	0.16	2.00	2.00	-31%
VAV system	CIBSE TRY	Base case scenario	0.40	0.74	0.00	0.00	-
		Minimum cooling energy consumption	0.25	0.16	2.00	2.00	-33%
	NOA TRY	Base case scenario	0.40	0.74	0.00	0.00	-
		Minimum cooling energy consumption	0.25	0.16	2.00	2.00	-29%

Table 4.1.1-5: The combination of factor levels minimising the use of mechanical cooling and the associated reduction over the cooling energy consumption of the BCS depending on the HVAC system and the climate for which it is simulated

The optimisation of the parameters of this group has a higher impact on the cooling than the heating energy use of the HVAC systems, as can be seen from tables 4.1.1-3 and 4.1.1-5.

4.1.1-3 Summary of the findings derived from the study of the effect of the factors contained in group A on the energy performance of the HVAC systems in both climates

It has been found that the TSC of the windows and the glazing percentage of the building have the highest impact on both the heating and the cooling energy use of the HVAC systems. The specification of a small glazing percentage reduces the heat losses to the external environment, while the installation of windows with a high TSC without external shading devices increases the solar gains during the winter period, minimising the space heating requirement. The cooling energy consumption, on the other hand, is more sensitive to the design factors of this group than the heating energy use. The optimization results have illustrated a clear trend for low TSCs and small glazing percentages to provide tight control of the incoming solar radiation over the summer months and avoid potential overheating problems. The addition of external shading devices is not necessary when the above two factors are set close to their minimum level, as suggested by figure 4.1.1-4.

4.1.2 The effect of the design variables associated with the thermal resistance and the air tightness of the building envelope (group B) on the energy performance of the HVAC systems

The aim of this study is to analyse the relationship between the parameters associated with the thermal resistance and the air tightness of the building envelope and the energy consumption of the HVAC systems when they are simulated for the CIBSE TRY and the NOA TRY respectively. Secondary aims include the identification of the combinations of factor levels that minimize the annual cooling and heating energy consumption of each system in both climates.

The design factors contained in this group and their range of values are presented in table 4.1.2-1:

Factors	Values		
	Standard	Minimum	Maximum
Factor A: Wall U-value (W/m^2K)	0.35	0.18	0.70
Factor B: Infiltration rate (ach)	0.50	0.25	2.00
Factor C: Window U-value (W/m^2K)	2.10	1.20	5.80

Table 4.1.2-1: The range of values of the three factors of group B

The parameters shown in this table are correlated with the annual heating and cooling energy consumption of the VAV system and the FCU system respectively. This procedure is repeated for both climates, so eight response surface models are developed in total. The models constructed in this study are presented in appendix H, section H.1.2.

Sections 4.1.2-1 and 4.1.2-2 discuss the effect of the parameters of group B on the annual heating and cooling energy use of the HVAC systems respectively, in both climates for which the simulations are carried out. The findings of this study are summarized in section 4.1.2-3.

4.1.2-1 The effect of the parameters of group B on the heating energy consumption of the HVAC systems, when they are simulated for the CIBSE TRY and the NOA TRY respectively

The effect of all the parameters related to the air tightness and the thermal resistance of the building envelope on the heating energy consumption of the FCU system for the CIBSE TRY is illustrated in figure 4.1.2-1:

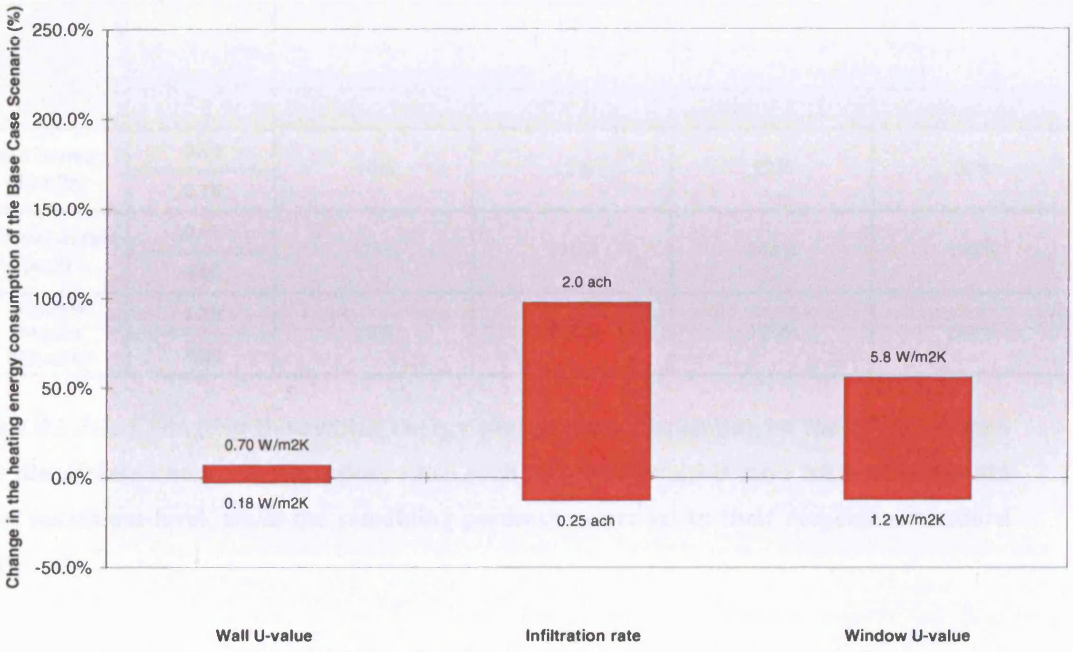

Figure 4.1.2-1: The effect of all the parameters of group B on the annual heating energy consumption of the BCS, when the FCU system is simulated for the CIBSE TRY

Figure 4.1.2-1 shows that the heating energy use is considerably more sensitive to the infiltration rate and the window U-value than the wall U-value. The increase of the infiltration rate[3] from 0.25 to 2.0 ach more than doubles the heating energy use of the FCU system. Also, opting for a window U-value of 5.8 instead of 1.2 W/m^{2}K results in approximately 78% higher heating energy use. It is clear that increasing the infiltration rate of the building or the U-value of the windows results in higher heat losses to the external environment and, hence, increases the demand for space heating. Similarly, setting the U-value of the external walls to 0.70 as opposed to 0.18 W/m^{2}K results in 10% higher heating

[3] **Note:** It should be remembered that the infiltration rate changes from 0.25 ach to 2.0 ach only in the perimeter zones of the building, while it is always held constant at 0.0 ach in the core zones.

energy consumption. The wall U-value has a limited effect on the heating energy use, since the net wall area (i.e. excluding the area of the windows) is a rather small percentage of the total surface area of the building.

The effect of all the parameters of this group on the heating energy consumption of both HVAC systems when they are simulated for the CIBSE TRY and the NOA TRY respectively is summarised in table 4.1.2-2:

Factor	Min and Max Level	Impact on heating energy use (%)			
		FCU system		VAV system	
		CIBSE TRY	NOA TRY	CIBSE TRY	NOA TRY
Wall U-value (W/m2K)	0.18	10%	13%	22%	32%
	0.70				
Infiltration rate (ach)	0.25	127%	170%	304%	486%
	2.00				
Window U-value (W/m2K)	1.20	78%	107%	190%	307%
	5.80				

Table 4.1.2-2: Change in the heating energy consumption, depending on the HVAC system and the climate under consideration, when each factor of group B rises from its minimum to its maximum level, while the remaining parameters are set to their respective standard level.

As can be seen from table 4.1.2-2, the sensitivity of the heating energy consumed by both HVAC systems particularly to factors B and C increases when the simulations are carried out for the NOA TRY as opposed to the CIBSE TRY. It should be borne in mind that the former is a cooling-dominated climate, which means that the amount of heating energy consumed, particularly when the parameters of this group are set to their minimum level (i.e. when the building is well-insulated and airtight) is trivial. However, increasing the values of the design factors under consideration affects the heat losses during the night, when the external temperature drops, resulting in a relatively higher increase of space heating energy in the following day, when the simulations are carried out for the Athens than for the London typical weather conditions.

It is also clear that the heating energy consumption of the VAV system is considerably more sensitive to the design factors associated with the thermal resistance and the air tightness of the building envelope than the FCU system heating energy use, in both climates. It should be remembered that a similar conclusion was derived from the study of the effect of the parameters of group A on the heating energy consumption of the HVAC systems (section 4.1.1-1).

4.1.2-1.1 The factor settings of group B minimising the heating energy consumption depending on the type of HVAC system and the climate for which the simulations are carried out

A well-insulated and airtight building envelope retains the heat inside the building, minimising the demand for space heating, as can be seen from table 4.1.2-3:

HVAC system	Climate	Scenario	Factor Levels			Reduction in heating energy over the BCS (%)
			Wall U-value (W/m^2K)	Infiltration rate (ach)	Window U-value (W/m^2K)	
FCU system	CIBSE TRY	Base case scenario	0.35	0.50	2.10	-
		Minimum heating energy consumption	0.18	0.25	1.20	-27%
	NOA TRY	Base case scenario	0.35	0.50	2.10	-
		Minimum heating energy consumption	0.18	0.25	1.20	-35%
VAV system	CIBSE TRY	Base case scenario	0.35	0.50	2.10	-
		Minimum heating energy consumption	0.18	0.25	1.20	-53%
	NOA TRY	Base case scenario	0.35	0.50	2.10	-
		Minimum heating energy consumption	0.18	0.25	1.20	-70%

Table 4.1.2-3: The combination of factor levels minimising the requirement for space heating and the associated reduction over the heating energy consumption of the BCS, depending on the type of HVAC system and the climate for which it is simulated

4.1.2-2 The effect of the parameters of group B on the cooling energy consumption of the HVAC systems when they are simulated for the CIBSE TRY and the NOA TRY respectively

The effect of all the parameters of group B on the cooling energy consumption of the FCU system for the CIBSE TRY is shown in figure 4.1.2-2:

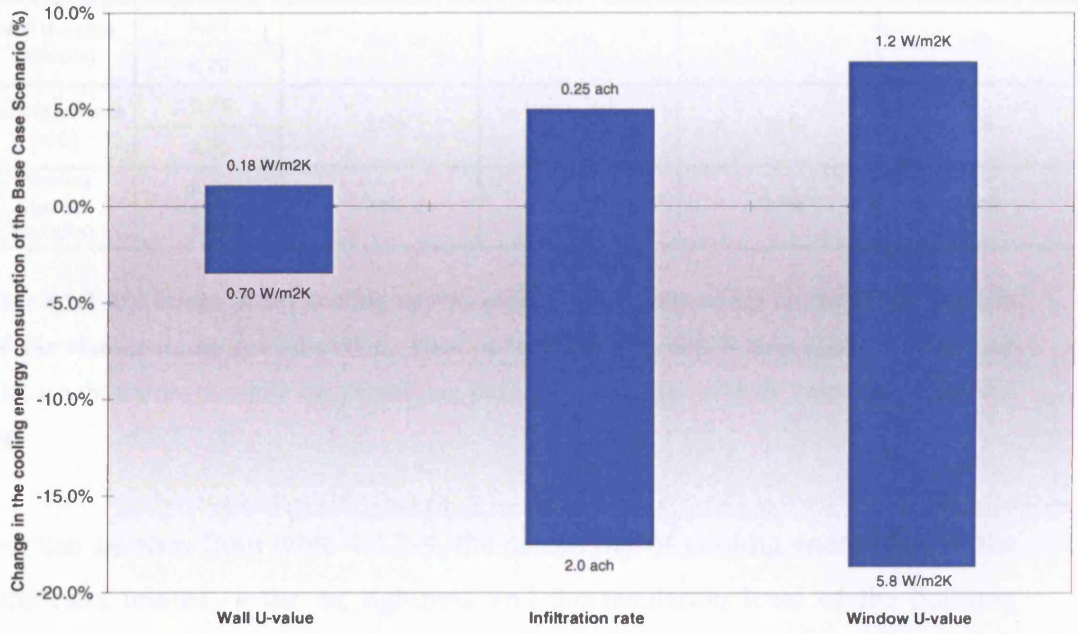

Figure 4.1.2-2: The effect of all the parameters of group B on the cooling energy consumption of the BCS, when the FCU system is simulated for the CIBSE TRY

Figure 4.1.2-2 illustrates that the cooling energy consumption of the FCU system drops by approximately 24% when the U-value of the windows increases from 1.2 to 5.8 W/m^{2}K and 21% when the infiltration rate of the building rises from 0.25 to 2.0 ach respectively. It seems that releasing part of the heat trapped inside the building to the external environment helps to reduce the overheating problems, and, hence, the demand for mechanical cooling, during the milder periods of the year, when the external temperature is lower than the temperature inside the building. Moreover, the increase of the wall U-value from 0.18 to 0.70 W/m^{2}K results in approximately 5% lower cooling energy consumption, as illustrated in this figure. It is obvious that the wall U-value has a moderate effect on both the cooling and the heating energy consumption of the FCU system.

The effect of all the design factors of this group on the cooling energy consumption of both HVAC systems when they are simulated for the London and the Athens climate respectively is summarised in table 4.1.2-4:

Factor	Min and Max Level	Impact on cooling energy use (%)			
		FCU system		VAV system	
		CIBSE TRY	NOA TRY	CIBSE TRY	NOA TRY
Wall U-value (W/m2K)	0.18	-4%	-2%	-3%	-1%
	0.70				
Infiltration rate (ach)	0.25	-21%	-7%	-14%	1%
	2.00				
Window U-value (W/m2K)	1.20	-24%	-14%	-17%	-9%
	5.80				

Table 4.1.2-4: Change in the cooling energy consumption, depending on the HVAC system and the climate under consideration, when each factor of group B rises from its minimum to its maximum level, while the remaining parameters are set to their respective standard level

As can be seen from table 4.1.2-4, the sensitivity of cooling energy use to the parameters related to the air tightness and the insulation level of the building envelope drops considerably when either the FCU system or the VAV system is simulated for the NOA TRY in place of the CIBSE TRY. On top of this, the increase of the infiltration rate, while the remaining two design factors of this group are held constant at their standard value, leads to a small increase in cooling energy use when the VAV system is simulated for the Athens typical climatic conditions. This is clearly due to the higher external temperatures involved in the Athens weather file (in comparison with the CIBSE TRY), which are close to or even higher than the temperature inside the building for a considerable part of the summer period. As a result, the reduction of the thermal resistance of the external building envelope or the increase of the infiltration rate of the building to allow part of the internal heat gains to be exhausted to the external environment is not as effective in the Athens as in the London climate.

The interaction term BC affects the cooling energy consumption of both HVAC systems in a similar way, when the simulations are carried out for the CIBSE TRY. For example, the effect the infiltration rate (factor B) of the building and the U-value of the windows (factor C) on the cooling energy use of the FCU system for the CIBSE TRY is shown in figure 4.1.2-3:

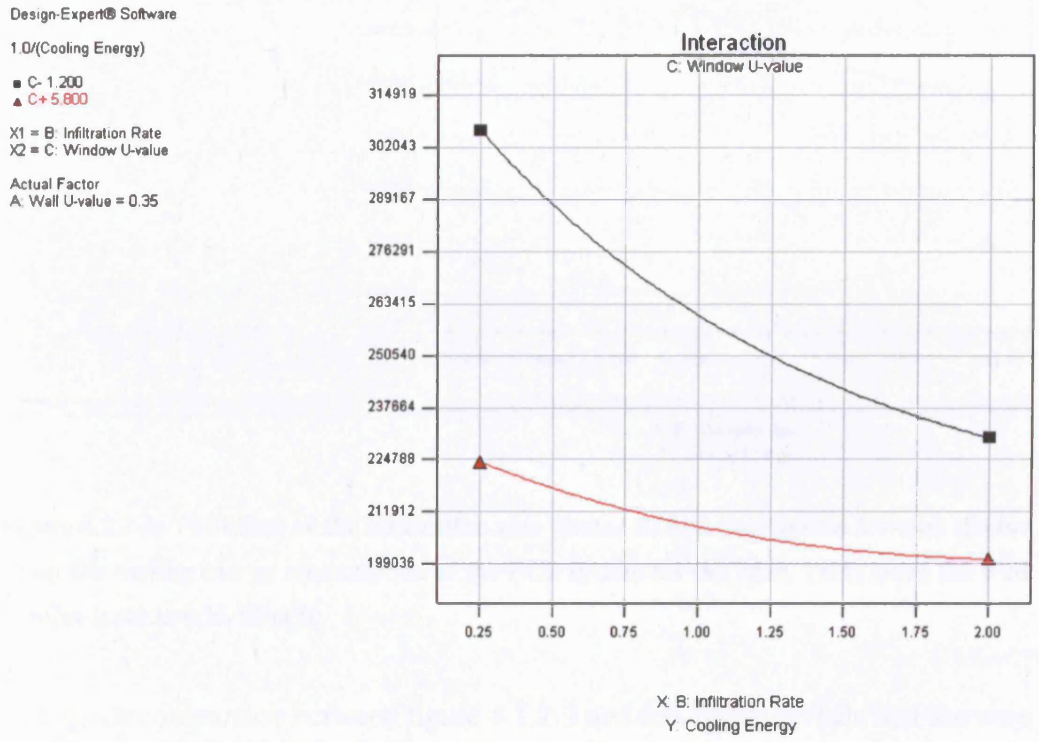

Figure 4.1.2-3: The effect of the infiltration rate (factor B) and the window U-value (factor C) on the cooling energy consumption of the FCU system for the CIBSE TRY, when the wall U-value (factor A) is kept constant at 0.35 W/m^{2}K (i.e. the standard value of this parameter)

Figure 4.1.2-3 shows that changing the infiltration rate from 0.25 to 2.0 ach reduces the cooling energy use for both levels of the window U-value. In addition, the infiltration rate has a higher impact on the cooling energy consumption when the window U-value is 1.2 W/m^{2}K as opposed to 5.8 W/m^{2}K, as indicated by the steeper slope of the black line in comparison with the red line shown in the above interaction plot.

The effect of the interaction term BC on the cooling energy consumption of the FCU system for the NOA TRY, on the other hand, is shown in figure 4.1.2-4:

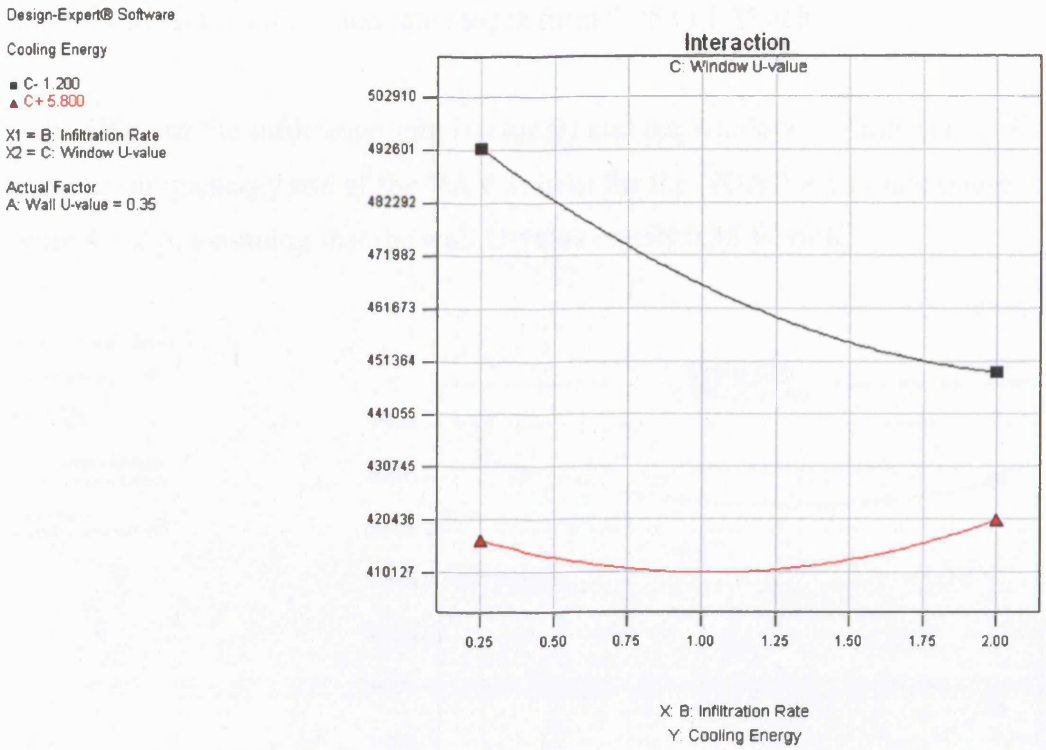

Figure 4.1.2-4: The effect of the infiltration rate (factor B) and the window U-value (factor C) on the cooling energy consumption of the FCU system for the NOA TRY, when the wall U-value is set to 0.35 W/m^{2}K

A quick comparison between figure 4.1.2-3 and this figure reveals that the way the infiltration rate affects the cooling energy use of FCU system when the window U-value equals 5.8 W/m^{2}K, is different in each climate. Thus, in such a case, figure 4.1.2-3 illustrates that the cooling energy use is minimised when the infiltration rate is 2.0 ach. Figure 4.1.2-4, on the other hand, shows that the cooling energy use drops as the infiltration rate changes from 0.25 to 0.75 ach, while it starts to rise again when the infiltration rate gets higher than 1.25 ach approximately. As explained earlier, the increase of the infiltration rate allows part of the excessive internal heat gains to be exhausted to the external environment reducing potential overheating problems. However, it seems that due to the high external temperatures and solar gains of the NOA TRY, after a certain point the heat introduced inside the building from the external environment overcomes the heat losses, leading to a small increase in cooling energy use. Figure 4.1.2-4 shows that the minimum cooling energy consumption,

for a wall U-value of 0.35 W/m^{2}K and a window U-value of 5.8 W/m^{2}K, is achieved when the infiltration rate ranges from 0.75 to 1.25 ach.

The effect of the infiltration rate (factor B) and the window U-value (factor C) on the cooling energy use of the VAV system for the NOA TRY is illustrated in figure 4.1.2-5, assuming that the wall U-value equals 0.35 W/m^{2}K:

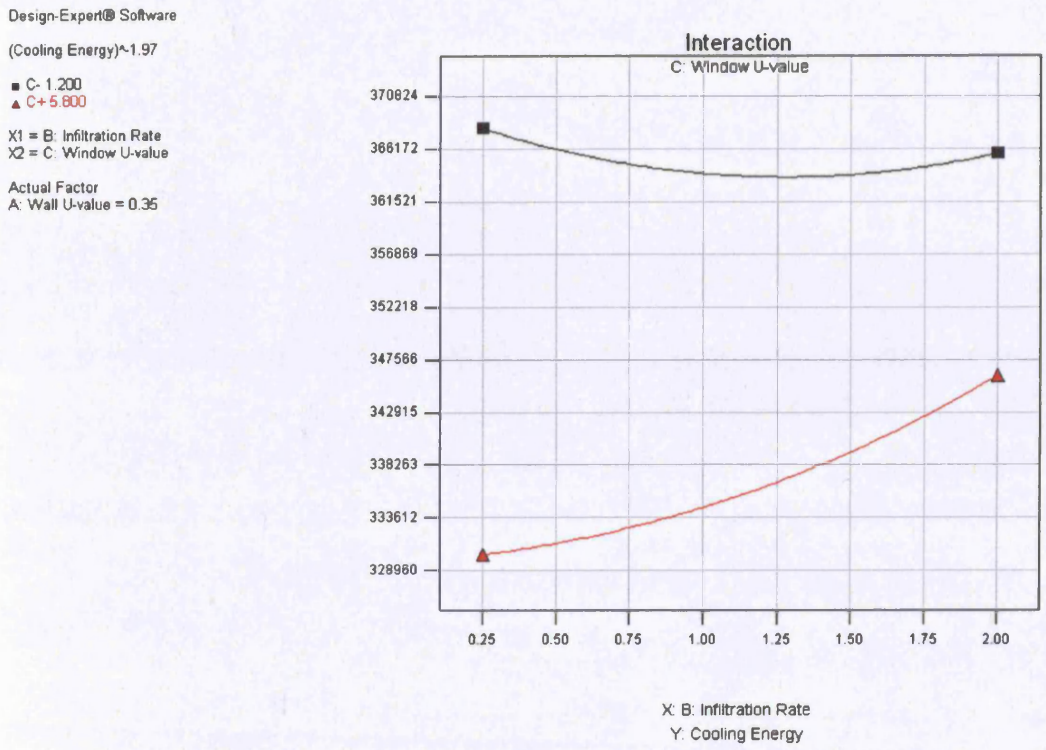

Figure 4.1.2-5: The effect of the infiltration rate (factor B) and the window U-value (factor C) on the cooling energy consumption of the VAV system for the NOA TRY, when the wall U-value (factor A) is 0.35 W/m^{2}K

Clearly, the way the interaction term BC affects the cooling energy consumption depends not only on the climate for which the simulations are carried out, as indicated in figures 4.1.2-3 and 4.1.2-4, but on the type of HVAC system that is simulated for the NOA TRY as well, as can be seen from figures 4.1.2-4 and 4.1.2-5. Thus, the shape of the line shown in figure 4.1.2-5 when the window U-value is 1.2 W/m^{2}K indicates that the cooling energy use drops as the infiltration rate changes from 0.25 to 1.0 ach, while it starts to rise again when the infiltration rate is set higher than 1.5 ach, since the heat gains from the

external environment overcome the heat losses through the building envelope. On the other hand, changing the infiltration rate from 0.25 to 2.0 ach increases the cooling energy use (by approximately 15,800 kWh) when the window U-value is 5.8 W/m^2K. This is the first time that the cooling energy use is minimised for an infiltration rate of 0.25 ach, as can be seen from all the interaction plots included in this section. It seems that in this case the heat gains from the external environment are higher than the heat losses for the entire range of values of the infiltration rate.

4.1.2-2.1 The factor settings of group B minimising the cooling energy consumption depending on the HVAC system and the climate for which it is simulated

The design option leading to the minimum cooling energy consumption and the associated energy savings over the BCS, depending on the HVAC system and the climate under consideration are shown in table 4.1.2-5:

HVAC system	Climate	Scenario	Factor Levels			Reduction in cooling energy over the BCS (%)
			Wall U-value (W/m^2K)	Infiltration rate (ach)	Window U-value (W/m^2K)	
FCU system	CIBSE TRY	Base case scenario	0.35	0.50	2.10	-
		Minimum cooling energy consumption	0.70	2.00	5.80	-25%
	NOA TRY	Base case scenario	0.35	0.50	2.10	-
		Minimum cooling energy consumption	0.70	0.88	5.80	-12%
VAV system	CIBSE TRY	Base case scenario	0.35	0.50	2.10	-
		Minimum cooling energy consumption	0.70	2.00	5.80	-22%
	NOA TRY	Base case scenario	0.35	0.50	2.10	-
		Minimum cooling energy consumption	0.70	0.25	5.80	-8%

Table 4.1.2-5: The combination of factor levels minimising the use of mechanical cooling and the associated reduction over the cooling energy consumption of the BCS depending on the type of HVAC system and the climate for which it is simulated

Table 4.1.2-5 shows that the cooling energy consumption of the HVAC systems for the CIBSE TRY is minimised when all the parameters of this group are set to their maximum level. Increasing the U-value of the walls & windows and the infiltration rate of the building allows part of the excessive heat gains

from the occupants, equipment and lighting to be exhausted to the external environment, thereby reducing the demand for mechanical cooling throughout the milder periods of the year.

The cooling energy consumption of both systems for the NOA TRY is also minimised when the wall and window U-values are set to their maximum level. The optimum value of the infiltration rate, however, differs depending on the type of HVAC system that is simulated for this climate. As can be seen from table 4.1.2-5, the infiltration rate is set to 0.88 ach (i.e. between 0.75 and 1.25 ach) when the FCU system is simulated for the NOA TRY, while it is equal to 0.25 ach, when the VAV system is simulated for the Athens typical weather conditions. This is due to the way that the infiltration rate affects the cooling energy consumption in this climate, when the window U-value is 5.8 W/m^2K, as shown in figure 4.1.2-4 for the FCU system and figure 4.1.2-5 for the VAV system respectively[4].

The optimisation of the factors of group B has a higher impact on the heating than the cooling energy use of the HVAC systems, as can be seen from tables 4.1.2-3 and 4.1.2-5.

[4] **Note:** It should be remembered that figures 4.1.2-4 & 4.1.2-5 are valid for a wall U-value of 0.35 W/m^2K. However, the U-value of the external walls has a small effect on the cooling energy use of both systems, while this effect does not change a lot depending on the level of the infiltration rate or the window U-value (in other words, the interaction terms AB and AC are not particularly 'strong'). As a result, both figures are expected to remain pretty much the same regardless of the wall U-value.

4.1.2-3 Summary of the findings derived from the study of the effect of the factors contained in group B on the energy performance of the HVAC systems in both climates

To sum up, the infiltration rate has the highest impact on the heating energy use of both HVAC systems, followed by the window U-value. The specification of a well-insulated, airtight building minimises the heating energy consumption of both HVAC systems regardless of the climate for which they are simulated. It has also been found that the annual cooling energy consumption is considerably less sensitive to the parameters of this group than the heating energy use. The window U-value has the highest impact on the cooling energy consumption of both systems followed by the infiltration rate. The optimization results have illustrated that there are some differences in the factor settings minimising the cooling energy use depending on the type of HVAC system and the climate for which it is simulated. The main reason for these differences lies in the way that the infiltration rate interacts with the window U-value in their effect on the cooling energy consumption of each system, depending on the climate under consideration.

4.1.3 The effect of the design variables related to the internal heat gains of the office building (group C) on the energy performance of the HVAC systems

This study investigates the effect of the internal heat gains from lighting, office equipment and occupants on the energy performance of the FCU system and the VAV system when they are simulated for the CIBSE TRY and the NOA TRY respectively. Secondary aims include the identification of factor levels that minimize the annual heating and cooling energy consumption of each system in both climates.

The respective minimum, maximum and standard values of the design variables of this group are shown in table 4.1.3-1:

Factors	Values		
	Standard	Minimum	Maximum
Factor A: Equipment gains (W/m^2)	15.0	10.0	25.0
Factor B: Lighting gains (W/m^2)	12.0	6.5	20.0
Factor C: Occupancy density (m^2 per person)	10	5	20

Table 4.1.3-1: The range of values of the design factors of group C

The parameters shown in this table are correlated with the annual heating and cooling energy use of the HVAC systems in both climates under consideration. The eight response surface models developed in this study can be found in appendix H, section H.1.3.

Sections 4.1.3-1 and 4.1.3-2 contain the analysis of the effect of the three parameters of group C on the heating and cooling energy consumption of the HVAC systems respectively, in both climates for which they are simulated. The findings of this study are summarized in section 4.1.3-3.

4.1.3-1 The effect of the parameters of group C on the heating energy consumption of the HVAC systems, when they are simulated for the CIBSE TRY and the NOA TRY respectively

The effect of all the parameters related to the internal heat gains of the office building on the heating energy consumption of the FCU system for the CIBSE TRY is illustrated in figure 4.1.3-1:

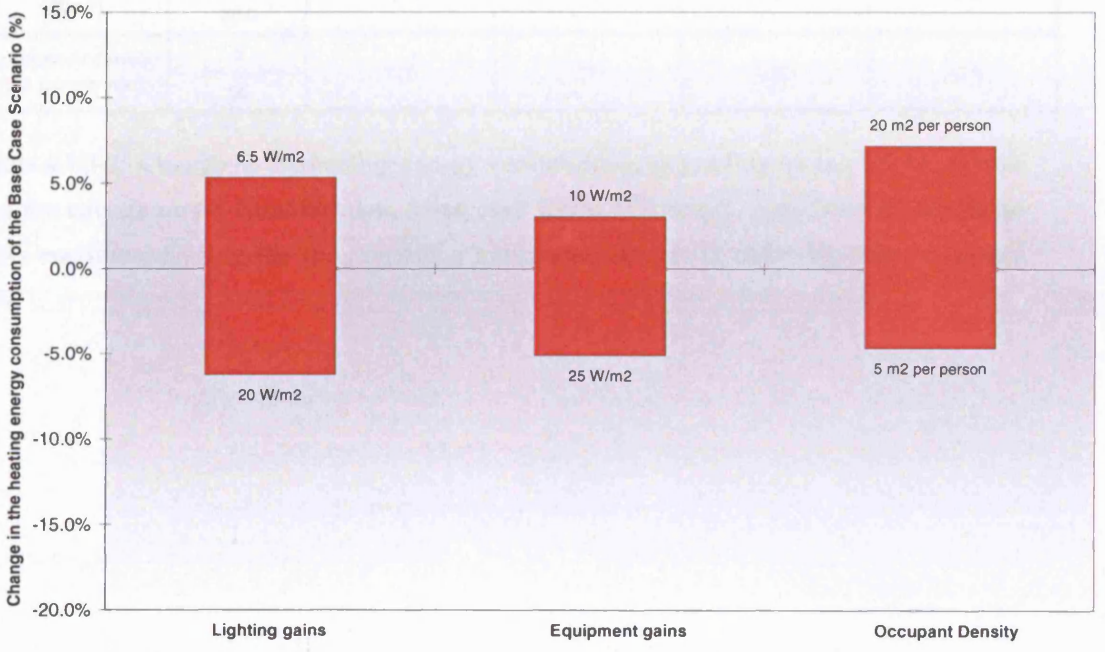

Figure 4.1.3-1: The effect of all the parameters of group C on the annual heating energy consumption of the BCS, when the FCU system is simulated for the CIBSE TRY

Figure 4.1.3-1 shows that the increase of the heat emitted by office equipment from 10 to 25 W/m^2 results in 8% lower heating energy consumption. Similarly, setting the lighting heat gains to 20 as opposed to 6.5 W/m^2 leads to 11% lower heating energy use. On the other hand, increasing the occupancy density from 5 to 20 m^2 per person, or, in other words, decreasing the number of occupants, results in limited sensible heat gains and, hence, 12% higher heating energy consumption.

The effect of all the parameters of this group on the heating energy consumption of both HVAC systems when they are simulated for the CIBSE TRY and the NOA TRY respectively is summarised in table 4.1.3-2:

Factor	Min and Max Level	Impact on heating energy use (%)			
		FCU system		VAV system	
		CIBSE TRY	NOA TRY	CIBSE TRY	NOA TRY
Lighting gains (W / m2)	6.5	-11%	-9%	-26%	-23%
	20.0				
Equipment gains (W/m2)	10.0	-8%	-4%	-19%	-8%
	25.0				
Occupancy density (m2 per person)	5	12%	7%	32%	16%
	20				

Table 4.1.3-2: Change in the heating energy consumption, depending on the HVAC system and the climate under consideration, when each factor of group C rises from its minimum to its maximum level, while the remaining parameters are set to their respective standard level

4.1.3-1.1 The factor settings of group C minimising the heating energy consumption depending on the type of HVAC system and the climate for which the simulations are carried out

Setting the internal heat gains from occupants, lighting and office equipment close to their maximum level, results in up to 29% lower heating energy use than the BCS, depending on the HVAC system and the climate under consideration, as shown in table 4.1.3-3:

HVAC system	Climate	Scenario	Factor Levels			Reduction in heating energy over the BCS (%)
			Lighting gains (W/m2)	Equipment gains (W/m2)	Occupant Density (m2 per person)	
FCU system	CIBSE TRY	Base case scenario	12.0	15.0	10	-
		Minimum heating energy consumption	20.0	25.0	5	-10%
	NOA TRY	Base case scenario	12.0	15.0	10	-
		Minimum heating energy consumption	20.0	25.0	5	-9%
VAV system	CIBSE TRY	Base case scenario	12.0	15.0	10	-
		Minimum heating energy consumption	20.0	25.0	5	-29%
	NOA TRY	Base case scenario	12.0	15.0	10	-
		Minimum heating energy consumption	20.0	25.0	5	-21%

Table 4.1.3-3: The combination of factor levels minimising the requirement for space heating and the associated reduction over the heating energy use of the BCS, depending on the HVAC system and the climate for which it is simulated

4.1.3-2 The effect of the parameters of group C on the cooling energy consumption of the HVAC systems when they are simulated for the CIBSE TRY and the NOA TRY respectively

The effect of all the parameters of group C on the cooling energy consumption of the FCU system for the CIBSE TRY is shown in figure 4.1.3-2:

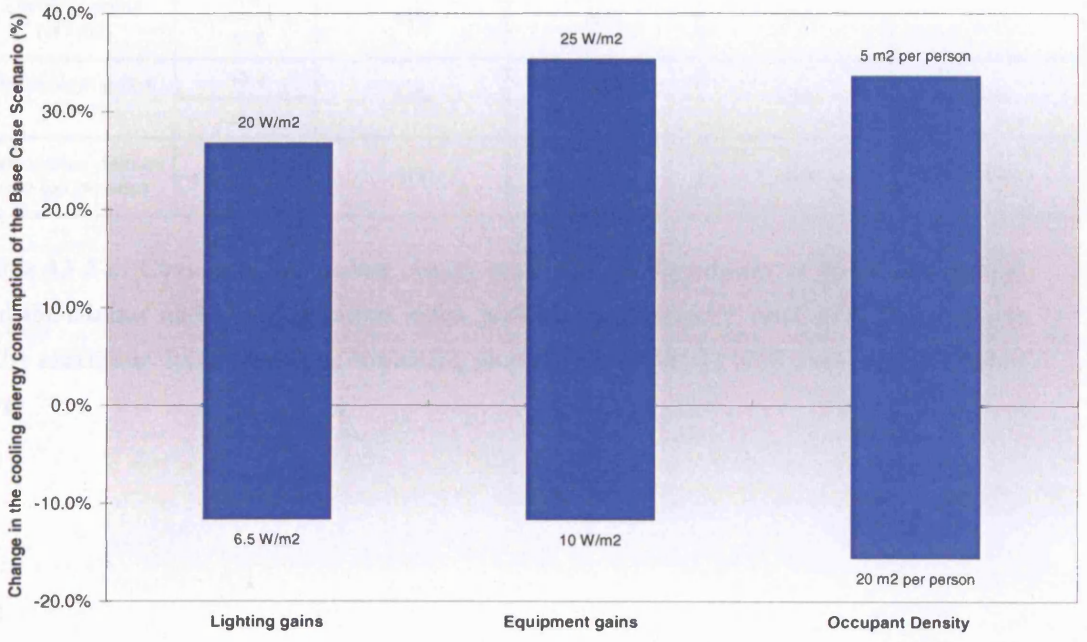

Figure 4.1.3-2: The effect of all the design factors of group C on the cooling energy consumption of the BCS, when the FCU system is simulated for the CIBSE TRY

Figure 4.1.3-2 indicates that the cooling energy consumption of the FCU system rises by approximately 53% when the equipment heat gains increase from 10 to 25 W/m^2 and 44% when the lighting gains increase from 6.5 to 20 W/m^2, respectively. On the other hand, the increase of the occupant density from 5 to 20 m^2 per person results in lower sensible heat gains due to the reduction of the number of occupants. In such a case the cooling energy consumption drops by approximately 37%, as can be seen from this figure. It is obvious that the cooling energy consumption is considerably more sensitive to all the parameters of group C than the heating energy use of the FCU system.

The effect of all the design factors of this group on the cooling energy consumption of both HVAC systems when they are simulated for the London and the Athens typical weather conditions respectively is summarised in table 4.1.3-4:

Factor	Min and Max Level	Impact on cooling energy use (%)			
		FCU system		VAV system	
		CIBSE TRY	NOA TRY	CIBSE TRY	NOA TRY
Lighting gains (W / m2)	6.5	44%	28%	30%	21%
	20.0				
Equipment gains (W/m2)	10.0	53%	33%	37%	26%
	25.0				
Occupancy density (m2 per person)	5	-37%	-27%	-28%	-24%
	20				

Table 4.1.3-4: Change in the cooling energy consumption, depending on the HVAC system and the climate under consideration, when each factor of group C rises from its minimum to its maximum level, while the remaining parameters are set to their respective standard level

4.1.3-2.1 The factor settings of group C minimising the cooling energy consumption depending on the HVAC system and the climate for which it is simulated

The simultaneous reduction of the heat emitted by lights, office equipment and occupants has a high impact on the cooling energy use of both HVAC systems, as shown in table 4.1.3-5:

HVAC system	Climate	Scenario	Factor Levels			Reduction in cooling energy over the BCS (%)
			Lighting gains (W/m2)	Equipment gains (W/m2)	Occupant Density (m2 per person)	
FCU system	CIBSE TRY	Base case scenario	12.0	15.0	10	-
		Minimum cooling energy consumption	6.5	10.0	20	-42%
	NOA TRY	Base case scenario	12.0	15.0	10	-
		Minimum cooling energy consumption	6.5	10.0	20	-29%
VAV system	CIBSE TRY	Base case scenario	12.0	15.0	10	-
		Minimum cooling energy consumption	6.5	10.0	20	-33%
	NOA TRY	Base case scenario	12.0	15.0	10	-
		Minimum cooling energy consumption	6.5	10.0	20	-25%

Table 4.1.3-5: The combination of factor levels minimising the use of mechanical cooling and the associated reduction over the cooling energy consumption of the BCS depending on the HVAC system and the climate for which it is simulated

4.1.3-3 Summary of the findings derived from the study of the effect of the factors contained in group C on the energy performance of the HVAC systems in both climates

It has been found that all the parameters associated with the internal heat gains of the office building have a high impact on the energy performance of the HVAC systems. In other words, all the design factors under consideration are equally important to designers. The cooling energy consumption is, however, more sensitive to the parameters of group C than the heating energy use. As a result, the minimisation of the heat generated by lights, office equipment and occupants leads to a considerable reduction in cooling energy use over the BCS.

4.2 HVAC system related parameters

4.2.1 The effect of the parameters related to the control of the internal air temperature (group D) on the energy performance of the HVAC systems

The aim of this study is to investigate the effect of the parameters associated with the control of the internal air temperature on the energy performance of the HVAC systems when they are simulated for the London and the Athens typical weather conditions respectively. Secondary aims include the identification of the temperature control settings that minimize the annual heating and cooling energy consumption of each system in both climates.

The design variables studied in this section and their range of values is displayed in table 4.2.1-1:

HVAC system	Factors	Values		
		Standard	Minimum	Maximum
VAV system	Factor A: Heating zone air temperature (°C)	20	18	22
	Factor B: Cooling zone air temperature (°C)	24	22	26
	Factor C: Temperature difference (ΔT) between the supply and the zone air (°C)	8	**6**	**10**
FCU system	Factor A: Heating zone air temperature (°C)	20	18	22
	Factor B: Cooling zone air temperature (°C)	24	22	26
	Factor C: Temperature difference (ΔT) between the supply and the zone air (°C)	8	**0**	**8**

Table 4.2.1-1: The specified range of values for the parameters associated with the temperature control settings of the VAV system and the FCU system respectively

As can be seen from table 4.2.1-1, the range of values for the temperature difference (ΔT) between the supply and zone air (factor C) differs depending on the type of HVAC system considered. This is due to the fact that each system uses a different approach to control the temperature inside the building. In short, the VAV system supplies the air to each zone at an identical, constant temperature, while its volume flow rate[5] is varied to meet the prevailing zone

[5] **Note:** The fresh and return air streams are mixed in variable proportions in the VAV system, in order to make use of the 'free' cooling capacity of the fresh air, particularly in mild weather conditions.

cooling load. Heating, on the other hand, is provided using terminal re-heaters located around the building. The ΔT between the supply and the zone air is usually set between 6°C and 10°C for this HVAC system, as illustrated in table 4.2.1-1. In the FCU system, the minimum fresh air quantity (for ventilation purposes) is supplied to the building zones at a constant temperature via a central ductwork system, while the fan coil units re-circulate the room air providing heating or cooling, depending on the zone requirements. In this case, the ΔT between the fresh and the zone air usually ranges from 0°C to 8°C, as shown in table 4.2.1-1. It should be remembered that more details regarding the specification of the range of values for the parameters of this group can be found in section 3.3.2, chapter 3.

The three temperature control set-points shown above are correlated with the annual heating & cooling energy use of the HVAC systems in both climates under consideration. The eight response surface models constructed in this study are presented in appendix H, section H.2.1.

Sections 4.2.1-1 and 4.2.1-2 analyse the effect of the three parameters of group D on the heating and cooling energy use of the HVAC systems respectively, in both climates for which the simulations are carried out. The findings of this study are summarized in section 4.2.1-3.

4.2.1-1 The effect of the parameters of group D on the heating energy consumption of the HVAC systems, when they are simulated for the CIBSE TRY and the NOA TRY respectively

The effect of all the parameters associated with the control of the internal air temperature on the heating energy consumption of the FCU system for the CIBSE TRY is illustrated in figure 4.2.1-1:

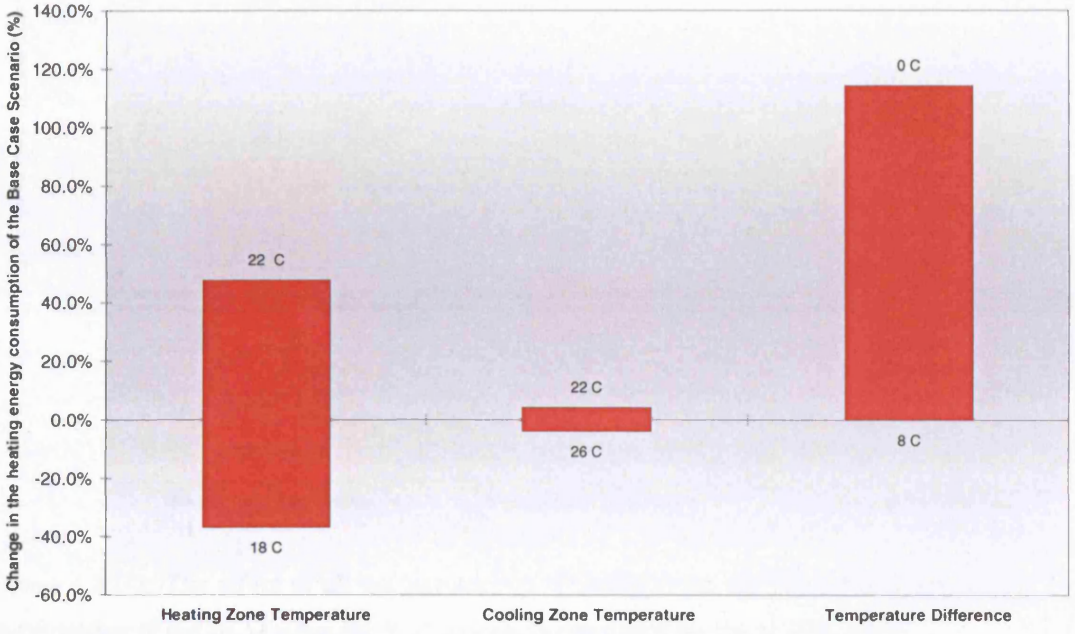

Figure 4.2.1-1: The effect of all the parameters of group D on the annual heating energy consumption of the BCS, when the FCU system is simulated for the CIBSE TRY

Figure 4.2.1-1 shows that the heating energy consumption of the FCU system is considerably more sensitive to the heating zone temperature set-point and the ΔT between the supply and the zone air than the cooling zone temperature set-point. The heating energy use increases by a factor of 2.3 when the temperature threshold below which heating is provided rises from 18˚C to 22˚C. In addition, setting the ΔT between the supply and zone air to 8˚C as opposed to 0˚C decreases the heating energy use by approximately 53%. On the other hand, the heating energy drops by just 8% when the cooling zone temperature set-point rises from 22˚C to 26˚C. It seems that the increase of the temperature limit above which cooling becomes available helps to maintain a warm internal environment

until the next morning when heating kicks in, thereby resulting in lower heating energy use over the period of the year that both heating and cooling is provided.

The effect of the parameters of this group on the heating energy use of the VAV system for the CIBSE TRY is illustrated in figure 4.2.1-2:

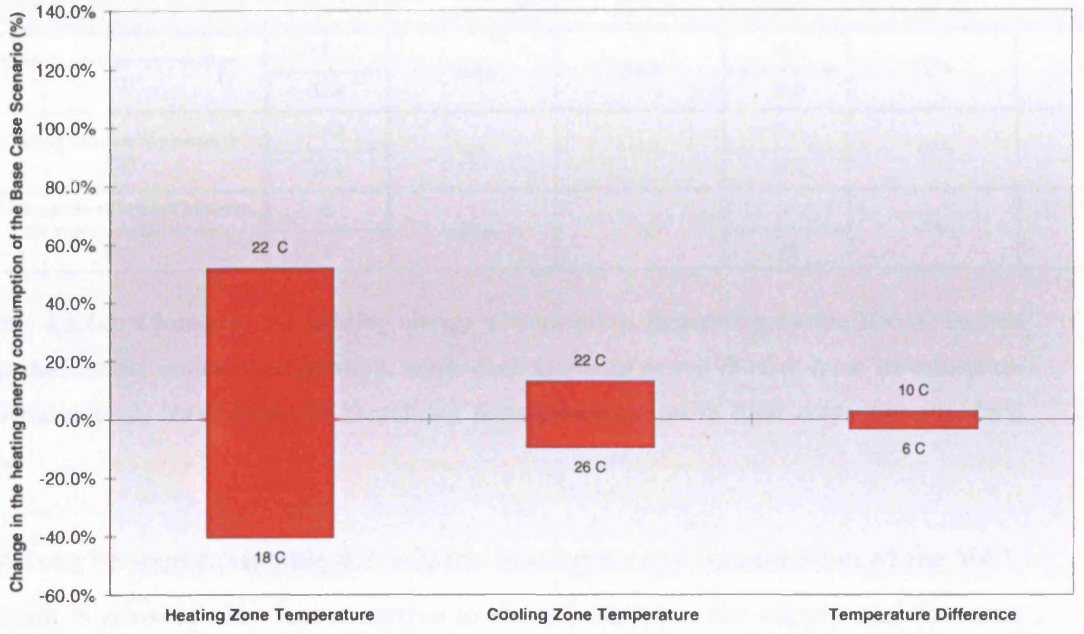

Figure 4.2.1-2: The effect of all the parameters of group D on the annual heating energy consumption of the BCS, when the VAV system is simulated for the CIBSE TRY

As can be seen from figure 4.2.1-2, the heating zone temperature set-point has a dominating effect on the VAV system heating energy use. Setting this parameter to 22°C instead of 18°C increases the heating energy consumption of the VAV system by a factor of 2.6 approximately. The heating energy drops by 20%, on the other hand, when the cooling zone temperature set-point rises from 22°C to 26°C. Also, the increase of the ΔT between the supply and zone air from 6°C to 10°C lowers the temperature of the supply air quantity, thereby increasing the heating energy consumed by the re-heat coils[6] by approximately 7%.

[6] **Note:** It should be remembered that the VAV system does not incorporate an inherent heating ability. As the zone air temperature drops, the system reduces the volume of the supply air until a minimum (which is set in this work to the minimum fresh air requirement for ventilation purposes) is reached. Upon further reduction of the zone temperature, the supply air quantity remains constant and the re-heat coils take over to warm the air.

The effect of all the parameters associated with the control of the internal air temperature on the heating energy consumption of both HVAC systems when they are simulated for the CIBSE TRY and the NOA TRY respectively is summarised in table 4.2.1-2:

Factor	Impact on heating energy use (%)					
	Min and Max Level	FCU system		Min and Max Level	VAV system	
		CIBSE TRY	NOA TRY		CIBSE TRY	NOA TRY
Heating zone air temperature (°C)	18.0	134%	298%	18.0	155%	404%
	22.0			22.0		
Cooling zone air temperature (°C)	22.0	-8%	-16%	22.0	-20%	-42%
	26.0			26.0		
Temperature difference between the supply and zone air (°C)	0	-53%	-73%	6	7%	8%
	8			10		

Table 4.2.1-2: Change in the heating energy consumption, depending on the HVAC system and the climate under consideration, when each factor of group D rises from its minimum to its maximum level, while the remaining parameters are set to their respective standard level

As can be seen from table 4.2.1-2, the heating energy consumption of the VAV system is considerably less sensitive to the ΔT between the supply and the zone air than the heating energy use of the FCU system. However, it should be remembered that both the range of values and the 'role' of this factor on the temperature control strategy of each system differ, as explained in the previous section.

The effect of the interaction term involving the heating zone temperature set-point (factor A) and the ΔT between the supply and the zone air (factor C) on the heating energy consumption of the FCU system for the CIBSE TRY is illustrated in figure 4.2.1-3:

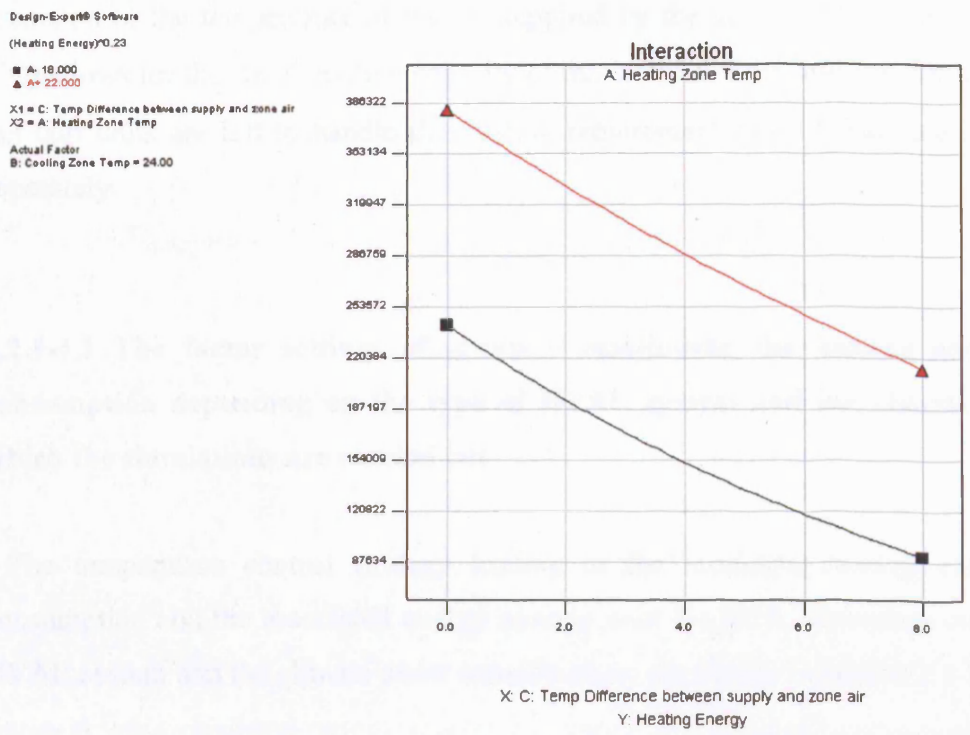

Figure 4.2.1-3: The effect of the heating zone temperature set-point (factor A) and the ΔT between the supply and zone air (factor C) on the heating energy use of the FCU system for the CIBSE TRY, when the cooling zone temperature (factor B) is set to 24°C (i.e. the standard value of this parameter)

Figure 4.2.1-3 shows that setting the ΔT between the supply and zone air to 8°C as opposed to 0°C (i.e. transferring part of the total heating load from the central AHU to the fan coil units located in the building zones) reduces the heating energy consumption by up to 168,000 kWh, depending on the specified heating zone temperature set-point. It is clear that the amount of energy consumed by the central heating coil dominates the annual heating energy use of the FCU system when the fresh air is heated to the zone temperature set-point (i.e. ΔT = 0°C). Therefore, this temperature control strategy is particularly energy wasteful, (as also illustrated in figure 4.2.1-1), since not only the total heating energy use does not correspond to the actual heating requirements of the building zones, but the potential overheating problems created for most of the working day[7] also increase the demand for mechanical cooling. On the other hand, the

[7] **Note:** It should be remembered that heating is mainly required for the first morning hours to compensate for the low temperatures that occur inside the building during night-time. On the other hand, cooling is usually required for the rest of the day due to the combination of high solar and internal heat gains with the well-insulated building envelope.

reduction of the temperature of the air supplied by the central AHU (i.e. ΔT = 8°C) allows for the 'free' cooling capacity of the fresh air to be utilized, while the fan coil units are left to handle the heating requirement of each building zone separately.

4.2.1-1.1 The factor settings of group D minimising the heating energy consumption depending on the type of HVAC system and the climate for which the simulations are carried out

The temperature control strategy leading to the minimum heating energy consumption and the associated energy savings over the BCS, depending on the HVAC system and the climate under consideration, are shown in table 4.2.1-3:

HVAC system	Climate	Scenario	Factor Levels			Reduction in heating energy over the BCS (%)
			Heating zone air temperature (°C)	Cooling zone air temperature (°C)	Temperature difference (°C)	
FCU system	CIBSE TRY	Base case scenario	*20.0*	*24.0*	*8.0*	-
		Minimum heating energy consumption	18.0	26.0	8.0	-39%
	NOA TRY	Base case scenario	*20.0*	*24.0*	*8.0*	-
		Minimum heating energy consumption	18.0	26.0	8.0	-58%
VAV system	CIBSE TRY	Base case scenario	*20.0*	*24.0*	*8.0*	-
		Minimum heating energy consumption	18.0	26.0	6.0	-47%
	NOA TRY	Base case scenario	*20.0*	*24.0*	*8.0*	-
		Minimum heating energy consumption	18.0	26.0	6.0	-70%

Table 4.2.1-3: The temperature control strategy minimising the requirement for space heating and the associated reduction over the heating energy consumption of the BCS, depending on the HVAC system and the climate for which it is simulated

Table 4.2.1-3 illustrates that setting the heating and cooling zone temperature to 18°C and 26°C respectively, reduces the amount of heating energy consumed by both HVAC systems. The optimum level of the remaining factor is different, however, for each HVAC system. Setting the ΔT between the supply and zone air to 8°C (i.e. the maximum level of this parameter) when the FCU system is considered, reduces the amount of energy consumed by the central heating coil and, hence, the total heating energy use of this system, while the fan coil units

are left to handle the heating requirement of each zone of the building separately. The optimum value of this parameter for the VAV system, on the other hand, is equal to 6°C. Minimising the ΔT between the supply and the zone air, increases the temperature of the supply air quantity and, hence, reduces the amount of energy consumed by the re-heat coils of this system.

4.2.1-2 The effect of the parameters of group D on the cooling energy consumption of the HVAC systems when they are simulated for the CIBSE TRY and the NOA TRY respectively

The effect of all the parameters of group D on the cooling energy consumption of the FCU system for the CIBSE TRY is shown in figure 4.2.1-4:

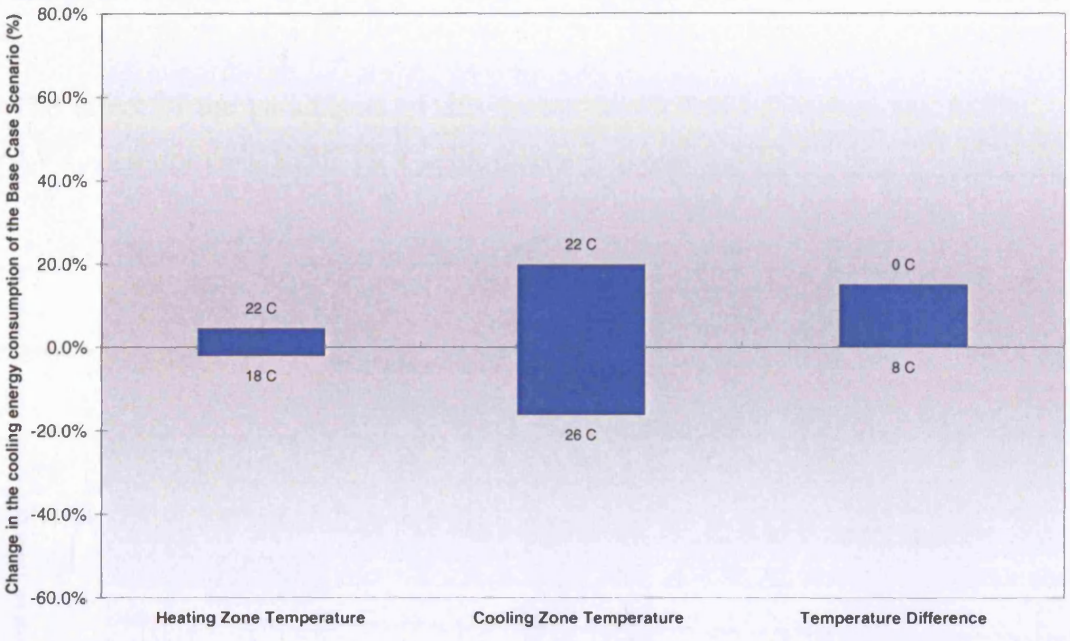

Figure 4.2.1-4: The effect of all the parameters of group D on the cooling energy consumption of the BCS, when the FCU system is simulated for the CIBSE TRY

Figure 4.2.1-4 indicates that the cooling zone temperature set-point has the highest impact on the cooling energy consumption of the FCU system. The cooling energy use drops by approximately 30%, when this parameter is set to 26°C instead of 22°C. The increase of the ΔT between the fresh and zone air

from 0°C to 8°C (i.e. transferring part of the total cooling load from the fan coil units to the central AHU), results in approximately 13% lower cooling energy use, as also shown in this figure. The cooling energy consumption is considerably less sensitive to the ΔT between the supply and zone air than the heating energy use of the FCU system. Nevertheless, it is clear that setting this parameter to 8°C (instead of 0°C) allows for the 'free' cooling potential of the fresh air to be utilized, thereby reducing the total cooling energy consumption of the VAV system. In addition, changing the heating zone temperature set-point from 18°C to 22°C results in approximately 7% higher cooling energy use. It seems that the maintenance of the internal temperature at a high level during the first morning hours (when heating is usually required) leads to overheating problems for the rest of the working day, particularly when high solar and internal heat gains coincide, thereby increasing the use of mechanical cooling over the part of the year that both heating and cooling is available.

The effect of the parameters of this group on the cooling energy use of the VAV system for the CIBSE TRY is illustrated in figure 4.2.1-5:

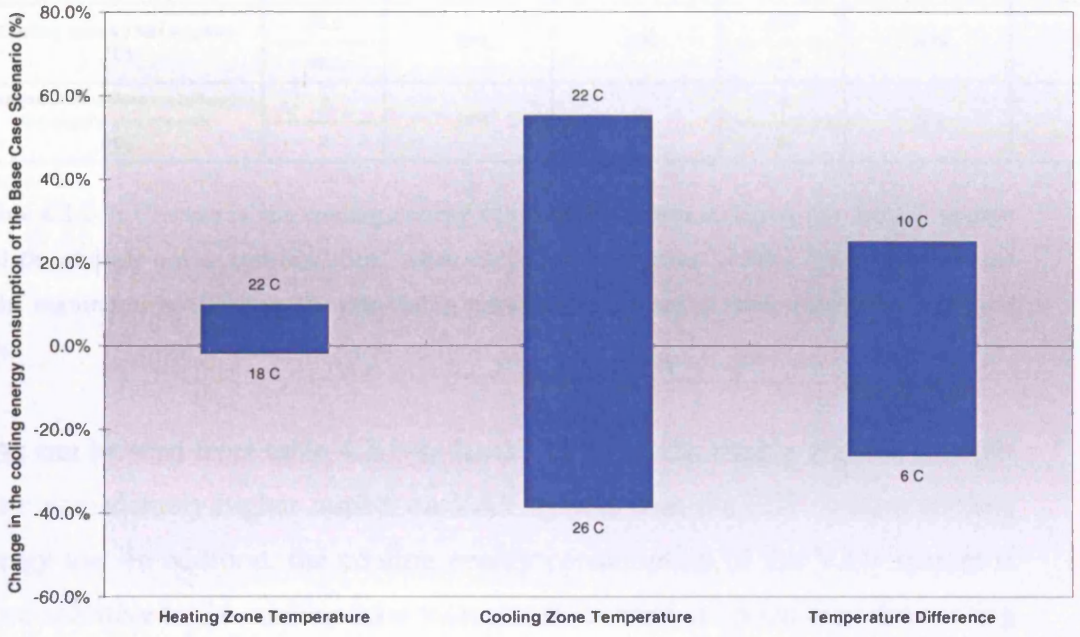

Figure 4.2.1-5: The effect of all the parameters of group D on the annual cooling energy consumption of the BCS, when the VAV system is simulated for the CIBSE TRY

Figure 4.2.1-5 shows that the cooling zone temperature set-point and the ΔT between the supply and the zone air have the highest impact on the cooling energy consumption of the VAV system. The cooling energy use of this system drops by approximately 61%, when the temperature threshold above which cooling becomes available is set to 26°C as opposed to 22°C. In addition, the increase of the ΔT between the supply and the zone air from 6°C to 10°C results in a lower temperature set-point for the central cooling coil, increasing the cooling energy consumption by approximately 70%. On the other hand, changing the heating zone temperature set-point from 18°C to 22°C results in just 10% higher cooling energy use.

The effect of all the parameters of group D on the cooling energy consumption of both HVAC systems when they are simulated for the London and the Athens climate respectively is summarised in table 4.2.1-4:

Factor	Impact on cooling energy use (%)					
	Min and Max Level	FCU system		Min and Max Level	VAV system	
		CIBSE TRY	NOA TRY		CIBSE TRY	NOA TRY
Heating zone air temperature (°C)	18.0	7%	2%	18.0	10%	5%
	22.0			22.0		
Cooling zone air temperature (°C)	22.0	-30%	-23%	22.0	-60%	-37%
	26.0			26.0		
Temperature difference between the supply and zone air (°C)	0	-13%	-6%	6	70%	19%
	8			10		

Table 4.2.1-4: Change in the cooling energy consumption, depending on the HVAC system and the climate under consideration, when each factor of group D rises from its minimum to its maximum level, while the remaining parameters are set to their respective standard level

As can be seen from table 4.2.1-4, the ΔT between the supply and the zone air has a considerably higher impact on VAV system than the FCU system cooling energy use. In addition, the cooling energy consumption of the VAV system is more sensitive to the cooling zone temperature control set-point than the cooling energy use of the FCU system, in both climates, given that the other two parameters are set to their standard level. It should be remembered that the total cooling load is handled by the central AHUs serving the building when the VAV

system is installed. As a result, potential changes to the temperature control settings of this system affect both the air quantities handled by the AHUs and, of course, the total amount of energy consumed by the central cooling coils. In the FCU system, on the other hand, the main part of the total cooling load is handled locally by the fan coil units, while the remaining (small part) is handled by the central AHU supplying the minimum fresh air quantity (for ventilation purposes) to the building zones. The simulation results show, however, that the respective changes in the cooling zone temperature set-point of this system affect mainly the amount of energy consumed by the central cooling coil[8], while the energy use of the fan coil units and, hence, the total cooling energy consumption of the FCU system is relatively less sensitive to the parameter under consideration.

Table 4.2.1-4 also indicates that the sensitivity of the cooling energy consumption to the parameters of this group drops when the HVAC systems are simulated for the Athens in place of the London climate. This is clearly due to the combination of high external temperatures and solar gains involved in the former, which leads to a high amount of cooling energy use for all the settings of the parameters of this group.

[8] **Note:** It should be remembered that in the FCU system: (central cooling coil temperature set-point) = (zone temperature set-point) – (ΔT between the fresh and the zone air).

4.2.1-2.1 The factor settings of group D minimising the cooling energy consumption depending on the HVAC system and the climate for which it is simulated

The temperature control strategy leading to the minimum cooling energy consumption and the associated energy savings over the BCS, depending on the HVAC system and the climate under consideration are shown in table 4.2.1-5:

HVAC system	Climate	Scenario	Factor Levels			Reduction in cooling energy over the BCS (%)
			Heating zone air temperature (°C)	Cooling zone air temperature (°C)	Temperature difference (°C)	
FCU system	CIBSE TRY	Base case scenario	*20.0*	*24.0*	*8.0*	-
		Minimum cooling energy consumption	18.0	26.0	8.0	-18%
	NOA TRY	Base case scenario	*20.0*	*24.0*	*8.0*	-
		Minimum cooling energy consumption	18.0	26.0	8.0	-13%
VAV system	CIBSE TRY	Base case scenario	*20.0*	*24.0*	*8.0*	-
		Minimum cooling energy consumption	18.0	26.0	6.0	-59%
	NOA TRY	Base case scenario	*20.0*	*24.0*	*8.0*	-
		Minimum cooling energy consumption	18.0	26.0	6.0	-28%

Table 4.2.1-5: The combination of factor levels minimising the use of mechanical cooling and the associated reduction over the cooling energy consumption of the BCS depending on the HVAC system and the climate for which it is simulated

Table 4.2.1-5 illustrates that maximising the temperature limit above which cooling becomes available reduces the amount of energy consumed by both HVAC systems, while setting the heating zone temperature as low as possible helps to maintain a relatively 'cool' internal environment, thereby reducing potential overheating problems during the working day, for the period of the year that both heating and cooling is available. Also, the ΔT between the supply and the zone air is set to 8°C for the FCU system, allowing for the utilisation of the 'free' cooling capacity of the fresh air. Setting this parameter to 6°C for the VAV system, on the other hand, results in a high temperature control set-point for the central cooling coils and, hence, reduces the amount of cooling energy consumed by this system.

4.2.1-3 Summary of the findings derived from the study of the effect of the factors contained in group D on the energy performance of the HVAC systems in both climates

It has been found that the heating energy consumption of the FCU system is particularly sensitive to the heating zone temperature set-point and the ΔT between the supply and the zone air, while the cooling zone temperature set-point has the highest impact on the cooling energy use of this system. On the other hand, the heating zone temperature set-point has a dominating effect on the heating energy consumption of the VAV system, while the cooling zone temperature set-point and the ΔT between the supply and the zone air have the highest effect on the cooling energy use of this system. Both the heating and cooling energy consumption of each HVAC system are minimized for the same temperature control strategy. The optimum value of the ΔT between the supply and the zone air differs, however, depending on the HVAC system under consideration. This is due to the fact that both the range of values and the 'role' of this parameter on the control of the internal air temperature are different for each system, as explained at the outset of this study.

4.2.2 The effect of the parameters associated with the provision of night ventilation throughout the cooling period (group E) on the energy performance of the HVAC systems

The aim of this study is to investigate the effect of the parameters associated with the night ventilation strategy implemented over the summer period (i.e. June, July and August) on the energy performance of the FCU system and the VAV system, when they are simulated for the London and the Athens climate respectively. Secondary aims include the identification of factor settings that minimize the annual energy consumption of each system in both climates.

The parameters studied in this section and their range of values are displayed in table 4.2.2-1:

Factors	Values		
	Standard	Minimum	Maximum
Factor A: Ventilation rate (ach)	-	5.0	10.0
Factor B: Duration of ventilation (hours)	-	4	10

Table 4.2.2-1: The range of values of the factors of group E

Details concerning the chosen range values for the parameters shown in this table can be found in section 3.3.2, chapter 3. It should be remembered that the required fresh air quantity is distributed around the perimeter zones of the building during the night, using only natural means, while the core zones are served using the central fans of the HVAC systems.

The parameters of this group are correlated with the cooling energy use of the VAV system and the FCU system respectively. This procedure is repeated for both climates, so four response surface models are developed in total. These models can be found in appendix H, section H.2.2.

Section 4.2.2-1 presents the calculation of the electricity consumed by the central fans serving the core zones of the building, as mentioned above. Section 4.2.2-2 discusses the effect of the parameters of group E on the energy

performance of the HVAC systems in both climates for which the simulations are carried out. The findings of this study are summarized in section 4.2.2-3.

4.2.2-1 Calculation of the fan energy consumption for the provision of night ventilation

The amount of energy consumed by the central fans operating during the night can be estimated by multiplying the number of hours of operation by the fan power developed when the required fresh air quantity flows through the system. The fan power is calculated using the following equation:

$$\text{Fan Power} = \frac{Air\_Power}{n} = \frac{(FTP) \times Q}{n} \quad (1)$$

The efficiency of the fans simulated in TAS is n = 0.78[9], so the problem is reduced to the estimation of the fan total pressure (FTP) and the fresh air flow rate Q. Sections 4.2.2-1.1 and 4.2.2-1.2 contain the calculation of the electricity consumed by the central fans of the VAV system and the FCU system, respectively.

4.2.2-1.1 Calculation of the energy consumption of the central fans of the VAV system serving the core zones of the building

The volumetric flow rate Q (m^3 / s) for both the minimum and the maximum (night) ventilation rate shown in table 4.2.2-1 is calculated in the following:

A. The total fresh air flow rate (m^3 / s) when the number of air changes is 5.0, is equal to: Q_{Atot} = (Number of ach) x (Total Volume) = $5.0 \times (16831) \approx 84155$ m^3 / hr or 23.4 m^3 / s.

[9] **Note:** This is the default value of the fan efficiency in the TAS database, corresponding to a backward curved centrifugal fan, as explained in section 3.3.2, chapter 3.

B. The total fresh air flow rate (m^3 / s) when the number of air changes is 10.0, is equal to: $Q_{Btot} = 46.8\ m^3 / s$.

It is worth mentioning that the term 'Total Volume' stands for the volume of all the core zones of the case study building.

It is assumed that the required fresh air quantity is supplied to the core zones of the building during the night using the three central AHUs located on the roof. Each unit will be supplying:

$$\text{A. } Q_A = \frac{Q_{Atot}}{3} = \frac{23.4}{3} = 7.8\ m^3 / s$$

$$\text{B. } Q_B = \frac{Q_{Btot}}{3} = \frac{46.8}{3} = 15.6\ m^3 / s$$

For any given ducting system: $\frac{\Delta P_1}{\Delta P_2} = \frac{(Q_1)^2}{(Q_2)^2}$ (2)

Using equation (2) for the characteristic behaviour of a ductwork system, it is possible to calculate the pressure ΔP_2 when the volumetric flow rate equals Q_A=7.8 m^3 / s or Q_B=15.6 m^3 / s, as illustrated in table 4.2.2-2 and 4.2.2-3 for the CIBSE TRY and the NOA TRY respectively:

Air Handling Units	Base case scenario			A. Night ventilation @ 5.0 ach			B. Night ventilation @ 10.0 ach		
	Supply Fans (Pa)	Return Fans (Pa)	Q (m^3 /s)	Supply Fans (Pa)	Return Fans (Pa)	Q_A (m^3 /s)	Supply Fans (Pa)	Return Fans (Pa)	Q_B (m^3 /s)
AHU_1	677	162	23	78	19	7.8	311	75	15.6
AHU_2	668	156	24	71	16	7.8	282	66	15.6
AHU_3	660	156	24	70	16	7.8	279	66	15.6

Table 4.2.2-2: FTP for the VAV system simulated for the CIBSE TRY, when the night ventilation rate equals (A) 5.0 ach and (B) 10.0 ach respectively

Air Handling Units	Base case scenario			A. Night ventilation @ 5.0 ach			B. Night ventilation @ 10.0 ach		
	Supply Fans (Pa)	Return Fans (Pa)	Q (m^3 /s)	Supply Fans (Pa)	Return Fans (Pa)	Q_A (m^3 /s)	Supply Fans (Pa)	Return Fans (Pa)	Q_B (m^3 /s)
AHU_1	681	156	27	57	13	7.8	227	52	15.6
AHU_2	677	156	28	53	12	7.8	210	48	15.6
AHU_3	672	156	28	52	12	7.8	209	48	15.6

Table 4.2.2-3: FTP for the VAV system simulated for the NOA TRY, when the night ventilation rate equals (A) 5.0 ach and (B) 10.0 ach respectively

Using equation (1) and the FTPs illustrated in tables 4.2.2-2 and 4.2.2-3, it is possible to estimate the fan power (W) for both night ventilation rates under consideration.

In addition, assuming that night ventilation is provided for 10 hours per night or 660 hours per year[10], the annual fan energy consumption will be:
(Fan Energy Consumption) = (Fan Power) x 660.

Both the fan power and the fan energy consumption are presented in table 4.2.2-4 and 4.2.2-5 for the CIBSE TRY and the NOA TRY respectively:

Air Handling Units	A. Night ventilation @ 5.0 ach				B. Night ventilation @ 10.0 ach			
	Supply Fan Power (W)	Return Fan Power (W)	Supply Fan Energy Consumption (kWh)	Return Fan Energy Consumption (kWh)	Supply Fan Power (W)	Return Fan Power (W)	Supply Fan Energy Consumption (kWh)	Return Fan Energy Consumption (kWh)
AHU_1	779	186	514	123	6229	1491	4111	984
AHU_2	706	165	466	109	5645	1318	3725	870
AHU_3	697	165	460	109	5577	1318	3681	870
	A. Total Fan Energy Consumption (kWh)		1780		B.Total Fan Energy Consumption (kWh)		14241	

Table 4.2.2-4: Fan power and energy use for the VAV system simulated for the CIBSE TRY, when the night ventilation rate equals: (A) 5.0 ach and (B) 10.0 ach respectively

[10] **Note:** It should be remembered that night ventilation is provided for 5 days per week during the cooling period (i.e. June, July and August) or, in other words, for 66 days per year.

Air Handling Units	A. Night ventilation @ 5.0 ach				B. Night ventilation @ 10.0 ach			
	Supply Fan Power (W)	Return Fan Power (W)	Supply Fan Energy Consumption (kWh)	Return Fan Energy Consumption (kWh)	Supply Fan Power (W)	Return Fan Power (W)	Supply Fan Energy Consumption (kWh)	Return Fan Energy Consumption (kWh)
AHU_1	568	130	375	86	4547	1042	3001	687
AHU_2	525	121	347	80	4203	968	2774	639
AHU_3	521	121	344	80	4172	968	2753	639
	A.Total Fan Energy Consumption (kWh)		1312		B.Total Fan Energy Consumption (kWh)		10494	

Table 4.2.2-5: Fan power and energy use for the VAV system simulated for the NOA TRY, when the night ventilation rate equals: (A) 5.0 ach and (B) 10.0 ach respectively

It is, of course, possible to estimate the fan energy consumption for all the combinations of the ventilation rate (factor A) and the duration of ventilation (factor B) using the procedure illustrated in this section.

4.2.2-1.2 Calculation of the energy consumed by the central fans serving the core zones of the building, when the FCU system is considered

The central fans of the FCU system were sized so that they deliver the minimum fresh air quantity (i.e. 8 l / s per person) for ventilation purposes, which is equal to 9.1 m^3 / s for the BCS. Assuming that night ventilation is provided at 5.0 ach, (i.e. the minimum ventilation rate shown in table 4.2.2-1), the central AHU must supply 23.4 m^3 / s or in other words, a 2.6 times higher flow rate than the BCS. It is obvious that such a flow rate exceeds the capacity limits of the AHU installed in the case study building.

It seems that in order to supply a ventilation flow rate of 23.4 m^3 / s (i.e. 5 ach) or 46.8 m^3 / s (i.e. 10 ach) over the night, it would be necessary to size the central fans installed in the case study building using one of these flow rates instead of a flow rate of 9.1 m^3 / s. However, this would increase not only the initial & operating cost of the fans but the overall energy use of the system as well, since the (larger in this case) fans would operate at a flow rate of 23.4 m^3 /s (or 46.8 m^3 /s) only for three months of the year (i.e. the cooling period when night ventilation is provided), while for the rest of the time they would simply supply the minimum fresh air quantity.

It was, therefore, decided to set the night ventilation rate for the core zones of the building to 1.5 ach. This is close to the maximum ventilation rate that can be supplied to these zones, without exceeding the capacity limits of the single AHU that serves the case study building when the FCU system is considered.

Using equation (2) for the characteristic behaviour of a ductwork system, it is possible to calculate the pressure ΔP_2 when the volumetric flow rate equals Q = 7.0 m^3 / s (i.e. 1.5 ach). The estimated pressure is illustrated in table 4.2.2-6 and 4.2.2-7 for the CIBSE TRY and the NOA TRY, respectively:

Air Handling Units	Base case scenario			Night ventilation @ 1.5 ach		
	Supply Fans (Pa)	Return Fans (Pa)	Q (m^3/s)	Supply Fans (Pa)	Return Fans (Pa)	Q (m^3/s)
AHU_1	421	197	9.1	249	117	7.0

Table 4.2.2-6: FTP for the FCU system simulated for the CIBSE TRY, when the night ventilation rate equals 1.5 ach

Air Handling Units	Base case scenario			Night ventilation @ 1.5 ach		
	Supply Fans (Pa)	Return Fans (Pa)	Q (m^3/s)	Supply Fans (Pa)	Return Fans (Pa)	Q (m^3/s)
AHU_1	474	197	9.1	280	117	7.0

Table 4.2.2-7: FTP for the FCU system simulated for the NOA TRY, when the night ventilation rate equals 1.5 ach

Using equation (1) and the FTPs presented in tables 4.2.2-6 and 4.2.2-7, it is possible to estimate the fan power (W) for the night ventilation rate under consideration. The fan energy use is then calculated by multiplying the fan power by the 660 hours of operation, as explained in section 4.2.2-1.1. Both the fan power and the fan energy use are presented in table 4.2.2-8 and 4.2.2-9 for the London and the Athens climate, respectively:

Air Handling Units	Night ventilation @ 1.5 ach			
	Supply Fan Power (W)	Return Fan Power (W)	Supply Fan Energy Consumption (kWh)	Return Fan Energy Consumption (kWh)
AHU_1	2236	1046	1476	690
	Total Fan Energy Consumption (kWh)		2166	

Table 4.2.2-8: Fan power and energy use for the FCU system simulated for the CIBSE TRY, when the night ventilation rate equals 1.5 ach

Air Handling Units	Night ventilation @ 1.5 ach			
	Supply Fan Power (W)	Return Fan Power (W)	Supply Fan Energy Consumption (kWh)	Return Fan Energy Consumption (kWh)
AHU_1	2517	1046	1661	690
	Total Fan Energy Consumption (kWh)		2352	

Table 4.2.2-9: Fan power and energy use for the FCU system simulated for the NOA TRY, when the night ventilation rate equals 1.5 ach

The FCU system (night) fan energy consumption can be estimated for the entire range of values of the duration of ventilation (factor B), using the procedure described above.

4.2.2-2 The effect of the parameters of group E on the cooling energy consumption of the HVAC systems, when they are simulated for the CIBSE TRY and the NOA TRY respectively

The effect of the parameters of group E on the cooling energy use of the FCU system for the CIBSE TRY is illustrated in figure 4.2.2-1. This plot usually shows how the cooling energy is affected as each factor moves from its respective value for the BCS, while the remaining parameters are held constant at their standard value. However, in this case night ventilation is not provided in the BCS. As a result, figure 4.2.2-1 shows the effect of each factor on the cooling energy use of the BCS, while the other factor is held constant at its mid-level[11].

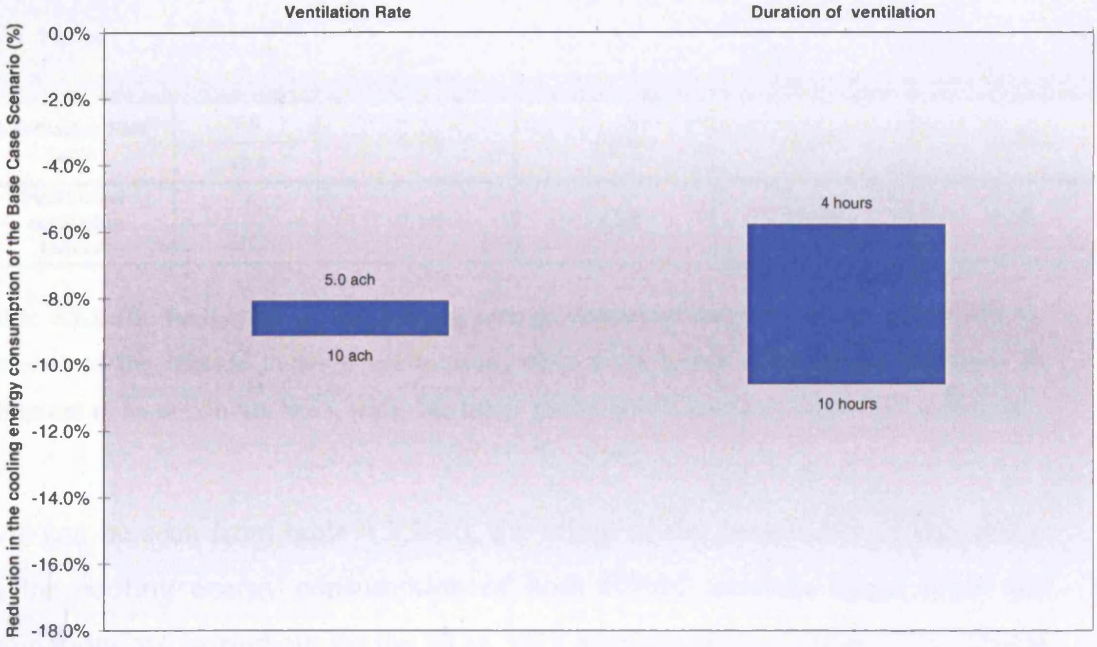

Figure 4.2.2-1: The effect of the parameters of group E on the cooling energy consumption of the BCS, when the FCU system is simulated for the CIBSE TRY

As explained in section 4.2.2-1.2, due to the capacity limits of the AHU serving the case study building when the FCU system is considered, the night ventilation rate ranges from 5 to 10 ach only in the perimeter, (natural ventilation), while it is held constant at 1.5 ach in the core zones of the building (mechanical ventilation). Figure 4.2.2-1 shows that the cooling energy use of this HVAC

[11] **Note:** Mid-value = (Minimum value + Maximum value) / 2

system is considerably more sensitive to the number of hours that night ventilation is provided than the ventilation rate. The introduction of fresh air into the building at a ventilation rate of 7.5 ach, (i.e. the mid-level of factor A), for 10 instead of 4 hours, results in 5% lower cooling energy use. On the other hand, the cooling energy consumption drops by just 1% when the ventilation rate changes from 5 to 10 ach, while night ventilation is provided for 7 hours (i.e. the mid-level of factor B).

The effect of all the parameters of this group on the cooling energy consumption of both HVAC systems when they are simulated for the London and the Athens climate respectively is summarised in table 4.2.2-10:

Factor	Min and Max Level	Impact on cooling energy use (%)			
		FCU system		VAV system	
		CIBSE TRY	NOA TRY	CIBSE TRY	NOA TRY
Ventilation Rate (ach)	5.0	-1.1%	-0.4%	-2.5%	-0.6%
	10.0				
Duration of ventilation (hours)	4	-5.1%	-1.3%	-7.6%	-1.7%
	10				

Table 4.2.2-10: Reduction in the cooling energy consumption, depending on the HVAC system and the climate under consideration, when each factor of group E rises from its minimum to its maximum level, while the other parameter is set to its respective mid-level

As can be seen from table 4.2.2-10, the effect of the parameters of this group on the cooling energy consumption of both HVAC systems drops when the simulations are carried out for the NOA TRY in place of the CIBSE TRY. This is clearly due to the high ambient temperatures involved in the climate of Athens.

4.2.2-2.1 The factor settings of group E minimising the cooling energy consumption depending on the HVAC system and the climate for which it is simulated

The night ventilation strategy resulting in the minimum cooling energy use and the associated energy savings over the BCS, depending on the HVAC system and the climate under consideration are shown in table 4.2.2-11:

HVAC system	Climate	Scenario	Factor Levels		Reduction in cooling energy over the BCS (%)
			Ventilation Rate (ach)	Period of ventilation (hours)	
FCU system	CIBSE TRY	Base case scenario	-	-	-
		Minimum cooling energy consumption	*10.0*	*10*	-11%
	NOA TRY	Base case scenario	-	-	-
		Minimum cooling energy consumption	*10.0*	*10*	-3%
VAV system	CIBSE TRY	Base case scenario	-	-	-
		Minimum cooling energy consumption	*10.0*	*10*	-16%
	NOA TRY	Base case scenario	-	-	-
		Minimum cooling energy consumption	*10.0*	*10*	-4%

Table 4.2.2-11: The combination of factor levels minimising the use of mechanical cooling and the associated reduction over the cooling energy consumption of the BCS depending on the type of HVAC system and the climate for which it is simulated

As can be seen from the night ventilation strategy displayed in table 4.2.2-11, the combination of a high ventilation rate with the provision of fresh air for several hours during the night, when the building is unoccupied, helps to maintain a cool internal environment until the following working day, thereby reducing the demand for mechanical cooling. The impact of this night ventilation strategy on the cooling energy consumption of both HVAC systems is particularly high when the simulations are carried out for the London climate, as can be seen from the last column of table 4.2.2-11.

Taking into consideration, on the other hand, the electricity consumed by the central fans of the FCU system (as illustrated in tables 4.2.2-8 and 4.2.2-9), the

maximum energy savings[12] over the BCS drop to approximately 10% and 2.6% for the CIBSE TRY and the NOA TRY respectively. The additional energy cost due to the fans operating during the night is trivial, since they are constantly supplying only a ventilation rate of 1.5 ach, while they serve only the core zones of the building.

Taking into account the electricity consumed by the central fans of the VAV system operating at a ventilation rate of 10 ach, (as illustrated in tables 4.2.2-4 & 4.2.2-5), the maximum energy savings over the BCS drop to 5% and 1.4%, when this system is simulated for the London and the Athens climate respectively. It is clear that the energy cost of the central fans serving the core zones during the night is significant in this case, due to the high (night) ventilation rate supplied by the VAV system (i.e. 10 ach).

Table 4.2.2-10 illustrated that the ventilation rate (factor A) has a rather trivial effect on the cooling energy consumption of the VAV system. This means that the cooling energy savings over the BCS will not be considerably reduced if fresh air is introduced into the building at a ventilation rate lower than 10 ach. For example, the provision of night ventilation for 10 hours at a ventilation rate of 5.0 ach results in approximately 14% lower cooling energy consumption than the BCS, when the VAV system is simulated for the CIBSE TRY. On the other hand, factor A seems to have a high impact on the amount of energy consumed by the central fans serving the core zones of the building. As can be seen from table 4.2.2-4 (or 4.2.2-5), the provision of fresh air at a ventilation rate of 5 ach as opposed to 10 ach for 10 hours during the night using the central fans of the VAV system, results in 87.5% lower (fan) electricity consumption. It is, therefore, clear that the optimum night ventilation strategy for the VAV system involves the provision of night ventilation for 10 hours at a ventilation rate of 5 ach. In such a case, the energy savings (including both the cooling energy use and the electricity consumed by the fans operating during the night) over the

[12] **Note:** In this case, the energy consumed by the central fans operating during the night is first added to the annual cooling energy consumption of the FCU system, and then the energy savings over the BCS are calculated. It is, of course, assumed that both the chiller and the central fans operate on electricity.

BCS are equal to approximately 13% and 3.3% when the VAV system is simulated for the London and the Athens climate respectively.

4.2.2-3 Summary of the findings derived from the study of the effect of the factors contained in group E on the energy performance of the HVAC systems in both climates

To sum up, it was decided to use a natural ventilation strategy for the perimeter zones and fan-assisted ventilation for the core zones of the case study building, in order to avoid the potential problems associated with the movement of the desired fresh air quantity through the deep-plan core zones, using only natural means. It has been found that the period of ventilation has a considerably higher effect on the cooling energy consumption of both HVAC systems than the ventilation rate.

The optimization results have illustrated that night ventilation should be provided for 10 hours (per day) in both climates, regardless of the HVAC system installed. The night ventilation rate is set to 10 ach in the perimeter zones of the building, while it is limited to only 1.5 ach in the cores zones, since the capacity limit of the AHU supplying the fresh air around the building when the FCU system is considered does not allow for the provision of a higher ventilation rate than this.

On the other hand, the night ventilation rate is set to 5 ach in both the perimeter and the core zones of the building when the VAV system is installed. Although the specification of a higher ventilation rate than this does not have a significant impact on the cooling energy use, it has been found that it increases considerably the amount of electricity consumed by the central fans of the VAV system, serving the core zones of the building during the night.

4.2.3 The effect of the parameters related to the plant performance and operation (group F) on the energy performance of the HVAC systems

The aim of this study is to investigate the effect of the parameters related to the operation schedule and the efficiency of the plant on the energy performance of the HVAC systems when they are simulated for the London and the Athens climate respectively. Secondary aims include the identification of factor levels that minimize the annual heating and cooling energy consumption of each system in both climates.

The parameters studied in this section and their range of values are displayed in table 4.2.3-1:

Factors	Values		
	Standard	Minimum	Maximum
Factor A: Boiler efficiency (%)	85%	75%	95%
Factor B: Chiller COP	2.5	1.9	5.2
Factor C: HVAC system operation schedule (hours)	10	9	17

Table 4.2.3-1: The range of values of the factors of group F

The factors shown in this table are correlated with the heating & cooling energy consumption of the FCU system and the VAV system respectively. This procedure is repeated for both climates, so eight response surface models are developed in total. These models can be found in appendix H, section H.2.3.

Sections 4.2.3-1 and 4.2.3-2 analyse the effect of the parameters of group F on the heating and cooling energy consumption of the HVAC systems respectively in both climates for which they are simulated. The findings obtained from this study are summarized in section 4.2.3-3.

4.2.3-1 The effect of the parameters of group F on the heating energy consumption of the HVAC systems, when they are simulated for the CIBSE TRY and the NOA TRY respectively

The effect of the parameters associated with the plant performance & operation on the heating energy consumption of the FCU system for the CIBSE TRY is illustrated in figure 4.2.3-1:

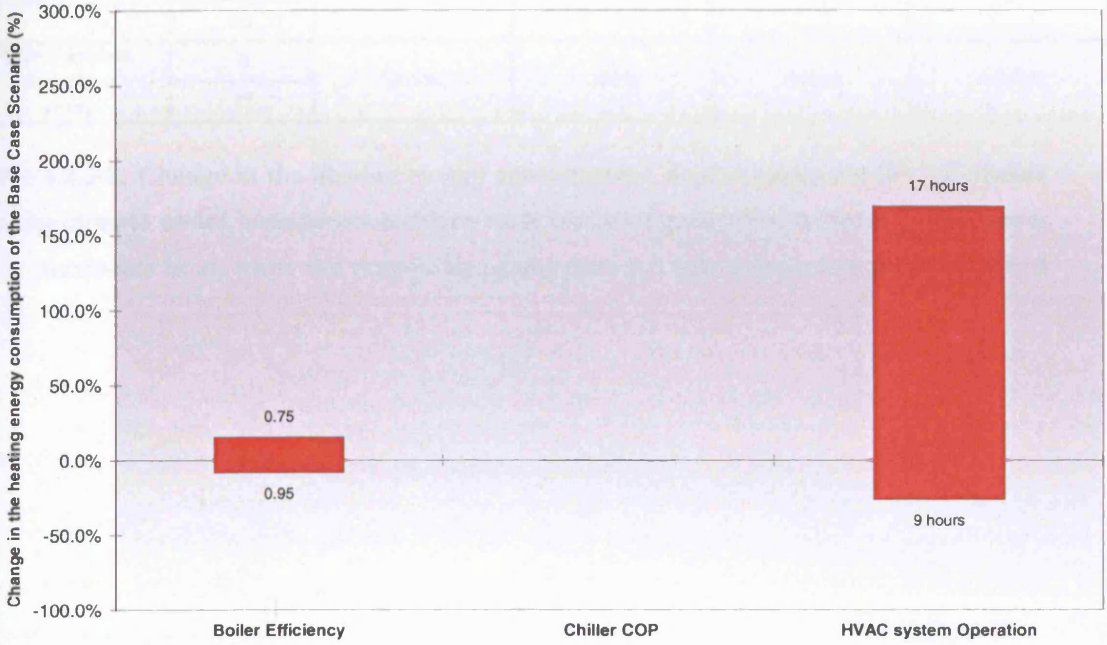

Figure 4.2.3-1: The effect of the parameters of group F on the heating energy consumption of the BCS, when the FCU system is simulated for the CIBSE TRY

As can be seen from this figure, the number of hours that the plant operates has a dominating effect on the heating energy consumption of the FCU system. The heating energy use of this HVAC system increases by a factor of 3.6 approximately when the heating plant operates for 17 hours as opposed to 9 hours per day. It is clear that maintaining the internal temperature throughout the building at a constant level for most of the day is a particularly energy wasteful control strategy. On the other hand, increasing the efficiency of the boiler from 0.75 to 0.95 results in approximately 21% lower heating energy consumption.

The effect of the parameters of this group on the heating energy consumption of both HVAC systems when they are simulated for the CIBSE TRY and the NOA TRY respectively is summarised in table 4.2.3-2:

Factor	Min and Max Level	Impact on heating energy use (%)			
		FCU system		VAV system	
		CIBSE TRY	NOA TRY	CIBSE TRY	NOA TRY
Boiler Efficiency (%)	75%	-21%	-21%	-21%	-21%
	95%				
Chiller COP	1.9	-	-	-	-
	5.2				
HVAC system operation (hrs)	9	265%	388%	536%	1100%
	17				

Table 4.2.3-2: Change in the heating energy consumption, depending on the HVAC system and the climate under consideration, when each factor of group F rises from its minimum to its maximum level, while the remaining parameters are set to their respective standard level

4.2.3-1.1 The factor settings of group F minimising the heating energy consumption depending on the type of HVAC system and the climate for which the simulations are carried out

Installing a high efficiency condensing boiler (i.e. boiler efficiency = 95%) and operating the heating plant for 9 hours per day results in considerably lower heating energy use than the BCS, as can be seen from table 4.2.3-3:

HVAC system	Climate	Scenario	Factor Levels			Reduction in heating energy over the BCS (%)
			Boiler Efficiency (%)	Chiller COP	HVAC system operation (hours)	
FCU system	CIBSE TRY	Base case scenario	*0.85*	*2.50*	*10*	-
		Minimum heating energy consumption	0.95	-	9	-33%
	NOA TRY	Base case scenario	*0.85*	*2.50*	*10*	-
		Minimum heating energy consumption	0.95	-	9	-41%
VAV system	CIBSE TRY	Base case scenario	*0.85*	*2.50*	*10*	-
		Minimum heating energy consumption	0.95	-	9	-46%
	NOA TRY	Base case scenario	*0.85*	*2.50*	*10*	-
		Minimum heating energy consumption	0.95	-	9	-61%

Table 4.2.3-3: The combination of factor levels minimising the requirement for space heating and the associated reduction over the heating energy consumption of the BCS, depending on the HVAC system and the climate for which it is simulated

4.2.3-2 The effect of the parameters of group F on the cooling energy consumption of the HVAC systems when they are simulated for the CIBSE TRY and the NOA TRY respectively

The effect of the parameters of group F on the cooling energy consumption of the FCU system for the CIBSE TRY is shown in figure 4.2.3-2:

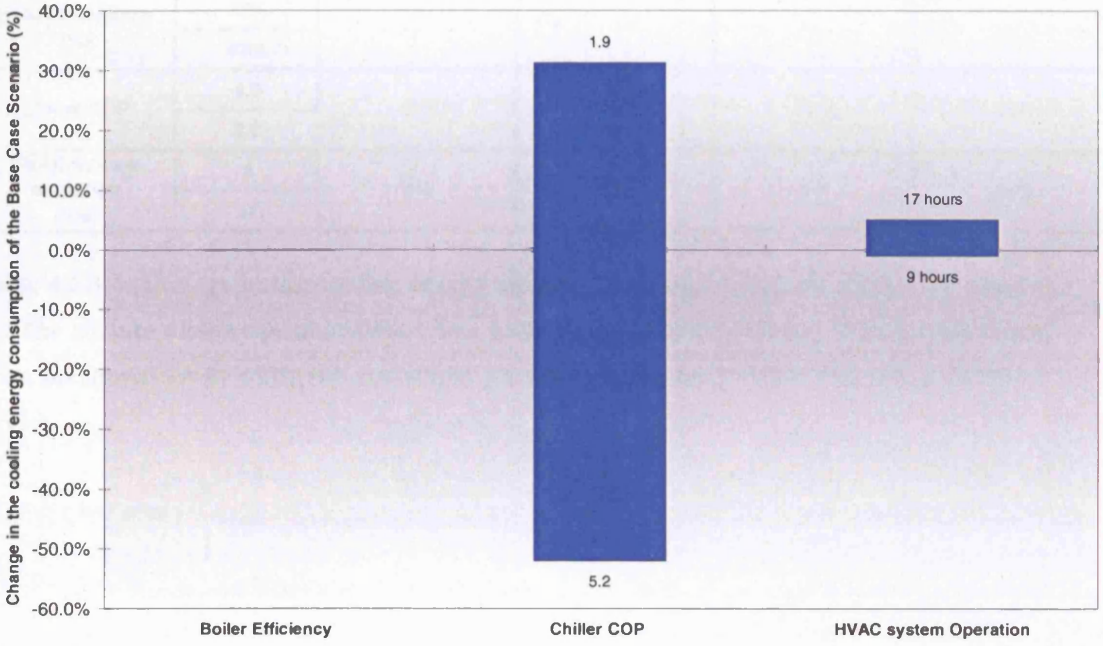

Figure 4.2.3-2: The effect of the parameters of group F on the cooling energy consumption of the BCS, when the FCU system is simulated for the CIBSE TRY

Figure 4.2.3-2 shows that the cooling energy use of the FCU system is considerably more sensitive to the COP of the chiller than the number of the hours that the plant operates. The cooling energy consumption of this system drops by approximately 63% when the chiller COP increases from 1.90 to 5.20. On the other hand, the operation of the plant for 17 hours instead of 9 hours per day, results in just 4% higher cooling energy consumption, since the cooling requirement of the building drops considerably outside the normal occupation period.

The effect of all the design factors of this group on the cooling energy consumption of both HVAC systems when they are simulated for the London and the Athens typical weather conditions respectively is summarised in table 4.2.3-4:

Factor	Min and Max Level	Impact on cooling energy use (%)			
		FCU system		VAV system	
		CIBSE TRY	NOA TRY	CIBSE TRY	NOA TRY
Boiler Efficiency (%)	75%	-	-	-	-
	95%				
Chiller COP	1.9	-63%	-63%	-63%	-63%
	5.2				
HVAC system operation (hrs)	9	4%	14%	8%	17%
	17				

Table 4.2.3-4: Change in the cooling energy consumption, depending on the HVAC system and the climate under consideration, when each factor of group F rises from its minimum to its maximum level, while the remaining parameters are set to their respective standard level

4.2.3-2.1 The factor settings of group F minimising the cooling energy consumption depending on the HVAC system and the climate for which it is simulated

The installation of a high efficiency water cooled chiller (i.e. COP = 5.2) in combination with the operation of the plant for 9 hours per day, approximately halves the cooling energy consumption of the BCS, as shown in table 4.2.3-5:

HVAC system	Climate	Scenario	Factor Levels			Reduction in cooling energy over the BCS (%)
			Boiler Efficiency (%)	Chiller COP	HVAC system operation (hours)	
FCU system	CIBSE TRY	Base case scenario	*0.85*	*2.50*	*10*	-
		Minimum cooling energy consumption	-	5.20	9	-52%
	NOA TRY	Base case scenario	*0.85*	*2.50*	*10*	-
		Minimum cooling energy consumption	-	5.20	9	-53%
VAV system	CIBSE TRY	Base case scenario	*0.85*	*2.50*	*10*	-
		Minimum cooling energy consumption	-	5.20	9	-53%
	NOA TRY	Base case scenario	*0.85*	*2.50*	*10*	-
		Minimum cooling energy consumption	-	5.20	9	-53%

Table 4.2.3-5: The combination of factor levels minimising the use of mechanical cooling and the associated reduction over the cooling energy consumption of the BCS depending on the HVAC system and the climate for which it is simulated

It should be stressed that this reduction is mainly due to the dominating effect of the chiller COP (factor B) on the cooling energy use of both HVAC systems which remains approximately the same in both climates[13] for which the simulations are carried out.

[13] **Note:** In a real application, the ambient temperatures affect the condensing temperatures and, hence, the overall efficiency of the chilled water system. However, the operating points of a chiller, such as the condensing and evaporating temperatures are not considered by B-TAS. A single chiller COP is therefore assumed, which is taken to apply at all external temperatures (as a seasonal average). In addition, B-TAS cannot simulate the energy performance of auxiliary systems such as chilled water & condenser water pumps or cooling tower fans.

4.2.3-3 Summary of the findings derived from the study of the effect of the factors contained in group F on the energy performance of the HVAC systems in both climates

To sum up, the number of hours that the plant operates has the highest impact on the heating energy consumption of the HVAC systems. As mentioned in chapter 3 (section 3.3.2), on average most HVAC systems installed in real office buildings run twice as long as the most conservative estimate of the occupancies served[14]. Table 4.2.3-2 has shown that the operation of the heating plant for most of the day (i.e. for 17 hours) is very energy wasteful for both systems and climates considered in this study. On the other hand, the chiller COP has a dominating effect on the cooling energy consumption of the HVAC systems. The installation of a high efficiency condensing boiler (i.e. boiler efficiency = 95%) and a water cooled chiller with a high seasonal COP (i.e. a COP of 5.2) reduces the heating and cooling energy use of both systems respectively. In addition, the operation of the plant for as short a time as possible (e.g. for 9 hours) has a positive impact on both the heating and the cooling energy use of the HVAC systems.

[14] **Note:** Ian Knight, Gavin Dunn, Size does matter, Building Services Journal, August 2004, pg. 34-36.

4.2.4 The effect of the design factors associated with the fan size and efficiency (group G) on the energy performance of the HVAC systems

The aim of this study is to investigate the effect of the parameters related to the size & efficiency of the central fans on the energy performance of the HVAC systems, when they are simulated for the London and the Athens climate, respectively. Secondary aims include the identification of factor settings that minimize the energy consumption of each system in both climates.

The parameters studied in this section and their range of values are displayed in table 4.2.4-1 and 4.2.4-2 for the VAV system and the FCU system, respectively:

HVAC system	Climate	Factors	Values		
			Standard	Minimum	Maximum
VAV system	CIBSE TRY	Factor A: Fan Efficiency (%)	78%	45%	90%
		Factor B: Motor Efficiency (%)	90%	75%	95%
		Factor C: Fan Total Pressure (FTP) - Supply Fan (Pa)	677	500	1500
		Factor D: Fan Total Pressure (FTP) - Extract Fan (Pa)	162	120	360
	NOA TRY	Factor A: Fan Efficiency (%)	78%	45%	90%
		Factor B: Motor Efficiency (%)	90%	75%	95%
		Factor C: Fan Total Pressure (FTP) - Supply Fan (Pa)	681	500	1500
		Factor D: Fan Total Pressure (FTP) - Extract Fan (Pa)	156	120	360

Table 4.2.4-1: The range of values of the four factors of group G for the VAV system

HVAC system	Climate	Factors	Values		
			Standard	Minimum	Maximum
FCU system	CIBSE TRY	Factor A: Fan Efficiency (%)	78%	45%	90%
		Factor B: Motor Efficiency (%)	90%	75%	95%
		Factor C: Fan Total Pressure (FTP) - Supply Fan (Pa)	421	300	900
		Factor D: Fan Total Pressure (FTP) - Extract Fan (Pa)	197	140	420
	NOA TRY	Factor A: Fan Efficiency (%)	78%	45%	90%
		Factor B: Motor Efficiency (%)	90%	75%	95%
		Factor C: Fan Total Pressure (FTP) - Supply Fan (Pa)	474	300	900
		Factor D: Fan Total Pressure (FTP) - Extract Fan (Pa)	197	140	420

Table 4.2.4-2: The range of values of the four parameters of group G for the FCU system

It should be remembered that details concerning the selection of the minimum, maximum and standard values for the FTP of the central fans can be found in section 3.3.2 of chapter 3.

The four parameters of group G are correlated with the fan energy consumption of the FCU system and the VAV system respectively. This procedure is repeated for both climates, so four response surface models are developed in total. Also, the simulations performed in B-TAS for the VAV system illustrated that the parameters under consideration affect the energy consumed by the central cooling coils to condition the air quantity supplied to the building zones. As a result, two more regression models are developed, approximating the relationship between the parameters of this group and the cooling energy use of the VAV system in both climates. All the aforementioned models are presented in appendix H, section H.2.4.

The analysis of the effect of the four parameters of group G on the fan energy consumption of the HVAC systems in both climates for which they are simulated, takes place in section 4.2.4-1. Also, section 4.2.4-2 discusses the effect of the factors of this group on the cooling energy consumption of the VAV system in both climates. The findings obtained from this study are summarized in section 4.2.4-3.

4.2.4-1 The effect of the parameters of group G on the fan energy consumption of the HVAC systems, when they are simulated for the CIBSE TRY and the NOA TRY respectively

The effect of the four parameters related to the fan size & performance on the fan energy consumption of the FCU system for the CIBSE TRY is illustrated in figure 4.2.4-1:

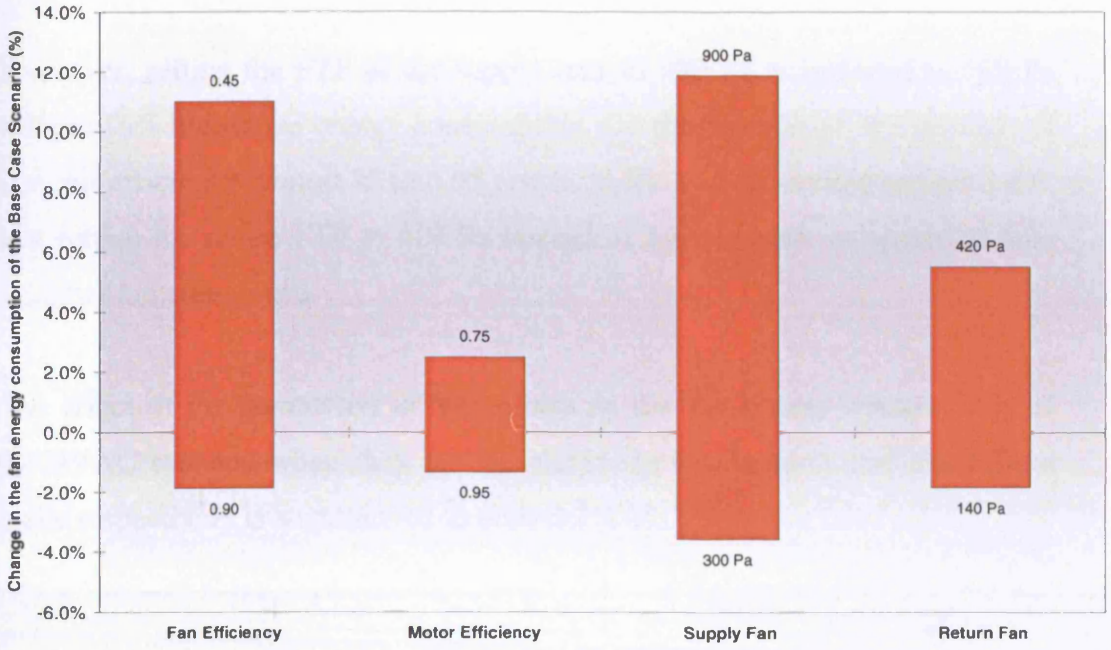

Figure 4.2.4-1: The effect of the four parameters of group G on the annual fan energy consumption of the BCS, when the FCU system is simulated for the CIBSE TRY

Figure 4.2.4-1 indicates that the fan efficiency and the supply FTP have a relatively higher effect on the fan energy use than the remaining two factors. Before looking at the effect of the fan efficiency on the energy consumption, it is worth mentioning that B-TAS estimates the FCU system fan energy use using the equation[15]: (Fan energy) = (Fan Power) x (Run hours) $= (\frac{\Delta P \times Q}{n_f}) \times$ (Run hours) *(1)*, where ΔP *(Pa)* is the total pressure rise across the (supply and return) fan at the design flow rate, while Q (m^3 / s) is the volume flow rate (i.e. the minimum

[15] **Note:** B-TAS Reference Manual, EDSL Documentation

fresh air quantity for ventilation purposes) and n_f is the fan efficiency. It should also be stressed that the program does not recalculate all the parameters in order to leave the heating/cooling loads unchanged when the fan efficiency is altered, but it leaves the volume flow rate and the fan total pressure constant, and just looks at the reduction or increase in the energy required due to the efficiency or inefficiency of the fans. Thus, the fan energy consumption of the FCU system drops by approximately 12%, when the fan efficiency increases from 0.45 to 0.90, as shown in figure 4.2.4-1.

Moreover, setting the FTP of the supply fans to 900 Pa as opposed to 300 Pa results in 16% higher fan energy consumption. On the other hand, the increase of the motor efficiency from 0.75 to 0.95 results in fan energy savings equal to 4%, while setting the return FTP to 420 Pa instead of 140 Pa leads to approximately 7% higher fan energy use.

The effect of the parameters of this group on the fan energy consumption of both HVAC systems when they are simulated for the London and the Athens climate respectively is summarised in table 4.2.4-3:

Factor	Impact on fan energy use (%)					
	Min and Max Level	FCU system		Min and Max Level	VAV system	
		CIBSE TRY	NOA TRY		CIBSE TRY	NOA TRY
Fan Efficiency (%)	45%	-12%	-12%	45%	-49%	-50%
	90%			90%		
Motor Efficiency (%)	75%	-4%	-4%	75%	-21%	-21%
	95%			95%		
Supply FTP (Pa)	300	16%	14%	500	146%	152%
	900			1500		
Return FTP (Pa)	140	7%	7%	120	33%	33%
	420			360		

Table 4.2.4-3: Change in the fan energy consumption, depending on the HVAC system and the climate under consideration, when each factor of group G rises from its minimum to its maximum level, while the remaining parameters are set to their respective standard level

Table 4.2.4-3 indicates that the VAV system fan energy use is considerably more sensitive to the parameters of group G than the FCU system fan energy consumption. This is due to the fact that the parameters displayed in table 4.2.4-2 affect only the amount of electricity consumed by the central fans of the FCU

system to move the minimum fresh air quantity throughout the building, while the energy consumed by the fan coil units, (which accounts for most of the total fan energy use of this system), remains the same. On the other hand, the total air quantity, which is usually much higher than the minimum fresh air requirement for ventilation purposes, is supplied around the building using only the central fans of the VAV system. As a result, the parameters shown in table 4.2.4-1 affect the total fan energy consumption of this system.

4.2.4-1.1 The factor settings of group G minimising the fan energy consumption depending on the type of HVAC system and the climate for which the simulations are carried out

Keeping the size of the fans used to move the air throughout the building as small as possible and opting for high fan and motor efficiencies minimises the fan energy use of both HVAC systems, as shown in table 4.2.4-4:

HVAC system	Climate	Scenario	Factor Levels				Reduction in fan energy over the BCS (%)
			Fan Efficiency (%)	Motor Efficiency (%)	Supply Fan (Pa)	Return Fan (Pa)	
FCU system	CIBSE TRY	Base case scenario	0.78	0.90	421	197	-
		Minimum fan energy consumption	0.90	0.95	300	140	-6%
	NOA TRY	Base case scenario	0.78	0.90	474	197	-
		Minimum fan energy consumption	0.90	0.95	300	140	-7%
VAV system	CIBSE TRY	Base case scenario	0.78	0.90	677	162	-
		Minimum fan energy consumption	0.90	0.95	500	120	-38%
	NOA TRY	Base case scenario	0.78	0.90	681	156	-
		Minimum fan energy consumption	0.90	0.95	500	120	-39%

Table 4.2.4-4: The combination of factor levels minimising the fan energy use and the associated reduction over the fan energy consumption of the BCS, depending on the HVAC system and the climate for which it is simulated

It is worth mentioning that the VAV system consumes up to 46% and 64% less fan energy than the FCU system when the base case and the optimum values of the factors of this group are considered respectively[16]. It should be remembered

[16] **Note:** The absolute values of the fan energy use for both the base case and the optimum factor settings of group G are presented in appendix F.

that the VAV system adjusts the volume of the supply air quantity depending on the zone requirements resulting in significant fan energy savings in comparison to systems that operate with a large, constant volume of air. The FCU system central fan energy consumption, on the other hand, is lower than the VAV system fan energy use, since only the minimum fresh air quantity (for ventilation purposes) is supplied around the building. However, if the energy consumed by all the fan coil units located around the building is taken into account, the total fan energy use of this system exceeds the VAV system fan energy consumption, as mentioned above.

4.2.4-2 The effect of the parameters of group G on the cooling energy consumption of the VAV system when it is simulated for the CIBSE TRY and the NOA TRY respectively

The effect of the parameters of group G on the VAV system cooling energy use for the CIBSE TRY is illustrated in figure 4.2.4-2:

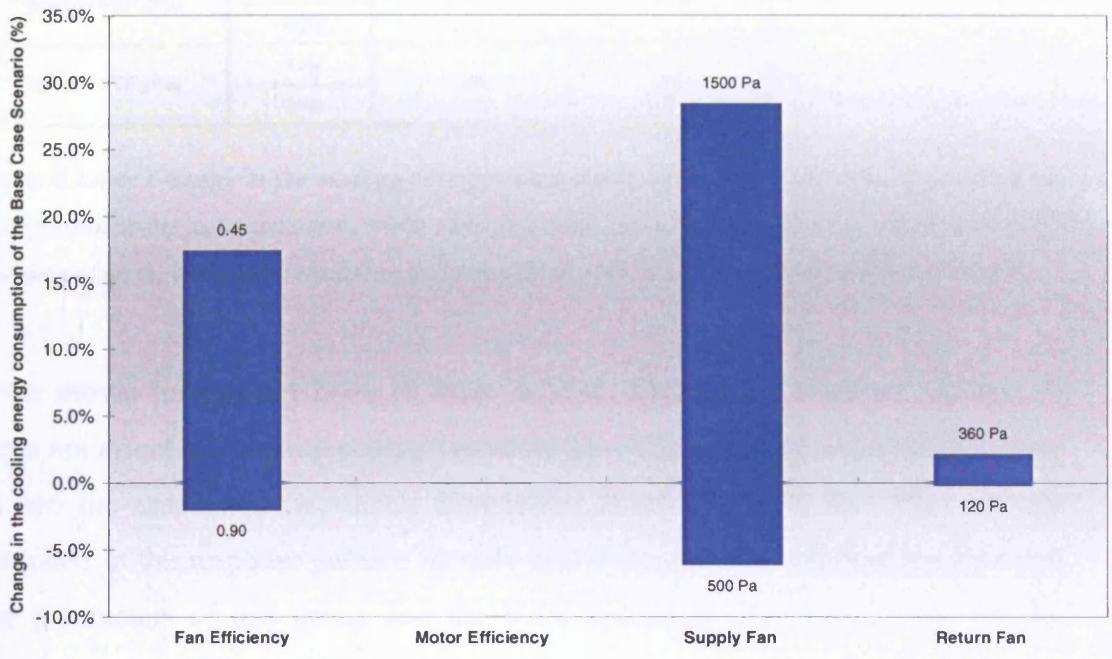

Figure 4.2.4-2: The effect of the parameters of group G on the annual cooling energy consumption of the BCS, when the VAV system is simulated for the CIBSE TRY

Figure 4.2.4-2 shows that the FTP of the supply fans and the fan efficiency have the highest impact on the cooling energy use of this system. The cooling energy consumption increases by 37% when the supply FTP is set to 1500 Pa as opposed to 500 Pa. In addition, the increase of the fan efficiency from 0.45 to 0.90 leads to cooling energy savings of approximately 17%. On the other hand, setting the return FTP to 360 Pa instead of 120 Pa increases the mechanical cooling requirement by just 2%.

The effect of the parameters of this group on the VAV system cooling energy use when this is simulated for the London and the Athens climate respectively is summarised in table 4.2.4-5:

Factor	Impact on cooling energy use (%)		
	Min and Max Level	VAV system	
		CIBSE TRY	NOA TRY
Fan Efficiency (%)	45%	-17%	-10%
	90%		
Motor Efficiency (%)	75%	0%	0%
	95%		
Supply FTP (Pa)	500	37%	18%
	1500		
Return FTP (Pa)	120	2%	2%
	360		

Table 4.2.4-5: Change in the cooling energy consumption of the VAV system, depending on the climate under consideration, when each factor of group G rises from its minimum to its maximum level, while the remaining parameters are set to their respective standard level

As shown in figure 4.2.4-4 or table 4.2.4-5, the motor efficiency (factor B) does not affect the cooling energy consumption of this system. As a result, factor B and the associated two-factor interaction terms (i.e. BA, BC, BD) are not included in the response surface models approximating the relationship between the parameters of this group and the VAV system cooling energy use for the London and the Athens climate respectively.

4.2.4-2.1 The factor settings of group G minimising the cooling energy consumption of the VAV system depending on the climate for which it is simulated

Both the cooling and the fan energy consumption of the VAV system are minimised for the same factor settings, as can be seen from tables 4.2.4-4 and 4.2.4-6.

HVAC system	Climate	Scenario	Factor Levels				Reduction in cooling energy over the BCS (%)
			Fan Efficiency (%)	Motor Efficiency (%)	Supply Fan (Pa)	Return Fan (Pa)	
VAV system	CIBSE TRY	Base case scenario	0.78	0.90	677	162	-
		Minimum cooling energy consumption	0.90	-	500	120	-7%
	NOA TRY	Base case scenario	0.78	0.90	681	156	-
		Minimum cooling energy consumption	0.90	-	500	120	-5%

Table 4.2.4-6: The combination of factor levels minimising the VAV system cooling energy use and the associated reduction over the cooling energy consumption of the BCS depending on the climate under consideration

4.2.4-3 Summary of the findings derived from the study of the effect of the factors contained in group G on the energy performance of the HVAC systems in both climates

It has been found that the total pressure of the supply fans and the fan efficiency have a higher impact on the fan energy consumption of both HVAC systems than the motor efficiency and the extract FTP. The sensitivity of the fan energy use to the four parameters associated with the fan size & efficiency drops considerably when the FCU system as opposed to the VAV system is simulated either for the London or the Athens climate. This is due to the fact that the parameters of this group affect only the energy used by the central fans of the FCU system to move the fresh air around the building, and not the considerable amount of electricity consumed by the fan coil units located in the building zones[17]. Also, the parameters of group G affect the energy consumed by the central cooling coils of the VAV system[18] to condition the supply air quantity. The fan efficiency and the supply FTP have the highest impact on the annual cooling energy use. The specification of high efficiency fans & motors and low-pressure supply & return fans minimises the annual energy use of both systems.

[17] **Note:** The amount of electricity consumed by the fan coil units dominates the total fan energy use of the FCU system in both climates. For example, the fan coil unit energy use accounts for approximately 85% and 92% of the total fan energy consumption of this HVAC system, when the base case and the optimum values of the four parameters of this group are taken into consideration respectively.

[18] **Note:** The motor efficiency is the only exception, since it does not affect the cooling energy use of this HVAC system.

4.2.5 The effect of the design factors associated with the humidification of the supply air quantity (group H) on the energy performance of the HVAC systems

The aim of this study is to investigate the effect of the parameters related to the humidification of the supply air quantity on the energy performance of the HVAC systems, when they are simulated for the London and the Athens climate, respectively. Secondary aims include the identification of factor settings that minimize the annual energy consumption of each system in both climates.

A central steam humidifier powered by electricity, is used to control the RH of the air. The parameters associated with the humidification process along with their range of values are presented in table 4.2.5-1:

Factors	Values		
	Standard	Minimum	Maximum
Factor A: Humidification set-point (%)	-	40%	50%
Factor B: Proportional band (%)	-	5%	10%
Factor C: Period of humidification	-	Heating season	All year

Table 4.2.5-1: The range of values of the parameters of group H

Details concerning the selection of the minimum & maximum values of the parameters shown in this table can be found in chapter 3, section 3.3.2. It is worth mentioning, however, that the period of humidification (factor C) is treated as a categorical factor, which means that it takes only a certain number of discrete levels. As can be seen from table 4.2.5-1, the steam humidifier is set to operate either for the heating season (i.e. for 6 months in total), or for the whole year.

The energy consumed for the humidification of the air is the only response variable in this study, since the effect of the parameters shown in table 4.2.5-1 on the heating or cooling energy use of the HVAC systems is trivial. As a result, the factors of this group are correlated with the humidification energy use of the

HVAC systems in both climates under consideration. The four response surface models constructed in this study can be found in appendix H, section H.2.5.

The effect of the parameters of group H on the energy performance of the HVAC systems in both climates for which they are simulated is analyzed in section 4.2.5-1. The findings of this study are summarized in section 4.2.5-2.

4.2.5-1 The effect of the parameters of group H on the humidification energy use of the HVAC systems, when they are simulated for the CIBSE TRY and the NOA TRY respectively

As explained in the analysis of the previous groups of factors, it is possible to illustrate in the same plot the way that each factor affects the annual energy use, given that the rest of the parameters under consideration are held constant at a reference level, which is usually the standard, (i.e. the value of each factor in the BCS), or the mid-value of each parameter. In this study, however, the period of humidification (factor C) is treated as a categorical factor with only two levels (i.e. there is no mid-value, while the supply air quantity is not humidified in the BCS, as shown in table 4.2.5-1). This means that only the effect of the remaining two (numerical) factors can be illustrated in the same plot, which must be repeated for both levels of factor C. Taking into consideration, however, that the period of humidification interacts with both the humidification set-point (factor A) and the proportional band (factor B), it was decided to study directly the effect of these two interaction terms (i.e. AC & BC) on the humidification energy use, using two interaction plots.

The effect of the RH set-point (factor A) and the period of humidification (factor C) on the humidification energy use of the FCU system for the CIBSE TRY, given that the proportional band is set to 7.5% (i.e. factor B is set to its mid-level), is illustrated in figure 4.2.5-1:

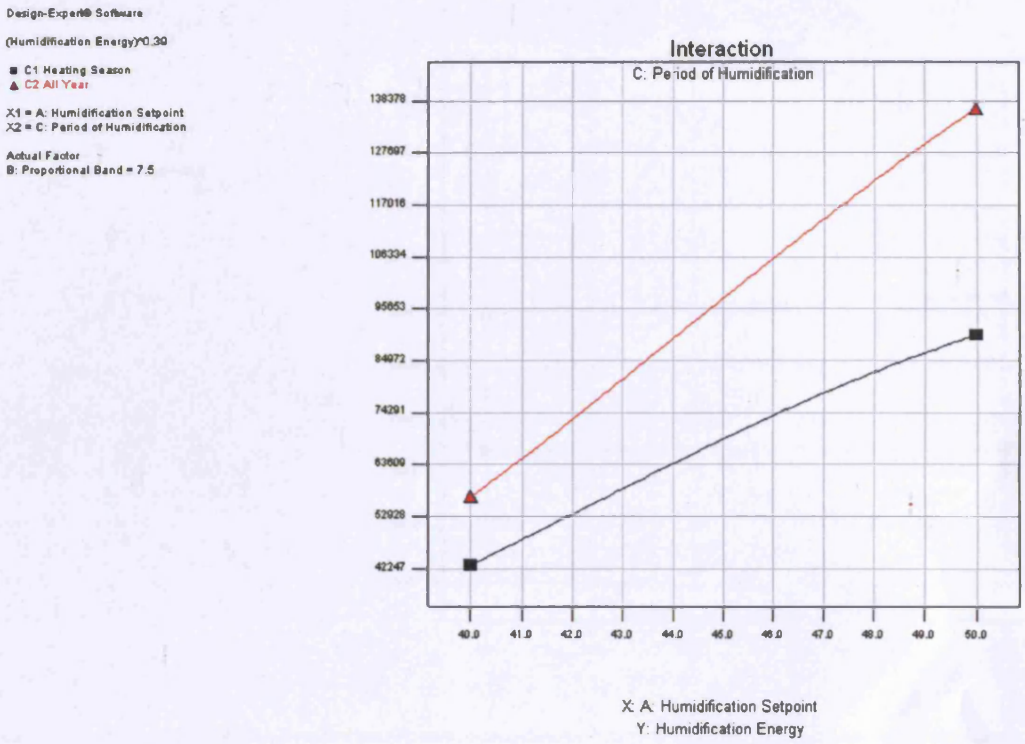

Figure 4.2.5-1: The effect of the RH set-point (factor A) and the period of humidification (factor C) on the humidification energy use of the FCU system for the CIBSE TRY, given that the proportional band (factor B) equals 7.5%

Figure 4.2.5-1 shows that changing the set-point for RH control from 40% to 50% increases the humidification energy use by approximately 47,300 kWh when the steam humidifier operates for the heating season, and 79,900 kWh when the humidifier operates for the whole year. In addition, it is worth mentioning that the amount of energy consumed when the humidifier operates at 50% (± 7.5% / 2) for the heating season is considerably higher than the energy used when the minimum level of RH maintained is 40% (± 7.5% / 2) throughout the year. It is clear that the provision of humidification at a high RH set-point can be very energy wasteful.

The effect of adding a proportional band (factor B) over the RH set-point on the energy use of the FCU system for the CIBSE TRY, when the steam humidifier operates for the heating season as compared to all year humidification (factor C) is illustrated in figure 4.2.5-2, for a RH set-point of 45% (i.e. factor A is set to its mid-level):

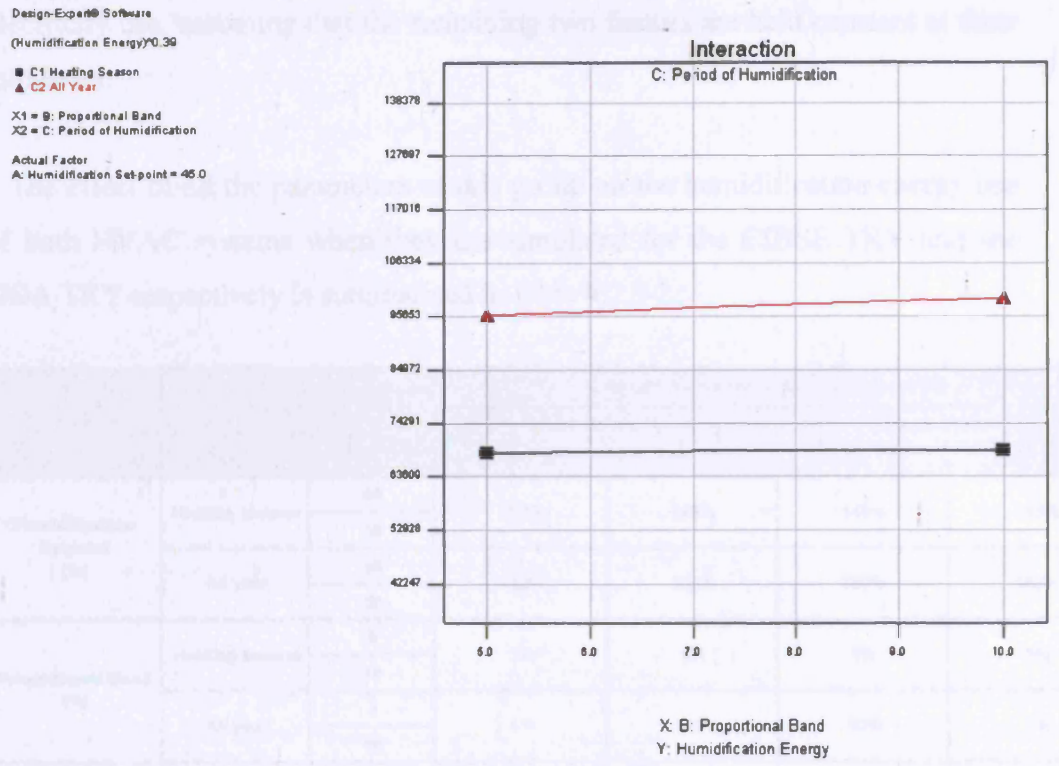

Figure 4.2.5-2: The effect of the proportional band (factor B) and the period of humidification (factor C) on the humidification energy use of the FCU system for the CIBSE TRY, given that the RH set-point (factor A) is 45%

As can be seen from figure 4.2.5-2, setting the proportional band to 10% instead of 5% increases the humidification energy use by approximately 3,400 kWh when the humidifier operates for 12 months as opposed to 580 kWh when the humidifier operates for the heating period. Clearly, the increase of the proportional band leads to slightly higher energy use for the humidification of the supply air quantity, particularly when the humidification process is extended over the year. This is due to the fact that the steam humidifier attempts to maintain the RH of the supply air quantity at RH set-point + (proportional band) / 2 for the largest part of the operation period[19].

It is also worth mentioning that the operation of the steam humidifier throughout the year as opposed to the heating season results in 42% higher

[19] **Note:** For example, when the RH set-point equals 45% and the proportional band is set to 10%, the steam humidifier maintains the humidity of the air between 40% and 50% (i.e. 45% ± 5%). However it seems that the humidifier operates at 45% + 5% for the largest part of the operation period, since the increase of the proportional band leads to higher electricity use, as mentioned above.

electricity use, assuming that the remaining two factors are held constant at their mid-level.

The effect of all the parameters of this group on the humidification energy use of both HVAC systems when they are simulated for the CIBSE TRY and the NOA TRY respectively is summarised in table 4.2.5-2:

Factor	Min and Max Level		Impact on humidification energy use (%)			
			FCU system		VAV system	
			CIBSE TRY	NOA TRY	CIBSE TRY	NOA TRY
Humidification Setpoint (%)	Heating season	40	110%	149%	148%	163%
		50				
	All year	40	140%	156%	160%	162%
		50				
Proportional Band (%)	Heating season	5	1%	3%	3%	1%
		10				
	All year	5	4%	6%	10%	5%
		10				
Period of Humidification (months)	Heating season		42%	31%	135%	39%
	All year					

Table 4.2.5-2: Change in the humidification energy use, depending on the HVAC system and the climate under consideration, when each factor of group H rises from its minimum to its maximum level, while the remaining parameters are set to their respective mid-level[20]

As can be seen from table 4.2.5-2, the RH set-point and the period of humidification have the highest impact on the humidification energy use of both systems. Also, the effect of the period of humidification on the amount of energy consumed by the steam humidifier drops when either the FCU system or the VAV system is simulated for the Athens as opposed to the London climate. The FCU system provides humidification of the minimum fresh air quantity, (for ventilation purposes), supplied by the central ductwork system. It should be stressed that the operation of this HVAC system is exactly the same in both climates. Thus, the aforementioned reduction shows that the requirement for humidification outside the heating season is lower when the simulations are carried out for the NOA TRY in place of the CIBSE TRY.

[20] **Note:** As explained earlier, factor C is a categorical factor with only two levels, which means that it has no mid-value. As a result, table 4.2.5-2, shows the effect of the humidification set-point (factor A) and the proportional band (factor B) on the humidification energy use, depending on the type of HVAC system and the climate for which the simulations are carried out, for both levels of the period of humidification (factor C).

The VAV system, on the other hand, handles much higher air quantities than the minimum fresh air requirement throughout the year. In addition, the way that this system operates during the simulation period differs depending on the climatic conditions. In general, the VAV system supplies the air to each zone at an identical, constant temperature, while its volume flow rate is varied to meet the prevailing zone cooling load. One of the advantages of this system is that it can exploit the free cooling capacity of the fresh air by mixing variable proportions of return and fresh air, in order to achieve the required supply air temperature, (ranging from 12°C to 16°C throughout the year for the BCS), without invoking the central cooling coils. This happens mainly when the simulations are carried out for the London climate, due to the mild external conditions that allow this HVAC system to achieve the desired supply air temperature with minimum use of mechanical cooling, for most of the time. The way that the VAV system operates in the CIBSE TRY has a positive impact not only on the cooling energy use, but also on the amount of energy consumed for the adjustment of the internal humidity, which is lower when the simulations are carried out for this climate than for the NOA TRY, given that the steam humidifier operates during the heating season. Extending, however, the humidification process throughout the year leads to a considerably higher increase in the humidification energy use of the VAV system in the CIBSE TRY than in the NOA TRY, due the high requirement for humidification outside the heating season in the former of the two climates, as explained above. Keeping also in mind that the VAV system handles much larger air quantities throughout the year than the FCU system, it can be seen from table 4.2.5-2 that the humidification energy of the former is more sensitive to the period of humidification than the energy use of the latter, particularly when the simulations are carried out for the CIBSE TRY.

4.2.5-1.1 The factor settings of group H minimising the amount of energy consumed in the humidification process, depending on the type of HVAC system and the climate for which the simulations are carried out

Table 4.2.5-3 indicates that the humidification energy use of the HVAC systems is minimised when the RH set-point and the proportional band are set to their lower level, while the steam humidifier operates only for the minimum period considered (i.e. for six months).

HVAC system	Climate	Scenario	Factor Levels			Humidification Energy (kWh)
			Humidification setpoint (%)	Proportional band (%)	Period of humidification	
FCU system	CIBSE TRY	Minimum humidification energy consumption	40	5	Heating Season	42319
	NOA TRY	Minimum humidification energy consumption	40	5	Heating Season	29123
VAV system	CIBSE TRY	Minimum humidification energy consumption	40	5	Heating Season	66549
	NOA TRY	Minimum humidification energy consumption	40	5	Heating Season	101620

Table 4.2.5-3: The combination of factor levels minimising the amount of energy consumed by the steam humidifier, depending on the HVAC system and the climate for which it is simulated

The effect of the parameters of this group on the total carbon emissions of the base case scenario is assessed in section 5.1.3-5 of chapter 5.

4.2.5-2 Summary of the findings derived from the study of the effect of the factors contained in group H on the energy performance of the HVAC systems in both climates

To sum up, the RH set-point and the period of humidification have the highest impact on the humidification energy use of both HVAC systems. Setting the humidifier to maintain a minimum RH of 40%±2.5% for the heating season only, minimises the energy consumption of both HVAC systems, regardless of the climatic conditions. It should be stressed, however, that the increase of the level of minimum humidity control and the prolongation of the humidification

process outside the heating season can lead to a considerable waste of energy for both systems.

4.3 Summary of the findings derived from the study of each group of factors

This chapter has assessed the effect of each group of parameters on the energy performance of the HVAC systems in both climates. The way that the design factors of each group interact in their effect on the annual energy use has been illustrated through a number of plots. The changes in the impact of the parameters of each group on the energy use depending on the type of HVAC system and the climate under consideration have been discussed, while the combinations of factor levels leading to the minimum energy consumption have been identified. The findings obtained from the study of each building related group of parameters have been summarised at the end of sections 4.1.1 to 4.1.3, while the findings derived from the study of each HVAC system associated group of factors have been summarised at the end of sections 4.2.1 to 4.2.5.

The following chapter presents the factor settings of each group minimising the overall carbon emissions as well as the associated reduction over the carbon performance of the BCS depending on the type of HVAC system and the climate for which the simulations are carried out. The alternative factor settings leading to near-optimum carbon performance are also provided through a number of trade-off diagrams.

Chapter 5: The factor settings of each group minimizing the overall carbon emissions of the HVAC systems, depending on the climate for which they are simulated

5.0 Aims of the chapter

The effect of the design factors contained in each of the eight chosen groups on the annual energy consumption of the HVAC systems was discussed in chapter 4. In addition, the factor settings minimizing the annual heating and cooling energy consumption of each system were identified. However, it was shown that in many cases the parameters under consideration do not affect both the heating and the cooling energy use in the same way (e.g. the window U-value or the infiltration rate). In other words, the combination of factor levels minimizing one response variable may have the opposite effect on the other. Therefore, the final decision concerning the optimum factor settings should not be made before the overall carbon emissions for both the heating and the cooling energy use are taken into consideration.

This chapter presents the factor settings of each group minimizing the overall carbon emissions of the HVAC systems and the associated reduction over the carbon performance of the base case scenario (BCS), depending on the type of HVAC system and the climate under consideration. Recommendations concerning the combinations of factor levels providing near-optimum carbon performance are also given through a number of trade-off diagrams.

Section 5.1 discusses the carbon performance of the BCS, depending on the HVAC system installed in the case study building and the weather data for which the simulations are carried out. Sections 5.2.1 to 5.2.3 identify the optimum factor settings of each of the groups associated with the building load, while sections 5.3.1 to 5.3.5 present the optimum factor levels of each of the HVAC system related group of parameters. Finally, section 5.4 summarizes the findings of this chapter.

5.1 The carbon performance of the HVAC systems in the base case scenario

The annual heating & cooling energy consumption and the associated carbon emissions of the BCS, given that cooling runs on electricity, while heating operates on gas, are presented in table 5.1-1, for both HVAC systems and climates under consideration:

Climate	HVAC system	Annual energy use		Carbon emissions			Difference in carbon emissions between the VAV system and the FCU system		
		Heating energy consumption (kWh)	Cooling energy consumption (kWh)	Boiler carbon emissions (kgC)	Chiller carbon emissions (kg C)	Total carbon emissions (kgC)	Difference in boiler emissions (%)	Difference in chiller emissions (%)	Difference in total carbon emissions (%)
CIBSE TRY	VAV system	108076	127741	5620	16223	21843	-25%	-52%	-47%
	FCU system	144279	267686	7503	33996	41499	-	-	-
NOA TRY	VAV system	25818	358596	1343	45542	46884	-31%	-23%	-23%
	FCU system	37457	464764	1948	59025	60973	-	-	-

Table 5.1-1: The annual energy and carbon performance of the VAV system and the FCU system in the BCS, when the simulations are carried out for the CIBSE TRY and the NOA TRY respectively

As can be seen from table 5.1-1, the VAV system is 47% less carbon intensive than the FCU system, when both of them are simulated for the CIBSE TRY. The breakdown of the energy consumption shows that the former consumes 25% less heating energy and 52% less cooling energy than the latter, mainly due to the utilization of recirculation as a form of heat recovery (during the winter months) and the exploitation of the free cooling capacity of the outdoor air (mainly under mild weather conditions).

The simulation of both HVAC systems for the Athens in place of the London climate results in up to 76% lower heating energy consumption. The combination of high external temperatures and solar gains involved in the NOA TRY is clearly responsible for the low space heating requirement in this climate. On the other hand, the FCU system cooling energy consumption increases by 74%, while the cooling energy use of the VAV system is approximately tripled, when the simulations are carried out for the Athens as opposed to the London typical weather conditions. It is obvious that the above change in the climate for which the simulations are carried out has a considerably higher impact on the cooling energy consumption of the latter of the two HVAC systems. The reason is that the VAV system cannot make use of the

'free' cooling capacity of the fresh air in the NOA TRY, (at least not for the same amount of time as in the CIBSE TRY), due to the high outdoor temperatures involved in this climate. As a result, both systems have got to rely on mechanical cooling, for most of the time, in order to maintain the desired thermal comfort conditions in the cooling dominated climate of Athens. As can be seen from table 5.1-1, the difference both in the cooling energy use and the overall carbon emissions between the two systems is considerably reduced when they are simulated for the NOA TRY than for the CIBSE TRY. Nevertheless, the VAV system is more energy efficient than the FCU system in both climates.

5.2 The effect of each of the groups of parameters associated with the building load on the total carbon emissions of the HVAC systems

5.2.1 The design factors associated with the solar gains through the transparent building elements (group A)

The optimum values[1] of the parameters of group A and their impact on the carbon performance of the BCS, depending on the HVAC system and the climate for which the simulations are carried out, are illustrated in table 5.2.1-1:

Scenario	Climate	HVAC system	Factor levels				Impact on the total cabron emissions of the BCS		
			Glazing ratio (0 -1)	Total shading coefficient	Overhang depth (m)	Sidefin depth (m)	Change in the boiler emissions of the BCS (%)	Change in the chiller emissions of the BCS (%)	Change in the total carbon emissions of the BCS (%)
Factor settings of group A minimising the total carbon emissions	CIBSE TRY	VAV system	*0.25*	*0.16*	*0.00*	*1.80*	26%	-32%	-17%
		FCU system	*0.25*	*0.16*	*0.00*	*1.30*	14%	-33%	-24%
	NOA TRY	VAV system	*0.25*	*0.16*	*1.10*	*2.00*	75%	-29%	-26%
		FCU system	*0.25*	*0.16*	*1.20*	*2.00*	42%	-31%	-29%

Table 5.2.1-1: The impact of the optimum factor values of group A on the carbon emissions of the BCS, depending on the HVAC system installed and the climate for which it is simulated

The optimization results suggest that both the glazing percentage of the building and the TSC the windows should be set close to their minimum level. As explained in section 4.1.1, minimizing the glazing percentage of the building helps to deal with both the heat losses during the winter months and the solar gains over the summer period. On the other hand, the specification of a TSC close to 0.16 minimises the solar gains through the transparent building elements throughout the year. This helps to reduce the requirement for mechanical cooling, but, on the other hand, it has a negative impact on the heating energy use of the BCS, as shown in table 5.2.1-1. Despite the increase in heating energy use, however, the total carbon emissions are lower than the BCS, as can be seen from the last column of this table. This is due to the fact that the use of mechanical cooling results in high carbon emissions that

[1] **Note:** The optimisation of the total carbon emissions is also carried out in Design Expert, using the response surface models approximating the relationship between the parameters of each group and the annual heating and cooling energy consumption of the HVAC systems respectively, and the simultaneous optimization technique developed by Derringer and Suich, as explained in chapter 3 (section 3.2.2).

dominate the overall carbon performance of both systems[2], particularly when they are simulated for the Athens climate.

The optimum values of the overhang & the side-fin depth, on the other hand, differ depending on the HVAC system and the climate under consideration, as shown in table 5.2.1-1. However, the effect of the external shading devices on the cooling energy consumption of both systems is trivial, particularly when the TSC of the windows is set close to its minimum level, as shown in section 4.1.1. In other words, the removal of both the overhangs and the side-fins illustrated in table 5.2.1-1 has a negligible effect on the overall carbon emissions, given that the other two factors are set to their optimum level.

There are, of course, several alternative design options leading to near-optimum carbon performance. This is clearly due to the interactions between the design factors under consideration. It is possible to identify the near-optimum factor settings using the response surface models developed in section 4.1.1. For example, the effect of the glazing percentage of the building and the TSC of the windows on the total carbon emissions of the BCS, given that the remaining two factors are set to their respective optimum level, is shown in figures 5.2.1-1 to 5.2.1-4, depending on the HVAC system and the climate for which the simulations are carried out.

[2] **Note:** The absolute values of the energy consumption and the associated carbon emissions for all the groups of parameters can be found in appendix F.

Figure 5.2.1-1: The effect of the glazing percentage and the TSC on the total carbon emissions of the BCS, given that the remaining parameters are set to their optimum level, when the VAV system is simulated for the CIBSE TRY

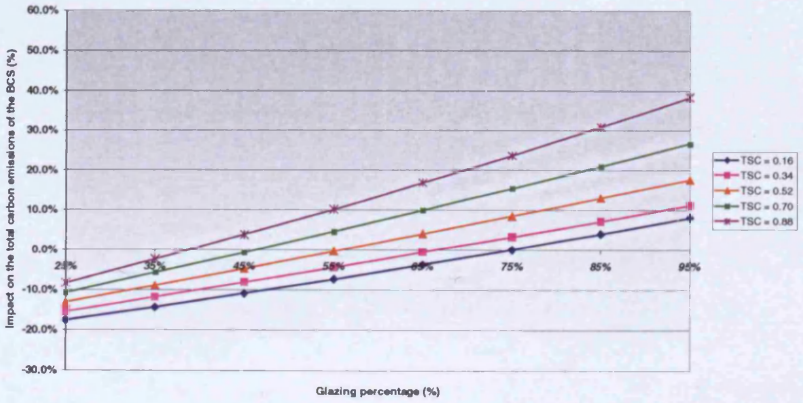

Figure 5.2.1-2: The effect of the glazing percentage and the TSC on the total carbon emissions of the BCS, given that the remaining parameters are set to their optimum level, when the FCU system is simulated for the CIBSE TRY

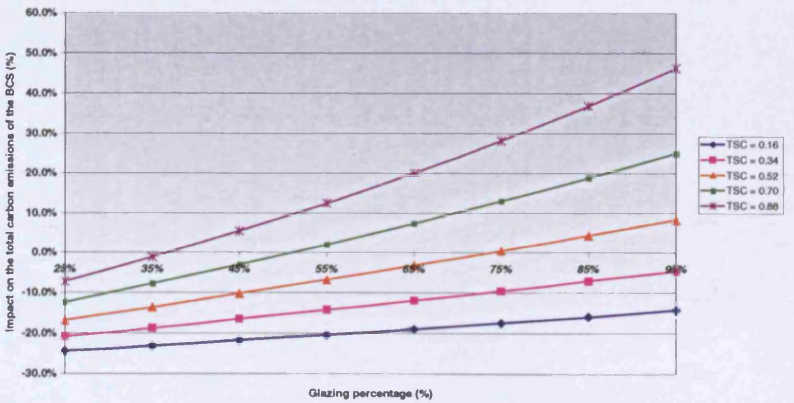

Figure 5.2.1-3: The effect of the glazing percentage and the TSC on the total carbon emissions of the BCS, given that the remaining parameters are set to their optimum level, when the VAV system is simulated for the NOA TRY

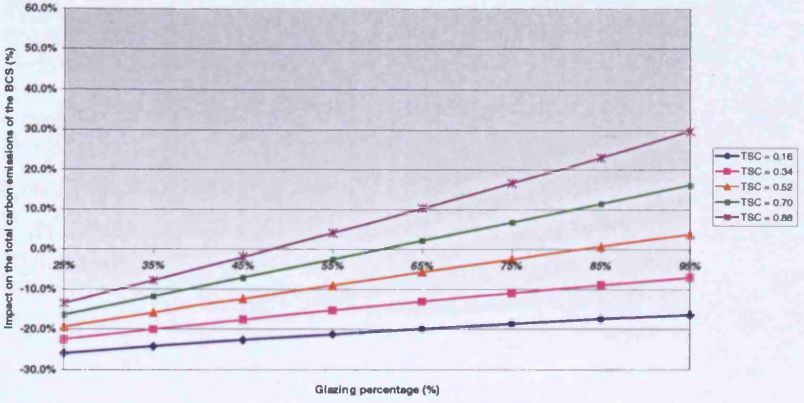

Figure 5.2.1-4:The effect of the glazing percentage and the TSC on the total carbon emissions of the BCS, given that the remaining parameters are set to their optimum level, when the FCU system is simulated for the NOA TRY

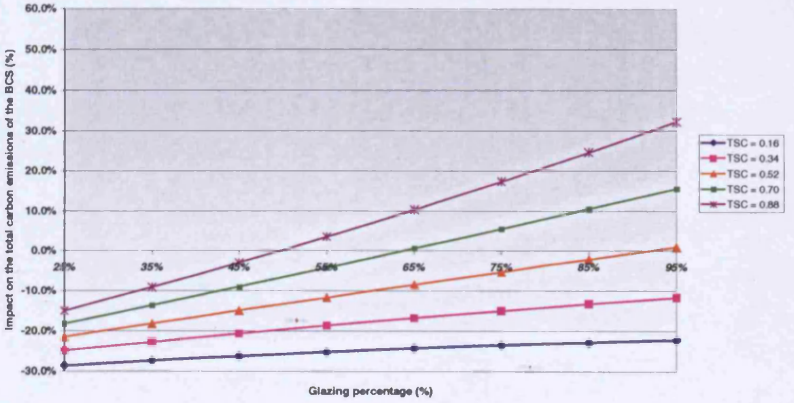

As can be seen from figures 5.2.1-1 and 5.2.1-3, minimising the TSC of the windows leads to near-optimum carbon emissions as long as the glazing percentage of the building does not exceed 45% and 75%, when the VAV system is simulated for the CIBSE TRY and the NOA TRY respectively. Furthermore, minimising the glazing percentage of the building results in near-optimum carbon performance given that the TSC of the windows is lower than 0.70 and 0.52, when this HVAC system is simulated for the London and the Athens climate respectively.

Figure 5.2.1-2 shows that setting the TSC of the windows to 0.16 leads to near-optimum carbon emissions provided that the glazing percentage is not higher than 75%, when the FCU system is simulated for the CIBSE TRY. Figure 5.2.1-4, on the other hand, illustrates that near-optimum carbon emissions can be achieved for the entire range of values of the glazing percentage, given that the TSC of the windows is minimised, when this HVAC system is simulated for the NOA TRY. Both figures under consideration also indicate that setting the glazing percentage of the building to 25% leads to near-optimum carbon performance, as long as the TSC of the windows does not exceed 0.52. Clearly, there are differences in the factor settings leading to near-optimum carbon emissions due to the changes in the sensitivity of both the heating & the cooling energy use to factors A and B, depending on the HVAC system and the climate under consideration (section 4.1.1).

5.2.1-1 The effect of the parameters of group A on the daylight performance of the building

Another factor that the designer should take into consideration, besides the energy efficiency of the final project, is the availability of daylight inside the building, since this affects not only the visual comfort of the occupants but the use of artificial lighting as well.

A conventional measure of the available daylight inside a building is the daylight factor, which is equal to the total daylight illuminance reaching a reference point in the building expressed as a percentage of the total daylight illuminance from an unobstructed sky [1]. In general, a room with an average daylight factor of 5% or more is assumed to be well-daylit and bright. When the average daylight factor is between 2% and 5%, the artificial lighting should be arranged to take advantage of the available daylight. To this end automatic control of lights can be utilized so that artificial lighting is switched off when the available daylight level is sufficient, while careful positioning of the luminaires so that they preserve the daylit character of the room is also required [2]. On the other hand, when the daylight factor is lower than 2% the room appears dull and underlit, so permanent supplementary electric lighting is usually required.

The BCO Guide 2000 [3] states that the optimum visual comfort standards for the office workplace are:

- Average daylight factor >2% - 5%
- Minimum daylight factor > 0.5%

It is clear that both the glazing percentage (i.e. the size of the apertures) and the depth of the external shading devices, which are classified in group A, can affect the available daylight levels inside the building. The TSC[3] is directly related to the total solar transmittance, which is the fraction of solar radiant heat at normal incidence that is transferred through the window construction by both direct transmittance and

[3] **Note:** The TSC is equal to the total solar transmittance divided by 0.87, i.e. it is derived by comparing the glass under consideration with clear float glass (3 or 4 mm thick) having a total solar transmittance of 0.87. It is the summation of the short wave shading coefficient (i.e. the direct transmittance divided by 0.87) and the long wave shading coefficient (i.e. the fraction of the solar absorptance that is dissipated inwards, divided by 0.87) [2].

inward flowing (via re-radiation and convection) absorbed energy [2], [4], and not the light transmittance of the glass, which stands for the fraction of visible light at normal incidence which is transmitted through the glazing [4]. However, the reduction of the TSC or the total solar transmittance of the glass usually leads to a decrease in the transmission of the visible part of the solar spectrum [2].

For example, figure 5.2.1-5, displays a large number of combinations of solar shading coefficients and daylight transmissions for various types of double-glazed windows [4]:

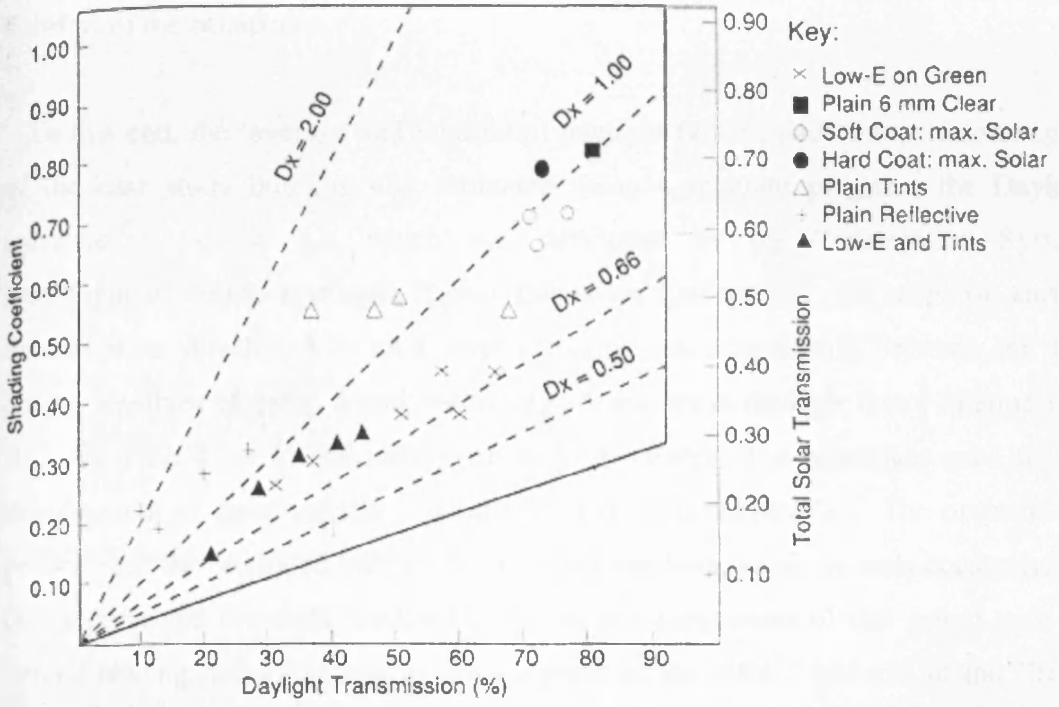

Figure 5.2.1-5: The possible combinations of solar shading coefficients and daylight transmissions for double-glazed windows[4] [4]

Clearly, the daylight transmission is quite similar to the shading coefficient for most of the actual glass products displayed in figure 5.2.1-5. The same conclusion can also be derived from a large number of window constructions provided in the Pilkington web-site [5], which are presented in appendix G. Therefore, it can be assumed that the

[4] **Note:** The ratio of the shading coefficient to the daylight transmission is the transmitted daylight's index of coolness D_x. The lower this number the cooler is the light [4].

light transmission of the glass is equal to the total shading coefficient for the purposes of this study.

TAS is not capable of evaluating the daylight levels inside the building, nor is it possible to schedule the use of artificial lighting (on an hourly basis) over the simulation year so that the lights are turned off when sufficient daylight is available. As a result, it was decided to simulate the worst case scenario, i.e. assume that the lights are constantly on throughout the occupation period[5]. Nevertheless, it would be useful to have a general idea of the effect that the four parameters of group A will have on the daylight performance of the case study building and, hence, the visual comfort of the occupants.

To this end, the (average and minimum) daylight factor inside the perimeter zones of the case study building was estimated using a separate program, the Daylight software [6] - version 4.1, which was developed by the Construction Systems Development Group at Anglia Higher Education College [1]. Six response surface models were developed in total, approximating the relationship between the four design variables of group A and the average & minimum daylight factor of zone 1 (or 3, 7, 9), zone 4 (or 6) and zone 2 (or 8)[7] respectively. The procedure used for the development of these models is described in detail in appendix I. The optimization process was then repeated taking into consideration both the six models constructed in this section and the eight models correlating the parameters of this group with the annual heating & cooling energy consumption of the HVAC systems in the CIBSE TRY and the NOA TRY respectively (section 4.1.1), so that both the daylight performance of the building and the energy performance of the systems can be kept as close to their optimum level as possible.

[5] **Note:** Keeping in mind that the case study building is deep plan it is realized that most of the lights would be permanently on anyway.
[6] **Note:** A short description of the main features of this program can be found in appendix I.
[7] **Note:** The zone(s) included in the parentheses have the same daylight performance as the respective zone outside the parentheses. A plan of a typical floor of the case study building can be found in appendix I.

Design expert was used to carry out the simultaneous optimization of the energy use of the systems and the daylight performance of all the perimeter zones of the building. The optimization goals which were introduced in the statistical software as the criteria required for the optimization of the visual comfort of the occupants in the case study office building, are in line with the design recommendations of the BCO Guide 2000 [3], as can be seen from table 5.2.1-2[8]:

Typical Perimeter Zones	BCO Guide 2000 Recommendations		Optimisation Goals		
				Lower limit	Upper Limit
Zone 1	Average DF (%)	>2% - 5%	Average DF (%)	2.1	5.0
	Minimum DF (%)	> 0.5%	Minimum DF (%)	0.6	5.4
Zone 4	Average DF (%)	>2% - 5%	Average DF (%)	2.1	5.0
	Minimum DF (%)	> 0.5%	Minimum DF (%)	0.6	3.9
Zone 2	Average DF (%)	>2% - 5%	Average DF (%)	2.1	5.0
	Minimum DF (%)	> 0.5%	Minimum DF (%)	0.6	4.7

Table 5.2.1-2: The optimisation criteria concerning the daylight performance of the perimeter zones of the case study building

[8] **Note:** The upper limit set for the minimum DF of each zone corresponds to the maximum value of this parameter that was observed in the simulations carried out with the Daylight software.

The factor values ensuring that the daylight performance of the building is in line with the recommendations of the BCO Guide 2000, while keeping, at the same time, the total carbon emissions of the HVAC systems as close to their minimum level as possible, are shown in table 5.2.1-3:

Scenario	Climate	HVAC system	Factor levels				Annual energy use		Carbon emissions			Perimeter zones DFs					
			Glazing ratio (0 -1)	Total shading coefficient	Overhang depth (m)	Sidefin depth (m)	Heating energy consumption (kWh)	Cooling energy consumption (kWh)	Boiler carbon emissions (kgC)	Chiller carbon emissions (kg C)	Total carbon emissions (kgC)	Zone 1 AVG DF (%)	Zone 1 MIN DF (%)	Zone 4 AVG DF (%)	Zone 4 MIN DF (%)	Zone 2 AVG DF (%)	Zone 2 MIN DF (%)
Factor settings of group A minimising the total carbon emissions, while keeping, at the same time, the daylight performance of the building in line with the BCO Guide 2000	CIBSE TRY	VAV system	0.25	0.76	0.70	0.00	104549	111711	5437	14187	19624	4.9	1.5	2.9	0.8	2.1	0.7
		FCU system	0.40	0.37	0.00	0.00	163315	207155	8492	26309	34801	3.8	1.0	2.2	0.7	2.1	0.6
	NOA TRY	VAV system	0.25	0.68	0.50	0.00	28570	308894	1486	39230	40715	4.6	1.4	2.6	0.7	2.1	0.6
		FCU system	0.95	0.16	0.00	0.00	71412	360743	3713	45814	49528	3.5	1.0	2.1	0.7	2.2	0.9

Table 5.2.1-3: The revised factor settings of group A maintaining both the total carbon emissions of the HVAC systems and the daylight performance of the building as close to their optimum level as possible, when the simulations are carried out for the CIBSE TRY and the NOA TRY respectively

As can be seen from table 5.2.1-3, the TSC of the windows and /or the glazing percentage of the building need to take higher values than the ones shown in table 5.2.1-1, in order to allow for some compromise between the energy consumption of the HVAC systems and the daylight performance of the building. The effect that the new factor settings have on the carbon performance of the BCS is shown in table 5.2.1-4:

Scenario	Climate	HVAC system	Factor levels				Impact on the total cabron emissions of the BCS		
			Glazing ratio (0 -1)	Total shading coefficient	Overhang depth (m)	Sidefin depth (m)	Change in the boiler emissions of the BCS (%)	Change in the chiller emissions of the BCS (%)	Change in the total carbon emissions of the BCS (%)
Factor settings of group A minimising the total carbon emissions, while keeping, at the same time, the daylight performance of the building in line with the BCO Guide 2000	CIBSE TRY	VAV system	*0.25*	*0.76*	*0.70*	*0.00*	-3%	-13%	-10%
		FCU system	*0.40*	*0.37*	*0.00*	*0.00*	13%	-23%	-16%
	NOA TRY	VAV system	*0.25*	*0.68*	*0.50*	*0.00*	11%	-14%	-13%
		FCU system	*0.95*	*0.16*	*0.00*	*0.00*	91%	-22%	-19%

Table 5.2.1-4: The effect of the revised factor values, (taking into consideration the daylight performance of the building), on the carbon emissions of the BCS, depending on the HVAC system and the climate under consideration

Clearly, the combinations of factor levels shown in table 5.2.1-4 lead to lower[9] total carbon savings over the BCS than the factor settings illustrated in table 5.2.1-1. Nevertheless, the revised factor settings of this group are close to the alternative combinations of factor levels leading to near-optimum carbon performance, which were discussed in the previous section, while they keep the daylight performance of the building in line with the recommendations of the BCO Guide 2000, as shown in the last six columns of table 5.2.1-3, satisfying the visual comfort of the occupants working in an office environment.

It is worth mentioning that both the factor settings displayed in table 5.2.1-1 and the combinations of factor levels shown in table 5.2.1-4 will be considered in the next chapter, in order to assess their effect on the total carbon savings (over the BCS) achieved when the parameters of group A are combined with the rest of the groups of factors in order to reach the overall optimum design solution.

[9] **Note:** It should be remembered that lights are assumed to be constantly on over the occupation period in the simulations carried out in TAS. However, had a proper control system been installed so that the lights are not used when sufficient daylight is available in the perimeter zones of the building, it is clear that the lighting & cooling energy use and, hence, the overall carbon emissions would probably have been lower for the factor settings shown in table 5.2.1-3 than the combinations of factor levels illustrated in table 5.2.1-1.

5.2.2 The design factors associated with the thermal resistance and the air tightness of the building envelope (group B)

Table 5.2.2-1 shows that there are differences in the optimum values of the parameters of group B, depending on the type of HVAC system and the climate for which it is simulated. This has to do with the way that the wall & window U-values and the infiltration rate affect the heating and cooling energy consumption in each case.

Scenario	Climate	HVAC system	Factor levels			Impact on the total carbon emissions of the BCS		
			Wall U-value (W/m^2K)	Infiltration rate (ach)	Window U-value (W/m^2K)	Change in the boiler emissions of the BCS (%)	Change in the chiller emissions of the BCS (%)	Change in the total carbon emissions of the BCS (%)
Factor settings of group B minimising the total carbon emissions	CIBSE TRY	VAV system	*0.18*	*0.25*	*1.20*	-53%	8%	-8%
		FCU system	*0.27*	*0.25*	*5.70*	37%	-16%	-6%
	NOA TRY	VAV system	*0.19*	*0.25*	*5.80*	113%	-8%	-4%
		FCU system	*0.70*	*0.40*	*5.80*	75%	-12%	-9%

Table 5.2.2-1: The effect of the optimum factor settings of group B on the carbon emissions of the BCS, depending on the HVAC system and the climate under consideration

The optimum values of the infiltration rate indicate that there is a tendency towards high standards of air tightness. This is mainly due to the fact that this factor has the highest impact on the heating energy use of both systems, so having a high infiltration rate would increase the demand for space heating.

On the other hand, the optimum level of the U-value of the building envelope depends on the HVAC system and the climate under consideration. The heating energy use of the VAV system is more sensitive to the parameters in question than the heating energy consumption of the FCU system, (in both climates), as shown in section 4.1.2. Therefore, the U-value of both walls and windows is minimised when the VAV system is simulated for the CIBSE TRY, to retain the heat inside the building. The heating energy consumption drops by 53%, in such a case, as shown in table 5.2.2-1. The optimum factor settings have a negative impact on the cooling energy use, as expected, but the total carbon emissions are 8% lower than the BCS, as can be seen from the last column of this table. In all the remaining cases, there is trend for high window and/or wall U-values to release part of the internal heat gains to the

external environment and, hence, reduce the demand for mechanical cooling. Despite the increase in heating energy use, due to the poorly insulated building envelope, the total carbon emissions are kept lower than the BCS, as illustrated in table 5.2.2-1.

It is also worth mentioning that the infiltration rate is set higher than its minimum value when the FCU system is simulated for the NOA TRY, as can be seen from table 5.2.2-1. This has to do with the fact that the minimum cooling energy use of this system is achieved for an infiltration rate ranging from 0.75 to 1.25 ach, when the window U-value is set to 5.8 W/m^{2}K, as shown in section 4.1.2 (i.e. figure 4.1.2-4, displaying the effect of the interaction term BC on the cooling energy consumption). Keeping in mind that emphasis is shifted towards the reduction of cooling energy use when the FCU system is simulated for the Athens climate, it becomes clear that the infiltration rate should be higher than 0.25 ach in this case (i.e. the value minimising only the heating energy use of this system, as shown in section 4.1.2).

The increase over the optimum total carbon emissions when each parameter is set higher (or lower) than its optimum level is shown in figures 5.2.2-1 to 5.2.2-4, depending on the type of HVAC system and the climate for which it is simulated:

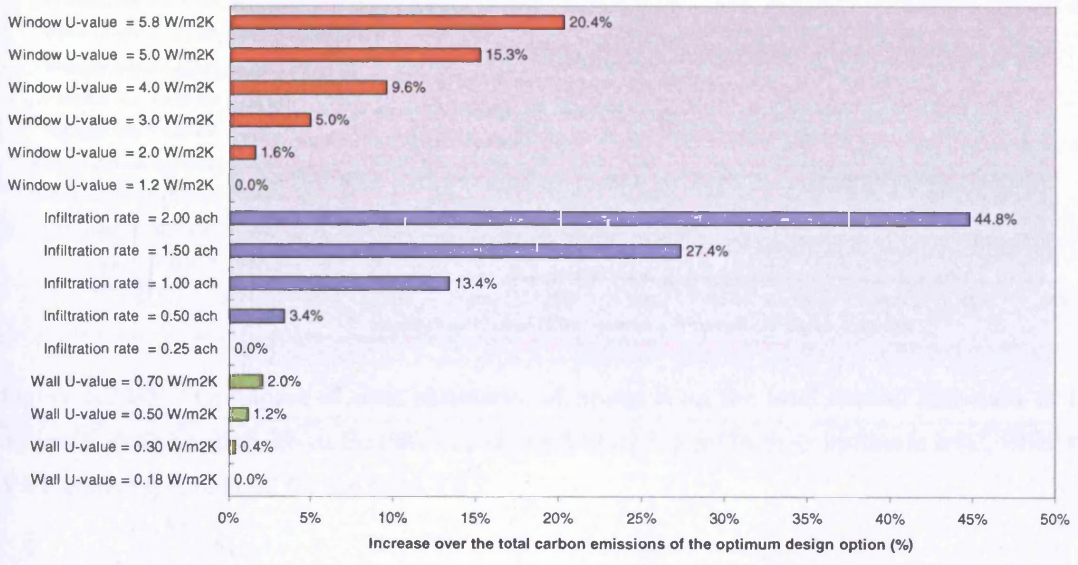

Figure 5.2.2-1: The impact of each parameter of group B on the total carbon emissions of the optimum design option, given that the remaining factors are set to their optimum level, when the VAV system is simulated for the CIBSE TRY

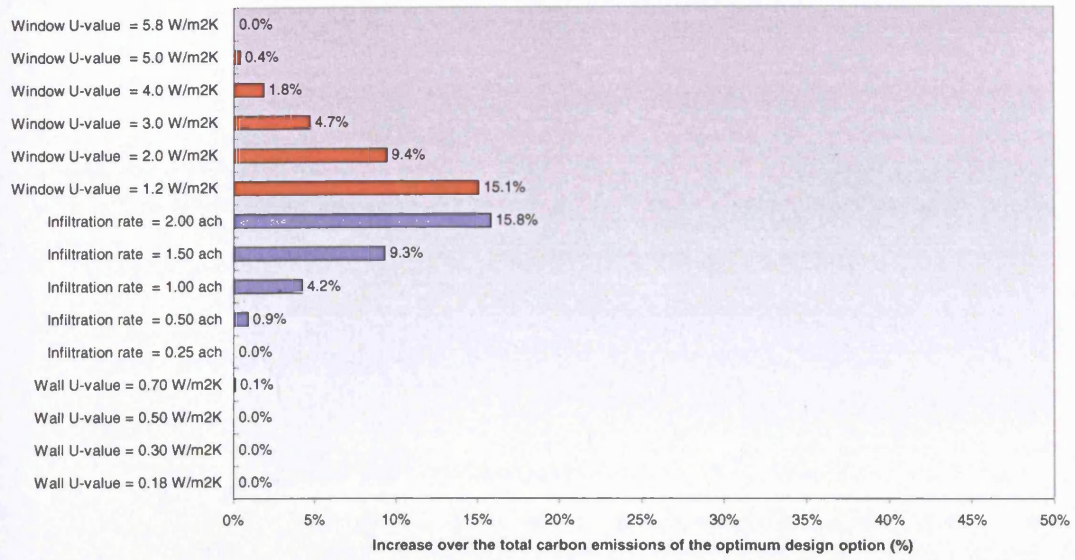

Figure 5.2.2-2: The impact of each parameter of group B on the total carbon emissions of the optimum design option, given that the remaining factors are set to their optimum level, when the FCU system is simulated for the CIBSE TRY

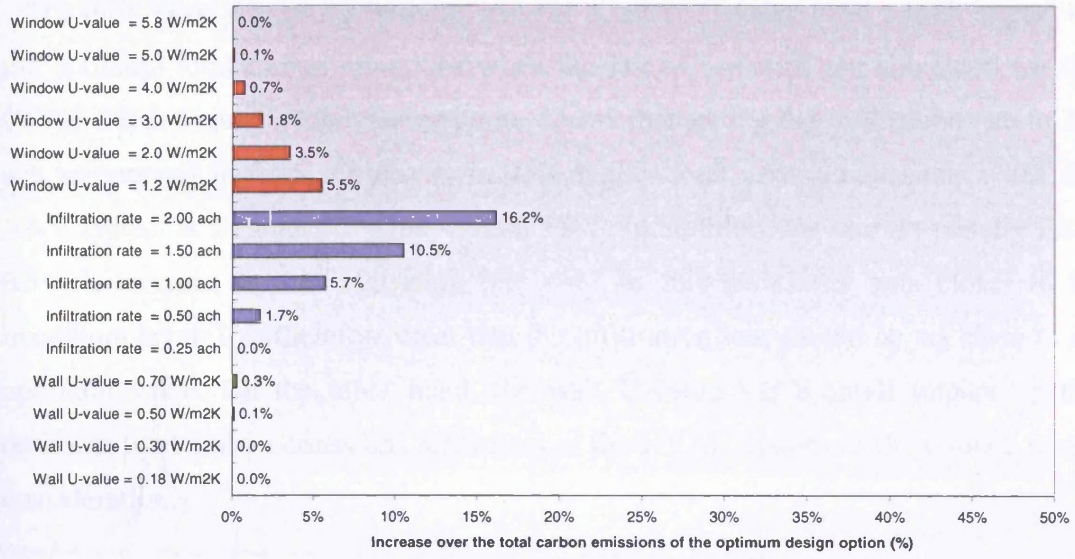

Figure 5.2.2-3: The impact of each parameter of group B on the total carbon emissions of the optimum design option, given that the remaining factors are set to their optimum level, when the VAV system is simulated for the NOA TRY

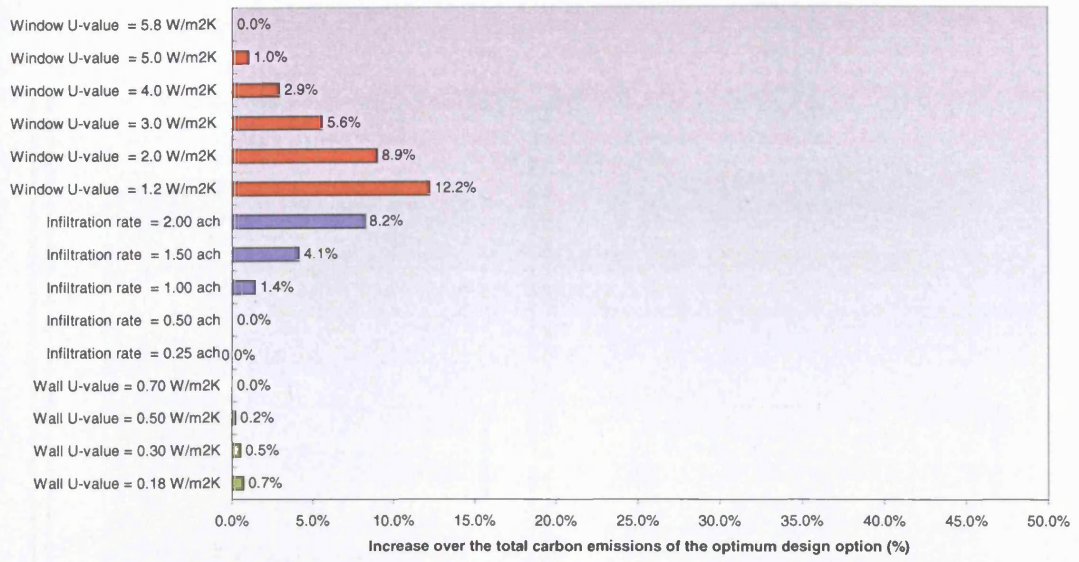

Figure 5.2.2-4: The impact of each parameter of group B on the total carbon emissions of the optimum design option, given that the remaining factors are set to their optimum level, when the FCU system is simulated for the NOA TRY

The infiltration rate of the building and the window U-value have a high impact on the optimum total carbon emissions when the HVAC systems are simulated for the CIBSE TRY. Figure 5.2.2-1, for example, shows that setting the infiltration rate to 2.0 ach as opposed to 0.25 ach results in 45% higher total carbon emissions when the VAV system is simulated for the CIBSE TRY. In addition, the carbon penalty for a 0.5 ach increase in the infiltration rate rises as this parameter gets closer to its maximum level. It is therefore clear that the infiltration rate should be set close to its optimum value. On the other hand, the wall U-value has a small impact on the optimum total carbon emissions regardless of the HVAC system or the climate under consideration.

There are several alternative combinations of the window U-value and the wall U-value resulting in near optimum carbon performance. The effect of these two factors on the total carbon emissions of the BCS, given that the infiltration rate is set to its optimum level, is shown in figures 5.2.2-5 to 5.2.2-8, depending on the HVAC system and the climate under consideration.

Figure 5.2.2-5: The effect of the wall U-value and the window U-value on the total carbon emissions of the BCS, given that the infiltration rate is set to its optimum level, when the VAV system is simulated for the CIBSE TRY

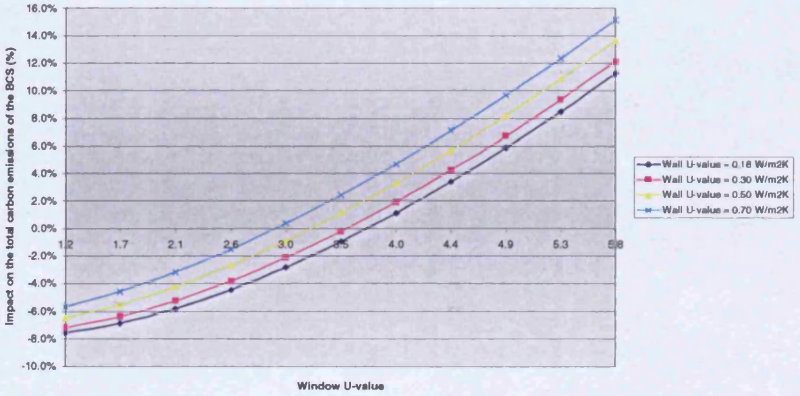

Figure 5.2.2-6: The effect of the wall U-value and the window U-value on the total carbon emissions of the BCS, given that the infiltration rate is set to its optimum level, when the FCU system is simulated for the CIBSE TRY

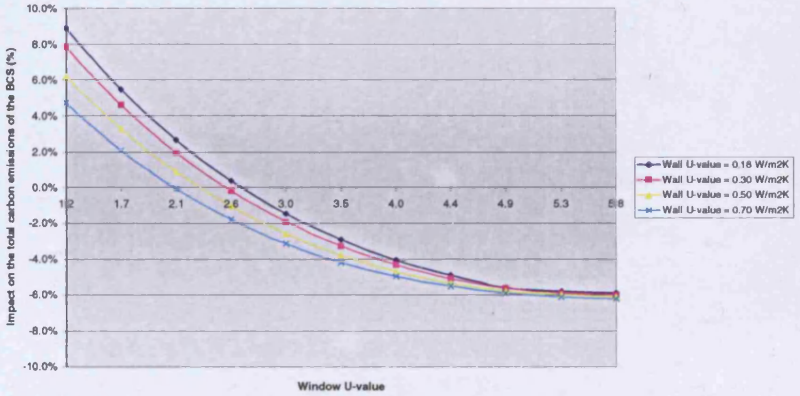

Figure 5.2.2-7: The effect of the wall U-value and the window U-value on the total carbon emissions of the BCS, given that the infiltration rate is set to its optimum level, when the VAV system is simulated for the NOA TRY

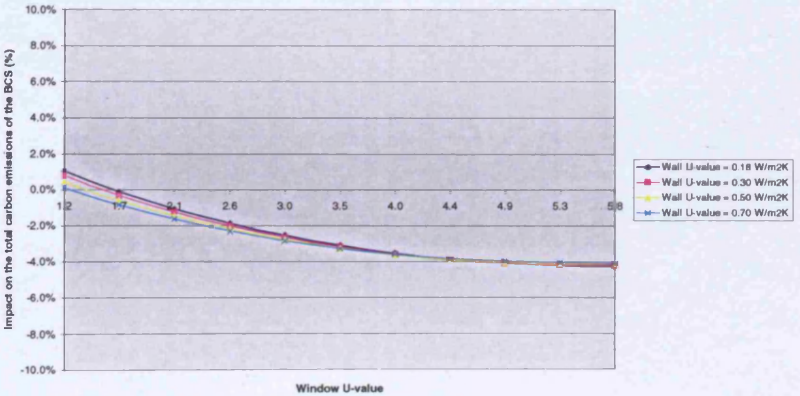

Figure 5.2.2-8: The effect of the wall U-value and the window U-value on the total carbon emissions of the BCS, given that the infiltration rate is set to its optimum level, when the FCU system is simulated for the NOA TRY

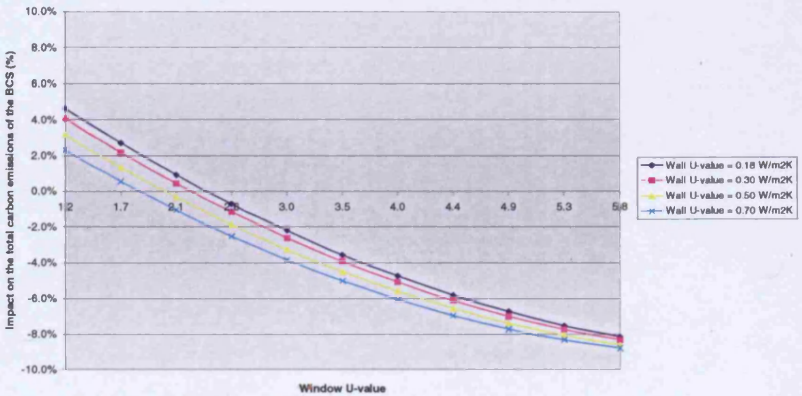

The specification of a well-insulated building envelope is necessary only when the VAV system is simulated for the CIBSE TRY, as can be seen from figure 5.2.2-5. The reason is that the increase in heating energy use when high window and wall U-values are specified can offset the cooling energy savings over the BCS in this case. Figure 5.2.2-5 suggests that aiming for a wall U-value lower than 0.30 W/m^2K leads to near-optimum carbon performance, given that the window U-value does not exceed 1.7 W/m^2K. There is a clear trend for high window U-values in all the other cases in order to limit the use of mechanical cooling. For example, figures 5.2.2-6 to 5.2.2-8 indicate that opting for a window U-value equal or higher than 4.9 W/m^2K leads to near-optimum carbon savings over the BCS. The choice of the wall U-value, on the other hand, makes little difference in the total carbon emissions, particularly when the window U-value is higher than 3.50 W/m^2K, as can be seen from figures 5.2.2-6 to 5.2.2-8.

5.2.3 The design factors associated with the internal heat gains of the office building (group C)

Table 5.2.3-1 shows that the carbon performance of the HVAC systems is optimised in both climates when the internal heat gains of the office building are set close to their minimum level.

Scenario	Climate	HVAC system	Factor levels			Impact on the total carbon emissions of the BCS		
			Lighting gains (W/m^2)	Equipment gains (W/m^2)	Occupant Density (m^2 per person)	Change in the boiler emissions of the BCS (%)	Change in the chiller emissions of the BCS (%)	Change in the total carbon emissions of the BCS (%)
Factor settings of group C minimising the total carbon emissions	CIBSE TRY	VAV system	*6.5*	*10.0*	*20*	58%	-33%	-10%
		FCU system	*6.5*	*10.0*	*20*	26%	-42%	-30%
	NOA TRY	VAV system	*6.5*	*10.0*	*20*	31%	-25%	-23%
		FCU system	*6.5*	*10.0*	*20*	11%	-29%	-28%

Table 5.2.3-1: The effect of the optimum factor settings of group C on the carbon emissions of the BCS, depending on the HVAC system and the climate under consideration

As expected, the reduction of the heat generated by lights, office equipment and occupants results in lower internal temperatures and, hence, increases the requirement for space heating. Keeping in mind, however, that the cooling energy use leads to higher carbon emissions than the heating energy consumption, it becomes clear that the main priority of the designer, (as far as this group of factors in concerned), should be the reduction of the demand for mechanical cooling throughout the year.

The increase over the optimum carbon emissions when each parameter is set higher (or lower) than its optimum level is shown in figures 5.2.3-1 to 5.2.3-4, depending on the type of HVAC system and the climate for which it is simulated:

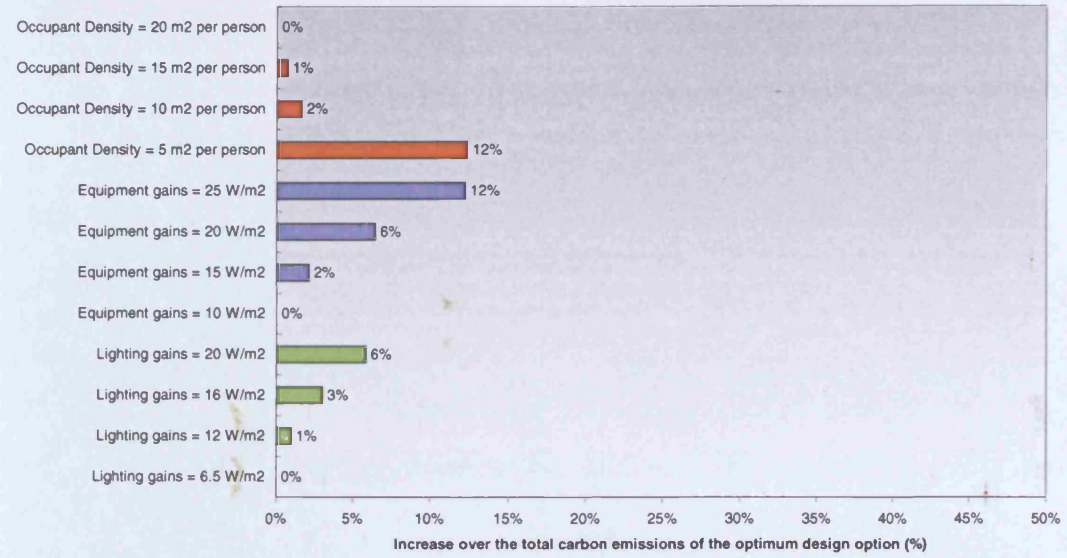

Figure 5.2.3-1: The impact of each parameter of group C on the total carbon emissions of the optimum design option, given that the remaining factors are set to their optimum level, when the VAV system is simulated for the CIBSE TRY

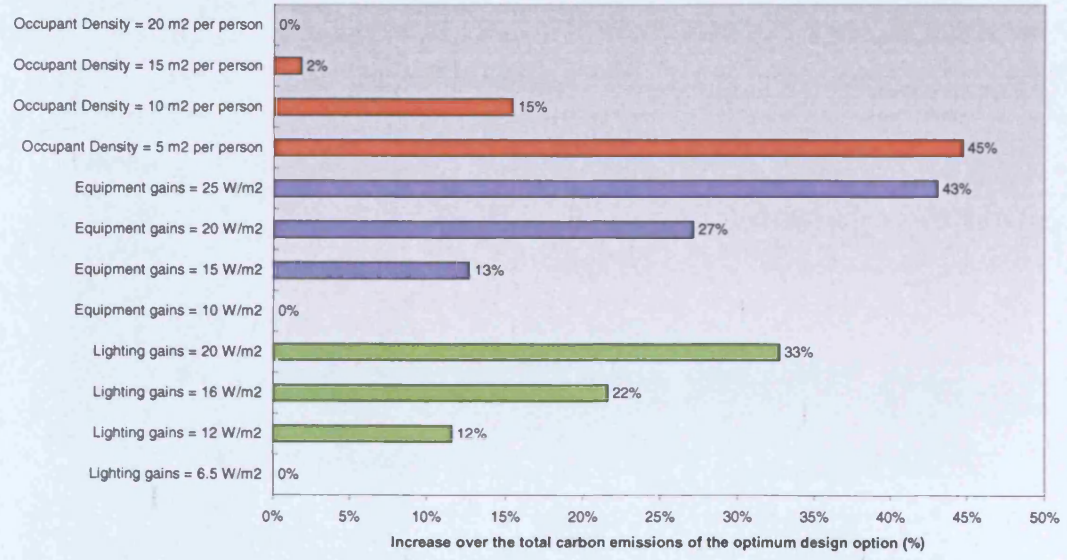

Figure 5.2.3-2: The impact of each parameter of group C on the total carbon emissions of the optimum design option, given that the remaining factors are set to their optimum level, when the FCU system is simulated for the CIBSE TRY

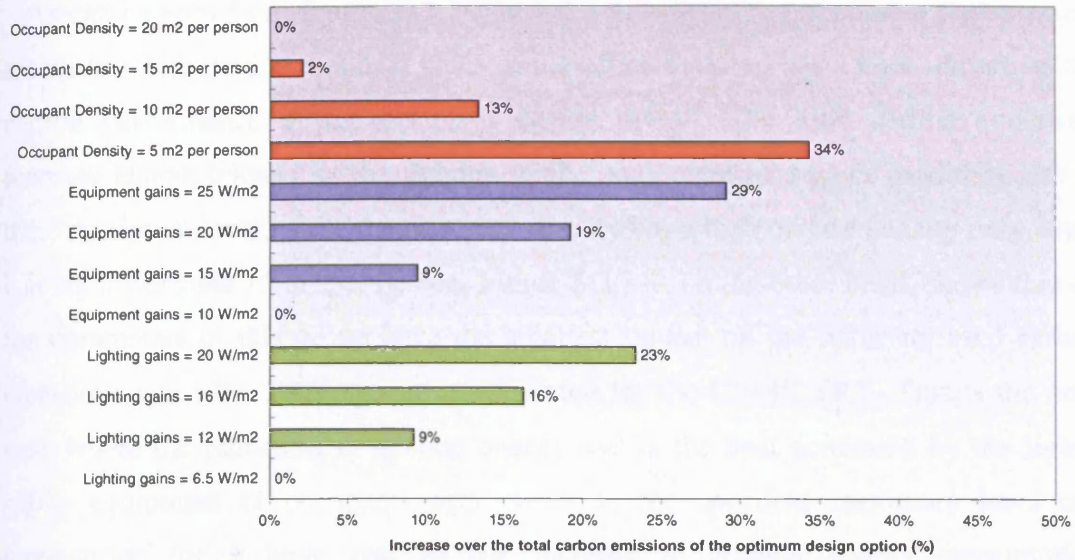

Figure 5.2.3-3: The impact of each parameter of group C on the total carbon emissions of the optimum design option, given that the remaining factors are set to their optimum level, when the VAV system is simulated for the NOA TRY

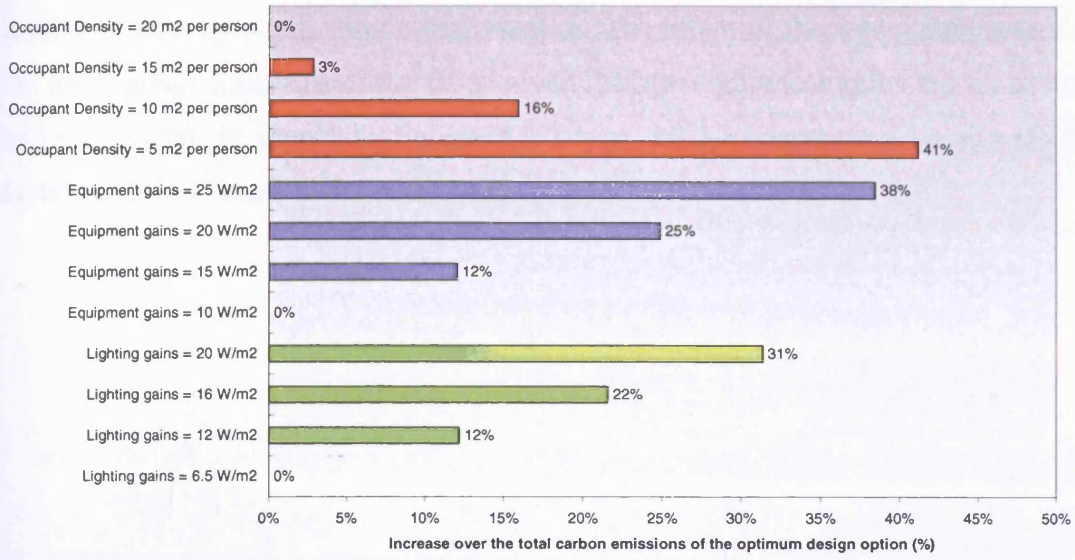

Figure 5.2.3-4: The impact of each parameter of group C on the total carbon emissions of the optimum design option, given that the remaining factors are set to their optimum level, when the FCU system is simulated for the NOA TRY

As can be seen from figures 5.2.3-2 to 5.2.3-4, maximising each of the parameters associated with the internal heat gains of the office building has a high impact on the carbon performance of the optimum design option. The total carbon emissions increase almost linearly as the lighting or the equipment heat gains gradually rise to their maximum level, while the occupant density has a high carbon penalty only when it is set lower than 15 m^2 per person. Figure 5.2.3-1, on the other hand, shows that all the parameters of this group have the smallest impact on the optimum total carbon emissions when the VAV system is simulated for the CIBSE TRY. This is the only case where the reduction in heating energy use as the heat generated by the lights, office equipment or occupants gets closer to the specified maximum level can compensate for a large part of the increase in cooling energy consumption maintaining the increase over the optimum total carbon emissions at a relatively low level.

There are several combinations of the lighting gains and the occupant density leading to near-optimum carbon performance. The effect of these two parameters on the total carbon emissions of the BCS, given that the equipment gains are set to their optimum value, is shown in figures 5.2.3-5 to 5.2.3-8, depending on the HVAC system and the climate under consideration.

Figure 5.2.3-5: The effect of the lighting gains and the occupant density on the total carbon emissions of the BCS, given that the equipment heat gains are set to their optimum level, when the VAV system is simulated for the CIBSE TRY

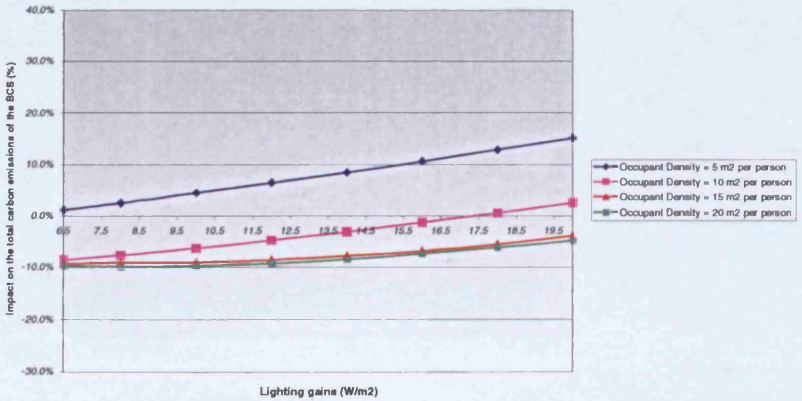

Figure 5.2.3-6: The effect of the lighting gains and the occupant density on the total carbon emissions of the BCS, given that the equipment heat gains are set to their optimum level, when the FCU system is simulated for the CIBSE TRY

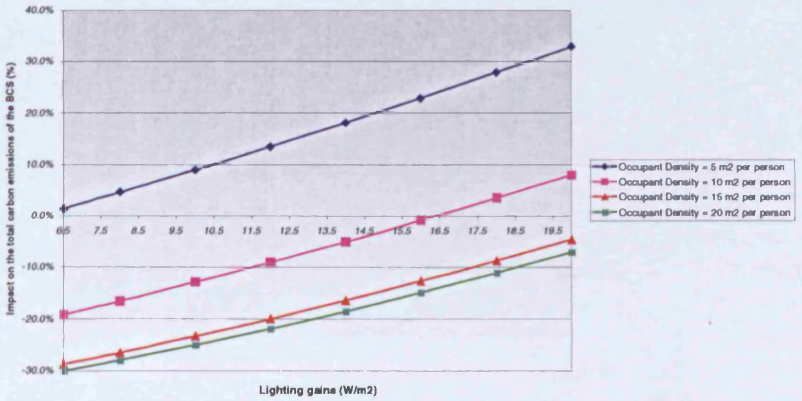

Figure 5.2.3-7: The effect of the lighting gains and the occupant density on the total carbon emissions of the BCS, given that the equipment heat gains are set to their optimum level, when the VAV system is simulated for the NOA TRY

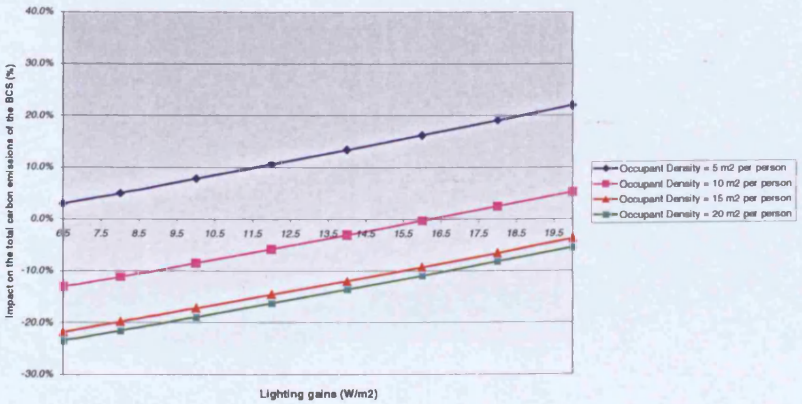

Figure 5.2.3-8: The effect of the lighting gains and the occupant density on the total carbon emissions of the BCS, given that the equipment heat gains are set to their optimum level, when the FCU system is simulated for the NOA TRY

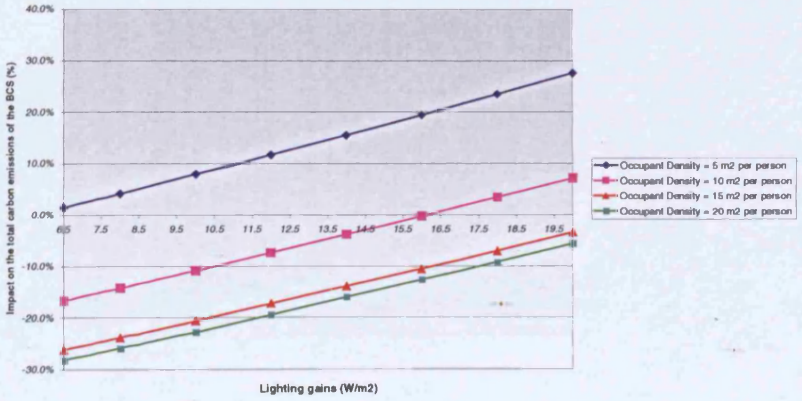

As can be seen from figures 5.2.3-6 to 5.2.3-8, the specification of an occupant density ranging from 15 to 20 m^2 per person results in near-optimum carbon emissions, given that the lighting gains do not exceed 8.5 W/m^2. On the other hand, figure 5.2.3-5 suggests that near optimum carbon performance is achieved when the occupant density is equal to or higher than 10 m^2 per person and the lighting gains range from 6.5 to 8.5 W/m^2.

Clearly, there is a trend for low internal heat gains, particularly from lighting and office equipment, since they create overheating problems especially during the summer months when they are combined with high solar heat gains and ambient temperatures. Energy efficient lights (e.g. fluorescent lamps in efficient luminaries [7]) should, therefore, be installed, while it should be also kept in mind that the use of daylight sensors or occupancy sensors, which can switch off the lights when not required, or simply the provision of good local individual control of artificial lighting can further reduce both the impact that the lights have on the cooling energy use and the amount of electricity consumed by them. Also, designers should recommend the use of low energy office equipment (e.g. use LCD screens which consume 80% less energy than conventional CRT monitors, or laptops instead of desktop computers, install low-energy printers or combination copier/printer/fax machines, etc [7]). It is, of course, important that the energy saving features are enabled during the installation procedure, while the office equipment must be switched off at the end of the working day or during long periods of inactivity. In addition, figures 5.2.3-5 to 5.2.3-8 show that low cooling energy use is ensured throughout the year, when the occupant density is close to 15 m^2 per person, (i.e. quite close to current standard values for office buildings in the UK [3]) or for higher values of this parameter.

5.3 The effect of each of the groups of parameters related to the design & operation of the HVAC systems on the total carbon emissions

5.3.1 The parameters associated with the control of the internal air temperature (group D)

The optimum temperature control strategy and the impact that it has on the carbon performance of the BCS, depending on the HVAC system and the climate under consideration, can be seen in table 5.3.1-1:

Scenario	Climate	HVAC system	Factor levels			Impact on the total carbon emissions of the BCS		
			Heating zone air temperature (°C)	Cooling zone air temperature (°C)	Temperature difference (°C)	Change in the boiler emissions of the BCS (%)	Change in the chiller emissions of the BCS (%)	Change in the total carbon emissions of the BCS (%)
Factor settings of group D minimising the total carbon emissions	CIBSE TRY	VAV system	*18*	*26*	*6*	-47%	-59%	-56%
		FCU system	*18*	*26*	*8*	-39%	-18%	-22%
	NOA TRY	VAV system	*18*	*26*	*6*	-70%	-28%	-29%
		FCU system	*18*	*26*	*8*	-58%	-13%	-15%

Table 5.3.1-1: The effect of the optimum temperature control strategy on the carbon emissions of the BCS, depending on the HVAC system and the climate under consideration

The optimum zone temperature control settings are the same for both systems and climates, as indicated in table 5.3.1-1. On the other hand, the optimum level of the temperature difference (ΔT) between the supply and the zone air differs, depending on the HVAC system studied. This is due to the fact that the range of values and the 'role' of this parameter on the control of the internal air temperature are different for each HVAC system, as explained in section 4.2.1[10].

As can be seen from the breakdown of the total carbon savings over the BCS, the optimum temperature control strategy reduces both the heating and the cooling energy use of the BCS. In addition, table 5.3.1-1 indicates that both the chiller and the total carbon savings over the BCS are particularly high in both climates for which the VAV

[10] **Note:** It should be remembered that the ΔT between the supply and the zone air has a high impact on the cooling energy consumption of the VAV system and the heating energy use of the FCU system respectively. In short, the minimisation of the ΔT between the supply and the zone air results in a high temperature control set-point for the central cooling coil and, hence, reduces the amount of cooling energy consumed by the VAV system. Regarding the FCU system, maximising the ΔT between the supply and the zone air not only reduces the heating energy consumption of the central heating coil but it also allows for the 'free' cooling capacity of the supply air quantity to be utilised, while the fan coil units handle the heating or cooling requirement of each zone of the building separately.

system is simulated. This is due to the high impact that both the cooling zone temperature set-point and the ΔT between the supply and the zone air have on the cooling energy use of this system, as shown in section 4.2.1.

The increase over the optimum carbon emissions when each temperature control set-point is set higher (or lower) than its optimum level is shown in figures 5.3.1-1 to 5.3.1-4, depending on the type of HVAC system and the climate for which it is simulated:

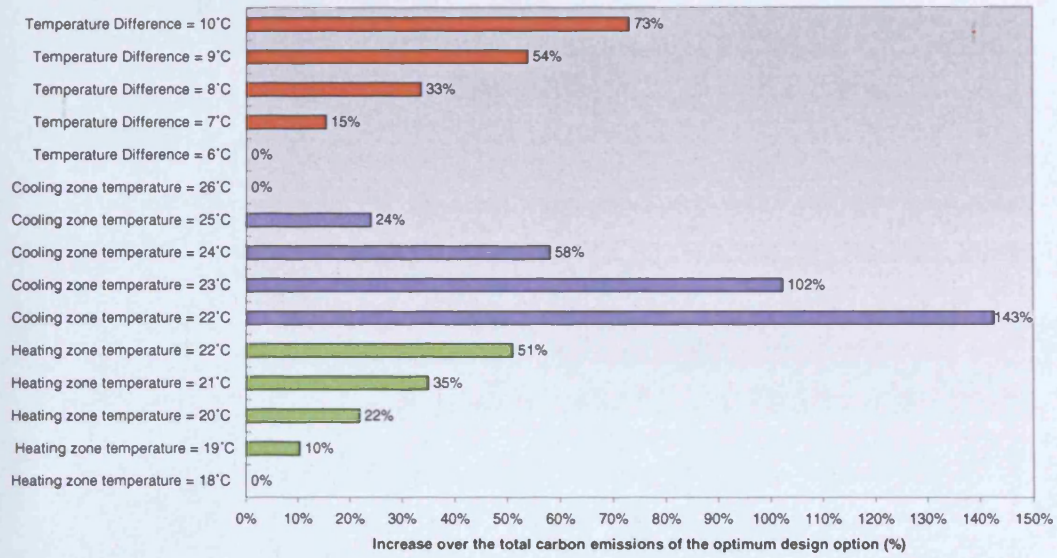

Figure 5.3.1-1: The impact of each parameter of group D on the total carbon emissions of the optimum design option, given that the remaining factors are set to their optimum level, when the VAV system is simulated for the CIBSE TRY

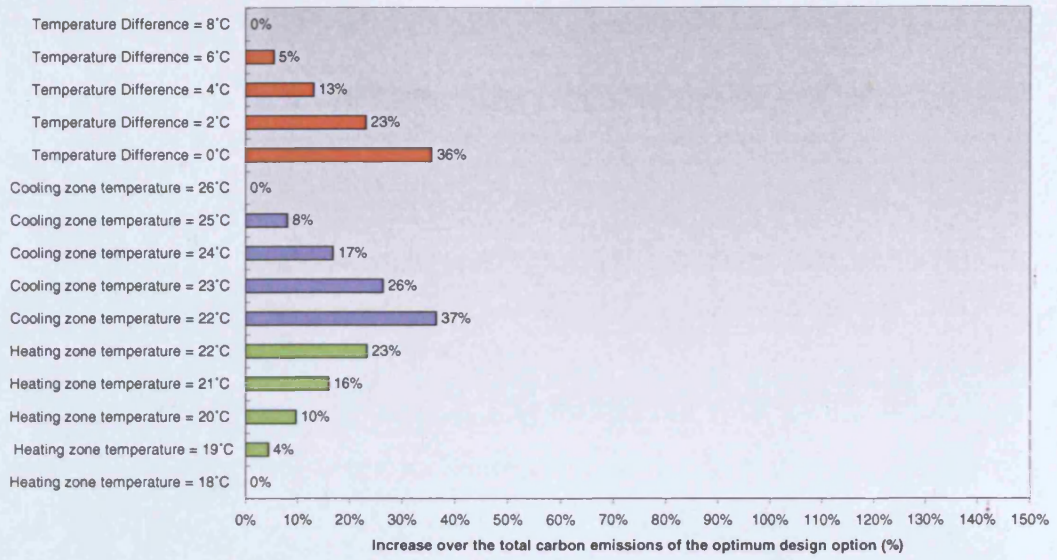

Figure 5.3.1-2: The impact of each parameter of group D on the total carbon emissions of the optimum design option, given that the remaining factors are set to their optimum level, when the FCU system is simulated for the CIBSE TRY

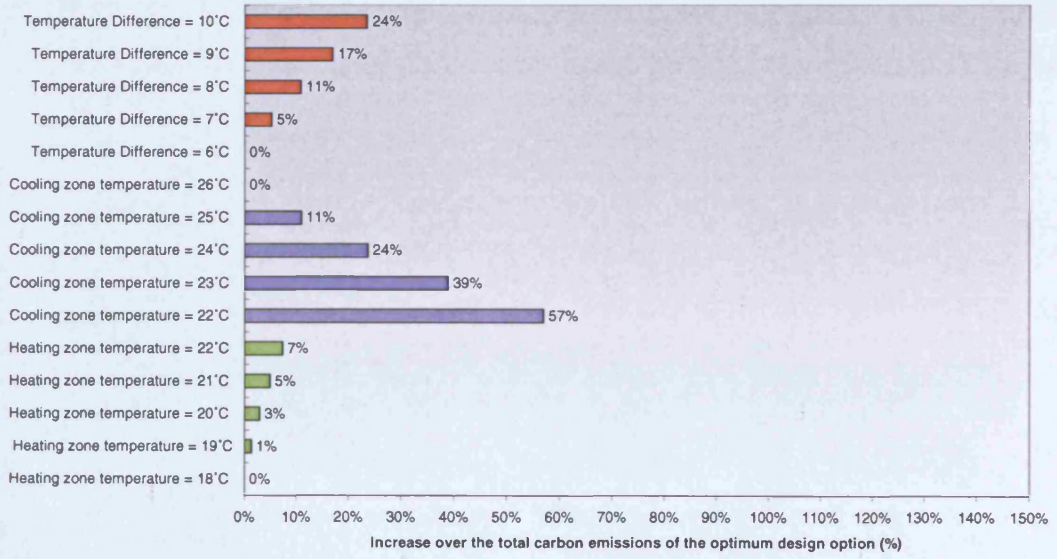

Figure 5.3.1-3: The impact of each parameter of group D on the total carbon emissions of the optimum design option, given that the remaining factors are set to their optimum level, when the VAV system is simulated for the NOA TRY

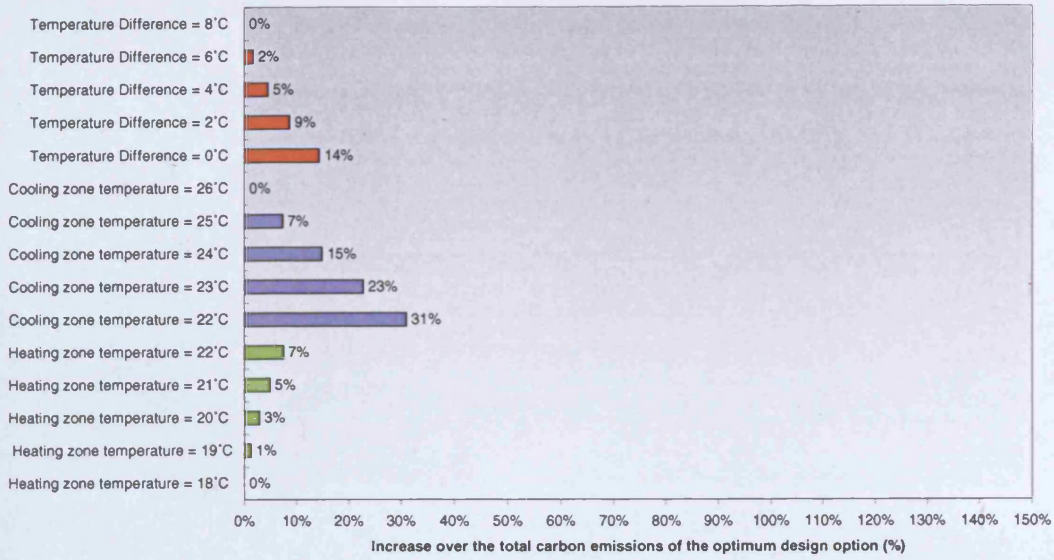

Figure 5.3.1-4: The impact of each parameter of group D on the total carbon emissions of the optimum design option, given that the remaining factors are set to their optimum level, when the FCU system is simulated for the NOA TRY

As can be seen from figure 5.3.1-1, the three parameters associated with the control of the internal temperature have a particularly high impact on the optimum total carbon emissions when the VAV system is simulated for the CIBSE TRY. The carbon penalty is up to 28% for a 1°C reduction in the cooling zone temperature set-point and up to 16% for a 1°C increase in the ΔT between the supply and the zone air respectively, as illustrated in figure 5.3.1-1. On the other hand, the carbon penalty for a 1°C increase in the heating zone temperature set-point is up to 12%, when the VAV system is simulated for this climate.

Figure 5.3.1-2, on the other hand, shows that the carbon penalty is approximately 8% when the cooling zone temperature set-point drops by 1°C and up to 6% when the heating zone temperature set-point increases by 1°C. It should also be remembered that the ΔT between the supply and the zone air has a high impact on the heating energy consumption of the FCU system. The effect of this parameter on the optimum total carbon emissions increases considerably when it is set lower than 4°C, as can be seen from figure 5.3.1-2.

The simulation of the VAV system for the NOA TRY in place of the CIBSE TRY leads to low heating energy use. As a result, the increase of the heating zone temperature set-point (over its optimum value) has a small carbon penalty, as shown in figure 5.3.1-3. This is also true for the effect of both the heating zone temperature set-point and the ΔT between the supply and the zone air on the optimum total carbon emissions of the FCU system when it is simulated for the Athens climate, as illustrated in figure 5.3.1-4. On the other hand, the specification of a low cooling zone temperature set-point has a high carbon impact when both HVAC systems are simulated for this climate. It is therefore clear that this parameter should be set to its optimum value (i.e. 26°C), regardless of the HVAC system and the climate for which the simulations are carried out.

There are some alternative combinations of the heating zone temperature set-point and the ΔT between the supply and the zone air leading to near-optimum carbon performance. The effect of these two parameters on the total carbon emissions of the BCS, given that the cooling zone temperature is set to its optimum level, is shown in figures 5.3.1-5 to 5.3.1-8, depending on the HVAC system and the climate under consideration.

Figure 5.3.1-5: The effect of the heating zone temp. and the ΔT between the supply and the zone air on the total carbon emissions of the BCS, given that the remaining factor is set to its optimum level, when the VAV system is simulated for the CIBSE TRY

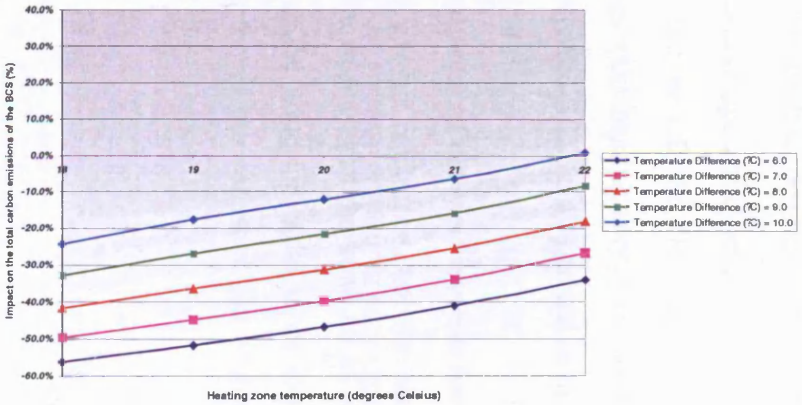

Figure 5.3.1-6: The effect of the heating zone temp. and the ΔT between the supply and the zone air on the total carbon emissions of the BCS, given that the remaining factor is set to its optimum level, when the FCU system is simulated for the CIBSE TRY

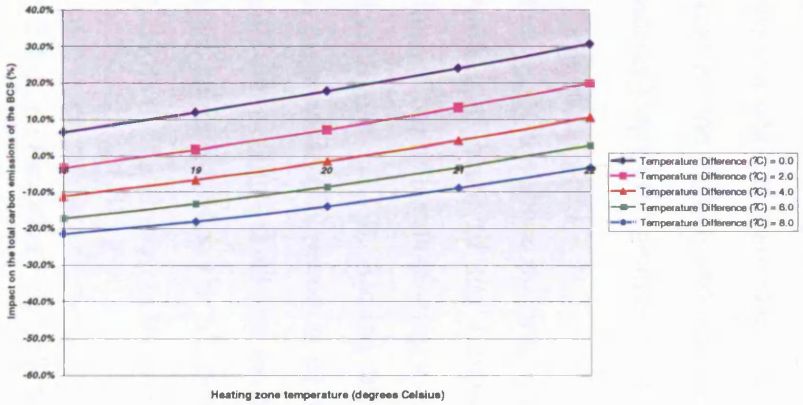

Figure 5.3.1-7: The effect of the heating zone temp. and the ΔT between the supply and the zone air on the total carbon emissions of the BCS, given that the remaining factor is set to its optimum level, when the VAV system is simulated for the NOA TRY

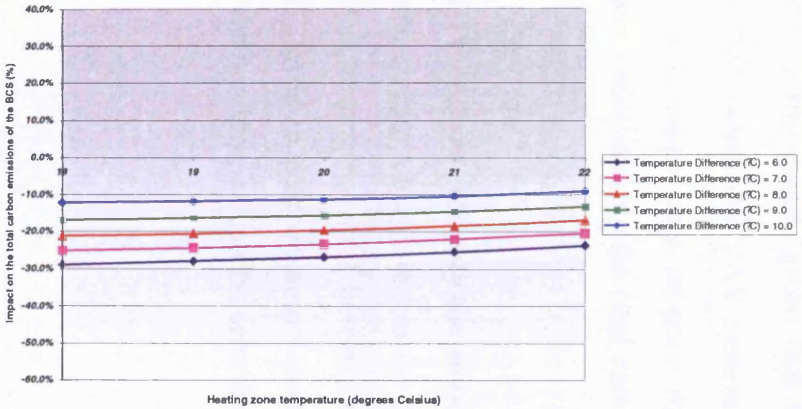

Figure 5.3.1-8: The effect of the heating zone temp. and the ΔT between the supply and the zone air on the total carbon emissions of the BCS, given that the remaining factor is set to its optimum level, when the FCU system is simulated for the NOA TRY

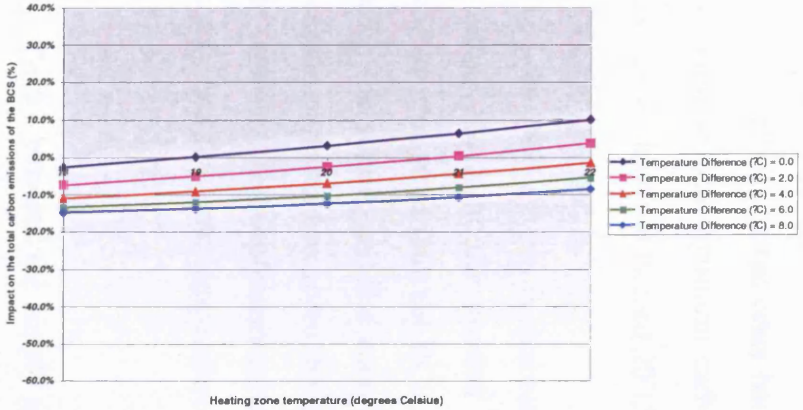

As can be seen from figure 5.3.1-6, opting for a ΔT between the supply and the zone air equal to or lower than 2°C leads to higher total carbon emissions than the BCS, for most of the values of the heating zone temperature set-point. This is clearly due to the high impact of both these parameters on the amount of heating energy consumed by the FCU system when it is simulated for the CIBSE TRY. Setting, on the other hand, the ΔT between the supply and the zone air to 8°C leads to near-optimum carbon performance as long as the heating zone temperature set-point does not exceed 20°C.

The reduction of the space heating requirement when the FCU system is simulated for the Athens in place of the London climate, allows for a higher number of combinations of factor levels leading to lower total carbon emissions than the BCS, as illustrated in figure 5.3.1-8. Aiming for a ΔT between the supply and the zone air equal to or higher than 6°C results in near-optimum carbon performance given that the heating zone temperature does not exceed 20°C. In addition, near-optimum carbon emissions are achieved when the ΔT between the supply and the zone temperature is set to 8°C, while the heating zone temperature is not higher than 21°C.

Figure 5.3.1-5, on the other hand, shows that setting the ΔT between the supply and the zone air to 6°C results in near-optimum carbon performance, given that the heating zone temperature set-point does not exceed 20°C when the VAV system is simulated for the CIBSE TRY. Specifying a higher zone temperature set-point than this increases the heating energy use and, hence, reduces considerably the total carbon savings over the BCS, as illustrated in this figure.

The simulation of the VAV system for the NOA TRY, reduces not only the amount of heating energy consumed, but the sensitivity of the cooling energy use to the ΔT between the supply and the zone air as well. Therefore, aiming for a ΔT between the supply and the zone air equal to or lower than 7°C, leads to near optimum carbon emissions for all the values of the heating zone air temperature, as can be seen from figure 5.3.1-7.

5.3.2 The parameters associated with the provision of night ventilation throughout the cooling period (group E)

The optimum night ventilation strategy and the impact that it has on the total carbon emissions of the BCS, depending on the HVAC system and the climate under consideration is shown in table 5.3.2-1:

Scenario	Climate	HVAC system	Factor levels		Impact on the total carbon emissions of the BCS			
			Ventilation rate (ach)	Period of ventilation (hours)	Change in the boiler emissions of the BCS (%)	Change in the chiller emissions of the BCS (%)	Change in the fan emissions (for night ventilation) of the BCS (%)	Change in the total carbon emissions of the BCS (%)
Factor settings of group E minimising the total carbon emissions	CIBSE TRY	VAV system	*5.0*	*10*	-	-14%	-	-9%
		FCU system	*10.0*	*10*	-	-11%	-	-8%
	NOA TRY	VAV system	*5.0*	*10*	-	-4%	-	-3%
		FCU system	*10.0*	*10*	-	-3%	-	-3%

Table 5.3.2-1: The effect of the optimum night ventilation strategy on the carbon emissions of the BCS, depending on the HVAC system and the climate under consideration

As can be seen from this table, the period of ventilation is set to 10 hours for both HVAC systems and climates, to maintain the internal temperature at a low level over the night and, hence, reduce the demand for mechanical cooling during the following day. The ventilation rate is set to 5 ach (i.e. the minimum value of this parameter) for the VAV system. It should be remembered that a natural ventilation strategy is used for the perimeter zones of the building, while the core zones are served by the central fans of this HVAC system. As explained in section 4.2.2, the night ventilation rate has a high impact on the electricity consumption of the central fans and should, therefore, be set close to its minimum value.

The fresh air is, on the other hand, supplied to the perimeter zones of the building, through natural means, at a ventilation rate of 10 ach, in order to maximise the effect of this parameter on the cooling energy use of the FCU system, as shown in section 4.2.2. The impact of the central fans of this HVAC system on the total carbon emissions is quite small, since they operate at a constant ventilation rate of 1.5 ach, serving the core zones of the building. It is not possible to specify a higher ventilation rate than this, for the core zones, due to the capacity limit of the central AHU

supplying the minimum fresh air quantity around the building when the FCU system is considered.

Table 5.3.2-1 illustrates that the total carbon savings over the BCS when the HVAC systems are simulated for the NOA TRY are only 3%. This is due to the small impact that the parameters of this group have on the cooling energy use of both systems when the simulations are carried out for the Athens climate, as shown in section 4.2.2.

The effect of the night ventilation rate and the period of ventilation on the total carbon emissions[11] of the BCS is presented in figures 5.3.2-1 to 5.3.2-4, depending on the HVAC system and the climate for which the simulations are carried out.

[11] **Note:** The total carbon emissions include the annual heating & cooling energy use, as well as the amount of electricity consumed by the central fans of the HVAC systems serving the core zones of the building during the night.

Figure 5.3.2-1: The effect of the ventilation rate and the period of ventilation on the total carbon emissions of the BCS, when the VAV system is simulated for the CIBSE TRY

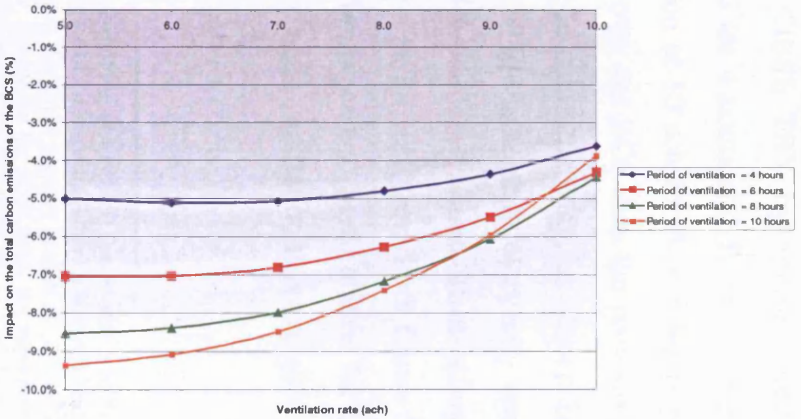

Figure 5.3.2-2: The effect of the ventilation rate and the period of ventilation on the total carbon emissions of the BCS, when the FCU system is simulated for the CIBSE TRY

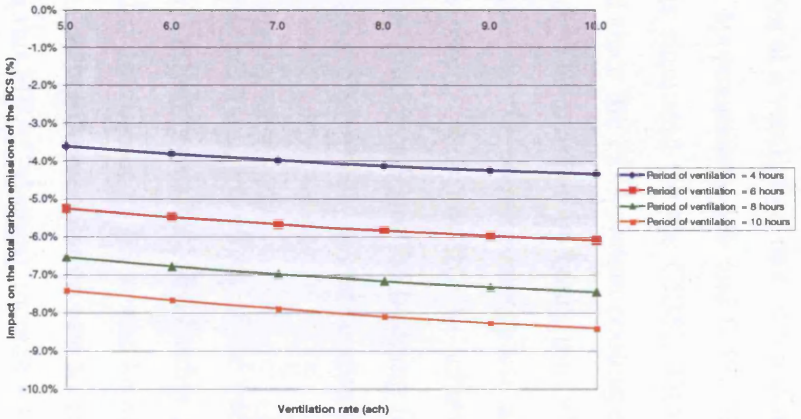

Figure 5.3.2-3: The effect of the ventilation rate and the period of ventilation on the total carbon emissions of the BCS, when the VAV system is simulated for the NOA TRY

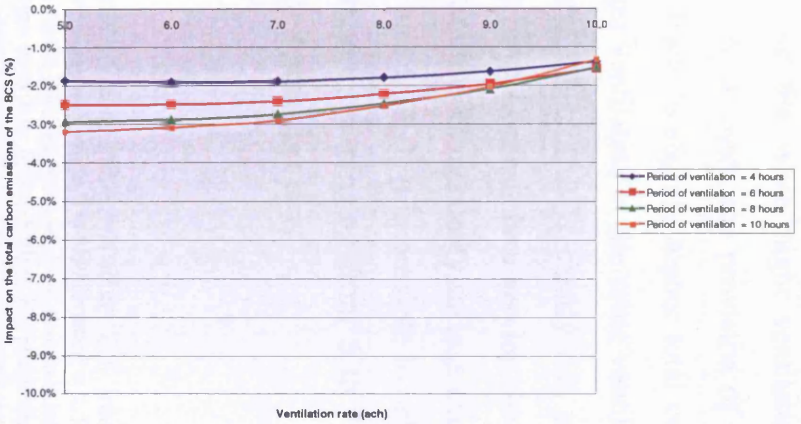

Figure 5.3.2-4: The effect of the ventilation rate and the period of ventilation on the total carbon emissions of the BCS, when the FCU system is simulated for the NOA TRY

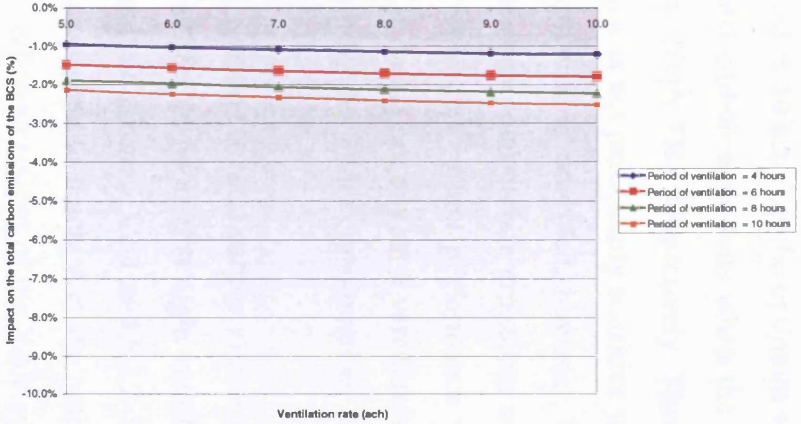

As can be seen from figures 5.3.2-2 and 5.3.2-4, the effect of the ventilation rate on the total carbon emissions of the FCU system[12] is trivial, regardless of the number of hours that night ventilation is provided. For example, the provision of night ventilation at a ventilation rate of 5 ach as opposed to 10 ach (i.e. the optimum value) leads to approximately 1% and 0.4% higher total carbon emissions when the FCU system is simulated for the CIBSE TRY and the NOA TRY respectively. This was expected since the FCU system cooling energy use is not particularly sensitive to this parameter. The number of hours that night ventilation is provided, however, has a high impact on the cooling energy use and, hence, the total carbon emissions of this HVAC system. It is possible to achieve near-optimum carbon performance when fresh air is introduced into the building for 8 to 10 hours per day, at a ventilation rate ranging from 5 to 10 ach, as can be seen from both figures under consideration.

On the other hand, the effect of the ventilation rate on the total carbon emissions of the VAV system increases considerably as the number of hours that night ventilation is provided gets closer to 10, as can be seen from both figure 5.3.2-1 and 5.3.2-3. For example, setting the ventilation rate to 10 ach as opposed to 5 ach, (i.e. the optimum value for this HVAC system), increases the total carbon emissions of the VAV system for the CIBSE TRY by approximately 1.5% and 6% when night ventilation is provided for 4 hours and 10 hours respectively. As a result, the provision of night ventilation at 10 ach for 6 or 8 hours per day leads to slightly higher total carbon savings over the BCS than the provision of night ventilation at the same ventilation rate for 10 hours per day, as shown in figure 5.3.2-1. This is clearly due to the increase in the amount of electricity consumed by the central fans serving the core zones of the building, which offsets a large part of the cooling energy savings over the BCS. As can be seen from both figure 5.3.2-1 and 5.3.2-3, it is possible to achieve near-optimum carbon performance for a ventilation rate ranging from 5 to 7 ach, given that night ventilation is provided at least for 8 hours per day.

[12] **Note:** It should be remembered that in this case the ventilation rate ranges from 5 to 10 ach only around the perimeter zones of the building (where it is supplied through natural means), while it is held constant at 1.5 ach in the core zones, due to the capacity limit of the central AHU serving the building when the FCU system is installed. In the VAV system, on the other hand, the ventilation rate ranges from 5 to 10 ach both in the perimeter zones (where it is supplied through natural means) and the core zones (where it is supplied through mechanical means).

5.3.3 The parameters associated with the plant operation schedule and performance (group F)

As discussed in section 4.2.3, opting for a high efficiency condensing boiler (i.e. a boiler efficiency close to 95%) results in low heating energy use, while, on the other hand, the utilisation of a water cooled chiller with a high COP (i.e. a COP close to 5.2) reduces the annual cooling energy consumption. On top of this, the operation of the plant for 9 hours per day reduces both the heating and the cooling energy consumption of the HVAC systems. Table 5.3.3-1 illustrates that the optimisation of the parameters of this group leads to considerably lower heating and cooling energy consumption than the BCS in all cases.

Scenario	Climate	HVAC system	Factor levels			Impact on the total carbon emissions of the BCS		
			Boiler efficiency (%)	Chiller COP	HVAC system operation (hours)	Change in the boiler emissions of the BCS (%)	Change in the chiller emissions of the BCS (%)	Change in the total carbon emissions of the BCS (%)
Factor settings of group F minimising the total carbon emissions	CIBSE TRY	VAV system	*95%*	*5.20*	*9*	-46%	-53%	-51%
		FCU system	*95%*	*5.20*	*9*	-33%	-52%	-49%
	NOA TRY	VAV system	*95%*	*5.20*	*9*	-61%	-53%	-53%
		FCU system	*95%*	*5.20*	*9*	-41%	-53%	-53%

Table 5.3.3-1: The effect of the optimum factor settings of group F on the carbon emissions of the BCS, depending on the HVAC system and the climate under consideration

The increase over the optimum total carbon emissions when each parameter of this group is set higher (or lower) than its optimum value is shown in figures 5.3.3-1 to 5.3.3-4, depending on the type of HVAC system and the climate for which it is simulated:

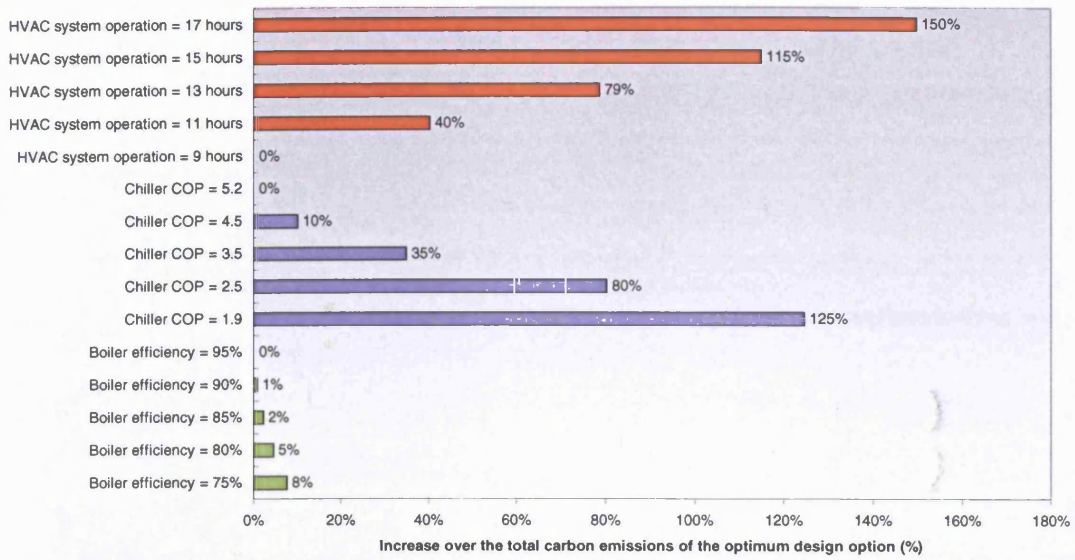

Figure 5.3.3-1: The impact of each parameter of group F on the total carbon emissions of the optimum design option, given that the remaining factors are set to their optimum level, when the VAV system is simulated for the CIBSE TRY

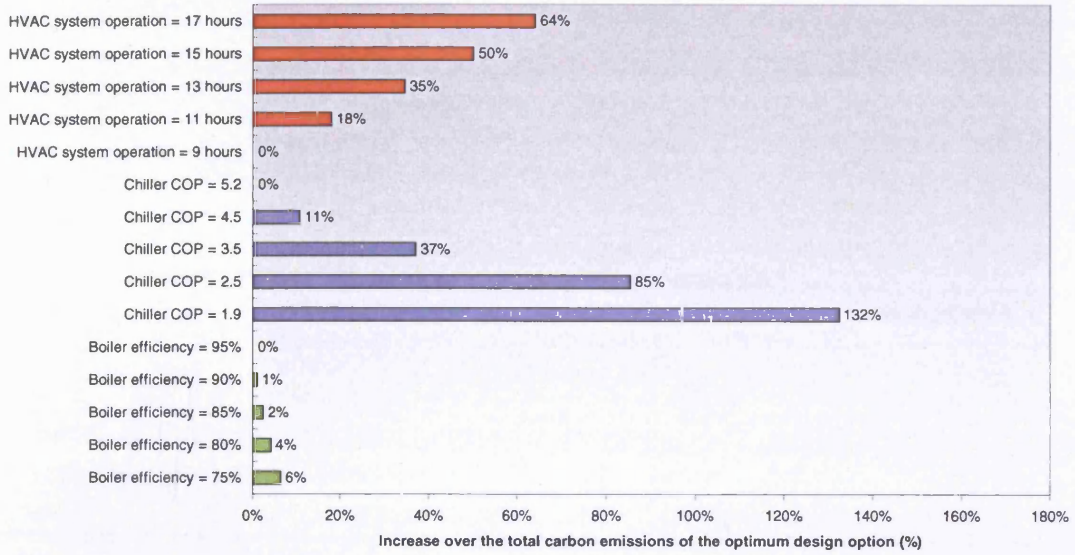

Figure 5.3.3-2: The impact of each parameter of group F on the total carbon emissions of the optimum design option, given that the remaining factors are set to their optimum level, when the FCU system is simulated for the CIBSE TRY

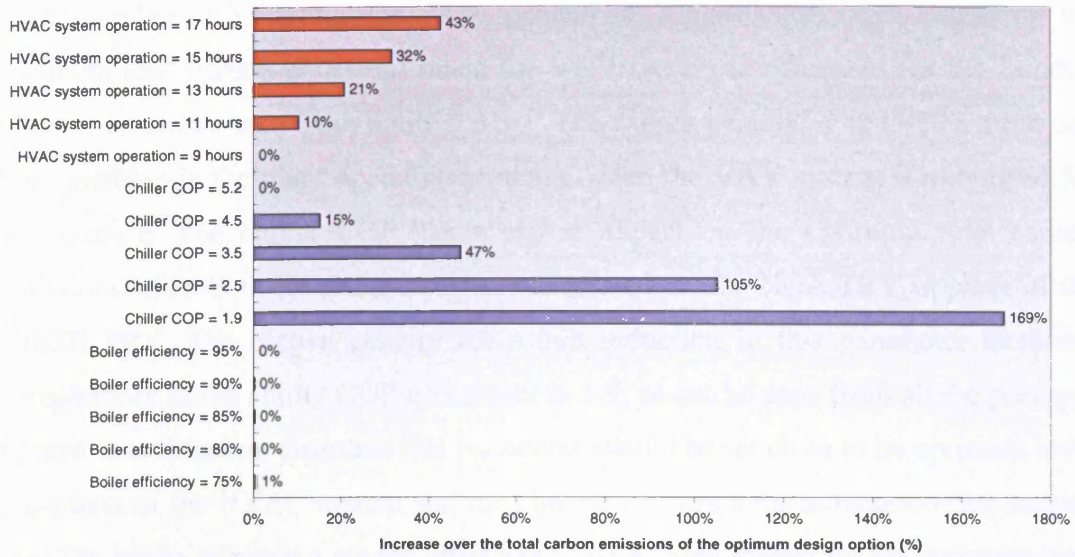

Figure 5.3.3-3: The impact of each parameter of group F on the total carbon emissions of the optimum design option, given that the remaining factors are set to their optimum level, when the VAV system is simulated for the NOA TRY

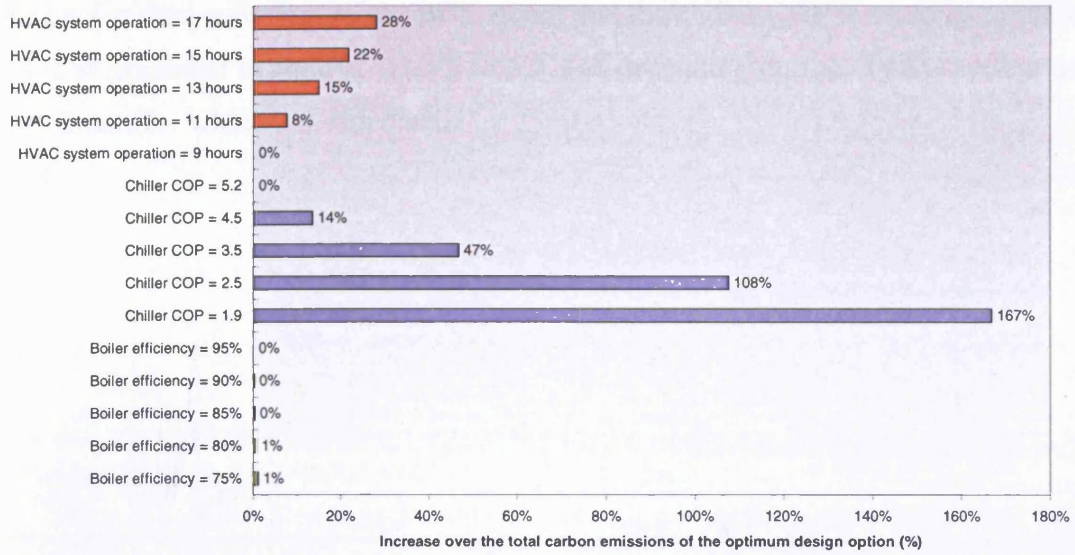

Figure 5.3.3-4: The impact of each parameter of group F on the total carbon emissions of the optimum design option, given that the remaining factors are set to their optimum level, when the FCU system is simulated for the NOA TRY

The number of hours that the plant operates has a particularly high impact on the optimum total carbon emissions when the VAV system is simulated for the London climate, as can be seen from figure 5.3.3-1. The carbon penalty is up to 20% for a one hour increase in the plant operation schedule when the VAV system is simulated for this climate. The chiller COP has a higher impact on the optimum total carbon emissions when both HVAC systems are simulated for the NOA TRY in place of the CIBSE TRY. The carbon penalty for a unit reduction in this parameter increases considerably as the chiller COP gets closer to 1.9, as can be seen from all the previous figures. It is therefore clear that this parameter should be set close to its optimum level regardless of the HVAC system and the climate for which the simulations are carried out. The boiler efficiency, on the other hand, has a small impact on the optimum total carbon emissions, particularly when the HVAC systems are simulated for the Athens typical weather conditions.

The effect of the boiler efficiency and the number of hours that the plant operates on the total carbon emissions of the BCS, given that the chiller COP is set to its optimum level, is presented in figures 5.3.3-5 to 5.3.3-8, depending on the HVAC system and the climate for which it is simulated.

Figure 5.3.3-5: The effect of the boiler efficiency and the number of hours the plant operates on the total carbon emissions of the BCS, given that the chiller COP is set to its optimum level, when the VAV system is simulated for the CIBSE TRY

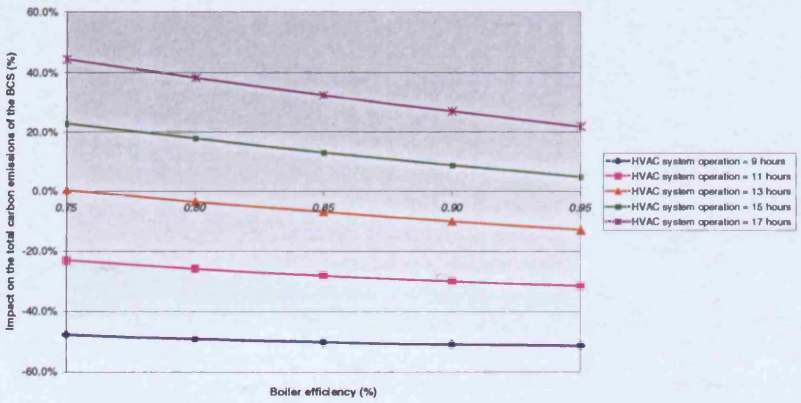

Figure 5.3.3-6: The effect of the boiler efficiency and the number of hours the plant operates on the total carbon emissions of the BCS, given that the chiller COP is set to its optimum level, when the FCU system is simulated for the CIBSE TRY

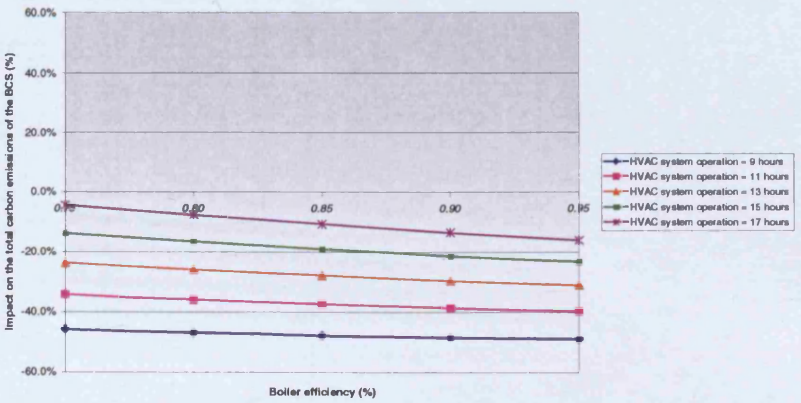

Figure 5.3.3-7: The effect of the boiler efficiency and the number of hours the plant operates on the total carbon emissions of the BCS, given that the chiller COP is set to its optimum level, when the VAV system is simulated for the NOA TRY

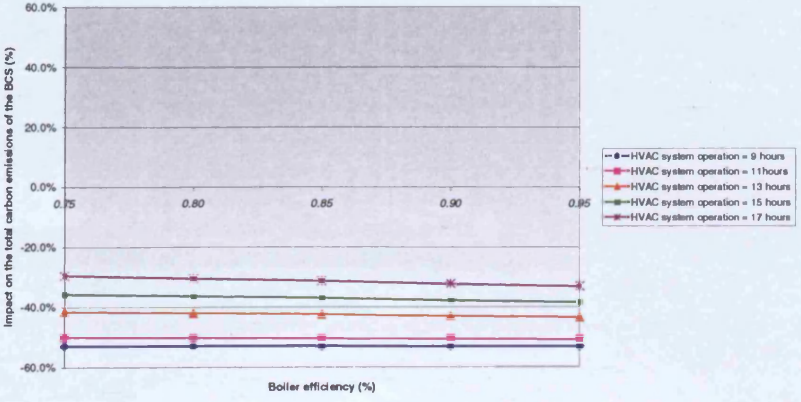

Figure 5.3.3-8: The effect of the boiler efficiency and the number of hours the plant operates on the total carbon emissions of the BCS, given that the chiller COP is set to its optimum level, when the FCU system is simulated for the NOA TRY

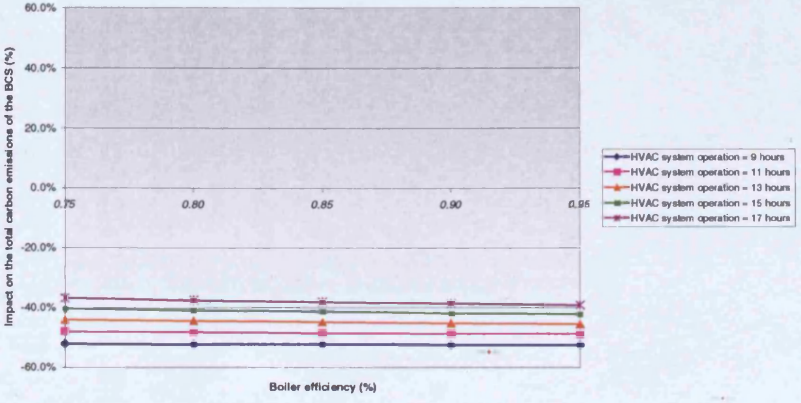

It should be stressed that the two parameters involved in the four figures shown above affect mainly the part of the total carbon emissions associated with the operation of the boiler. Given the low space heating requirement in the cooling-dominated climate of Athens it can be seen from figures 5.3.3-7 and 5.3.3-8 that most of the combinations of the boiler efficiency and the number of hours of plant operation have a limited effect on the total carbon savings over the BCS in this climate. Figure 5.3.3-5, on the other hand, shows that this is the only case where the operation of the plant for 15 hours or more leads to higher carbon emissions than the BCS, regardless of the boiler efficiency. This is clearly due to the high impact of the number of hours that the plant operates on the heating energy use of the VAV system when it is simulated for the CIBSE TRY.

In general, figures 5.3.3-5 and 5.3.3-6 suggest that it is possible to achieve near-optimum carbon emissions when the plant operates for 9 hours, regardless of the efficiency of the boiler. On the other hand, figures 5.3.3-7 and 5.3.3-8 indicate that near-optimum carbon performance can be achieved for the entire range of values of the boiler efficiency, as long as the plant operation does not exceed 13 hours and 14 hours, respectively.

This study illustrated that the maintenance of the internal temperature at a constant level for most of day can be particularly energy wasteful. It should be stressed that, theoretically, the operation of the heating plant for a couple of hours outside the normal plant operation schedule should be recommended when 'optimum start' is utilised. In such a case, the plant provides heating for a number of hours in advance of the occupation period, (pre-heat period), so that the zone design condition is gradually reached before the start of the normal plant operation schedule. This operation strategy should lead to a relatively lower amount of heating energy than the energy that would have been required in order to achieve the zone desired condition in a single hour (i.e. as soon as the plant starts to operate). However, B-TAS[13] (version 8.40) does not allow for the simulation of this plant control function. Nevertheless, the effect of such an operation strategy on the overall carbon performance of the HVAC

[13] **Note:** A brief study included in appendix J, shows that B-TAS version 8.40 cannot simulate 'Optimum Start', despite the provision of input parameters associated with this aspect of the plant operation in A-TAS.

systems under consideration would have been trivial since the emissions associated with the operation of the boiler are in most cases a small part of the total carbon emissions, as mentioned earlier.

5.3.4 The parameters associated with the fan size and efficiency (group G)

Table 5.3.4-1 indicates that opting for high fan and motor efficiencies, (e.g. close to 90% and 95% respectively), and keeping the size of the supply & return fans as small as possible minimises the total carbon emissions of both HVAC systems.

Scenario	Climate	HVAC system	Factor levels				Impact on the total carbon emissions of the BCS			
			Fan efficiency (%)	Motor efficiency (%)	Supply fan (Pa)	Return fan (Pa)	Change in the boiler emissions of the BCS (%)	Change in the chiller emissions of the BCS (%)	Change in the fan emissions of the BCS (%)	Change in the total carbon emissions of the BCS (%)
Factor settings of group G minimising the total carbon emissions	CIBSE TRY	VAV system	0.90	0.95	500	120	-	-7%	-38%	-15%
		FCU system	0.90	0.95	300	140	-	0%	-6%	-2%
	NOA TRY	VAV system	0.90	0.95	500	120	-	-5%	-39%	-12%
		FCU system	0.90	0.95	300	140	-	-1%	-7%	-2%

Table 5.3.4-1: The effect of the optimum factor settings of group G on the carbon emissions of the BCS[14], depending on the HVAC system and the climate under consideration

As can be seen from table 5.3.4-1, the optimisation of the factors associated with the size & efficiency of the fans results in a small reduction in total carbon emissions over the BCS in both climates for which the FCU system is simulated. This is due to the fact that the parameters of this group affect mainly the amount of energy used by the central fans of this HVAC system to supply the minimum fresh air quantity around the building, and not the energy consumed by the fan coil units located in the building zones, which dominates the total fan energy use of the FCU system.

The increase over the optimum carbon emissions when each parameter of this group is set higher (or lower) than its optimum value is shown in figures 5.3.4-1 to 5.3.4-4, depending on the type of HVAC system and the climate for which it is simulated:

[14] **Note:** It is worth mentioning that the carbon emissions associated with the electricity consumed by the fans of each system in the BCS are added to the carbon emissions related to the heating & cooling energy use first, and then the calculation of the total carbon savings over the BCS, (for the optimum factor settings of this group), takes place.

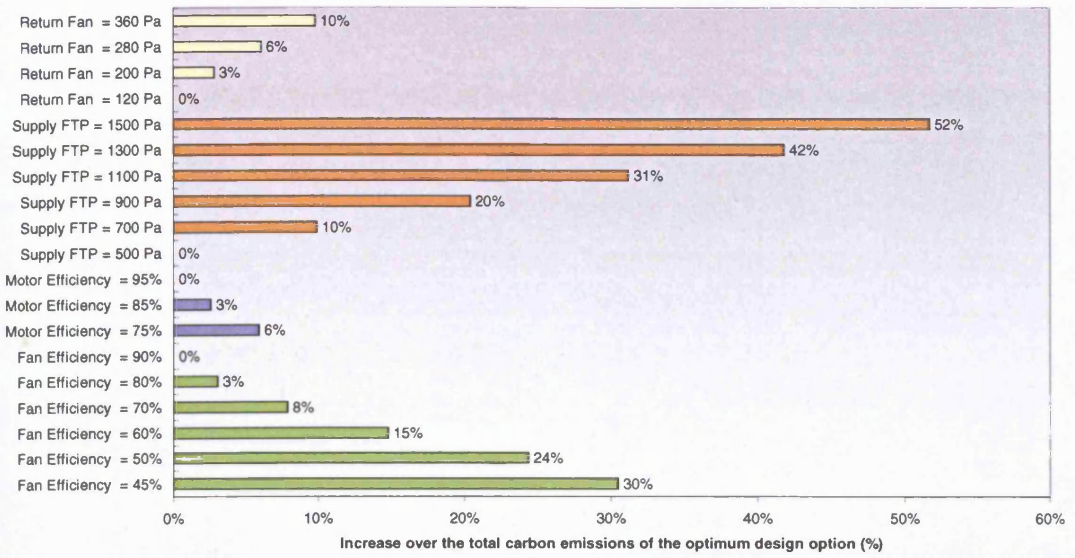

Figure 5.3.4-1: The impact of each parameter of group G on the total carbon emissions of the optimum design option, given that the remaining factors are set to their optimum level, when the VAV system is simulated for the CIBSE TRY

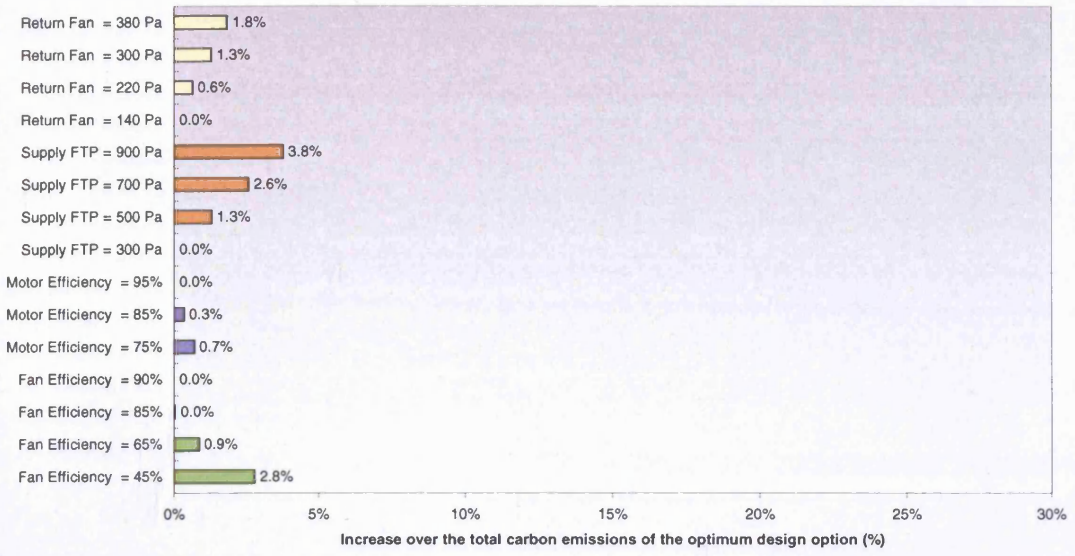

Figure 5.3.4-2: The impact of each parameter of group G on the total carbon emissions of the optimum design option, given that the remaining factors are set to their optimum level, when the FCU system is simulated for the CIBSE TRY

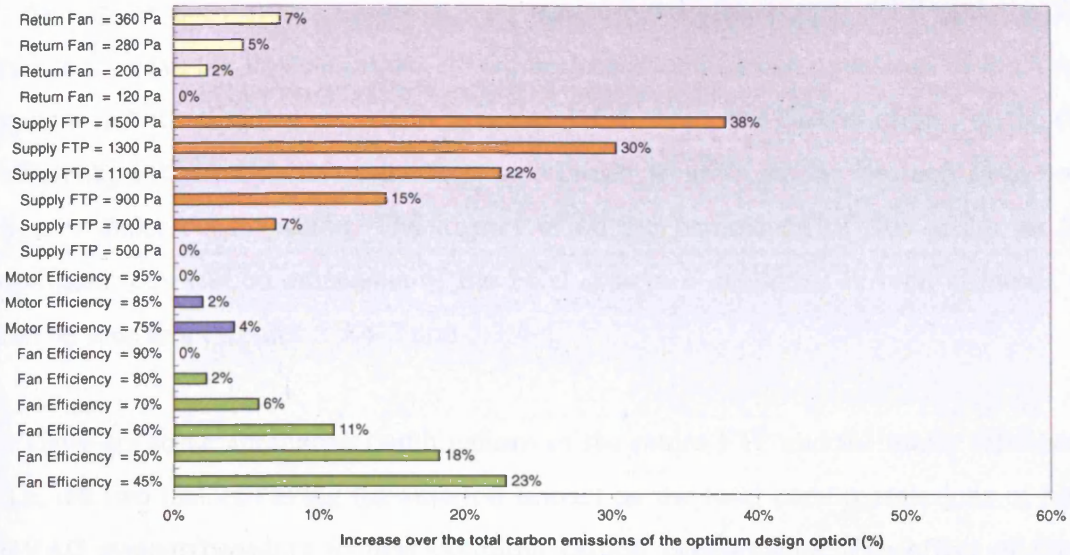

Figure 5.3.4-3: The impact of each parameter of group G on the total carbon emissions of the optimum design option, given that the remaining factors are set to their optimum level, when the VAV system is simulated for the NOA TRY

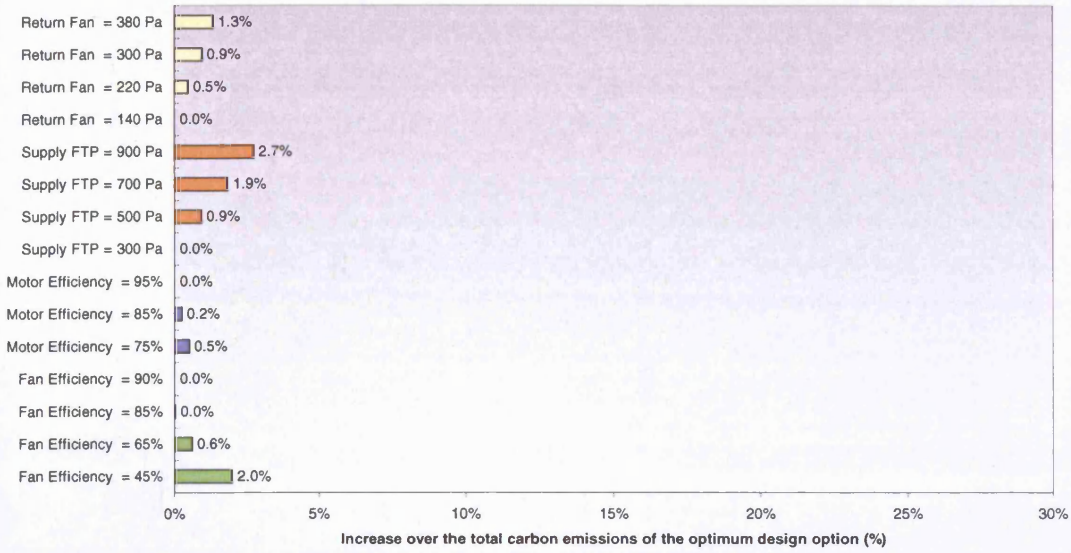

Figure 5.3.4-4: The impact of each parameter of group G on the total carbon emissions of the optimum design option, given that the remaining factors are set to their optimum level, when the FCU system is simulated for the NOA TRY

As can be seen from figures 5.3.4-1 and 5.3.4-3, the supply FTP and the fan efficiency have the highest impact on the optimum total carbon emissions of the VAV system in both climates for which it is simulated. Also, the carbon impact of the fan efficiency increases as this parameter gets closer to 45%, as can be seen from both figures under consideration. The impact of all the parameters of this group on the optimum total carbon emissions of the FCU system is moderate in both climates, as can be seen from figures 5.3.4-2 and 5.3.4-4.

There are some alternative combinations of the return FTP and the motor efficiency (i.e. the two factors having the smallest impact on the total carbon emissions of both HVAC systems) leading to near-optimum carbon performance. The effect of these two parameters on the total carbon emissions of the BCS, given that the remaining two factors are held constant at their respective optimum level, is presented in figures 5.3.4-5 to 5.3.4-8, depending on the HVAC system and the climate under consideration.

Figure 5.3.4-5: The effect of the return FTP and the motor efficiency on the total carbon emissions of the BCS, given that the remaining two factors are set to their optimum level, when the VAV system is simulated for the CIBSE TRY

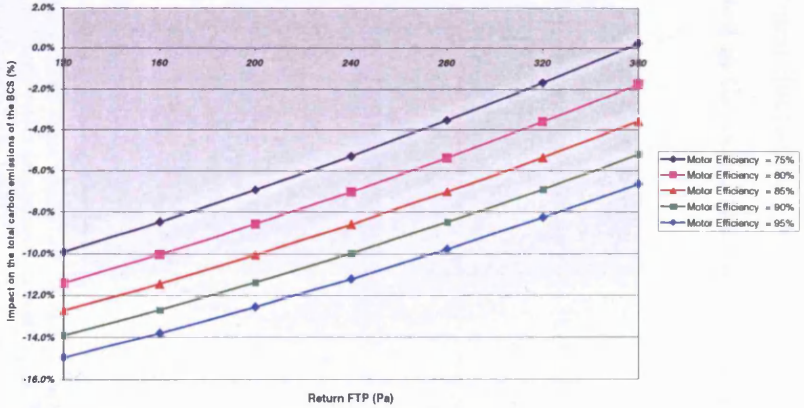

Figure 5.3.4-6: The effect of the return FTP and the motor efficiency on the total carbon emissions of the BCS, given that the remaining two factors are set to their optimum level, when the FCU system is simulated for the CIBSE TRY

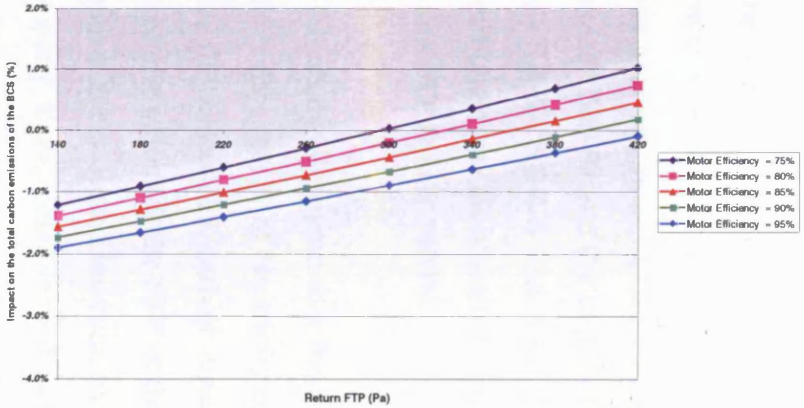

Figure 5.3.4-7: The effect of the return FTP and the motor efficiency on the total carbon emissions of the BCS, given that the remaining two factors are set to their optimum level, when the VAV system is simulated for the NOA TRY

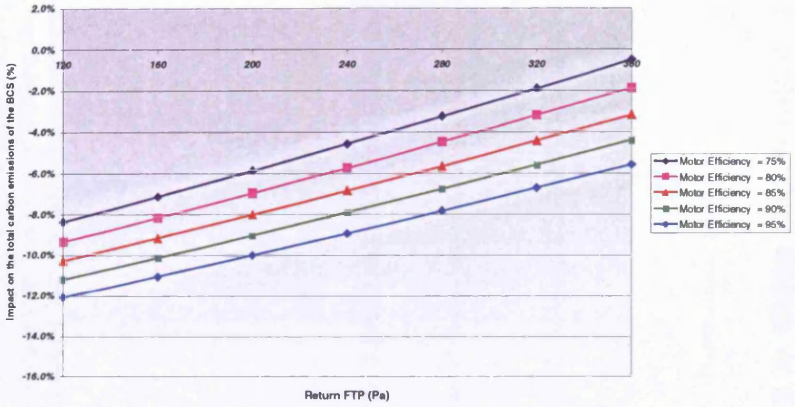

Figure 5.3.4-8: The effect of the return FTP and the motor efficiency on the total carbon emissions of the BCS, given that the remaining two factors are set to their optimum level, when the FCU system is simulated for the NOA TRY

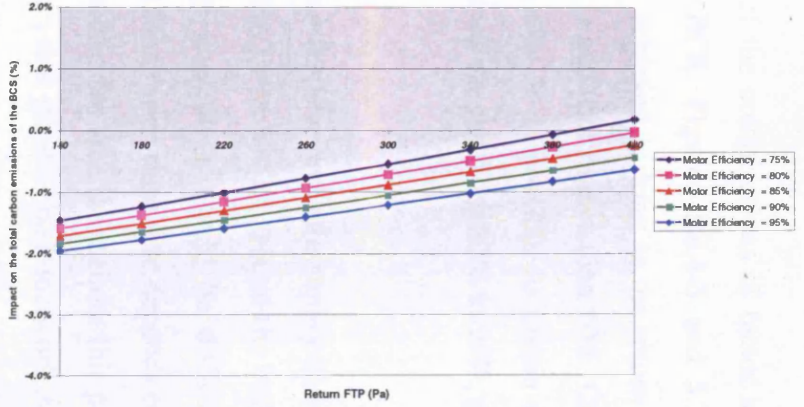

As can be seen from these four figures, most of the combinations of factor levels lead to lower total carbon emissions than the BCS. Figures 5.3.4-5 and 5.3.4-7 indicate that near-optimum carbon emissions are achieved as long as the return FTP does not exceed 200 Pa and the motor efficiency is equal or higher than 90%. On the other hand, figures 5.3.4-6 and 5.3.4-8 suggest that it is possible to obtain near-optimum carbon emissions when the motor efficiency ranges from 80% to 95%, given that the return FTP equals 140 Pa.

Clearly, this study illustrated that there is a trend for low pressure supply & return fans to reduce the amount of electricity consumed to move the air around the building and, hence, the associated carbon emissions. In general, it would be difficult to suggest a specific value for the FTP of the central fans, since their size depends on the requirements of the project. However, by changing the fan size throughout this purely theoretical study, it was possible to show the impact that good or bad ductwork design has on the fan energy consumption of the HVAC systems, as also explained in chapter 3 (section 3.3.2). The engineer should therefore pay particular attention to the selection and placement of the duct fittings in the ductwork system, as well as to the AHU component losses, since they can significantly increase the size of the fans (e.g. a complicated ductwork system involving a large number of duct fittings or a dirty filter located in the AHU can lead to excessive FTP[15]).

[15] **Note:** As can be seen from appendices A and B, there are large differences in the pressure drop figures found in the literature for each AHU component as well as in the pressure loss factors for the various duct fittings, so they should be chosen carefully to keep the size of the supply & return fans as small as possible.

5.3.5 The parameters associated with the humidification of the supply air quantity (group H)

Table 5.3.5-1 illustrates that setting both the RH set-point and the proportional band to their lower level (i.e. 40% ± 2.5%) and operating the steam humidifier only for the minimum period considered (i.e. for six months), minimises the total carbon emissions of the HVAC systems, when humidification is provided.

Scenario	Climate	HVAC system	Factor levels			Impact on the total carbon emissions of the BCS			
			Humidification setpoint (%)	Proportional band (%)	Period of humidification	Change in the humidification emissions of the BCS (%)	Change in the boiler emissions of the BCS (%)	Change in the chiller emissions of the BCS (%)	Change in the total carbon emissions of the BCS (%)
Factor settings of group H minimising the total carbon emissions	CIBSE TRY	VAV system	40	5	Heating Season	-	0%	0%	39%
		FCU system	40	5	Heating Season	-	0%	0%	13%
	NOA TRY	VAV system	40	5	Heating Season	-	0%	0%	28%
		FCU system	40	5	Heating Season	-	0%	0%	6%

Table 5.3.5-1: The effect of the optimum factor settings of group H on the carbon emissions of the BCS[16], depending on the HVAC system and the climate under consideration

As can be seen from this table, the chosen factor settings of this group lead to higher total carbon emissions than the BCS due to the energy consumed for the humidification of the air. The energy cost of humidification is considerably higher for the VAV system than the FCU system in both climates. This is due to the fact that the former is required to handle large air quantities, (mixing fresh and re-circulated air), which vary throughout the year depending on the requirements of the building zones, while the latter provides humidification of the minimum fresh air quantity, (for ventilation purposes), which is supplied throughout the building by the central ductwork system.

[16] **Note:** The steam humidifier operates on electricity (i.e. a value of 0.127 kg C / kWh of delivered energy is assumed) [6].

As shown in section 4.2.5, the RH set-point has the highest impact on the amount of energy consumed in the humidification process and, hence, the total carbon emissions of the HVAC systems[17]. It is therefore clear that this parameter should be set close to its optimum level. The effect of the proportional band and the period of humidification on the total carbon emissions of the BCS, given that the RH set-point is set to 40%, is displayed in figures 5.3.5-1 to 5.3.5-4, depending on the HVAC system and the climate for which it is simulated.

[17] **Note:** For example, specifying a RH set-point of 50% as opposed to 40%, while the proportional band is set to 5% and the steam humidifier operates for the heating season (i.e. the remaining two parameters are set to their optimum level), increases the total carbon emissions by up to 42% and 13% for the VAV system and the FCU system respectively, depending on the climate for which the simulations are carried out.

Figure 5.3.5-1: The effect of the proportional band and the period of humidification on the total carbon emissions of the BCS, given that the remaining factor is set to its optimum level, when the VAV system is simulated for the CIBSE TRY

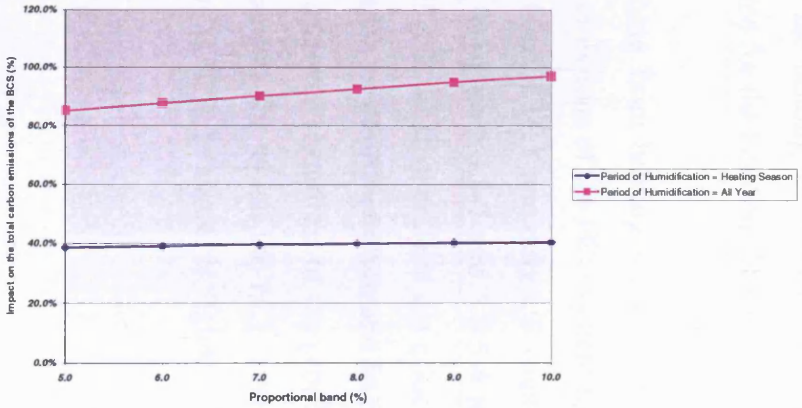

Figure 5.3.5-2: The effect of the proportional band and the period of humidification on the total carbon emissions of the BCS, given that the remaining factor is set to its optimum level, when the FCU system is simulated for the CIBSE TRY

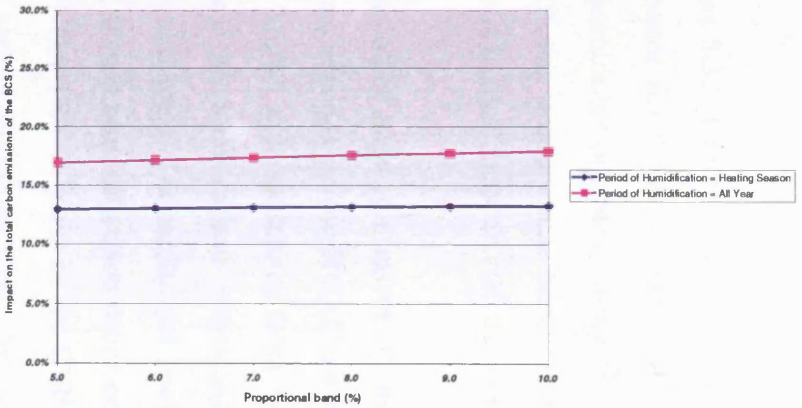

Figure 5.3.5-3: The effect of the proportional band and the period of humidification on the total carbon emissions of the BCS, given that the remaining factor is set to its optimum level, when the VAV system is simulated for the NOA TRY

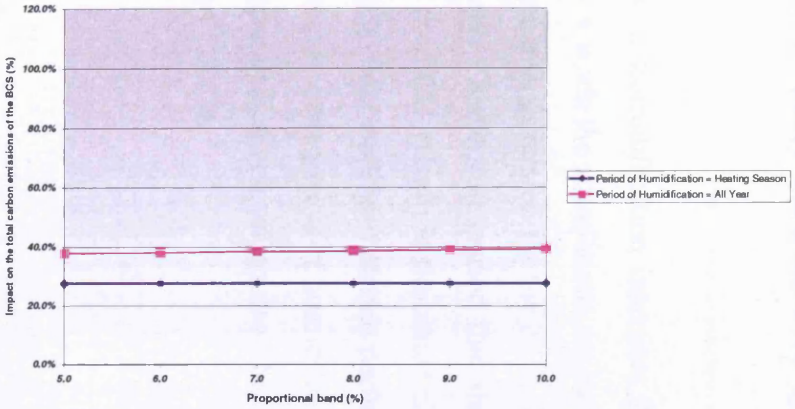

Figure 5.3.5-4: The effect of the proportional band and the period of humidification on the total carbon emissions of the BCS, given that the remaining factor is set to its optimum level, when the FCU system is simulated for the NOA TRY

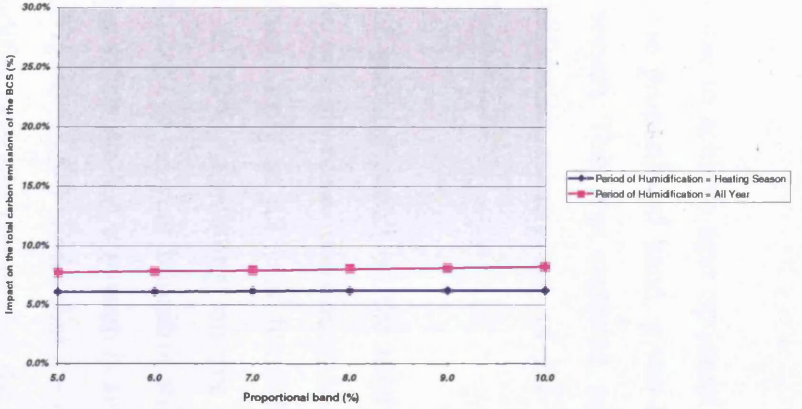

Figures 5.3.5-1 to 5.3.5-4 show that it is possible to achieve near optimum carbon performance for the entire range of values of the proportional band, given that the steam humidifier operates during the heating season. This was expected, since the effect of the proportional band on the humidification energy use of the HVAC systems is in most cases trivial, as shown in section 4.2.5.

On the other hand, the effect of the period of humidification on the total carbon emissions depends on the HVAC system and the climate under consideration. Figure 5.3.5-1 shows that switching from heating season only to all year humidification increases the total carbon emissions by up to 42%, depending on the chosen proportional band. The additional environmental cost of all year humidification over heating season humidification drops considerably when the VAV system is simulated for the NOA TRY in place of the CIBSE TRY. Figure 5.3.5-3 shows that the increase in total carbon emissions when the steam humidifier operates throughout the year as opposed to the heating season only, is up to 9%. This has to do with the effect of the outdoor conditions on the way that this system operates throughout the year, as explained in section 4.2.5. Nevertheless, it is clear that the provision of humidification outside the heating season should be avoided, particularly when the VAV system is simulated for the London climate.

Switching from heating season only to all year humidification increases the total carbon emissions of the FCU system by up to 4% when the simulations are carried out for the CIBSE TRY and only 2% when this system is simulated for the NOA TRY, as shown in figure 5.3.5-2 and 5.3.5-4 respectively. Clearly, the period that the steam humidifier is set to operate is not critical when the FCU system is simulated either for the London or the Athens climate. In other words, near-optimum carbon performance can be achieved regardless of the proportional band or the period of humidification, in both climates for which the FCU system is simulated, given, of course, that the RH set-point is 40%, as shown in figures 5.3.5-2 and 5.3.5-4.

In section 5.1, which contains a discussion on the carbon performance of the two HVAC systems for the BCS, it was shown that the VAV system is 47% and 23% less carbon intensive than the FCU system, when the simulations are carried out for the CIBSE TRY and the NOA TRY respectively. This difference drops to 35% and 8% for the London and the Athens climate respectively, when the steam humidifier is set to maintain a minimum RH of 40% ± 2.5% for the heating period. Keeping, therefore, in mind that the humidification process is much more carbon intensive for the VAV system than the FCU system, particularly when the steam humidifier operates throughout the year, it can be seen that it may be possible to turn the carbon scales in favour of the FCU system depending on the values of the parameters of this group. The effect of the RH set-point and the period of humidification (i.e. the two parameters that have the highest impact on the amount of energy consumed by the steam humidifier and, hence, the overall carbon performance of the HVAC systems) on the difference[18] in total carbon emissions between the VAV system and the FCU system, given that the proportional band is set to its optimum level, is presented in figure 5.3.5-5 for the CIBSE TRY and figure 5.3.5-6 for the NOA TRY respectively.

[18] **Note:** The difference (%) in total carbon emissions is set as follows: (VAV system total carbon emissions – FCU system total carbon emissions) / (FCU system total carbon emissions)

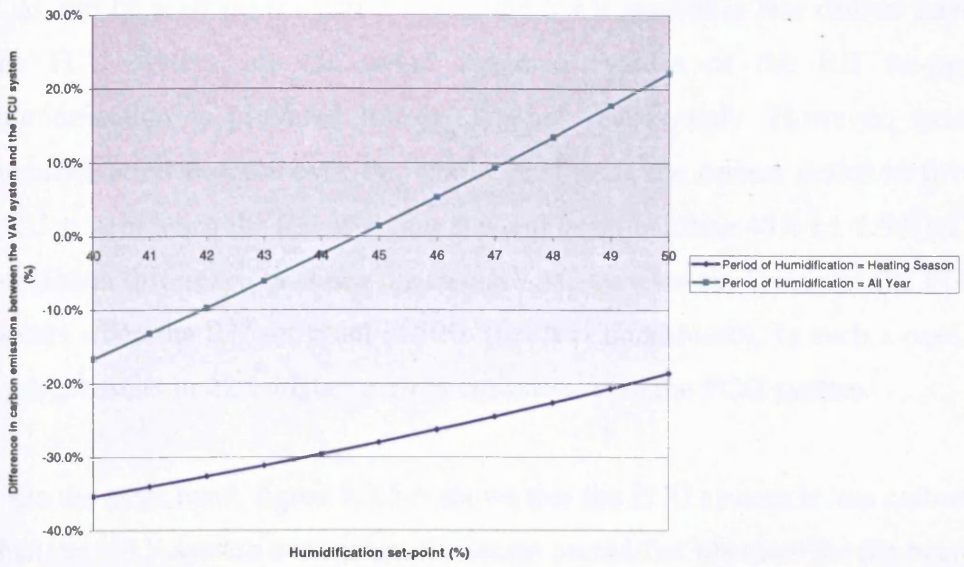

Figure 5.3.5-5: The effect of the RH set-point and the period of humidification on the difference in total carbon emissions between the VAV system and the FCU system, for a proportional band of 5%, when both systems are simulated for the CIBSE TRY

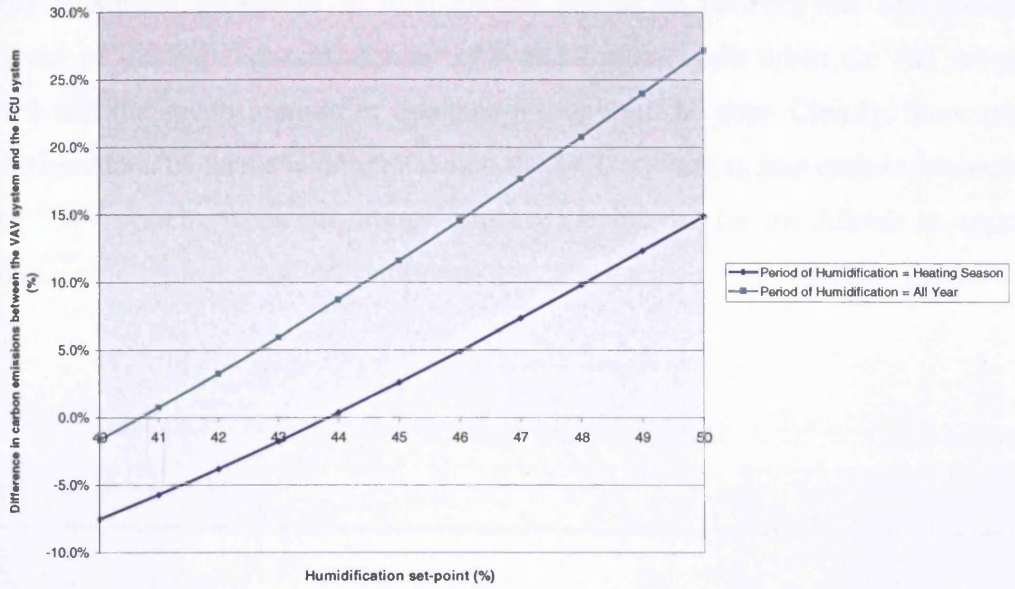

Figure 5.3.5-6: The effect of the RH set-point and the period of humidification on the difference in total carbon emissions between the VAV system and the FCU system, for a proportional band of 5%, when the simulations are carried out for the NOA TRY

As can be seen from figure 5.3.5-5, the VAV system is less carbon intensive than the FCU system for the entire range of values of the RH set-point, when humidification is provided for the heating season only. However, extending the humidification process over the whole year turns the carbon scales in favour of the FCU system when the RH set-point is equal or higher than 45% (± 2.5%). Clearly, the maximum difference between the two HVAC systems (in favour of the FCU system) occurs when the RH set-point is 50% (i.e. it is maximised). In such a case, the VAV system results in 22% higher carbon emissions than the FCU system.

On the other hand, figure 5.3.5-6 shows that the FCU system is less carbon intensive than the VAV system even when the steam humidifier operates for the heating season only, given that the RH set-point is higher than 44% (± 2.5%). In addition, switching from heating season only to all year humidification turns the carbon scales in favour of the FCU system when the RH set-point is equal or higher than 41% (± 2.5%), or in other words, for most of the values of the RH set-point displayed in figure 5.3.5-6. The maximum difference in total carbon emissions between the two systems (in favour of the FCU system) equals 27% and occurs again when the RH set-point is 50% and the steam humidifier operates throughout the year. Clearly, there are more combinations of factor levels for which the FCU system is less carbon intensive than the VAV system, when the simulations are carried out for the Athens as opposed to the London typical weather conditions.

5.4 Summary of findings

This chapter has identified the values of the parameters contained in each of the eight chosen groups that minimise the total carbon emissions of the HVAC systems in both climates for which they are simulated. The effect of the optimum factor settings on the carbon performance of the BCS depending on the HVAC system and the climate under consideration has been discussed, while the alternative combinations of factor levels leading to near-optimum carbon emissions have been presented through a number of trade-off diagrams.

As explained in chapter 3, (section 3.3.1), groups A and B contain the parameters associated with the building envelope cooling load, while group C consists of the factors related to the internal cooling load. The optimum factor settings of each of these groups are summarised in table 5.4-1:

Scenario		Base case scenario				Optimum factor settings			
Climate		CIBSE TRY		NOA TRY		CIBSE TRY		NOA TRY	
HVAC system		VAV system	FCU system	VAV system	FCU system	VAV system	FCU system	VAV system	FCU system
Group A (no daylight)	Glazing ratio (0 -1)	0.40	0.40	0.40	0.40	0.25	0.25	0.25	0.25
	Total shading coefficient	0.74	0.74	0.74	0.74	0.16	0.16	0.16	0.16
	Overhang depth (m)	0.00	0.00	0.00	0.00	0.00	0.00	1.10	1.20
	Sidefin depth (m)	0.00	0.00	0.00	0.00	1.80	1.30	2.00	2.00
Group A (with daylight)	Glazing ratio (0 -1)	0.40	0.40	0.40	0.40	0.25	0.40	0.25	0.95
	Total shading coefficient	0.74	0.74	0.74	0.74	0.76	0.37	0.68	0.16
	Overhang depth (m)	0.00	0.00	0.00	0.00	0.70	0.00	0.50	0.00
	Sidefin depth (m)	0.00	0.00	0.00	0.00	0.00	0.00	0.00	0.00
Group B	Wall U-value (W/m^2K)	0.35	0.35	0.35	0.35	0.18	0.27	0.19	0.70
	Infiltration rate (ach)	0.50	0.50	0.50	0.50	0.25	0.25	0.25	0.40
	Window U-value (W/m^2K)	2.10	2.10	2.10	2.10	1.20	5.70	5.80	5.80
Group C	Lighting gains (W/m^2)	12.0	12.0	12.0	12.0	6.5	6.5	6.5	6.5
	Equipment gains (W/m^2)	15.0	15.0	15.0	15.0	10.0	10.0	10.0	10.0
	Occupant Density (m^2 per person)	10	10	10	10	20	20	20	20

Table 5.4-1: The base case and the optimum factor settings of each of the groups associated with the building load

The impact of the optimum factor settings of each group on the overall carbon performance of the BCS depending on the HVAC system installed in the case study building is presented in figure 5.4-1 for the CIBSE TRY and figure 5.4-2 for the NOA TRY.

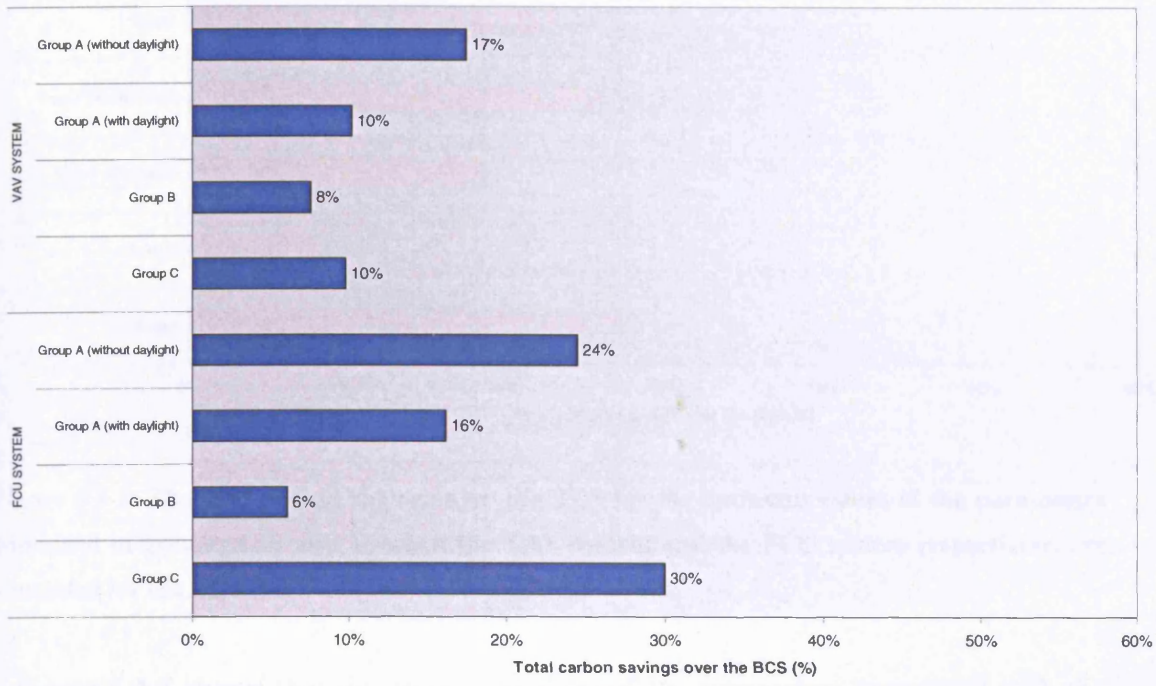

Figure 5.4-1: The total carbon savings over the BCS for the optimum factor settings of groups A, B and C, when the VAV system and the FCU system respectively, are simulated for the CIBSE TRY

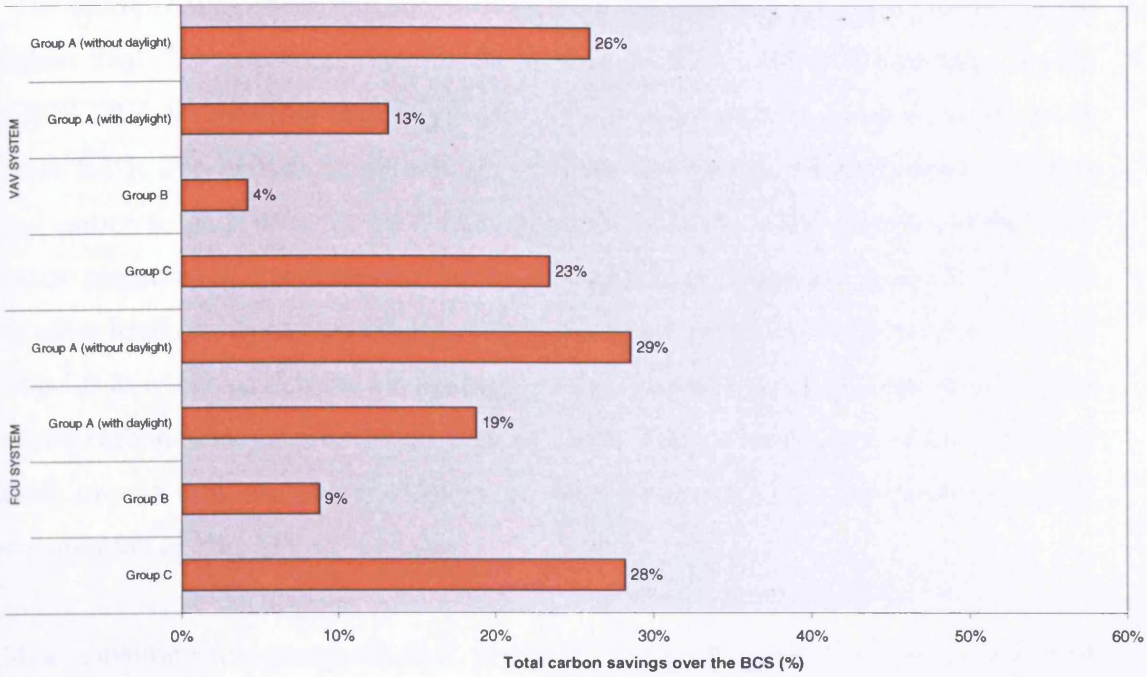

Figure 5.4-2: The total carbon savings over the BCS for the optimum values of the parameters contained in groups A, B and C, when the VAV system and the FCU system respectively, are simulated for the NOA TRY

Figure 5.4-1 shows that the optimum values of the parameters associated with the solar gains through the windows of the building (group A) lead to the highest reduction in total carbon emissions over the BCS, when the VAV system is simulated for the CIBSE TRY. The total carbon savings over the BCS drop, however, when the revised factor settings of group A (table 5.4-1), which ensure that the daylight performance of the perimeter zones of the building is in line with the BCO Guide 2000 recommendations, are taken into consideration. This is mainly due to the negative impact that the increase in the glazing percentage of the building and/or the TSC of the windows over their respective minimum level has on the cooling energy savings over the BCS. Nevertheless, the revised factor settings of this group still lead to the highest total carbon savings over the BCS, along with the optimum values of the parameters associated with the heat generated by occupants, lights and office equipment (group C), as can be seen from figure 5.4-1.

The minimisation of the internal heat gains of the building (group C) results in the highest total carbon savings over the BCS when the FCU system is simulated for the CIBSE TRY, followed by the optimisation of the parameters of group A, as shown in figure 5.4-1. The chosen factor settings of these two groups similarly lead to higher total carbon savings over the BCS than group B when the VAV system and the FCU system respectively, are simulated for the NOA TRY, as illustrated in figure 5.4-2. On the other hand, the optimum values of the parameters associated with the insulation of the walls & windows and the air-tightness of the building (group B) lead to the lowest overall carbon savings over the BCS in all cases. This is mainly due to the relatively small impact that the design factors of this group have on the cooling energy consumption of both HVAC systems.

The remaining five groups D, E, F, G and H contain the parameters associated with the design & operation of the HVAC systems. The optimum factor settings of each of these groups are summarized in table 5.4-2:

Scenario		Base case scenario				Optimum factor settings			
Climate		CIBSE TRY		NOA TRY		CIBSE TRY		NOA TRY	
HVAC system		VAV system	FCU system	VAV system	FCU system	VAV system	FCU system	VAV system	FCU system
Group D	Heating zone air temperature (°C)	20	20	20	20	18	18	18	18
	Cooling zone air temperature (°C)	24	24	24	24	26	26	26	26
	Temperature difference (°C)	8	8	8	8	6	8	6	8
Group E	Ventilation rate (ach)	-	-	-	-	5.0	10.0	5.0	10.0
	Period of ventilation (hours)	-	-	-	-	10	10	10	10
Group F	Boiler Efficiency (%)	85%	85%	85%	85%	95%	95%	95%	95%
	Chiller COP	2.50	2.50	2.50	2.50	5.20	5.20	5.20	5.20
	HVAC system operation (hours)	10	10	10	10	9	9	9	9
Group G	Fan efficiency (%)	78%	78%	78%	78%	90%	90%	90%	90%
	Motor efficiency (%)	90%	90%	90%	90%	95%	95%	95%	95%
	Supply fan (Pa)	677	421	681	474	500	300	500	300
	Return fan (Pa)	162	197	156	197	120	140	120	140
Group H	Humidification setpoint (%)	-	-	-	-	40	40	40	40
	Proportional band (%)	-	-	-	-	5	5	5	5
	Period of humidification	-	-	-	-	Heating season	Heating season	Heating season	Heating season

Table 5.4-2: The base case and the optimum factor settings of each of the groups related to the design and operation of the HVAC systems

The impact of the optimum factor settings of each group on the overall carbon performance[19] of the BCS depending on the HVAC system installed in the case study building is presented in figure 5.4-3 for the CIBSE TRY and figure 5.4-4 for the NOA TRY.

[19] **Note:** The total carbon savings displayed in the following two graphs include the boiler and chiller savings over the BCS. This is true for all groups of factors, apart from group E (which contains the factors related to night ventilation). In this group, the carbon emissions associated with the small amount of electricity consumed by the central fans (over the night), when the optimum night ventilation strategy is implemented, have been included in the chiller emissions of the HVAC systems.

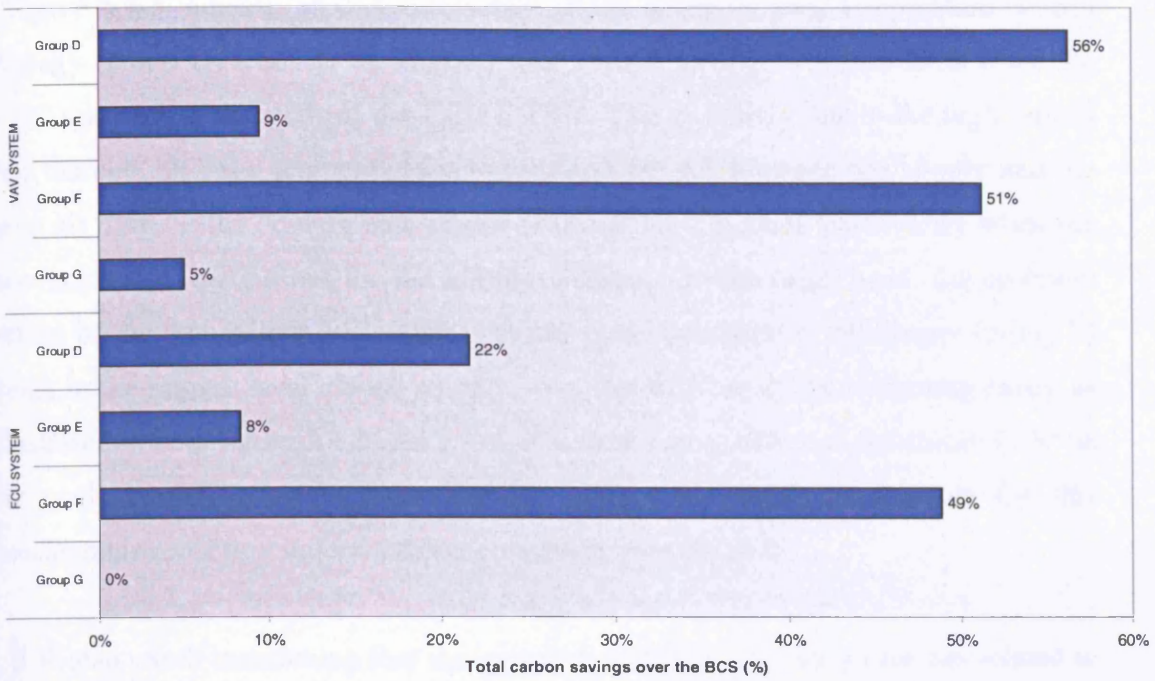

Figure 5.4-3: The total carbon savings over the BCS for the optimum factor settings of groups D, E, F and G, when the VAV system and the FCU system respectively, are simulated for the CIBSE TRY

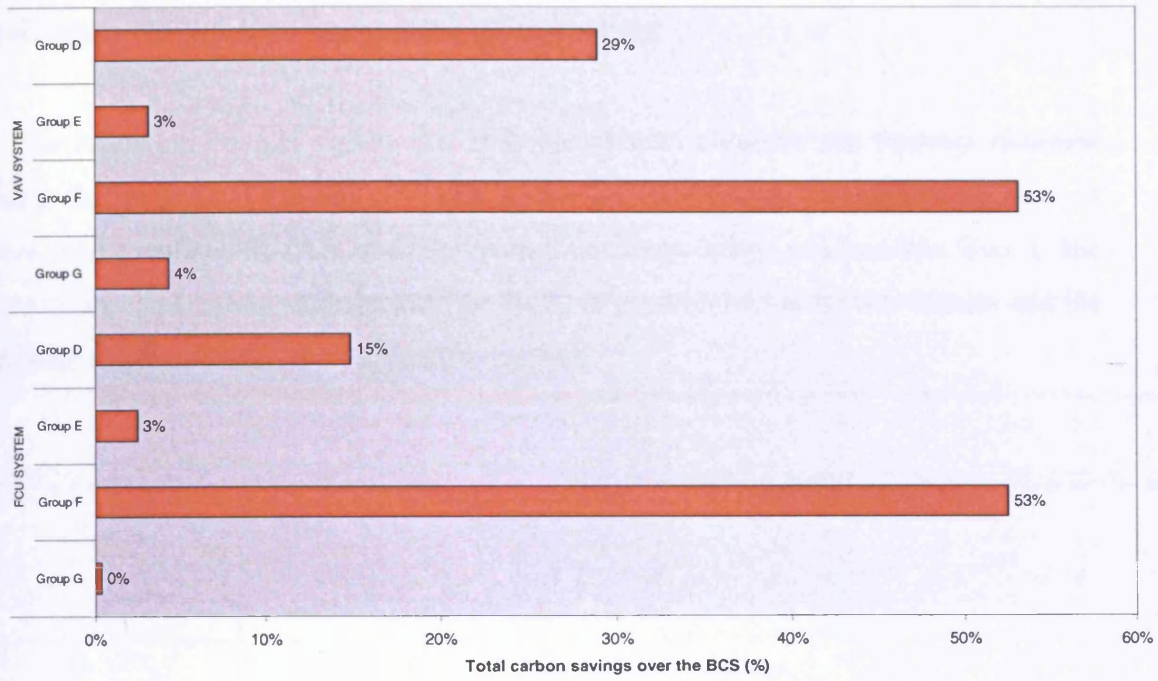

Figure 5.4-4: The total carbon savings over the BCS for the optimum values of the parameters contained in groups D, E, F and G, when the VAV system and the FCU system respectively, are simulated for the NOA TRY

Figure 5.4-3 indicates that the utilisation of the optimum zone temperature control strategy (group D) leads to the highest total carbon savings over the BCS when the VAV system is simulated for the CIBSE TRY. This is mainly due to the high impact that the cooling zone temperature set-point and the ΔT between the supply and the zone air have on the cooling energy use of this HVAC system, particularly when the simulations are carried out for the London climate. On the other hand, the optimum values of the parameters associated with the plant operation & efficiency (group F) result in the highest total carbon savings over the BCS in all the remaining cases, as illustrated in both figure 5.4-3 and 5.4-4. The dominating effect of the chiller COP on the cooling energy use of both HVAC systems is mainly responsible for this considerable reduction in total carbon emissions over the BCS.

It is also worth mentioning that the optimum values of the design factors related to the humidification of the supply air quantity (group H) are not included in figures 5.4-3 and 5.4-4, since they have a negligible effect on the carbon emissions associated with both the heating and the cooling energy use. However, the parameters of this group affect the amount of energy consumed by the steam humidifier increasing the total carbon emissions of the BCS by up to 39%, depending on the HVAC system and the climate for which the simulations are carried out.

The following chapter shows that it is possible to combine the findings obtained from the individual studies of each group of parameters, through a number of scenarios simulated in TAS, until the overall optimum design solution that leads to the maximum total carbon savings over the BCS, depending on the HVAC system and the climate under consideration, is finally reached.

References

[1] Birch, S., I. Frame. 1991, The Use and Evaluation of a Computer Program for the Investigation of the Daylight and Sunlight Performance of Buildings. Proceedings of Building Simulation '91: 139-144.

[2] David Button, Brian Pye, Glass in Building: A Guide to Modern Architectural Glass Performance, Butterworth Architecture; 1993

[3] BCO Guide 2000 – Best Practice in the specification for offices, British Council for Offices, 2000

[4] Timothy Edward Johnson, Low-E Glazing Design Guide, Chapter 5: Product Performance, figure 5-1, pg 47, Butterworth Architecture, April 1991

[5] Pilkington web-site: http://www.pilkington.com/

[6] Energy Consumption Guide 19: Energy use in offices, Best Practice Programme

[7] Good Practice Guide 276: Managing for a better environment, Best Practice Programme

Chapter 6: The overall optimum design solution depending on the HVAC system and the climate for which the simulations are carried out

6.0 Aims of the chapter

Chapter 5 presented the factor settings of each group that minimise the total carbon emissions of the VAV system and the FCU system respectively, in both climates for which they are simulated. This chapter shows that it is possible to combine the findings obtained from the study of each group of parameters through eight scenarios simulated in TAS, in order to reach gradually the overall optimum design solution, which maximises the total carbon savings over the BCS, depending on the HVAC system and the climate under consideration. Section 6.1 discusses the simulation results of the first two scenarios, which combine the findings derived from groups A to C in order to optimise the building load, while section 6.2 analyses the results of scenarios 3 to 6, which make use of the findings obtained from groups D to H in order to optimise the design & operation of the HVAC systems. Section 6.3 presents the results of the final two scenarios (i.e. 7 and 8), which combine the chosen values of both the building and the HVAC system related parameters in order to reach the overall optimum design solution, as mentioned above. Finally, section 6.4 summarises the findings of this chapter.

6.1 The combination of factor levels optimising the building load

Two scenarios are simulated in this section. Scenario 1 combines the optimum values of the factors associated with the solar gains through the windows (group A) and the parameters related to the internal heat gains of the office building (group C). It should be remembered that the study of each of the group of parameters classified in this category, carried out in the previous chapter, illustrated that the two aforementioned groups of factors lead to considerably higher total carbon savings over the BCS than the parameters associated with the thermal resistance and the air

tightness of the building envelope (i.e. group B). Scenario 2, on the other hand, considers the optimum values of all the parameters associated with the building load, (i.e. groups A, C & B). Section 6.1.1 discusses the effect of scenarios 1 and 2 on the total carbon emissions of the BCS when the daylight performance of the building is not taken into account, while section 6.1.2 analyses the effect of these two scenarios on the overall carbon performance of the BCS when the daylight performance of the perimeter zones of the building is considered, respectively.

6.1.1 The factor settings optimising the building load when the daylight performance of the building is not taken into consideration

The optimum values of the parameters involved in scenarios 1 and 2 are displayed in table 6.1.1-1:

Scenarios		Climate		CIBSE TRY		NOA TRY	
		HVAC system		VAV system	FCU system	VAV system	FCU system
Scenario 2	Scenario 1	Group A (no daylight)	Glazing ratio (0 -1)	0.25	0.25	0.25	0.25
			Total shading coefficient	0.16	0.16	0.16	0.16
			Overhang depth (m)	0.00	0.00	1.10	1.20
			Sidefin depth (m)	1.80	1.30	2.00	2.00
		Group C	Lighting gains (W/m^2)	6.5	6.5	6.5	6.5
			Equipment gains (W/m^2)	10.0	10.0	10.0	10.0
			Occupant Density (m^2 per person)	20	20	20	20
		Group B	Wall U-value (W/m^2K)	0.18	0.27	0.19	0.70
			Infiltration rate (ach)	0.25	0.25	0.25	0.40
			Window U-value (W/m^2K)	1.20	5.70	5.80	5.80

Table 6.1.1-1: The values of the design factors involved in scenario 1 and 2 respectively, depending on the HVAC system and the climate under consideration

The effect of scenarios 1 and 2 on the total carbon emissions of the BCS is presented in tables 6.1.1-2 to 6.1.1-5, depending on the HVAC system and the climate under consideration.

Scenario	Annual energy use		Carbon emissions			Impact on the total carbon emissions of the BCS		
	Heating energy consumption (kWh)	Cooling energy consumption (kWh)	Boiler carbon emissions (kgC)	Chiller carbon emissions (kg C)	Total carbon emissions (kgC)	Change in the boiler emissions of the BCS (%)	Change in the chiller emissions of the BCS (%)	Change in the total carbon emissions of the BCS (%)
Scenario 1: Combination of groups A & C	227159	45293	11812	5752	17564	110%	-65%	-20%
Scenario 2: Combination of groups A & C & B	125916	51151	6548	6496	13044	17%	-60%	-40%

Table 6.1.1-2: The effect of scenarios 1 and 2 on the total carbon emissions of the BCS, when the VAV system is simulated for the CIBSE TRY

Scenario	Annual energy use		Carbon emissions			Impact on the total carbon emissions of the BCS		
	Heating energy consumption (kWh)	Cooling energy consumption (kWh)	Boiler carbon emissions (kgC)	Chiller carbon emissions (kg C)	Total carbon emissions (kgC)	Change in the boiler emissions of the BCS (%)	Change in the chiller emissions of the BCS (%)	Change in the total carbon emissions of the BCS (%)
Scenario 1: Combination of groups A & C	230562	83605	11989	10618	22607	60%	-69%	-46%
Scenario 2: Combination of groups A & C & B	279928	78616	14556	9984	24540	94%	-71%	-41%

Table 6.1.1-3: The effect of scenarios 1 and 2 on the total carbon emissions of the BCS, when the FCU system is simulated for the CIBSE TRY

Scenario	Annual energy use		Carbon emissions			Impact on the total carbon emissions of the BCS		
	Heating energy consumption (kWh)	Cooling energy consumption (kWh)	Boiler carbon emissions (kgC)	Chiller carbon emissions (kg C)	Total carbon emissions (kgC)	Change in the boiler emissions of the BCS (%)	Change in the chiller emissions of the BCS (%)	Change in the total carbon emissions of the BCS (%)
Scenario 1: Combination of groups A & C	68010	174585	3537	22172	25709	163%	-51%	-45%
Scenario 2: Combination of groups A & C & B	96132	168233	4999	21366	26364	272%	-53%	-44%

Table 6.1.1-4: The effect of scenarios 1 and 2 on the total carbon emissions of the BCS, when the VAV system is simulated for the NOA TRY

Scenario	Annual energy use		Carbon emissions			Impact on the total carbon emissions of the BCS		
	Heating energy consumption (kWh)	Cooling energy consumption (kWh)	Boiler carbon emissions (kgC)	Chiller carbon emissions (kg C)	Total carbon emissions (kgC)	Change in the boiler emissions of the BCS (%)	Change in the chiller emissions of the BCS (%)	Change in the total carbon emissions of the BCS (%)
Scenario 1: Combination of groups A & C	69857	205136	3633	26052	29685	86%	-56%	-51%
Scenario 2: Combination of groups A & C & B	113967	201314	5926	25567	31493	204%	-57%	-48%

Table 6.1.1-5: The effect of scenarios 1 and 2 on the total carbon emissions of the BCS, when the FCU system is simulated for the NOA TRY

Scenario 1 leads to considerably higher heating energy use than the BCS in all cases, due to the minimisation of the internal heat gains of the building (group C) and the TSC of the windows (group A). The increase of the heating energy consumption of the VAV system by a factor of two approximately, offsets a large part of the respective cooling energy savings over the BCS, limiting the total carbon savings to 20%, when this system is simulated for the CIBSE TRY, as shown in table 6.1.1-2. In all the remaining cases, however, the reduction in cooling energy use dominates, leading to considerably lower total carbon emissions than the BCS, as shown in tables 6.1.1-3 to 6.1.1-5.

Table 6.1.1-2 illustrates that scenario 2 results in considerably higher total carbon savings over the BCS than scenario 1, when the VAV system is simulated for the CIBSE TRY. This is due to the minimisation of the U-values of the walls & windows and the specification of high standards of air tightness, (i.e. the optimum values of the factors of group B, shown in table 6.1.1-1), which lead to approximately 45% lower heating energy consumption than scenario 1. In all the remaining cases, however, scenario 2 results in lower total carbon savings over the BCS than scenario 1, (or, in other words, scenario 2 leads to higher total carbon emissions than scenario 1), as can be seen from tables 6.1.1-3 to 6.1.1-5.

As explained in section 5.2.2, which studied the effect of the parameters of group B on the total carbon emissions of the HVAC systems, the specification of a well-insulated building envelope is necessary only when the VAV system is simulated for the CIBSE TRY, since the associated reduction in the heating energy requirement offsets the increase in cooling energy use, leading to lower total carbon emissions than the BCS (table 5.2.2-1). In all the remaining cases, it was shown that opting for high window and / or wall U-values reduces both the cooling energy use and the total carbon emissions of the BCS. In this section, however, the combination of the optimum values of the parameters of groups A and C has already increased the heating energy consumption of the BCS, as can be seen from scenario 1 in tables 6.1.1-3 to 6.1.1-5. As a result, the specification of a badly insulated building envelope in scenario 2, (table 6.1.1-1), leads to slightly higher total carbon emissions than scenario 1, since the reduction in cooling energy is offset by the considerable increase in heating energy consumption, as shown in the three tables mentioned above.

Scenario 2b is, therefore, simulated, where both the wall and the window U-values are set to their minimum level, as illustrated in table 6.1.1-6:

Scenarios	Climate		CIBSE TRY		NOA TRY	
	HVAC system		VAV system	FCU system	VAV system	FCU system
Scenario 2b	Group A (no daylight)	Glazing ratio (0 -1)	-	0.25	0.25	0.25
		Total shading coefficient	-	0.16	0.16	0.16
		Overhang depth (m)	-	0.00	1.10	1.20
		Sidefin depth (m)	-	1.30	2.00	2.00
	Group C	Lighting gains (W/m^2)	-	6.5	6.5	6.5
		Equipment gains (W/m^2)	-	10.0	10.0	10.0
		Occupant Density (m^2 per person)	-	20	20	20
	Group B	Wall U-value (W/m^2K)	-	0.18	0.18	0.18
		Infiltration rate (ach)	-	0.25	0.25	0.40
		Window U-value (W/m^2K)	-	1.20	1.20	1.20

Table 6.1.1-6: The values of the parameters involved in scenario 2b, depending on the type of HVAC system and the climate under consideration

The effect of scenario 2b on the total carbon emissions of the BCS is presented in tables 6.1.1-7 to 6.1.1-9, depending on the HVAC system and the climate under consideration.

Scenario	Annual energy use		Carbon emissions			Impact on the total carbon emissions of the BCS		
	Heating energy consumption (kWh)	Cooling energy consumption (kWh)	Boiler carbon emissions (kgC)	Chiller carbon emissions (kg C)	Total carbon emissions (kgC)	Change in the boiler emissions of the BCS (%)	Change in the chiller emissions of the BCS (%)	Change in the total carbon emissions of the BCS (%)
Scenario 1: Combination of groups A & C	230562	83605	11989	10618	22607	60%	-69%	-46%
Scenario 2b: Combination of groups A & C & B, but with minimum U-values for both walls and windows	154283	91209	8023	11584	19606	7%	-66%	-53%

Table 6.1.1-7: The effect of scenarios 1 and 2b on the total carbon emissions of the BCS, when the FCU system is simulated for the CIBSE TRY

Scenario	Annual energy use		Carbon emissions			Impact on the total carbon emissions of the BCS		
	Heating energy consumption (kWh)	Cooling energy consumption (kWh)	Boiler carbon emissions (kgC)	Chiller carbon emissions (kg C)	Total carbon emissions (kgC)	Change in the boiler emissions of the BCS (%)	Change in the chiller emissions of the BCS (%)	Change in the total carbon emissions of the BCS (%)
Scenario 1: Combination of groups A & C	68010	174585	3537	22172	25709	163%	-51%	-45%
Scenario 2b: Combination of groups A & C & B, but with minimum U-values for both walls and windows	32946	173354	1713	22016	23729	28%	-52%	-49%

Table 6.1.1-8: The effect of scenarios 1 and 2b on the total carbon emissions of the BCS, when the VAV system is simulated for the NOA TRY

Scenario	Annual energy use		Carbon emissions			Impact on the total carbon emissions of the BCS		
	Heating energy consumption (kWh)	Cooling energy consumption (kWh)	Boiler carbon emissions (kgC)	Chiller carbon emissions (kg C)	Total carbon emissions (kgC)	Change in the boiler emissions of the BCS (%)	Change in the chiller emissions of the BCS (%)	Change in the total carbon emissions of the BCS (%)
Scenario 1: Combination of groups A & C	69857	205136	3633	26052	29685	86%	-56%	-51%
Scenario 2b: Combination of groups A & C & B, but with minimum U-values for both walls and windows	49083	206513	2552	26227	28779	31%	-56%	-53%

Table 6.1.1-9: The effect of scenarios 1 and 2b on the total carbon emissions of the BCS, when the FCU system is simulated for the NOA TRY

As can be seen from tables 6.1.1-7 to 6.1.1-9, scenario 2b reduces both the heating energy use and the total carbon emissions of scenario 1, or in other words, the specification of a well-insulated building envelope maximises the total carbon savings over the BCS, when the parameters of groups A, C and B are combined. On the other hand, it seems that the improvement in total carbon emissions over scenario 1 is moderate, when either the VAV system or the FCU system is simulated for the NOA TRY, as can be seen from tables 6.1.1-8 and 6.1.1-9.

6.1.2 The factor settings optimising the building load when the daylight performance of the building is taken into account

The optimum values of the parameters involved in scenarios 1 and 2, when the daylight performance of the building is taken into consideration, are summarised in table 6.1.2-1:

Scenarios		Climate		CIBSE TRY		NOA TRY	
		HVAC system		VAV system	FCU system	VAV system	FCU system
Scenario 2	Scenario 1	Group A (with daylight)	Glazing ratio (0 -1)	*0.25*	*0.40*	*0.25*	*0.95*
			Total shading coefficient	*0.76*	*0.37*	*0.68*	*0.16*
			Overhang depth (m)	*0.70*	*0.00*	*0.50*	*0.00*
			Sidefin depth (m)	*0.00*	*0.00*	*0.00*	*0.00*
		Group C	Lighting gains (W/m^2)	*6.5*	*6.5*	*6.5*	*6.5*
			Equipment gains (W/m^2)	*10.0*	*10.0*	*10.0*	*10.0*
			Occupant Density (m^2 per person)	*20*	*20*	*20*	*20*
		Group B	Wall U-value (W/m^2K)	*0.18*	*0.27*	*0.19*	*0.70*
			Infiltration rate (ach)	*0.25*	*0.25*	*0.25*	*0.40*
			Window U-value (W/m^2K)	*1.20*	*5.70*	*5.80*	*5.80*

Table 6.1.2-1: The values of the parameters involved in scenario 1 and 2 respectively, when the daylight performance of the building is taken into account, depending on the HVAC system and the climate under consideration

The effect of scenarios 1 and 2 on the total carbon emissions of the BCS is presented in tables 6.1.2-2 to 6.1.2-5, depending on the HVAC system and the climate under consideration.

Scenario	Annual energy use		Carbon emissions			Impact on the total carbon emissions of the BCS		
	Heating energy consumption (kWh)	Cooling energy consumption (kWh)	Boiler carbon emissions (kgC)	Chiller carbon emissions (kg C)	Total carbon emissions (kgC)	Change in the boiler emissions of the BCS (%)	Change in the chiller emissions of the BCS (%)	Change in the total carbon emissions of the BCS (%)
Scenario 1: Combination of groups A & C	172370	66954	8963	8503	17466	59%	-48%	-20%
Scenario 2: Combination of groups A & C & B	87490	75117	4549	9540	14089	-19%	-41%	-35%

Table 6.1.2-2: The effect of scenarios 1 and 2 on the total carbon emissions of the BCS, taking into consideration the daylight performance of the building, when the VAV system is simulated for the CIBSE TRY

Scenario	Annual energy use		Carbon emissions			Impact on the total carbon emissions of the BCS		
	Heating energy consumption (kWh)	Cooling energy consumption (kWh)	Boiler carbon emissions (kgC)	Chiller carbon emissions (kg C)	Total carbon emissions (kgC)	Change in the boiler emissions of the BCS (%)	Change in the chiller emissions of the BCS (%)	Change in the total carbon emissions of the BCS (%)
Scenario 1: Combination of groups A & C	221396	105054	11513	13342	24854	53%	-61%	-40%
Scenario 2: Combination of groups A & C & B	308990	90836	16067	11536	27604	114%	-66%	-33%

Table 6.1.2-3: The effect of scenarios 1 and 2 on the total carbon emissions of the BCS, taking into consideration the daylight performance of the building, when the FCU system is simulated for the CIBSE TRY

Scenario	Annual energy use		Carbon emissions			Impact on the total carbon emissions of the BCS		
	Heating energy consumption (kWh)	Cooling energy consumption (kWh)	Boiler carbon emissions (kgC)	Chiller carbon emissions (kg C)	Total carbon emissions (kgC)	Change in the boiler emissions of the BCS (%)	Change in the chiller emissions of the BCS (%)	Change in the total carbon emissions of the BCS (%)
Scenario 1: Combination of groups A & C	41160	215832	2140	27411	29551	59%	-40%	-37%
Scenario 2: Combination of groups A & C & B	61920	203893	3220	25894	29114	140%	-43%	-38%

Table 6.1.2-4: The effect of scenarios 1 and 2 on the total carbon emissions of the BCS, taking into consideration the daylight performance of the building, when the VAV system is simulated for the NOA TRY

Scenario	Annual energy use		Carbon emissions			Impact on the total carbon emissions of the BCS		
	Heating energy consumption (kWh)	Cooling energy consumption (kWh)	Boiler carbon emissions (kgC)	Chiller carbon emissions (kg C)	Total carbon emissions (kgC)	Change in the boiler emissions of the BCS (%)	Change in the chiller emissions of the BCS (%)	Change in the total carbon emissions of the BCS (%)
Scenario 1: Combination of groups A & C	97226	235578	5056	29918	34974	160%	-49%	-43%
Scenario 2: Combination of groups A & C & B	197920	226061	10292	28710	39002	428%	-51%	-36%

Table 6.1.2-5: The effect of scenarios 1 and 2 on the total carbon emissions of the BCS, taking into consideration the daylight performance of the building, when the FCU system is simulated for the NOA TRY

Most of the conclusions derived from the analysis of scenarios 1 and 2 (or 2b) in section 6.1.1, are also valid for this section. In short, the optimum values of the parameters of group B, (table 6.1.2-1), involved in scenario 2, lead to considerably lower heating energy use and, hence, lower total carbon emissions than scenario 1, when the VAV system is simulated for the CIBSE TRY, as illustrated in table 6.1.2-2. The remaining three tables indicate that scenario 2 leads to higher heating energy use than scenario 1, due to the adoption of high U-values for the building envelope (table 6.1.2-1). Despite this fact however, the total carbon emissions of scenario 2 remain slightly lower than scenario 1, when the VAV system is simulated for the NOA TRY, as can be seen from table 6.1.2-4. This is due to the positive impact that the high TSC, chosen when the daylight performance of the building is taken into account, (the TSC of the windows is set to 0.68 instead of 0.16, as can be seen from table 6.1.2-1 and 6.1.1-1 respectively), has on the heating energy consumption of this HVAC system. Therefore, scenario 2b, which minimises the U-values of the walls & windows, is simulated only for the FCU system in this section.

The optimum values of the parameters involved in scenario 2b are illustrated in table 6.1.2-6:

Scenarios	Climate		CIBSE TRY		NOA TRY	
	HVAC system		VAV system	FCU system	VAV system	FCU system
Scenario 2b	Group A (with daylight)	Glazing ratio (0 -1)	-	*0.40*	-	*0.95*
		Total shading coefficient	-	*0.37*	-	*0.16*
		Overhang depth (m)	-	*0.00*	-	*0.00*
		Sidefin depth (m)	-	*0.00*	-	*0.00*
	Group C	Lighting gains (W/m^2)	-	*6.5*	-	*6.5*
		Equipment gains (W/m^2)	-	*10.0*	-	*10.0*
		Occupant Density (m^2 per person)	-	*20*	-	*20*
	Group B	Wall U-value (W/m^2K)	-	*0.18*	-	*0.18*
		Infiltration rate (ach)	-	*0.25*	-	*0.40*
		Window U-value (W/m^2K)	-	*1.20*	-	*1.20*

Table 6.1.2-6: The values of the parameters involved in scenario 2b, when the daylight performance of the building is taken into consideration, depending on the climate for which the FCU system is simulated

The effect of scenario 2b on the total carbon emissions of the BCS when the FCU system is simulated for the CIBSE TRY and the NOA TRY is presented in table 6.1.2-7 and 6.1.2-8 respectively.

Scenario	Annual energy use		Carbon emissions			Impact on the total carbon emissions of the BCS		
	Heating energy consumption (kWh)	Cooling energy consumption (kWh)	Boiler carbon emissions (kgC)	Chiller carbon emissions (kg C)	Total carbon emissions (kgC)	Change in the boiler emissions of the BCS (%)	Change in the chiller emissions of the BCS (%)	Change in the total carbon emissions of the BCS (%)
Scenario 1: Combination of groups A & C	221396	105054	11513	13342	24854	53%	-61%	-40%
Scenario 2b: Combination of groups A & C & B, but with minimum U-values for both walls and windows	144495	121331	7514	15409	22923	0%	-55%	-45%

Table 6.1.2-7: The effect of scenarios 1 and 2b on the total carbon emissions of the BCS, taking into consideration the daylight performance of the building, when the FCU system is simulated for the CIBSE TRY

Scenario	Annual energy use		Carbon emissions			Impact on the total carbon emissions of the BCS		
	Heating energy consumption (kWh)	Cooling energy consumption (kWh)	Boiler carbon emissions (kgC)	Chiller carbon emissions (kg C)	Total carbon emissions (kgC)	Change in the boiler emissions of the BCS (%)	Change in the chiller emissions of the BCS (%)	Change in the total carbon emissions of the BCS (%)
Scenario 1: Combination of groups A & C	97226	235578	5056	29918	34974	160%	-49%	-43%
Scenario 2b: Combination of groups A & C & B, but with minimum U-values for both walls and windows	60144	240422	3127	30534	33661	61%	-48%	-45%

Table 6.1.2-8: The effect of scenarios 1 and 2b on the total carbon emissions of the BCS, taking into consideration the daylight performance of the building, when the FCU system is simulated for the NOA TRY

The specification of a well insulated building envelope in scenario 2b results in lower total carbon emissions (or in higher total carbon savings over the BCS) than scenario 1, as can be seen from tables 6.1.2-7 and 6.1.2-8. However, this improvement is moderate when the FCU system is simulated for the NOA TRY, as shown in the latter of the two tables. It is therefore concluded, from both sections 6.1.1 and 6.1.2, that the minimisation of the U-values of the walls and windows is worthwhile only when the HVAC systems are simulated for the London climate.

The comparison of the overall carbon performance of the three scenarios discussed in sections 6.1.1 and 6.1.2 shows that scenarios 1, 2 and 2b discussed in this section result in up to 18%, 26% and 15% lower[1] total carbon savings over the BCS than the respective scenarios shown in the previous section, depending on the HVAC system and the climate under consideration. This is mainly due to the negative impact that the high values of the TSC of the windows and / or the glazing percentage of the building, specified when the daylight performance of the perimeter zones is taken into consideration, have on the cooling energy savings over the BCS, as can be seen from the respective versions of scenarios 1, 2 and 2b presented in sections 6.1.1 and 6.1.2.

[1] **Note:** There is only one exception, as can be seen from the two versions of scenario 1 for the VAV system when this is simulated for the CISBE TRY (tables 6.1.1-2 and 6.1.2-2). In such a case the high value of the TSC, which is specified when the daylight performance of the building is taken into account, has a negative impact on the use of mechanical cooling, but, on the other hand, it reduces the amount of heating energy consumed, in comparison with the original version of scenario 1 (i.e. without consideration of the daylight performance of the building). As a result, the heating energy savings offset part of the increase in the cooling energy use leading to approximately the same total carbon savings over the BCS for both versions of this scenario, as shown in table 6.1.1-2 and table 6.1.2-2, respectively.

6.2 The combination of factor levels optimising the design & operation of the HVAC systems

As mentioned earlier, this section deals with the parameters associated with the design & operation of the HVAC systems (i.e. groups D, E, F, G and H). Four scenarios are simulated in total. Scenario 3 considers the optimum values of the parameters associated with the control of the air temperature inside the building (group D) and the factors related to the plant operation & performance (group F). It should be remembered that the individual studies of each of group of parameters, carried out in chapter 5, illustrated that the two groups of factors mentioned above lead to higher total carbon savings over the BCS than the remaining groups of parameters classified in this category. Scenario 4 combines the parameters involved in the previous scenario with the optimum values of the factors related to the provision of night ventilation (group E). Scenario 5 combines all the previous groups of parameters with the optimum values of the factors associated with the efficiency and the size of the central fans of the HVAC systems (group G). Finally, scenario 6 represents the optimum combination of all the HVAC system related parameters, assuming that the supply air quantity is humidified (i.e. it combines the optimum values of the factors contained in groups D, F, E, G and H).

The optimum values of the design factors involved in scenarios 3 to 6 are shown in table 6.2-1:

Scenarios	Climate		CIBSE TRY		NOA TRY	
	HVAC system		VAV system	FCU system	VAV system	FCU system
Scenario 6 / Scenario 5 / Scenario 4 / Scenario 3	Group D	Heating zone air temperature (°C)	18	18	18	18
		Cooling zone air temperature (°C)	26	26	26	26
		Temperature difference (°C)	6	8	6	8
	Group F	Boiler efficiency (%)	95%	95%	95%	95%
		Chiller COP	5.20	5.20	5.20	5.20
		HVAC system operation (hours)	9	9	9	9
	Group E	Ventilation rate (ach)	5.0	10.0	5.0	10.0
		Period of ventilation (hours)	10	10	10	10
	Group G	Fan efficiency (%)	90%	90%	90%	90%
		Motor efficiency (%)	95%	95%	95%	95%
		Supply fan (Pa)	500	300	500	300
		Return fan (Pa)	120	140	120	140
	Group H	Humidification setpoint (%)	40	40	40	40
		Proportional band (%)	5	5	5	5
		Period of humidification	Heating season	Heating season	Heating season	Heating season

Table 6.2-1: The values of the parameters involved in scenario 3, 4, 5 and 6 respectively, depending on the HVAC system and the climate under consideration

The effect of scenarios 3, 4, 5 and 6 on the total carbon emissions of the BCS is presented in tables 6.2-2 to 6.2-5, depending on the HVAC system and the climate under consideration.

Scenario	Annual energy use			Carbon emissions				Impact on the total carbon emissions of the BCS		
	Humidification energy consumption (kWh)	Heating energy consumption (kWh)	Cooling energy consumption (kWh)	Humidification Carbon Emissions (kg C)	Boiler carbon emissions (kgC)	Chiller carbon emissions (kg C)	Total carbon emissions (kgC)	Change in the boiler emissions of the BCS (%)	Change in the chiller emissions of the BCS (%)	Change in the total carbon emissions of the BCS (%)
Scenario 3: Combination of groups D & F	-	27777	25002	-	1444	3175	4620	-74%	-80%	-79%
Scenario 4: Combination of groups D & F & E	-	27561	20273	-	1433	2801	4234	-74%	-83%	-81%
Scenario 5: Combination of groups D & F & E & G	-	28174	18626	-	1465	2592	4057	-74%	-84%	-81%
Scenario 6: Combination of groups D & F & E & G & H	55021	28174	18626	6988	1465	2592	11044	-74%	-84%	-49%

Table 6.2-2: The effect of scenarios 3, 4, 5 and 6 on the total carbon emissions of the BCS, when the VAV system is simulated for the CIBSE TRY

Scenario	Annual energy use			Carbon emissions				Impact on the total carbon emissions of the BCS		
	Humidification energy consumption (kWh)	Heating energy consumption (kWh)	Cooling energy consumption (kWh)	Humidification Carbon Emissions (kg C)	Boiler carbon emissions (kgC)	Chiller carbon emissions (kg C)	Total carbon emissions (kgC)	Change in the boiler emissions of the BCS (%)	Change in the chiller emissions of the BCS (%)	Change in the total carbon emissions of the BCS (%)
Scenario 3: Combination of groups D & F	-	57599	106406	-	2995	13514	16509	-60%	-60%	-60%
Scenario 4: Combination of groups D & F & E	-	57682	91103	-	2999	11845	14845	-60%	-65%	-64%
Scenario 5: Combination of groups D & F & E & G	-	59451	90569	-	3091	11777	14869	-59%	-65%	-64%
Scenario 6: Combination of groups D & F & E & G & H	46286	59449	90575	5878	3091	11778	20748	-59%	-65%	-50%

Table 6.2-3: The effect of scenarios 3, 4, 5 and 6 on the total carbon emissions of the BCS, when the FCU system is simulated for the CIBSE TRY

Scenario	Annual energy use			Carbon emissions				Impact on the total carbon emissions of the BCS		
	Humidification energy consumption (kWh)	Heating energy consumption (kWh)	Cooling energy consumption (kWh)	Humidification Carbon Emissions (kg C)	Boiler carbon emissions (kgC)	Chiller carbon emissions (kg C)	Total carbon emissions (kgC)	Change in the boiler emissions of the BCS (%)	Change in the chiller emissions of the BCS (%)	Change in the total carbon emissions of the BCS (%)
Scenario 3: Combination of groups D & F	-	2583	124160	-	134	15768	15903	-90%	-65%	-66%
Scenario 4: Combination of groups D & F & E	-	2586	116424	-	134	14953	15087	-90%	-67%	-68%
Scenario 5: Combination of groups D & F & E & G	-	2653	110842	-	138	14244	14382	-90%	-69%	-69%
Scenario 6: Combination of groups D & F & E & G & H	128739	2653	110843	16350	138	14244	30732	-90%	-69%	-34%

Table 6.2-4: The effect of scenarios 3, 4, 5 and 6 on the total carbon emissions of the BCS, when the VAV system is simulated for the NOA TRY

Scenario	Annual energy use			Carbon emissions				Impact on the total carbon emissions of the BCS		
	Humidification energy consumption (kWh)	Heating energy consumption (kWh)	Cooling energy consumption (kWh)	Humidification Carbon Emissions (kg C)	Boiler carbon emissions (kgC)	Chiller carbon emissions (kg C)	Total carbon emissions (kgC)	Change in the boiler emissions of the BCS (%)	Change in the chiller emissions of the BCS (%)	Change in the total carbon emissions of the BCS (%)
Scenario 3: Combination of groups D & F	-	9213	192536	-	479	24452	24931	-75%	-59%	-59%
Scenario 4: Combination of groups D & F & E	-	9245	183696	-	481	23628	24109	-75%	-60%	-60%
Scenario 5: Combination of groups D & F & E & G	-	9950	182653	-	517	23496	24013	-73%	-60%	-61%
Scenario 6: Combination of groups D & F & E & G & H	39536	9950	182652	5021	517	23496	29034	-73%	-60%	-52%

Table 6.2-5: The effect of scenarios 3, 4, 5 and 6 on the total carbon emissions of the BCS, when the FCU system is simulated for the NOA TRY

Scenario 3 results in considerably lower total carbon emissions than the BCS, particularly when the VAV system is simulated for the CIBSE TRY, as can be seen from table 6.2-2. This is mainly due to the high impact that the parameters associated with the control of the zone air temperature (group D) have on the cooling energy consumption of this HVAC system when it is simulated for the London climate.

The implementation of the optimum night ventilation strategy (group E) in scenario 4, results in up to 10% and 5% lower total carbon emissions than scenario 3 when the HVAC systems are simulated for the CIBSE TRY and the NOA TRY respectively. This is due to the effect that the parameters of group E have on the cooling energy consumption of both HVAC systems, which drops when the simulations are carried out for the Athens in place of the London typical weather conditions.

The difference in total carbon emissions between scenarios 4 and 5 is small in all cases, as can be seen from tables 6.2-2 to 6.2-5. It should be remembered, however, that the parameters associated with the fan size and efficiency (group G), involved in scenario 5, have their highest impact on the amount of energy consumed by the central fans of both HVAC systems to move the air around the building. The fan energy savings over the BCS for scenario 5[2] range from 21% to 24% depending on the type of HVAC system and the climate under consideration.

[2] **Note:** It is worth mentioning that the aforementioned reduction in fan energy use over the BCS, (in scenario 5, which is a combination of groups D, F, E and G), is not only due to the optimisation of the four parameters associated with the size & the efficiency of the central fans (group G), but also due to the reduction of the number of hours that the fans of the VAV system and the FCU system, (including both the central fans and the small fans located in the fan coil units), operate from 10 to 9, as the optimum value of the HVAC system operation schedule (group F) dictates (see table 6.2-1).

Scenario 6 increases the total carbon emissions of scenario 5 by up to a factor of 2.7 and 1.4, depending on the climate for which the VAV system and the FCU system is simulated respectively. The carbon impact of the parameters associated with the air humidification (group H) is much higher for the VAV system than the FCU system, in both climates, due to the larger air quantities that the former is required to handle throughout the year in comparison with the latter which provides humidification of the minimum fresh air quantity for ventilation purposes.

6.3 The combination of factor levels optimising both the building load and the design & operation of the HVAC systems

This section considers both the building and the HVAC system related parameters. Two scenarios are simulated in TAS. Scenario 7 investigates the effect of the optimum values of the design factors related to the building load and the design & operation of the HVAC systems on the total carbon emissions of the BCS, assuming that the supply air quantity is not humidified. In other words, this scenario combines the chosen values of the parameters involved in scenario 2 (i.e. groups A, C and B) and scenario 5 (i.e. groups D, F, E and G) that were simulated in section 6.1 and 6.2 respectively. On the other hand, scenario 8 illustrates the effect of the optimum values of the design factors contained in all eight groups on the total carbon emissions of the BCS. In other words, scenario 8 combines the optimum values of the parameters involved in scenario 2 (i.e. groups A, C and B) and scenario 6 (i.e. groups D, F, E, G and H), which were discussed in section 6.1 and 6.2 respectively.

Section 6.3.1 analyses the effect of scenarios 7 & 8 on the overall carbon performance of the BCS, assuming that the daylight performance of the perimeter zones of the building is not taken into consideration, while section 6.3.2 discusses the effect of these two scenarios on the total carbon emissions of the BCS when the daylight performance of the building is taken into account, respectively.

6.3.1 The factor settings optimising both the building load and the design & operation of the HVAC systems when the daylight performance of the building is not considered

The optimum values of the parameters involved in scenarios 7 and 8 are summarized in table 6.3.1-1:

Scenarios		Climate		CIBSE TRY		NOA TRY	
		HVAC system		VAV system	FCU system	VAV system	FCU system
Scenario 8	Scenario 7	Group A (no daylight)	Glazing ratio (0 -1)	0.25	0.25	0.25	0.25
			Total shading coefficient	0.16	0.16	0.16	0.16
			Overhang depth (m)	0.00	0.00	1.10	1.20
			Sidefin depth (m)	1.80	1.30	2.00	2.00
		Group C	Lighting gains (W/m^2)	6.5	6.5	6.5	6.5
			Equipment gains (W/m^2)	10.0	10.0	10.0	10.0
			Occupant density (m^2 per person)	20	20	20	20
		Group B	Wall U-value (W/m^2K)	0.18	0.18	0.19	0.70
			Infiltration rate (ach)	0.25	0.25	0.25	0.40
			Window U-value (W/m^2K)	1.20	1.20	5.80	5.80
		Group D	Heating zone air temperature (°C)	18	18	18	18
			Cooling zone air temperature (°C)	26	26	26	26
			Temperature difference (°C)	6	8	6	8
		Group F	Boiler efficiency (%)	95%	95%	95%	95%
			Chiller COP	5.20	5.20	5.20	5.20
			HVAC system operation (hours)	9	9	9	9
		Group E	Ventilation rate (ach)	5.0	10.0	5.0	10.0
			Period of ventilation (hours)	10	10	10	10
		Group G	Fan efficiency (%)	90%	90%	90%	90%
			Motor efficiency (%)	95%	95%	95%	95%
			Supply fan (Pa)	500	300	500	300
			Return fan (Pa)	120	140	120	140
		Group H	Humidification setpoint (%)	40	40	40	40
			Proportional band (%)	5	5	5	5
			Period of humidification	Heating season	Heating season	Heating season	Heating season

Table 6.3.1-1: The values of the parameters involved in scenario 7 and 8 respectively, depending on the HVAC system and the climate under consideration

The effect of scenarios 7 and 8 on the total carbon emissions of the BCS is presented in tables 6.3.1-2 to 6.3.1-5, depending on the HVAC system and the climate for which it is simulated.

Scenario	Annual energy use			Carbon emissions				Impact on the total carbon emissions of the BCS		
	Humidification energy consumption (kWh)	Heating energy consumption (kWh)	Cooling energy consumption (kWh)	Humidification Carbon Emissions (kg C)	Boiler carbon emissions (kgC)	Chiller carbon emissions (kg C)	Total carbon emissions (kgC)	Change in the boiler emissions of the BCS (%)	Change in the chiller emissions of the BCS (%)	Change in the total carbon emissions of the BCS (%)
Scenario 7: Combination of scenario 2 and scenario 5	-	41624	5174	-	2164	883	3048	-61%	-95%	-86%
Scenario 8: Combination of scenario 2 and scenario 6	21572	41606	5174	2740	2164	883	5786	-62%	-95%	-74%

Table 6.3.1-2: The effect of scenarios 7 and 8 on the total carbon emissions of the BCS, when the VAV system is simulated for the CIBSE TRY

Scenario	Annual energy use			Carbon emissions				Impact on the total carbon emissions of the BCS		
	Humidification energy consumption (kWh)	Heating energy consumption (kWh)	Cooling energy consumption (kWh)	Humidification Carbon Emissions (kg C)	Boiler carbon emissions (kgC)	Chiller carbon emissions (kg C)	Total carbon emissions (kgC)	Change in the boiler emissions of the BCS (%)	Change in the chiller emissions of the BCS (%)	Change in the total carbon emissions of the BCS (%)
Scenario 7: Combination of scenario 2b and scenario 5	-	65982	14713	-	3431	2144	5575	-54%	-94%	-87%
Scenario 8: Combination of scenario 2b and scenario 6	31186	65981	14713	3961	3431	2144	9535	-54%	-94%	-77%

Table 6.3.1-3: The effect of scenarios 7 and 8 on the total carbon emissions of the BCS, when the FCU system is simulated for the CIBSE TRY[3]

Scenario	Annual energy use			Carbon emissions				Impact on the total carbon emissions of the BCS		
	Humidification energy consumption (kWh)	Heating energy consumption (kWh)	Cooling energy consumption (kWh)	Humidification Carbon Emissions (kg C)	Boiler carbon emissions (kgC)	Chiller carbon emissions (kg C)	Total carbon emissions (kgC)	Change in the boiler emissions of the BCS (%)	Change in the chiller emissions of the BCS (%)	Change in the total carbon emissions of the BCS (%)
Scenario 7: Combination of scenario 2 and scenario 5	-	26406	46524	-	1373	6076	7449	2%	-87%	-84%
Scenario 8: Combination of scenario 2 and scenario 6	30957	26403	46523	3932	1373	6075	11380	2%	-87%	-76%

Table 6.3.1-4: The effect of scenarios 7 and 8 on the total carbon emissions of the BCS, when the VAV system is simulated for the NOA TRY

[3] **Note:** As can be seen both tables 6.3.1-1 and 6.3.1-3, the U-values of the walls & windows are minimized when the FCU system is simulated for the CIBSE TRY. This is due to the fact that the adoption of a well-insulated building envelope (i.e. scenario 2b) has a considerable effect on the total carbon emissions when the simulations are carried out for the CIBSE TRY, as shown in section 6.1. For example, if high window and wall U-values had been specified in scenario 7, when the FCU system is simulated for the CIBSE TRY, the total carbon savings over the BCS would have been 78% instead of 87% (table 6.3.1-3). On the other hand, the minimization of the U-value of both the walls and windows is not particularly beneficial in terms of total carbon emissions when the HVAC systems are simulated for the NOA TRY, as shown in section 6.1. For example, had the wall & window U-values been minimized in scenario 7, when the VAV system is simulated for the NOA TRY, the total carbon savings over the BCS would have been 86% instead of 84% (table 6.3.1-4). Similarly, had a well-insulated building envelope been specified, when the FCU system is simulated for the NOA TRY, the total carbon savings over the BCS would have been 84% as opposed to 83% (table 6.3.1-5).

Scenario	Annual energy use			Carbon emissions				Impact on the total carbon emissions of the BCS		
	Humidification energy consumption (kWh)	Heating energy consumption (kWh)	Cooling energy consumption (kWh)	Humidification Carbon Emissions (kg C)	Boiler carbon emissions (kgC)	Chiller carbon emissions (kg C)	Total carbon emissions (kgC)	Change in the boiler emissions of the BCS (%)	Change in the chiller emissions of the BCS (%)	Change in the total carbon emissions of the BCS (%)
Scenario 7: Combination of scenario 2 and scenario 5	-	39834	62968	-	2071	8296	10367	6%	-86%	-83%
Scenario 8: Combination of scenario 2 and scenario 6	25645	39834	62973	3257	2071	8297	13625	6%	-86%	-78%

Table 6.3.1-5: The effect of scenarios 7 and 8 on the total carbon emissions of the BCS, when the FCU system is simulated for the NOA TRY

It is worth mentioning that scenario 7 results in up to 77% lower total carbon emissions than scenario 2, which combines the optimum values of the design factors associated only with the building load, and up to 63% lower total carbon emissions than scenario 5, which considers only the HVAC system related parameters (when humidification is not provided), depending on the type of HVAC system and the climate for which the simulations are carried out.

Scenario 8, on the other hand, increases the total carbon emissions of scenario 7, due to the amount of energy consumed in the humidification process, by up to 90% and 71% depending on the climate for which the VAV system and the FCU system is simulated respectively. Nevertheless, scenario 8 results in up to 57% lower total carbon emissions than scenario 2, while it reduces the total carbon emissions of scenario 6, (which considers the HVAC system associated parameters when the supply air quantity is humidified), by up to 63%, depending on the HVAC system and the climate under consideration. It is therefore concluded (from both scenario 7 and 8) that combining the values of the parameters optimising the building load with the factor settings optimising the design & operation of the HVAC systems, results in a considerable improvement in the overall carbon performance of all the scenarios studied in sections 6.1.1 and 6.2.

It should also be stressed that scenario 8 reduces the humidification energy of scenario 6 by up to 76% for the VAV system and up to 35% for the FCU system, depending on the climate for which the simulations are carried out. This implies that the parameters associated with the humidification of the supply air quantity interact with the design factors related to the building load, reducing the amount of energy consumed for the adjustment of the RH of the air.

6.3.2 The factor settings optimising both the building load and the design & operation of the HVAC systems when the daylight performance of the building is taken into account

The optimum values of the parameters involved in scenarios 7 and 8, when the daylight performance of the building is taken into consideration, are displayed in table 6.3.2-1:

Scenarios		Climate		CIBSE TRY		NOA TRY	
		HVAC system		VAV system	FCU system	VAV system	FCU system
Scenario 8	Scenario 7	Group A (with daylight)	Glazing ratio (0 -1)	0.25	0.40	0.25	0.95
			Total shading coefficient	0.76	0.37	0.68	0.16
			Overhang depth (m)	0.70	0.00	0.50	0.00
			Sidefin depth (m)	0.00	0.00	0.00	0.00
		Group C	Lighting gains (W/m^2)	6.5	6.5	6.5	6.5
			Equipment gains (W/m^2)	10.0	10.0	10.0	10.0
			Occupant density (m^2 per person)	20	20	20	20
		Group B	Wall U-value (W/m^2K)	0.18	0.18	0.19	0.70
			Infiltration rate (ach)	0.25	0.25	0.25	0.40
			Window U-value (W/m^2K)	1.20	1.20	5.80	5.80
		Group D	Heating zone air temperature (°C)	18	18	18	18
			Cooling zone air temperature (°C)	26	26	26	26
			Temperature difference (°C)	6	8	6	8
		Group F	Boiler efficiency (%)	95%	95%	95%	95%
			Chiller COP	5.20	5.20	5.20	5.20
			HVAC system operation (hours)	9	9	9	9
		Group E	Ventilation rate (ach)	5.0	10.0	5.0	10.0
			Period of ventilation (hours)	10	10	10	10
		Group G	Fan efficiency (%)	90%	90%	90%	90%
			Motor efficiency (%)	95%	95%	95%	95%
			Supply fan (Pa)	500	300	500	300
			Return fan (Pa)	120	140	120	140
		Group H	Humidification setpoint (%)	40	40	40	40
			Proportional band (%)	5	5	5	5
			Period of humidification	Heating season	Heating season	Heating season	Heating season

Table 6.3.2-1: The values of the parameters involved in scenario 7 and 8 respectively, when the daylight performance of the building is taken into account, depending on the HVAC system and the climate under consideration

The effect of scenarios 7 and 8 on the total carbon emissions of the BCS is presented in tables 6.3.2-2 to 6.3.2-5, depending on the HVAC system and the climate under consideration.

Scenario	Annual energy use			Carbon emissions				Impact on the total carbon emissions of the BCS		
	Humidification energy consumption (kWh)	Heating energy consumption (kWh)	Cooling energy consumption (kWh)	Humidification Carbon Emissions (kg C)	Boiler carbon emissions (kgC)	Chiller carbon emissions (kg C)	Total carbon emissions (kgC)	Change in the boiler emissions of the BCS (%)	Change in the chiller emissions of the BCS (%)	Change in the total carbon emissions of the BCS (%)
Scenario 7: Combination of scenario 2 and scenario 5	-	23050	8901	-	1199	1356	2555	-79%	-92%	-88%
Scenario 8: Combination of scenario 2 and scenario 6	32862	23051	8901	4173	1199	1356	6729	-79%	-92%	-69%

Table 6.3.2-2: The effect of scenarios 7 and 8 on the total carbon emissions of the BCS, taking into consideration the daylight performance of the building, when the VAV system is simulated for the CIBSE TRY

Scenario	Annual energy use			Carbon emissions				Impact on the total carbon emissions of the BCS		
	Humidification energy consumption (kWh)	Heating energy consumption (kWh)	Cooling energy consumption (kWh)	Humidification Carbon Emissions (kg C)	Boiler carbon emissions (kgC)	Chiller carbon emissions (kg C)	Total carbon emissions (kgC)	Change in the boiler emissions of the BCS (%)	Change in the chiller emissions of the BCS (%)	Change in the total carbon emissions of the BCS (%)
Scenario 7: Combination of scenario 2b and scenario 5	-	61053	23984	-	3175	3321	6496	-58%	-90%	-84%
Scenario 8: Combination of scenario 2b and scenario 6	36494	61051	23996	4635	3175	3322	11132	-58%	-90%	-73%

Table 6.3.2-3: The effect of scenarios 7 and 8 on the total carbon emissions of the BCS, taking into consideration the daylight performance of the building, when the FCU system is simulated for the CIBSE TRY

Scenario	Annual energy use			Carbon emissions				Impact on the total carbon emissions of the BCS		
	Humidification energy consumption (kWh)	Heating energy consumption (kWh)	Cooling energy consumption (kWh)	Humidification Carbon Emissions (kg C)	Boiler carbon emissions (kgC)	Chiller carbon emissions (kg C)	Total carbon emissions (kgC)	Change in the boiler emissions of the BCS (%)	Change in the chiller emissions of the BCS (%)	Change in the total carbon emissions of the BCS (%)
Scenario 7: Combination of scenario 2 and scenario 5	-	13273	58492	-	690	7595	8286	-49%	-83%	-82%
Scenario 8: Combination of scenario 2 and scenario 6	46122	13274	58473	5857	690	7593	14141	-49%	-83%	-70%

Table 6.3.2-4: The effect of scenarios 7 and 8 on the total carbon emissions of the BCS, taking into consideration the daylight performance of the building, when the VAV system is simulated for the NOA TRY

Scenario	Annual energy use			Carbon emissions				Impact on the total carbon emissions of the BCS		
	Humidification energy consumption (kWh)	Heating energy consumption (kWh)	Cooling energy consumption (kWh)	Humidification Carbon Emissions (kg C)	Boiler carbon emissions (kgC)	Chiller carbon emissions (kg C)	Total carbon emissions (kgC)	Change in the boiler emissions of the BCS (%)	Change in the chiller emissions of the BCS (%)	Change in the *total carbon* emissions of the BCS (%)
Scenario 7: Combination of scenario 2 and scenario 5	-	80037	69318	-	4162	9102	13264	114%	-85%	-78%
Scenario 8: Combination of scenario 2 and scenario 6	22259	80036	69318	2827	4162	9102	16091	114%	-85%	-74%

Table 6.3.2-5: The effect of scenarios 7 and 8 on the total carbon emissions of the BCS, taking into consideration the daylight performance of the building, when the FCU system is simulated for the NOA TRY

The conclusions derived from the analysis of scenarios 7 and 8 that took place in section 6.3.1, are also valid for this section.

The comparison of the overall carbon performance of the scenarios presented in sections 6.3.1 and 6.3.2 indicates that scenarios 7 and 8 discussed in this section result in up to 6% and 8% lower[4] total carbon savings over the BCS than the respective two scenarios shown in the previous section, depending on the HVAC system and the climate under consideration. It should be remembered that a similar conclusion was derived from section 6.1.2.

[4] **Note:** There is only one exception, as can be seen from the two versions of scenario 7 for the VAV system when this is simulated for the CISBE TRY (illustrated in table 6.3.2-2 and 6.3.1-2 respectively). In this case, the increase in cooling energy use due to the high value of the TSC of the windows, which is specified in the revised version of scenario 7 to ensure that the daylight performance of the perimeter zones of the building is in line with the BCO Guide 2000 recommendations, is offset by the reduction in heating energy consumption, resulting in approximately 3% higher total carbon savings over the BCS than the original version of scenario 7, as can be seen from tables 6.3.2-2 and 6.3.1-2 respectively.

6.4 Summary of findings

The previous sections have illustrated that it is possible to combine the findings obtained from the study of each group of parameters, (carried out in chapters 4 & 5), through eight scenarios simulated in TAS, until the overall optimum design solution, which maximises the total carbon savings over the BCS, is finally reached. This procedure has been repeated for both HVAC systems and climates under consideration. In general, it has been shown that the overall carbon performance of each scenario is not a simple summation of the performances of the groups of factors that it consists of. The interaction of the parameters involved in each of these scenarios in their effect on the annual (heating, cooling or humidification) energy use of the HVAC systems is clearly responsible for this. Only in a few cases has it proved necessary to make some changes to the chosen factor settings (i.e. the U-values of the walls and windows), but even in these cases the changes made to the factor levels were based on the knowledge gained through the analysis of the individual groups of factors. Clearly, obtaining the overall optimum solution through a number of sequential stages (i.e. scenarios 1 to 8) has helped to understand the interaction between the various groups of parameters and their relative magnitude in the total carbon savings over the BCS, depending on the HVAC system and the climate under consideration.

To sum up, the first two scenarios consider the optimum values of the parameters associated with the building load. The comparison of the overall carbon performance of these scenarios shows that the combination of the optimum values of the design factors associated with the solar gains through the windows (group A) with the parameters related to the internal heat gains of the office building (group C) is mainly responsible for the reduction in total carbon emissions over the BCS, when the HVAC systems are simulated for the NOA TRY. Although the parameters associated with the air tightness and the thermal resistance of the building envelope (group B) have a small impact on the use of mechanical cooling, (as shown in chapter 5), it has been found that their combination with the optimum values of the factors of groups A and C is particularly beneficial, in terms of total carbon emissions, when the simulations are carried out for the London climate. This is due to the positive impact that the minimisation of the U-values of the walls and windows and the specification of high

standards of air tightness have on the amount of heating energy consumed by both HVAC systems when they are simulated for the CIBSE TRY.

Taking into consideration the daylight performance of the perimeter zones of the building reduces considerably the total carbon savings (over the BCS) of the first two scenarios, in most cases. This is mainly due to the negative impact of the revised values of the TSC of the windows and the glazing percentage of the building (group A) on the use of mechanical cooling.

Scenarios 3, 4, 5 and 6 consider the optimum values of the HVAC system related parameters. The comparison of the overall carbon performance of these scenarios shows that the combination of the optimum values of the factors related to the control of the internal air temperature (group D) with the parameters associated with the plant operation & performance (group F) is responsible for the largest part of the maximum reduction in total carbon emissions over the BCS. The parameters of these two groups should therefore be the main priority of the designers, regardless of the HVAC system or the climate under consideration. It should also be stressed that scenario 5, which optimises the design & operation of the HVAC systems when humidification is not provided, results in higher total carbon savings over the BCS than scenario 2, which optimises the building load. This shows that the design of the building should not be the only concern of architects / engineers, since the choice, design & operation of the HVAC system has a significant contribution in the overall energy performance of the final project.

Scenario 7 represents the overall optimum design solution for the case study building, combining the chosen values of both the building and the HVAC system related factors, given, however, that the supply air quantity is not humidified. Scenario 8, on the other hand, combines the optimum values of all the parameters under consideration, assuming that the supply air quantity is humidified. The two final scenarios result in considerably lower total carbon emissions than both the combination of factor levels optimising the building load (i.e. scenario 2) and the factor settings optimising the design and operation of the HVAC systems (i.e. scenario 6 or 5 depending on whether humidification is provided or not). It should also be stressed that scenario 8 leads to lower humidification energy use than scenario

6, suggesting that the combination of the building related factors with the parameters associated with the HVAC system design & operation has a positive impact on the amount of energy consumed in the humidification process. It is therefore clear that the optimisation process should take into consideration both the design of the building and the performance & operation of the HVAC system installed, in order to keep the total carbon emissions of the case study building as low as possible.

Finally, taking into consideration the daylight performance of the perimeter zones of the building reduces the total carbon savings (over the BCS) of scenarios 7 & 8, as expected. However, the difference in total carbon savings (over the BCS) between the two versions of scenarios 7 & 8 (i.e. with and without consideration of the daylight performance of the perimeter zones of the building) is in most cases moderate. This is clearly due to the interaction of the design factors associated with the solar gains through the windows (group A) with the rest of the parameters involved in the scenarios mentioned above. It is therefore recommended to opt for the factor settings providing a satisfactory daylight performance for the case study building.

Chapter 7: Conclusions / Further Research

7.0 Aims of the chapter

This chapter presents the conclusions derived from the study of the effect of the eight groups of design factors on the energy performance of the VAV system and the FCU system when they are simulated for the London and the Athens climate respectively. Section 7.1 briefly compares the overall results of the thesis with the findings obtained from the past studies, which were reviewed in chapter 2. Section 7.2 presents the conclusions of the thesis, while section 7.3 provides a few recommendations regarding future research on the design of low-energy buildings through computer simulation.

7.1: Comparison of the overall results of the thesis with the findings obtained from past studies

The second chapter of the thesis provided a critical review of past studies on the assessment of the effect of a number of design factors on the energy performance of air-conditioned buildings through computer simulation. The last section of this chapter summarized the weaknesses of the previous studies to ensure that the investigation carried out in the thesis would avoid the same mistakes and be able to provide a more comprehensive and practical solution to the problem.

It is difficult to compare in detail the findings of these studies with the overall results of the thesis, since there are several differences in the case study building and its HVAC systems, the weather conditions, the dynamic simulation tool and the methodology that was used in each case. Nevertheless, there are some basic findings which are valid for most of the past studies considered in chapter 2 and the current investigation. These findings are summarised in the following:

- The annual energy use is affected by a number of design factors of both an architectural and an engineering nature that interact with each other to determine the overall energy performance of the building (section 2.2).
- The energy consumption of air conditioned commercial buildings is dominated by the cooling function (sections 2.2, 2.4, 2.5 & 2.6).
- The building related factors that should be the main priority of designers include the shading coefficient of the windows, the glazing percentage and the internal heat gains (sections 2.2, 2.4, 2.5 & 2.7), while some of the HVAC system related parameters that should receive critical attention during the design process include the cooling thermostat set-point, the chiller COP, the fan static pressure and the fan efficiency (sections 2.4 & 2.5).
- The choice of the HVAC system (section 2.6) and the type of climate (section 2.7) have a considerable impact on the overall energy performance of the case study building.
- The application of optimization techniques in the thermal design of buildings allows for significant energy savings. In addition, the optimum design solution is not unique. The study of the interactions between the design variables under consideration helps to identify alternative combinations of factor levels leading to near-optimum energy performance (sections 2.7 & 2.8).

The methodology employed in this research has, of course, resulted in a more detailed assessment of the relationship between a number of building & HVAC system related parameters and the energy consumption of an air conditioned office building than the previous studies, providing the designers with some valuable information on the likely combinations of design variables that will lead to low energy use, for two types of HVAC system in two different climates. The conclusions of the thesis are presented in the following section.

7.2 Conclusions

This study has investigated the effect of 25 design factors of both an architectural and an engineering nature on the energy performance of a notional air-conditioned office building, employing either a VAV system with terminal re-heaters or a four-pipe fan coil system with fresh air supply from a central plant, through computer simulation. This investigation has been carried out for the typical weather conditions of London (UK) and Athens (Greece). The main conclusions which are set out below can also be used as guidelines for the building designers / engineers, who are aware of the need to service the heating, ventilating and air conditioning requirements of an office building with the minimum environmental cost. A summary of these design recommendations in tabular form can also be found in appendix N.

The comparison of the overall energy performance of the HVAC systems in the base case scenario shows that the VAV system is more energy efficient than the FCU system, in both climates. The VAV system is approximately 47% less carbon intensive than the FCU system when the simulations are carried out for the CIBSE TRY, mainly due to the utilization by the former of recirculation as a form of heat recovery (in the winter months) and the exploitation of the free cooling capacity of the fresh air (in mild conditions). The difference in carbon emissions between the two HVAC systems is considerably reduced when the simulations are carried out for the NOA TRY, since both of them have got to rely on mechanical cooling, for most of the time, in order to maintain the desired thermal comfort conditions in a cooling dominated climate such as this.

The adjustment of the RH of the air reduces the difference in carbon emissions between the two HVAC systems in both climates, while it is possible to turn the carbon scales in favour of the FCU system depending on the values of the parameters associated with the humidification of the supply air quantity. For example, the simulations carried out for the NOA TRY show that the VAV system produces 27% more carbon than the FCU system when humidification to a minimum RH of 50% is provided all year. The humidification process is very carbon intensive particularly for the VAV system, due to the larger air quantities

that this system is required to handle throughout the year compared to the FCU system which provides humidification of the minimum fresh air quantity for ventilation purposes. It is recommended to set the RH set-point to 40%, regardless of the HVAC system and the climate under consideration, in order to reduce the energy cost of humidification. The choice of the proportional band has a negligible effect on the overall carbon performance of both systems. The humidification process should normally not be extended outside the heating season (i.e. six months in total), particularly when the VAV system is simulated for the CIBSE TRY. The period of humidification is not so critical, on the other hand, when the FCU system is simulated either for the London or the Athens typical weather data.

The parameters associated with the solar gains through the transparent building elements and the internal heat gains of the building should receive critical attention, particularly when the HVAC systems are simulated for the NOA TRY. Neglecting daylight availability considerations, the optimization trend is towards small glazing percentages (i.e. close to 25%) and low window shading coefficients (i.e. close to 0.16), in both climates, in order to reduce the use of mechanical cooling. The addition of external shading devices is not necessary when the previous two parameters are held close to their minimum level. On the other hand, minimizing the two design factors under consideration has a negative impact on the daylight performance of the perimeter zones of the building. The glazing percentage and / or the TSC of the windows need to take higher values than their respective minimum level in order to allow for some compromise between the energy consumption of the HVAC systems and the daylight performance of the building. For example, the glazing percentage is set to 40% and 95%, while the TSC of the windows is equal to 0.37 and 0.16, when the FCU system is simulated for the CIBSE TRY and the NOA TRY respectively. The revised settings of these two design factors have a negative impact mainly on the amount of cooling energy consumed and, hence, the total carbon emissions, but the optimization results show that this effect diminishes when the optimum values of all the parameters considered in the thesis are combined.

The heat generated by office equipment, lights and occupants has a high impact on the use of mechanical cooling. Setting the heat gains from lighting, equipment and occupants to their respective maximum as opposed to their minimum level increases the total carbon emissions by up to 33%, 43% and 45% respectively, depending on the HVAC system and the climate under consideration. It is therefore recommended to keep the equipment heat gains close to 10 W/m^2, while the lighting heat gains should ideally range from 6.5 to 8.5 W/m^2. The installation of energy efficient lights, (e.g. fluorescent lamps in energy efficient luminaires) and the use of low energy office equipment, (e.g. LCD screens, laptops instead of desktop computers, combination of copier/printer/fax machines, etc), is, therefore, necessary to achieve the targets set above. In addition, keeping the occupant density close to 15 m^2 / person or higher contributes considerably to the reduction of the cooling requirement. The trade-off diagrams presented in chapter 5 can be used to identify more combinations of factor levels resulting in near-optimum carbon performance depending on the HVAC system and the climate for which the simulations are carried out.

The parameters associated with the U-value of the building envelope and the air-tightness of the building affect mainly the heating energy use. There is a tendency towards low infiltration rates (i.e. 0.25 - 0.40 ach) in both climates. It has been found that the carbon penalty for a 0.5 ach increase in the infiltration rate rises as this parameter gets closer to 2.0 ach. The increase in total carbon emissions when the infiltration rate is set to 2.0 ach as opposed to 0.25 ach reaches 45% when the VAV system is simulated for the CIBSE TRY. On the other hand, the combination of all the design factors related to the building load illustrates that it is worthwhile to invest in a well-insulated building only when the HVAC systems are simulated for the CIBSE TRY. In such a case, the window U-value should be held as close to 1.2 W/m^2K as possible, while the choice of the wall U-value is not so critical, particularly when the other two parameters are set close to their optimum level.

The total carbon savings over the base case scenario when the optimum values of all the parameters associated with the building load are combined and the daylight performance of the building is taken into consideration range from 35%

to 45%, depending on the HVAC system and the climate for which it is simulated.

Emphasis should also be given to the parameters associated with the control of the internal air temperature, as well as to the factors related to the plant performance and operation. The cooling zone temperature should be set close to 26°C. The carbon impact for a 1°C reduction in this temperature set-point is up to 28% depending on the HVAC system and the climate for which it is simulated. The recommendations concerning the remaining two parameters associated with the temperature control strategy depend on the HVAC system and the climate under consideration. In general, the increase of the temperature difference between the supply and the zone air allows for the 'free' cooling potential of the fresh air quantity to be utilized, reducing, at the same time, the heating energy consumption of the FCU system by up to 82%, depending on the level the heating zone temperature set-point and the climate for which the simulations are carried out. Setting the ΔT between the supply and the zone air to 8°C (i.e. the maximum level) leads to near optimum carbon performance, given that the heating zone temperature set-point does not exceed 20°C and 21°C when the FCU system is simulated for the London and the Athens climate respectively. The ΔT between the supply and the zone air should be as low as possible, on the other hand, to reduce the cooling energy consumption of the VAV system. Thus, the ΔT between the supply and the zone air should be set to 6°C, while the heating zone temperature set-point should not exceed 20°C, when the VAV system is simulated for the CIBSE TRY. Also, maintaining the ΔT between the supply and the zone air at or below 7°C, leads to near optimum carbon emissions for the entire range of values of the heating zone temperature set-point (i.e. 18°C to 22°C), when the VAV system is simulated for the NOA TRY. The above recommendations provide the designers / engineers with some flexibility regarding the chosen temperature control strategy, allowing them to ensure low energy use for both HVAC systems and climates under consideration, without deviating a lot from the high quality internal environment desired in a contemporary air conditioned office building.

It is recommended to opt for a water cooled chiller with a seasonal COP as high as possible (i.e. close to 5.2). It has been shown that the carbon penalty for a unit reduction in this parameter increases considerably as the COP gets closer to 1.9. The installation of a chiller with a COP of 1.9 as opposed to 5.2 approximately doubles and triples the total carbon emissions of the HVAC systems when they are simulated for the London and the Athens typical weather conditions respectively. Also, the plant should operate for as short a time as possible (e.g. for 9 hours) when the HVAC systems are simulated for the CIBSE TRY. The carbon penalty for a one hour increase in the plant operation schedule reaches 20% when the VAV system is simulated for this climate. On the other hand, the plant operation should not exceed 13 and 14 hours when the VAV system and the FCU system, respectively, are simulated for the NOA TRY. The choice of the boiler efficiency is not critical when the above recommendations are taken into consideration.

The night ventilation strategy considered in this study combines the provision of fresh air to the perimeter zones of the building through natural means with the use of the central fans of the HVAC systems to serve the core zones, in order to avoid the potential problems associated with the movement of fresh air through these deep plan zones. The implementation of such a night ventilation strategy contributes to the reduction of cooling energy use and, hence, the total carbon emissions, particularly when the simulations are carried out for the CIBSE TRY. It is recommended to introduce the fresh air into the building for no less than 8 hours per night. The night ventilation rate is not critical as far as the perimeter zones of the building are concerned, but it should not exceed the capacity limit of the central AHU serving the core zones when the FCU system is considered. On the other hand, the ventilation rate should not be higher than 7 ach when the VAV system is installed, in order to limit the amount of the electricity consumed by the central fans serving the core zones of the case study building.

The parameters associated with the fan size & efficiency affect mainly the amount of electricity consumed by the central fans of the VAV system. It is recommended to opt for a fan and motor efficiency as high as possible, say, 90% and 95% respectively. Although the exact size of the supply & the return fans

depends on the requirements of the application, it is advised to select duct fittings and plant equipment that incur low pressure losses to the ductwork system. The effect of these four parameters on the total fan energy use of the FCU system, on the other hand, is negligible, since the amount of electricity consumed by the fan coil units located in the building zones dominates the overall fan energy consumption of this HVAC system.

The total carbon savings over the base case scenario when the optimum values of all the parameters associated with the design & operation of the HVAC systems are combined range from 61% to 81%, depending on the HVAC system and the climate for which it is simulated. However, the provision of humidity control to a min RH set-point of 40% for the winter period reduces the total carbon savings over the base case scenario by up to 50% for the VAV system and 22% for the FCU system due to the amount of electricity consumed by the steam humidifier. The humidification process is much more 'carbon expensive' for the former, as explained earlier.

The combination of both the building and the HVAC system related parameters results in total carbon savings ranging from 78% to 88% depending on the type of HVAC system and the climate for which the simulations are carried out. The utilization of the humidity control strategy described above reduces the total carbon savings over the base case scenario by up to 22% for the VAV system and 13% for the FCU system. Clearly, the interaction of the design factors associated with the building load with the parameters related to the HVAC system design & operation reduces the energy cost of humidification. Also, the total carbon savings over the base case scenario when all the parameters are taken into consideration are higher than all the previous combinations of factor levels considering only the building related design factors or just the parameters associated with design & operation of the HVAC systems. It is therefore clear that the building design should be treated as a whole, since both the architecture and the engineering interact with each other to determine the overall energy performance of the building. Taking into consideration the design recommendations described above, can minimize the impact of the air conditioned office building on the environment.

The comparison of the overall carbon performance of the two HVAC systems for the optimum combination of all the parameters under consideration shows that the VAV system is 61% and 38% less carbon intensive than the FCU system when the simulations are carried out for the CIBSE TRY and the NOA TRY, respectively. It is clear that the answer to the question of which HVAC system is the most energy efficient remains the same whether the optimum or the starting base case set of parameters is taken into consideration. The VAV system should, therefore, be the first choice in both climates, assuming that the environmental performance of the HVAC system is the main concern. However, the implementation of the humidification strategy described earlier reduces the difference in total carbon emissions between the two HVAC systems to 40% and 12% when the simulations are carried out for the London and the Athens typical weather conditions, respectively. The VAV system is still more energy efficient than the FCU system. However, the specification of high RH set-points combined with the needless operation of the steam humidifier during mild weather conditions can turn the carbon scales in favour of the FCU system.

7.3 Future Research

The limitations of this study along with a few recommendations concerning future research on the assessment of the design factors that affect the energy consumption of buildings, through computer simulation, are considered in the following:

- The number of floors and the aspect ratio of the case study building were kept the same throughout the current investigation. Further research would be required to study the effect of different building forms on the HVAC system energy use.
- This research work investigated the effect of two climates, a cooling-dominated climate and a temperate climate on the HVAC system energy / carbon performance. It would be interesting if a future study of this type considered a heating-dominated climate as well. This type of climate, however, is expected to have a smaller impact on the total carbon emissions than the climates considered in the current study, since the overall energy performance of large air conditioned office buildings, such as the one considered here, is dominated by the cooling function.
- The methodology adopted in the thesis can be applied to other types of buildings. Given, for example, that dwellings account for 28% of the UK's total carbon dioxide emissions as well as the expected increase in the number of domestic properties with air conditioning over the coming years [1], [2], it would be interesting to carry out a similar parametric analysis for a typical air conditioned residence. It is expected that the climate and the parameters associated with the design of the building envelope will have a considerable impact on the annual energy use, since residences are 'skin-load' dominated, while internal loads are relatively insignificant compared to commercial buildings [3].
- The two HVAC systems that took part in this investigation are very popular world-wide, being suitable for a variety of applications, while they are also very flexible in terms of the range of heating and cooling loads that they are capable of handling. More types of HVAC systems can be involved in a future study including contemporary systems that

promise low energy use, such as the displacement ventilation (DV) system and the Termodeck hollow core floor slab mechanical ventilation system. It should be stressed, however, that the satisfactory operation of these systems relies on several design guidelines concerning both the construction of the building and the design & control strategy of the system itself (e.g. the building should be airtight and well-insulated, the supply air temperature and the air velocity in the occupied zone should not exceed certain limits when the DV system is concerned [7], [8], etc). Careful selection of the design factors that will take part in the parametric investigation and their range of values is therefore required to ensure that the strict design guidelines concerning the DV or the Termodeck system are met, and to avoid potential thermal discomfort problems or disruption of the intended operation of these systems.

- This study concentrated on the effect of a number of building and system related design factors on the energy / carbon performance of two HVAC systems. Future research work can also evaluate the impact that the chosen factors have on the cost of the design project. Although energy efficiency should always come first, many clients will opt for the environmentally friendly design solution only if it does not involve a significantly higher cost. The economic evaluation of alternative design options should not, however, be based only on the initial acquisition cost, since this does not necessarily minimize the total cost over the whole life of the asset [4]. In fact, it seems that there is an unwritten rule which holds that whatever project design options cost less to acquire will tend to cost more to operate and conversely [4], [5]. It is therefore clear that all the expenditure incurred in respect of the asset during its operational life should be considered whenever a comparison of asset alternatives is undertaken, taking also into account the "time value of money" (i.e. the fact that a pound today does not have the same value as a pound in the distant future [5]). This is the Life-Cycle Costing (LCC) approach, which aims to optimize the cost of acquiring, owning and operating physical assets over their useful lives by attempting to quantify all the significant costs involved in that life, using the present value technique [4] (i.e. a process in which all costs, both future and present, are expressed in terms

of the same time frame: the present [5]). The methodology adopted in the thesis can therefore be used to quantify the impact of the chosen design factors on the LCC of the building (i.e. the new response variable Y), which is a single measure of the overall cost that takes into consideration all the cost components associated with each design option, (i.e. each combination of factor levels), including capital costs, electricity and fuel costs, maintenance costs as well as capital replacement costs and the time they occur. It is obvious, however, that detailed information concerning the cost components mentioned above for all the design points (or, in other words, for all the combinations of factor levels) required to model the relationship between the design parameters and the new response variable needs to be obtained first, in order to carry out such a study.

- Given the high standards of thermal comfort and air quality demanded by occupants working in a contemporary air-conditioned office building, it would be interesting if a future study could evaluate the impact that the building design or the control & operation of the HVAC system installed will have on each of these two response functions. It is clear, however, that a suitable simulation tool that is capable of assessing the effect of the chosen design factors on the thermal comfort conditions or the air quality inside the building model in detail throughout the year should be chosen in such a case.

In spite of its limitations, the present study has illustrated that the application of statistical & optimization techniques in the design of buildings through computer simulation allows for significant energy / carbon savings. It has also been shown that the type of climate, the design of the building and the choice & operation of the HVAC system are key factors that determine the overall energy performance of the building. The implementation of the energy efficiency measures described in detail in the previous section requires good collaboration between the engineer and the architect, particularly at the conceptual stage of the design process, when the design decisions carry the most effect. However, it should also be stressed that it is the responsibility of the building manager and the occupants to ensure that the operation of the building and the associated HVAC system is carried out in accordance with the design specifications throughout the year. It is therefore

important to raise the awareness and motivate the occupants to use energy in an efficient way, maintain the HVAC system properly, invest in energy improvement measures when the opportunity arises (e.g. refurbishment, plant replacement, etc) and review the operation schedules and control strategies throughout the year to ensure low energy use and, hence, reduce the impact of the building on the environment [6].

References

[1] Act fast, say climate experts: New climate change report urges the government to act swiftly to meet the 2050 CO_2 emissions target, Building Services Journal, April 2005, pg. 6

[2] Ian Knight, Gavin Dunn, Size does matter, Building Services Journal, August 2004, pg. 34-36

[3] Mohammad S. Al-Homoud, Optimum Thermal Design of Air-Conditioned Residential Buildings, *Building and Environment*, Vol. 32, No. 3, 203-210, 1997

[4] David G. Woodward, *Life-cycle costing – theory, information acquisition and application, International Journal of Project Management*, Vol. 15, No 6, pp. 335 – 344, 1997.

[5] Marlin S. Addison, *"User-Friendly" Life-Cycle Costing: The BLCC Procedure in an Easy-to-Use Spreadsheet*, U.S. DOE Pollution Prevention Conference, Albuquerque, NM, 1999

[6] Energy Consumption Guide 19: Energy use in offices, Best Practice Programme

[7] Tariq Abbas, Displacement Ventilation and Static Cooling Devices, Code of Practice 17/99

[8] Hakon Skistad, Displacement Ventilation, Research Studies Press LTD, June 1994

Appendices

Appendix A: Duct sizing calculations

A.1 AHU specification and ductwork schematics for the HVAC systems installed in the case study building

A.1.1 AHU specification and typical duct layouts for the VAV system

The total air quantity which must be supplied throughout the case study building by the VAV system was found to be equal to 70.7 m^3/s and 82.9 m^3/s when the simulations are carried out for the CIBSE TRY and the NOA TRY, respectively. Keeping in mind that both air quantities are very high, research was conducted in order to collect information concerning the range of air quantities which are usually handled by air handling units (AHUs) used in commercial applications. The findings of this research are summarized in table A-1:

Manufacturer	Type of AHU	Capacity Range (m^3/s)
IAC (www.iacl.co.uk/uk/index.htm)	custom engineered low-noise AHUs	3.5 to 18
Airfridge (www.airfridge.com)	Central Station AHUs	0.48 to 7.9
York International (www.York.com)	Curbak AHUs	0.5 to 28
	Pace Custom AHUs	1.4 to 47
Fyrogenis (www.Fyrogenis.gr)	MFE AHUs	0.42 - 26.4

Table A-1: The capacity range (in m^3/s) of various AHUs suitable for commercial buildings

It is clear that the majority of packaged air handling units for central HVAC systems cannot handle a total air quantity of 71 m^3/s (or 83 m^3/s). As a result, large commercial buildings have got to use a number of AHUs, in order to supply the total required air quantity.

It was, therefore, decided to use three AHUs in total, so that each unit serves two floors of the case study building. The first option that was considered involved placing only one AHU on the rooftop and the other two in the intermediate floors of the building in order to reduce the length of the vertical ducts. However the developer would probably argue against such a design solution since a considerable part of useful office space would have been occupied by these units[1].

Another option that was considered concerned the placement of all units on the rooftop, so that the vertical ducts were placed outside the building next to the external wall. The downside of this option is the extra cost involved, since all the vertical ducts need to be well-insulated.

[1] **Note:** According to the technical guide supplied by *FYROGENIS* [6], the length of the *MFE AHU* models ranges from 5.5-10 m, while the width ranges from 0.7 – 5.0 m depending on the total air quantity handled.

Taking into consideration the problems associated with the previous design options it was decided to place all the AHUs on the rooftop of the office building, as shown in figure A-1:

Figure A-1: The positions of the three AHUs on the rooftop plan of the case study building

As can be seen from figure A-1, the vertical ducts for all the AHUs run inside the building, (next to the external wall), in the middle of the small side of the floor plan. The first AHU serves the first and ground floor, the second AHU serves the third and second floor, while the third AHU serves the fifth and fourth floor of the building, as shown in figure A-2:

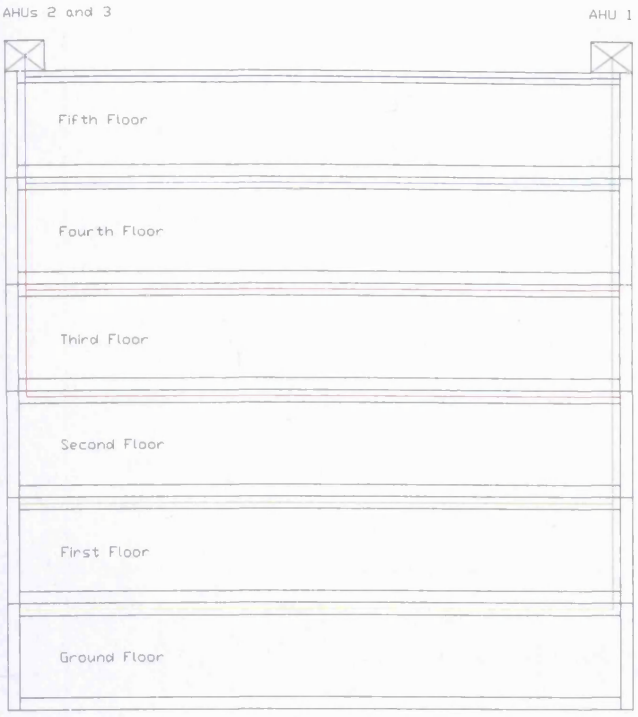

Figure A-2: Section through the middle of the small side of the case study building showing that AHU 1 serves the first and ground floors (green line), AHU 2 serves the third and second floors (red line), while AHU 3 serves the fifth and fourth floors (blue line) of the building

It is clear that the ductwork system schematics are the same for all the floors of the building. The index run for AHU 3 which serves the two top floors of the case study building is shown in figure A-3, while both the supply and extract duct layouts for the fourth floor of the building are presented in figure A-4, as an example:

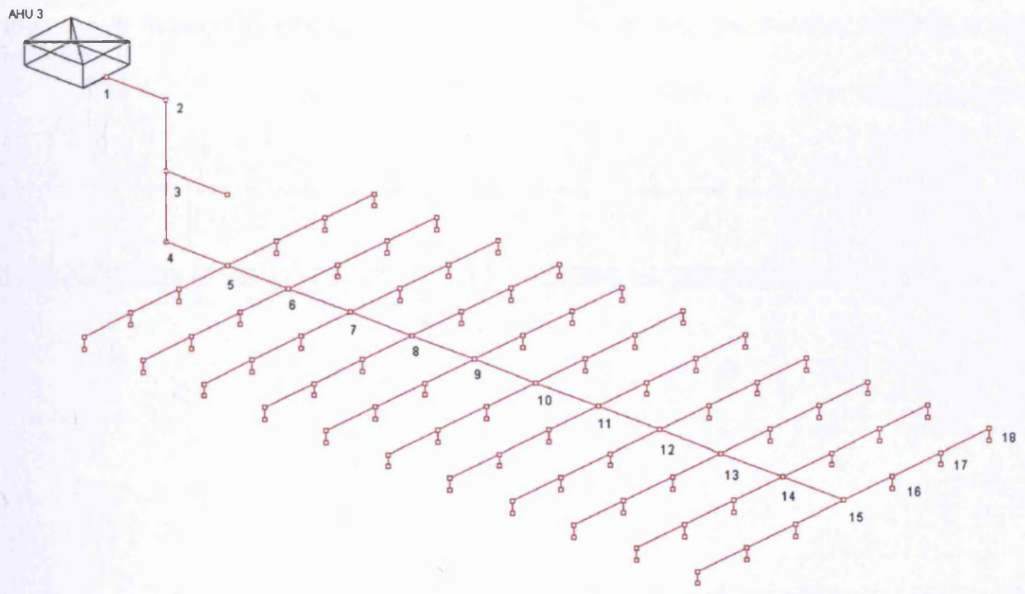

Figure A-3: Index run for AHU 3 which serves the fifth and fourth floor of the building

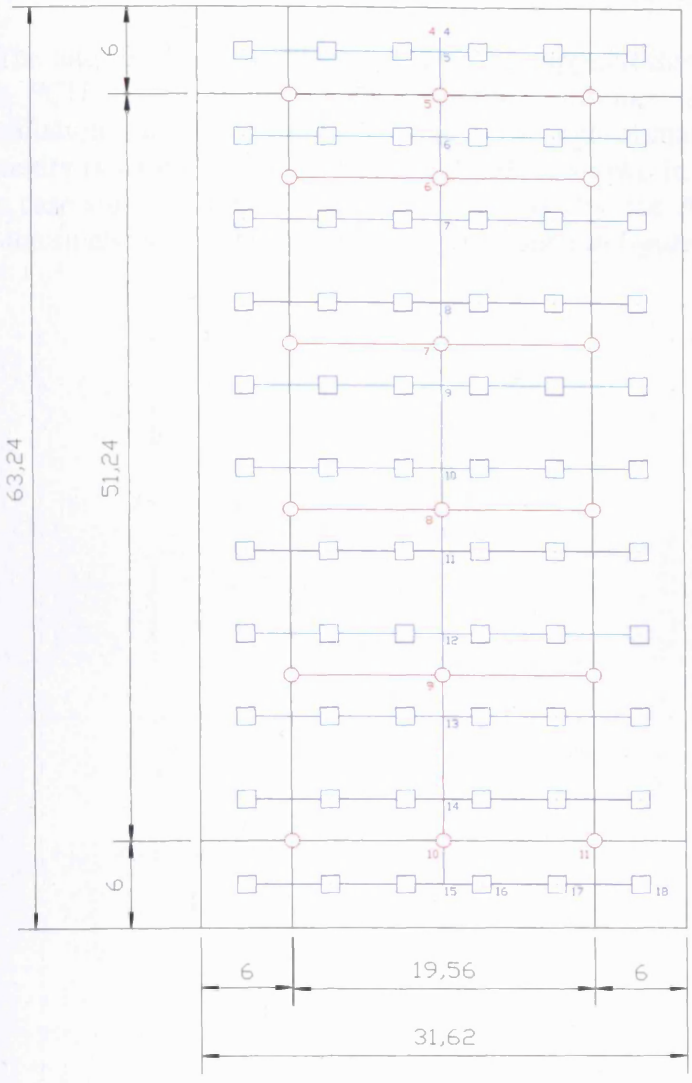

Figure A-4: Supply (blue line) and extract (red line) duct layout for the fourth floor of the building

A.1.2 AHU specification and ductwork schematics for the FCU system

The total fresh air quantity that must be supplied throughout the building when the FCU system is installed, (i.e. the minimum fresh air requirement for ventilation purposes), equals 9.13 m^3/s, in both climates. It is clear that this air quantity is within the typical range of values shown in section A.1.1. As a result, the case study building is served in this case by one AHU located in the middle of the small side of the rooftop, as can be seen in figure A-5:

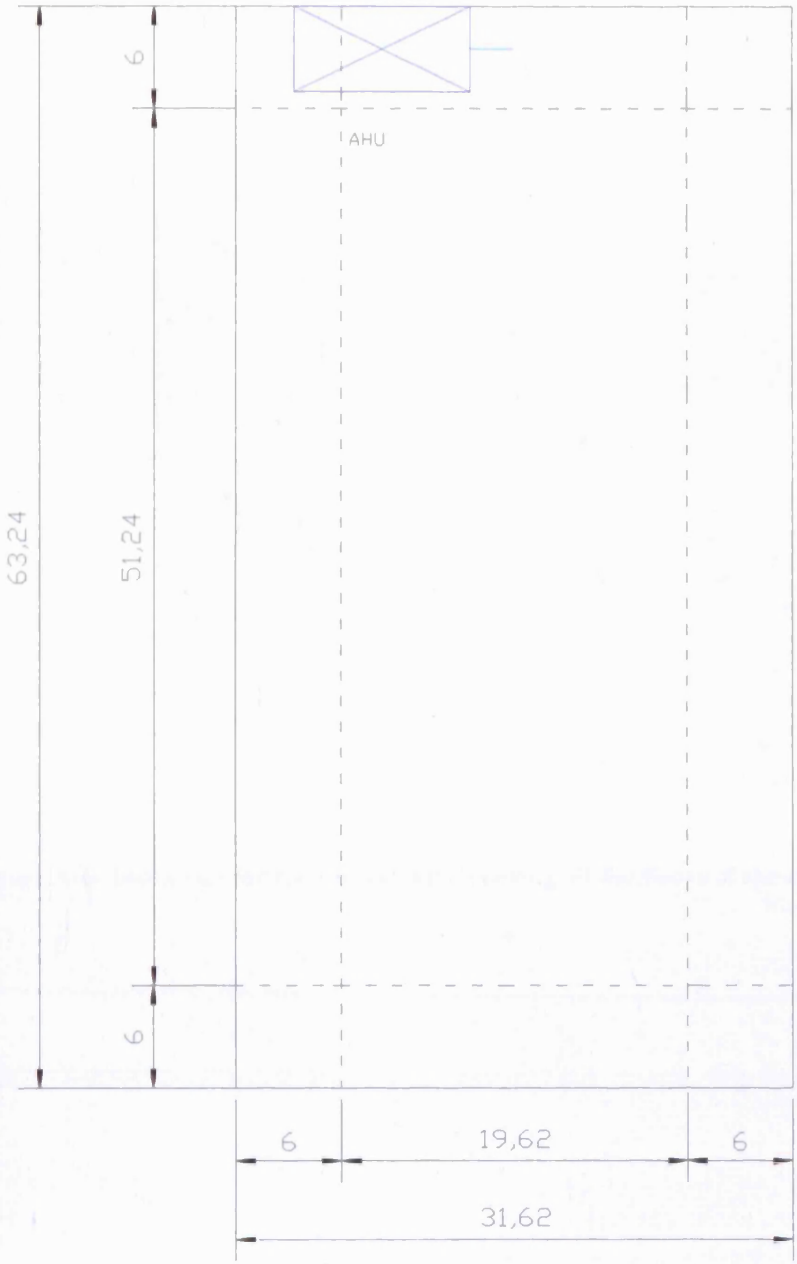

Figure A-5: The AHU which serves the entire building, when the FCU system is installed, is located in the middle of the small side of the rooftop plan

The main duct enters the building at the middle of the small side of the rooftop plan as shown in figure A-5, and runs throughout the entire building serving all floors. The ductwork system schematic is the same for all the floors of the building. The index run is presented in figure A-6 while the supply and the extract duct layout for the ground floor are shown in figure A-7, as an example:

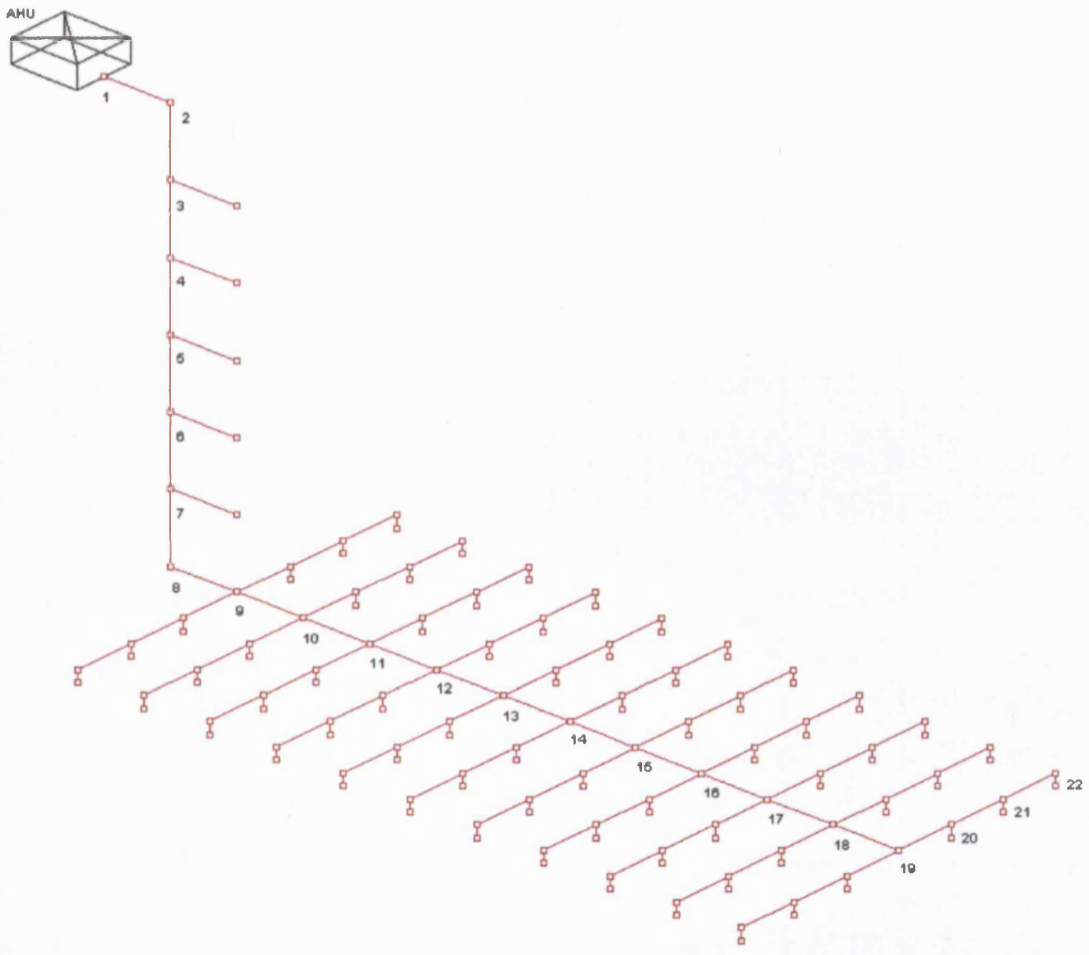

Figure A-6: Index run for the central AHU serving all the floors of the case study building

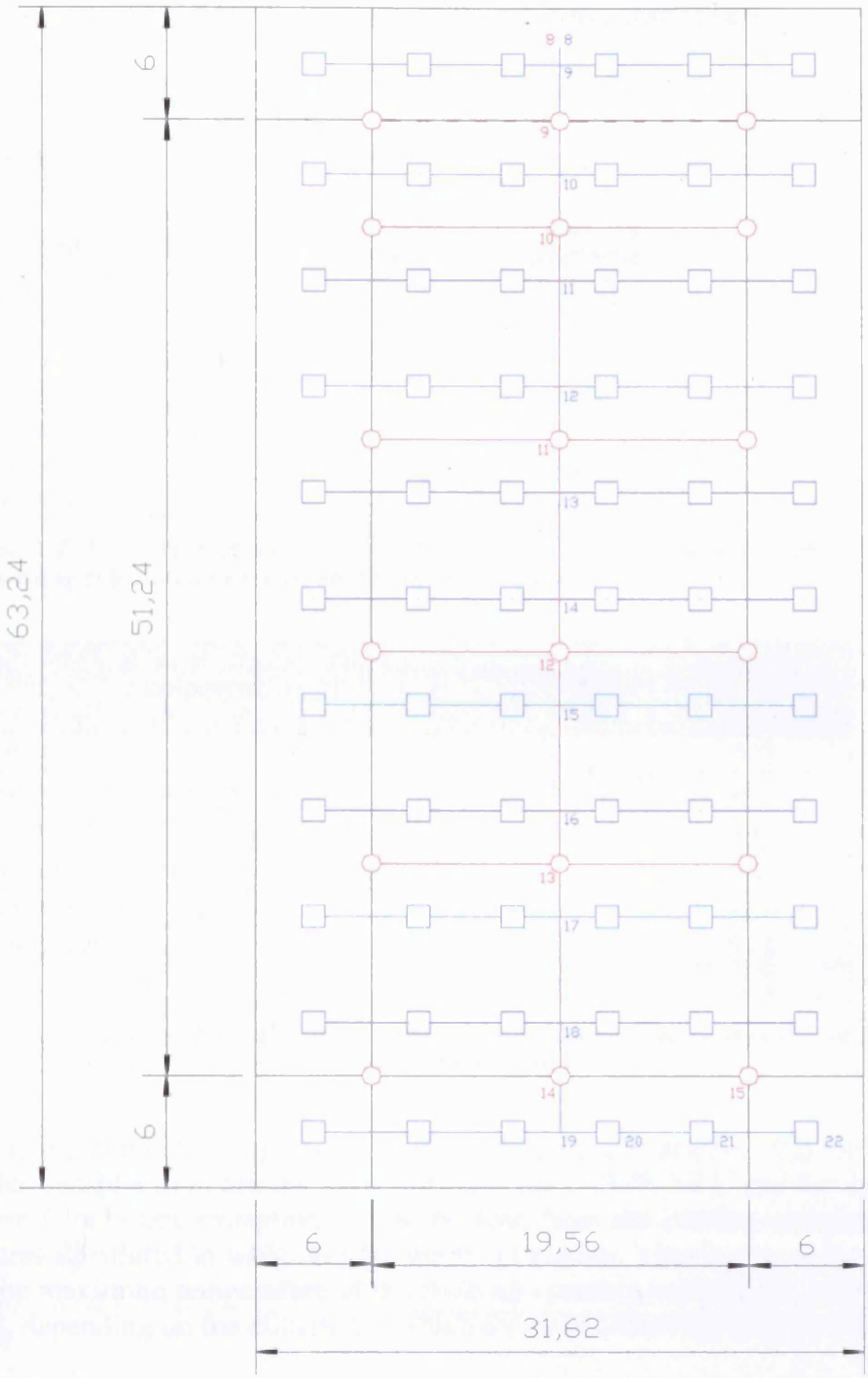

Figure A-7: Supply (blue line) and extract (red line) duct layout for the ground floor

A.2 Air Pressure drop for various plant/system components

The pressure drop figures that were used in the duct sizing calculations carried out for the VAV and the FCU system are shown in tables A-2 and A-3, respectively:

Equipment	Air velocity limit (m/s)	Pressure drop (Pa)
Mixing box [6]	2.5	45.0
Filter [6]	2.5	85.0
Cooling coil (4 rows) [6]	2.5	105.9
Humidifier [6]	2.5	18.0
VAV terminal box [7]	5.0	85.0
Supply grille [4]	5.0	50.0
Extract grille [2]	5.0	25.0

Table A-2: Pressure drop and air velocity limits for various pieces of equipment used in the duct sizing calculations carried out for the VAV system

Equipment	Air velocity limit (m/s)	Pressure drop (Pa)
Filter [6]	2.5	85.0
Heating coil (single row) [6]	2.5	28.0
Cooling coil (6 rows) - CIBSE TRY [6]	2.5	158.8
Cooling coil (8 rows) - NOA TRY [6]	2.5	211.7
Humidifier [6]	2.5	18.0
Supply grille [4]	5.0	50.0
Extract grille [2]	5.0	25.0

Table A-3: Pressure drop and air velocity limits for various pieces of equipment used in the duct sizing calculations performed for the FCU system

It is worth mentioning that the pressure drop figures displayed in the two tables under consideration are the same for both the CIBSE TRY and the NOA TRY. There is only one exception, as can be seen from the cooling coil pressure drop figures illustrated in table A-3 for the FCU system. This is due to the difference in the maximum temperature of the fresh air quantity entering the central cooling coil, depending on the climate for which the simulations are carried out [6].

It should be stressed that manufacturers produce a large variety of AHU components (e.g. heating or cooling coils, filters, etc) designed to meet the requirements of many different applications. This results in a range of different pressure losses for the same AHU component. For example, the pressure drop figures (in Pa) for a number of AHU components obtained from various sources (i.e. journals, books, manufacturer web sites or technical guides) are presented in table A-4:

AHU Components	Air Pressure Drop in Pa					
	Source [1]	Source [2]	Source [3]	Source [4]	Source [5]	Source [6]
Mixing Box	-	-	-	-	-	45
Heating Coil	10[1]	40 – 100[2]	50[3]	20[4]	15	28[15]
Cooling Coil	80[5]	-	150[6]	20[7]	130	105.9 -211.7[8]
Filter	120 – 200[9]	50 - 250[10]	90[11]	75[12]	100 – 250[13]	86[14]
Humidifier	-	-	-	-	-	18

Table A-4: Air pressure drop figures for a number of AHU components derived from various sources

Table A-4 notes:
1: This is a single row heating coil
2: The low value refers to efficient design and the high value to poor design
3: This value refers to a face velocity of 3.0 m/s
4: This value refers to a face velocity of 3.5 m/s
5: The pressure drop is for a cooling coil including an eliminator
6: This value is for a face velocity of 2.0 m/s
7: This value is for a face velocity of 3.5 m/s
8: The low value is for a cooling coil with 4 rows and the high value is for a cooling coil with 8 rows
9: The low value refers to panel filter (dirty), while the high value refers to a bag filter (dirty)
10: The low value refers to an old filter and efficient design, while the high value refers to an old filter and poor design
11: This value is for a face velocity of 1.5 m/s
12: This is for a face velocity of 2.5 m/s
13: The low value is for a panel filter and high value is for a bag filter
14: This value is for a bag filter
15: This value is for a single row heating coil

It should also be noted that all the figures taken from sources [5] and [6] refer to a face velocity of 2.5 m/s, while the velocity limit for the figures derived from source [1] is not known.

It is clear that there are significant differences between the figures quoted in the literature for the same AHU component. A direct comparison between the figures presented in table A-4 is not possible due to the differences in a number of parameters associated with a specific component (e.g. the face velocity or the number of rows of a coil), as can be seen from the notes illustrated above. It was therefore decided to use the pressure losses derived from *FYROGENIS* [6], since this was the only source providing figures for all the plant components under consideration and for the same velocity limit.

A.3 Description of the duct sizing calculation procedure

The duct sizing calculation was based on the following equation of Colebrook-White [3]:

$$Q = -4 \cdot (N_3 \cdot \Delta P \cdot d^5)^{1/2} \times \log_{10}\left(\frac{k_s}{3.7 \cdot d} + \frac{N_4 \cdot d}{(N_3 \cdot \Delta P \cdot d^5)^{1/2}}\right)$$

or

$$Q = -4 \cdot \sqrt{N_3 \cdot \Delta P} \cdot d^{2.5} \times \log_{10}\left(\frac{k_s}{3.7 \cdot d} + \frac{N_4}{\sqrt{N_3 \cdot \Delta P} \cdot d^{1.5}}\right) \quad (1)$$

where:

Q is the rate of airflow in m^3/s
ΔP is the pressure drop in Pa / m
d is the internal diameter of the duct in m
$k_s = 0.15 \times 10^{-3}$ m is the absolute roughness of the duct
$\rho = 1.2$ kg / m^3 is the air density
$\mu = 1.8 \times 10^{-5}$ N × s / m^2 (or kg / m × s) is the dynamic viscosity

$$N_3 = \frac{\pi^2}{32 \cdot \rho} = 0.257020948 \quad (2)$$

$$N_4 = \frac{1.255 \cdot \pi \cdot \mu}{4 \cdot \rho} = 1.478512043 \times 10^{-5} \quad (3)$$

From (1) $\xrightarrow{(2)\wedge(3)}$

$$Q = -2.0279 \cdot \Delta P \cdot d^{2.5} \times \log_{10}\left(\frac{4.0541 \times 10^{-5}}{d} + \frac{2.9164 \times 10^{-5}}{\sqrt{\Delta P} \cdot d^{1.5}}\right)$$

Before proceeding to the description of the calculation procedure, it should be mentioned that the methodology used is based on a modified spreadsheet presented in chapter 6 of *Air conditioning: A practical introduction* [4]. An example of such a spreadsheet is presented in table A-5. The column numbers mentioned in the following description of the calculation procedure refer to this table.

The main steps of the calculation are the following:

- the duct length L (m) and the volumetric flow rate Q (m^3/s) are input in the first two columns for each section of the index run (i.e. the run of ductwork with the largest pressure drop).
- The maximum velocity V (m/s) and pressure drop rate ΔP (Pa/m) are inserted in columns *(3)* and *(4)*, for each duct section. The velocity and pressure drop limits are in accordance with table 3-16 - section 3.6 (e.g. for the fan coil supply system presented in table A-5, the sizing limits are 5 m/s and 1.0 Pa/m, respectively).

- In column *(5)* the program calculates the duct diameter D (m) required for each section in order to carry the actual volumetric air flow of column *(2)* with the maximum velocity of column *(3)* using the equation: $D = \sqrt{\frac{4 \cdot Q}{\pi \cdot V}}$
- In column *(6)* the maximum capacity of each duct is calculated using the Colebrook-White equation that correlates the volumetric air flow Q (m^3/s) with the pressure drop rate ΔP (Pa/m) and the diameter D (m), while in column *(7)* the difference between the maximum carrying capacity (column *(6)*) and the actual capacity Q (column *(2)*) is expressed as Q error (%). The error can be reduced by changing the limiting velocity or the limiting pressure drop rate. The trial and error procedure stops when the error Q is as close to zero as possible.
- The likely diameter D is entered in column *(8)* using increments of 50 mm. The program then calculates in column *(9)* the likely velocity V using the equation $V = \frac{4 \cdot Q}{\pi \cdot D^2}$ where Q is the actual volumetric flow rate and D the likely diameter.
- The dimensions of the equivalent rectangular duct are entered in columns *(10)* and *(11)*, while the aspect ratio is calculated in column *(12)*. The dimensions are chosen so that the aspect ratio is lower than 3.0, to reduce the frictional losses. The equivalent duct diameter is calculated automatically in column *(13)* [2], using the equation: $d = 1.265 \times \left[\frac{(a \cdot b)^3}{a + b}\right]^{0.2}$ (*CIBSE Guide, volume C: Reference Data*), while the actual velocity is calculated in column *(14)*, using the equation $V = \frac{4 \cdot Q}{\pi \cdot D^2}$, where Q is the actual volumetric flow rate (column *(2)*), and D is the equivalent diameter.
- In column *(17)* the maximum capacity is re-calculated using the Colebrook-White equation that correlates (this time) the volumetric air flow Q (m^3/s) with the actual pressure drop rate ΔP (Pa/m) shown in column *(15)* and the equivalent diameter D (m) (which is re-entered in column *(16)* in m), while in column *(18)* the difference between the maximum carrying capacity (column *(17)*) and the actual capacity (column *(2)*) is expressed as Q error (%). The error can be reduced by changing the actual pressure drop rate in column *(15)*. The trial and error procedure stops when the error Q is as close to zero as possible. This procedure is used to estimate the actual pressure drop rate (column *(15)*), which can be significantly different to the maximum drop rate of column *(4)* due to the rounding up of the diameter.
- The duct pressure (Pa) is calculated in column *(19)* by multiplying the actual pressure drop rate (Pa/m) by the length (m) of each duct section.
- In column *(20)*, the summation of all the velocity pressure loss factors ζ is inserted for all the fittings included in each duct section.

[2] **Note:** Columns *(10)* – *(13)* are not taken into consideration when the shape of the ducts is circular (e.g. in the VAV supply system).

- The velocity pressure (Pa) is calculated in column *(21)*, using the equation $P_v = \frac{1}{2} \times \rho \times V^2$, where ρ=1.21 kg/m^3 is the density of the air and V (m/s) is the actual velocity (column *(14)*).
- The pressure losses (Pa) due to the duct fittings are calculated in column *(22)*, by multiplying the summation of the velocity pressure loss factors by the velocity pressure of each duct section.
- The pressure losses (Pa) due to equipment such as filters or heating coils are entered in column *(23)*.
- The total pressure (Pa) for each duct section is calculated in column *(24)*, as the summation of the pressure losses due to straight duct sections, fittings and equipment.
- Finally, the FTP (fan total pressure) is calculated as the summation of the total pressure for each duct section.

											Rectangular Ducts										Fitting Pressure Losses			Equipment Plant Pressure	Total Pressure
		Length	Q	Max velocity	Max ΔP	D	Max Q	Q error	Likely D	Likely V	Width	Depth	Aspect ratio	Equiv D	Actual V	Actual ΔP	D	Max Q	Q error	Duct press	Fitting ζ	P_V	$\zeta * P_V$		
		(m)	(m^3/s)	(m/s)	(Pa/m)	(m)	(m^3/s)	(%)	(m)	(m/s)	(mm)	(mm)	<3.0	(mm)	(m/s)	(Pa/m)	(m)	(m^3/s)	(m^3/s)	(Pa)		(Pa)	(Pa)	(Pa)	(Pa)
		1	2	3	4	5	6	7	8	9	10	11	12	13	14	15	16	17	18	19	20	21	22	23	24
AHU	AHU containing heating coil, cooling coil, filter, humidifier and supply fan	10.00	9.129	2.50	0.0257	2.16	9.13	-0.01	2.200	2.40	2500.00	1600.00	1.56	2192	2.42	0.0237	2.19	9.13	0.00	0.24	5.38	3.51	18.90	289.8	308.94
Vertical Duct Sections	1 to 2	2.00	9.129	5.00	0.1415	1.52	9.13	0.00	1.550	4.84	1600.00	1250.00	1.28	1555	4.81	0.1283	1.555	9.13	0.01	0.26	0.29	13.86	4.02	0.0	4.28
	2 to 3	1.00	9.129	5.00	0.1415	1.52	9.13	0.00	1.550	4.84	1600.00	1250.00	1.28	1555	4.81	0.1283	1.555	9.13	0.01	0.13	0.01	13.86	0.17	0.0	0.29
	3 to 4	3.50	7.607	5.00	0.1578	1.39	7.61	0.01	1.400	4.94	1300.00	1250.00	1.04	1404	4.92	0.1513	1.404	7.61	0.00	0.53	0.07	14.50	0.96	0.0	1.49
	4 to 5	3.50	6.086	5.00	0.1804	1.24	6.09	0.00	1.250	4.96	1300.00	1000.00	1.30	1253	4.93	0.1744	1.253	6.09	-0.01	0.61	0.08	14.59	1.11	0.0	1.72
	5 to 6	3.50	4.564	5.00	0.2145	1.08	4.57	-0.02	1.100	4.80	1200.00	850.00	1.41	1109	4.73	0.1864	1.109	4.56	0.02	0.65	0.09	13.40	1.26	0.0	1.91
	6 to 7	3.50	3.043	5.00	0.2739	0.88	3.04	-0.01	0.900	4.78	900.00	750.00	1.20	904	4.74	0.2480	0.904	3.04	-0.02	0.84	0.05	13.49	0.67	0.0	1.51
	7 to 8	3.50	1.521	5.00	0.4163	0.62	1.52	0.01	0.650	4.59	700.00	500.00	1.40	650	4.59	0.3367	0.650	1.52	0.01	1.18	0.29	12.64	3.67	0.0	4.84
Ground Floor Duct Sections	8 to 9	1.00	1.521	5.00	0.4163	0.62	1.52	0.01	0.650	4.59	700.00	500.00	1.40	650	4.59	0.3367	0.650	1.52	0.01	0.34	0.01	12.64	0.10	0.0	0.44
	9 to 10	5.86	1.385	5.00	0.4408	0.59	1.39	0.01	0.600	4.90	600.00	500.00	1.20	603	4.86	0.4100	0.603	1.39	-0.01	2.40	0.06	14.15	0.82	0.0	3.22
	10 to 11	5.69	1.246	5.00	0.4700	0.56	1.25	0.01	0.600	4.41	600.00	500.00	1.20	603	4.37	0.3365	0.603	1.25	0.00	1.91	0.01	11.45	0.11	0.0	2.03
	11 to 12	5.69	1.108	5.00	0.5050	0.53	1.11	0.01	0.550	4.66	500.00	500.00	1.00	551	4.65	0.4222	0.551	1.11	0.00	2.40	0.07	12.98	0.86	0.0	3.26
	12 to 13	5.69	0.969	5.00	0.5479	0.50	0.97	0.01	0.500	4.93	800.00	350.00	1.71	501	4.91	0.5248	0.501	0.97	0.00	2.99	0.07	14.49	0.99	0.0	3.97
	13 to 14	5.69	0.830	5.00	0.6020	0.46	0.83	0.01	0.500	4.23	600.00	350.00	1.71	501	4.21	0.2932	0.501	0.83	0.00	2.24	0.02	10.64	0.26	0.0	2.49
	14 to 15	5.69	0.691	5.00	0.6733	0.42	0.69	0.00	0.450	4.35	500.00	350.00	1.43	459	4.17	0.4304	0.459	0.69	0.00	2.45	0.08	10.45	0.86	0.0	3.31
	15 to 16	5.69	0.553	5.00	0.7720	0.38	0.55	0.02	0.400	4.40	450.00	300.00	1.50	403	4.33	0.5413	0.403	0.55	0.01	3.08	0.10	11.26	1.15	0.0	4.23
	16 to 17	5.69	0.414	5.00	0.9220	0.32	0.41	0.02	0.350	4.30	400.00	250.00	1.60	346	4.39	0.6690	0.346	0.41	0.00	3.81	0.14	11.58	1.67	0.0	5.47
	17 to 18	5.69	0.275	4.67	1.0000	0.27	0.28	0.00	0.300	3.89	300.00	250.00	1.20	301	3.86	0.4238	0.301	0.28	-0.01	3.55	0.06	8.93	0.45	0.0	4.00
	18 to 19	5.86	0.136	3.92	1.0000	0.21	0.14	0.01	0.250	2.78	300.00	175.00	1.71	251	2.77	0.4247	0.251	0.14	-0.01	2.49	1.18	4.59	5.40	0.0	7.89
	19 to 20	2.45	0.068	3.29	1.0000	0.16	0.07	-0.01	0.200	2.17	225.00	150.00	1.50	201	2.14	0.3483	0.201	0.07	0.00	0.85	-0.07	2.74	-0.19	0.0	0.66
	20 to 21	4.90	0.046	2.99	1.0000	0.14	0.05	-0.02	0.150	2.63	150.00	125.00	1.20	151	2.61	0.7195	0.151	0.05	0.00	3.53	0.03	4.08	0.13	0.0	3.65
	21 to 22	5.46	0.025	2.54	1.0000	0.11	0.02	-0.01	0.150	1.40	150.00	125.00	1.20	151	1.39	0.2314	0.151	0.02	0.01	1.26	0.24	1.16	0.28	50.0	51.54
																								FTP (Pa):	421.15

Table A-5: Duct sizing calculation spreadsheet for the FCU supply system, when this is simulated for the CIBSE TRY (velocity limit = 5.0 m/s, pressure drop limit = 1.0 Pa / m)

A.4 Duct sizing results - Fan Total Pressure

A.4.1 Duct sizing results for the VAV system

The total pressure of the supply and return fans for the VAV system, as estimated via the duct sizing calculations, is presented in table A-6, for both climates:

Weather data	AHU number	Floors served	Supply Fan (Pa)	Return Fan (Pa)
CIBSE TRY	1	First and Ground	677	162
	2	Third and Second	668	156
	3	Fifth and Fourth	660	156
NOA TRY	1	First and Ground	681	156
	2	Third and Second	677	156
	3	Fifth and Fourth	672	156

Table A-6: FTP of the supply and return fans of the VAV system for both the CIBSE TRY and the NOA TRY

As can be seen from table A-6, the differences in the size of the supply and return fans depending on the climate under consideration are small, since the duct pressure losses (estimated by multiplying the pressure drop rate by the length of each duct section) and the pressure losses due to the chosen duct fittings (calculated by multiplying the summation of the relevant velocity pressure loss factors ζ by the velocity pressure of each duct section) are fairly similar[3] for both climates.

A.4.2 Duct sizing results for the FCU system

The FTP of the central fans moving the fresh air around the case study building, as estimated via the duct sizing calculations, is shown in table A-7 for both climates:

Weather data	AHU number	Floors served	Supply Fan (Pa)	Return Fan (Pa)
CIBSE TRY	1	Ground - Fifth	421	197
NOA TRY	1	Ground - Fifth	474	197

Table A-7: FTP (Pa) of the central supply and return fan of the FCU system for both the CIBSE TRY and the NOA TRY

As can be seen from table A-7, the increase in the FTP of the supply fan when the simulations are carried out for the NOA TRY as opposed to the CIBSE TRY is mainly due to the large central cooling coil required for this climate, (i.e. an 8 row coil involving a pressure drop of 211.7 Pa instead of a 6 row coil involving a

[3] **Note:** It should also be remembered that the pressure drop due to the AHU components is the same in both climates, as shown in table A-1.

pressure drop of 158.8 Pa, which was used for the CIBSE TRY), as shown in section A.2.

In addition, a brief investigation was carried out regarding the typical size of the small fan located in each of the fan coil units installed throughout the case study building.

In the Final Report to the California Institute for Energy Efficiency titled "Efficient Thermal Energy Distribution in Commercial Buildings" [8] an attempt was made to characterize the stock of commercial buildings, their thermal distribution systems and their energy consumption in California. Some computer simulations were also performed using DOE-2 in order to compare the fan and pump power consumption of a VAV system, a four-pipe fan coil system and a packaged constant-air-volume system. Each of the four-pipe fan coil units simulated was assumed to provide a fixed quantity of outside air for ventilation along with re-circulated air, which was conditioned by the corresponding heating or cooling coils contained within each unit. Friction losses in this report were taken equal to 57 Pa for each fan coil unit, assuming negligible duct runs, causing no additional friction losses.

On the other hand, *Carrier*, provides several data for a variety of fan coil unit types. The fan static pressure depending on the type of unit is illustrated in table A-8:

Manufacturer	Type of AHU	Fan Static Pressure (Pa)
Carrier (www.uk.carrier.com)	CARRIER 42UK compact fan coil units	60
	CARRIER 42EL Aqualia fan coil units	50
	CARRIER 42N room fan coil units	60 or 70

Table A-8: Fan static pressure for a variety of fan coil units produced by Carrier (UK)

Although it is difficult to compare the values found in the literature due to the variety in the characteristics of the available types of fan coil units, it seems that the maximum static pressure for four-pipe fan coil units usually ranges from 50 to 70 Pa. As a result, it was decided to assume a value of 60 Pa for each of the fan coil units placed throughout the building (i.e. the mid-value of the range of values shown above).

The total number of the fan coil units installed in the case study building was based on the assumption that there is 1 fan coil unit per 49 m^2 (approximated to a 6×8.2 m^2 space, where 6 m is the depth of the perimeter office zone and 8.2 m is the width of one or two structural bays). The number of fan coil units per zone and the respective fan total pressures, as they were introduced in B-TAS, are presented in table A-9:

Floors:	Ground	First	Second	Third	Fourth	Fifth	Orientation	Number of Fan Coil Units	FTP (Pa)
Zones:	*1*	*10*	*19*	*28*	*37*	*46*	*SW*	1	60
	2	*11*	*20*	*29*	*38*	*47*	*S*	6	360
	3	*12*	*21*	*30*	*39*	*48*	*SE*	1	60
	4	*13*	*22*	*31*	*40*	*49*	*W*	2	120
	5	*14*	*23*	*32*	*41*	*50*	*CORE*	20	1200
	6	*15*	*24*	*33*	*42*	*51*	*E*	2	120
	7	*16*	*25*	*34*	*43*	*52*	*NW*	1	60
	8	*17*	*26*	*35*	*44*	*53*	*N*	6	360
	9	*18*	*27*	*36*	*45*	*54*	*NE*	1	60

Table A-9: Number of fan coil units and FTP (Pa) of the fans located in each zone of the case study office building

References

[1] Roderic Bunn, Let's get specific about fan power, Building Services Journal, August 1999

[2] Lars J. Nilsson, Air-handling energy efficiency and design practices, Energy and Buildings 22, 1995, 1-13

[3] Jones W P, Air Conditioning Applications and Design, Arnold, London, 2nd edition, 1997, pg 420.

[4] David V. Chadderton, Air conditioning: A practical introduction, London; New York: E & FN Spon, 1997

[5] Envirotec Ltd, http://www.envirotec.co.uk/airhandlingunits/env.htm

[6] FYROGENIS Air Handling Units (Series MFB and MFE-MFD) Technical Guide

[7] VAV terminal units, www.celmec.com.au

[8] M. Modera, H. Feustel, N.Matson, C. Huizenga, F. Bauman, E. Avens, T. Borgers, Efficient Thermal Energy Distribution in Commercial Buildings, Final Report to California Institute for Energy Efficiency, May 1994 (Revised in August 1999)

Appendix B: The variation in the FTP of the HVAC systems under consideration depending on the choice of duct fittings and the energy consequences

B.1 The effect of the duct fittings used in Appendix A6 of CIBSE Guide B3 on the FTP and the fan energy consumption of the FCU and the VAV system

The new edition of CIBSE Guide C (2001) [1] provides comprehensive information on pressure loss factors for a large number of duct fittings and is considered as the most detailed and authoritative source for such data [2]. The designer can, therefore, choose from a variety of components for the same type of duct fitting (e.g. 90° branch tees, 90° shoe branch tees, 90° bell-mouth branch tees, 90° swept branch tees, etc) the one that best suites the application under consideration. The pressure loss factors (or ζ factors) are specified in detail for each of these fittings, while in some cases ζ factors from more than one source are provided for the same duct component (e.g. the branch flow $\zeta_{c\text{-}b}$ factor for 90° branch tees & diverging flow can be obtained either from Idelchik or SMACNA).

Appendix A6 [3] of CIBSE Guide B3: Ductwork (2002) illustrates a duct sizing calculation example based on a generic supply system serving six private offices. The calculation of pressure losses through the various duct fittings is based on data contained in section 4 of the new CIBSE Guide C (2001) [1]. Although details of the HVAC system or the duct sizing method used are not given[4], the example illustrates how the ζ factors are estimated from the various tables of CIBSE Guide C [1].

Although the source of pressure loss data is the same for both the calculations carried out in the thesis and the Appendix A6 [3], the choice of fittings often differs. On top of this, there are also some differences in the shape of the ducts between the two calculations. The generic supply system presented in Appendix A6 [3] consists mainly of rectangular ducts. However, this doesn't include the duct branches which were assumed to be circular[5], since as is explained in section A6.1.2.10 (of Appendix A6 [3]), it is more convenient to make the final connection to a diffuser by a flexible duct [3]. The length of the final flexible ducts is taken equal to 0.4 m (i.e. as small as possible since their pressure loss is high), while the associated pressure drop is taken as 8 times that of a smooth duct (i.e. flexible duct loss = 8 x (smooth duct loss)) [3]. On the other hand, the shape of all ducts is circular for the supply and rectangular for the extract VAV system, respectively, as shown in table 3-16 (chapter 3). As far as the FCU system is concerned, the shape of the ducts is rectangular for both the supply and the extract system.

[4] **Note:** The duct sizing method utilized in Appendix A6 [3] seems to be the constant velocity method, since the calculation is based on a number of velocity limits depending on the section of the system, while pressure loss limits are not taken into consideration.

[5] **Note:** As a result, the worked example contained in Appendix A6 [3] makes use of both rectangular and circular duct fittings for the same supply ductwork system.

The main differences in the duct fittings chosen in the two duct sizing calculations are summarized in table B-1:

	Thesis Calculation			Appendix A6 - Section A6.1 worked example		
Duct Fitting Type	**CIBSE Guide C Fitting**	**Section**	**Table**	**CIBSE Guide C Fitting**	**Section**	**Table**
Bend (Rectangular Ducts)	Rectangular Mitred elbows with vanes	4.10.3.8	4.71	Short Radius Bends with splitter vanes	4.10.3.2	4.63
Bend (Circular Ducts)	90 Smooth radius round elbow	4.10.5.1	4.115	90 Segmented Bend	4.10.5.2	4.119
Tee (Recangular Ducts)	90 branch tees: rectangular from rectangular	Diverging Flows - 4.10.3.21 (b)	4.85 & 4.87	90 shoe branch tees: rectangular from rectangular	Diverging Flows - 4.10.3.22 (b)	4.90 & 4.91
		Converging Flows - 4.10.3.21 (a)	4.83 & 4.84		Converging Flows - 4.10.3.22 (a)	4.88 & 4.89
	-			90 shoe branch tees: circular from rectangular	Diverging Flows - 4.10.4.5 (b)	4.113 & 4.114
					Converging Flows - 4.10.4.5 (a)	4.111 & 4.112
	-			90 branch tees: circular from rectangular	Diverging Flows - 4.10.4.4 (b)	4.108 & 4.110
					Converging Flows - 4.10.4.4 (a)	4.106 & 4.107
Tee (Circular Ducts)	90 branch tees: circular from circular	Diverging Flows - 4.10.5.12 (b)	4.133 & 4.135	-		
		Converging Flows - 4.10.5.12 (a)	4.131 & 4.132			

Table B-1: Duct fittings chosen for the duct sizing calculations performed in the thesis and Appendix A6 of CIBSE Guide B3

Some useful notes regarding table B-1 are the following:

- Table B-1 includes only duct fitting types which are common in the ductwork schematic designed for each calculation, and for which different fittings were chosen from CIBSE Guide C. For example, regarding the rectangular bends, a rectangular mitred elbow with vanes was chosen in the thesis, while a short radius bend with splitter vanes was assumed in Appendix A6.
- In some cases there are differences in the estimation of the ζ factor, even for duct fittings appearing in the ductwork schematics in both calculations, such as the symmetrical expansions or contractions. For example, the ζ factor for symmetrical expansions (rectangular ducts) is obtained from section 4.10.3.17 - table 4.79 of CIBSE Guide C in both calculations, with regard to the included angle θ, the area ratio A_2 / A_1 (i.e. large duct area / small duct area) and the Re number. In appendix A6, the angle θ was taken equal to 45° (i.e. the maximum taper recommended in HVCA specification DW/144), while in the thesis the same angle was taken equal to 30°. Moreover, in Appendix A6 the calculation of the Re number was differentiated depending on the point of the ductwork system and the associated temperature of the air, while in the thesis-related calculations the estimation of the Re number was based on standard conditions (i.e. air @ 20°C). However, the choice of included angle θ is not important as stated in appendix A6, while the estimation of the Re number for different temperature conditions does not result in significantly different ζ factors. (In appendix A6, it is also stated that it is even possible to obtain a speculative value from the respective table and avoid the whole calculation, particularly for small expansions or contractions). Therefore, the differences in the computation of the pressure loss factor for such duct components are ignored.

As can be seen from table B-1, the differences regarding the chosen duct fittings in the two calculations are mainly in bends and tees. Although there are no specific rules regarding which fitting should be taken from CIBSE Guide C[6] when a bend or a tee is concerned, it is observed that the ζ factor between two fittings of the same type can often be quite different. For clarity, the ζ factors for the fittings displayed in table B-1 are briefly presented in the following:

Bend (Rectangular Ducts)

The ζ factor associated with a **rectangular mitred elbow with vanes** (*section 4.10.3.8 -table 4.71*) for a single skin vane and a velocity limit of 5 m/s is 0.24. For the highest velocity limit c = 12.5 m/s, the ζ factor drops to 0.20.

On the other hand, the ζ factor for a **short radius bend with vanes** (*section 4.10.3.2 – table 4.63*) when r/w = 1.0 (DW/144 standard bend radius is r = w) and for a single turning vane ranges from 0.04 to 0.09 depending on the ratio h / w (i.e. the dimensions of the duct section). For 2 turning vanes the pressure loss factor ranges from 0.01 to 0.03, while for 3 turning vanes the ζ factor drops to 0.01 for all h /w values included in table 4.63.

Bend (Circular Ducts)

The ζ factor for a **90° smooth radius round elbow** (*section 4.10.5.1 – table 4.115*) when r / d = 1.0 equals 0.24. The maximum value of this pressure loss factor is 1.2, for r/d = 0.5

On the other hand, the ζ factor for a **90° segmented bend** *(section 4.10.5.2 – table 4.119)* and r / d = 1.0 is provided only for two duct sizes. When d = 250 mm (4 sections), the pressure loss factor ranges from 0.24 to 0.38 depending on the Re number. On the other hand, when d = 400 mm (4 sections), the ζ factor ranges from 0.213 to 0.31 depending also on the Re number.

Tee (circular or rectangular ducts)

Diverging Flows: The straight duct factor $\zeta_{c\text{-}s}$[7] is the same for all duct shapes (e.g. rectangular or circular), including 90° branch tees: circular from rectangular (i.e. tees where the main duct is rectangular but the branch is circular). On the other hand, the branch factor $\zeta_{c\text{-}b}$ for tees with shoe branches is in general **lower** than for tees without a shoe branch, for all shapes of ducts. Depending on the ratios q_b / q_c and A_b / A_c (i.e. branch / combined flow) the branch factor $\zeta_{c\text{-}b}$ for a

[6] **Note:** In the worked example illustrated in Appendix A6, a tee with a shoe branch is obtained for a certain point of the duct schematic, while a tee without a shoe branch is chosen for the next similar point in the same schematic without any apparent reason for the difference in these two choices. (If the choice of fitting was based on the minimization of ζ factor, all the tees illustrated in appendix A6 should involve a shoe branch).

[7] **Note:** In general the subscript *c* stands for 'combined', the subscript *s* stands for 'straight', while the subscript *b* stands for 'branch'.

tee without a shoe branch can be twice as high as the respective factor for a tee with a shoe branch.

Converging Flows: The straight duct factor $\zeta_{s\text{-}c}$ for a tee with a shoe is in general lower than the respective factor of a tee without a shoe branch. The difference depends on the shape of the duct and the parameters required for the estimation of the ζ factor under consideration. For example, for a **rectangular tee without a shoe branch** *(section 4.10.3.21 – table 4.83)* the $\zeta_{s\text{-}c} = 0.46$ when $q_s / q_c = 0.6$, while for a **rectangular tee with a shoe branch** *(section 4.10.3.22 – table 4.88)* the value of $\zeta_{s\text{-}c}$ drops to 0.29. Similarly, the branch factor $\zeta_{b\text{-}c}$ for tees with shoe branches is in general lower than for tees without a shoe branch, for all shapes of ducts. Depending on the ratios q_b / q_c and A_b / A_c (i.e. branch / combined flow) the branch factor $\zeta_{b\text{-}c}$ for a tee without a shoe branch can be up to approximately two-times as high as the respective factor for a tee with a shoe branch.

It is obvious that there are some significant differences in the pressure loss factors of the duct fittings contained in table B-1. As a result the choice of fittings can lead to different total pressure losses through the same supply or extract ductwork system. Of course it would be difficult to 'guess' the effect of a fitting contained in table B-1 on the total pressure of the system, since that depends on the number of such fittings in the duct schematic, the velocity of the air (and, hence, the velocity pressure) passing through the fitting under consideration, and the values of the parameters required to estimate the value of ζ from the respective table of CIBSE Guide C, as was explained earlier.

It was, therefore, decided to repeat the duct sizing calculations[8] for both the FCU system and the first AHU of the VAV system (as an example) using as similar as possible duct fittings to the worked example of Appendix A6 [3], (also presented in the respective columns of table B-1), in order to study their effect on the total pressure. To be more specific, the changes made to the duct sizing calculations for each system were the following:

FCU system: It should be stressed that both the supply and the extract ductwork system involve the same duct shape (i.e. rectangular) and are sized using the same criteria, so the changes described in this paragraph are the same for both the supply & the extract system. Thus, the duct branches were changed to circular while the final connection to a supply or extract diffuser (for the supply and the extract system respectively), was made by a flexible duct with length equal to 0.4 m and a pressure drop equal to 8 times that of a smooth duct, as described earlier. The tees involved in the duct schematic were assumed to be 90° shoe branch tees: rectangular from rectangular or 90° shoe branch tees circular from rectangular, depending on the shape of the branch. All rectangular bends were designed to be short radius bends with vanes, while the circular bend at the final connection to the diffuser was assumed to be a 90° segmented bend.

[8] **Note:** It should be remembered that the duct shape and the duct sizing criteria used to perform the calculations for both the FCU system and the VAV system are summarized in table 3-16 - section 3.6 of chapter 3.

VAV system: All the ducts of the supply system are circular, so the only change here was the addition of a flexible duct for the final connection with the supply diffuser. The tees involved in the supply system were assumed to be 90° shoe branch tees: circular from circular. The circular bend at the final connection to the diffuser was designed to be a 90° segmented bend. However, the rest of the circular bends included in the supply ductwork system could not be changed to 90° segmented bends since the respective duct sizes were much higher than 250 or 400 mm (the only sizes for which ζ factors are available in table 4.119 of CIBSE Guide C, as explained earlier). On the other hand, the VAV extract system has similar characteristics to the FCU supply or extract system, so the changes described earlier regarding the calculations carried out for the FCU system were also applied here.

The pressure of the supply & extract fans for both HVAC systems when the duct fittings described in the worked example of Appendix A6 are also adopted in the duct sizing calculations performed in the thesis is illustrated in table B-2:

	FCU system		VAV system (First AHU)	
	Supply Fan (kPa)	Extract Fan (kPa)	Supply Fan (kPa)	Extract Fan (kPa)
Base case scenario: Using the duct fittings of CIBSE Guide C (2001)	0.421	0.197	0.677	0.162
Scenario 1: Using the duct fittings of Appendix A6	0.415	0.180	0.668	0.139
Change over the base case scenario (%)	-1.4%	-8.6%	-1.3%	-14.2%

Table B-2: The effect of the duct fittings shown in table B-1 (i.e. under column Appendix A6 – Section A6.1) on the FTP of the central supply & extract fans of the FCU and the VAV system (CIBSE TRY)

As can be seen from table B-2, the reduction in the FTP of the supply fans of both HVAC systems over the base case scenario (BCS) is quite small. The main reason for this result is that even though the fittings for tees were changed in both HVAC systems (i.e. they were replaced with 90° shoe branch tees), the straight flow factor $\zeta_{c\text{-}s}$, which dominates the index run, remained the same[9]. In addition, the circular bends in the supply VAV system could not be changed from 90° smooth radius elbows to 90° segmented bends (as suggested in table B-1) due to the large size of the ducts, as was explained above. However, even if the aforementioned replacement of circular bends was possible the change in the FTP of the supply VAV system would not have been significant, since the ζ factors for the two duct fittings under consideration are very similar, as was described earlier.

The reduction in the FTP of the extract fans over the BCS is considerably higher, reaching 14.2% for the VAV system (scenario 1). This was anticipated since both the straight flow ($\zeta_{s\text{-}c}$) and branch flow factors ($\zeta_{b\text{-}c}$), for converging flows, are much lower when a tee with a shoe branch is used instead of a tee without a shoe branch. On top of this, the pressure loss factors for rectangular short radius bends with vanes are much lower than the ζ factors for rectangular mitred elbows with vanes, as was mentioned earlier. On the other hand, though,

[9] **Note:** It should be remembered that the factor $\zeta_{c\text{-}s}$ for **diverging** flows, as provided by CIBSE Guide C, is the same regardless of the shape of the ducts or the presence of a shoe branch.

this reduction in pressure of the extract fans is not expected to be very beneficial in terms of fan energy use since both the size and, hence, the contribution of these fans to the total fan energy consumption of the BCS was already quite small.

The total energy consumption of the VAV[10] and the FCU system when the original fan sizes and the reduced fan sizes (based on the duct fittings used in the worked example of Appendix A6 [3]) are used, respectively, is illustrated in table B-3:

		Heating Energy Consumption (kWh)	Cooling Energy Consumption (kWh)	Supply Fan (kWh)	Return Fan (kWh)	Fan Coil Units (kWh)	Total Fan Energy Consumption (kWh)
FCU system	Base case scenario: Using the duct fittings of CIBSE Guide C (2001)	144279	267686	14289	6686	117446	138421
	Scenario 1: Using the fittings of Appendix A6	144375	267639	14085	6109	117434	137628
	Change over the base case scenario (%)	-	-	-1.4%	-8.6%	0.0%	-0.6%
VAV system	Base case scenario: Using the duct fittings of CIBSE Guide C (2001)	108076	127741	60083	14200	-	74283
	Scenario 1: Using the fittings of Appendix A6	108162	127241	59300	12199	-	71499
	Change over the base case scenario (%)	-	-	-1.3%	-14.1%	-	-3.7%

Table B-3: The effect of the duct fittings described in Appendix A6 (also presented in table B-1) on the annual fan energy use, when the simulations are carried out for the CIBSE TRY

As can be seen from scenario 1, the reduction in fan energy use over the BCS is greater for the extract than the supply fans in both systems, as anticipated. However, if the total fan energy consumption is taken into consideration then the reduction is approximately 3.7% for the VAV system and only 0.6% for the FCU system.

To sum up, the use of the duct fittings presented in the worked example in Appendix A6 [3], (also summarized in table B-1), proved to be beneficial[11] for the size of the fans of both HVAC systems. The reduction in FTP was greater for the extract than the supply fans, as shown in table B-2. However, the predicted energy consumption data for both systems illustrated that the overall savings in fan energy use were rather small. This was due to the lower contribution of the extract fans (in comparison with the supply fans) to the total fan energy use, as can be seen from the simulation results for both the base case scenario and scenario 1, presented in table B-3.

[10] **Note:** It should be stressed that the fan sizes for the remaining two AHUs serving the rest of the building floors when the VAV system is installed, were 'quickly estimated' by reducing the original fan sizes via the percentages shown in table B-2 (i.e. VAV system – first AHU: 1.3% for the supply fan and 14.2% for the extract fan), since the duct schematics for all the floors of the building are the same. Moreover, the energy consumption of the supply or the extract fans of the VAV system, as illustrated in table B-3, is the summation of all the supply or extract fans contained in all three AHUs.

[11] **Note:** To be more specific the addition of the flexible duct in the final connection with the supply or extract grille and the use of 90° segmented bends increased the pressure losses over the BCS, but if all the changes made to the sizing of each system are taken into consideration, their effect certainly proved to be beneficial since the size of the fans for both HVAC systems was reduced.

B.2 The effect of the duct fittings obtained from the old CIBSE Guide C (1986) on both the FTP and the fan energy consumption of the FCU and the VAV system

The old version of the CIBSE Guide C: Reference Data (1986) [4] provides a limited choice of duct fittings, (in comparison with the recent version of the same CIBSE Guide [1]), while in some cases the specification of pressure loss factors raises questions due to the lack of sufficient information (e.g. the ζ factors for rectangular or circular tees seem to be the same for both diverging and converging flows, the ζ factors for gradual enlargements seem to depend on the included angle θ alone and not the duct area ratio, the straight flow ζ factor for circular duct 90° tees is not specified, implying that it is equal to zero, etc). Nevertheless, it was decided to carry out a similar investigation as in the previous section, using the duct fittings contained in the old CIBSE Guide C [1] (i.e. the main source for pressure loss data before 2001) in order to study their effect on the FTP of both the FCU and the VAV system.

The main differences in the duct fittings chosen from each version of the CIBSE Guide C are described in the following:

Louvred duct entry and mesh screen

CIBSE Guide C (2001): The ζ factor associated with the pressure losses through a **louvred duct entry** *(Section 4.10.3.32 - table 4.104)* is specified in association with a number of parameters concerning the shape and geometry of the louvres. Taking case a, $x_1 / x = 0.9$ and $h_1 / h = 0.7$ the ζ factor is found equal to 4.8.

The ζ factor which accounts for the losses occurring when the fresh air passes through a **mesh screen** *(section 4.10.3.29 - table 4.102)* ranges from 0.32 to 82 depending on the free area ratio. Assuming a free area ratio of 70%, it is taken equal to 0.58.

CIBSE Guide C (1986): The ζ factor for a **louvred duct entry** *(table C4.35 – page C4-64)* is specified in association with the shape of the louvres and the free area ratio. Taking case a (i.e. assuming the same shape of louvres as in the calculation carried out with the new duct fittings) and a free area ratio of 0.70, the ζ factor is taken equal to 2.40. It is clear that the pressure loss factor for the louvred duct entry obtained from this Guide is half of the respective value derived from the new CIBSE Guide.

On the other hand, the ζ factor for a **wire mesh** *(table C4.35 – page C4-64)* ranges from 0.3 – 17 depending on the free area ratio. Assuming a free area ratio of 0.70, the ζ factor is found equal to 0.6.

Bend (Rectangular Ducts)

CIBSE Guide C (2001): The ζ factor for a **rectangular mitred elbow with vanes** *(section 4.10.3.8 -table 4.71)* and a velocity limit of 5 m/s is equal to 0.24 (single skin vane), as was also mentioned in section B.1.

CIBSE Guide C (1986): The ζ factor ranges from 0.2 to 1.25 for a variety of **rectangular mitre bends** *(table C4.35 – page C4-65).* Assuming a mitre bend with vanes similar as the one chosen from the new CIBSE Guide C, the ζ factor is taken equal to 0.35.

Bend (Circular Ducts)

CIBSE Guide C (2001): The ζ factor for a **90° smooth radius round elbow** *(section 4.10.5.1 – table 4.115)* when r / d = 1.0 equals 0.24, as was also mentioned in section B.1.

CIBSE Guide C (1986): The ζ factor for a **90° circular duct**[12] *(table C4.35 – page C4-65)* ranges from 0.22 to 0.46 depending on the number of pieces (segments) and the ratio r / d. For 4 pieces (HVCA standard) and r / d = 1.0 the ζ factor is taken equal to 0.42. It is clear that the ζ factor for this duct fitting is approximately twice as high as the respective factor derived from the new version of the CIBSE Guide C.

Tee (circular or rectangular ducts)

CIBSE Guide C (2001) - Diverging Flows: The straight duct factor $\zeta_{c\text{-}s}$ for **90° branch tees** ranges from -0.064 to 0.40 depending on the straight flow ratio q_s / q_c and the area ratio A_b / A_c (i.e. branch flow / combined flow). The ζ factors are the same for both rectangular *(section 4.10.3.21 (b) – table 4.85)* and circular ducts *(section 4.10.5.12 (b) – table 4.133).* The branch flow factor $\zeta_{c\text{-}b}$ ranges from 0.81 to 3.6 for rectangular ducts *(4.10.3.21 (b) – table 4.87)* and 0.82 to 2.5 for circular ducts *(4.10.5.12 (b) – table 4.135)* depending on the branch flow ratio q_b / q_c and the area ratio A_b / A_c (i.e. branch flow / combined flow).

CIBSE Guide C (2001) - Converging Flows: The straight duct factor $\zeta_{s\text{-}c}$ for **90° branch tees** ranges from 0.0 to 0.60 for rectangular ducts *(section 4.10.3.21 (a) – table 4.83)* and 0.0 to 0.79 for circular ducts *(section 4.10.5.12 (a) – table 4.131)* depending on the straight flow ratio q_s / q_c. The branch flow factor $\zeta_{b\text{-}c}$ for rectangular ducts *(section 4.10.3.21 (a) – table 4.84)*, ranges from -0.75 to 5.13 depending on the combined flow velocity c_c and the branch flow ratio q_b / q_c[13]. On the other hand, the respective branch flow factor $\zeta_{b\text{-}c}$ for circular ducts *(section 4.10.5.12 (a) – table 4.132)* ranges from -0.52 to 101 depending on the area ratio A_b / A_c and the branch flow ratio q_b / q_c.

[12] **Note:** This is the only fitting of this type available in table C4.35 for circular ducts, so it was not possible to select a duct component more similar as the one derived from the new CIBSE Guide C.

[13] **Note:** It should be stressed that the values of the branch flow factor included in table 4.84 are valid only for $A_s = A_c = 2 \times A_b$. Alternatively the branch flow factor can be estimated from the Idelchik equations (section 4.10.2.21 (a) – page 4-102) which also cover other branch areas.

CIBSE Guide C (1986): The straight flow ζ factor for **90° branch tees** and rectangular ducts *(table C4.35 – page C4-65)* ranges from 0.02 to 0.44 depending on the velocity ratio of the straight flow to the combined flow. On the other hand, the branch flow factor ranges from 0.45 – 1.60 depending on the velocity ratio of the branch flow to the combined flow. The straight flow factor for circular ducts *(table C4.35 – page C4-65)* is equal to zero. On the other hand, the branch flow factor ranges from 1.4 to 3.7 (i.e. it is much higher than the respective pressure loss factor for rectangular ducts) depending on the velocity ratio of the branch flow to the combined flow.

A major difference between the two CIBSE Guides regarding the specification of pressure loss factors for all types of tees is that in the old CIBSE Guide C the ζ factors are used in conjunction with the velocity pressure of the branch flow, while in the new CIBSE Guide C they refer to the velocity pressure of the combined flow. Moreover, the old CIBSE Guide does not differentiate between diverging and converging flows as far as the ζ factors for tees are concerned.

Enlargements

CIBSE Guide C (2001): The pressure loss factors for **symmetrical expansions** are specified in correlation with the ratio of the large area to the small area, the included angle θ and the Re number. They range from 0.16 to 0.96 for rectangular ducts (section 4.10.3.17 – table 4.79) and 0.14 to 1.02 for circular ducts (section 4.10.5.8 – table 4.125). Assuming an angle θ = 30°, the pressure loss factor ranges from 0.265 to 0.76 for rectangular ducts and 0.194 to 0.807 for circular ducts.

CIBSE Guide C (1986): The ζ factors for **abrupt enlargements** (table C4.35 – page C4-64) range from 0.09 to 0.56 depending on the ratio of the small area to the large area. On the other hand, the pressure loss factors for **gradual symmetrical expansions** range from 0.3 to 1.0 depending on the angle θ[14]. It must be stressed that the latter ζ factors are multiplying factors, which are applied to the respective pressure loss factors for abrupt enlargements. (Assuming an angle θ = 30°, the multiplying ζ factor equals 0.6 for circular ducts and 0.8 for rectangular ducts, respectively). Applying these multiplying ζ factors to the pressure loss factors for abrupt enlargements results in much lower ζ factors than the respective values for symmetrical expansions provided by the new version of CIBSE Guide C.

Contractions

CIBSE Guide C (2001): The pressure loss factors for symmetrical contractions (section 4.10.3.18 – table 4.80 for rectangular ducts and section 4.10.5.9 – table 4.126 for circular ducts) range from 0.04 to 0.43 depending on the ratio of the small area to the large area and the included angle θ. The range of values is the

[14] **Note:** The range of values is the same for both rectangular and circular ducts but the individual values of the ζ factor for a specific angle θ are slightly different is some cases.

same for both rectangular and circular ducts. Assuming an angle $\theta = 30^{\circ}$ the range of values of this ζ factor drops to 0.04 - 0.05.

CIBSE Guide C (1986): The ζ factors for **abrupt contractions** (table C4.35 – page C4-64) range from 0.09 to 0.37 depending on the ratio of the small area to the large area. On the other hand, the ζ factors for **gradual symmetrical contractions** range from 0.02 to 0.07 depending on the angle θ. The latter factors are directly applied to the velocity pressure of the small area (i.e. they are not related to the pressure loss factors of abrupt contractions). For an angle $\theta = 30^{\circ}$ the ζ factor for a gradual contraction equals 0.02. Clearly, the pressure loss factor for gradual symmetrical contractions (and $\theta = 30^{\circ}$) is approximately half of the respective values derived from the new CIBSE Guide (i.e. $\zeta = 0.04 - 0.05$).

The pressure of the supply & extract fans for both HVAC systems when the duct fittings contained in CIBSE Guide C (1986) are also adopted in the duct sizing calculations performed in the thesis, is illustrated in table B-4:

	FCU system		VAV system (First AHU)	
	Supply Fan (kPa)	Extract Fan (kPa)	Supply Fan (kPa)	Extract Fan (kPa)
Base case scenario: Using the duct fittings of CIBSE Guide C (2001)	0.421	0.197	0.677	0.162
Scenario 2: Using the duct fittings of CIBSE Guide C (1986)	0.427	0.106	0.684	0.085
Change over the base case scenario (%)	1.4%	-46.2%	1.0%	-47.5%

Table B-4: The effect of duct fittings contained in the old version of CIBSE Guide C on the FTP of the central supply & extract fans of both the VAV and the FCU system (CIBSE TRY)

As can be seen from scenario 2, the FTP of the supply fan of the VAV system is 1.0% higher than the BCS, despite the reduction in the pressure loss factors for the louvred duct entry and the symmetrical contractions over the original calculation as well as the minimisation of the straight flow factor ($\zeta_{c\text{-}s}$) for 90°circular tees[15]. The increase in the supply FTP (over the original calculation) is attributed to the high pressure loss factor for circular bends (the ζ factor derived from the old CIBSE Guide for this fitting is twice as high as the respective factor taken from the new version of CIBSE Guide C, as explained earlier), as well as the particularly high branch flow ($\zeta_{c\text{-}b}$) factors for circular tees.

The FTP of the supply fan of the FCU system has also increased by 1.4% over the BCS, as illustrated in the same table. In this case, the reduction in the pressure loss factors for the louvred duct entry, the symmetrical contractions and the branch flow ($\zeta_{c\text{-}b}$) of rectangular tees over the original calculation was more than compensated by the increase in the ζ factors for the rectangular bends and the straight flow ($\zeta_{c\text{-}s}$) of rectangular tees, resulting in slightly higher total pressure for the supply duct system than the BCS.

[15] **Note:** The straight flow ζ factor for 90°circular tees is equal to zero, as suggested in table C4.35 of the old CIBSE Guide C (1986) [4].

On the other hand, the FTP of the extract fans is reduced approximately to half for both HVAC systems, as illustrated by scenario 2 in table B-4. This is due to the considerable reduction in the pressure loss factors related to the straight flow ($\zeta_{s\text{-}c}$) of rectangular tees and the symmetrical expansions over the original calculation, which was based on the fittings derived from the new version of CIBSE Guide C.

The total energy consumption of the VAV and the FCU system when the original fan sizes and the fan sizes based on the duct fittings of the old version of CIBSE Guide C are used, respectively, is presented in table B-5:

		Heating Energy Consumption (kWh)	Cooling Energy Consumption (kWh)	Supply Fan (kWh)	Return Fan (kWh)	Fan Coil Units (kWh)	Total Fan Energy Consumption (kWh)
FCU system	Base case scenario: Using the duct fittings of CIBSE Guide C (2001)	144279	267686	14289	6686	117446	138421
	Scenario 2: Using the duct fittings of CIBSE Guide C (1986)	144181	267783	14493	3598	117473	135564
	Change over the base case scenario (%)	-	-	1.4%	-46.2%	0.0%	-2.1%
VAV system	Base case scenario: Using the duct fittings of CIBSE Guide C (2001)	108076	127741	60083	14200	-	74283
	Scenario 2: Using the duct fittings of CIBSE Guide C (1986)	108091	127699	60717	7460	-	68177
	Change over the base case scenario (%)	-	-	1.1%	-47.5%	-	-8.2%

Table B-5: The effect of the duct fittings of the old CIBSE Guide C on the annual fan energy use, when the simulations are carried out for the CIBSE TRY

As can be seen from scenario 2 in table B-5, the energy consumed by the supply fans is slightly higher than the BCS for both HVAC systems, while the amount of energy used by the return fans has been reduced by 46% for the FCU system and 48% for the VAV system, respectively. However, if the total fan energy use is taken into consideration then the reduction over the BCS is approximately 2% for the FCU system and 8% for the VAV system respectively. It is clear that the effect of the duct fittings derived from the old CIBSE Guide C on the annual fan energy use is moderate, despite the fact that size of the extract fans was approximately halved for both HVAC systems, as shown in table B-4. This is due to the small contribution of the return fans to the total fan energy use as can be seen from the BCS and scenario 2 for both HVAC systems, presented in table B-5.

To sum up, the use of the duct fittings contained in the old version of CIBSE Guide C resulted to more or less the same total pressure for the supply fans, while the size of the extract fans was approximately halved for both HVAC systems. The predicted energy consumption data for both systems shown in table B-5 illustrated that the overall savings in fan energy use were moderate, particularly for the FCU system. This was due to the small contribution of the extract fans in the total fan energy use, as can be seen from the results of both scenarios presented in table B-5. Nevertheless, even if the reduction in the overall fan energy use was higher than scenario 2, the use of the old version of CIBSE Guide C would still not be recommended due to the limited number of duct fittings provided and the lack of sufficient information regarding the specification of some pressure loss factors, as explained earlier in this section.

References

[1] CIBSE Guide C: Reference Data, The Chartered Institution of Building Services Engineers, London, 2001, Section 4.10: Pressure loss factors for ductwork, pages 96 -117.

[2] CIBSE (Chartered Institution of Building Services Engineers) web-site: http://www.cibse.org/index.cfm?go=publications.view&PubID=3&L1=164

[3] CIBSE Guide B3: Ductwork, The Chartered Institution of Building Services Engineers, London, 2002, Appendix A6: Ductwork sizing and associated calculations – worked example, pages 1-13.

[4] CIBSE Guide C: Reference Data, The Chartered Institution of Building Services Engineers, London, 1986, Table C4.35, pages C4-64 & 65.

Appendix C: Specification of heating, cooling and intermediate period in A-TAS

The calendar function found in A-TAS allows the user to divide the simulation year into a number of periods for which different occupation data, plant operation schedules, window opening schedules, etc, can be specified.

Using this calendar function the simulation year[16] was initially divided into two periods (most common assumption):

Heating Period: January, February, March, October, November and December

Cooling Period: April, May, June, July, August and September

The HVAC system provides heating for the six months comprising the heating period (with respect to a lower temperature limit equal to 20°C) and cooling for the rest of the year (with respect to an upper temperature threshold equal to 24°C). In other words, the aim of the system is to maintain the internal temperature between 20°C and 24°C throughout the year, in order to satisfy the thermal comfort requirements of the occupants.

The room temperature frequency, (in hours in the specified month), during the occupation period (i.e. 9:00 – 17:00), for 5 days a week – 52 weeks a year is presented in tables C-1 to C-3 for three representative zones (a typical core zone, a typical south zone and a typical north zone, respectively) located in the third floor of the case study building, assuming that the simulation year is divided into the heating and cooling period specified above:

Zone 32 (Core Zone)

	Temperature Band (Degrees Celcius)	Jan	Feb	Mar	Apr	May	Jun	Jul	Aug	Sep	Oct	Nov	Dec
ZONE 32 (CORE)	18 to 19	0	0	0	0	0	0	0	0	0	0	0	0
	19 to 20	0	0	0	0	0	0	0	0	0	0	0	0
	20 to 21	0	0	0	0	0	0	0	0	0	0	0	0
	21 to 22	1	0	0	0	0	0	0	0	0	0	0	0
	22 to 23	1	0	0	0	0	0	0	0	0	0	0	0
	23 to 24	8	1	0	189	207	189	198	207	180	0	0	0
	24 to 25	9	4	0	0	0	0	0	0	0	0	0	2
	25 to 26	6	15	3	0	0	0	0	0	0	1	0	9
	26 to 27	12	6	3	0	0	0	0	0	0	1	0	5
	27 to 28	18	14	9	0	0	0	0	0	0	2	0	8
	28 to 29	58	30	8	0	0	0	0	0	0	2	1	23
	29 to 30	43	36	6	0	0	0	0	0	0	4	5	31
	30 to 31	32	29	19	0	0	0	0	0	0	7	9	47
	31 to 32	19	37	34	0	0	0	0	0	0	7	15	38
	32 to 33	0	8	48	0	0	0	0	0	0	13	16	26
	33 to 34	0	0	50	0	0	0	0	0	0	17	26	0
	34 to 35	0	0	15	0	0	0	0	0	0	28	49	0
	35 to 36	0	0	3	0	0	0	0	0	0	48	46	0
	36 to 37	0	0	0	0	0	0	0	0	0	35	28	0
	37 to 38	0	0	0	0	0	0	0	0	0	18	3	0
	38 to 39	0	0	0	0	0	0	0	0	0	21	0	0
	39 to 40	0	0	0	0	0	0	0	0	0	3	0	0

Table C-1: Zone 32 (core zone) temperature frequency (in hours in the specified month) throughout the occupation period for 5 days a week, 52 weeks a year (A-TAS results)

[16] **Note:** The A-TAS simulation results presented in this appendix refer to the CIBSE TRY (London)

As can be seen from table C-1, there is net cooling demand for the whole year, since the internal temperature rises above 24°C for several hours during the heating period. As expected, the high internal heat gains from occupants, lighting and office equipment in combination with the fact that the core zone has zero losses to the external environment, create overheating problems over the heating period.

Zone 29 (South Zone)

ZONE 29 (SOUTH)	Temperature Band (Degrees Celcius)	Jan	Feb	Mar	Apr	May	Jun	Jul	Aug	Sep	Oct	Nov	Dec
	17 to 18	0	0	0	0	1	0	0	0	0	0	0	0
	18 to 19	0	0	0	1	1	0	0	0	0	0	0	0
	19 to 20	0	0	0	3	4	0	0	0	0	0	0	0
	20 to 21	61	43	13	1	0	0	0	0	0	0	8	56
	21 to 22	25	18	2	3	4	1	0	0	2	0	6	28
	22 to 23	26	21	15	3	5	1	0	0	7	4	8	32
	23 to 24	36	17	14	178	192	187	198	207	171	4	10	27
	24 to 25	22	16	21	0	0	0	0	0	0	8	10	10
	25 to 26	9	16	11	0	0	0	0	0	0	5	12	7
	26 to 27	4	14	20	0	0	0	0	0	0	6	16	7
	27 to 28	10	7	26	0	0	0	0	0	0	8	29	4
	28 to 29	5	4	15	0	0	0	0	0	0	21	28	7
	29 to 30	2	4	19	0	0	0	0	0	0	22	17	2
	30 to 31	2	7	10	0	0	0	0	0	0	21	6	4
	31 to 32	4	4	11	0	0	0	0	0	0	30	7	2
	32 to 33	1	3	4	0	0	0	0	0	0	24	6	3
	33 to 34	0	4	2	0	0	0	0	0	0	6	9	0
	34 to 35	0	1	4	0	0	0	0	0	0	8	8	0
	35 to 36	0	1	4	0	0	0	0	0	0	9	2	0
	36 to 37	0	0	3	0	0	0	0	0	0	11	3	0
	37 to 38	0	0	3	0	0	0	0	0	0	7	3	0
	38 to 39	0	0	1	0	0	0	0	0	0	1	4	0
	39 to 40	0	0	0	0	0	0	0	0	0	10	5	0
	40 to 41	0	0	0	0	0	0	0	0	0	2	1	0

Table C-2: Zone 29 (south zone) annual temperature frequency (in hours in the specified month) over the occupation period, for 5 days a week, 52 weeks a year (A-TAS results)

Table C-2 similarly indicates that there is a net cooling demand for the whole year. Moreover, the internal temperatures that occur in zone 29 are in several occasions higher than the internal temperatures of zone 32. The main reason for this temperature difference is the effect of the solar gains through the south-orientated windows of zone 29. It seems that the solar gains through the glazed elements in combination with the internal heat gains are higher than the heat losses to the external environment through the well-insulated building envelope, leading to excessive internal temperatures.

On the other hand, there is a heating demand for a few hours in April and May, as can be seen from table C-2. It seems that the building cools down during night-time (losing heat to the external environment) due to the relatively low external temperatures that occur in April and May. A small amount of heating is, therefore, required for the first hours in the morning to bring the internal temperature close to 20°C, i.e. the lower temperature limit set for the heating period. For example, figure C-1 shows that the building cools down during night-time, on April 30th. As a result, the internal temperature at 9:00 am equals 17.3°C, (as highlighted in this figure), which means that a small amount of heating is required to maintain the internal temperature at or above 20°C.

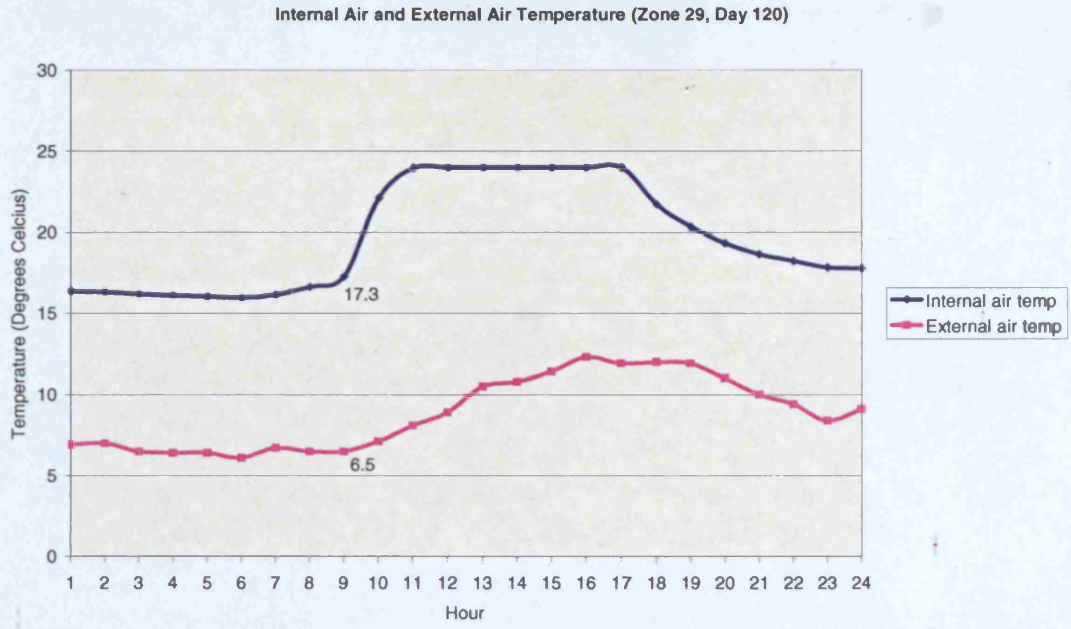

Figure C-1: Internal and outside temperature for zone 29 on April 30th. A small amount of heating is required for the first hour of the occupation period to bring the internal temperature to 20°C

Zone 35 (North Zone)

	Temperature Band (Degrees Celcius)	Jan	Feb	Mar	Apr	May	Jun	Jul	Aug	Sep	Oct	Nov	Dec
ZONE 35 (NORTH)	17 to 18	0	0	0	4	1	0	0	0	0	0	0	0
	18 to 19	0	0	0	8	2	0	0	0	0	0	0	0
	19 to 20	0	0	0	4	3	0	0	0	0	0	0	0
	20 to 21	129	99	26	2	3	0	0	0	3	12	26	113
	21 to 22	34	29	10	4	6	2	0	1	10	7	12	45
	22 to 23	31	27	33	9	7	1	0	5	6	5	18	28
	23 to 24	13	16	29	158	185	186	198	201	161	6	33	3
	24 to 25	0	8	42	0	0	0	0	0	0	10	42	0
	25 to 26	0	1	37	0	0	0	0	0	0	18	44	0
	26 to 27	0	0	17	0	0	0	0	0	0	31	19	0
	27 to 28	0	0	4	0	0	0	0	0	0	34	4	0
	28 to 29	0	0	0	0	0	0	0	0	0	32	0	0
	29 to 30	0	0	0	0	0	0	0	0	0	25	0	0
	30 to 31	0	0	0	0	0	0	0	0	0	18	0	0
	31 to 32	0	0	0	0	0	0	0	0	0	9	0	0

Table C-3: Zone 35 (north zone) temperature frequency (in hours in the specified month) throughout the occupation period for 5 days a week, 52 weeks a year (A-TAS results)

Table C-3 implies that zone 35 has a lower cooling demand than zones 32 and 29. The internal temperature rises above 24°C for four months outside the designated cooling period (i.e. February, March, October and November). This was anticipated since zone 35 (north zone), has lower solar gains than zone 29 (south zone), and higher heat losses to the external environment than zone 32 (core zone). Thus, the internal temperature in zone 35 is in general lower than the temperature that occurs in both zones mentioned above[17]. Nevertheless, the high internal heat gains in combination with the well-insulated building envelope still create overheating problems for several hours in February, March, October and

[17] **Note:** The maximum temperature is approximately 40°C in zone 32 and 41°C in zone 29, while in zone 35 it reaches 32°C.

November, as mentioned above. In other words, cooling is again required at least for part of the heating period.

On the other hand, there is a small heating demand in April and May, since the internal temperature falls below 20°C, as can be seen from table C-3. The number of hours that the internal temperature falls below 20°C and, hence, the heating demand of zone 35 is higher than zone 29, due to the low solar gains of the north orientated zone, that could offset part of the heat losses to the external environment keeping the internal temperature at a higher level for the first morning hours. Moreover, it has been observed that the internal temperature falls below 20°C, for a small number of hours in September (not only in March and April), in all the north orientated zones located in the ground floor, as well as in most of the corner north-east or north-west zones throughout the rest of the building floors. For example, the internal temperature in zone 8 (north zone), which is located in the ground floor of the case study building is provided in table C-4:

ZONE 8 (NORTH)	Temperature Band (Degrees Celcius)	Jan	Feb	Mar	Apr	May	Jun	Jul	Aug	Sep	Oct	Nov	Dec
	15 to 16	0	0	0	2	0	0	0	0	0	0	0	0
	16 to 17	0	0	0	7	2	0	0	0	0	0	0	0
	17 to 18	0	0	0	7	4	0	0	0	0	0	0	0
	18 to 19	0	0	0	0	2	0	0	0	3	0	0	0
	19 to 20	0	0	0	5	3	2	0	1	6	0	0	0
	20 to 21	133	103	29	1	7	1	0	2	8	22	38	130
	21 to 22	35	31	13	10	7	3	2	6	3	3	10	38
	22 to 23	28	23	43	7	5	2	2	2	0	5	29	18
	23 to 24	11	14	24	150	177	181	194	196	160	10	45	3
	24 to 25	0	8	50	0	0	0	0	0	0	20	40	0
	25 to 26	0	1	25	0	0	0	0	0	0	24	27	0
	26 to 27	0	0	14	0	0	0	0	0	0	30	9	0
	27 to 28	0	0	0	0	0	0	0	0	0	34	0	0
	28 to 29	0	0	0	0	0	0	0	0	0	29	0	0
	29 to 30	0	0	0	0	0	0	0	0	0	16	0	0
	30 to 31	0	0	0	0	0	0	0	0	0	14	0	0

Table C-4: Zone 8 (north zone) temperature frequency (in hours in the specified month) throughout the occupation period for 5 days a week, 52 weeks a year (A-TAS results)

To sum up, the high internal heat gains in combination with the well-insulated building envelope create a net cooling demand throughout the building for the whole year. As a result, cooling should be available for the heating period as well, in order to keep the internal temperature between 20°C and 24°C throughout the year. Moreover, there is a small heating demand mainly for the first morning hours during April, May and also in September. It seems that the building cools down during night-time due to the low external temperatures that occur for certain days during these months, requiring a small amount of heating at the beginning of the occupation period. Therefore, heating should also be provided in April, May and September, which were initially categorized in the cooling period.

As a result, the simulation year was finally divided into the following periods:

Heating Period: January, February, March, October, November and December
Both heating and cooling are available for the heating period.

Intermediate Period: April, May and September
Both heating and cooling are available for the intermediate period. However, heating will only be required for a few hours, mainly during the beginning of the occupancy period, so the heating energy consumption is expected to be low for these months.

Cooling Period: June, July, August
Only cooling is available for this period.

It is worth mentioning that A-TAS uses a generic and rather simplified model of the HVAC system (which is based on a limited number of parameters including the heating set-point, cooling set-point, control band, heating capacity and cooling capacity) to assess the system behaviour and performance. This approach is quite adequate for the investigation of issues related to thermal design of the building. However, when it is required to investigate the performance of a particular HVAC system installed in the building, this generic model cannot be considered adequate in every case, since it does not have the flexibility to represent the full range of influences that the system may exert on the building [1]. In such a case B-TAS, the HVAC system simulation software, which allows the simulation of the system to be assessed in relation with the dynamic simulation of the building in A-TAS, should be used. B-TAS uses the A-TAS results[18] as a starting point and adjusts them to take account of the differences between the generic model of the HVAC system in A-TAS and the detailed model designed in B-TAS, taking, at the same time, into consideration the history of zone temperatures and loads [1].

For example, the VAV system simulations performed in B-TAS indicated that the cooling energy consumption, for several months in the heating period (as this was specified in A-TAS), is practically reduced to zero. This is due to the fact that the VAV system makes use of the free cooling capacity of the fresh air. Thus, variable proportions of fresh and re-circulated air are mixed so that the internal temperature in all the building zones remains below 24°C without invoking the cooling coils located in the central AHUs. In other words, even though mechanical cooling is always available, as shown earlier, it is not really used for a large part of the simulation year, when the VAV system is installed in the case study building. This shows that the simulation of the chosen HVAC system in B-TAS is necessary in order to obtain a more accurate estimation of the total energy consumption of the air-conditioned building than this provided by A-TAS.

References

[1] B-Tas Reference Manual, EDSL Documentation

[18] **Note:** For example, the heating, cooling and intermediate period and the relevant set-points as specified in A-TAS are passed to B-TAS via a Building Simulation Output file which contains all the relevant information from the A-TAS simulation required to perform the simulation of the HVAC system in B-TAS.

Appendix D: The effect of different ventilation options in A-TAS on the internal temperatures and the annual cooling energy consumption

As explained in section 4.2.2, the perimeter zones of the building were treated using only natural means, while fan-assisted ventilation was deemed necessary to serve the core zones of the building. The control over the fresh air ventilation rate was achieved by changing the infiltration rate of the building (in A-TAS). It should be stressed that it is not possible to simulate the effect of mechanical ventilation during night-time on the annual energy use properly, since the HVAC system schematic as designed in B-TAS does not allow the specification of fans which will provide fresh air at a constant flow rate over the night. As a result, a manual calculation of the fan energy consumed for night ventilation was carried out in section 4.2.2-1.

On the other hand, A-TAS provides a number of alternative ventilation options (based on automatic or manual control of the apertures of the building) that can be used to evaluate the effect of night ventilation on the internal temperatures and the annual energy consumption. Two such options are described in the following paragraphs[19], including an explanation why it was decided not to use them in the main study.

The provision of fresh air over the night can be simulated in A-TAS using automatic control of the apertures of the building, based on zone temperature, external temperature and wind speed set-points. The automatic control of window opening was simulated as described in the following. As the dry-bulb temperature of the control zone rises above 18°C, the windows start to open. The openings will be 'fully open'[20] at 21°C and will remain fully open at all temperatures above 21°C. However the openings will start to close, if, at any time the external temperature is greater than the internal temperature. In particular, the apertures start to close when the two temperatures are equal, and will be fully closed when the external temperature is one full degree greater than the internal temperature. The wind speed will also start to close the windows as it increases above 5 m/s. The windows will be fully closed when the wind speed reaches 5.5 m/s. It was assumed that night ventilation, using the automatic control function described above, is provided for 10 hours (i.e. 21:00 – 7:00) per day.

Also, it is possible to introduce fresh air into the building by simply opening the windows for the same number of hours as in the automatic control strategy described above. The maximum openable proportion equals 60% in both ventilation strategies. The difference is that in the automatic control strategy the windows will be 60% open when the internal temperature is $\geq 21^{\circ}C$, while in the

[19] **Note:** It should be stressed that all the simulation results presented in this section refer to the CIBSE TRY.
[20] **Note:** The maximum openable proportion is specified by the user. The windows were first considered to be 'fully open' when the openable proportion equals 60% of the total window area. However, the simulations were repeated assuming a maximum openable proportion of 100% as well.

manual control strategy the openable proportion equals 60% for the whole period that night ventilation is provided.

The internal temperature of zone 2[21] for June 19th (i.e. a summer day with moderate external temperature) is shown in figure D-1, when night ventilation is not provided[22] and figures D-2 and D-3, when automatic and manual control of the openings is utilised respectively:

TABULAR OUTPUT

Building Name: MODEL Building Data File: CASESTUDY.bdf.01 Revisior
Time: 18:42:16 Date: 18:Nov:03 Consultant: Program:

Zone 2 Ground S
Day 170: Tuesday, Jun 19 (COOLING)
Weather File: UK_Hebtry.wfl

Time (24hr clock)	Temperature (deg C)	Sensible load (kw)	Humidity (%)	Latent load (kw)	Mean radiant temp. (deg C)	Resultant temp. (deg C)
1	21.2	0.00	47.0	0.00	23.1	22.2
2	20.9	0.00	48.0	0.00	22.8	21.9
3	20.6	0.00	48.6	0.00	22.5	21.6
4	20.3	0.00	49.0	0.00	22.3	21.3
5	20.4	0.00	48.6	0.00	22.5	21.5
6	20.9	0.00	46.9	0.00	23.0	22.0
7	21.8	0.00	44.4	0.00	23.8	22.8
8	22.9	0.00	40.7	0.00	25.1	24.0
9	24.0	-1.64	38.5	0.00	27.3	25.7
10	24.0	-12.78	44.0	0.00	30.0	27.0
11	24.0	-16.58	46.7	0.00	31.5	27.7
12	24.0	-17.17	48.9	0.00	31.5	27.7
13	24.0	-18.00	49.5	0.00	32.1	28.0
14	24.0	-15.89	48.9	0.00	30.7	27.3
15	24.0	-15.01	48.4	0.00	30.4	27.2
16	24.0	-13.69	49.5	0.00	29.7	26.8
17	24.0	-11.52	50.4	0.00	28.8	26.4
18	25.6	0.00	43.9	0.00	27.5	26.5
19	25.2	0.00	43.4	0.00	26.7	26.0
20	24.3	0.00	44.7	0.00	25.6	25.0
21	23.5	0.00	45.1	0.00	24.8	24.2
22	22.9	0.00	45.8	0.00	24.4	23.6
23	22.5	0.00	46.4	0.00	24.0	23.2
24	22.0	0.00	46.7	0.00	23.6	22.8

Sensible heating	0.0 kwh
Sensible cooling	122.3 kwh
Sensible total	122.3 kwh

Figure D-1: Zone 2 air temperature for June 19th when night ventilation is not provided (base case scenario)

[21] **Note:** This is a south zone located in the ground floor of the building.
[22] **Note:** It should be remembered that the building is occupied between 9:00 – 17:00, while the plant operates between 7:00 – 17:00.

TABULAR OUTPUT

Building Name: MODEL Building Data File: NAT1.bdf.01 Revisic
Time: 14:14:52 Date: 13:Nov:03 Consultant: Program

Zone 2 Ground S
Day 170: Tuesday, Jun 19 (COOLING)
Weather File: UK_Hebtry.wfl

Time (24hr clock)	Temper-ature (deg C)	Sensible load (kW)	Humidity (%)	Latent load (kW)	Mean radiant temp. (deg C)	Result-ant temp. (deg C)
1	18.2	0.00	57.9	0.00	21.2	19.7
2	18.2	0.00	57.6	0.00	21.1	19.6
3	18.1	0.00	56.5	0.00	20.9	19.5
4	18.1	0.00	55.8	0.00	20.8	19.4
5	18.1	0.00	56.0	0.00	20.9	19.5
6	18.2	0.00	55.2	0.00	21.3	19.8
7	18.5	0.00	53.6	0.00	22.0	20.2
8	21.3	0.00	44.5	0.00	23.7	22.5
9	24.0	-0.10	38.3	0.00	26.5	25.3
10	24.0	-11.86	43.9	0.00	29.4	26.7
11	24.0	-15.86	46.7	0.00	31.1	27.5
12	24.0	-16.59	48.9	0.00	31.1	27.6
13	24.0	-17.49	49.5	0.00	31.8	27.9
14	24.0	-15.45	48.9	0.00	30.4	27.2
15	24.0	-14.62	48.4	0.00	30.2	27.1
16	24.0	-13.33	49.5	0.00	29.5	26.7
17	24.0	-11.20	50.4	0.00	28.6	26.3
18	25.4	0.00	44.4	0.00	27.2	26.3
19	25.0	0.00	44.0	0.00	26.4	25.7
20	24.0	0.00	45.4	0.00	25.3	24.7
21	23.2	0.00	45.8	0.00	24.5	23.9
22	18.9	0.00	56.6	0.00	22.7	20.8
23	18.7	0.00	57.3	0.00	22.0	20.3
24	18.4	0.00	56.6	0.00	21.6	20.0

Sensible heating	0.0 kwh
Sensible cooling	116.5 kwh
Sensible total	116.5 kwh

Figure D-2: Zone 2 temperature for June 19th when the automatic control function is implemented

TABULAR OUTPUT

Building Name: MODEL Building Data File: TESTNAT1.bdf.01 Revisio
Time: 14:20:09 Date: 13:Nov:03 Consultant: Program

Zone 2 Ground S
Day 170: Tuesday, Jun 19 (COOLING)
Weather File: UK_Hebtry.wfl

Time (24hr clock)	Temper-ature (deg C)	Sensible load (kW)	Humidity (%)	Latent load (kW)	Mean radiant temp. (deg C)	Result-ant temp. (deg C)
1	14.6	0.00	73.6	0.00	18.9	16.8
2	14.2	0.00	74.0	0.00	18.5	16.4
3	13.4	0.00	75.4	0.00	18.0	15.7
4	12.7	0.00	77.7	0.00	17.5	15.1
5	13.5	0.00	75.4	0.00	17.8	15.7
6	14.7	0.00	69.2	0.00	18.5	16.6
7	16.3	0.00	61.8	0.00	19.7	18.0
8	19.6	0.00	49.5	0.00	21.9	20.7
9	22.7	0.00	41.5	0.00	24.9	23.8
10	24.0	-9.86	43.9	0.00	28.4	26.2
11	24.0	-14.52	46.7	0.00	30.3	27.2
12	24.0	-15.47	48.9	0.00	30.5	27.3
13	24.0	-16.48	49.5	0.00	31.2	27.6
14	24.0	-14.56	48.9	0.00	29.9	26.9
15	24.0	-13.79	48.4	0.00	29.7	26.8
16	24.0	-12.55	49.5	0.00	29.0	26.5
17	24.0	-10.48	50.4	0.00	28.1	26.0
18	25.0	0.00	45.5	0.00	26.5	25.8
19	24.4	0.00	45.4	0.00	25.7	25.1
20	23.4	0.00	47.0	0.00	24.5	24.0
21	22.6	0.00	47.6	0.00	23.7	23.2
22	17.3	0.00	62.3	0.00	21.6	19.4
23	16.8	0.00	64.5	0.00	20.7	18.7
24	15.9	0.00	66.0	0.00	19.9	17.9

Sensible heating	0.0 kwh
Sensible cooling	107.7 kwh
Sensible total	107.7 kwh

Figure D-3: Zone 2 air temperature for June 19th when all windows are kept open (60% openable proportion) for 10 hours during the night (i.e. manual control of windows)

It is obvious that the internal temperature during the period that night ventilation is provided (i.e. 21:00 – 7:00) is considerably lower in figure D-3 than in figure D-2. This is due to the fact that the windows are kept closed as long as the internal temperature is lower than 18°C when the automatic control function is used, so the internal temperature never drops below 18°C in this case, as can be seen from figure D-2. On the other hand, the cooling requirement is reduced or even eliminated for the first morning hours when the windows are manually controlled, (e.g. see the sensible cooling load for hours 9 and 10 in figure D-2 and D-3 respectively). Therefore, the use of a low temperature set-point, below which the windows are kept closed, is not really useful since the internal temperature is not particularly low[23], even for a rather 'cool' summer night, as can be seen from figure D-3 where the apertures remain open throughout the night. Moreover, when a low temperature limit is imposed, the cooling load is kept quite close to the base case scenario (see figures D-1 and D-2), which means that the provision of night ventilation through automatic control of windows is not particularly effective.

In addition, the internal temperature of zone 2 for July 5th (hottest day with low external air velocity) is shown in figure D-4, when night ventilation is not provided, and figures D-5 and D-6 when automatic and manual control of the apertures is implemented, respectively:

TABULAR OUTPUT

Building Name: MODEL Building Data File: CASESTUDY.bdf.01 Revision:
Time: 19:07:52 Date: 18:Nov:03 Consultant: Program:

Zone 2 Ground S
Day 186: Thursday, Jul 5 (COOLING)
Weather File: UK_Hebtry.wfl

Time (24hr clock)	Temper-ature (deg C)	Sensible load (kW)	Humidity (%)	Latent load (kW)	Mean radiant temp. (deg C)	Result-ant temp. (deg C)
1	23.7	0.00	60.1	0.00	24.8	24.2
2	23.5	0.00	61.0	0.00	24.6	24.1
3	23.4	0.00	61.6	0.00	24.5	23.9
4	23.2	0.00	62.4	0.00	24.4	23.8
5	23.3	0.00	62.6	0.00	24.6	23.9
6	23.8	0.00	62.2	0.00	25.2	24.5
7	24.7	0.00	60.2	0.00	26.3	25.5
8	24.0	-2.80	64.5	0.00	27.3	25.6
9	24.0	-4.10	66.0	0.00	28.0	26.0
10	24.0	-13.82	71.8	0.00	29.3	26.7
11	24.0	-16.31	77.3	0.00	30.4	27.2
12	24.0	-15.24	77.7	0.00	29.4	26.7
13	24.0	-13.37	77.9	0.00	29.0	26.5
14	24.0	-10.83	81.0	0.00	28.1	26.1
15	24.0	-14.01	80.6	0.00	29.8	26.9
16	24.0	-14.75	78.6	0.00	29.8	26.9
17	24.0	-13.85	78.0	0.00	28.9	26.5
18	26.5	0.00	65.3	0.00	28.2	27.3
19	26.2	0.00	61.1	0.00	27.3	26.8
20	25.3	0.00	59.7	0.00	26.4	25.8
21	24.3	0.00	59.3	0.00	25.5	24.9
22	23.5	0.00	58.2	0.00	25.0	24.3
23	23.0	0.00	57.4	0.00	24.6	23.8
24	22.6	0.00	56.4	0.00	24.2	23.4

Sensible heating	0.0 kWh
Sensible cooling	119.1 kWh
Sensible total	119.1 kWh

Figure D-4: Zone 2 air temperature for July 5th when night ventilation is not provided (base case scenario)

[23] **Note:** If the internal temperature was lower than 20° during the first morning hours that the building is occupied, heating would have been required to maintain optimum thermal comfort conditions. However, this is not the case even for summer night with rather low external temperatures, as can be seen from figure D-3.

TABULAR OUTPUT

Building Name: MODEL Building Data File: NAT1.bdf.01 Revisior
Time: 14:24:30 Date: 13:Nov:03 Consultant: Program:

Zone 2 Ground S
Day 186: Thursday, Jul 5 (COOLING)
Weather File: UK_Hebtry.wfl

Time (24hr clock)	Temper-ature (deg C)	Sensible load (kw)	Humidity (%)	Latent load (kw)	Mean radiant temp. (deg C)	Result-ant temp. (deg C)
1	20.4	0.00	74.4	0.00	22.8	21.6
2	20.2	0.00	75.3	0.00	22.6	21.4
3	20.1	0.00	75.8	0.00	22.4	21.2
4	19.9	0.00	76.8	0.00	22.3	21.1
5	19.7	0.00	78.6	0.00	22.4	21.1
6	20.5	0.00	79.4	0.00	23.0	21.8
7	21.3	0.00	76.4	0.00	24.1	22.7
8	24.0	-0.25	66.1	0.00	26.1	25.0
9	24.0	-2.88	67.0	0.00	27.2	25.6
10	24.0	-12.82	72.2	0.00	28.7	26.4
11	24.0	-15.45	77.5	0.00	29.9	27.0
12	24.0	-14.51	77.7	0.00	28.9	26.5
13	24.0	-12.71	77.9	0.00	28.6	26.3
14	24.0	-10.23	81.0	0.00	27.7	25.9
15	24.0	-13.42	80.6	0.00	29.4	26.7
16	24.0	-14.19	78.6	0.00	29.4	26.7
17	24.0	-13.34	78.0	0.00	28.6	26.3
18	26.2	0.00	66.4	0.00	27.7	27.0
19	25.8	0.00	62.4	0.00	26.8	26.3
20	24.9	0.00	61.2	0.00	25.8	25.3
21	23.8	0.00	60.9	0.00	25.0	24.4
22	19.0	0.00	68.3	0.00	23.0	21.0
23	18.5	0.00	68.5	0.00	22.2	20.3
24	18.4	0.00	67.3	0.00	21.7	20.1

Sensible heating	0.0 kwh
Sensible cooling	109.8 kwh
Sensible total	109.8 kwh

Figure D-5: Zone 2 air temperature for July 5th when the automatic control function is utilized

TABULAR OUTPUT

Building Name: MODEL Building Data File: TESTNAT1.bdf.01 Revis
Time: 14:28:00 Date: 13:Nov:03 Consultant: Progr

Zone 2 Ground S
Day 186: Thursday, Jul 5 (COOLING)
Weather File: UK_Hebtry.wfl

Time (24hr clock)	Temper-ature (deg C)	Sensible load (kw)	Humidity (%)	Latent load (kw)	Mean radiant temp. (deg C)	Result-ant temp. (deg C)
1	20.2	0.00	75.3	0.00	22.6	21.4
2	19.9	0.00	76.4	0.00	22.3	21.1
3	19.8	0.00	77.0	0.00	22.1	21.0
4	19.6	0.00	78.3	0.00	22.0	20.8
5	19.3	0.00	80.6	0.00	22.0	20.7
6	20.3	0.00	80.3	0.00	22.7	21.5
7	21.3	0.00	76.7	0.00	23.9	22.6
8	24.0	-0.02	66.1	0.00	25.9	24.9
9	24.0	-2.65	67.0	0.00	27.0	25.5
10	24.0	-12.59	72.2	0.00	28.6	26.3
11	24.0	-15.22	77.5	0.00	29.8	26.9
12	24.0	-14.30	77.7	0.00	28.8	26.4
13	24.0	-12.52	77.9	0.00	28.5	26.2
14	24.0	-10.05	81.0	0.00	27.6	25.8
15	24.0	-13.23	80.6	0.00	29.3	26.7
16	24.0	-14.01	78.6	0.00	29.3	26.7
17	24.0	-13.16	78.0	0.00	28.5	26.2
18	26.1	0.00	66.8	0.00	27.6	26.8
19	25.7	0.00	62.9	0.00	26.6	26.2
20	24.7	0.00	61.7	0.00	25.6	25.2
21	23.7	0.00	61.4	0.00	24.8	24.2
22	17.5	0.00	73.8	0.00	22.4	19.9
23	16.4	0.00	77.8	0.00	21.1	18.8
24	16.0	0.00	78.1	0.00	20.4	18.2

Sensible heating	0.0 kwh
Sensible cooling	107.7 kwh
Sensible total	107.7 kwh

Figure D-6: Zone 2 air temperature for July 5th when the manual control strategy is used

As can be seen from figures D-5 and D-6, the lowest internal temperatures, during the period that night ventilation is provided, occur when the windows are manually controlled. Also, the total daily cooling load is slightly lower in figure D-6, where the windows are 60% open for the whole period that night ventilation is provided, than figure D-5, where the windows open gradually as the internal temperature rises from 18°C to 21°C. It is therefore clear that the upper temperature limit set when the automatic control function is utilised is not necessary, since the internal temperature reaches 21°C just for one hour, even for the hottest day of the year (i.e. hour 7 - figure D-5).

To sum up, it was shown that the automatic control function, as simulated in A-TAS, is less effective than the simplest night ventilation strategy which involves opening the windows for a certain number of hours without imposing any temperature control limits. It is clear that the upper temperature limit is not necessary since the internal temperature rarely reaches or exceeds 21°C even for the hottest day of the year, while the use of a lower temperature limit of 18°C leads to cooling energy use which is quite close to the base case scenario where night ventilation is not provided.

On the other hand, a few problems common in both ventilation strategies described above are the following:

1. There is no control over the ventilation rate. As a result, the fresh air ventilation rate takes some rather unusual values, particularly for the small corner zones of the building, as illustrated in figure D-7:

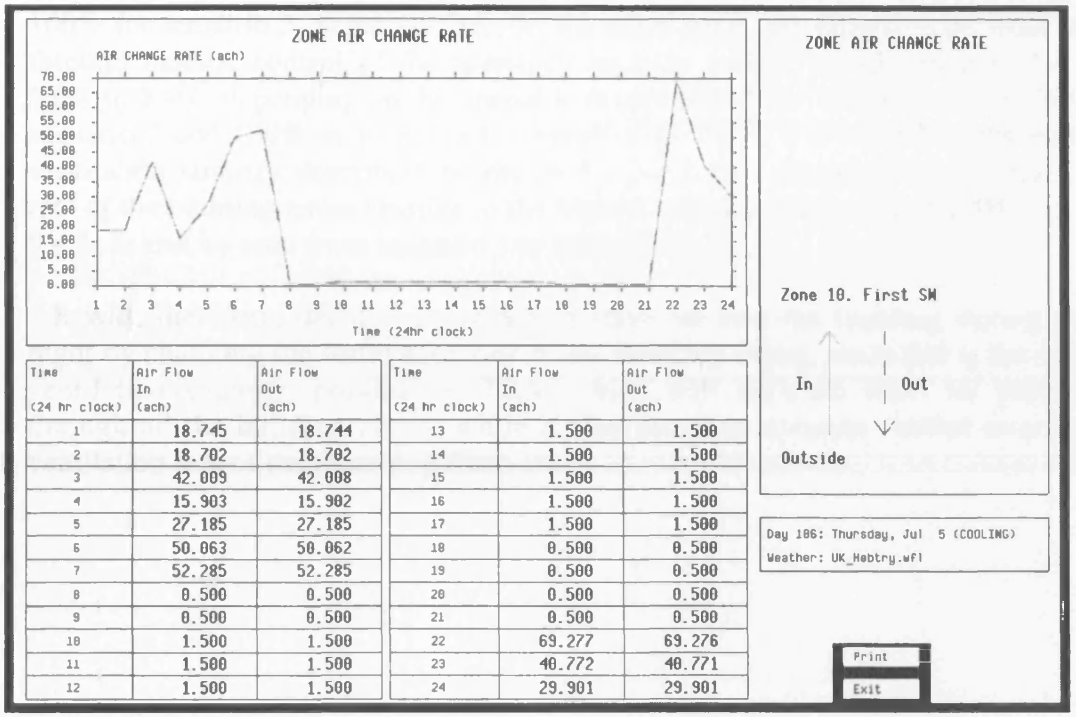

Time (24 hr clock)	Air Flow In (ach)	Air Flow Out (ach)	Time (24 hr clock)	Air Flow In (ach)	Air Flow Out (ach)
1	18.745	18.744	13	1.500	1.500
2	18.702	18.702	14	1.500	1.500
3	42.009	42.008	15	1.500	1.500
4	15.903	15.902	16	1.500	1.500
5	27.185	27.185	17	1.500	1.500
6	50.063	50.062	18	0.500	0.500
7	52.285	52.285	19	0.500	0.500
8	0.500	0.500	20	0.500	0.500
9	0.500	0.500	21	0.500	0.500
10	1.500	1.500	22	69.277	69.276
11	1.500	1.500	23	40.772	40.771
12	1.500	1.500	24	29.901	29.901

Figure D-7: The fresh air ventilation rate (ach) for zone 10 (i.e. a corner SW zone located in the first floor of the building) on July 5th, when the automatic control function is utilised

2. The incoming fresh air passes only through the perimeter zones since there are not any apertures in the internal walls surrounding the core zone of the building[24]. As a result, the effect of night ventilation (despite the rather huge ventilation rates displayed above) on the total cooling energy consumption or the carbon emissions of the VAV system[25] is quite small, as shown in table D-1:

Scenarios	Factor Levels		Annual Energy Use			Carbon Emissions					
	Ventilation Rate (ach)	Period of ventilation (hours)	Heating Energy Consumption (kWh)	Cooling Energy Consumption (kWh)	Fan energy consumed for night ventilation (kWh)	Boiler Carbon emissions (kgC)	Chiller Carbon emissions (kg C)	Fan Carbon emissions (kgC)	Total Carbon emissions (kgC)	Cooling energy savings (%)	Total carbon savings (%)
Base case scenario	-	-	108076	127741	-	5620	16223	-	21843	-	-
Scenario 1: Optimum night ventilation strategy described in sections 4.2.2-2.1 and 5.3.2	5.0	10	107768	109849	1780	5604	13951	226	19781	-14.0%	-9.4%
Scenario 2: All windows 60% open	varies	10	106701	119778	-	5548	15212	-	20760	-6.2%	-5.0%
Scenario 3: Automatic control of windows (max openable proportion = 60%)	varies	10	106514	124026	-	5539	15751	-	21290	-2.9%	-2.5%
Scenario 4: All windows 100% open	varies	10	106747	118972	-	5551	15109	-	20660	-6.9%	-5.4%
Scenario 5: Automatic control of windows (max openable proportion = 100%)	varies	10	106511	123699	-	5539	15710	-	21248	-3.2%	-2.7%

Table D-1: VAV system energy consumption and carbon emissions using the night ventilation strategies described in this appendix and the ventilation strategy derived from section 4.2.2-2.1

As can be seen from table D-1, the A-TAS automatic control function described earlier results in carbon savings up to 2.7%, depending on the maximum openable proportion of the windows (i.e. 60% for scenario 3 and 100% for scenario 5, respectively). On the other hand, the provision of fresh air through manual control of the apertures leads to carbon savings ranging from 5.0% to 5.4%, depending on the openable proportion of the windows (i.e. 60% in scenario 2 and 100% in scenario 4, respectively). Thus, it is clear that the night ventilation strategy described in section 4.2.2-2.1 (i.e. changing the infiltration rate of the building zones) results in the highest carbon savings over the BCS (i.e. 9.4%, as can be seen from scenario 1 in table D-1).

It was, therefore, decided to introduce fresh air into the building during the night by changing the infiltration rate of the building zones, since this is the only ventilation strategy, possible in TAS, which will simulate fresh air passing through all the building zones, while it also provides accurate control over the ventilation rate of the incoming fresh air.

[24] **Note:** Even if there were openings in the internal walls, it would have been difficult to move the fresh air through the deep plan core zones using only natural means.

[25] **Note:** The conclusions derived from this investigation are the same for both HVAC systems, so it was decided to present only the simulations results for the VAV system in table D-1, as an example.

Appendix E: Calculation of the office equipment heat gains

The office equipment heat gains (W/m^2) for the case study building can be estimated using the worksheet provided in appendix 1 of the *Good Practice Guide 276: Managing for a better environment, Best Practice Programme*, as stated in chapter 3, section 3.3.1. The rough calculation example contained in GPG 276 is based on typical values for mid-range office equipment. These typical figures for the number of items of office equipment per occupant, the daily operating & idling hours and the operating and idling low-power rate of consumption (depending on the type of equipment) are also adopted for the calculation carried out for the case study office building in this study, as shown in table E-1:

	Office Equipment	PCs	Printers	Copiers	Fax Machines	Scanners	Vending Machines	
(1)	Number of pieces of equipment (For 1200 persons)	1200	360	60	36	36	36	
(2)	Number of operating hours (hrs)	3.2	1.6	1.6	1	1	1	
(3)	Rate of consumption in operating mode (W)	125	300	1400	300	25	1700	
(4) = (1) x (2) x (3)	Operating Energy Consumption (Wh)	480000	172800	134400	10800	900	61200	
(5)	Number of idling hours (hrs)	4.8	6.4	6.4	7	7	7	
(6)	[a]. Rate of consumption in idling mode when energy saving features are not enabled (W)	120	90	200	30	20	300	
(7)	[b]. Rate of consumption in idling mode when energy saving features are enabled (W)	45	15	100	10	12	100	
(8)= (1) x (5) x (6)	[a]. Idling Energy Consumption (Wh)	691200	207360	76800	7560	5040	75600	
(9)= (1) x (5) x (7)	[b]. Idling Energy Consumption (Wh)	259200	34560	38400	2520	3024	25200	
(10) = (4) + (8)	[a]. Total Daily Energy Consumption (Wh)	1171200	380160	211200	18360	5940	136800	
(11) = (4) + (9)	[b]. Total Daily Energy Consumption (Wh)	739200	207360	172800	13320	3924	86400	Total (W / m^2):
(12) = (10) / 8 hrs x 12000 m^2	[a]. Equipment Power Load (W/m^2)	12.2	4.0	2.2	0.2	0.1	1.4	20.0
(13) = (11) / 8 hrs x 12000 m^2	[b]. Equipment Power Load (W/m^2)	7.7	2.2	1.8	0.1	0.0	0.9	12.7

Table E-1: Calculation of the office equipment heat gains (W/m^2) using the worksheet provided in GPG 276

The calculation of the total daily energy consumption (Wh) and the equipment load (W/m^2) depending on whether the energy saving features are enabled or not, is explained in the first column of table E-1. The total power load of the office equipment equals 20 W/m^2 when the energy saving features are not enabled and 13 W/m^2 when the energy saving features are enabled respectively, as can be seen from the last column of the table.

Appendix F: Absolute values of the energy use and carbon emissions for the optimum factor settings of each group

The energy consumption data and the associated carbon emissions for both the base case and the optimum factor values of each group of parameters are illustrated in the following 8 tables:

Scenario	Climate	HVAC system	Factor levels				Annual energy use		Carbon emissions		
			Glazing ratio (0 -1)	Total shading coefficient	Overhang depth (m)	Sidefin depth (m)	Heating energy consumption (kWh)	Cooling energy consumption (kWh)	Boiler carbon emissions (kgC)	Chiller carbon emissions (kg C)	Total carbon emissions (kgC)
Base case scenario	CIBSE TRY	VAV system	*0.40*	*0.74*	*0.00*	*0.00*	108076	127741	5620	16223	21843
		FCU system	*0.40*	*0.74*	*0.00*	*0.00*	144279	267686	7503	33996	41499
	NOA TRY	VAV system	*0.40*	*0.74*	*0.00*	*0.00*	25818	358596	1343	45542	46884
		FCU system	*0.40*	*0.74*	*0.00*	*0.00*	37457	464764	1948	59025	60973
Factor settings of group A minimising the total carbon emissions	CIBSE TRY	VAV system	*0.25*	*0.16*	*0.00*	*1.80*	136071	86312	7076	10962	18037
		FCU system	*0.25*	*0.16*	*0.00*	*1.30*	164846	179389	8572	22782	31354
	NOA TRY	VAV system	*0.25*	*0.16*	*1.10*	*2.00*	45258	255057	2353	32392	34746
		FCU system	*0.25*	*0.16*	*1.20*	*2.00*	53282	321328	2771	40809	43579

Table F-1: The energy consumption data and the associated carbon emissions for both the base case and the optimum factor settings of group A, depending on the HVAC system and the climate under consideration

Scenario	Climate	HVAC system	Factor levels			Annual energy use		Carbon emissions		
			Wall U-value (W/m^2K)	Infiltration rate (ach)	Window U-value (W/m^2K)	Heating energy consumption (kWh)	Cooling energy consumption (kWh)	Boiler carbon emissions (kgC)	Chiller carbon emissions (kg C)	Total carbon emissions (kgC)
Base case scenario	CIBSE TRY	VAV system	*0.35*	*0.50*	*2.10*	108076	127741	5620	16223	21843
		FCU system	*0.35*	*0.50*	*2.10*	144279	267686	7503	33996	41499
	NOA TRY	VAV system	*0.35*	*0.50*	*2.10*	25818	358596	1343	45542	46884
		FCU system	*0.35*	*0.50*	*2.10*	37457	464764	1948	59025	60973
Factor settings of group B minimising the total carbon emissions	CIBSE TRY	VAV system	*0.18*	*0.25*	*1.20*	50524	138299	2627	17564	20191
		FCU system	*0.27*	*0.25*	*5.70*	197827	226020	10287	28705	38992
	NOA TRY	VAV system	*0.19*	*0.25*	*5.80*	54985	331067	2859	42046	44905
		FCU system	*0.70*	*0.40*	*5.80*	65586	411058	3410	52204	55615

Table F-2: The energy consumption data and the associated carbon emissions for both the base case and the optimum factor settings of group B, depending on the HVAC system and the climate under consideration

Scenario	Climate	HVAC system	Factor levels			Annual energy use		Carbon emissions		
			Lighting gains (W/m^2)	Equipment gains (W/m^2)	Occupant Density (m^2 per person)	Heating energy consumption (kWh)	Cooling energy consumption (kWh)	Boiler carbon emissions (kgC)	Chiller carbon emissions (kg C)	Total carbon emissions (kgC)
Base case scenario	CIBSE TRY	VAV system	*12.0*	*15.0*	*10*	108076	127741	5620	16223	21843
		FCU system	*12.0*	*15.0*	*10*	144279	267686	7503	33996	41499
	NOA TRY	VAV system	*12.0*	*15.0*	*10*	25818	358596	1343	45542	46884
		FCU system	*12.0*	*15.0*	*10*	37457	464764	1948	59025	60973
Factor settings of group C minimising the total carbon emissions	CIBSE TRY	VAV system	*6.5*	*10.0*	*20*	170593	85335	8871	10838	19708
		FCU system	*6.5*	*10.0*	*20*	182108	154252	9470	19590	29060
	NOA TRY	VAV system	*6.5*	*10.0*	*20*	33866	268956	1761	34157	35918
		FCU system	*6.5*	*10.0*	*20*	41737	327717	2170	41620	43790

Table F-3: The energy consumption data and the associated carbon emissions for both the base case and the optimum factor settings of group C, depending on the HVAC system and the climate under consideration

Scenario	Climate	HVAC system	Factor levels			Annual energy use		Carbon emissions		
			Heating zone air temperature (°C)	Cooling zone air temperature (°C)	Temperature difference (°C)	Heating energy consumption (kWh)	Cooling energy consumption (kWh)	Boiler carbon emissions (kgC)	Chiller carbon emissions (kg C)	Total carbon emissions (kgC)
Base case scenario	CIBSE TRY	VAV system	*20*	*24*	*8*	108076	127741	5620	16223	21843
		FCU system	*20*	*24*	*8*	144279	267686	7503	33996	41499
	NOA TRY	VAV system	*20*	*24*	*8*	25818	358596	1343	45542	46884
		FCU system	*20*	*24*	*8*	37457	464764	1948	59025	60973
Factor settings of group D minimising the total carbon emissions	CIBSE TRY	VAV system	*18*	*26*	*6*	56811	51954	2954	6598	9552
		FCU system	*18*	*26*	*8*	87536	220527	4552	28007	32559
	NOA TRY	VAV system	*18*	*26*	*6*	7670	259068	399	32902	33301
		FCU system	*18*	*26*	*8*	15824	402137	823	51071	51894

Table F-4: The energy consumption data and the associated carbon emissions for both the base case and the optimum factor settings of group D, depending on the HVAC system and the climate under consideration

Scenario	Climate	HVAC system	Factor Levels		Annual energy use			Carbon emissions			
			Ventilation rate (ach)	Period of ventilation (hours)	Heating energy consumption (kWh)	Cooling energy consumption (kWh)	Fan energy consumed for night ventilation (kWh)	Boiler carbon emissions (kgC)	Chiller carbon emissions (kg C)	Fan carbon emissions (kg C)	Total carbon emissions (kgC)
Base case scenario	CIBSE TRY	VAV system	-	-	108076	127741	-	5620	16223	-	21843
		FCU system	-	-	144279	267686	-	7503	33996	-	41499
	NOA TRY	VAV system	-	-	25818	358596	-	1343	45542	-	46884
		FCU system	-	-	37457	464764	-	1948	59025	-	60973
Factor settings of group E minimising the total carbon emissions	CIBSE TRY	VAV system	*5.0*	*10*	107768	109849	1780	5604	13951	226	19781
		FCU system	*10.0*	*10*	144826	238034	2166	7531	30230	275	38036
	NOA TRY	VAV system	*5.0*	*10*	25902	345501	1312	1347	43879	167	45392
		FCU system	*10.0*	*10*	37542	450269	2352	1952	57184	299	59435

Table F-5: The energy consumption data and the associated carbon emissions for both the base case and the optimum factor settings of group E, depending on the HVAC system and the climate under consideration

Scenario	Climate	HVAC system	Factor levels			Annual energy use		Carbon emissions		
			Boiler efficiency (%)	Chiller COP	HVAC system operation (hours)	Heating energy consumption (kWh)	Cooling energy consumption (kWh)	Boiler carbon emissions (kgC)	Chiller carbon emissions (kg C)	Total carbon emissions (kgC)
Base case scenario	CIBSE TRY	VAV system	*85%*	*2.50*	*10*	108076	127741	5620	16223	21843
		FCU system	*85%*	*2.50*	*10*	144279	267686	7503	33996	41499
	NOA TRY	VAV system	*85%*	*2.50*	*10*	25818	358596	1343	45542	46884
		FCU system	*85%*	*2.50*	*10*	37457	464764	1948	59025	60973
Factor settings of group F minimising the total carbon emissions	CIBSE TRY	VAV system	*95%*	*5.20*	*9*	57967	60230	3014	7649	10663
		FCU system	*95%*	*5.20*	*9*	97010	127437	5045	16184	21229
	NOA TRY	VAV system	*95%*	*5.20*	*9*	10049	168843	523	21443	21966
		FCU system	*95%*	*5.20*	*9*	22139	218956	1151	27807	28959

Table F-6: The energy consumption data and the associated carbon emissions for both the base case and the optimum factor settings of group F, depending on the HVAC system and the climate under consideration

Scenario	Climate	HVAC system	Factor levels				Annual energy use			Carbon emissions			
			Fan efficiency (%)	Motor efficiency (%)	Supply fan (Pa)	Return fan (Pa)	Heating energy consumption (kWh)	Cooling energy consumption (kWh)	Fan Energy Consumption (kWh)	Boiler Carbon emissions (kgC)	Chiller Carbon emissions (kg C)	Fan Carbon emissions (kg C)	Total carbon emissions (kgC)
Base case scenario	CIBSE TRY	VAV system	*78%*	*90%*	*677*	*162*	108076	127741	74283	5620	16223	9434	31277
		FCU system	*78%*	*90%*	*421*	*197*	144279	267686	138421	7503	33996	17579	59078
	NOA TRY	VAV system	*78%*	*90%*	*681*	*156*	25818	358596	106876	1343	45542	13573	60457
		FCU system	*78%*	*90%*	*474*	*197*	37457	464764	155304	1948	59025	19724	80696
Factor settings of group G minimising the total carbon emissions	CIBSE TRY	VAV system	*90%*	*95%*	*500*	*120*	109765	118330	46215	5708	15028	5869	26605
		FCU system	*90%*	*95%*	*300*	*140*	147444	266467	129483	7667	33841	16444	57953
	NOA TRY	VAV system	*90%*	*95%*	*500*	*120*	26273	342239	65637	1366	43464	8336	53166
		FCU system	*90%*	*95%*	*300*	*140*	39184	462348	144614	2038	58718	18366	79122

Table F-7: The energy consumption data and the associated carbon emissions for both the base case and the optimum factor settings of group G, depending on the HVAC system and the climate under consideration

Scenario	Climate	HVAC system	Factor levels				Annual energy use			Carbon emissions		
			Humidification setpoint (%)	Proportional band (%)	Period of humidification	Humidification energy consumption (kWh)	Heating energy consumption (kWh)	Cooling energy consumption (kWh)	Humidification Carbon Emissions (kg C)	Boiler carbon emissions (kgC)	Chiller carbon emissions (kg C)	Total carbon emissions (kgC)
Base case scenario	CIBSE TRY	VAV system	-	-	-	-	108076	127741	-	5620	16223	21843
		FCU system	-	-	-	-	144279	267686	-	7503	33996	41499
	NOA TRY	VAV system	-	-	-	-	25818	358596	-	1343	45542	46884
		FCU system	-	-	-	-	37457	464764	-	1948	59025	60973
Factor settings of group H minimising the total carbon emissions	CIBSE TRY	VAV system	*40*	*5*	*Heating Season*	66549	108103	127684	8452	5621	16216	30289
		FCU system	*40*	*5*	*Heating Season*	42319	144282	267677	5375	7503	33995	46872
	NOA TRY	VAV system	*40*	*5*	*Heating Season*	101620	25818	358673	12906	1343	45551	59800
		FCU system	*40*	*5*	*Heating Season*	29123	37459	464755	3699	1948	59024	64670

Table F-8: The energy consumption data and the associated carbon emissions for both the base case and the optimum factor settings of group H, depending on the HVAC system and the climate under consideration

Appendix G: Window constructions data published by Pilkington

This appendix contains a number of window constructions presented in the Pilkington web-site (http://www.pilkington.com/), which illustrate that the daylight transmittance is in most cases very close to the Total Shading Coefficient (TSC) of the window construction, as explained in section 5.2.1-1 (chapter 5).

	Light		Solar Radiant Heat				Shading Coefficient			U value (W/m²K)	U value (W/m²K)	Sound Insulation		Mass	Unit Maximum Sizes†		
	Transmittance	Reflectance	Direct Transmittance	Reflectance	Absorptance	Total Transmission	Short Wavelength	Long Wavelength	Total	Air-filled	Argon-filled	R_w (dB)	R_w (dB)	(kg/m²)	Annealed (mm)	Toughened (mm)	Descriptive Code
Pilkington Insulight™ (with 6mm Pilkington K Glass™ inner pane and 16mm cavity – unless otherwise indicated)																	
Pilkington Optifloat™ Clear																	
*4mm	0.75	0.17	0.60	0.16	0.24	0.72	0.69	0.14	0.83	1.7	1.5	29	31	20	2400 x 1300	1500 x 2200	75/72
6mm	0.74	0.17	0.55	0.15	0.30	0.69	0.63	0.16	0.79	1.7	1.5	30	33	30	2400 x 4000	2000 x 4000	73/69
Pilkington Optiwhite™																	
*4mm	0.76	0.17	0.64	0.18	0.18	0.77	0.75	0.14	0.89	1.7	1.5	29	31	20	2400 x 1300	1500 x 2200	76/77
6mm	0.76	0.17	0.61	0.17	0.22	0.76	0.71	0.16	0.87	1.7	1.5	30	33	30	2400 x 4000	2000 x 4000	76/76
Pilkington Optifloat™																	
6mm 75/79 Green	0.62	0.13	0.34	0.08	0.58	0.43	0.39	0.10	0.49	1.7	1.5	30	33	30	2400 x 4000	2000 x 4000	62/43
6mm 49/58 Bronze	0.41	0.08	0.31	0.08	0.61	0.42	0.36	0.12	0.48	1.7	1.5	30	33	30	2400 x 4000	2000 x 4000	41/42
6mm 43/58 Grey	0.36	0.07	0.31	0.08	0.61	0.42	0.36	0.12	0.48	1.7	1.5	30	33	30	2400 x 4000	2000 x 4000	36/42
Pilkington Arctic Blue™																	
6mm	0.47	0.10	0.28	0.07	0.65	0.36	0.32	0.09	0.41	1.7	1.5	30	33	30	2400 x 4000	2000 x 4000	47/36
Pilkington EverGreen™																	
6mm	0.55	0.11	0.27	0.07	0.66	0.35	0.31	0.09	0.40	1.7	1.5	30	33	30	2400 x 4000	2000 x 4000	55/35
Pilkington Suncool™ Classic																	
6mm 14/25 (Silver)	0.13	0.30	0.09	0.27	0.64	0.15	0.10	0.07	0.17	1.6	1.4	30	33	30	2400 x 3600	2000 x 3500	13/15
6mm 20/34 (Silver)	0.17	0.24	0.11	0.22	0.67	0.18	0.13	0.08	0.21	1.7	1.4	30	33	30	2400 x 3600	2000 x 3500	17/18
6mm 30/39 (Blue)	0.25	0.17	0.16	0.18	0.66	0.23	0.18	0.08	0.26	1.7	1.4	30	33	30	2400 x 3600	2000 x 3500	25/23
6mm 32/49 (Grey)	0.26	0.13	0.20	0.11	0.69	0.29	0.23	0.10	0.33	1.7	1.4	30	33	30	2400 x 3600	2000 x 3500	26/29

Table G-1: Performance Data Pilkington Insulight with 6 mm Pilkington K Glass Inner Pane

	Light		Solar Radiant Heat				Shading Coefficient			U value (W/m^2K)	U value (W/m^2K)	Sound Insulation		Mass	Unit Maximum Sizes†		
	Transmittance	Reflectance	Direct Transmittance	Reflectance	Absorptance	Total Transmission	Short Wavelength	Long Wavelength	Total	Air-filled	Argon-filled	R_w (dB)	R_w (dB)	(kg/m²)	Annealed (mm)	Toughened (mm)	Descriptive Code
Pilkington Insulight™ (with 6mm Pilkington Optifloat™ clear inner pane and 16mm cavity – unless otherwise indicated)																	
Pilkington Optifloat™ Clear																	
*4mm	0.81	0.15	0.69	0.13	0.18	0.75	0.79	0.07	0.86	2.7	2.6	29	31	20	1300 x 2400	1500 x 2200	81/75
6mm	0.80	0.15	0.64	0.12	0.24	0.72	0.74	0.09	0.83	2.7	2.6	30	33	30	2400 x 4000	1500 x 2200	80/72
Pilkington Optiwhite™																	
*4mm	0.83	0.15	0.75	0.14	0.11	0.81	0.86	0.07	0.93	2.7	2.6	29	31	20	1300 x 2400	1500 x 2200	83/81
6mm	0.82	0.15	0.71	0.14	0.15	0.79	0.82	0.09	0.91	2.7	2.6	30	33	30	2400 x 4000	1500 x 2200	82/79
Pilkington Optifloat™																	
6mm 75/59 Green	0.67	0.11	0.39	0.08	0.53	0.47	0.45	0.09	0.54	2.7	2.6	30	33	30	2400 x 4000	2000 x 4000	67/47
6mm 49/58 Bronze	0.44	0.07	0.37	0.07	0.56	0.46	0.43	0.10	0.53	2.7	2.6	30	33	30	2400 x 4000	2000 x 4000	44/46
6mm 43/58 Grey	0.39	0.07	0.36	0.07	0.53	0.46	0.41	0.12	0.53	2.7	2.6	30	33	30	2400 x 4000	2000 x 4000	39/46
Pilkington Arctic Blue™																	
6mm	0.50	0.09	0.32	0.07	0.61	0.41	0.37	0.10	0.47	2.7	2.6	30	33	30	2400 x 4000	2000 x 4000	50/41
Pilkington EverGreen™																	
6mm	0.59	0.10	0.30	0.07	0.63	0.39	0.34	0.11	0.45	2.7	2.6	30	33	30	2400 x 4000	2000 x 4000	59/39
Pilkington Suncool™ Classic																	
6mm 14/25 (Silver)	0.14	0.30	0.10	0.27	0.63	0.17	0.11	0.08	0.19	2.2	2.0	30	33	30	2400x3600	2000 x 3500	14/17
6mm 20/34 (Silver)	0.18	0.24	0.13	0.22	0.65	0.20	0.15	0.08	0.23	2.3	2.2	30	33	30	2400x3600	2000 x 3500	18/20
6mm 30/39 (Blue)	0.27	0.17	0.18	0.17	0.65	0.26	0.21	0.09	0.30	2.4	2.3	30	33	30	2400x3600	2000 x 3500	27/26
6mm 32/49 (Grey)	0.28	0.13	0.23	0.11	0.66	0.32	0.26	0.11	0.37	2.5	2.3	30	33	30	2400x3600	2000 x 3500	28/32
Pilkington Suncool™ High Performance																	
6mm 66/33 (Brilliant)	0.66	0.14	0.31	0.31	0.38	0.36	0.36	0.05	0.41	1.3	1.0	30	33	30	2400 x 3600	2000 x 3500	66/36
6mm 50/25 (Brilliant)	0.50	0.15	0.24	0.32	0.44	0.27	0.28	0.03	0.31	1.4	1.1	30	33	30	2400 x 3600	2000 x 3500	50/27
6mm 65/39 (Titan)	0.65	0.20	0.36	0.28	0.36	0.39	0.41	0.04	0.45	1.4	1.1	30	33	30	2400 x 3600	2000 x 3500	65/39
6mm 63/45 (Clear)	0.63	0.22	0.36	0.31	0.33	0.43	0.41	0.08	0.49	1.4	1.1	30	33	30	2400 x 3600	2000 x 3500	64/43
6mm 52/44 (Neutral)	0.55	0.08	0.36	0.13	0.51	0.44	0.41	0.10	0.51	1.6	1.4	30	33	30	2400 x 3600	2000 x 3500	55/44
6mm 42/29 (Silver)	0.45	0.44	0.23	0.45	0.32	0.28	0.26	0.06	0.32	1.4	1.1	30	33	30	2400 x 3600	2000 x 3500	45/28
**6mm 35/25 (Green)	0.38	0.29	0.17	0.18	0.65	0.27	0.20	0.11	0.31	1.4	1.1	30	33	30	2400 x 3600	2000 x 3500	38/27
**6mm 24/25 (Bronze)	0.24	0.14	0.14	0.18	0.68	0.23	0.16	0.10	0.26	1.4	1.1	30	33	30	2400 x 3600	2000 x 3500	24/23
**6mm 20/24 (Grey)	0.22	0.13	0.14	0.18	0.68	0.23	0.16	0.10	0.26	1.4	1.1	30	33	30	2400 x 3600	2000 x 3500	22/23
**6mm 28/23 (Blue)	0.28	0.19	0.14	0.14	0.72	0.23	0.16	0.10	0.26	1.4	1.1	30	33	30	2400 x 3600	2000 x 3500	28/23

In conjunction with notes under table 4.

Table G-2: Performance Data Pilkington Insulight with 6 mm Pilkington Optifloat Clear Inner Pane

	Light		Solar Radiant Heat				Shading Coefficient			U value (W/m^2K)	U value (W/m^2K)	Sound Insulation		Mass	Unit Maximum Sizes†		
	Transmittance	Reflectance	Direct Transmission	Reflectance	Absorptance	Total Transmission	Short Wavelength	Long Wavelength	Total	Air-filled	Argon-filled	R_w (dB)	R_w (dB)	(kg/m²)	Annealed (mm)	Toughened (mm)	Descriptive Code
Pilkington Insulight™ (with 6mm Pilkington Optitherm™ SN inner pane coating to surface 3 and 16mm cavity – unless otherwise indicated)																	
Pilkington Optifloat™ Clear																	
*4mm	0.79	0.12	0.53	0.23	0.24	0.63	0.61	0.11	0.72	1.4	1.1	29	31	20	2400x1300	1500x2200	79/63
6mm	0.78	0.11	0.50	0.21	0.29	0.61	0.57	0.13	0.70	1.4	1.1	30	33	30	2400x4000	2000x4000	78/61
Pilkington Optiwhite™																	
*4mm	0.81	0.12	0.57	0.28	0.15	0.68	0.66	0.12	0.78	1.4	1.1	29	31	20	2400x1300	1500x2200	81/68
6mm	0.80	0.11	0.55	0.27	0.18	0.67	0.63	0.14	0.77	1.4	1.1	30	33	30	2400x4000	2000x4000	80/67
Pilkington Optifloat™																	
6mm 75/59 Green	0.66	0.09	0.33	0.08	0.59	0.41	0.38	0.09	0.47	1.4	1.1	30	33	30	2400x4000	2000x4000	66/41
6mm 49/58 Bronze	0.43	0.06	0.28	0.10	0.62	0.36	0.32	0.09	0.41	1.4	1.1	30	33	30	2400x4000	2000x4000	43/36
6mm 43/58 Grey	0.38	0.06	0.27	0.11	0.62	0.36	0.31	0.10	0.41	1.4	1.1	30	33	30	2400x4000	2000x4000	38/36
Pilkington Arctic Blue™																	
6mm	0.49	0.07	0.27	0.07	0.66	0.34	0.31	0.08	0.39	1.4	1.1	30	33	30	2400x4000	2000x4000	49/34
Pilkington EverGreen™																	
6mm	0.58	0.08	0.26	0.07	0.67	0.33	0.30	0.08	0.38	1.4	1.1	30	33	30	2400x4000	2000x4000	58/33
Pilkington Suncool™ Classic																	
6mm 14/25 (Silver)	0.14	0.30	0.09	0.27	0.64	0.14	0.05	0.10	0.15	1.4	1.1	30	33	30	2400x3600	2000x3500	14/14
6mm 20/34 (Silver)	0.18	0.24	0.11	0.22	0.67	0.16	0.13	0.06	0.19	1.4	1.1	30	33	30	2400x3600	2000x3500	18/16
6mm 30/39 (Blue)	0.26	0.17	0.15	0.18	0.67	0.22	0.18	0.07	0.25	1.4	1.1	30	33	30	2400x3600	2000x3500	26/22
6mm 32/49 (Grey)	0.27	0.12	0.18	0.13	0.69	0.25	0.21	0.08	0.29	1.4	1.1	30	33	30	2400x3600	2000x3500	27/25

Table G-3: Performance Data Pilkington Insulight with 6 mm Pilkington Optitherm SN Inner Pane

	Light		Solar Radiant Heat				Shading Coefficient			U value (W/m^2K)	U value (W/m^2K)	Sound Insulation		Mass	Unit Maximum Sizes†		
	Transmittance	Reflectance	Direct Transmission	Reflectance	Absorptance	Total Transmission	Short Wavelength	Long Wavelength	Total	Air-filled	Argon-filled	R_w (dB)	R_A (dB)	(kg/m²)	Annealed (mm)	Toughened (mm)	Descriptive Code
Pilkington Insulight™ (with 6mm Pilkington Optitherm™ S2 inner pane coating to surface 3 and 16mm cavity – unless otherwise indicated)																	
Pilkington Optifloat™ Clear																	
*4mm	0.71	0.11	0.38	0.31	0.31	0.53	0.44	0.17	0.61	1.3	1.1	29	31	20	2400x1300	1500x2200	71/53
6mm	0.70	0.11	0.36	0.28	0.36	0.52	0.41	0.19	0.60	1.3	1.0	30	33	30	2400x4000	2000x4000	70/52
Pilkington Optiwhite™																	
*4mm	0.73	0.11	0.40	0.39	0.21	0.56	0.46	0.18	0.64	1.3	1.1	29	31	20	2400x1300	1500x2200	73/56
6mm	0.72	0.11	0.38	0.38	0.24	0.55	0.44	0.19	0.63	1.3	1.0	30	33	30	2400x4000	2000x4000	72/55
Pilkington Optifloat™																	
6mm 75/59 Green	0.59	0.09	0.26	0.09	0.65	0.38	0.30	0.14	0.44	1.3	1.0	30	33	30	2400x4000	2000x4000	59/38
6mm 49/58 Bronze	0.39	0.06	0.20	0.13	0.67	0.31	0.23	0.13	0.36	1.3	1.0	30	33	30	2400x4000	2000x4000	39/31
6mm 43/58 Grey	0.35	0.06	0.19	0.14	0.67	0.30	0.22	0.12	0.34	1.3	1.0	30	33	30	2400x4000	2000x4000	35/30
Pilkington Arctic Blue™																	
6mm	0.44	0.07	0.21	0.08	0.71	0.31	0.24	0.12	0.36	1.3	1.0	30	33	30	2400x4000	2000x4000	44/31
Pilkington EverGreen™																	
6mm	0.52	0.08	0.22	0.07	0.71	0.31	0.25	0.11	0.36	1.3	1.0	30	33	30	2400x4000	2000x4000	52/31
Pilkington Suncool™ Classic																	
6mm 14/25 (Silver)	0.13	0.30	0.06	0.27	0.67	0.12	0.07	0.07	0.14	1.3	1.0	30	33	30	2400x3600	2000x3500	13/12
6mm 20/34 (Silver)	0.16	0.24	0.08	0.23	0.69	0.14	0.09	0.07	0.16	1.3	1.0	30	33	30	2400x3600	2000x3500	16/14
6mm 30/39 (Blue)	0.23	0.16	0.12	0.18	0.70	0.19	0.14	0.08	0.22	1.3	1.0	30	33	30	2400x3600	2000x3500	23/19
6mm 32/49 (Grey)	0.24	0.12	0.13	0.14	0.73	0.22	0.15	0.10	0.25	1.3	1.0	30	33	30	2400x3600	2000x3500	24/22

U values for argon gas-filled cavities based on 100% gas fill. U values for other % gas fills are available on request.
* with 4mm inner pane
** with 6mm Pilkington Suncool™ High Performance coating on surface 3
† Maximum sizes are for guidance only, please consult with processor for details. These are not recommended glazing sizes.
Descriptive Code – A pair of numbers signifying the properties of glazing. The first number is the visible light transmittance and the second is the total solar radiant heat transmittance.

Note: Pilkington Optitherm™ S2 is a very high performance low emissivity glass manufactured to special order and is therefore generally only available for larger commercial projects.

Table G-4: Performance Data Pilkington Insulight with 6 mm Pilkington Optitherm S2 Inner Pane

Appendix H: The response surface models approximating the relationship between the design factors of each group and the energy consumption of the VAV system and the FCU system, in both climates

Sections H.1.1 to H.1.3 present the response surface models approximating the relationship between the design factors contained in each of the groups related to the building load and the energy performance of the VAV system and the FCU system, respectively, in both the CIBSE TRY and the NOA TRY. Also, sections H.2.1 to H.2.5 contain the response surface models correlating the parameters classified in each of the groups related to the design & operation of the HVAC systems with the energy consumption of the VAV system and the FCU system, respectively, depending on the climate for which the simulations are carried out. A few summary statistics along with the validation results for all the fitted regression models are finally presented in section H.3.

H.1 Building load related parameters

H.1.1 The design variables associated with the solar gains through the transparent building elements (Group A)

The procedure that is followed in order to correlate the four parameters of group A with the annual heating & cooling energy consumption of the VAV system and the FCU system, in both climates, is briefly described in the following bullet points, as an example:

- It is assumed that the relationship between the four parameters of this group and the response variables of interest can be approximated by a second-order regression model. The range of values specified for each of the four parameters under consideration (shown in table 4.1.1-1, in section 4.1.1) is strict, which means that the axial distance α cannot be extended beyond the experimental region defined by the upper and lower limits of each factor. In other words, the axial distance α equals 1, (region of interest = region of operability), so a Face Centered Design[26] (FCD) [1] is suitable for this case.
- A FCD involving four parameters consists of 25 design points (i.e. combinations of factor levels). The number of parameters contained in group A as well as their minimum and maximum values are introduced into Design-Expert, which uses this information to determine the factor levels for each of the 25 design points. The values of the factors for each of these design points become input parameters to TAS which estimates the response variables of interest (in this case the annual heating and cooling energy consumption).
- The TAS energy predictions for all the design points are finally input into Design-Expert which carries out step-by-step statistical analysis, suggesting which type of regression model provides best fit for the data.

[26] **Note:** It should be remembered that details regarding the Face Centered and the Central Composite Designs, which represent the most popular class of second order designs, can be found in section 3.2.1, chapter 3.

The factor levels for each design point as well as the TAS energy predictions when the VAV system is simulated for the CIBSE TRY, are shown in table H.1.1-1 as an example:

Point Type	Independent Variables				Response Variables	
	Glazing Percentage (%)	Total Shading Coefficient	Overhang Depth (m)	Sidefin Depth (m)	Heating energy (kWh)	Cooling energy (kWh)
Axial	0.60	0.16	1.00	1.00	184710	88328
Fact	0.25	0.16	2.00	2.00	137623	85848
Axial	0.60	0.52	1.00	2.00	144041	113191
Fact	0.25	0.88	2.00	0.00	104311	110211
Axial	0.60	0.52	1.00	0.00	139770	115779
Fact	0.95	0.88	0.00	2.00	124510	187494
Axial	0.60	0.52	2.00	1.00	146437	111392
Axial	0.25	0.52	1.00	1.00	118808	97509
Fact	0.25	0.88	0.00	0.00	97500	119069
Fact	0.25	0.88	2.00	2.00	110179	106083
Fact	0.25	0.88	0.00	2.00	102896	115006
Fact	0.95	0.16	2.00	0.00	228566	89912
Axial	0.60	0.52	0.00	1.00	137020	122229
Center	0.60	0.52	1.00	1.00	142013	114451
Fact	0.95	0.16	0.00	0.00	223079	93253
Axial	0.95	0.52	1.00	1.00	164066	131670
Fact	0.95	0.88	2.00	2.00	134216	162541
Fact	0.95	0.16	0.00	2.00	226288	92281
Fact	0.95	0.16	2.00	2.00	231855	88995
Fact	0.25	0.16	0.00	2.00	135658	87073
Fact	0.95	0.88	0.00	0.00	118914	193651
Axial	0.60	0.88	1.00	1.00	114192	142808
Fact	0.25	0.16	2.00	0.00	136114	86486
Fact	0.25	0.16	0.00	0.00	133984	87639
Fact	0.95	0.88	2.00	0.00	128106	169262

Table H.1.1-1: VAV system annual heating and cooling energy use when the simulations are carried out for the CIBSE TRY

As mentioned earlier, the TAS energy predictions for all the design points contained in the table shown above are input into Design-Expert, which carries out step-by-step statistical analysis to provide the regression model that best fits the data.

The response surface models correlating the four parameters of group A with the annual heating and cooling energy consumption of the VAV system, when this is simulated for the CIBSE TRY, are the following:

1.0/Sqrt(Heating Energy) =

+2.92415E-003

-1.30376E-003 * Glazing Percentage

+5.72966E-004 * Total Shading Coefficient

-1.27678E-005 * Overhang Depth

-1.01950E-005 * Sidefin Depth

+2.65542E-004 * Glazing Percentage^2

-7.30533E-005 * Total Shading Coefficient^2

+4.88229E-006 * Overhang Depth^2

+2.35038E-006 * Sidefin Depth^2

+6.41713E-004 * Glazing Percentage * Total Shading Coefficient

-1.66050E-006 * Glazing Percentage * Overhang Depth

+7.19391E-006 * Glazing Percentage * Sidefin Depth

-5.72248E-005 * Total Shading Coefficient * Overhang Depth

-4.11755E-005 * Total Shading Coefficient * Sidefin Depth

+3.30619E-007 * Overhang Depth * Sidefin Depth

(Cooling Energy)$^{0.25}$ =

+13.41983

-0.10794 * Glazing Percentage

+1.12930 * Total Shading Coefficient

+0.059621 * Overhang Depth

-2.38073E-003 * Sidefin Depth

-0.37777 * Total Shading Coefficient^2

+2.89354 * Glazing Percentage * Total Shading Coefficient

-0.11541 * Glazing Percentage * Overhang Depth

-0.21508 * Total Shading Coefficient * Overhang Depth

-0.070015 * Total Shading Coefficient * Sidefin Depth

The response surface models correlating the four parameters of this group with the heating and cooling energy consumption of the FCU system, when this is simulated for the CIBSE TRY, are the following:

1.0/(Heating Energy) =

+6.58208E-006

-3.16380E-006 * Glazing Percentage

+1.08189E-006 * Total Shading Coefficient

-4.60622E-008 * Overhang Depth

+9.23939E-009 * Sidefin Depth

+4.77563E-007 * Glazing Percentage^2

-5.99633E-008 * Total Shading Coefficient^2

+1.72382E-008 * Overhang Depth^2

-8.83977E-009 * Sidefin Depth^2

+2.28428E-006 * Glazing Percentage * Total Shading Coefficient

+1.87031E-010 * Glazing Percentage * Overhang Depth

+5.24205E-009 * Glazing Percentage * Sidefin Depth

-1.62587E-007 * Total Shading Coefficient * Overhang Depth

-7.89027E-008 * Total Shading Coefficient * Sidefin Depth

-3.50544E-010 * Overhang Depth * Sidefin Depth

Log_{10}(Cooling Energy) =

+5.23088

-0.030797 * Glazing Percentage

+0.10102 * Total Shading Coefficient

+8.99665E-003 * Overhang Depth

+1.32681E-004 * Sidefin Depth

+0.40780 * Glazing Percentage * Total Shading Coefficient

-0.015615 * Glazing Percentage * Overhang Depth

-0.033805 * Total Shading Coefficient * Overhang Depth

-9.79170E-003 * Total Shading Coefficient * Sidefin Depth

The response surface models correlating the parameters under consideration with the VAV system heating and cooling energy use, when this is simulated for the NOA TRY, are the following:

$$\begin{aligned}
\text{Log}_{10}(\text{Heating Energy}) = {} & \\
& +4.60071 \\
& +0.41671 \ * \text{Glazing Percentage} \\
& -0.32434 \ * \text{Total Shading Coefficient} \\
& +2.39585\text{E-}003 \ * \text{Overhang Depth} \\
& +1.84458\text{E-}003 \ * \text{Sidefin Depth} \\
& +0.068087 \ * \text{Total Shading Coefficient}^2 \\
& -0.44404 \ * \text{Glazing Percentage} * \text{Total Shading Coefficient} \\
& +0.042311 \ * \text{Total Shading Coefficient} * \text{Overhang Depth} \\
& +0.015460 \ * \text{Total Shading Coefficient} * \text{Sidefin Depth}
\end{aligned}$$

$$\begin{aligned}
\text{Log}_{10}(\text{Cooling Energy}) = {} & \\
& +5.37079 \\
& +0.073479 \ * \text{Glazing Percentage} \\
& +0.12752 \ * \text{Total Shading Coefficient} \\
& -7.90117\text{E-}003 \ * \text{Overhang Depth} \\
& -1.96255\text{E-}004 \ * \text{Sidefin Depth} \\
& -0.045423 \ * \text{Glazing Percentage}^2 \\
& -0.043232 \ * \text{Total Shading Coefficient}^2 \\
& +7.25112\text{E-}003 \ * \text{Overhang Depth}^2 \\
& +0.28849 \ * \text{Glazing Percentage} * \text{Total Shading Coefficient} \\
& -0.013014 \ * \text{Glazing Percentage} * \text{Overhang Depth} \\
& -0.025031 \ * \text{Total Shading Coefficient} * \text{Overhang Depth} \\
& -6.94840\text{E-}003 \ * \text{Total Shading Coefficient} * \text{Sidefin Depth}
\end{aligned}$$

The response surface models correlating the four parameters of group A with the FCU system heating and cooling energy use, when this is simulated for the NOA TRY, are the following:

$(\text{Heating Energy})^{-0.5} =$

+1.01582E-004

-4.19329E-005 * Glazing Percentage

+3.78200E-005 * Total Shading Coefficient

-7.11285E-007 * Overhang Depth

-4.50108E-007 * Sidefin Depth

+4.65175E-005 * Glazing Percentage * Total Shading Coefficient

+7.21348E-007 * Glazing Percentage * Overhang Depth

+5.60691E-007 * Glazing Percentage * Sidefin Depth

-5.43946E-006 * Total Shading Coefficient * Overhang Depth

-2.21745E-006 * Total Shading Coefficient * Sidefin Depth

+1.28698E-008 * Overhang Depth * Sidefin Depth

$(\text{Cooling Energy})^{-0.14} =$

+0.17125

-3.07762E-003 * Glazing Percentage

-6.89617E-003 * Total Shading Coefficient

+3.53835E-004 * Overhang Depth

+8.11580E-006 * Sidefin Depth

+2.27429E-003 * Glazing Percentage^2

+2.03162E-003 * Total Shading Coefficient^2

-3.51223E-004 * Overhang Depth^2

-0.017118 * Glazing Percentage * Total Shading Coefficient

+7.08166E-004 * Glazing Percentage * Overhang Depth

+1.48625E-003 * Total Shading Coefficient * Overhang Depth

+4.01779E-004 * Total Shading Coefficient * Sidefin Depth

H.1.2 The design variables associated with the thermal resistance and the air tightness of the building (Group B)

The response surface models correlating the three parameters of group B with the annual heating and cooling energy consumption of the VAV system, when this is simulated for the CIBSE TRY, are the following:

$$(\text{Heating Energy})^{0.63} =$$

$$
\begin{aligned}
&+242.54412 \\
&+428.30808 \ * \text{Wall U-value} \\
&+1006.95977 \ * \text{Infiltration Rate} \\
&+303.01567 \ * \text{Window U-value} \\
&+8.03353 \ * \text{Infiltration Rate}^2 \\
&-4.64117 \ * \text{Window U-value}^2 \\
&-28.96033 \ * \text{Wall U-value} * \text{Infiltration Rate} \\
&-26.40021 \ * \text{Wall U-value} * \text{Window U-value} \\
&-10.15030 \ * \text{Infiltration Rate} * \text{Window U-value}
\end{aligned}
$$

$$1.0/(\text{Cooling Energy}) =$$

$$
\begin{aligned}
&+6.34874E\text{-}006 \\
&+5.40501E\text{-}007 \ * \text{Wall U-value} \\
&+1.03258E\text{-}006 \ * \text{Infiltration Rate} \\
&+4.81780E\text{-}007 \ * \text{Window U-value} \\
&-1.01381E\text{-}007 \ * \text{Infiltration Rate}^2 \\
&-1.58489E\text{-}008 \ * \text{Window U-value}^2 \\
&-8.74524E\text{-}008 \ * \text{Wall U-value} * \text{Infiltration Rate} \\
&-4.76589E\text{-}008 \ * \text{Wall U-value} * \text{Window U-value} \\
&-2.73308E\text{-}008 \ * \text{Infiltration Rate} * \text{Window U-value}
\end{aligned}
$$

The response surface models correlating the three parameters of this group with the annual heating and cooling energy consumption of the FCU system, when this is simulated for the CIBSE TRY, are the following:

$$(\text{Heating Energy})^{0.2} =$$

$$+9.27108$$
$$+0.46521 * \text{Wall U-value}$$
$$+1.35568 * \text{Infiltration Rate}$$
$$+0.37668 * \text{Window U-value}$$
$$+0.059550 * \text{Wall U-value}^2$$
$$-0.075048 * \text{Infiltration Rate}^2$$
$$-9.13379E\text{-}003 * \text{Window U-value}^2$$
$$-0.077055 * \text{Wall U-value} * \text{Infiltration Rate}$$
$$-0.034868 * \text{Wall U-value} * \text{Window U-value}$$
$$-0.045489 * \text{Infiltration Rate} * \text{Window U-value}$$

$$1.0/(\text{Cooling Energy}) =$$

$$+2.41659E\text{-}006$$
$$+4.75113E\text{-}007 * \text{Wall U-value}$$
$$+1.06955E\text{-}006 * \text{Infiltration Rate}$$
$$+4.14036E\text{-}007 * \text{Window U-value}$$
$$-1.49332E\text{-}007 * \text{Infiltration Rate}^2$$
$$-1.75286E\text{-}008 * \text{Window U-value}^2$$
$$-1.01410E\text{-}007 * \text{Wall U-value} * \text{Infiltration Rate}$$
$$-4.26792E\text{-}008 * \text{Wall U-value} * \text{Window U-value}$$
$$-6.77325E\text{-}008 * \text{Infiltration Rate} * \text{Window U-value}$$

The response surface models correlating the parameters under consideration with the VAV system heating and cooling energy use, when this is simulated for the NOA TRY, are the following:

$(\text{Heating Energy})^{0.68}$ =

-219.93216

+337.24586 * Wall U-value

+1021.46834 * Infiltration Rate

+295.47113 * Window U-value

+119.35550 * Wall U-value^2

-2.86454 * Infiltration Rate^2

-3.47203 * Window U-value^2

-27.23052 * Wall U-value * Infiltration Rate

-22.47496 * Wall U-value * Window U-value

-1.39215 * Infiltration Rate * Window U-value

$(\text{Cooling Energy})^{-1.97}$ =

+9.45778E-012

+7.95521E-013 * Wall U-value

+8.75294E-013 * Infiltration Rate

+8.81159E-013 * Window U-value

-2.38644E-013 * Infiltration Rate^2

-3.69769E-014 * Window U-value^2

-1.97099E-013 * Wall U-value * Infiltration Rate

-6.86924E-014 * Wall U-value * Window U-value

-1.62655E-013 * Infiltration Rate * Window U-value

The response surface models correlating the three parameters of this group with the FCU system heating and cooling energy use, when this is simulated for the NOA TRY, are the following:

$$(\text{Heating Energy})^{0.5} =$$

$$+2710.58320$$
$$+1562.55932 * \text{Wall U-value}$$
$$+3849.74421 * \text{Infiltration Rate}$$
$$+1075.97657 * \text{Window U-value}$$
$$+38.36232 * \text{Wall U-value}^2$$
$$+333.56769 * \text{Infiltration Rate}^2$$
$$+12.28521 * \text{Window U-value}^2$$
$$+163.63367 * \text{Wall U-value} * \text{Infiltration Rate}$$
$$-27.48572 * \text{Wall U-value} * \text{Window U-value}$$
$$+181.11135 * \text{Infiltration Rate} * \text{Window U-value}$$

$$\text{Cooling Energy} =$$

$$+5.48862E+005$$
$$-35236.19110 * \text{Wall U-value}$$
$$-59091.15065 * \text{Infiltration Rate}$$
$$-30123.16553 * \text{Window U-value}$$
$$+3378.53386 * \text{Wall U-value}^2$$
$$+10680.01814 * \text{Infiltration Rate}^2$$
$$+1554.51586 * \text{Window U-value}^2$$
$$+8372.89377 * \text{Wall U-value} * \text{Infiltration Rate}$$
$$+3317.02899 * \text{Wall U-value} * \text{Window U-value}$$
$$+5923.27122 * \text{Infiltration Rate} * \text{Window U-value}$$

H.1.3 The design variables associated with the internal heat gains of the office building (Group C)

The response surface models correlating the three parameters of group C with the annual heating and cooling energy consumption of the VAV system, when this is simulated for the CIBSE TRY, are the following:

$$(\text{Heating Energy})^{-0.72} =$$
$$+2.10355E\text{-}004$$
$$+4.40076E\text{-}006 * \text{Lighting Gains}$$
$$+4.45082E\text{-}006 * \text{Equipment Gains}$$
$$-1.02433E\text{-}005 * \text{Occupant Density}$$
$$-5.88536E\text{-}008 * \text{Equipment Gains}^2$$
$$+1.83115E\text{-}007 * \text{Occupant Density}^2$$
$$-8.52012E\text{-}008 * \text{Lighting Gains} * \text{Equipment Gains}$$
$$+7.56931E\text{-}008 * \text{Lighting Gains} * \text{Occupant Density}$$
$$+1.03661E\text{-}007 * \text{Equipment Gains} * \text{Occupant Density}$$

$$(\text{Cooling Energy})^{0.99} =$$
$$+1.08168E+005$$
$$+2292.77134 * \text{Lighting Gains}$$
$$+2382.11207 * \text{Equipment Gains}$$
$$-7627.37757 * \text{Occupant Density}$$
$$+3.24169 * \text{Equipment Gains}^2$$
$$+205.20915 * \text{Occupant Density}^2$$
$$+2.30080 * \text{Lighting Gains} * \text{Equipment Gains}$$
$$-2.42239 * \text{Lighting Gains} * \text{Occupant Density}$$
$$-2.05655 * \text{Equipment Gains} * \text{Occupant Density}$$

The response surface models correlating the three parameters of this group with the annual heating and cooling energy consumption of the FCU system, when this is simulated for the CIBSE TRY, are the following:

$$
\begin{aligned}
(\text{Heating Energy})^{-2.18} = \\
&+5.09135E\text{-}012 \\
&+1.26773E\text{-}013 * \text{Lighting Gains} \\
&+7.70575E\text{-}014 * \text{Equipment Gains} \\
&-2.79584E\text{-}013 * \text{Occupant Density} \\
&+3.19585E\text{-}015 * \text{Occupant Density}^2 \\
&-3.86572E\text{-}015 * \text{Lighting Gains} * \text{Equipment Gains} \\
&+3.91009E\text{-}015 * \text{Lighting Gains} * \text{Occupant Density} \\
&+3.89110E\text{-}015 * \text{Equipment Gains} * \text{Occupant Density}
\end{aligned}
$$

$$
\begin{aligned}
\text{Sqrt(Cooling Energy)} = \\
&+500.53713 \\
&+7.26268 * \text{Lighting Gains} \\
&+8.19096 * \text{Equipment Gains} \\
&-24.88741 * \text{Occupant Density} \\
&-0.015622 * \text{Equipment Gains}^2 \\
&+0.63213 * \text{Occupant Density}^2 \\
&-0.026660 * \text{Lighting Gains} * \text{Equipment Gains} \\
&+0.027226 * \text{Lighting Gains} * \text{Occupant Density} \\
&+0.038734 * \text{Equipment Gains} * \text{Occupant Density}
\end{aligned}
$$

The response surface models correlating the parameters under consideration with the VAV system heating and cooling energy use, when this is simulated for the NOA TRY, are the following:

$$(\text{Heating})^{-1.99} =$$

$$+1.28811E\text{-}009$$
$$+5.61006E\text{-}011 * \text{Lighting Gains}$$
$$+3.00288E\text{-}011 * \text{Equipment Gains}$$
$$-9.93180E\text{-}011 * \text{Occupant Density}$$
$$+5.86585E\text{-}013 * \text{Lighting Gains}^2$$
$$-4.12694E\text{-}013 * \text{Equipment Gains}^2$$
$$+2.31139E\text{-}012 * \text{Occupant Density}^2$$
$$-2.00040E\text{-}013 * \text{Lighting Gains} * \text{Equipment Gains}$$
$$-1.10141E\text{-}013 * \text{Lighting Gains} * \text{Occupant Density}$$
$$+6.01726E\text{-}013 * \text{Equipment Gains} * \text{Occupant Density}$$

$$(\text{Cooling})^{0.82} =$$

$$+36505.89819$$
$$+431.34264 * \text{Lighting Gains}$$
$$+471.11731 * \text{Equipment Gains}$$
$$-1684.12123 * \text{Occupant Density}$$
$$-0.020926 * \text{Lighting Gains}^2$$
$$-0.10751 * \text{Equipment Gains}^2$$
$$+44.67070 * \text{Occupant Density}^2$$
$$-0.19514 * \text{Lighting Gains} * \text{Equipment Gains}$$
$$+0.47502 * \text{Lighting Gains} * \text{Occupant Density}$$
$$+0.45971 * \text{Equipment Gains} * \text{Occupant Density}$$

The response surface models correlating the parameters of group C with the FCU system heating and cooling energy use, when this is simulated for the NOA TRY, are the following:

$$(\text{Heating})^{-2.44} =$$

$$+6.29081E\text{-}012$$
$$+1.25342E\text{-}013 * \text{Lighting Gains}$$
$$+5.05379E\text{-}014 * \text{Equipment Gains}$$
$$-2.17429E\text{-}013 * \text{Occupant Density}$$
$$+4.14128E\text{-}015 * \text{Occupant Density}^2$$
$$-1.34715E\text{-}015 * \text{Lighting Gains} * \text{Equipment Gains}$$
$$+1.30818E\text{-}015 * \text{Lighting Gains} * \text{Occupant Density}$$
$$+1.59399E\text{-}015 * \text{Equipment Gains} * \text{Occupant Density}$$

$$\text{Sqrt(Cooling)} =$$

$$+674.73991$$
$$+6.51280 * \text{Lighting Gains}$$
$$+6.68391 * \text{Equipment Gains}$$
$$-22.54655 * \text{Occupant Density}$$
$$+0.58355 * \text{Occupant Density}^2$$
$$-0.014712 * \text{Lighting Gains} * \text{Equipment Gains}$$
$$+0.012178 * \text{Lighting Gains} * \text{Occupant Density}$$
$$+0.027188 * \text{Equipment Gains} * \text{Occupant Density}$$

H.2 HVAC system related parameters

H.2.1 The design variables associated with the air temperature control set-points of the HVAC systems (Group D)

The response surface models correlating the three parameters of group D with the annual heating and cooling energy consumption of the VAV system, when this is simulated for the CIBSE TRY, are the following:

1.0/(Heating Energy) =

+3.19452E-004

-5.62602E-005 * Heating Zone Temp

+1.44806E-005 * Cooling Zone Temp

-6.92738E-007 * Temp Difference

+3.10981E-006 * Heating Zone Temp^2

-1.62972E-008 * Cooling Zone Temp^2

-1.19070E-006 * Heating Zone Temp * Cooling Zone Temp

+2.04352E-008 * Heating Zone Temp * Temp Difference

+5.63918E-009 * Cooling Zone Temp * Temp Difference

-5.60615E-008 * Heating Zone Temp^3

+2.64773E-008 * Heating Zone Temp^2 * Cooling Zone Temp

1.0/(Cooling Energy) =

+1.13259E-003

-2.70161E-005 * Heating Zone Temp

-1.12473E-004 * Cooling Zone Temp

-1.57201E-005 * Temp Difference

+1.11587E-006 * Heating Zone Temp^2

+3.85732E-006 * Cooling Zone Temp^2

-1.75654E-006 * Temp Difference^2

+4.88333E-007 * Heating Zone Temp * Cooling Zone Temp

-2.04567E-007 * Heating Zone Temp * Temp Difference

+2.91215E-006 * Cooling Zone Temp * Temp Difference

-4.01037E-008 * Heating Zone Temp^3

-2.83221E-008 * Cooling Zone Temp^3

+1.90656E-009 * Temp Difference^3

+4.34453E-008 * Heating Zone Temp^2 * Cooling Zone Temp

+1.99593E-008 * Heating Zone Temp^2 * Temp Difference

-4.12051E-008 * Heating Zone Temp * Cooling Zone Temp^2

-4.14147E-009 * Heating Zone Temp * Temp Difference^2

-9.03823E-008 * Cooling Zone Temp^2 * Temp Difference

+8.11921E-008 * Cooling Zone Temp * Temp Difference^2

-1.91947E-008 * Heating Zone Temp * Cooling Zone Temp * Temp Difference

The response surface models correlating the three parameters of this group with the annual heating and cooling energy consumption of the FCU system, when this is simulated for the CIBSE TRY, are the following:

Heating Energy)$^{0.23}$ =

+1.72524

+1.12074 * Heating Zone Temp

+0.070512 * Cooling Zone Temp

-0.88246 * Temp Difference

-0.013327 * Heating Zone Temp^2

-4.55241E-003 * Heating Zone Temp * Cooling Zone Temp

+0.033609 * Heating Zone Temp * Temp Difference

-6.55719E-003 * Cooling Zone Temp * Temp Difference

Cooling Energy =

+1.15335E+006

+4998.37361 * Heating Zone Temp

-54527.40417 * Cooling Zone Temp

-6834.88194 * Temp Difference

+485.22222 * Heating Zone Temp^2

+889.72222 * Cooling Zone Temp^2

+381.89931 * Temp Difference^2

-715.09375 * Heating Zone Temp * Cooling Zone Temp

-356.82812 * Heating Zone Temp * Temp Difference

+252.57813 * Cooling Zone Temp * Temp Difference

The response surface models correlating the parameters under consideration with the VAV system heating and cooling energy use, when this is simulated for the NOA TRY, are the following:

Log_{10}(Heating Energy) =

+0.53368

+0.51724 * Heating Zone Temp

-0.20566 * Cooling Zone Temp

+0.021022 * Temp Difference

-0.010444 * Heating Zone Temp^2

+1.89725E-003 * Cooling Zone Temp^2

+5.29650E-004 * Temp Difference^2

+3.16637E-003 * Heating Zone Temp * Cooling Zone Temp

+2.01577E-005 * Heating Zone Temp * Temp Difference

-8.96659E-004 * Cooling Zone Temp * Temp Difference

1.0/Sqrt(Cooling Energy) =

+1.08954E-003

-1.21219E-004 * Heating Zone Temp

+5.62553E-005 * Cooling Zone Temp

+4.85959E-005 * Temp Difference

+4.04341E-006 * Heating Zone Temp * Cooling Zone Temp

+1.82343E-006 * Heating Zone Temp * Temp Difference

-5.04091E-006 * Cooling Zone Temp * Temp Difference

The response surface models correlating the three parameters of group D with the FCU system heating and cooling energy use, when this is simulated for the NOA TRY, are the following:

$(\text{Heating Energy})^{0.21}$ =

-0.14486

+0.89413 * Heating Design Zone Temp

-0.068742 * Cooling Design Zone Temp

-0.73617 * Temp Difference

-0.010835 * Heating Design Zone Temp^2

+1.75787E-003 * Cooling Design Zone Temp^2

+1.06843E-003 * Temp Difference^2

-1.50701E-003 * Heating Design Zone Temp * Cooling Design Zone Temp

+0.028635 * Heating Design Zone Temp * Temp Difference

-8.74445E-003 * Cooling Design Zone Temp * Temp Difference

Cooling Energy =

+1.59867E+006

-8632.47083 * Heating Design Zone Temp

-58846.76250 * Cooling Design Zone Temp

+3429.09583 * Temp Difference

+322.95833 * Heating Design Zone Temp^2

+566.70833 * Cooling Design Zone Temp^2

+315.17708 * Temp Difference^2

+57.21875 * Heating Design Zone Temp * Cooling Design Zone Temp

-388.39062 * Heating Design Zone Temp * Temp Difference

-83.26562 * Cooling Design Zone Temp * Temp Difference

H.2.2 The design variables associated with the provision of night ventilation over the cooling period (Group E)

The response surface model correlating the parameters of group E with the annual cooling energy consumption of the VAV system, when this is simulated for the CIBSE TRY, is the following:

(Cooling Energy)^3 =

+2.33049E+015

-5.54280E+013 * Ventilation rate

-1.35457E+014 * Period of ventilation

+2.28902E+012 * Ventilation rate^2

+5.69532E+012 * Period of ventilation^2

The response surface model correlating the parameters of this group with the annual cooling energy consumption of the FCU system, when this is simulated for the CIBSE TRY, is the following:

Cooling Energy =

+2.72540E+005

-1048.86667 * Ventilation rate

-4170.62963 * Period of ventilation

+45.49333 * Ventilation rate^2

+159.87037 * Period of ventilation^2

-28.46667 * Ventilation rate * Period of ventilation

The response surface model correlating the parameters under consideration with the VAV system cooling energy consumption use, when this is simulated for the NOA TRY, is the following:

Cooling Energy =

+3.61814E+005

-879.90000 * Ventilation rate

-2067.49074 * Period of ventilation

+37.33333 * Ventilation rate^2

+85.37037 * Period of ventilation^2

-14.16667 * Ventilation rate * Period of ventilation

The response surface model correlating the parameters of group E with the FCU system cooling energy use, when this is simulated for the NOA TRY, is the following:

Cooling Energy =

+4.67306E+005

-622.23333 * Ventilation rate

-2003.37963 * Period of ventilation

+29.01333 * Ventilation rate^2

+82.20370 * Period of ventilation^2

-19.03333 * Ventilation rate * Period of ventilation

H.2.3 The design variables associated with the plant performance & operation schedule (Group F)

The response surface models correlating the parameters of group F with the annual heating and cooling energy consumption of the VAV system, when this is simulated for the CIBSE TRY, are the following:

Heating Energy =

-4.61798E+005

-1.90825E+005 * Boiler Efficiency

+96272.20179 * HVAC system operation

+3.27721E+005 * Boiler Efficiency^2

-474.39286 * HVAC system operation^2

-49443.75000 * Boiler Efficiency * HVAC system operation

Log_{10}(Cooling Energy) =

+5.61279

-0.27033 * Chiller COP

+5.90844E-003 * HVAC system operation

+0.019412 * Chiller COP^2

-6.62379E-005 * HVAC system operation^2

-5.60331E-008 * Chiller COP * HVAC system operation

The response surface models correlating the parameters of this group with the annual heating and cooling energy consumption of the FCU system, when this is simulated for the CIBSE TRY, are the following:

Heating Energy =

-2.48079E+005

-3.56849E+005 * Boiler Efficiency

+85172.85804 * HVAC system operation

+3.52971E+005 * Boiler Efficiency^2

-559.51786 * HVAC system operation^2

-41601.87500 * Boiler Efficiency * HVAC system operation

Log_{10}(Cooling Energy) =

+5.93930

-0.27033 * Chiller COP

+6.76016E-003 * HVAC system operation

+0.019412 * Chiller COP^2

-1.73472E-004 * HVAC system operation^2

-4.46843E-008 * Chiller COP * HVAC system operation

The response surface models correlating the parameters of group F with the VAV system heating and cooling energy use, when this is simulated for the NOA TRY, are the following:

Heating Energy =

-2.59441E+005

+1.52819E+005 * Boiler Efficiency

+31363.06875 * HVAC system operation

-18474.37500 * Boiler Efficiency * HVAC system operation

1.0/(Cooling Energy) =

+4.70108E-008

+1.32612E-006 * Chiller COP

-7.82352E-009 * HVAC system operation

+3.00888E-010 * HVAC system operation^2

-2.08147E-008 * Chiller COP * HVAC system operation

The response surface models correlating the parameters under consideration with the FCU system heating and cooling energy use, when this is simulated for the NOA TRY, are the following:

Heating Energy =

-1.25370E+005

-79551.55357 * Boiler Efficiency

+29913.70804 * HVAC system operation

+1.02071E+005 * Boiler Efficiency^2

-248.20536 * HVAC system operation^2

-13819.37500 * Boiler Efficiency * HVAC system operation

Log_{10}(Cooling Energy) =

+6.14237

-0.27033 * Chiller COP

+9.64369E-003 * HVAC system operation

+0.019412 * Chiller COP^2

-9.89377E-005 * HVAC system operation^2

-2.53677E-008 * Chiller COP * HVAC system operation

H.2.4 The design variables associated with the fan size & performance (Group G)

The response surface models correlating the parameters of group G with the annual cooling and fan energy consumption of the VAV system, when this is simulated for the CIBSE TRY, are the following:

1.0/(Cooling Energy) =

+6.48574E-006

+8.44148E-006 * Fan Efficiency

-5.24833E-009 * Supply Fan

+5.11592E-010 * Return Fan

-5.10981E-006 * Fan Efficiency^2

+6.99792E-013 * Supply Fan^2

-3.25903E-012 * Return Fan^2

+2.01686E-009 * Fan Efficiency * Supply Fan

+2.02158E-010 * Fan Efficiency * Return Fan

+2.01998E-013 * Supply Fan * Return Fan

(Fan Energy)$^{0.09}$ =

+3.25943

-0.81295 * Fan Efficiency

-0.60931 * Motor Efficiency

+4.61799E-004 * Supply Fan

+5.16935E-004 * Return Fan

+0.31144 * Fan Efficiency^2

+0.17839 * Motor Efficiency^2

-8.28563E-008 * Supply Fan^2

-9.15526E-008 * Return Fan^2

+0.041338 * Fan Efficiency * Motor Efficiency

-2.36354E-005 * Fan Efficiency * Supply Fan

-3.23492E-005 * Fan Efficiency * Return Fan

-2.30188E-005 * Motor Efficiency * Supply Fan

-2.63403E-005 * Motor Efficiency * Return Fan

-1.85502E-007 * Supply Fan * Return Fan

The response surface models correlating the parameters under consideration with the annual cooling and fan energy consumption of the VAV system, when this is simulated for the NOA TRY, are the following:

$(\text{Cooling Energy})^{-1.29}$ =

+7.30763E-008

+5.43841E-008 * Fan Efficiency

-3.20322E-008 * Motor Efficiency

-2.97980E-011 * Supply Fan

-1.29472E-011 * Return Fan

-3.35607E-008 * Fan Efficiency^2

+1.88425E-008 * Motor Efficiency^2

+2.28809E-015 * Supply Fan^2

+1.38331E-011 * Fan Efficiency * Supply Fan

+6.09375E-012 * Fan Efficiency * Return Fan

+2.46898E-015 * Supply Fan * Return Fan

$(\text{Fan Energy})^{0.03}$ =

+2.94089

-0.67117 * Fan Efficiency

-0.48676 * Motor Efficiency

+3.83267E-004 * Supply Fan

+4.21105E-004 * Return Fan

+0.25894 * Fan Efficiency^2

+0.13983 * Motor Efficiency^2

-6.88507E-008 * Supply Fan^2

-7.76300E-008 * Return Fan^2

+0.030491 * Fan Efficiency * Motor Efficiency

-2.11049E-005 * Fan Efficiency * Supply Fan

-2.44161E-005 * Fan Efficiency * Return Fan

-1.70685E-005 * Motor Efficiency * Supply Fan

-1.90944E-005 * Motor Efficiency * Return Fan

-1.52552E-007 * Supply Fan * Return Fan

The response surface model correlating the four parameters of group G with the FCU system fan energy use, when this is simulated for the CIBSE TRY, is the following:

1.0/Sqrt(Fan Energy) =

+2.24700E-003

+1.23221E-003 * Fan Efficiency

+3.52131E-004 * Motor Efficiency

-9.54149E-007 * Supply Fan

-9.37226E-007 * Return Fan

-5.84536E-004 * Fan Efficiency^2

+7.24580E-011 * Supply Fan^2

-3.31855E-004 * Fan Efficiency * Motor Efficiency

+3.48164E-007 * Fan Efficiency * Supply Fan

+3.57919E-007 * Fan Efficiency * Return Fan

+2.61761E-007 * Motor Efficiency * Supply Fan

+2.69444E-007 * Motor Efficiency * Return Fan

+1.69695E-010 * Supply Fan * Return Fan

The response surface model correlating the four parameters of this group with the FCU system fan energy use, when this is simulated for the NOA TRY, is the following:

1.0/Sqrt(Fan Energy) =

+2.16707E-003

+1.08971E-003 * Fan Efficiency

+3.08928E-004 * Motor Efficiency

-8.38794E-007 * Supply Fan

-8.29462E-007 * Return Fan

-5.21433E-004 * Fan Efficiency^2

+5.24599E-011 * Supply Fan^2

-3.05746E-004 * Fan Efficiency * Motor Efficiency

+3.22282E-007 * Fan Efficiency * Supply Fan

+3.26385E-007 * Fan Efficiency * Return Fan

+2.40511E-007 * Motor Efficiency * Supply Fan

+2.46272E-007 * Motor Efficiency * Return Fan

+1.36026E-010 * Supply Fan * Return Fan

H.2.5 The design variables associated with the humidification of the supply air quantity (Group H)

The response surface models[27] correlating the parameters of group H with the humdification energy consumption of the VAV system, when this is simulated for the CIBSE TRY, are the following:

Period of Humidification Heating Season

Sqrt(Humidification Energy) =

-524.60961

+22.42930 * Humidification Setpoint

+4.45312 * Proportional Band

-0.079781 * Humidification Setpoint^2

-0.14887 * Proportional Band^2

-0.027435 * Humidification Setpoint * Proportional Band

Period of Humidification All Year

Sqrt(Humidification Energy) =

-789.89549

+31.67639 * Humidification Setpoint

+8.47741 * Proportional Band

-0.079781 * Humidification Setpoint^2

-0.14887 * Proportional Band^2

-0.027435 * Humidification Setpoint * Proportional Band

[27] **Note:** The reason for the development of two regression models (instead of one) is that the period of humidification (factor C) is treated as a categorical factor, which means that it takes a certain number of discrete levels (two levels in this case). Therefore, the first model is valid when humidification is provided for the heating season, while the second model is used when the humidifier operates throughout the year.

The response surface models correlating the parameters of of this group with the humdification energy consumption of the FCU system, when this is simulated for the CIBSE TRY, are the following:

Period of Humidification Heating Season

$(\text{Humidification Energy})^{0.39}$ =

-201.19820

+10.06897 * Humidification Setpoint

+0.81070 * Proportional Band

-0.086854 * Humidification Setpoint^2

-0.011088 * Proportional Band^2

-0.013194 * Humidification Setpoint * Proportional Band

Period of Humidification All Year

$(\text{Humidification Energy})^{0.39}$ =

-225.58627

+10.83044 * Humidification Setpoint

+1.00182 * Proportional Band

-0.086854 * Humidification Setpoint^2

-0.011088 * Proportional Band^2

-0.013194 * Humidification Setpoint * Proportional Band

The response surface models correlating the parameters under consideration with the VAV system humdification energy use, when this is simulated for the NOA TRY, are the following:

Period of Humidification Heating Season

$(\text{Humidification Energy})^{0.17}$ =

-1.34214

+0.24474 * Humidification Setpoint

-6.89976E-003 * Proportional Band

-1.76416E-003 * Humidification Setpoint^2

-1.83620E-004 * Proportional Band^2

+2.55855E-004 * Humidification Setpoint * Proportional Band

Period of Humidification All Year

$(\text{Humidification Energy})^{0.17}$ =

-1.25545

+0.24853 * Humidification Setpoint

-1.44635E-005 * Proportional Band

-1.76416E-003 * Humidification Setpoint^2

-1.83620E-004 * Proportional Band^2

+2.55855E-004 * Humidification Setpoint * Proportional Band

The response surface models correlating the parameters of group H with the FCU system humdification energy use, when this is simulated for the NOA TRY, are the following:

Period of Humidification Heating Season

$(\text{Humidification Energy})^{0.44}$ =

-306.30361

+14.31574 * Humidification Setpoint

-0.37066 * Proportional Band

-0.11000 * Humidification Setpoint^2

-0.017631 * Proportional Band^2

+0.020324 * Humidification Setpoint * Proportional Band

Period of Humidification All Year

$(\text{Humidification Energy})^{0.44}$ =

-328.15294

+15.06038 * Humidification Setpoint

+0.052142 * Proportional Band

-0.11000 * Humidification Setpoint^2

-0.017631 * Proportional Band^2

+0.020324 * Humidification Setpoint * Proportional Band

H.3 Summary statistics and evaluation results for all the response surface models

Table H.3-1 contains a few summary statistics for all the regression models[28] presented in sections H.1 and H.2. The type of response surface design and the number of design points [29] used to develop each model, as well as the transformation of the response variable Y (wherever this was necessary) is also displayed in this table.

Some of the terms shown in table H.3-1 are briefly explained in the following:

Type of model: As shown in sections H.1 and H.2, a quadratic or a 2FI (i.e. first-order plus two factor interactions) model was used in most cases. A cubic model was required only in one case[30]. The final models presented in table H.3-1, (and also shown in full detail in sections H.1 and H.2), involved the highest Pred-R^2 and the lowest PRESS, while they also displayed the best performance during the validation process.

Transformation of Y [1]: A mathematical conversion of the response value Y. In general, transformations are used in order to (a) stabilize the variance of the response, (b) make the distribution of the response variable closer to the normal distribution and (c) improve the fit of the model to the data. Sometimes a transformation is able to simultaneously accomplish more than one of the above objectives. The Box-Cox plot [1], [2] (produced by Design – Expert) was used in order to choose the transformations shown in table H.3-1.

PRESS [2], [3]: Predicted Residual Error Sum of Squares – A measure of how well the model fits each point in the design. The PRESS is computed by first predicting where each point should be from a model that contains all other points except the one in question. The squared residuals (i.e. the differences between the actual and the predicted values) are then summed. The smaller the PRESS statistic is, the better the predictability of the model. In other words, the objective is to minimize PRESS when evaluating alternative predictive models.

Predicted R-Squared [2], [3]: A measure of the amount of variation in new data explained by the model. It makes use of PRESS as shown in the following equation: Pred R-Squared = 1-(PRESS / SS_{total}), where SS_{total} is the total sum of squares, i.e. the sum of the squared differences between the response values and the overall mean. The closer this number is to 1.0, the better.

---

[28] **Note:** The regression models developed in the thesis are also known as 'metamodels', which are approximations of the detailed computer analysis code (TAS in this case) [3], as explained in section 3.2.3 in chapter 3.

[29] **Note:** It should be remembered that details regarding the Response Surface Methodology used in this study can be found in chapter 3.

[30] **Note:** A cubic model was used to approximate the relationship between the three parameters related to the temperature control set-points (group D) and the annual heating & cooling energy consumption of the VAV system, when this was simulated for the CIBSE TRY, as illustrated in section H2.1.

The validity of each of the fitted regression models was tested by running TAS for some additional combinations of the input variables[31], (different to the original set of design points), and then comparing the simulation output ($y_{TAS,i}$) with the predictions of the fitted regression model ($y_{M,i}$), using the following three model accuracy measures:

Average Absolute Error $= \dfrac{\sum_{i=1}^{n} | y_{M,i} - y_{TAS,i} | / y_{TAS,i}}{n}$, where n is the number of evaluation runs (i.e. TAS simulations).

Maximum Absolute Error $= \max \left(\dfrac{| y_{M,i} - y_{TAS,i} |}{y_{TAS,i}} \right)$

Root Mean Square Error (RMSE) $= \sqrt{\dfrac{\sum_{i=1}^{n} (y_{M,i} - y_{TAS,i})^2}{n}}$

The final response surface models displayed in table H.3-1 involved the lowest values for all three statistics described above.

[31] **Note:** The number of validation runs (i.e. TAS simulations) carried out to evaluate each model is also displayed in table H3-1.

	Group of Factors	Weather file	HVAC system	Summary statistics for the fitted regression models							Model evaluation			
				Response Variable (Y)	Response Surface Design	Number of design points (TAS simulations)	Type of Model	Transformation of Y	Predicted Rsquared	PRESS	Number of evaluation runs (TAS simulations)	Average Absolute Error (%)	Maximum Absolute Error (%)	RMSE
Building Level related parameters	Solar Gains	CIBSE TRY (London)	VAV	Heating Energy	Face Centered Design	25	Quadratic	Inverse Square Root	0.9934	1.65E-08	10	0.82%	1.64%	1242.8
				Cooling Energy	Face Centered Design	25	Quadratic	Power = 0.23	0.9960	0.069	10	1.23%	2.59%	2021.8
			FCU	Heating Energy	Face Centered Design	25	Quadratic	Inverse	0.9345	9.203E-14	10	0.41%	1.38%	912.1
				Cooling Energy	Face Centered Design	25	2FI	Log	0.9963	1.208E-03	10	1.22%	3.08%	4215.0
		NOA TRY (Athens)	VAV	Heating Energy	Face Centered Design	25	Quadratic	Log	0.9961	2.509E-03	10	1.59%	5.03%	650.2
				Cooling Energy	Face Centered Design	25	Quadratic	Log	0.9964	7.196E-04	10	0.84%	1.44%	3178.7
			FCU	Heating Energy	Face Centered Design	25	2FI	Power = -0.85	0.9931	6.472E-11	10	0.97%	2.80%	571.4
				Cooling Energy	Face Centered Design	25	Quadratic	Power = -0.14	0.9961	2.561E-06	10	0.93%	1.80%	4787.6
	Building Envelope	CIBSE TRY (London)	VAV	Heating Energy	Face Centered Design	15	Quadratic	Power = 0.63	0.9999	652.71	8	0.61%	1.26%	1431.0
				Cooling Energy	Face Centered Design	15	Quadratic	Inverse	0.9960	3.585E-14	8	0.48%	1.29%	768.0
			FCU	Heating Energy	Face Centered Design	15	Quadratic	Power = 0.20	0.9997	3.179E-03	8	0.25%	0.91%	866.4
				Cooling Energy	Face Centered Design	15	Quadratic	Inverse	0.9915	3.29E-14	8	0.43%	1.07%	1213.2
		NOA TRY (Athens)	VAV	Heating Energy	Face Centered Design	16	Quadratic	Power = 0.68	0.9999	894.16	8	0.86%	2.83%	465.9
				Cooling Energy	Face Centered Design	15	Quadratic	Power = -1.97	0.9817	2.01E-25	8	0.40%	0.94%	1734.4
			FCU	Heating Energy	3-Level Factorial	27	Quadratic	Power = 0.85	0.9997	1.50E+05	8	0.47%	0.99%	234.9
				Cooling Energy	3-Level Factorial	27	Quadratic	None	0.9733	4.34E+08	8	0.43%	1.25%	2614.6
	Internal Heat Gains	CIBSE TRY (London)	VAV	Heating Energy	Face Centered Design	15	Quadratic	Power = -0.72	0.9962	6.037E-11	8	1.80%	2.67%	2386.5
				Cooling Energy	Face Centered Design	15	Quadratic	Power = 0.99	0.9999	7.98E+05	8	1.52%	3.09%	2640.2
			FCU	Heating Energy	Face Centered Design	15	Quadratic	Power = -2.18	0.8656	1.79E-24	8	0.97%	4.55%	2866.8
				Cooling Energy	Face Centered Design	15	Quadratic	Square Root	0.9995	49.28	8	2.19%	4.37%	7971.8
		NOA TRY (Athens)	VAV	Heating Energy	Face Centered Design	15	Quadratic	Power = -1.99	0.9633	1.08E-19	8	0.81%	1.39%	257.3
				Cooling Energy	Face Centered Design	15	Quadratic	Power = 0.82	0.9999	2125B.14	8	1.31%	2.65%	6288.0
			FCU	Heating Energy	Face Centered Design	15	Quadratic	Power = -2.44	0.9130	9.526E-25	8	0.37%	0.81%	186.9
				Cooling Energy	Face Centered Design	15	Quadratic	Square Root	0.9996	30.62	8	1.53%	3.09%	9304.9
HVAC system related parameters	Temperature Control Setpoints	CIBSE TRY (London)	VAV	Heating Energy	D-optimal	33	Cubic	Inverse	0.9999	2.54E-14	10	0.16%	0.38%	243.5
				Cooling Energy	D-optimal	33	Cubic	Inverse	0.9954	2.76E-12	10	2.09%	6.37%	6081.0
			FCU	Heating Energy	Face Centered Design	15	Quadratic	Power=0.23	0.9995	0.017	8	0.34%	0.78%	1080.8
				Cooling Energy	Face Centered Design	15	Quadratic	None	0.9819	5.59E+08	8	0.56%	1.41%	2106.4
		NOA TRY (Athens)	VAV	Heating Energy	Face Centered Design	15	Quadratic	Log	0.9998	0.014	8	1.55%	2.53%	606.7
				Cooling Energy	Face Centered Design	15	2FI	Inverse Square Root	0.9736	1.16E-08	8	0.96%	2.34%	4615.7
			FCU	Heating Energy	Face Centered Design	15	Quadratic	Power=0.21	0.9995	0.017	8	0.88%	1.89%	925.1
				Cooling Energy	Face Centered Design	15	Quadratic	None	0.9616	1.58E+09	8	0.58%	1.08%	3289.1
	Night Ventilation	CIBSE TRY (London)	VAV	Cooling Energy	Face Centered Design	9	Quadratic	Power = 3	0.9996	2.59E+26	8	0.07%	0.13%	85.8
			FCU	Cooling Energy	Face Centered Design	9	Quadratic	None	0.9991	2.75E+05	8	0.03%	0.05%	74.9
		NOA TRY (Athens)	VAV	Cooling Energy	Face Centered Design	9	Quadratic	None	0.9934	3.96E+05	8	0.01%	0.01%	34.5
			FCU	Cooling Energy	Face Centered Design	9	Quadratic	None	0.9995	1.12E+05	8	0.00%	0.01%	20.6
	Plant Operation and Performance	CIBSE TRY (London)	VAV	Heating Energy	Face Centered Design	15	Quadratic	None	0.9999	3.07E+07	8	0.91%	2.94%	1186.0
				Cooling Energy	Face Centered Design	16	Quadratic	Log	1.0000	3.14E-11	8	0.50%	1.87%	815.3
			FCU	Heating Energy	Face Centered Design	15	Quadratic	None	0.9999	2.45E+07	8	0.82%	1.49%	1382.2
				Cooling Energy	Face Centered Design	15	Quadratic	Log	1.0000	3.28E-12	8	0.59%	1.73%	2221.7
		NOA TRY (Athens)	VAV	Heating Energy	Face Centered Design	15	2FI	None	0.9998	7.88E+06	8	2.23%	4.79%	965.9
				Cooling Energy	Face Centered Design	15	Quadratic	Inverse	1.0000	1.79E-17	8	0.06%	0.19%	369.0
			FCU	Heating Energy	Face Centered Design	15	Quadratic	None	0.9999	3.19E+06	8	0.86%	2.16%	364.6
				Cooling Energy	Face Centered Design	15	Quadratic	Log	1.0000	1.97E-12	8	0.58%	1.67%	3608.9
	Fan Size and Performance	CIBSE TRY (London)	VAV	Cooling Energy	Face Centered Design	25	Quadratic	Inverse	0.9986	5.43E-14	8	0.46%	1.04%	735.0
				Fan Energy	Face Centered Design	26	Quadratic	Power = 0.09	0.9994	2.33E-04	8	0.66%	1.45%	834.1
			FCU	Cooling Energy	-	-	-	-	-	-	8	-	-	-
				Fan Energy	Face Centered Design	26	Quadratic	Inverse Square Root	0.9961	1.97E-09	8	0.26%	0.82%	479.1
		NOA TRY (Athens)	VAV	Cooling Energy	Face Centered Design	25	Quadratic	Power = -1.29	0.9991	1.56E-18	8	0.23%	0.62%	1220.7
				Fan Energy	Face Centered Design	26	Quadratic	Power = 0.08	0.9994	1.56E-04	8	0.83%	2.17%	1395.5
			FCU	Cooling Energy	-	-	-	-	-	-	8	-	-	-
				Fan Energy	Face Centered Design	26	Quadratic	Inverse Square Root	0.9962	1.47E-09	8	0.26%	0.83%	639.6
	Humidification	CIBSE TRY (London)	VAV	Humidification Energy	Face Centered Design	18	Quadratic	Square Root	0.9999	39.31	8	0.19%	0.59%	428.9
			FCU	Humidification Energy	Face Centered Design	18	Quadratic	Power = 0.39	0.9999	0.32	8	1.36%	2.30%	1364.6
		NOA TRY (Athens)	VAV	Humidification Energy	Face Centered Design	18	Quadratic	Power = 0.16	0.9995	4.17E-03	8	0.61%	1.34%	1817.1
			FCU	Humidification Energy	Face Centered Design	18	Quadratic	Power = 0.44	0.9997	2.84	8	1.23%	2.84%	862.1

Table H.3-1: Summary statistics and evaluation results for the fitted regression models

References

[1] R.H. Myers, D.C. Montgomery, Response Surface Methodology: Process and Product Optimization Using Designed Experiments, Second Edition, 2002

[2] Design-Expert version 6 User's Guide, Stat-Ease (2000)

[3] R Mark J. Anderson & Patrick J. Whitcomb, RSM Simplified: Optimizing Processes Using Response Surface Methods for Design of Experiments, Productivity Press, 2005

Appendix I: The response surface models describing the relationship between the design variables of group A and the daylight performance of the perimeter zones of the building

The parameters related to the solar gains through the transparent building elements (group A) are correlated with the average and the minimum daylight factor (DF) of the perimeter zones of the building, respectively, in order to assess their effect on the daylight levels inside the case study building. The optimization process (carried out in Design-Expert) is then repeated taking into consideration both the energy consumption of the HVAC systems and the daylight performance of the perimeter zones of the building, as shown in section 5.2.1-1 (chapter 5). The process that is followed in order to model the relationship between the parameters of this group and the daylight performance of the building is described in this appendix.

The independent variables classified in group A include the glazing percentage, the TSC of the windows[32] and the depth of both the overhangs & the side-fins. The response variables are the average DF and the minimum DF of the perimeter zones of the building, which are shown in figure I-1, for a typical floor:

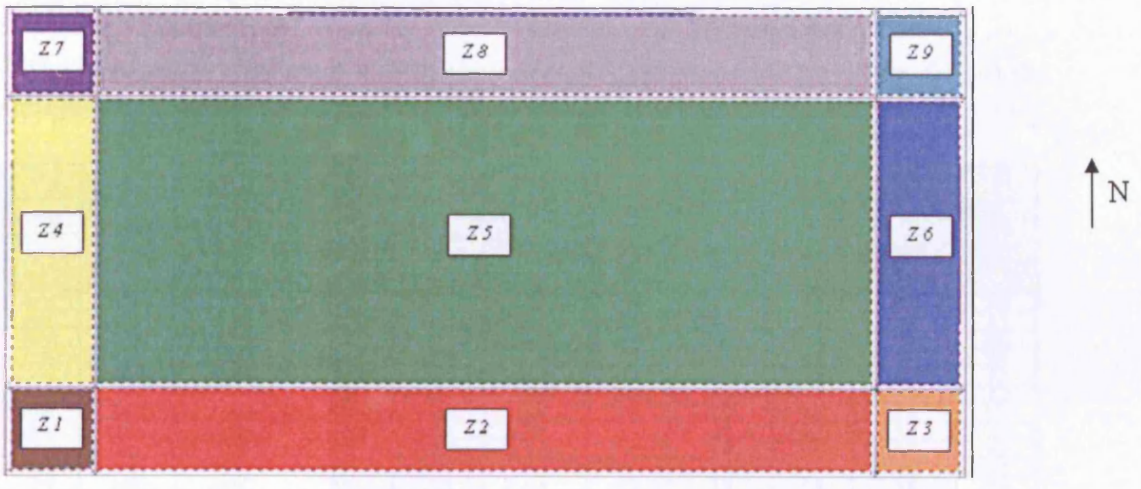

Figure I-1: The 8 perimeter zones and the single core zone for a typical floor plan[33] of the case study building

The four parameters mentioned above are correlated with the average & minimum DF of zone 1 (or 3, 7, 9), zone 4 (or 6) and zone 2 (or 8)[34], respectively, so six response surface models are developed in total. A Face Centered Design[35] is used to generate the data required for the development of

[32] **Note:** The TSC coefficient of the windows is assumed to be equal to the light transmission of the glass, as explained in section 5.2.1-1, (chapter 5).
[33] **Note:** The zone numbers displayed in this figure refer to the ground floor of the building.
[34] **Note:** As also mentioned in section 5.2.1-1, the zone(s) inside the parentheses have the same daylight performance as the respective zone outside the parenthesis. It should also be stressed that zones 4 & 6 are smaller than zones 2 & 8 (i.e. the depth and height is the same for all the perimeter zones of the building, but the width of zones 2 & 8 is greater than the width of zones 4 & 6). As a result, the daylight performance of these zones differs.
[35] **Note:** Details concerning the Response Surface Methodology used in this study can be found in chapter 3.

these models in an organized way. The factor levels for each design point are determined by Design Expert. The response variables for each of these design points are estimated using the Daylight software - version 4.1, which was developed by the Construction Systems Development Group at Anglia Higher Education College. This program is capable of analyzing the daylight behaviour within relatively simple architectural spaces taking into consideration a number of factors including the position, the size and the light transmission of windows and rooflights, the reflectances of the walls and the ceiling, the presence of internal obstructions, etc. Moreover, it is possible to simulate the effect of external obstructions, (such as other buildings located in the same site), in terms of position, size and reflectance [1]. The program divides the room into a grid of rectangles and calculates the daylight factor for a reference point in the centre of each rectangle at a height determined by the working plane (taken at 0.85 m). Besides the average DF, the Daylight software provides the ratio of min / max DF and the uniformity ratio[36], which is expressed as the ratio of the minimum to the average DF. It is also worth mentioning that the accuracy of this program was tested by comparing the software outputs with actual measurements taken in Maylandsea County Primary School in Essex, as well as with measurements taken in a physical model of this school tested under an artificial sky. Good correlation was found between the maximum and average daylight factors in all cases [1]. More details concerning the scientific basis as well as the evaluation of the program can be found in reference [1].

The average & minimum DF of the perimeter zones of the building, for all the simulations carried out in the Daylight software, are shown in table I-1:

Design Point Type	Independent Variabels				Response Variables					
					ZONE 1 (or 3, 7, 9)		ZONE 2 (or 8)		ZONE 4 (or 6)	
	Glazing Ratio (0 - 1)	TSC = Light Transmittance	Overhang Depth (m)	Sidefin Depth (m)	AVERAGE DF (%)	Min DF (%)	AVERAGE DF (%)	Min DF (%)	AVERAGE DF (%)	Min DF (%)
Axial	0.60	0.52	0.0	1.0	6.9	1.5	5.3	1.8	4.2	0.9
Fact	0.25	0.16	2.0	2.0	0.6	0.2	0.3	0.1	0.4	0.1
Axial	0.60	0.52	1.0	2.0	5.2	1.4	3.2	1.5	4.2	0.9
Fact	0.25	0.88	2.0	0.0	4.6	1.5	1.5	0.7	3.3	0.9
Axial	0.60	0.52	1.0	0.0	6.9	2.1	3.2	1.5	5.1	1.5
Fact	0.95	0.88	0.0	2.0	14.4	3.6	12.1	4.8	9.3	2.3
Axial	0.60	0.52	2.0	1.0	4.4	1.3	2.3	1.4	4.2	0.9
Axial	0.25	0.52	1.0	1.0	2.5	0.7	1.2	0.4	1.4	0.3
Fact	0.25	0.88	0.0	0.0	6.4	1.8	3.3	0.8	3.3	0.9
Fact	0.25	0.88	2.0	2.0	3.5	1.1	1.5	0.7	2.2	0.4
Fact	0.25	0.88	0.0	2.0	5.4	1.3	3.3	0.8	2.2	0.4
Fact	0.95	0.16	2.0	0.0	2.5	0.9	1.1	0.7	2.1	0.7
Axial	0.60	0.16	1.0	1.0	1.6	0.4	1.0	0.5	1.3	0.3
Fact	0.95	0.16	0.0	0.0	3.4	1.0	2.2	0.9	2.1	0.7
Axial	0.95	0.52	1.0	1.0	6.6	1.9	4.7	2.4	5.6	1.4
Fact	0.95	0.88	2.0	2.0	9.4	3.0	5.8	3.6	9.3	2.3
Fact	0.95	0.16	0.0	2.0	2.6	0.7	2.2	0.9	1.7	0.4
Fact	0.95	0.16	2.0	2.0	1.7	0.6	1.1	0.7	1.7	0.4
Fact	0.25	0.16	0.0	2.0	1.0	0.2	0.6	0.1	0.4	0.1
Fact	0.95	0.88	0.0	0.0	18.9	5.4	12.1	4.8	11.5	3.9
Axial	0.60	0.88	1.0	1.0	8.7	2.3	5.4	2.6	7.1	1.5
Fact	0.25	0.16	2.0	0.0	0.8	0.3	0.3	0.1	0.6	0.2
Fact	0.25	0.16	0.0	0.0	1.2	0.3	0.6	0.1	0.6	0.2
Fact	0.95	0.88	2.0	0.0	13.9	4.9	5.8	3.6	11.5	3.9
Center	0.60	0.52	1.0	1.0	5.2	1.4	3.2	1.5	4.2	0.9

Table I-1: The average and minimum DF of the perimeter zones of the building, for all the simulations carried out in the Daylight software

[36] **Note:** The uniformity ratio is a measure of the distribution of daylight and the quality of the lighting environment. In general, this factor should be equal or higher than 0.30, so that the daylight is considered reasonably uniform [1].

An example of the Daylight software output for zone 1, when the parameters of group A take the values determined by the first design point of table I-1, is shown in figure I-2:

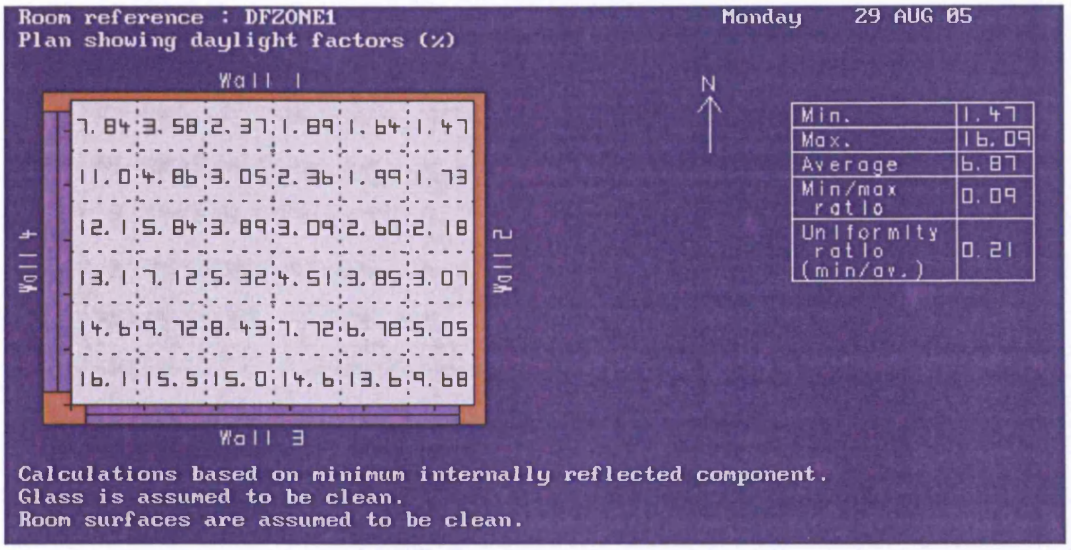

Figure I-2: Average and minimum daylight factor for zone 1, when the four parameters of group A are set to the values shown in the first design point of table I-1, as estimated by the Daylight software

The Daylight software predictions for all the design points illustrated in table I-1 are then input into Design-Expert which carries out step-by-step statistical analysis, suggesting which type of regression model provides best fit for the data.

For example, the response surface models correlating the four parameters of group A with the average and minimum DF of zone 1, respectively, are the following:

$$(\text{ZONE 1 AVR DF})^{-0.04} =$$

$$\begin{aligned}
&+1.05691 \\
&-0.15656 * \text{Glazing Percentage} \\
&-0.19811 * \text{TSC} \\
&+0.010459 * \text{Overhang Depth} \\
&+0.013134 * \text{Sidefin Depth} \\
&+0.079389 * \text{Glazing Percentage}^2 \\
&+0.10187 * \text{TSC}^2 \\
&-1.72815\text{E-}003 * \text{Overhang Depth}^2 \\
&-5.14405\text{E-}003 * \text{Sidefin Depth}^2 \\
&+5.33067\text{E-}003 * \text{Glazing Percentage} * \text{TSC} \\
&-7.05925\text{E-}004 * \text{Glazing Percentage} * \text{Overhang Depth} \\
&+2.78480\text{E-}003 * \text{Glazing Percentage} * \text{Sidefin Depth} \\
&-6.14433\text{E-}004 * \text{TSC} * \text{Overhang Depth} \\
&-5.06630\text{E-}004 * \text{TSC} * \text{Sidefin Depth} \\
&+9.95560\text{E-}004 * \text{Overhang Depth} * \text{Sidefin Depth}
\end{aligned}$$

(Pred-R^2 = 0.9987, PRESS = 3.641E-005) [37]

$$(\text{ZONE 1 MIN DF})^{-0.02} =$$

$$\begin{aligned}
&+1.05291 \\
&-0.068556 * \text{Glazing Percentage} \\
&-0.10124 * \text{TSC} \\
&+2.00662\text{E-}003 * \text{Overhang Depth} \\
&+0.011378 * \text{Sidefin Depth} \\
&+0.030000 * \text{Glazing Percentage}^2 \\
&+0.051455 * \text{TSC}^2 \\
&-1.65284\text{E-}004 * \text{Overhang Depth}^2 \\
&-4.26841\text{E-}003 * \text{Sidefin Depth}^2 \\
&+1.48476\text{E-}003 * \text{Glazing Percentage} * \text{TSC} \\
&-6.61612\text{E-}004 * \text{Glazing Percentage} * \text{Overhang Depth} \\
&+1.54032\text{E-}003 * \text{Glazing Percentage} * \text{Sidefin Depth} \\
&-1.47022\text{E-}004 * \text{TSC} * \text{Overhang Depth} \\
&-3.43919\text{E-}004 * \text{TSC} * \text{Sidefin Depth} \\
&+3.54537\text{E-}004 * \text{Overhang Depth} * \text{Sidefin Depth}
\end{aligned}$$

(Pred-R^2 = 0.9993, PRESS = 5.568E-006)

[37] **Note:** The definitions of the Pred-R^2 and PRESS statistics shown in the parenthesis are given in section H.3.

As mentioned earlier, the six response surface models developed through the procedure described in this appendix along with the models approximating the relationship between the parameters of group A and the energy consumption of the FCU system and the VAV system respectively, depending on the climate under consideration, are finally used by Design-Expert to identify the combinations of factor levels optimizing both the daylight performance of the building and the energy/carbon performance of the HVAC systems. The simultaneous optimization technique developed by Derringer and Suich is used to this end, as explained in section 3.2.2, chapter 3.

The model predictions are compared with the Daylight software results for the combinations of factor levels keeping both the daylight performance of the building and the carbon performance of the HVAC systems as close to their optimum level as possible[38], in table I-2, as an example:

Climate	HVAC system	Daylight software and model predictions	Factor levels				Perimeter zones daylight factors (DF)					
			Glazing Ratio (0 -1)	Total Shading Coefficient	Overhang Depth (m)	Sidefin Depth (m)	Zone 1 AVG DF (%)	Zone 1 MIN DF (%)	Zone 4 AVG DF (%)	Zone 4 MIN DF (%)	Zone 2 AVG DF (%)	Zone 2 MIN DF (%)
CIBSE TRY	VAV system	Daylight software predictions	*0.25*	*0.76*	*0.7*	*0.0*	4.7	1.4	2.9	0.8	2.0	0.6
		Model Predictions	*0.25*	*0.76*	*0.7*	*0.0*	4.9	1.5	2.9	0.8	2.1	0.7
	FCU system	Daylight software predictions	*0.40*	*0.37*	*0.0*	*0.0*	4.3	1.1	2.5	0.7	2.6	0.8
		Model Predictions	*0.40*	*0.37*	*0.0*	*0.0*	3.8	1.0	2.2	0.7	2.1	0.6
NOA TRY	VAV system	Daylight software predictions	*0.25*	*0.68*	*0.5*	*0.0*	4.4	1.3	2.6	0.7	2.0	0.6
		Model Predictions	*0.25*	*0.68*	*0.5*	*0.0*	4.6	1.4	2.6	0.7	2.1	0.6
	FCU system	Daylight software predictions	*0.95*	*0.16*	*0.0*	*0.0*	3.4	1.0	2.1	0.7	2.2	0.9
		Model Predictions	*0.95*	*0.16*	*0.0*	*0.0*	3.5	1.0	2.1	0.7	2.2	0.9

Table I-2: Comparison of the model predictions with the Daylight software results for the combinations of factor levels optimising both the daylight performance of the building and the carbon performance of the HVAC systems

As can be seen from table I-2, the predictions of the regression models are clearly in line with the Daylight software results.

References

[1] Birch, S., I. Frame. 1991, The Use and Evaluation of a Computer Program for the Investigation of the Daylight and Sunlight Performance of Buildings. Proceedings of Building Simulation '91: 139-144.

[38] **Note:** The HVAC system energy consumption / carbon emissions and the daylight performance of the building for the optimum combinations of factor levels are presented in table 5.2.1-4, section 5.2.1-1 (chapter 5).

Appendix J: The simulation of plant Optimum Start in TAS

A-TAS allows for the simulation of plant Optimum Start using a number of parameters specified in *Plant and Controls*. The operation of the Optimum Start controller is illustrated in figure J-1:

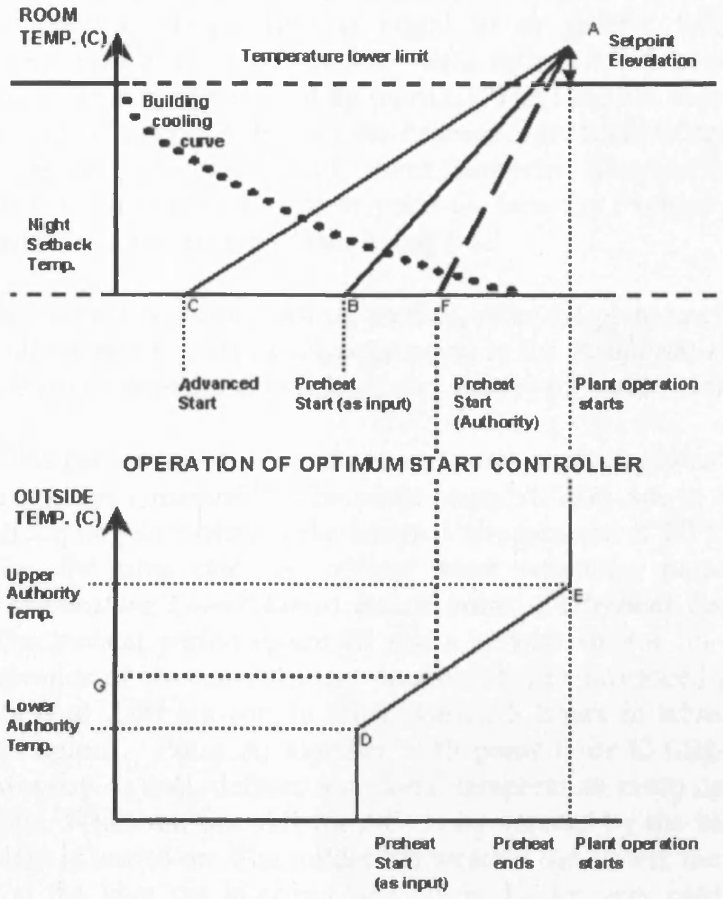

Figure J-1: The operation of the Optimum Start controller in A-TAS [1]

The parameters displayed in this figure are briefly described in the following [1]:

Preheat Start: This is the time corresponding to point B shown in figure J-1. This point represents the start of the preheat period for all days except Mondays.

Advanced Start: This is the time corresponding to point C shown in figure J-1. It represents the start of the preheat period for Mondays.

Night Setback Temperature: This is the temperature set-point that the heating plant attempts to maintain during hours that the plant would otherwise be off.

Lower and Upper Authority Temperatures: The values of these two parameters along with the value of a third factor called *External Authority* represent the influence of the outside air temperature on the *Preheat Start* (or the *Advanced*

Start) time. The *External Authority* takes values between 0 and 1. Lightweight buildings are more responsive to the external climate, and, therefore, need a higher setting for this parameter. Heavyweight buildings, on the other hand, have a large amount of thermal mass and, hence, require a lower setting for *External Authority* as they are less influenced by the external conditions. Assuming the *External Authority* has been set to 1 then figure J-1 works likes this: When the outside temperature is equal to or less than the *Lower Authority Temperature*, the *Preheat Start* time remains unchanged. (This is represented by point D). When the outside temperature is equal to or greater than the *Upper Authority Temperature*, the *Preheat Start* time moves to an hour before plant operation time. (This is represented by point E). The Line DE represents the effect that the outside temperature has on the *Preheat Start* time, when the outside temperature is between the *Lower* and *Upper Authority Temperatures*. For example, if the outside air temperature is at point G, then the *Preheat Start* time will move to point F, as can be seen from figure J-1.

Set-point Elevation: During preheat, after the plant has been turned on, the zone will attempt to attain a set-point equal to the *Temperature Lower Limit* defined in the zone's *Internal Conditions*, elevated by the value of this parameter.

The parameters described above are set accordingly to the recommendations of the A-TAS manual[39]. The plant starts at 7:00 am in the case study building, attempting to maintain the internal temperature at 20°C. These two parameters (i.e. the time that the normal plant operating period starts and the zone *Temperature Lower Limit*) define point A (*Preheat End*), shown in figure J-1. The preheat period (point B) starts at 4:00 am (or, in other words, 3 hours in advance of the normal plant operation). The advanced preheat period (point C) starts at 2:00 am (or, in other words, 5 hours in advance of the normal plant operation). Point A, together with point B or C (depending on whether it is Monday or not), defines a notional temperature ramp determining the plant start time. When the line AB (or AC) is intersected by the building cooling curve the plant is turned on. The milder the weather the slower the building will cool down and the later the interrupt will occur. Under very cold external conditions the building may cool down to the *Night Setback Temperature*[40] before *Advanced Start* or *Preheat Start* times. In these circumstances the *Night Setback* will be brought on until either point B or C is reached and the preheat period begins.

Having specified the parameters described above, the heating plant is sized in the *Design Day* simulation mode. In such a case, A-TAS carries out a building simulation for one or more *Design Days*[41] specified by the user to test the limits of the plant performance. The *Design Day* is run repeatedly until the sized plant no longer changes. This gives enough capacity to heat the zones so that they just reach the desired temperature set-point before the normal plant operating period

---

[39] **Note:** It is worth mentioning that the *External Authority* was set to 0.4, since the case study building is fairly heavyweight. The simulations were also carried out for an *External Authority* of 0.3, but the results were approximately the same.

[40] **Note:** The *Night Setback Temperature* is automatically set by the program to the lowest temperature that the *Optimum Start Control Zone,* (i.e. the zone where the internal sensor controlling the Optimum Start operation is situated), fell to in the A-TAS *Design Day* simulation mode.

[41] **Note:** The chosen *Design Day* for the simulations carried out in this appendix was February 14th, which is the day with the lowest external temperature in CIBSE TRY.

starts. The size of the plant is then fixed to the value estimated in the *Design Day* simulation and the building is simulated using the same Optimum Start settings for a full year. The Building Simulation Output (BSO) file produced by A-TAS is finally input into B-TAS in order to estimate the energy consumption of the HVAC system (i.e. the FCU system or the VAV system).

The hourly values of zone temperatures and sensible loads which were estimated in A-TAS (using Optimum Start) are passed to B-TAS through the BSO file, along with the plant operation or internal gain schedules and other information required to drive the simulation of the HVAC system designed in detail in B-TAS. However, since there are not any input parameters associated with Optimum Start available in B-TAS, (e.g. preheat & advanced start time, lower and upper authority temperature, night setback temperature, etc), it is not possible to manually specify this aspect of the plant operation nor is it clear whether the Optimum Start parameters specified in A-TAS are automatically transferred to B-TAS through the BSO file.

It was, therefore, decided to study the hourly values of the zone internal temperature during a winter day and check if the plant behaviour is the same in both programs. The air temperature in the *Optimum Start Control Zone* for February 14th (the coldest day of the simulation year) estimated using first the generic HVAC system model specified in A-TAS and then the detailed FCU system model designed in B-TAS, is presented in figure J-2:

Hour	A-TAS Internal Temperature	B-TAS Internal Temperature
1	12.2	12.2
2	12.1	12.1
3	12.0	12.0
4	11.9	11.9
5	17.9	11.5
6	19.4	11.2
7	20.0	11.1
8	20.0	20.0
9	20.0	20.0
10	20.0	20.0
11	20.0	20.3
12	20.0	20.9
13	20.0	21.5
14	20.0	21.3
15	20.0	21.2
16	20.0	21.1
17	20.0	20.9
18	15.6	15.9
19	14.3	14.3
20	13.6	13.6
21	13.3	13.2
22	13.0	12.9
23	12.9	12.8
24	12.8	12.7

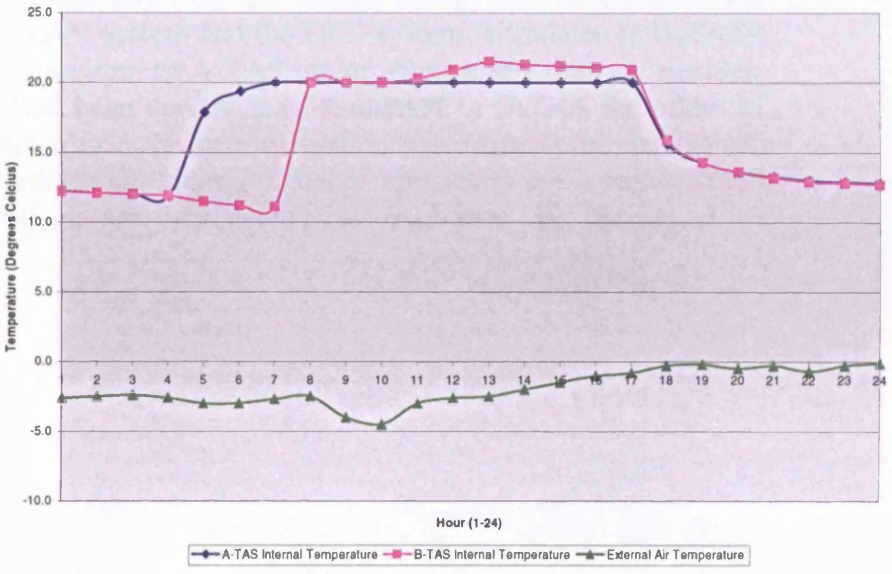

Figure J-2: Internal air temperature for zone 17 (North zone in the first floor of the case study building) on February 14th, as predicted by A and B-TAS respectively

The plant operates between 7:00 am – 17:00 pm in both programs (normal plant operating schedule). In addition, Optimum Start has been specified in A-TAS, which means that preheat will be provided during the first morning hours. The start of the preheat period has been set to 4:00 am (or Hour 5) in A-TAS, as explained earlier. As a result, the plant should provide heating between 4:00 am and 7:00 am so that the zone design condition (*Zone Lower Temperature Limit* =

20°C) is gradually reached before the start of the normal plant operating schedule. Indeed, the A-TAS predicted temperatures illustrate that the heating plant starts at 4:00 am on February 14th and the internal temperature progressively increases from 11.9°C to 20°C. On the other hand, the B-TAS predicted temperatures, also included in figure J-2, reveal that the heating plant remains inactive over the preheat period specified in A-TAS and starts to operate at 7:00 am (or Hour 8), as it was scheduled in the zone's *Internal Conditions*.

It is, therefore, clear that the plant behaviour is different in each program, (i.e. B-TAS ignores the preheat period specified in A-TAS), and, hence, the energy consumption data provided by B-TAS cannot be trusted in this case. The manual states that the building is simulated in A-TAS on the basis of an HVAC system model which is generic and relatively simple. B-TAS uses this model as a starting point and adds several detailed features in order to simulate the performance of a specific HVAC system (such as the VAV system or the FCU system simulated in this study). However, it seems that the specification of the Optimum Start in A-TAS provides an additional level of detail which cannot be mirrored in B-TAS due to the absence of suitable input parameters in the interface of this program. Keeping in mind that the Optimum Start is a detailed aspect of the plant operation, it would perhaps be better for this to be part of the input parameters of B-TAS, given that this is the detailed HVAC system analysis tool and not A-TAS.

It was, therefore, decided to investigate the effect of the number of hours that the plant operates during the day[42] on the annual energy consumption of the HVAC systems (i.e. the VAV system and the FCU system, simulated in B-TAS), ignoring the parameters provided in A-TAS under *Plant and Controls*. Besides, even if Optimum Start had been successfully simulated in B-TAS the effect of such a plant control strategy on the overall carbon performance of the HVAC systems would have been trivial, since the boiler emissions are a rather small percentage of the total carbon emissions, as explained in section 5.3.3 (chapter 5).

[42] **Note:** It should be remembered that details concerning the selection of the range of values for the plant operation schedule can be found in section 3.3.2, chapter 3.

Appendix K: The calculation of the hourly values of cloud cover for the NOA TRY

The NOA TRY (Athens – Greece) contains hourly values for both global and diffuse solar radiation, but there are no cloud cover measurements available. Section K.1 describes the calculation of daytime cloud cover from the global and diffuse solar radiation measurements, using the cloud-cover radiation model (CRM) developed by Karsten and Czeplak [1]. Section K.2, on the other hand, shows that it is possible to use the night-time cloud-cover data derived from a typical weather year for Athens (1979), which is contained in the TAS database, in order to fill the missing values of cloud cover in the NOA TRY.

K.1 The calculation of the hourly of values of daytime cloud cover for the NOA TRY [1]

Cloud cover is measured during daytime using a trained observer, while during the night, (within the UK), it is measured via laser cloud base recorders, which primarily record the height of the cloud passing overhead. These recorders can also be used on automatic weather stations to calculate the cloud amount based on the assumption that what passes overhead is representative of the rest of the sky. Detailed observations related to the type and state of the clouds are not, however, taken at every weather station. Clouds vary from thin, transparent cirrus which have a small effect on global radiation to thick and dark thunderstorm clouds, which may reduce the global radiation to 1% of its normal value. However, there are only a few stations where each cloud layer is separately observed, and at which both the type and the extent of each layer is recorded.

The number of weather stations measuring cloud cover is generally higher than the number of stations recording solar radiation data. As a result, many attempts have been made in the past to model the relationship between the insolation and the amount of sky covered by clouds[43]. The result of these efforts was the cloud-cover radiation model (CRM) which was developed by Kastern and Czeplak, using continuous hourly data for Hamburg for their research. The aforementioned researchers showed that the ratio of global radiation for any given cloud amount N (in octa[44]) to global radiation under a cloudless sky

[43] **Note:** In general, the record of duration of bright sunshine (where available) is a much better indicator of insolation than the cloudiness index. This is due to the fact that the continuous sunshine trace through the hour provides more detailed information than a spot reading of the cloud cover. Nevertheless, it would be useful to model the relationship between cloud cover and insolation, since many weather stations do not provide measurements of sunshine duration, (besides global or diffuse radiation), while cloud observations are usually available. It should be kept in mind however, that sunshine duration explains 70-85% of the insolation variance, while cloud cover seldom explains more than 70% and frequently less than 50% of the insolation variance.

[44] **Note:** The total cloud amount (cloud-cover) is measured in octas. The celestial dome is divided into 8 equal parts and then it is estimated how many eighths of the dome are covered by clouds.

(I_G / I_{Gc}) is independent of solar elevation, and can be estimated using the equation: $I_G / I_{Gc} = 1 - C \times (N/8)^D$ (1)

The global radiation under cloudless sky (I_{Gc}) depends on the solar altitude (*SOLALT*) and is estimated via the equation: $I_{Gc} = (A \times \sin SOLALT - B)$ (2)

The coefficients A, B, C and D for Hamburg are shown in table K.1-1. Gul and Muneer [1] observed an improvement in the performance of the model when it is based on locally fitted coefficients. As a result, they refitted these four coefficients for five UK locations, as also illustrated in table K.1-1:

Location	Latitude	A	B	C	D
Hamburg	58.3	910	30	0.75	3.4
Stornoway	58.2	979	45	0.73	3.4
Aldergrove	54.6	956	34	0.7	3.1
Finningley	53	902	36	0.71	3.7
Aberporth	52.1	1024	54	0.71	4.2
London	51.5	948	49	0.71	3.4

Table K.1-1: Coefficients for the CRM to be used in equations (1) and (2) [1]

On the other hand, the *SOLALT*, (involved in equation *(2)*), can be estimated using the following equation:

$$\sin SOLALT = \sin LAT \cdot \sin DEC + \cos LAT \cdot \cos DEC \cdot \cos GHA$$

where

- LAT is the latitude of the location,
- DEC is the solar declination[45] (i.e. the angle between the earth-sun vector and the equatorial plane).
- GHA is the Greenwich Hour Angle

Finally, the diffuse solar radiation is computed via the equation: $I_D / I_G = 0.3 + 0.7 \times (N/8)^2$ (3), while the beam component is estimated as the difference of global and diffuse solar radiation.

The validity of the CRM was checked using a 9-year hourly database (1985-93) for five UK sites and a 3-year database (1993-95) for two Swiss sites [1]. It was found that the model performs best for clear skies, while it has rather poor performance under overcast conditions. This is due to the fact that detailed data regarding the type of the cloud are not taken into consideration by this model. However, even if they were, such observations are not available in most weather stations, as mentioned earlier.

[45] **Note:** The solar declination and the Greenwich Hour Angle can be estimated using a number of equations some of which are very complicated for use in manual calculations. Muneer [1] has developed a program in FORTRAN which can be used for the estimation of these two parameters.

The NOA TRY does not contain any cloud cover measurements but, on the other hand, it provides hourly values for both global and diffuse solar radiation. The CRM provides a correlation between the solar radiation data and the cloud cover fraction, as shown above. The cloud cover N is involved in equations (1) and (3). However, only equation (3) takes into consideration both the global & diffuse solar radiation data, (which are available in the TRY for Athens), while it does not contain any coefficients that depend on the location of the measurements. Moreover, the ratio of diffuse to global radiation (I_D / I_G) is independent of the solar altitude (i.e. the elevation angle above the horizon), as can be seen from equation (3).

Before making use of this model, it was decided it to evaluate it for a number of days obtained from the only weather file for Athens, which is available in the TAS database. The GR_Athens_TRN weather file, which was translated into the TAS format from TRNSYS, another dynamic simulation tool, contains hourly values for both the cloud cover and the global & diffuse solar radiation for the calendar year 1979. The CRM predictions are compared with the hourly values of cloud cover, for both an overcast day (19/4/1979) and a sunny day (18/6/1979) derived from the TAS weather file for Athens, in table K.1-2, as an example:

Hour	Overcast day (19/4/1979)		Sunny day (18/6/1979)	
	Cloud-Cover (0 - 1)		Cloud-Cover (0 - 1)	
	TAS weather file	CRM - equation (3)	TAS weather file	CRM - equation (3)
5	0.97	0.20	0.15	0.24
6	1.00	1.00	0.22	0.15
7	1.00	1.00	0.25	0.27
8	1.00	1.00	0.25	0.32
9	1.00	1.00	0.25	0.35
10	0.88	0.34	0.28	0.29
11	1.00	0.74	0.27	0.31
12	1.00	1.00	0.26	0.32
13	1.00	0.77	0.26	0.33
14	0.92	0.48	0.26	0.32
15	1.00	0.83	0.26	0.31
16	1.00	1.00	0.24	0.27
17	1.00	1.00	0.2	0.18
18	0.97	1.00	0.16	0.65

Table K.1-2: Evaluation of the CRM (equation (3)) for an overcast day (19/4/1979) and a sunny day (18/6/1979) obtained from the GR_Athens_TRN weather file contained in the TAS database

As can be seen from table K.1-2, the values of cloud cover obtained from equation (3), (which makes use of both the global & diffuse radiation measurements provided by the GR_Athens_TRN weather file), are quite close to the measured could cover data contained in the TAS weather file, for most of the hours of the two chosen days. In addition, it seems that the CRM performs better under part-overcast or clear sky conditions (18/6/1979) than under overcast

conditions (19/4/1979). As mentioned earlier, the validation exercises carried out in the past had reached a similar conclusion.

Equation (3) of the cloud-cover radiation model was, therefore, used for the calculation of the hourly values of daytime cloud cover from the global and diffuse solar radiation measurements obtained from the NOA TRY.

K.2 The estimation of the night-time cloud cover hourly values for the NOA TRY

As explained in section K.1, the CRM was used for the estimation of the hourly values of cloud cover for the part of the day that solar radiation measurements are available. Keeping in mind, however, that TAS uses night-time cloud-cover (NCC) data to estimate night-time radiation loss to the night sky, it was decided to set the cloud cover for the part of the day that solar radiation measurements are not available to 0.0 (scenario 1), 0.5 (scenario 2) and 1.0 (scenario 3), respectively, in order to study the effect of NCC on the energy performance of the HVAC systems.

The effect of NCC on the energy/carbon performance of the HVAC systems is presented in table K.2-1:

		Annual energy use		Carbon emissions			Change in the carbon emissions of scenario 1		
HVAC system	Scenario	Heating energy consumption (kWh)	Cooling energy consumption (kWh)	Boiler carbon emissions (kgC)	Chiller carbon emissions (kg C)	Total carbon emissions (kgC)	Change in the boiler emissions of scenario 1 (%)	Change in the chiller emissions of scenario 1 (%)	Change in the total carbon emissions of scenario 1 (%)
FCU system	*Scenario 1: NCC = 0.0*	38344	473018	1994	60073	62067	-	-	-
	Scenario 2: NCC = 0.5	37305	475706	1940	60415	62355	-2.71%	0.57%	0.46%
	Scenario 3: NCC = 1.0	36389	478458	1892	60764	62656	-5.10%	1.15%	0.95%
VAV system	*Scenario 1: NCC = 0.0*	27997	365938	47930	46474	47930	-	-	-
	Scenario 2: NCC = 0.5	26516	367573	48061	46682	48061	-5.29%	0.45%	0.27%
	Scenario 3: NCC = 1.0	25080	369115	48182	46878	48182	-10.42%	0.87%	0.53%

Table K.2-1: The effect of night-time cloud-cover on the energy/carbon performance of the FCU system and the VAV system, respectively

As can be seen from table K.2-1, the inclusion of NCC in the NOA TRY has an impact mainly on the heating energy consumption of both systems. For example, the FCU system heating energy use drops by 5%, while the heating energy consumption of the VAV system is reduced by 10% when the NCC is set to 1.0 (scenario 3) as opposed to 0.0 (scenario 1). This was expected, since the building loses less heat, via radiative night cooling, to an overcast night sky than a clear night sky. On the other hand, the aforementioned change in the NCC results in approximately 1.0% higher cooling energy consumption for both HVAC systems, since the building retains the heat during the night (when NCC = 1.0) increasing the demand for cooling in the following day. However, the NOA TRY is a cooling dominated climate which means that the reduction in the carbon emissions associated with the heating energy use is more than compensated by the small increase in the carbon emissions associated with the use of mechanical cooling, resulting in just 1.0% higher total carbon emissions

for the FCU system and only 0.5% higher total carbon emissions for the VAV system, when the NCC is set to 1.0 (scenario 3) instead of 0.0 (scenario 1). In other words, it can be said that using the NOA TRY without night-time cloud-cover data is not expected to affect the total carbon emissions of the systems much, but, on the other hand, it will result in over-predicted heating energy consumption data, particularly for the VAV system. If more realistic predictions of the heating energy use are required, it is clear that NCC should be included. However, the problem in such a case lies in the choice of proper hourly values for the missing cloud cover data, since it is obvious that keeping the NCC constant at 0.5 or 1.0 is unrealistic.

As also mentioned in section K.1, the TAS weather database provides only one weather file for Athens, called 'GR_Athens_TRN", which contains hourly measurements for the calendar year 1979. A few summary statistics for the GR_Athens_TRN weather file and the NOA TRY, (when the NCC is set to 0.50), are presented in table K.2-2 and K.2-3, respectively:

Variable	Min.	Day of Min	Mean	Max.	Day of Max
Global solar (W/m^2)	0.00	1	188.76	967.00	161
Diffuse solar (W/m^2)	0.00	1	61.63	286.00	155
Cloud-Cover (0 -1)	0.00	276	0.44	1.00	3
Air Temp. (°C)	0.10	56	17.89	39.30	213
Wind Speed (m/s)	0.00	18	3.47	17.50	103
RH (%)	14.00	212	62.49	98.00	75

Table K.2-2: Summary statistics for the GR_Athens_TRN

Variable	Min.	Day of Min	Mean	Max.	Day of Max
Global solar (W/m^2)	0.00	1	187.18	1031.00	139
Diffuse solar (W/m^2)	0.00	1	73.23	833.00	90
Cloud-Cover (0 -1)	0.00	33	0.52	1.00	3
Air Temp. (°C)	1.10	77	17.55	37.60	195
Wind Speed (m/s)	0.00	18	3.26	19.90	322
RH (%)	15.00	197	63.12	98.00	310

Table K.2-3: Summary statistics for the NOA TRY when the NCC is held constant at 0.50

As can be seen from tables K.2-2 and K.2-3, the GR_Athens_TRN and the NOA TRY have very similar mean values for all the weather variables under consideration, while there are only a few large differences mainly in the min or max values of some of the weather parameters (e.g. in the min value of the air temperature).

The frequency distribution of the weather parameters included in the two tables shown above, (apart from the cloud cover), throughout the year for both weather files is presented in figures K.2-1 to K.2-10:

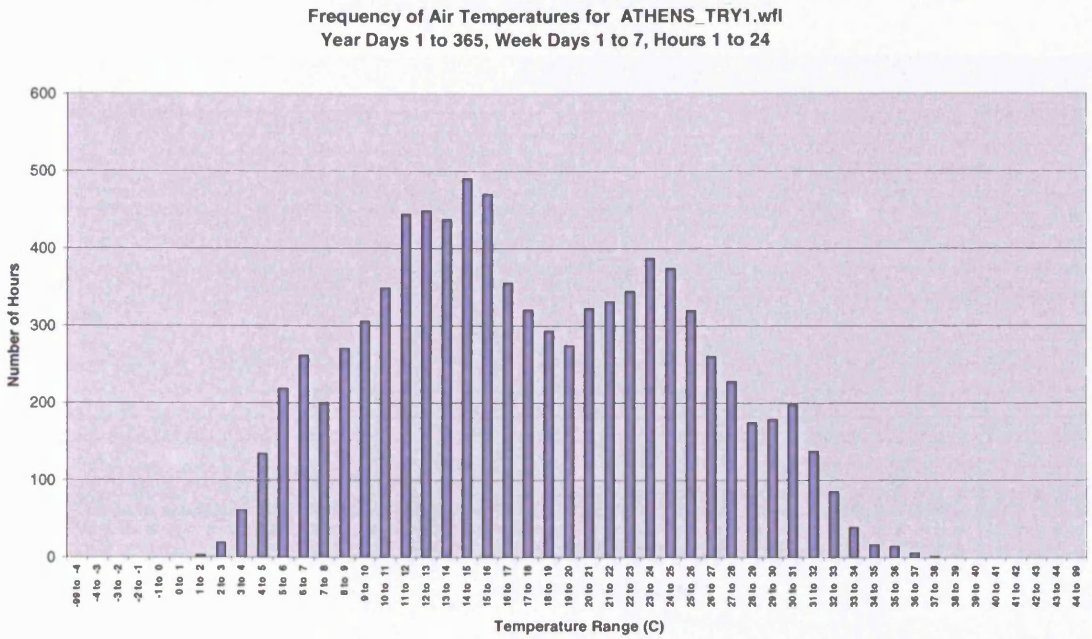

Figure K.2-1: Frequency distribution of the air temperature for the NOA TRY

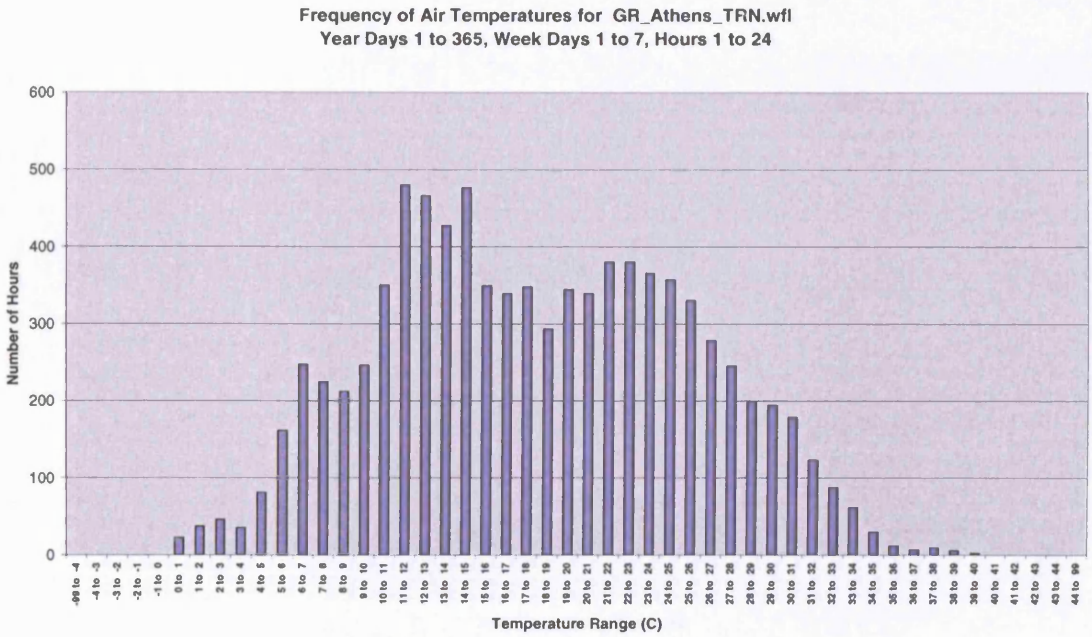

Figure K.2-2: Frequency distribution of the air temperature for the GR_Athens_TRN

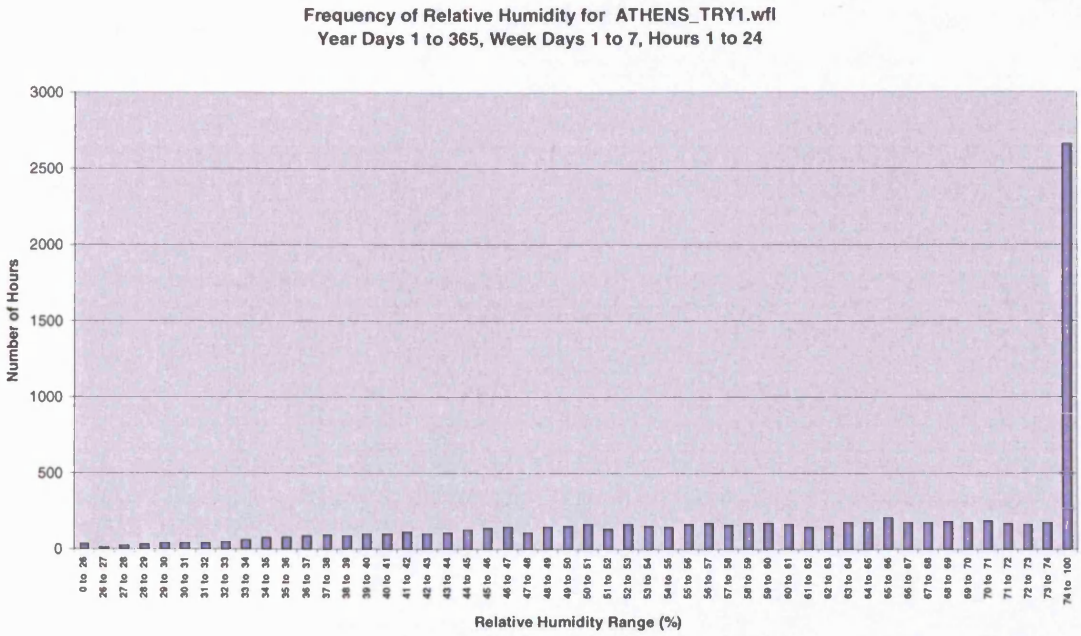

Figure K.2-3: Frequency distribution of the RH for the NOA TRY

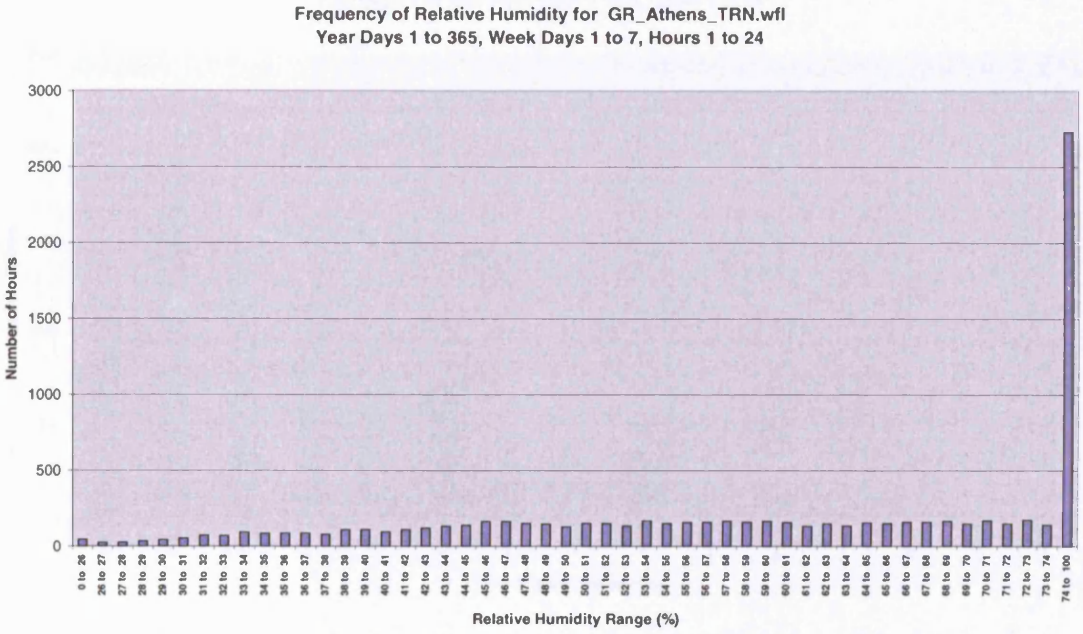

Figure K.2-4: Frequency distribution of the RH for the GR_Athens_TRN

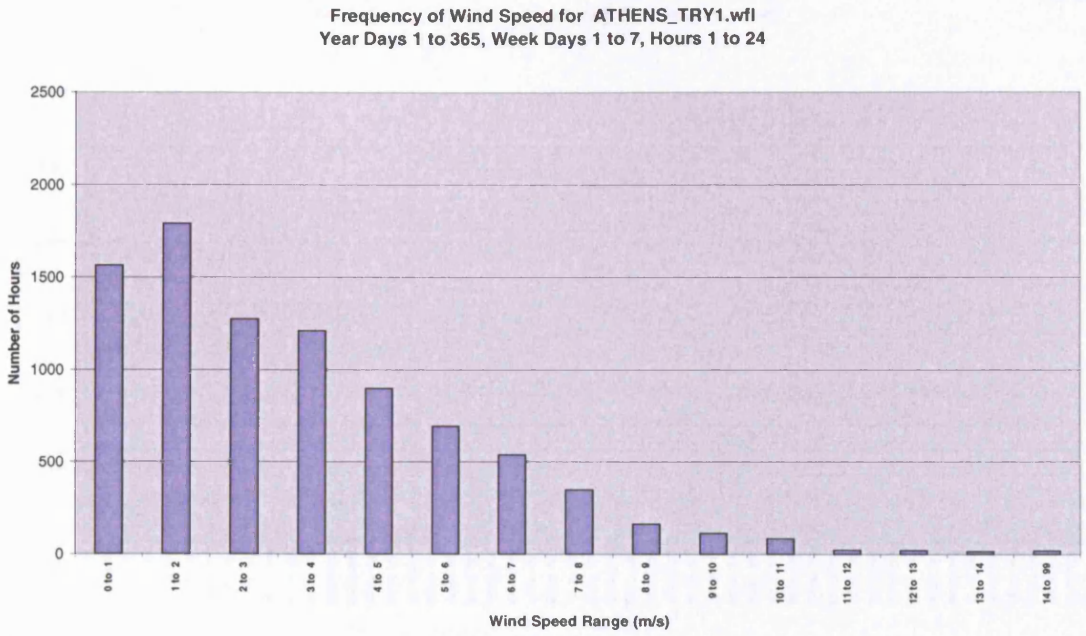

Figure K.2-5: Frequency distribution of the wind speed for the NOA TRY

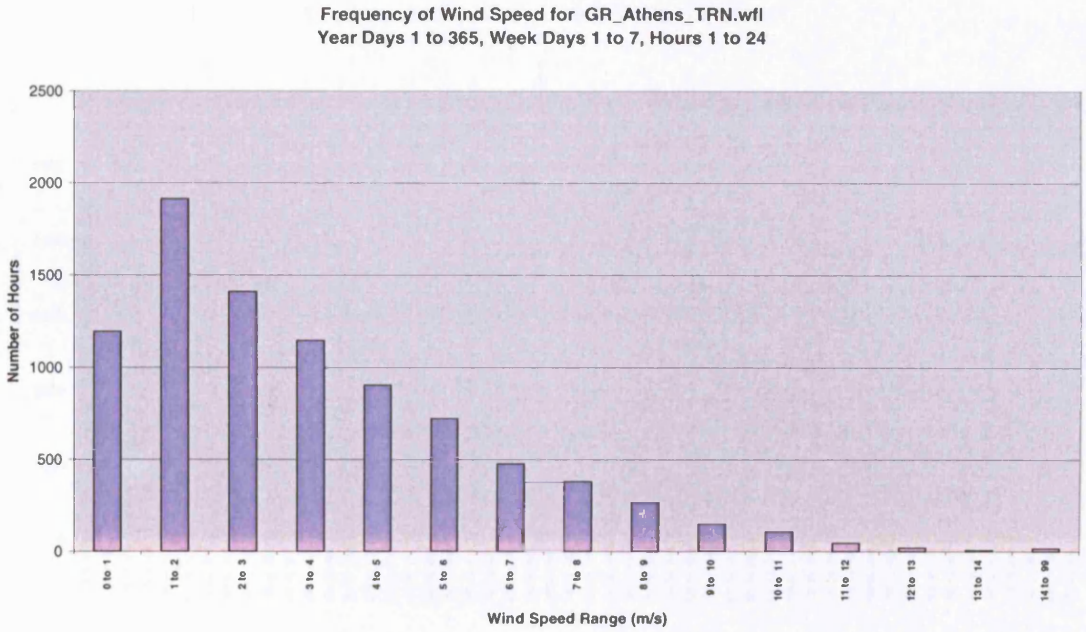

Figure K.2-6: Frequency distribution of the wind speed for the GR_Athens_TRN

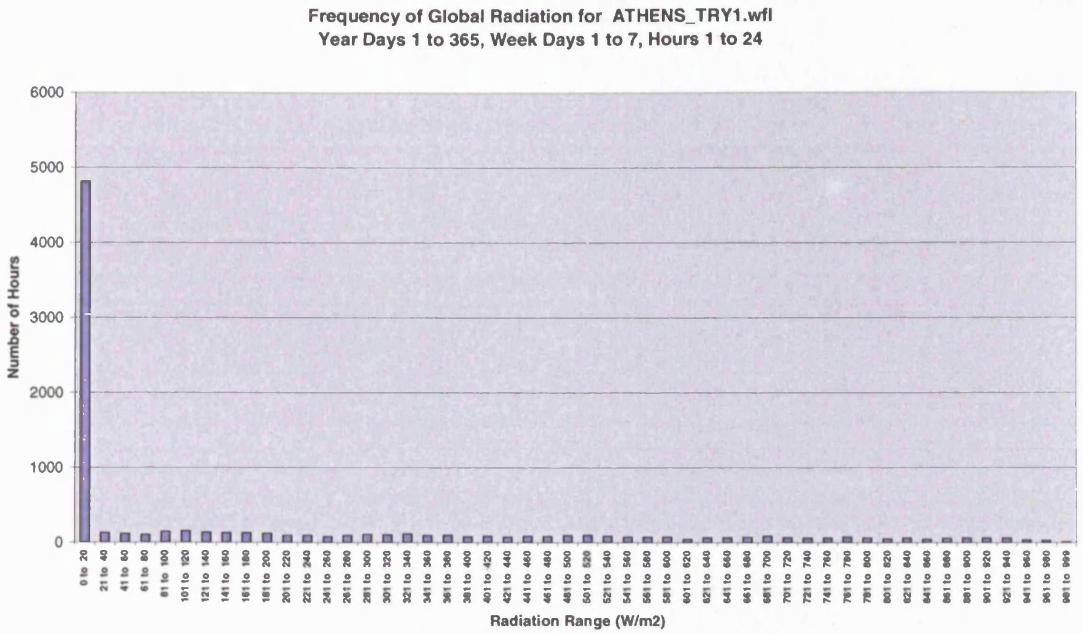

Figure K.2-7: Frequency distribution of the global radiation for the NOA TRY

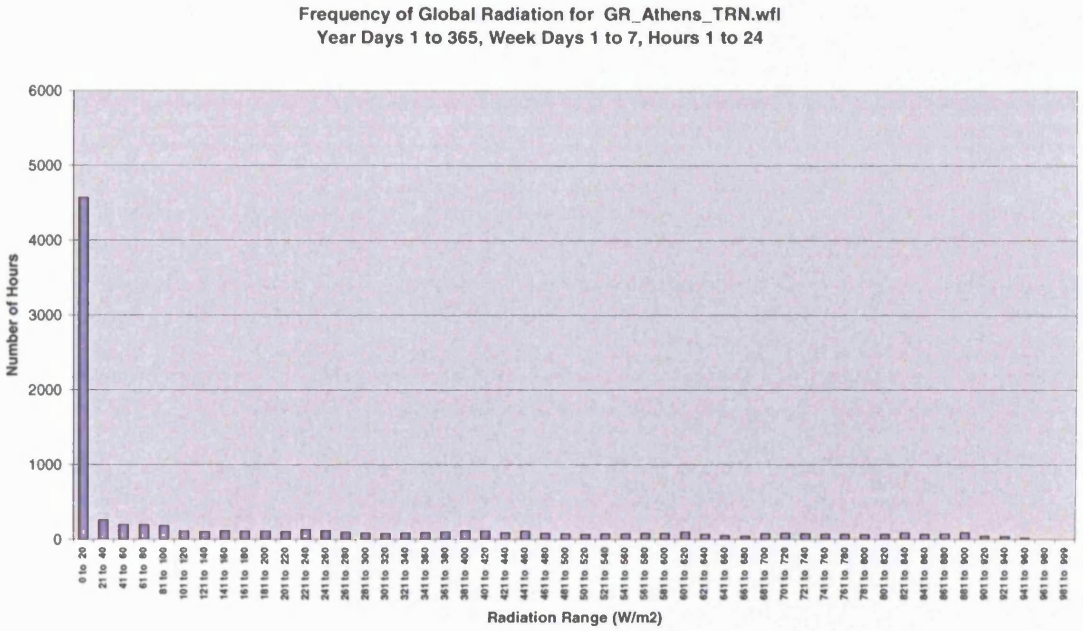

Figure K.2-8: Frequency distribution of the global radiation for the GR_Athens_TRN

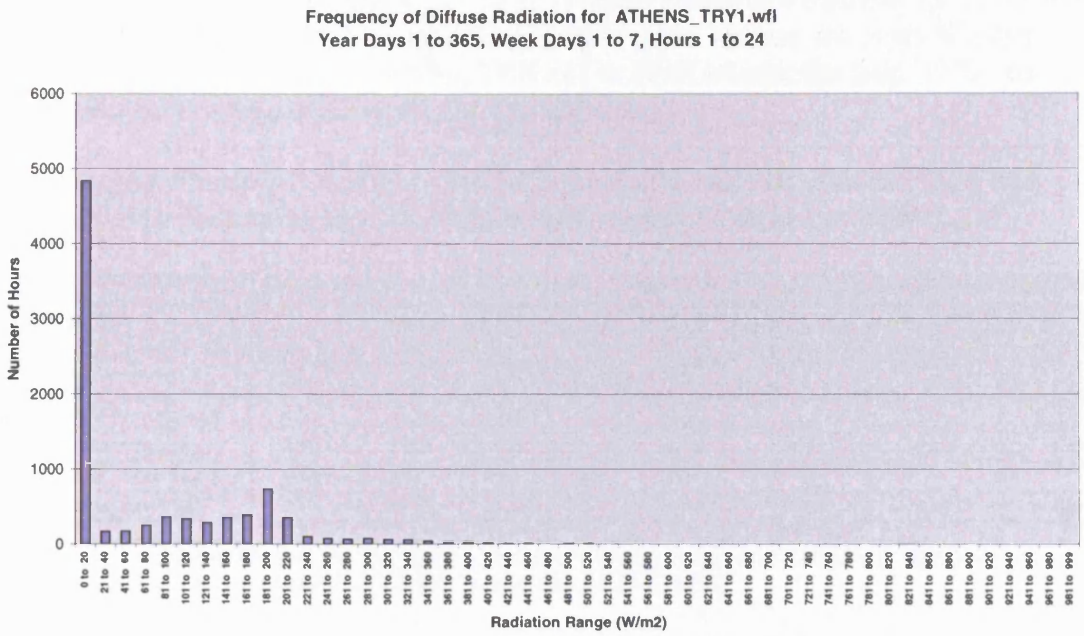

Figure K.2-9: Frequency distribution of the diffuse radiation for the NOA TRY

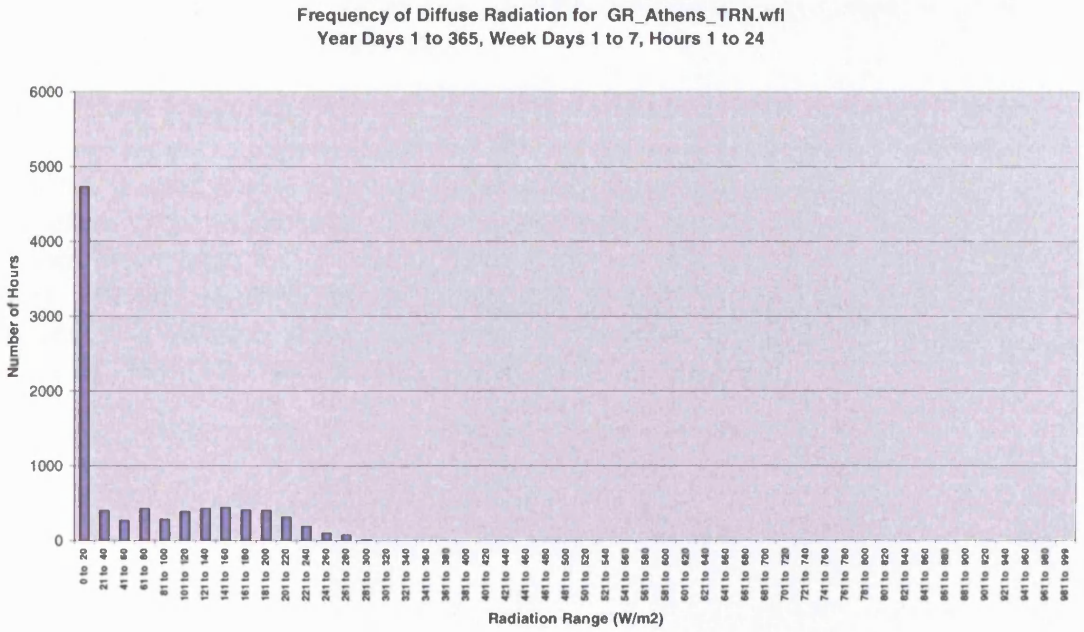

Figure K.2-10: Frequency distribution of the diffuse radiation for the GR_Athens_TRN

As can be seen from figures K.2-1 to K.2-10 the frequency distribution of the weather parameters under consideration is also quite similar for both weather files, indicating that the GR_Athens_TRN or, in other words, the year 1979 can be considered as a typical calendar year for Athens.

The energy consumption of both HVAC systems for the GR_Athens_TRN and the NOA TRY (assuming that the NCC is equal to 0.5) is shown in table K.2-4:

		Annual energy use		Carbon emissions			Change in the carbon emissions of scenario 2		
HVAC system	Scenario	Heating energy consumption (kWh)	Cooling energy consumption (kWh)	Boiler carbon emissions (kgC)	Chiller carbon emissions (kg C)	Total carbon emissions (kgC)	Change in boiler emissions (%)	Change in chiller emissions (%)	Change in total carbon emissions (%)
FCU system	*Scenario 2: NOA TRY (NCC = 0.5)*	37305	475706	1940	60415	62355	-	-	-
	Scenario 4: GR_Athens_TRN	33961	469824	61434	59668	61434	-8.96%	-1.24%	-1.48%
VAV system	*Scenario 2: NOA TRY (NCC = 0.5)*	26516	367573	48061	46682	48061	-	-	-
	Scenario 4: GR_Athens_TRN	20124	367809	47758	46712	47758	-24.11%	0.06%	-0.63%

Table K.2-4: Comparison of the energy/carbon performance of the two HVAC systems for the GR_Athens_TRN and the NOA TRY (when the NCC is 0.5)

Table K.2-4 shows that the energy/carbon performance of the HVAC systems is very similar for both the NOA TRY and the GR_Athens_TRN, (particularly as far as the cooling energy or the total carbon emissions are concerned), providing further evidence that the latter can also be considered representative of the typical weather conditions in Athens.

It is worth mentioning that the reason that the NOA TRY night-time cloud-cover was set to 0.5 instead of 0.0 or 1.0[46], for the comparison made in table K.2-4, is that in such a case the mean value of the cloud cover for the NOA TRY is very close to the mean value of this parameter for the GR_Athens_TRN, as can be seen from table K.2-3 (mean cloud cover = 0.52) and K.2-2 (mean cloud cover = 0.44), respectively. However, this is definitely not the case for the frequency distribution of the cloud cover, as illustrated in figure K.2-11 and K.2-12 for the NOA TRY and the GR_Athens_TRN, respectively:

[46] **Note:** Had the NCC been held constant at 0.0 for the NOA TRY, the mean value of the cloud cover for this climate would have been 0.24. Also, if the NCC had been set to 1.0 for the NOA TRY, the mean value of the cloud cover for this climate would have been equal to 0.79.

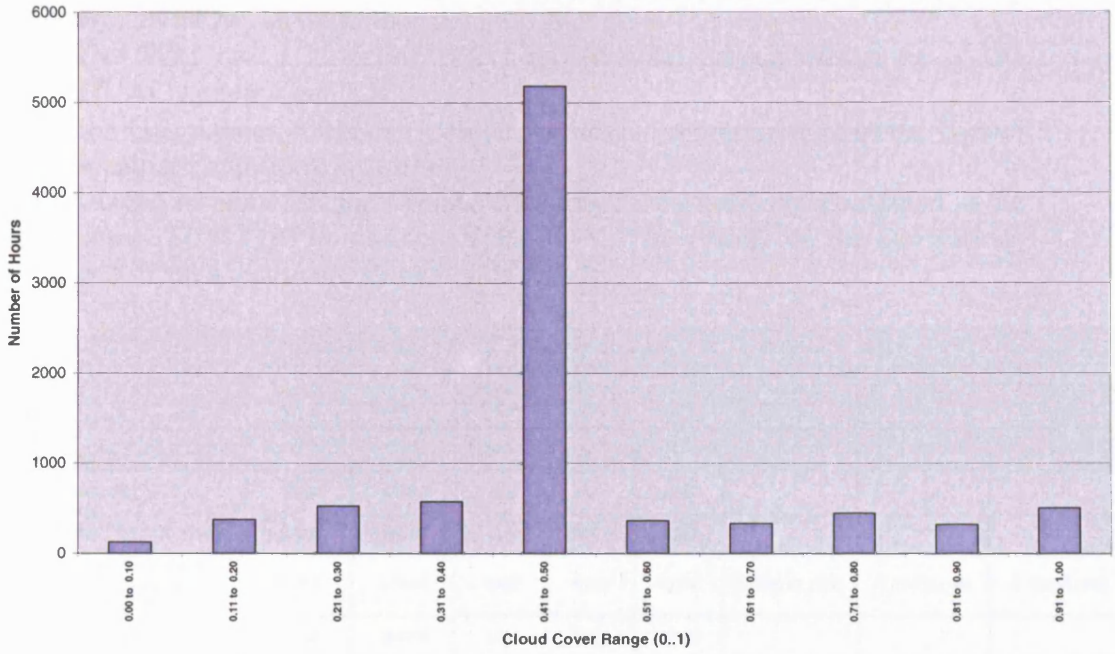

Figure K.2-11: Frequency distribution of the cloud cover for the NOA TRY (assuming that the NCC is held constant at 0.5)

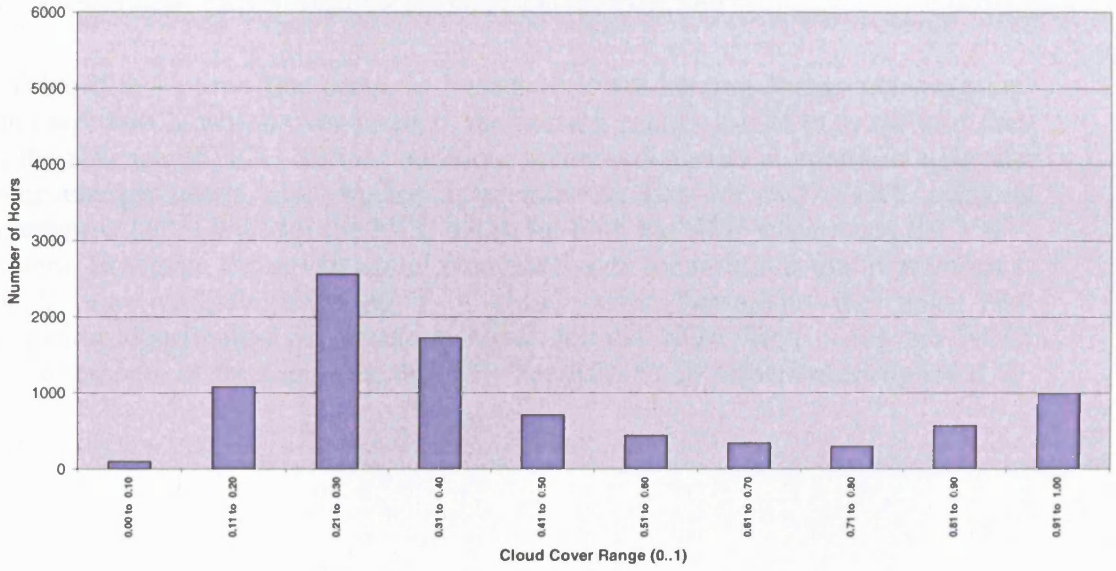

Figure K.2-12: Frequency distribution of the cloud cover for the GR_Athens_TRN

Figures K.2-11 and K.2-12 clearly show that the frequency distribution of the cloud cover is different in each weather file. The mean value of this weather parameter is very similar in both weather files due to the fact that the NCC is held constant at 0.5 for a large number of hours, (i.e. for the hours that there are no solar radiation data available), in the NOA TRY. It is obvious, however, that the frequency distribution of the cloud cover for this weather file is unrealistic, as shown in figure K.2-11.

Keeping, therefore, in mind that:

- the NCC has a moderate effect on the total carbon emissions of the HVAC systems (table K.2-1)
- the GR_Athens_TRN can also be considered representative of the typical weather conditions in Athens,

it was decided to input the night-time cloud-cover measurements contained in the GR_Athens_ TRN (1979) into the NOA TRY. The results of the simulations carried out in such a case are shown table K.2-5:

		Annual energy use		Carbon emissions			Change in the carbon emissions of scenarios 1 & 2		
HVAC system	Scenario	Heating energy consumption (kWh)	Cooling energy consumption (kWh)	Boiler carbon emissions (kgC)	Chiller carbon emissions (kg C)	Total carbon emissions (kgC)	Change in boiler emissions (%)	Change in chiller emissions (%)	Change in total carbon emissions (%)
FCU system	*Scenario 1: NOA TRY (NCC = 0)*	38344	473018	1994	60073	62067	-	-	-
	Scenario 2: NOA TRY (NCC = 0.5)	37305	475706	1940	60415	62355	-	-	-
	Scenario 5: NOA TRY with NCC measurements derived from the GR_Athens_TRN	37212	475108	1935	60339	62274	-0.25% (-2.95%)	-0.13% (0.44%)	-0.13% (0.33%)
VAV system	*Scenario 1: NOA TRY (NCC = 0)*	27997	366938	1456	46474	47930	-	-	-
	Scenario 2: NOA TRY (NCC = 0.5)	26516	367573	1379	46682	48061	-	-	-
	Scenario 5: NOA TRY with NCC measurements derived from the GR_Athens_TRN	26319	366995	1369	46608	47977	-0.74% (-5.99%)	-0.16% (0.29%)	-0.17% (0.10%)

Table K.2-5: HVAC system energy consumption and carbon emissions when the NCC data of the GR_Athens_TRN weather file are input into the NOA TRY[47]

Table K.2-5 shows that scenario 5 leads to lower heating energy consumption than scenario 1, which over-predicts the heating energy use of both systems due to the absence of NCC data. In addition, scenario 5 results in approximately the same energy/carbon performance as scenario 2, (i.e. the NOA TRY using a constant value of 0.50 for the NCC data), for both the FCU system and the VAV system. However, the advantage of scenario 5 over scenario 2 is that it provides a much more realistic distribution of cloud cover throughout the year. The frequency distribution of the cloud cover for the NOA TRY using the NCC measurements of the GR_Athens_TRN (scenario 5), is presented in figure K.2-13:

[47] **Note:** In the last three columns of table K.2-5, the number **outside** the parenthesis shows the change in the carbon emissions of scenario 2, while the number **inside** the parenthesis illustrates the change in the carbon emissions of scenario 1.

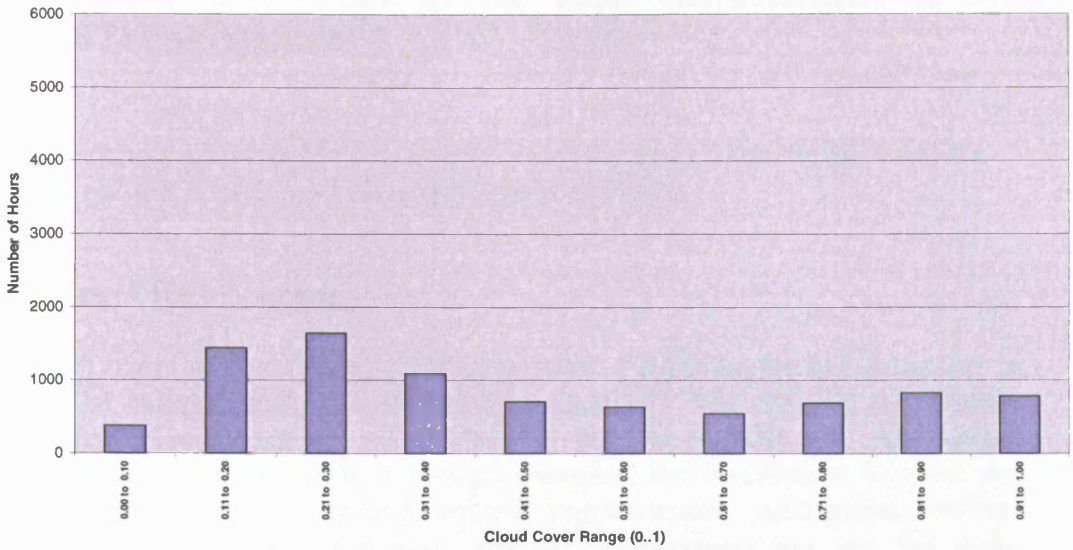

Figure K.2-13: Frequency distribution of the cloud cover for the NOA TRY using the NCC data of the GR_Athens_TRN

Figure K.2-13 shows that the frequency distribution of the cloud cover for the NOA TRY combining the daytime cloud cover data estimated using the CRM with the NCC data of the GR_Athens_TRN, is much closer to the frequency distribution of the same weather parameter for the GR_Athens_TRN (figure K.2-12) in comparison with figure K.2-11 (i.e. the unrealistic frequency distribution of the cloud cover based on a constant value of NCC = 0.5). Also, the mean value of the cloud cover for the NOA TRY using the NCC data of the GR_Athens_TRN is equal to 0.49, which is between the mean value of the cloud cover for the GR_Athens_TRN (i.e. 0.44, as shown in table K.2-2) and the average value of the same weather variable for the NOA TRY using a constant value of 0.50 for the NCC (i.e. 0.52, as shown in table K.2-3).

Therefore, it can be concluded that the input of the night-time cloud-cover data of the GR_Athens_TRN into the NOA TRY results in a frequency distribution of the cloud-cover close to that of a typical weather year for Athens (such as 1979, as shown earlier), as well as more realistic predictions of the heating energy consumption than those estimated using the NOA TRY without any measurements for the night-time cloud-cover (as shown in table K.2-5). Moreover, the calculation of the daytime cloud- cover using the CRM model, as shown in section K.1, helps to maintain a good relationship between this weather variable and the solar radiation measurements contained in the NOA TRY.

References

[1] Tariq Muneer, *Solar Radiation and Daylight Models: For the Energy Efficient Design of Buildings*, Elsevier – Butterworth Heinemann, Second Edition, 2004

Appendix L: Description of the main characteristics of the selected HVAC systems

This appendix provides a short description of the main characteristics and the operation of the HVAC systems considered in the thesis.

L.1 Types of HVAC systems

The provision of satisfactory thermal comfort conditions for the occupants is one of the primary priorities of building designers. The severity of climatic conditions in some regions of the world, (e.g. in tropical and sub-tropical climates), indicates that passive design measures are insufficient to meet the requirements of thermal comfort without supplementary mechanical cooling. Furthermore, even when the high external temperatures are not the main characteristic of a climate, (e.g. in temperate climates), the modern forms of buildings, (e.g. airtight buildings that aim to minimize the ingress of polluted air and noise from the external environment combined with high glazing ratios, extensive use of IT equipment, etc), create such internal conditions that the use of some form of air conditioning is the only option left to the designer in order to produce a tolerable state of comfort.

An HVAC system does not only provide space cooling, but is also capable of satisfying both the ventilation and heating requirements of the occupants. In addition, modern HVAC systems incorporate the functions of controlling the humidity, purity and movement of the air, in an attempt to respond to the current high standards of living and working conditions. As a result, a large number of systems, air handling components and equipment configurations have been developed for a variety of applications in the residential, the commercial and the industrial sectors.

The wide variety of systems does not allow the adoption of a general agreed classification system. Nevertheless, Jones [3] adopts a quite common arrangement, which classifies the HVAC systems into three basic categories:

- All-air systems
- Air-water systems
- Unitary systems

The main difference between the first two categories is the cooling medium by which the cooling energy of the systems is distributed to the spaces that require air conditioning [2].

All-air systems provide cooling (sensible and latent), heating and humidification, by supplying conditioned air to all zones served [4]. As a result, the supply volume airflow rate required to meet the load of each zone is typically much higher than the minimum ventilation requirement. The all-air systems include constant volume re-heat and sequence heat systems, roof top units, variable air volume (VAV) systems, multi-zone units and air curtains [3]. However, the VAV system is the principal type of all-air systems for new multi-

zone applications and is also considered as one of the dominant systems installed in office buildings both in the USA and the UK [2], [5].

In air-water systems both air and water are distributed to the individual zones to perform the cooling function [4]. This time though, the air quantity supplied from the central plant is usually the minimum required to meet the ventilation needs of the occupants. Although the supply air is still capable of providing some sensible cooling, the bulk of this is done by circulating chilled water through a heat exchange surface, which may be a coil that is part of an air terminal unit, or a separate component within the zone such as a radiation panel [2], [4]. This category includes fan coil systems, perimeter induction systems, chilled ceilings and chilled beams [3]. However, the fan coil system is considered the primary type of air-water systems for multi-zone applications, being suitable for both refurbished and new buildings [2].

Unitary air conditioners consist mainly of specially designed air handling components such as fans, coils, filters, etc, placed in air conditioning units, which are field designed to meet the needs of the user [4]. This category includes self-contained, air-cooled room air conditioners, split systems, cassette units and variable refrigerant volume systems, water-cooled air conditioning units, and water loop, air conditioning/ heat pump units [3]. The most popular unitary air conditioning units are considered to be the room air conditioners [3], which have low capital cost and offer considerable space savings eliminating both ductwork and plant rooms [4]. However, there is a limitation to the size of cooling loads and spaces that can be served by such systems. As a result, their most popular applications are in hotel rooms and in renovation of existing buildings, because there is less disruption to the occupants and reduction of lettable space, than with alternative central systems.

There are also some contemporary HVAC systems, which cannot be classified in one of the three categories mentioned above, and which are gaining in popularity mainly due to their low energy use potential.

The displacement ventilation (DV) system, is one of these systems, where the air is introduced via floor mounted outlets at a few degrees below the room design temperature. The supply air moves upwards at a low velocity, using a piston effect to take warm pollutants and heat gains with it, and is extracted at high level positions [1]. The result is a vertical stratification of temperature and pollutant concentration, so that the best conditions are achieved and maintained in the occupied zone [7]. Also, the DV system offers the possibility of low energy use mainly due to the provision of fresh air at relatively low flow rates, and the exploitation of the free cooling capacity of the fresh air quantity, since the temperature of the supply air is only a few degrees lower than the room air temperature, as also mentioned above [8]. It should be stressed that the satisfactory operation of this system relies on several design guidelines associated with both the construction of the building as well as the design and control strategy of the system itself. For example, the building should be airtight, while good external shading is also required to avoid disruption of the desired air flow pattern [1]. Additional design factors that should be considered include the air velocity in the occupied zone [9], [10], the vertical temperature gradient [10],

the selection and positioning of air terminal devices, etc. The main disadvantage of this system is the relatively low cooling loads it can deal with. As a result, the DV system is usually combined with chilled ceilings or chilled beams to increase the overall cooling capacity of the system [1]. In addition, the DV system cannot respond to the heating requirements of the perimeter zones of the building, so it may be necessary to install a separate heating system to deal with the heat losses through the building envelope [9].

The Termodeck hollow core floor slab mechanical ventilation system is another innovative HVAC system, which takes advantage of night-time ventilation techniques and the thermal storage capacity of the building structural mass, passing the fresh air through the cores of hollow floor planks, before it is introduced into the space [1]. As a result, the floor slab acts as a store of heat or 'coolth' that stabilizes the internal temperatures, providing a satisfactory indoor climate throughout the year. The energy consumption of the system is limited to the amount of fan energy required to move the air through the hollow core concrete floor planks. However, in some types of climate it may be necessary to treat the supply airflow rate at a conventional central air-handling plant providing filtration and heating or cooling [1]. It is worth mentioning that the Termodeck system relies on a well-insulated, airtight building, while the provision of dense internal walls also aids thermal retention and helps to increase the overall thermal mass of the building. The ceiling and (if possible) the floor slabs should be left exposed, since the majority of the cooling / heating effect is due to radiation and natural convection from the ceiling and floor surface [12]. A weakness of this system is that it cannot respond quickly to load changes in the space being served, due to the fact that the concrete mass maintains fairly stable air supply temperatures.

The following two sections contain the description of the main characteristics and the operation of the HVAC systems considered in the thesis. Section L.2 describes the main characteristics of the VAV system, which is the most popular all-air system, while section L.3 deals with the description of the fan coil system, which is the primary type of air-water system.

L.2 Variable air volume system

Most of the traditional all-air systems were based on the constant air volume (CAV) concept, which means that the volume flow rate of the supply air was kept constant to meet peak fresh air ventilation requirements, while the supply air temperature was varied to meet the prevailing zone cooling load [2].

CAV systems were very popular before the 1970s, due to the fact that the constant volume of air was very easy to control and problems like diffuser dumping and poor ventilation efficiency were not very likely to occur, providing a satisfactory internal environment for the occupants [5]. The main disadvantages of the system included the large amounts of fan energy required to distribute the constant volume of air around the building and the wasteful re-heating, which was necessary to avoid possible overcooling problems in some building zones [2]. Thus, the popularity of the CAV systems decreased dramatically during the energy crisis of the 1970s, when the energy cost became one of the primary concerns of HVAC system designers.

An alternative option to the design of all-air systems is the variable air volume (VAV) approach. Instead of varying the temperature of the supply air to meet the zone requirements, the air is supplied to each zone at an identical, constant temperature, while its volume flow rate is varied to meet the prevailing zone cooling load [2]. This task is achieved by controlling the air quantity, which is usually supplied to a group of diffusers via a terminal unit under thermostatic control [1]. A typical VAV terminal unit is illustrated in figure L-1:

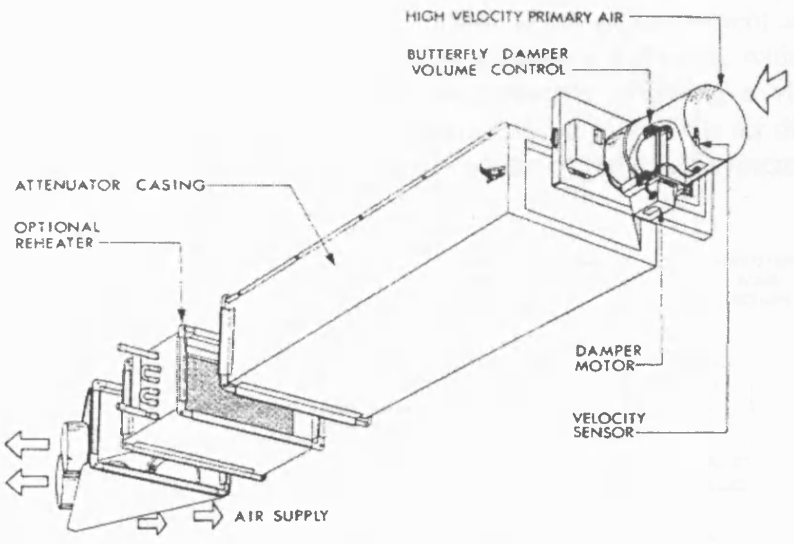

Figure L-1: Variable volume terminal unit [1]

The first all-air systems based on the VAV concept, appeared in the mid-1960s, in the USA. The development of VAV technology was rather slow at the beginning, and most of the VAV applications prior to the 1970s were limited to the USA.

VAV technology might have not originated in response to the rise in energy cost, in the mid-1970s, but it was certainly during this period that both engineers and HVAC manufacturers appreciated the potential of these HVAC systems to [1], [2]:

- reduce the fan energy required to distribute the air around the building.
- minimize the waste of energy for re-heating of the supply air quantity, to provide temperature control of the space.
- exploit the free cooling capacity of the fresh air by mixing variable proportions of return and fresh air, in order to achieve the required supply air temperature with minimal use of mechanical cooling. Particularly in temperate climates, the temperature of the outside air is low enough to achieve the desired supply air temperature with minimum mechanical cooling, for most of the year.
- achieve capital cost savings by reducing the plant size, since the load diversity is taken into consideration in system sizing.
- allow for architectural space savings, since the ductwork is sized to handle the air quantity required to offset the maximum simultaneous heat gain that could occur in the building, and not the sum of the air quantities demanded by the peak loads in each of the individual zones.

As a result, the development of the VAV system was rapid in the latter half of the 1970s and throughout the 1980s, while in the ten-year period between 1975-1985 the application of the VAV technology became widespread in the UK [2].

One of the problems of the first VAV systems was the poor performance of the air terminal devices when the supply air was reduced below 40% of the design flow rate, which resulted in loss of control of the air movement and possible cold draughts. The development of variable geometry diffusers, which are shown in figure L-2, helped to overcome these problems, allowing a volume flow rate reduction down to 25% of the maximum without loss of the air distribution in the space, and extended the potential applications of the VAV system [1], [4].

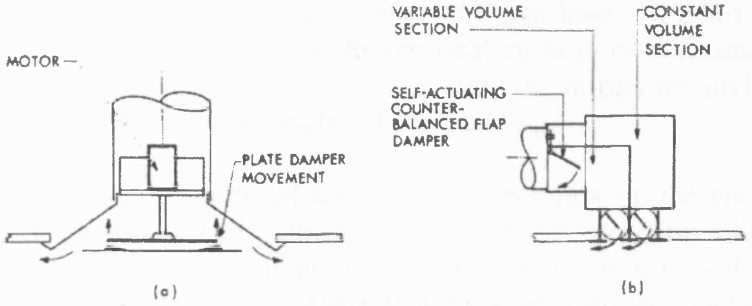

Figure L-2: Variable geometry supply diffusers: (a) variable orifice, (b) variable bypass [1]

Having overcome the problem of poor air distribution, the way was clear for the rapid growth of a variety of VAV system configurations. As a result, the VAV system is considered today one of the dominant HVAC systems both in the USA and the UK, being installed in a wide variety of building types including health centres, office and educational buildings [2].

It is quite difficult to name all the variations and hybrid or pseudo-VAV systems that have been developed since the 1970s. However, some of the most common VAV system configurations were developed in response to the fact that the VAV system does not incorporate an inherent heating ability. When the zone temperature falls, the VAV terminal unit reduces the supply volume flow rate, as the sensible heat gains diminish, until the minimum flow rate to meet the ventilation requirement is reached [3]. This means that a typical VAV system cannot meet the potential heating requirements mainly of the perimeter zones. As a result, three different VAV system configurations were developed to expand the application of the VAV technology to buildings where some form of heating is required.

The VAV system with compensated perimeter heating represents the cheapest and simplest solution for the provision of space heating when this is required. Thus, the VAV system copes with the heat gains from people, equipment, lights or solar radiation, and a secondary heating system, like radiators, is placed around the perimeter of the building. The radiators are fed with LTHW, the flow temperature of which is compensated against outside air temperature to deal with the heat losses through the building envelope [3].

The disadvantage of this arrangement is the waste of thermal energy which may occur, since the heating output of the radiators is related to the outside temperature, without taking into consideration the heat gains that could offset the heat losses. The addition of thermostatic radiator valves to take advantage of the beneficial heat gains does not produce the expected results, since the valves are self-acting with a slow response, and are not in the same control loop with the VAV terminals, which have a faster response [3].

The VAV system with terminal re-heaters is the most popular application of the VAV technology in office buildings, even though it involves higher capital cost than the previous VAV system configuration. When the zone air temperature falls, the VAV terminal reduces the volume of the supply airflow rate until the minimum is reached. Upon further reduction of the zone air temperature, the supply volume flow rate remains constant and the re-heat coil takes over to warm the air. Thus, the VAV system with terminal re-heaters consumes much less thermal energy than the CAV system, since only the minimum airflow rate is re-heated and only around the perimeter of the building.

There are several variations of this system depending on the configuration of the VAV terminal units. For example, apart from incorporating a heating coil in the terminal unit, it is also possible to add a secondary cooling coil to respond to the increased cooling requirements that usually arise from the extensive use of IT equipment in contemporary office buildings [1].

Another possibility is to introduce fans to the VAV terminal units to improve the control of air distribution at reduced airflow [3]. There are two types of fan-assisted VAV terminals, as can be seen in figure L-3 [1]:

- One that has the secondary fan in parallel with the primary air supply.
- An alternative one that has the secondary fan in series with the primary air supply.

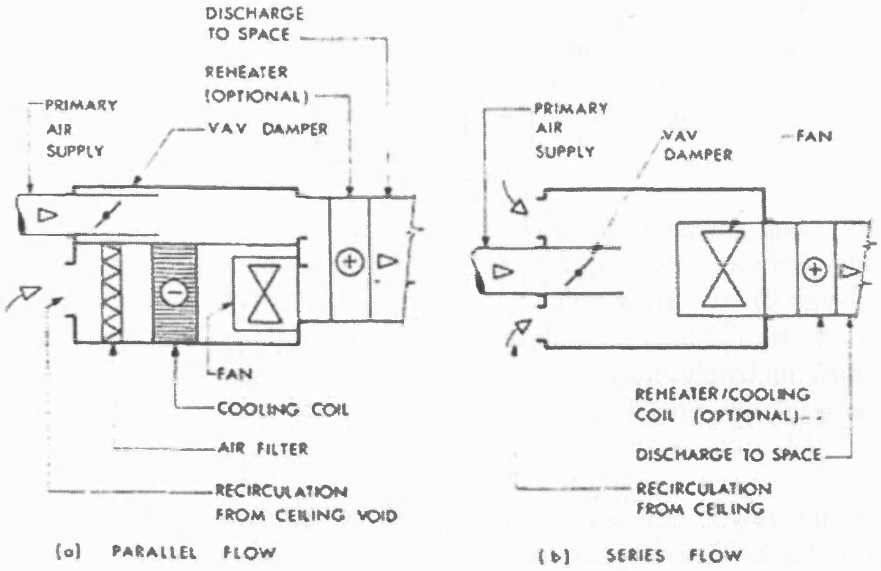

Figure L-3: Fan-assisted variable volume terminal devices [1]

In the parallel flow type, the secondary fan runs only when the cooling load exceeds a certain limit, using less fan energy than the series fan configuration, where the secondary fan runs continuously. On the other hand, this intermittent fan operation may cause more disturbance to the air distribution than the continuous running of the fan in the series flow arrangement [1].

Finally, the third type of VAV system, which is capable of providing space heating, is the dual-duct VAV system. In the dual-duct system the air handling unit supplies warm air through one duct and cold air though the other [4]. The control of temperature is achieved by mixing of the warm and cool air in proper proportions [4]. Thus, as the room temperature falls, the VAV terminal, which receives air only from the cold duct, reduces the volume flow rate to its minimum value. On further fall of the room temperature, air from the hot duct is mixed, under thermostatic control, with air from the cold duct, so that the total delivery of air at the room remains constant at its minimum value.

There are several variations of the dual-duct system. A common dual-duct system arrangement is to serve the perimeter zones using the dual duct supply and the interior zones using only a single duct supply of cool air [1]. This hybrid configuration is certainly more cost-effective since the supply of hot air is limited to the perimeter zones only [5].

Two more variations of the dual-duct system are based on the number of fans which are employed to supply the air to the spaces being served by the system. In dual-duct, single-fan systems a common supply fan serves both hot and cold ducts, whereas in dual-duct, dual-fan systems, there is a fan in both the hot and cold ducts. The choice of one of these two configurations is usually a matter of economics and space availability, with the single fan system requiring less space and cost [5].

The dual duct systems are quite popular in the USA, (where they are installed in office buildings, hotels, hospitals, schools and large laboratories), mainly due to their flexibility in satisfying multiple loads. On the other hand, the dual-duct systems are not so popular in the UK [4]. The main reason is the increased capital cost and the amount of ductwork required, which can be up to twice the size of a single duct VAV system [5].

To sum up, the VAV system is the most popular all-air system, and is widely used in commercial applications, providing satisfactory thermal comfort conditions in combination with low energy use. The ability of the system to reduce the volume of the supply air as the sensible heat gains diminish, allows for significant fan energy savings, while the mixing of re-circulated air with fresh air limits the use of mechanical cooling, especially during the intermediate seasons.

Additional advantages of the VAV system include the lower initial and operational costs, in comparison with other systems that provide individual space control, because it uses single runs of duct and requires relatively simple control at the air terminal [3]. Moreover, VAV systems are particularly popular in buildings subjected to long periods of cooling loads, while they can also be relatively easily adapted to changes in office partition layouts [5].

Finally, the inherent weakness of the system to provide space heating has been overcome with a number of different system configurations, the most popular of which is the addition of re-heat coils in the terminal VAV units. It should be stressed that only the minimum flow rate is re-heated avoiding the waste of heating energy.

A VAV system with terminal re-heaters is simulated in B-TAS as explained in section 3.5.2 (chapter 3).

L.3 Fan coil unit system

The fan coil unit (FCU) system is the principal type of air-water system, which has been in use world-wide since the early part of the 20th century. In the UK, it has been applied to a large number of office buildings since 1980 [3].

Fan coil units are basically small air handling plants, which can be installed in each room being conditioned, using either the manufacturer's sheet metal casings, or some form of concealment in purpose-designed enclosures [1], [3].

The units can be placed in the room either vertically or horizontally, as can be seen in figure L-4, depending on the requirements of the application. The most familiar are the vertical units, which are placed under a window, or on external walls to compensate for the heat losses through the building envelope. On the other hand, horizontal units are usually located above a suspended ceiling. They provide floor space savings, but they also require high floor to ceiling heights, since the void in which they are placed must be of sufficient depth to accommodate them [6].

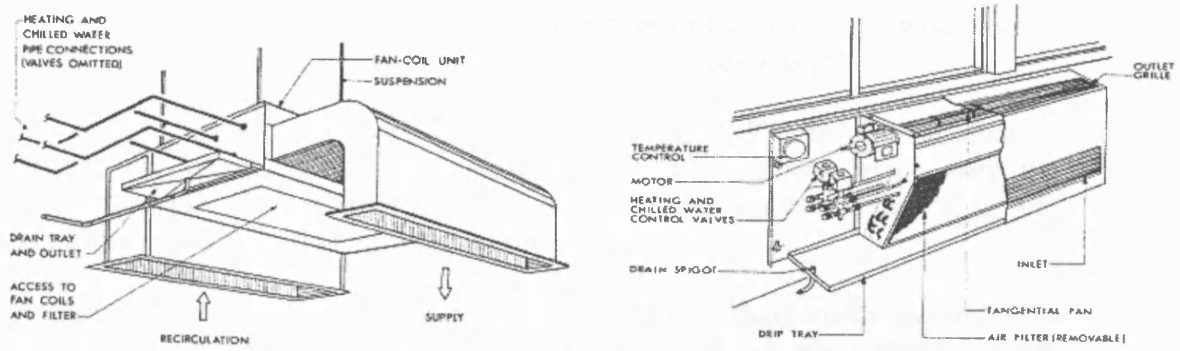

Figure L-4: Fan coil units fitted above a suspended ceiling or under a window [1]

The basic elements of a fan coil unit are a simple filter, a fan and a water-to-air heat exchange coil [1]. Space cooling is provided by continuous operation of the fan, which re-circulates the room air, blowing it over the cooling coil. However, there are several types of fan coil units which are also capable of providing space heating.

The two-pipe changeover fan coil units contain a single coil, which is supplied with chilled water in summer and heated water in winter from a common water circuit, connected to central heating and cooling plants via 3-port changeover valves [6]. This type of FCU system is suitable when the period of climate change between winter and summer is short, with little or no mid-season as, for example, in several parts of the USA [1]. However, two-pipe fan coil units are not very popular in the UK, where the lengthy spring and autumn characteristics of the climate create such internal conditions that some zones of the building may require heating, while others require cooling at the same time [1], [2], [11].

Four-pipe fan coil units incorporate separate heating and cooling coils, which are supplied with heated and chilled water, respectively [6]. Clearly, this is the most suitable option for temperate climates, since the fan coil terminal units are

capable of providing either heating or cooling depending on the requirements of each zone, throughout the year.

It should be stressed that fan coil units primarily re-circulate the room air. This means that the minimum fresh air quantity to meet the ventilation needs of the occupants must be provided independently.

The most common design option is to introduce pre-filtered and heated fresh air to the space through a ducted system from a central plant [1]. It is also possible to add a cooling coil to the central plant, to provide cooling and de-humidification of the air, allowing the fan coil units to perform only sensible cooling. The advantage of this solution is the elimination of the condensation problems that usually occur in the fan coil terminal units [3].

The fresh air supplied by the central AHU can either be ducted to the back of the fan coil units, which are typically located above the suspended ceiling, feeding the air into the ceiling diffusers, or it can be introduced into the space separately, via conventional air terminal devices. An advantage of supplying the air separately into the space via air terminal devices is the energy conservation that can be achieved in some applications or types of climate, by switching off the fan coil units when neither heating nor cooling is required [6].

It is also worth mentioning that the sizes of the AHU and the distribution network are much smaller than these of an all-air system, since only the minimum fresh air quantity required to meet the ventilation needs of the occupants is distributed around the building [6].

An alternative design option is to place the fan coil units under the windows and introduce the fresh air directly into each terminal unit via a purpose made hole in the wall. This is clearly the cheapest design option, since it does not require any ventilation ducts, and is also relatively easy to install in existing buildings [4]. On the other hand, dust and noise pollution can be introduced into the space, while there is also the possibility of unit overload due to wind pressure [1]. Furthermore, it may also lead to air leakage problems due to ill-fitting units, which may increase both heating and cooling loads. As a result, this system configuration cannot be recommended, since it is unable to meet today's stringent indoor air quality requirements [4].

Finally, a major advantage of the FCU system is the provision of accurate temperature control on a zone-by-zone basis [6]. Occasionally, basic control of individual fan coil units can be achieved by changing the fan speed or by switching the fan motor on and off [1]. For typical fan coil units there are three fan speeds: medium with an airflow of say 100%, low with 83% airflow and high with 118% airflow [11]. For free standing fan coil units installed in hotels or cellular offices, occupants may have access to the units and be able to change the fan settings [11]. As noise is related to the speed of the fan, most units are usually set to medium or low speed [11]. However, the most commonly adopted option is to run the fan motor continuously, (so that airflow and noise are uniform and, hence, not disturbing to the occupants [11]), and control either the water temperature via automatic valves, or the air temperature via mixing

dampers with actuators supplied with the fan coil unit [1], [6]. Although there are maintenance problems associated with valves blocking, it should be stressed that the air-side control is less energy efficient than the water-side control, since there is always a hot or cold coil operating simultaneously at full duty within the unit, while air leakage usually occurs at the coil dampers [6].

To sum up, the FCU system is the most popular air-water system, which utilizes both air and water to perform the cooling function. The fresh air is usually ducted to each fan coil unit from a central plant. The distribution of the minimum fresh air quantity around the building allows for smaller plant and duct sizes and lower central fan energy consumption than all-air systems. However, if the energy consumed by the large number of zone fan coil units is taken into consideration, the total energy consumption of this system is usually higher than all-air systems (e.g. a VAV system) [2]. Although the minimum fresh air quantity is still capable of doing some cooling, the bulk of this is done by circulating chilled water through the fan coils [2]. The main disadvantage of providing only the minimum fresh air quantity to the building is that it is not possible to take advantage of the free cooling capacity of the air. Water-side economy cycles are possible, but require the use of a cooling tower, which is usually the subject of stringent health and safety requirements [2]. On the other hand, the use of water as the primary cooling medium, allows for smaller cross sectional area of distribution pipes than that required for ductwork to accomplish the same cooling task, due to the greater specific heat and much greater density of water than of air [4].

The FCU system is also capable of providing space heating using either a single coil which is provided with heated or chilled water, or separate heating and cooling coils. The second option is more suitable for the UK due to the long mid-season between winter and summer, and the general variability of the weather.

The FCU system is, therefore, one of the most well suited HVAC systems for both new multi-zone applications and refurbishment projects, while it is very flexible in terms of the loads capable of being handling [1], [6]

A four-pipe FCU system with fresh air supply from a central plant is simulated in B-TAS, as shown in section 3.5.3 (chapter 3).

References

[1] Martin P L and Oughton D R, editors, Faber and Kell's Heating and Air-Conditioning of Buildings, Butterworths, London, 7th edition, 1989

[2] Keith Shepherd, VAV air conditioning systems, Blackwell Science, 1999

[3] Jones W P, Air Conditioning Applications and Design, Arnold, London, 2nd edition, 1997.

[4] McQuiston F C, Parker J D, Spitler J D, Heating, Ventilating and Air-Conditioning: Analysis and Design, 4th edition, 2000

[5] Steve Chen, Stanley Demster, Variable Air Volume Systems for Environmental Quality, McGraw-Hill Education, June 1995

[6] CIBSE Guide B2, Ventilation and air conditioning, Department of Trade and Industry, 2001

[7] Tariq Abbas, Displacement Ventilation and Static Cooling Devices, Code of Practice 17/99

[8] David Butler, Trends in air conditioning, *Building services Journal*, June 2001, pg. 43-47

[9] Atila Novoselac, Jelena Srebric, A Critical Review on the Performance and Design of Combined Cooled Ceiling and Displacement Ventilation Systems, *Energy and Buildings 34*, 2002, 497-509

[10] Hakon Skistad, Displacement Ventilation, Research Studies Press LTD, June 1994

[11] Levermore G J, Building Energy Management Systems: Applications to Low-Energy HVAC and Natural Ventilation Control, E & FN Spon, 2nd Edition, 2000

[12]: Roderic Bunn, Termodeck: the thermal flywheel, *Building Services Journal*, May 1991, pg.41-44

Appendix M: Selection of Building Simulation Tool

The aim of this appendix is to compare three of the most popular building simulation tools (TAS, IES Virtual Environment and EnergyPlus), in order to decide which is most suitable for this study.

M.1 Building Simulation – An Overview

Buildings are major energy consumers and, therefore, primary candidates for energy conservation efforts [1]. It is estimated that substantial savings can be achieved through energy efficient design of buildings and their systems. However, it is important to understand that the energy consumption of a building does not only depend on the performance of the envelope components (e.g. walls, roof, etc), or the HVAC and lighting systems, but also on their overall performance as an integrated system within the building [2]. These complex and dynamic relations that a building has with its environment and its systems need to be modeled, as accurately as possible, in order to understand how energy efficiency can be achieved. Computers, with their speed and accuracy, are becoming powerful tools which can analyze these complex relationships efficiently and accurately, and so can aid the design process.

The building simulation concept is certainly not new. The first attempts in the field were made in the 1960s and continued until the 1970s when computer simulation became the hot topic within the research community. During the period of the oil crisis, building simulation was considered to be the major tool to produce energy efficient buildings [2].

The passing of the oil crisis lessened the incentive for achieving energy efficiency. However, in the early eighties, the interest in building simulation received new impetus brought about mainly by the developments in desktop personal computers. During this period some of the most popular energy simulation tools like DOE-2 and ESP were created. However, most of them were used mainly for research purposes and were very rarely employed in building design practices due to the high cost and difficulties involved in their use [2].

The development and use of simulation tools has changed rapidly ever since. The beginning of the 1990s saw the growing global concern to protect the environment. The wasteful consumption of fossil fuels and the use of fluorocarbon-based refrigerants were considered to have a major impact on global warming and ozone depletion. Also, the design of airtight and well insulated building envelopes, in conjunction with the intensive use of computers or lighting, and the over-reliance on HVAC systems to achieve the required levels of comfort, has made energy conservation in buildings one of the first priorities for both engineers and architects. The 1990s can, therefore, be considered the starting point for the increasing use of building simulation tools in professional practices [2].

Nowadays, there is a vast selection of software tools that cover many aspects of building design ranging from electrical lighting design to room acoustics. However, the current use of energy related programs is dominated by those for the analysis of building energy consumption and the selection & sizing of HVAC equipment [3].

Taking into consideration that the main objective of the thesis is to study the effect of a number of building & HVAC system related design factors on the energy performance of a notional air conditioned office building, it was decided to study three of the most popular building simulation programs, (TAS, IES Virtual Environment and EnergyPlus), in order to choose the one that is the most suitable for this project.

Sections M.2 to M.4 contain a short description of the main features of each of the programs. In section M.5 the three software tools are compared in order to choose the one that serves the purpose of the study best.

M.2 EnergyPlus version 1.0.0.023

M.2.1 Description of the main features of the program

EnergyPlus is a new generation energy simulation tool that combines the best features from BLAST and DOE-2, along with new capabilities [4].

BLAST and DOE-2 are energy simulation programs with a large number of users both in the USA and the rest of the world. The main difference between the two is the calculation methodology. DOE-2 uses a room weighting factor approach, while BLAST uses a heat balance algorithm [5]. Depending on the application one algorithm might prove to be more accurate than the other. Nevertheless, both programs have provided building designers with reasonably good estimates for building thermal loads and energy consumption.

However, the continuous sponsorship of two fairly similar programs from the US government was criticized due to the effort, time and cost required for the maintenance and enhancement of both of them [4]. A good reason for that criticism was the fact that the development of both programs for several decades, (sometimes by multiple authors), had resulted in a 'spaghetti code'. This means that a potential user of the program needed to have years of experience working with the code and plenty of time, in order to be able to trace the data or a subroutine for a particular simulation capability spread throughout the program. The debate about the development or the merging of the two programs finally came to an end in 1996, when the US Department of Energy took the initiative to develop EnergyPlus.

It should be stressed that EnergyPlus is a new program, based on the most popular features of BLAST and DOE-2, as mentioned above, written in Fortran 90. The advantage of using Fortran instead of C/C++ as a programming language is that the former allows the creation of a modular program structure, which

makes the addition of new features or links to other programs a relatively easy task, even for developers with limited experience with the program [4], [5].

The simulation engine of EnergyPlus is based on a heat balance algorithm that originates from IBLAST, a research version of BLAST. The main assumption of the heat balance algorithm is that the zone air can be modeled as if it were well stirred with uniform temperature throughout, which might not reflect exactly the physical reality [5]. On the other hand, the only alternative to this is a computational fluid dynamic (CFD) model, which results in a much more complicated simulation of the movement of air [5]. Nevertheless, the heat balance approach is considered to be a very accurate building thermal simulation methodology within the research community [6], while the modular structure of EnergyPlus allows for the incorporation of a CFD model in a future version of the program, if that proves necessary.

A major advantage of EnergyPlus in comparison with its predecessors, is the integrated, (simultaneous loads and system), building simulation technique that it is based on, which allows more accurate temperature and thermal comfort predictions, due to the feedback from the HVAC module to the loads calculations. The structure of the program can be seen in figure M-1, while the simulation process used in EnegryPlus can be summarized in the following [4], [5]:

- The thermal loads are calculated using the heat balance algorithm at a user specified time step (the default is 15 min and the minimum is 10 min).
- The loads are passed to the building system simulation module at the same time step.
- The building systems simulation module with a variable time step, (down to one minute), calculates the HVAC system response.
- Finally, feedback from the building systems simulation module on loads not met is reflected in the next time step of the loads calculations with adjusted space temperatures, if that is necessary.

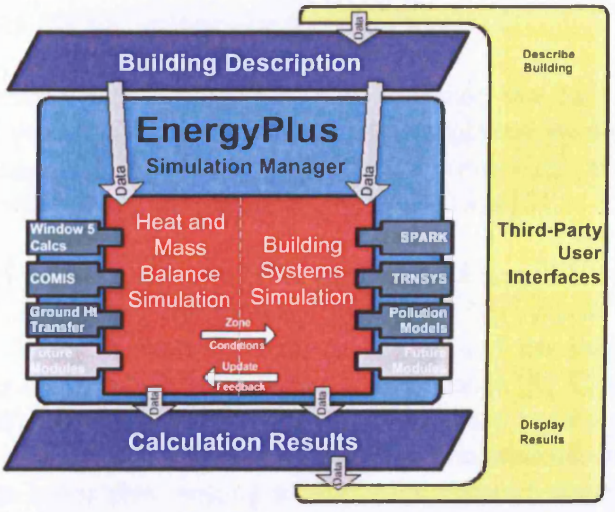

Figure M-1: Overall EnergyPlus structure [5]

In addition, the integrated simulation approach allows the evaluation of some processes that BLAST and DOE-2 could not simulate well, such as [4]:

- Realistic system controls.
- Moisture adsorption and desorption in building elements.
- Radiant heating and cooling systems.
- Interzone air flow.

Apart from the heat balance algorithm, which was the legacy of BLAST, three new modules based on the capabilities of DOE-2 were created for EnergyPlus [4], [5]:

- A daylighting simulation, which calculates interior daylight illuminance, glare from windows, electric lighting controls and reduction in the use of electric lighting. However, the daylighting calculations are limited to only two reference points for each zone in this version of the program.
- A detailed fenestration module, which incorporates capabilities like accurate angular dependence of transmission and absorption for both solar and visible radiation and temperature dependent U-value. Movable interior or exterior (but not mid-pane) blinds, or even electrochromic glazing can be simulated using this module.
- An anisotropic sky model, which includes non-isotropic radiance and luminance distribution of the sky as a function of sun position and cloud cover, allowing for a more accurate calculation of diffuse solar radiation on tilted surfaces.

Finally, a point that should be stressed is that EnergyPlus is primarily a simulation engine, which means that it does not include an interface. The main reason for this decision is the diversity of the potential users of the program [4]. Thus, the developers of the program left it to private industry to provide different interfaces that respond to the requirements of a highly diversified consumer market [4].

M.2.2 Simulation of HVAC systems in EnergyPlus

It should be stressed that EnergyPlus does not use the hardware template systems of DOE-2 and BLAST, which have been replaced by equivalent input file templates for major HVAC system types which allow users to define system configurations that differ from the 'default' configurations [5].

In general, the HVAC system simulation concept of EnergyPlus is based on air and fluid loops that imitate the network of ducts and pipes found in real buildings, and the ability to track fluid properties around the loop by means of characteristic points on the system schematic, called nodes [8]. Components such as fans, heating and cooling batteries, boilers, chillers, etc have also to be added in order to form a complete system [8]. The connections between these components and the loops they belong to are made through nodes, where fluid properties are evaluated and passed on to subsequent equipment. An example node diagram can be seen in figure M-2:

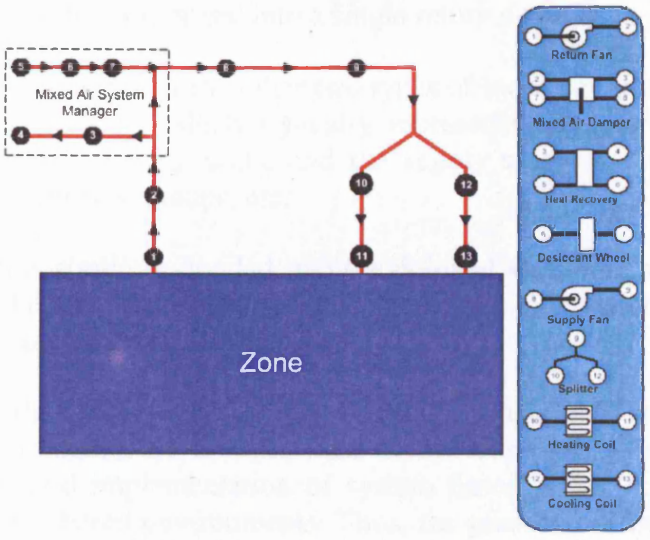

Figure M-2: Example node diagram [9]

As can be seen from figure M-2, there are nodes at the interface of the demand and the supply side of the loop, as well as input and output nodes for every system component [8].

There are three types of loop in EnergyPlus: The zone/air loop, the plant loop and the condenser loop.

The air loop simulates the air transport, conditioning and mixing, containing the associated components, such as supply fans, heating and cooling batteries, outside air economizer, etc. The air loop is connected to the zone through the zone equipment, which includes components like mixing dampers, fan powered VAV boxes, re-heat or re-cool coils, as well as high temperature radiant convective units, low temperature radiant panels and local convection units (e.g. fan coil units, air-to-air or water-to-air heat pumps, etc).

A simple example of an air/zone loop, representing a terminal re-heat system, is shown in figure M-3:

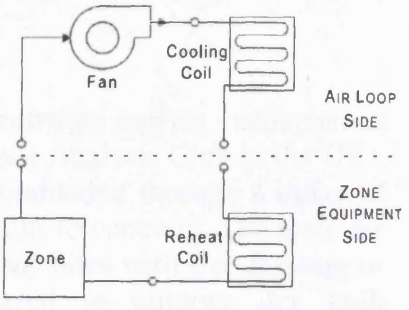

Figure M-3: Air/zone loop schematic illustrating a terminal re-heat system [8]

In general, the air loop is defined by the section of the zone/air loop that starts after the zone return air streams are combined and continues on until just before any air streams are branched off to individual zones [9]. On the other hand, the zone equipment side of the air/zone loop includes everything from where the

supply ducts are split to serve various zones, up through the point where the return ducts from these zones are mixed into a single return duct [9].

A similar concept is adopted for the other two types of loop. The plant loop is divided into the demand side, which typically represents the water side of equipment like heating or cooling coils, and the supply side, which includes equipment like boilers, chillers, pumps, etc.

The condenser loop is similarly divided into the demand side, which typically includes equipment like a chiller condenser, and the supply side which includes components like cooling towers, well water, etc.

The description of the EnergyPlus HVAC simulation engine shows that the system modeling environment of this software is not completely component based, but rather a hybrid implementation of system based, (like BLAST and DOE-2), and component based environments. Thus, the presence of fluid loops, which represent the network of pipes and ducts found in actual systems, provides the structural framework of system based models, while the presence of a number of components, which can be placed at several locations and be fully defined by the user, provide the flexibility characteristic of component based models [8].

M.2.3 Program validation

EnergyPlus has undergone extensive testing during the various steps of its development to ensure that the first public version of the program would have been as bug free as possible. The validation procedure included analytical, comparative, sensitivity and empirical tests. In most cases published test suites that included reference tests were used, in order to take advantage of the efforts of others to develop well-defined reproducible tests [7]. A summary of the testing procedures and the most interesting bugs that were found is presented in the following [7]:

Analytical Tests: BEPAC/BLAND Conduction

Analytical tests compare the building simulation software against mathematical solutions. BEPAC, (the Building Energy Performance Analysis Club in the UK), conduction tests provide analytical solutions for conduction through a range of thicknesses, for a variety of materials from aluminum to concrete. The tests are run with a cube made of the same material on all six sides with free floating or controlled inside temperature, which is subjected to outdoor dry bulb temperatures. One of these tests, with aluminum as the selected material, was applied to EnergyPlus, as a part of its validation procedure.

Analytical Tests: ASHRAE 1052 RP Building Fabric

The ASHRAE 1052 research project includes 16 tests that cover a variety of building envelope mechanisms including conduction, convection, solar gains, shading, infiltration, internal gains, radiant heat transfer and ground coupling.

These tests were applied to EnergyPlus, uncovering several bugs that raised questions requiring further investigation.

Comparative Tests: BESTEST / ASHRAE STD 140

Comparative tests compare the predictions of a number of dynamic simulation programs for a simple (but realistic), hypothetical building. The BESTEST suite[48] adopted in AHRAE STD 140 is a comparative set of tests performed on single-zone and double-zone simple rectangular building models, with variations in mass, windows, overhangs and fins. Reference results, (including annual and peak heating and cooling loads), for eight different simulation programs, are provided with the ASHRAE standard to serve as a comparison point for the testing of other simulation tools.

As an example, the annual cooling load predictions for low mass building construction are presented in figure M-4, showing that the EnergyPlus simulation results were within the range of other tested programs. In general though, this test suite helped to uncover several bugs of the software like, for example, a change required to the shade-fin surface coordinates.

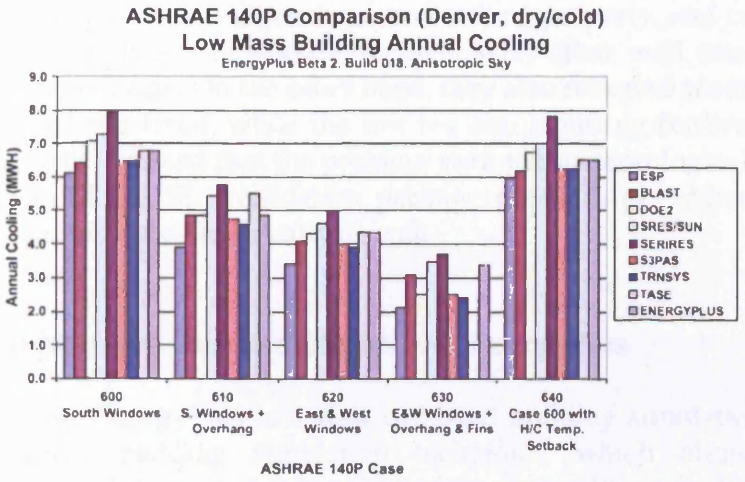

Figure M-4: Sample EnergyPlus comparative testing results [5]

Comparative/Analytical tests: HVAC BESTEST

The HVAC BESTEST suite, tests the cooling loads and electric power consumption for a single zone DX cooling system with a dry or wet coil under varying conditions of entering dry bulb, outdoor dry bulb, part-load ratio and sensible-heat-ratio. The results of these tests indicated some problems associated with the fan energy and humidity ratio that require further investigation.

[48] **Note:** The aim of these tests is to determine the amount of disagreement between the programs involved and diagnose the algorithmic sources of the differences observed. They can also be used to check a program against a previous version of itself after internal code modifications to ensure that only the intended changes actually resulted [22].

Sensitivity and Range tests

Sensitivity tests compare small input changes versus a baseline run, while range tests exercise the program over wide ranges of input values in order to confirm that the basic algorithm of the program functions properly, and identify potential errors in the code. These tests helped to eliminate several crashes of the program related mostly to the minimum and maximum specifications of input data.

Empirical tests: IEA Validation Suite

The IEA empirical validation test suite contains detailed information for two ten-day experiments, (October 17-26 with heating and May 21-30 without heating), using three highly monitored test rooms equipped with single glazing, double glazing and an opaque insulated panel. Although input files have been developed for this test package, there is a problem with the available solar data, which contain global and diffuse horizontal total radiation that must be converted to direct normal solar values in order to be used in EnergyPlus.

The variety of tests that have been applied to EnergyPlus showed in general that the main simulation algorithms are working properly, and confirmed that the simulation results are in good agreement with other well established building simulation programs. On the other hand, they also revealed several bugs, some of which have been fixed, while the rest remain, requiring further investigation. It should also be stressed that the problem with the meteorological data conversion in the case of the IEA validation package needs to be addressed, in order to validate the software empirically as well.

M.2.4 Summary of the characteristics of EnergyPlus

To sum up, EnergyPlus is a well validated building simulation tool, based on an integrated building simulation technique, which allows for accurate temperature and thermal comfort predictions. It combines the best capabilities of BLAST and DOE-2 and incorporates a modular structure, which makes the addition of new features or links to other programs a relatively easy task, avoiding the problems of the 'spaghetti' code. The HVAC system simulation environment of EnergyPlus is considered to be a hybrid implementation of component based and system based environments, which allows greater flexibility than the hardware templates of DOE-2 and BLAST, but still limits the choice of the user to a relatively small number of systems, in the first public version of the program[49]. The main criticism of the program seems to be the absence of an interface, since the developers of EnergyPlus decided to trust private industry with the task of providing interfaces that would respond to the requirements of different users.

[49] **Note:** Links to other HVAC system simulation tools are being prepared.

M.3 IES Virtual Environment version 4.0.1 (APACHE)

M.3.1 Description of the main features of the program

IES have developed Virtual Environment, a set of software tools that can be used for a number of applications ranging from the assessment of the thermal performance of a building to the design of evacuation routes in case of an emergency. However, APACHE simulation (APsim) and APACHE hvac (APhvac) are the most sophisticated tools of this package, which can be used for the evaluation of the thermal performance and the energy consumption of a building and its HVAC system. These two software tools are of particular interest for the thesis and will be studied further.

Before performing any of the aforementioned calculations, the user must create a 3D geometric representation of the building using ModelIT, which includes a comprehensive interface that allows the appropriate levels of complexity to be incorporated within a model with minimal effort [11].

An advantage of ModelIT is that it stores geometrical data, which can be supplemented with application specific data from the rest of the software tools [13]. Having not to re-enter the same data for each thermal application not only saves time, but also minimizes potential input errors [13]. The efficiency of input data can be further enhanced with the use of templates, which contain information such as building constructions, sets of internal gains, air exchanges, plant operation parameters, etc. The templates can be assigned to a single or a group of zones, avoiding again the repeated importation of the same data [13].

It is worth mentioning that Virtual Environment contains extensive libraries of materials, constructions and profiles that describe the time variation of casual gains, ventilation rates and plant set-points over the hours of a day and throughout the year. All these profiles or constructions can be directly accessed by the user, modified if necessary, and incorporated within a room thermal template. There is also the option to create a new material, construction or profile, if that is necessary.

The program also contains a rather limited library of complete weather files[50] covering mainly locations in Europe. These weather files can be accessed using a weather and site location editor called APlocate. This utility also provides the option to select a location from an extensive database, (containing information concerning mainly the latitude & longitude of the site, the height above sea level, etc), and define limited weather data suitable for heat gains and heat loss calculations[51] [14].

---

[50] **Note:** A complete weather file contains hourly values of several weather variables including dry-bulb temperature, wet-bulb temperature, direct beam solar radiation, etc and is used for the dynamic simulation of the building in APsim [12].

[51] **Note:** For heat loss calculations the weather data takes the form of a single outside winter design temperature, while for heat gains calculations the required weather data contain hourly dry-bulb temperatures, wet-bulb temperatures and solar data for one design day per month [12].

Having completed the description of the building thermal model, the user is presented with two options [12]:

- Perform industry-standard calculations and compliance tests, using APcalc.
- Perform dynamic simulation of the building, using APsim.

APcalc is a software utility that performs heat gain and heat loss calculations according to the procedures presented in CIBSE Guide A (1995, 1999, 2001) [15].

Heat losses by conduction, infiltration and mechanical ventilation are estimated, assuming steady state conditions and ignoring both casual and solar heat gains. The calculation optionally includes conduction heat gains from the adjacent rooms and the effects of mechanical and natural air exchanges [12]. The aim of heat losses calculations is to evaluate the zone heating requirements and the size of the heating plant.

Heat gains by conduction, infiltration and mechanical ventilation are calculated for 24 hours of the design day of each month, taking into account both casual and solar gains [15]. Heat gains from the adjacent rooms can also be taken into consideration using the modified U-value method. In addition, two enhancements of the 'simple model' described in the CIBSE guide can be applied [15]:

- External shading can be taken into consideration using the data contained in the shading files generated by the relevant utilities of the package.
- The solar gain factor methodology used in the 'simple model' can be replaced by a different approach that estimates solar gains more accurately and allows the software to deal with a greater variety of glazing types.

The main aim of this calculation is to estimate the room cooling requirements, while there is also the option to define the ventilation supply conditions based on the calculated cooling loads [12].

APsim is the dynamic thermal simulation program developed by IES, which makes use of a finite difference technique[52] that results in a comprehensive simulation of the building performance [16]. The thermal conditions throughout the building are determined during a time step, which ranges from 10 minutes to 1 minute, by balancing the sensible and latent heat flows entering and leaving each air mass and building surface [17]. During each time step the heat transfer processes, modeled individually for each building element, are integrated with models of room heat gains, air exchanges and plant operation.

Heat gains from people, equipment and lights are input in W/m^2, while their variation with time is specified using the relevant profiles, derived from the program database, or created by the user.

Air exchanges are divided into three categories: infiltration, mechanical ventilation and natural ventilation. They can be specified in APsim, (in ach),

[52] **Note:** In general, the finite difference technique uses several nodes to represent each layer of a building element as well as the space air mass. The differential equations describing mass, momentum and energy conservation are solved at each of these nodes to determine the correct temperatures [16].

while their variation with time is determined creating the relevant profile. Alternatively, the flow of air through openings in the building envelope can be simulated more accurately with Macroflo, a program used for the design and appraisal of naturally ventilated and mixed-mode buildings. Macroflo can be run independently or in conjunction with APsim through a link, exchanging data at run-time to achieve a fully integrated simulation of air and thermal exchanges [12].

Similarly, the plant operation can be modeled either by assuming idealized room control, or by performing detailed system simulation with APhvac [17]. In the first case, the user is prompted to define temperature and humidity set-points and determine the plant operation profile, while APsim runs in stand alone mode, assuming that the plant has either unlimited or limited capacity[53]. Alternatively, APhvac can be coupled to APsim to model accurately the performance of the air conditioning or mechanical ventilation system of the building[17], as explained in detail in the following section.

If the building incorporates shading devices, shading calculations can be performed using Suncast or Suncast Lite.

Hourly shading data describing the exposure of both exterior and interior building surfaces to beam solar radiation are generated by Suncast for the 15th day of selected months, and are stored in a shading file. If this file is linked to APsim, the program uses these data to modify the beam component of solar radiation and, when the beam solar radiation enters the building through glazing, to assign it to interior surfaces. If one of these surfaces is itself glazed, the radiation is traced on through this element to other receiving surfaces beyond and so on. The process is called solar tracking [17].

Suncast Lite also generates monthly shading data, which are stored in a similar shading file. However, the capabilities of this program are limited to external shading only, which means that it does not perform any solar tracking calculations [17].

Alternatively, shading calculations can be performed by APsim itself in a stand alone mode, for construction based shading applying only to glazed components and not to opaque surfaces, like the previous two cases.

Finally, another important feature of APsim worth mentioning is the incorporation of an efficient ground heat loss algorithm, which allows the program to model the involved heat flows in three planes, bearing in mind that 3-D predictions of heat losses to the earth are considered to be closest to reality [18]. The accuracy of this algorithm was validated empirically, comparing the results of the program with data obtained from a structure with 100% earth-contact, which was monitored for two months. The predictions of the program showed very good agreement with the monitored data [18].

[53] **Note:** The capacity limits are specified by the user.

M.3.2 Simulation of HVAC systems in APACHE hvac

APhvac can be used for the estimation of the fuel consumption of the building's heating and cooling systems as well as the analysis of the performance of the HVAC system and controls under a range of operating conditions [20]. The simulation engine of the program is completely component based imposing minimal restrictions on the user in the definition of an HVAC schematic. The interface of the program includes a grid where the user can place the various components that form the HVAC schematic, as can be seen in figure M-5 [20].

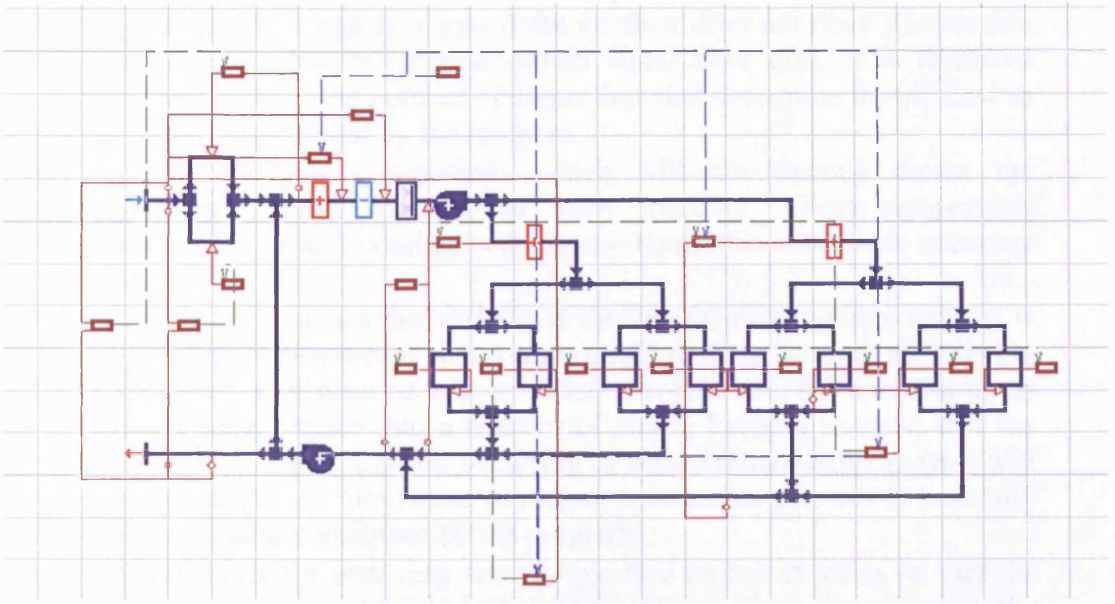

Figure M-5: Example of an HVAC system schematic in APhvac [19]

The majority of system components are presented graphically in the form of 'tiles'. Each tile contains a set of parameters characterizing the operation of the component it represents. The program database includes heating and cooling coils, spray humidifiers, fans, dampers, etc. There are also some components such as chillers or boilers that do not appear on the system schematic, but are linked, instead, to the rest of the components through text references [19].

Having assembled the HVAC system from its basic components, the next step is to determine its operation, which is governed by controllers. The user has got to overlay the controllers on top of the HVAC schematic in order to determine the operation of the various components and move the air through the system network. Each of these controllers has as input, a time switch profile and, optionally, a physical variable (this is the sensor signal which can, for example, be temperature, humidity, etc). The output of the controller is again a signal, which can be either logical or numerical. The logical control signal will be ON or OFF, depending on the sensed variable and the parameters of the sensor. The numerical signal can be, for example, the off-coil temperature of a heating battery. It is also possible to link controllers together so that the final signal is the product of a rather complex set of decisions [19].

It is obvious that the user can specify a large number of HVAC systems choosing the desired combination of components. The complexity of the systems is limited only by the components available by the program and some basic principles regarding their connection, which the user should keep in mind. The most important of these principles are the following [19]:

- Each HVAC system requires a minimum number of controllers that define the flow of air through the system network. At junctions, the program must know the flow at all branches except one, which can be specified by subtraction or addition. On top of this, the program does not check for over specification of flow rate, which means that it is possible to generate meaningless output if the air flow does not obey Kirchhoff's law (i.e. flow into a junction should equal flow out). It is therefore important to keep the number of controllers that determine the air flow to the minimum required by the program.
- There are certain components which will not operate unless the appropriate control strategy has been specified. These components include heating and cooling coils, spray humidifiers and heat recovery units.
- The program assumes that as long as the supply air enters the zone, it is fully mixed, which means that it cannot differentiate between air entering from a ceiling diffuser or a floor outlet. Nevertheless, the user can try to divide a single space into a number of zones, keeping in mind that the mechanisms of heat transfer occurring in such a situation, (e.g. stack and system induced air movement or radiant heat exchange), can at best only be approximately analyzed by the program.
- In some cases the user may want to put two rooms in series so that the outlet from one room feeds into the inlet of the other. For example, the extraction of room air through a ceiling void can be simulated by defining the occupied space and the ceiling void as two separate zones and connecting them in series. However, the program limits the number of the rooms that can be chained together to two.

M.3.3 Program validation

APACHE took part in the major empirical validation exercise carried out by the International Energy Agency (IEA) in 1993 [31], which included 17 detailed thermal simulation programs from 8 countries. The program predictions were compared with high quality measurements taken from a number of test rooms which were chosen to be a good thermal compromise between the needs for realism and experimental accuracy.

The IEA exercise provided a snap-shot of the capabilities of the dynamic simulation programs in thermal modelling of buildings. In particular, the benchmarks that were developed assessed the reliability of the programs to predict heat transfer through the building fabric [31]. None of the program predictions were within the estimated uncertainty bands on all occasions, but even in such a case, the values produced by some programs were much closer to the measurements than others. It is, therefore, clear that some programs performed much better than others. APACHE was one of the programs that

performed well, providing predictions consistent with the measured data, which were within the uncertainty bands in most cases.

In addition, APACHE took part in an Anglo-French research project[54] aiming to identify and remedy the causes of poor predictive performance in four thermal simulation programs [32]. To this end high quality measurements were taken for two double-glazed test rooms[55] heated by an oil-filled electric radiator. The key building performance parameters measured were the room air and surface temperatures.

The predictions of the programs were compared against the measured parameters mentioned above, using two advanced analysis techniques. The main feature of both techniques was that they disaggregated errors due to different sources of energy helping the analyst to focus on the algorithms related to these sources in order to identify possible mistakes [32]. Differences were observed between the measurements and the predictions of all programs in the air temperature. Both methods mentioned above indicated that the main source of this error was the inaccurate modeling of the heater and its dynamics. This revealed the need for an improved method for the modeling of heat sources of various types taking into account both the radiant and convective components of heat input as well as the storage effects of the heater if appropriate [32]. In addition, some programs predicted higher or lower floor temperatures than the measured data or the rest of the programs[56]. The prediction of solar radiation and its distribution to the enclosing surfaces was found to be the most likely source of error in this case.

Finally, an inter-model comparison of APACHE and TRNSYS was carried out with particular reference to HVAC plant and control system modelling [38]. The basis of comparison was a seven-zone constant air volume (CAV) system. The building model constructed in both programs included four additional zones which were heated and naturally ventilated. The HVAC system included a primary air conditioning plant consisting of a mixing damper, (set with 28% minimum fresh air), and a pre-cooling coil, while terminal heating and cooling coils were installed in each of the seven air conditioned zones. Both programs were set up using the same building, plant and meteorological input data. However, TRNSYS required additional detailed plant information, (e.g. chilled water and hot water coils required valve characteristic and water flow specifications), due to the rigorous nature of its modelling of certain system components [38].

The CAV system was simulated for two months (January & July), while the results for a 3-day winter and 3-day summer period were only considered in the comparative analysis. The simulation results included air temperatures and relative humidities for strategic points around the system network, as well as for

[54] **Note:** APACHE version 7.2 took part to this project [32] while APACHE version 6.52 (older version) was involved in the IEA validation exercise [31].
[55] **Note:** The measured data sets were taken from the EMC test rooms which were also used in the IEA empirical validation exercise described earlier and other studies [32].
[56] **Note:** It was observed that CLIM2000 over-estimated, while APACHE under-estimated the influence of solar radiation on the floor temperature [32].

two air-conditioned zones on opposite orientations of the building (i.e. a South-facing and a North-facing zone) [38].

Certain groups of results compared very well, for example, the zone air-conditions for the winter period. On the other hand, comparative zone air conditions in summer and plant air conditions in winter contained some significant inconsistencies. In the former case, the reason for the observed inconsistencies was the inadequate capacity of the zone cooling coil in TRNSYS, suggesting that the sizing method used by this program needed refinement [38]. In the latter case, the reason was the major effect of an artificial control loop parameter[57] input in APACHE on the plant performance, raising questions regarding the proper choice of value for this parameter [38].

M.3.4 Summary of the characteristics of APACHE

In general, IES have developed a set of comprehensive software tools that cover a variety of aspects of the building design, incorporating a user-friendly interface, which allows the user to design complicated building models with minimal effort, and perform a number of calculations without having to repeat the same input data. The dynamic simulation of the building model is performed by APsim, which makes use of a finite difference technique that results in a comprehensive simulation of the building thermal performance. APsim can be run in a stand alone mode or in conjunction with other software tools, exchanging data at run time, to achieve a detailed assessment of the airflow through the openings in the building envelope, or the effect of solar shading on the internal temperatures and the heating or cooling requirements of the zones. The analysis of the performance of the HVAC system is performed by APhvac, which can also be run independently, or be integrated with the dynamic simulation of the building by APsim. The simulation environment of APhvac is fully component based, allowing the user to simulate a large number of HVAC systems making the appropriate combinations of system components. However, the program imposes some restrictions on the simulation of HVAC systems, including the definition of the airflow through the system by the user, the rough estimation of certain heat transfer processes related to stack or system induced air movement and radiant heat exchange, as well as the limitation of the number of zones that can be chained together[58].

[57] **Note:** This parameter acts to retard the change in control signal in a time-step [38].
[58] **Note:** In other words, the outlet from one room feeding into the inlet of another is limited to two, as also explained earlier.

M.4 EDSL TAS version 8.40

M.4.1 Description of the main features of the program

TAS is a software package for the thermal analysis of buildings developed by Environmental Design Solutions Ltd (EDSL). The package consists mainly of 3D-TAS, a building design modeler, A-TAS, a thermal and energy analysis tool, B-TAS, an HVAC systems simulator and Ambiens, a 2D computational fluid dynamics (CFD) program.

TAS is considered to be a comprehensive design tool for the simulation of a building's energy and thermal comfort performance and is widely used in Europe. It is particularly popular in the UK, as can be seen from table M-1, which estimates the use of some of the most well known simulation tools in several countries[59] [25].

tool	*lpm*	*"home" market*	*category*	*focus*
TeknoSim	100	Sweden	manufacturer, low cost	Single-zone indoor climate equipment sizing
IDA ICE	22	Sweden	commercial, high cost	Multi-zone indoor climate and energy
TSBI3	30	Denmark	semi-commercial, high cost	Multi-zone indoor climate and energy
TAS	5	U.K.	commercial, high cost	Multi-zone indoor climate and energy
ESP-r	1	U.K.	academic, free	Multi-zone indoor climate and energy
HAP	17	U.S.A	manufacturer, medium cost	Multi-zone energy and equipment sizing
DOE-2	5	U.S.A.	semi-commercial, low cost	Multi-zone energy and equipment sizing
Energy10	4	U.S.A.	semi-commercial, low cost	Few-zone energy, mainly architectural use
TRNSYS	4	U.S.A.	semi-commercial, high cost	Multi-zone indoor climate and energy

Table M-1: Number of single user licences per million of inhabitants (lpm) for a selection of building simulation tools [25]

The first task of a potential user of TAS is the creation of a 3D model of the building using 3D-TAS. The main role of 3D-TAS is to prepare data for the thermal simulation of the building in A-TAS. Thus, apart from the building geometry interface, the program also provides facilities for [26]:

- assigning 'building elements'[60] to walls, floors and ceilings.
- placing apertures for air flow calculations.
- defining the zones[61] of the building model.

A problem of the interface of 3D-TAS is that it restricts the user to the design of models of fairly simple geometry. It is quite clear that it cannot be compared with the interface of CAD software. However, the priorities of the two types of software are quite different. CAD is a detailed architectural tool that aims for

[59] **Note:** The accuracy of this table is rather limited since the author has in some cases estimated the percentage of a given total number of licences that corresponds to a specific 'home' market [25]. Nevertheless, it can provide an indication of the popularity of several simulation tools in different countries.
[60] **Note:** In general, a 'building element' contains information concerning (a) the thermal properties of the component, (b) its thickness (which takes part to the calculation of areas and volumes) and (c) its colour (which helps to identify the element in the perspective views of the 3D building model) [27].
[61] **Note:** A zone is identified as the region of the building in which the air temperature and humidity are assumed to be uniform [27].

geometrical realism. 3D-TAS, on the other hand, is a simple design tool that aims to produce a building model for thermal analysis. Thus, in the latter case, complex shapes can be simplified making sure that surface areas, aspects and contained volumes are reserved so that the heat conduction, thermal capacity and dominant spatial relationships remain the same [30]. This is why even though a DXF/DWG file can be imported and used as a background image, (e.g. a reference floor), to trace over, it is recommended that the user should first remove all the unnecessary details from the DXF file.

The building model is directly linked to A-TAS, a thermal simulation tool that uses the response factor method for the transient analysis of the building structure, which provides accurate results requiring up to 10 times less simulation time than finite difference methods [24].

The simulation technique used by A-TAS is based on the tracing of the thermal state of the building through hourly snapshots that allow the influences of the numerous thermal processes occurring in the building, (e.g. the heat transfer through the building fabric by conduction or convection, the long-wave radiation exchange, the effect of solar radiation that is reflected, transmitted or absorbed by the various building elements, the internal heat gains from people, equipment or lights, the heat losses or gains via infiltration, natural ventilation and air movement through the various zones, etc), to be properly accounted for. All these thermal processes are represented by a number of equations, which are solved simultaneously with respect to the energy conservation theorem, to generate air temperatures, surface temperatures and room loads. The procedure is repeated for each hour of the simulation period in order to give a detailed picture of the way the building will perform under extreme design conditions or throughout a typical year [23], [27].

The thermal simulation of the building, as described above, can be carried out over a whole year using real weather data. A-TAS includes an extensive climate database containing hourly weather files for many different regions of the world. Also, there is a utility allowing the conversion of different types of weather files to TAS format. Furthermore, it is possible to introduce hourly weather files from METEONORM, which is a comprehensive meteorological reference incorporating an extensive catalogue of meteorological data and calculation procedures for solar engineering applications and system design at any desired location in the globe [39].

Having defined the building thermal model and its location, the user has got to specify the constructions of the building elements. The program provides a library of materials and constructions, which can be modified if necessary. There is also the option to create new materials for which the user must enter a minimum number of parameters, while the rest can be calculated by the program.

The next task of the user is the specification of the internal conditions including casual gains, infiltration & mechanical ventilation air changes and environmental control settings. The program provides a rather limited database of internal conditions, which means that in most cases new ones will be created. The basic parameters that the user must specify include:

- The internal heat gains from people, equipment and lights in W/m^2.
- The infiltration rate in air changes per hour (ach). If the building is mechanically ventilated, the user also specifies the fresh air that enters the zone via this system in ach[62].
- The temperature and humidity set-points of the plant. There is also the option to simulate the effects of proportional control, frost protection and advanced/optimum start on the plant performance. The size of the heating and cooling plant can either be specified by the user or estimated by the program.

The variation of all the aforementioned parameters with time for each hour of the day is user defined for three day types: Weekday, Saturday and Sunday. However, additional day types can be created if that is necessary[63]. The calendar function is used to assign each day type to one or more days of the simulation year, as well as to create new day types, as mentioned above [27].

The user can similarly schedule the opening of windows in case of a naturally ventilated building. By generating a natural ventilation air flow network between the apertures in the building model, TAS is capable of carrying out fast and stable simultaneous building simulation with integrated bulk air flow even for large commercial buildings [24]. The aperture air flow model takes account of the pressure flow characteristics of apertures, wind and stack pressures and any prescribed air flows [23]. Wind driven ventilation rates and direction are calculated for each hour of the simulation period using the hourly values of wind speed and direction contained in the weather file. By simultaneously calculating internal air temperatures, the effects of buoyancy forces are also integrated into the analysis, while the interaction between mechanical ventilation and natural ventilation forces can also be taken into consideration [24].

Furthermore, the aperture opening can be controlled with respect to a number of parameters, including the zone temperature, the outside temperature and the wind speed, allowing the simulation of BEMS operation or mixed mode ventilation strategies [27].

Solar shading of the building can be modeled by specifying shading devices such as side-fins, overhangs and external, internal or mid-pane blinds. Overhangs and side- fins can be applied to both opaque and glazed building elements, taking into consideration the effects of diffuse shading, which if ignored, can add up to 2°C to the predicted internal temperatures [24]. This shading effect can also be combined with shadow calculations performed when exiting from 3D-TAS [27]. These calculations take into account both external shading (by the subject building or the surrounding buildings), and internal solar tracking. This means that the program can track the distribution of the admitted solar radiation among the zone's surfaces, by modeling the repeated bouncing of radiation around the zone. If any of the zone surfaces incorporates transparent elements, part of the radiation will be transmitted to the adjacent zone. This part of radiation will be dealt with in the distribution which will take place in the adjacent zone.

---

[62] **Note:** This parameter serves to obtain an estimate of the total load on the air handling system serving the building without using B-TAS, the detailed system analysis software [27].
[63] **Note:** The maximum number of day types equals 7.

The simulation of the building can now be performed either for a single day or for a whole year. In the latter case the user is presented with two modes of simulation [27]:

- The sequential mode, where the performance of the building is simulated for a sequence of days. If required, A-TAS can also size the heating and cooling plant on the basis of the maximum heating and cooling requirements encountered in the process of achieving the specified temperature lower and upper limits during the plant operating periods.
- The design day mode, where the building is simulated for a specified set of days chosen by the user to test the limits of plant performance. Sizing is always performed in this mode, while the user is presented with various options, (e.g. preconditioning period and optimum start), which can give a generous margin of over capacity to the plant or not.

Finally, in the sequential simulation mode, a Building Simulation Output (BSO) file is generated, which can be used as a systems loads file for B-TAS [27].

M.4.2 Simulation of HVAC systems in B-TAS

B-TAS is a software tool, which simulates the energy performance of HVAC systems. It is a component-based simulation program that allows the systems to be assembled graphically from a number of components, as can be seen in figure M-6. Each of these components represents a set of relationships between system variables such as mass flows, temperatures, humidities, etc, which can be solved simultaneously using iterative techniques [28].

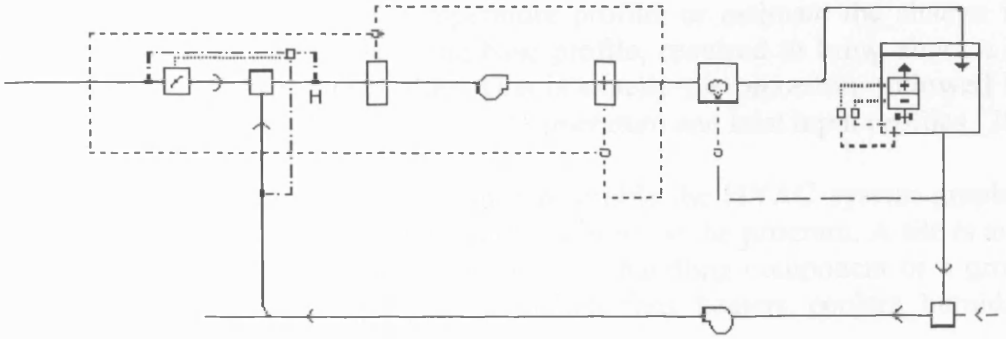

Figure M-6: Example of an HVAC system schematic in B-TAS [28]

B-TAS provides two modes of simulation [28]:

- The design point simulation, which does not require a building simulation in A-TAS. It allows for the investigation of system performance under design conditions. The only required parameters in this case are specifications for zone sensible and latent loads.

- The loads file simulation, which allows the performance of the system to be assessed in relation to the dynamic performance of the building, and requires the generation of a loads file from A-TAS.

The complicated factor in performing the zone sensible balance in the loads file simulation is its dynamic nature. Thus, the sensible load at a particular time step depends not only on the conditions at that moment, but on what has occurred before as well, since the building fabric has the ability to store heat and release it at a later time. The analysis of the dynamic behaviour of building fabric is the main objective of A-TAS and forms the starting point for the joint simulation of the building and its systems in B-TAS loads file simulation. The approach of each simulation tool is the following [28]:

- In A-TAS the building is simulated on the basis of a simple model of the HVAC system, which makes use of a limited number of parameters, (i.e. heating and cooling set-points, control band, heating and cooling plant capacities), to characterize its behaviour throughout the simulation period.
- In B-TAS, the system behaviour is simulated more accurately, since the simplified model of A-TAS may not have the flexibility to represent the full range of influences that the system may put on the building.

Consequently, the approach of B-TAS is to use the A-TAS results as a starting point, and adjust them to take account of the differences between the generic model of A-TAS and the detailed model of B-TAS. Because of the dynamic nature of the building response, this adjustment should also take into consideration the history of zone temperatures and loads as well as their instantaneous values [28]. The solution adopted is based on zone weighting factors, which are sets of numbers that embody the dynamic thermal characteristics of the zone for the purposes of system simulation [28]. Knowing the weighting factors it is possible to calculate the zone heat input profile required to produce a given temperature profile, or estimate the change in the heat input profile relative to some base profile, required to bring about a given change in the temperature profile. This is exactly the procedure followed by B-TAS, with A-TAS providing the base temperature and heat input profiles [28].

As mentioned earlier, the user must assemble the HVAC system graphically from a selection of 'tiles' included in the library of the program. A tile is an icon displaying a graphic representation of an air handling component or a group of components [28]. The tile categories include fans, heaters, coolers, humidifiers, zones, etc.

Having designed the HVAC system, the user must determine the control strategy by placing control arcs on the system schematic. The control arc is a graphical representation of a control device, which consists of (a) a dashed line, (representing the sensor arc), attached to a duct symbol, (b) a box representing the controller itself and (c) a dotted line, (representing the signal arc), attached to an air handling component [28].

The next task of the user is to set the appropriate parameters for each system component and controlling device (e.g. air handling component capacities,

controller set-points, etc). However, the program can simplify this procedure, providing the following facilities [28]:

- As mentioned before, some of the tiles represent groups of components, which may also incorporate control arcs. Thus, the user can choose directly a tile representing, for example, an air handling unit consisting of a fan, a heating and a cooling battery, or a temperature optimizer, which is basically a mixing box incorporating the appropriate controllers that enable the mixing of the fresh and return air streams in variable proportions with respect to the target temperature set as the parameter of the sensor. Similarly, the user can choose from a number of zone tiles, which represent several systems, including VAV, CAV, fan coil unit systems, etc. These simplifications in system design not only save time, but also reduce the possibility of input error and increase the confidence of the user towards the simulation of more complicated systems and control strategies.
- There is a selection of duct network tiles, which provide a concise way of representing systems incorporating repeating elements[64]. As a result, it is possible to simulate HVAC systems serving a large number of zones in multi-storey buildings, avoiding complex system schematics.
- Several component parameters can be sized automatically by the program in the course of a simulation with respect to certain imposed demands.

Having specified the system parameters, the program is able to start the simulation and perform a number of tasks, including the assessment of the system's environmental performance, analysis of energy conservation options, plant sizing, etc.

M.4.3 Program validation

TAS was also one of the dynamic simulation tools that took part in the empirical validation exercise described in section M.3.3, which was carried out in 1993 by the International Energy Agency (IEA) [31]. The test rooms used in this study were carefully constructed, the monitoring equipment and procedures were of high standard, and the data produced by the Energy Monitoring Company (EMC) were of high quality, meeting the stringent criteria set by IEA [24].

It is worth mentioning that EDSL was first involved with the EMC datasets in 1990, when a 'blind' investigation trial[65] on TAS was carried out [31]. It was concluded from this study that TAS was capable of reproducing the performance of the test rooms well. In absolute terms the predictive performance of TAS was better than other programs that were also tested against these datasets, while in

[64] **Note:** For example, any part of the HVAC system schematic that is positioned between the outlet of a distributor network and the inlet of a collector network is considered to be replicated a user-specified number of times [28].

[65] **Note:** In a 'blind' study, the modellers have no knowledge of the actual measured performance of the test rooms. This provides a clear snapshot of the program capabilities when used in a very similar way to that adopted in a real design situation [31]. It also helps to reveal program weaknesses and avoid ambiguities which can be introduced when the modellers are able to fit predictions to the measured data [31]. It should be stressed that the first phase of the IEA validation exercise was also carried out in this way.

In all cases the TAS simulation results were consistent with the monitored data illustrating the predicted accuracy of the software.

TAS was also empirically validated using monitored data collected from the Passive House Darmstad-Kranichstein[66], for a hot summer period of 25 days (July 1995) [29]. The validation calculations showed good correspondence between the measured and the simulated temperatures. The calculated daily mean temperatures differed from the measured values by 0.1-0.5 K, while for the majority of time the temperature curve corresponded exactly with the measured data, illustrating that TAS is capable of depicting the thermal performance of a building realistically [29].

Apart from the aforementioned validation tests, TAS has also been successfully used in a number of prestigious projects. Some examples include [24]:

- The PowerGen HQ, which incorporates a BEMS that controls the window opening with respect to the air temperature in particular zones. TAS has successfully simulated this ventilation control strategy providing results quite close to the actual performance of the building.
- The Cheltenham and Cloucester College of Higher Education Learning Centre, which uses a mechanical ventilation system via a Termodeck hollow core ceiling slab and the BRE Environmental Office of the Future that uses a natural ventilation strategy based on solar chimneys.

TAS software was, finally, part of a study conducted for the Building Research Establishment and Property Services Agency (PSA) of the UK Department of the Environment [33]. This study assessed and compared the capabilities of 16 computer simulation programs to model plant and controls for building services engineering applications. The total number of programs participating in the study was narrowed down to 3 using a multiple stage process of outline evaluation and filtering for detailed investigation [33]. TAS was one of the three programs that reached this stage, meeting most of the criteria set by PSA. The other two chosen programs were APACHE (considered in section M.3) and TRNSYS, as can be seen from table M-2.

[66] **Note:** TAS version 8.0 was involved in this study [29], while TAS version 7.52 (older version) took part in the IEA validation exercise [31].